# EMERGING INFECTIOUS DISEASES®

CDC
Centers for Disease Control and Prevention

## Bacterial Infections

May 2023

**Franz Xaver Winterhalter (1805–1873), *Princess Alice (1843–78), later Grand Duchess of Hesse*, 1861.**
Oil on canvas, 46.9 in x 34.9 in/119.0 cm x 88.6 cm. Royal Collection Trust, Buckingham Palace, London, United Kingdom.

# EMERGING INFECTIOUS DISEASES®





Emerging Infectious Diseases is published monthly by the Centers for Disease Control and Prevention, 1600 Clifton Rd NE, Mailstop H16-2, Atlanta, GA 30329-4027, USA. Telephone 404-639-1960; email, eideditor@cdc.gov

# EMERGING INFECTIOUS DISEASES®

**Bacterial Infections** **May 2023**


## On the Cover

**Franz Xaver Winterhalter (1805–1873). *Princess Alice (1843–78), later Grand Duchess of Hesse*, 1861**. Oil on canvas, 46.9 in x 34.9 in/119.0 cm x 88.6 cm. Royal Collection Trust, Buckingham Palace, London, United Kingdom.

About the Cover p. 1085

## Synopses



## Research



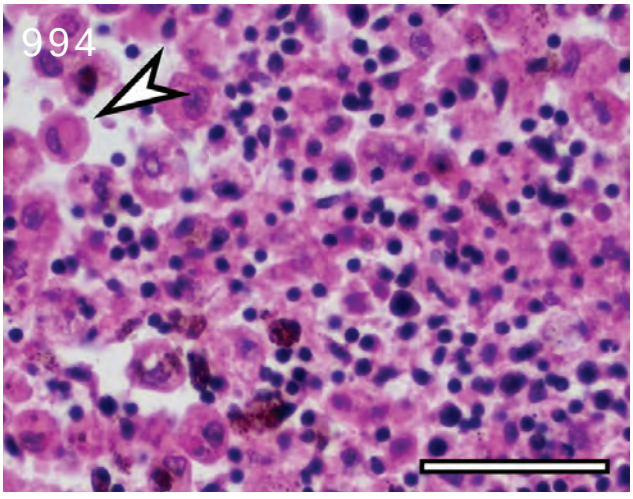




## Dispatches



EMERGING INFECTIOUS DISEASES®
May 2023



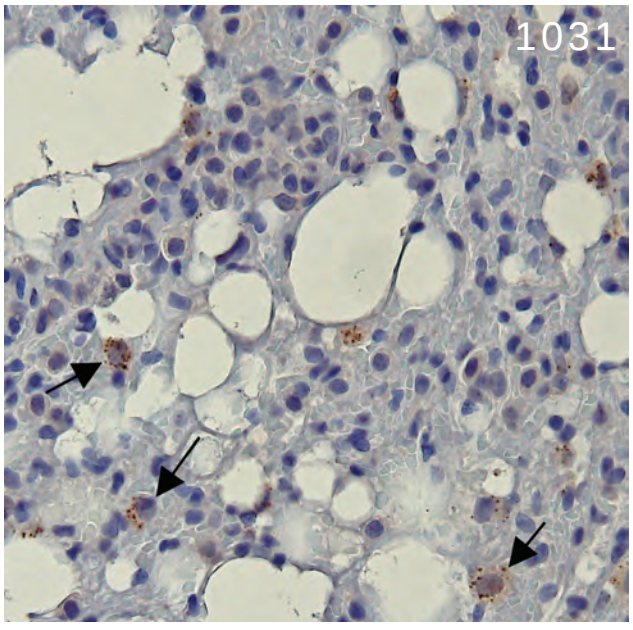


EMERGING INFECTIOUS DISEASES®
May 2023



## Research Letters



## Comment Letter



## About the Cover



## Online Report



## Correction

**Vol. 26, No. 12**



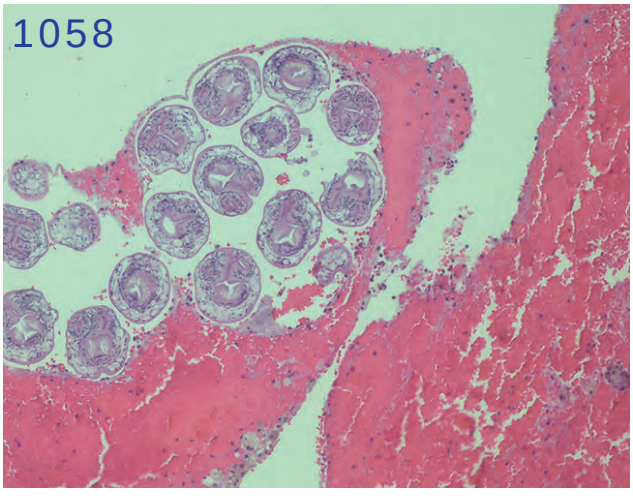

# DAVID J. SENCER CDC MUSEUM

History·Legacy·Innovation

Dr. David J. Sencer, Mrs. Mountin and Jim Collins celebrate CDC's 25th anniversary, 1961.

# CDC at 75

## January 9, 2023–July 28, 2023

## TEMPORARY EXHIBITIONS GALLERY

**Opening January 9, *CDC at 75* is a commemorative exhibition that tells unique stories about the work of this fabled agency and provides a glimpse into the breadth and depth of CDC's history and vast accomplishments. It features rarely seen objects, documents, and media taken from the CDC Museum's rich collections and archives.**

### Hours

Monday–Wednesday: 9 a.m.–5 p.m.
Thursday: 9 a.m.–7 p.m.
Friday: 9 a.m.–5 p.m.
Closed weekends and federal holidays

### Location

1600 Clifton Road, NE
Atlanta, GA
30329-4021
Phone (404) 639-0830

Admission and parking free • Vehicle inspection required
Government-issued photo ID required for adults over the age of 18
Passport required for non-U.S. citizens

# Trends in and Risk Factors for Recurrent *Clostridioides difficile* Infection, New Haven County, Connecticut, USA, 2015–2020

Chinenye M. Okafor, Paula Clogher, Danyel Olson, Linda Niccolai, James Hadler


In support of improving patient care, this activity has been planned and implemented by Medscape, LLC and *Emerging Infectious Diseases*. Medscape, LLC is jointly accredited with commendation by the Accreditation Council for Continuing Medical Education (ACCME), the Accreditation Council for Pharmacy Education (ACPE), and the American Nurses Credentialing Center (ANCC), to provide continuing education for the healthcare team.

Medscape, LLC designates this Journal-based CME activity for a maximum of 1.0 *AMA PRA Category 1 Credit(s)*™. Physicians should claim only the credit commensurate with the extent of their participation in the activity.

Successful completion of this CME activity, which includes participation in the evaluation component, enables the participant to earn up to 1.0 MOC points in the American Board of Internal Medicine's (ABIM) Maintenance of Certification (MOC) program. Participants will earn MOC points equivalent to the amount of CME credits claimed for the activity. It is the CME activity provider's responsibility to submit participant completion information to ACCME for the purpose of granting ABIM MOC credit.

All other clinicians completing this activity will be issued a certificate of participation. To participate in this journal CME activity: (1) review the learning objectives and author disclosures; (2) study the education content; (3) take the post-test with a 75% minimum passing score and complete the evaluation at https://www.medscape.org/journal/eid; and (4) view/print certificate. For CME questions, see page 1088.

**Release date: April 13, 2023; Expiration date: April 13, 2024**

### Learning Objectives

Upon completion of this activity, participants will be able to:

- Assess trends in the epidemiology of *Clostridioides difficile* infection
- Analyze race and study year as risk factors for recurrent *Clostridioides difficile* infection
- Evaluate chronic health conditions as risk factors for recurrent *Clostridioides difficile* infection
- Evaluate specific medications or medication classes as risk factors for recurrent *Clostridioides difficile* infection

**CME Editor**

**Jude Rutledge, BA,** Technical Writer/Editor, Emerging Infectious Diseases. *Disclosure: Jude Rutledge has no relevant financial relationships.*

**CME Author**

**Charles P. Vega, MD,** Health Sciences Clinical Professor of Family Medicine, University of California, Irvine School of Medicine, Irvine, California. *Disclosure: Charles P. Vega, MD, has the following relevant financial relationships: GlaxoSmithKline; Johnson & Johnson Pharmaceutical Research & Development, L.L.C.*

**Authors**

***Chinenye M. Okafor, MD, MPH; Paula Clogher, MPH, CHES; Danyel Olson MS, MPH; Linda Niccolai, PhD;*** and ***James Hadler, MD, MPH***

Author affiliations: Yale School of Public Health, New Haven, Connecticut, USA (C.M. Okafor, L. Niccolai, J. Hadler); Connecticut Emerging Infections Program, New Haven (P. Clogher, D. Olson, L. Niccolai, J. Hadler); Yale Institute of Global Health, New Haven (L. Niccolai)
DOI: https://doi.org/10.3201/eid2905.221294

Recurrent *Clostridioides difficile* infection (RCDI) causes an increased burden on the healthcare system. We calculated RCDI incidence and identified factors associated with RCDI cases in New Haven County, Connecticut, USA, during 2015–2020 by using data from population-based laboratory surveillance. A subset of *C. difficile* cases had complete chart reviews conducted for RCDI and potentially associated variables. RCDI was defined as a positive *C. difficile* specimen occurring 2–8 weeks after incident *C. difficile* infection. We compared cases with and without RCDI by using multiple regression. RCDI occurred in 12.0% of 4,301 chart-reviewed *C. difficile* cases, showing a U-shaped time trend with a sharp increase in 2020, mostly because of an increase in hospital-onset cases. Malignancy (odds ratio 1.51 [95% CI 1.11–2.07]) and antecedent nitrofurantoin use (odds ratio 2.37 [95% CI 1.23–4.58]) were medical risk factors for RCDI. The 2020 increase may reflect the impact of the COVID-19 pandemic.

*Clostridioides difficile* infection (CDI) is one of the most common causes of healthcare-associated infection (*1*) and can result in serious illness and death (*2*). CDI is classified into 3 types on the basis of epidemiology: healthcare facility–onset (HCFO), community-onset healthcare facility–associated (CO-HCFA), and community-associated (CA) CDI (*1*). Both HCFO and CO-HCFA are healthcare-associated CDIs, differing in where a person is located at symptom onset. Despite evidence of decreasing healthcare-associated CDI cases in the United States, CA-CDI incidence appears to be stable (*3*).

Recurrent CDI (RCDI), defined as an episode of symptom onset and a positive assay result after an episode with a positive assay result in the previous 2–8 weeks (*4*), is associated with increased burden on the healthcare system and increased medical costs (*2*). As many as an estimated 30% of CDI case-patients will experience a first recurrence, with increasing risk for recurrence after the previous episode (*2*). Specific to RCDI, studies have demonstrated that older age and female sex increase the risk for recurrence (*2*). CDI episodes have been shown to have worse outcomes with each subsequent recurring episode (*2*,*5*). Prior studies have described the possible factors that may increase the risk for recurrence as microbiologic factors (*6*–*9*), clinical characteristics (*5*,*10*–*15*), or epidemiologic factors (*15*). Studies mostly limited to older populations also describe social factors, such as living environment, that may be linked to RCDI (*16*) and readmission (*17*), as well as receipt of additional antibiotics (*16*) after CDI. An increasing percentage of cases that are CA-CDI (*3*) could potentially mean an increase in RCDI attributable to the community despite evidence of overall reduction in RCDI cases (*2*).

Determining trends in RCDI and both predisposing and treatment factors associated with recurrence will provide insight into the effectiveness of measures to prevent RCDI, especially given its burden on the healthcare system. Observations from previous studies of increasing cases of RCDI among CA incident cases while RCDI decreases among healthcare-associated incident CDI (*3*) may require a reexamination of the measures for managing CDI among those with CA-CDI. Because of the COVID-19 pandemic and the consequent increase in hospital admissions (*18*), an increase in RCDI is expected among those with healthcare-associated CDI, but the extent and associated factors are largely unexplored. We aimed to describe the sociodemographic characteristics, clinical underlying conditions and medical history, and medication history up to the point of incident CDI of the population with RCDI in New Haven County, Connecticut, USA, during 2015–2020. Additional objectives were to examine trends in RCDI stratified by epidemiologic class (HCFO, CO-HCFA, or CA) and identify possible factors associated with RCDI in the study population.

## Methods

### Study Population and Design

Our study used data from the Healthcare-Associated Infections Community Interface (HAIC) Program of the Connecticut Emerging Infectious Program collected during January 2015–December 2020. The HAIC program and its CDI surveillance system are described elsewhere (*1*). In brief, the CDI surveillance program, following a common protocol established by Emerging Infectious Program (EIP) sites in other states, monitors the population-based incidence and incidence trends of CDI through active laboratory surveillance of New Haven County residents, regardless of the location of their CDI diagnosis. A RCDI case was defined as a positive laboratory test for CDI in a person with an incident case 2–8 weeks after the defining positive laboratory test in the incident case.

### Epidemiologic Class

The process of assigning epidemiologic class has been described elsewhere (*1*). In brief, a case was classified as either HCFO or community-onset. HCFO was assigned if it was a hospital-onset CDI (positive stool specimen collected >3 days after hospital admission) or long-term care facility (LTCF) onset (positive stool specimen collected in an LTCF or from an LTCF resident admitted to a hospital). Community-onset was defined by a positive stool specimen collected when

a person was an outpatient or within 3 days of their hospital admission. Community-onset CDI was further classified into CA if no healthcare facility visit in the prior 12 weeks was reported; all other community-onset cases were considered CO-HCFA (*1*,*3*). CO-HCFA and HCFO cases were considered healthcare-associated CDI.

### Case Selection

A total of 7,023 incident CDI cases occurred during the study period. All CA-CDI and CO-HCFA cases, and a variable (but no lower than 1:10) random selection of HCFO-CDI cases underwent complete chart reviews at EIP sites (*1*). In determining RCDI incidence and associated factors, we excluded 430 cases without a complete chart review (usually because medical charts were unavailable for abstraction after several attempts at retrieval). We then excluded 74 cases for which an epidemiologic class was not determined and 2,218 HCFO cases not selected for chart review. The final denominator for RCDI incidence and associated factors was 4,301 cases.

We compared characteristics of index CDI cases selected for the study of RCDI and those not selected (Appendix Table 1, https://wwwnc.cdc.gov/EID/article/29/5/22-1294-App1.pdf) and observed that a significantly lower percentage of case-patients selected for analysis had HCFO classification (14.2% vs. 86.2%); they also were younger (median age 65 vs. 75 years) and had a lower mortality rate (3.8% vs. 10.5%). Because of the significantly lower percentage of HCFO cases among selected cases, a consequence of including all CA and CO-HCFA CDI cases but only a sample of HCFO cases, we then conducted a comparison of HCFO cases included and excluded in the final analysis; that review showed no significant difference in sex, ethnicity, and mortality rate between selected and excluded HCFO case-patients. However, we noted significantly higher proportions of White persons (77.1% vs. 66.6%), younger persons (median age 73 vs. 75 years), and those who had incident CDI in 2020 (36.0% vs. 5.1%) among included compared with excluded HCFO case-patients (Appendix Table 2).

### Participant Characteristics

Medical records abstraction was carried out by trained EIP personnel. For this study, we classified the retrieved information into categories of sociodemographic factors, medication history, medical history, clinical exposures, and treatment received and outcome.

Sociodemographic variables included age, sex, and race (grouped as White; Black; Asian, American Indian, or Pacific Islander; and mixed race or unknown race). Mixed race within available data was a combination of either Black and White race (n = 5) or Black and American Indian race (n = 1). Ethnicity was grouped into non-Hispanic and Hispanic categories.

Medication history included medications taken within the 12 weeks before a positive incident CDI sample. Medications included proton pump inhibitors, histamine receptor 2 blockers, antibiotics, and immunotherapeutic agents. Immunotherapeutic agents included steroids, chemotherapy agents, and other immunosuppressants. Antibiotics were classified into the different drug classes: penicillin, macrolides, aminoglycosides, cephalosporins, fluoroquinolones, trimethoprim or trimethoprim/sulfamethoxazole, carbapenem, glycopeptide, tetracycline, nitroimidazole, and nitrofurans (Appendix Table 3).

Medical history included history of CDI, immunocompromised states (including HIV with or without AIDS; diabetes mellitus; primary immunodeficiency; solid organ transplant, hematopoietic stem cell transplant, or both), cerebrovascular accidents (CVA) (including stroke and transient ischemic attacks), chronic cognitive deficits or dementia, and malignancies (including hematologic and solid organ malignancy with or without metastasis). Treatment variables included vancomycin, metronidazole, fidaxomicin, stool transplant, probiotics, and >1 treatment course duration.

Clinical data relevant to determining epidemiologic class (clinical exposures) included CDI as reason for admission and whether patients had an emergency department visit, dialysis, or surgery within 12 weeks before sample collection. Because the case report form changed from 2017 to 2018 with respect to treatment variables, only treatment data from 2018–2020 are included in this analysis.

### Primary Outcome

The primary outcome was recurrence of CDI, which we defined as a positive CDI sample using either or both of toxin assay or molecular assay and occurring 2–8 weeks after an episode of incident CDI. We defined incident CDI as a positive diagnostic stool specimen using either or both of toxin assay and molecular assay of any resident of New Haven County who was >1 year of age. We classified CDI cases occurring after 8 weeks of incident CDI as new incident cases and CDI cases occurring within 2 weeks of incident CDI as duplicate cases (*1*). We collected all information on the primary outcome, including information on whether death occurred within 90 days, through medical chart abstraction. We validated mortality data by using the Connecticut death registry database.

### Data Analysis

We calculated annual incidence rates of CDI, excluding RCDI, overall and by epidemiologic class, by using the New Haven County population for each year as a denominator. We calculated incidence rates for RCDI (cases/100 initial cases), overall and by epidemiologic class, by using CDI cases selected for analysis as denominators for each study year. We excluded cases in which the patient died within 2 weeks of incident CDI from the denominator. We compared demographic, clinical, medical, and treatment characteristics of patients with CDI with and without recurrence and then compared distribution of the same characteristics among patients with RCDI, stratified by epidemiologic class. We used the Kruskal-Wallis test for continuous variables and $\chi^2$ (Fisher exact test if cell frequency was $\leq$5) for categoric variables.

Multivariable logistic regression involved the addition of prespecified domains in a sequential manner. We selected covariates for the multivariable regression on the basis of statistical significance at $p = 0.05$ in the comparison of case-patients with and without RCDI. Multivariable model building used forward elimination, enabling visualization of the effect of each category on the overall model (*19*).

Model 1 encompassed year of incident CDI, age, sex, race, and ethnicity. Race variables were Black compared with White and multiracial or unknown race compared with White. Model 2 includes year of incident CDI, age, sex, race, ethnicity, use of proton pump inhibitors, histamine 2 receptor blockers, antibiotics, penicillin, cephalosporin, tetracycline, nitroimidazole, nitrofuran, and immunotherapy, as well as previous CDI episode, immunocompromised state, CVA, malignancies, chronic cognitive deficit or dementia, admission because of CDI, emergency department visit, dialysis, and surgery. Model 3 encompassed the epidemiologic classes in addition to variables in model 2. Results from the regression models are presented as odds ratio (OR) of RCDI for each covariate and its 95% CI. We conducted all statistical analysis by using SAS version 9.4 (SAS Institute) with 2-tailed tests of significance at $\alpha = 0.05$ level. Analyses of surveillance data obtained and conducted by Yale EIP staff have been granted a blanket exemption from Yale institutional review board review.

## Results

### Incidence Rates of CDI and RCDI

A total of 7,023 incident CDI cases occurred during 2015–2020, of which 4,301 cases had a complete chart review. The incidence rate of CDI had a downward trend during the study years, ranging from 165.2 cases/100,000 persons in 2015 to 107.8 cases/100,000 persons in 2020 (median 140.2 cases/100,000 persons). The incidence of RCDI was U-shaped across the study period: 18.1 cases/100 incident cases in 2015, dropping to 13.2–12.1 cases/100 incident cases during 2016–2019, then rising to 16.9 cases/100 incident cases in 2020 (Figure 1).

When stratified according to epidemiologic class, the incidence of total CDI cases showed a fluctuating pattern but overall decreases in HCFO and CA-CDI over time. The overall U-shaped incidence of RCDI was contributed to mainly by CA and HCFO CDI; the increase in 2020 was largely contributed to by a sharp 37.3% increase in HCFO CDI during 2019–2020 (Figure 2). Throughout the study period, the rate of recurrent CA-CDI cases generally remained consistently below the rate of RCDI among HCFO cases. Overall, 12.0% of 4,301 CDI cases with complete chart reviews had RCDI. By epidemiologic class, the recurrence rate was 13.6% for HCFO-CDI, 14.1% for CO-HCFA-CDI, and 10.5% for CA-CDI.

### Sociodemographic and Clinical Characteristics of Patients with RCDI

Among the 4,301 CDI cases with complete chart reviews, the median age of patients was 65.0 years; 61.9% of patients were female, 73.7% were White, and 8.4% were Hispanic. RCDO occurred in 12.0% of cases. A significantly higher proportion of patients with RCDI were older (median age 70.0 vs. 64.0 years), female (66.0% vs. 61.3%), White, and non-Hispanic and had incident CDI cases classified as healthcare-associated CDI (HCFO and CO-HCFA) (Table 1, 2). The only underlying condition that was significantly higher among case-patients with RCDI was a history of malignancy. Among antecedent medicines, only antecedent antibiotic use in aggregate, and specifically, cephalosporins, tetracyclines, and nitrofurans, were significantly more frequent among patients with RCDI. No specific treatment for the incident CDI case was significant, so specific treatment was not included in modeling (Table 2).

When we compared cases with RCDI by epidemiologic class of the incident CDI episode, we noted that a significantly higher proportion in HCFO case-patients were older (median age 74.0 years), White, and non-Hispanic (Table 3). This group also had a significantly higher proportion of persons with CVA and immunocompromised states, including diabetes mellitus. Proportions of persons with malignancies, a history of nitrofurantoin use, incident CDI as reason for admission, and emergency department use were significantly higher among the CO-HCFA CDI class.

### Factors Associated with RCDI

The multivariable models indicated that Black race when compared to White race and year of incident CDI (except 2020) when compared to 2015 were associated with lower odds of RCDI (Table 4). The associations for incident CDI occurring in 2016 (compared with 2015) was attenuated in the final model, but results remained significant for 2017 (OR 0.43 [95% CI 0.26–0.73]), 2018 (OR 0.60 [95% CI 0.37–0.97]), and 2019 (OR 0.50 [95% CI 0.30–0.84]) (all compared with 2015) and for Black race compared with White race (OR 0.50 [95% CI 0.30–0.83]). When year of incident CDI was regressed as an ordinal variable (i.e., 2015 to 2020 represented by numbers 1 to 6 and regressed as is), we observed no statistical significance in the univariate analysis and multivariable results for all 3 models. In the final model, case-patients with malignancies were 51% more likely to have RCDI (OR 1.51 [95% CI 1.11–2.07]), whereas nitrofurantoin use before an incident CDI episode had 137% higher odds for RCDI (OR 2.37 [95% CI 1.23–4.58]).

## Discussion

We observed a general reduction in CDI incidence over the entire study period and an increase in incidence rates of RCDI from 2019 to 2020 despite initial decreases from 2015 to 2018. When stratified by epidemiologic class of CDI, the increase in RCDI was largely attributable to an increase in recurrent HCFO-CDI in 2020 and, to a lesser extent, small, gradual increases in recurrence rates for CA-CDI during 2018–2020. After adjusting for year of incident CDI, sex, age, race, ethnicity, medication history, underlying conditions, clinical exposures, treatment, and epidemiologic class of incident CDI, we observed significantly increased risk for RCDI among case-patients who were admitted for non-CDI reasons and those with a history of malignancy and nitrofurantoin use.

This study highlights that the observed decrease in incidence of RCDI from 2015 to 2018 adds to the published literature by emphasizing a lower rate of RCDI overall (*12*) and in all epidemiologic classes of RCDI (*3*) and reflecting a continued decrease in RCDI from before 2015 (*20*). The decrease in RCDI may be attributable to current measures for managing and preventing RCDI, including restrictions on prescription of fluroquinolones (*3*,*21*), infection control measures (*22*), and possibly adherence to approved treatment guidelines (*23*), being effective enough to produce a notable reduction in RCDI rates. Studies of RCDI rates in 2020 are scarce; thus, this study provides early possible evidence of increasing rates

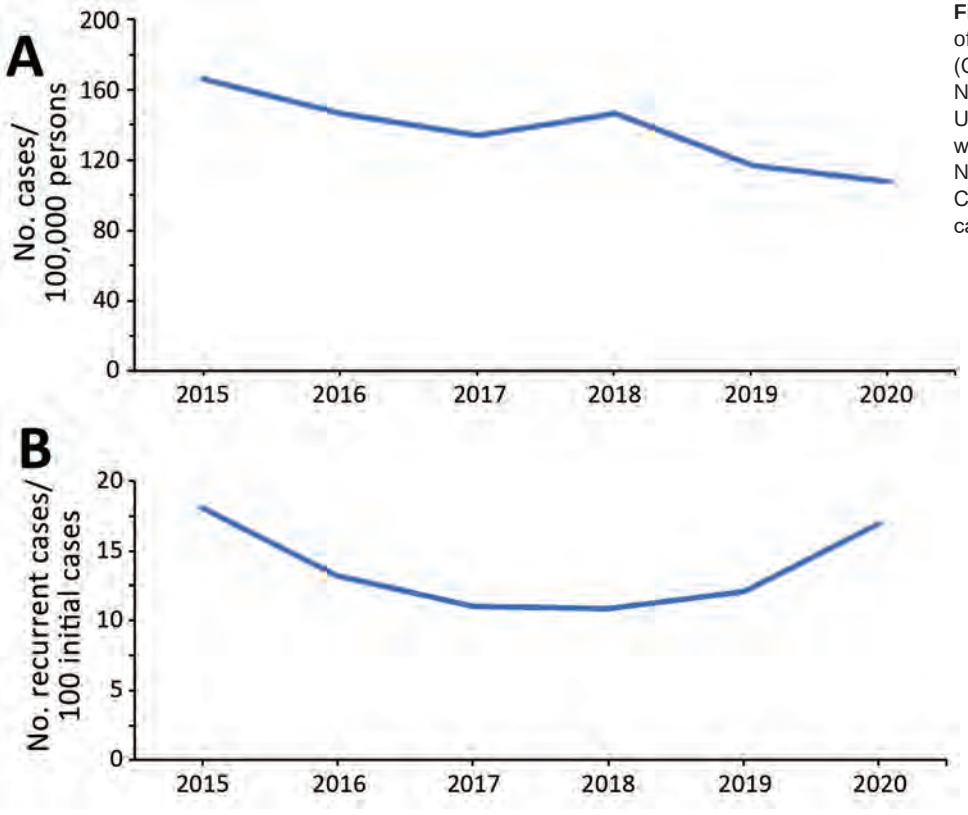


**Figure 1.** Annual incidence rates of *Clostridioides difficile* infection (CDI) (A) and recurrent CDI (B), New Haven County, Connecticut, USA, 2015–2020. CDI cases were all reported CDI cases in New Haven County. Recurrent CDI cases were available only for cases with complete chart reviews.

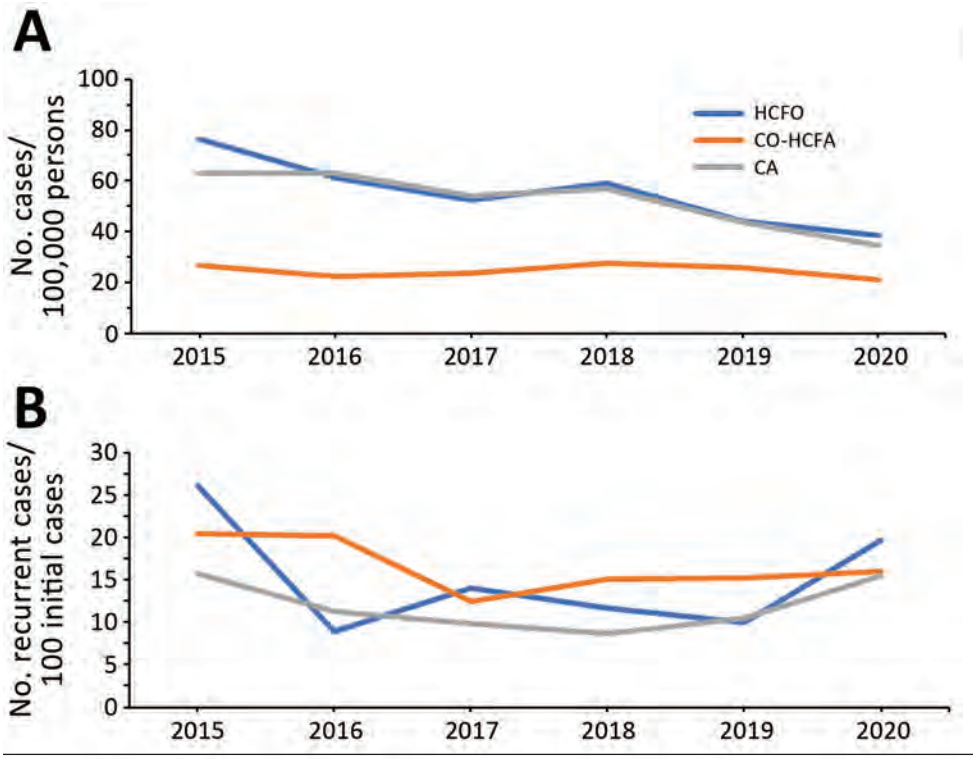


**Figure 2.** Annual incidence rates of *Clostridioides difficile* infection (CDI) (A) and recurrent CDI (B), by epidemiologic class, New Haven County, Connecticut, USA, 2015–2020. Recurrent CDI cases were available only for cases with complete chart reviews. Epidemiologic class of incident cases was not available for 74 cases because medical records were not available. CA, community-associated; CO-HCFA, community-onset healthcare facility–associated; HCFO, healthcare facility–onset.

of RCDI from 2019 to 2020. Although the CDI case report form changed in 2019 (*24*) and improvements were made in the laboratory techniques for detection of CDI, those factors would not explain the increase in RCDI occurring from 2019 to 2020 without a similar pattern occurring from 2018 to 2019. Given that the major distinguishing factor between the year 2019 and 2020 was the COVID-19 pandemic, the increase in 2020 could be related to that. Of note, a recent US study found that, although the incidence of several healthcare-associated infections increased during periods of high COVID hospital admissions, incident CDI did not (*25*). However, that study did not specifically look at RCDI.

Prior studies have suggested that persons with a history of malignancy (*26*), prior antibiotic use (*21*,*27*), increasing age (*23*,*28*), female sex (*28*), and White race (*28*) have an increased risk for CDI recurrence. Although our study shows that these factors are important predictors of RCDI, adjusting for

**Table 1.** Demographic characteristics of persons with incident CDI, stratified by occurrence of recurrent CDI, New Haven County, Connecticut, USA, 2015–2020*

| Characteristic | Total | Recurrent CDI, n = 515 | No recurrent CDI, n = 3,786 | p value |
|---|---|---|---|---|
| Year of incident CDI | | | | 0.002 |
| 2015 | 751 (17.5) | 115 (22.3) | 636 (16.8) | 0.002 |
| 2016 | 744 (17.3) | 86 (16.7) | 658 (17.4) | NS |
| 2017 | 685 (15.9) | 68 (13.2) | 617 (16.3) | NS |
| 2018 | 789 (18.3) | 77 (15.0) | 712 (18.8) | 0.03 |
| 2019 | 632 (14.7) | 68 (13.2) | 564 (14.9) | NS |
| 2020 | 700 (16.3) | 101 (19.6) | 599 (15.8) | 0.03 |
| Age, y, median (IQR) | 65.0 (26.0) | 70.0 (23.0) | 64.0 (26.0) | <0.001 |
| Sex | | | | 0.04 |
| M | 1,640 (38.1) | 175 (34.0) | 1,465 (38.7) | |
| F | 2,661 (61.9) | 340 (66.0) | 2,321 (61.3) | |
| Race | | | | |
| White | 3,169 (73.7) | 419 (81.4) | 2,750 (72.6) | <0.001 |
| Black | 430 (10.0) | 34 (6.6) | 396 (10.5) | 0.006 |
| Asian, American Indian, or Pacific Islander | 38 (0.9) | 1 (0.2) | 37 (1.0) | NS |
| Mixed race or unknown | 664 (15.4) | 61 (11.8) | 603 (15.9) | 0.02 |
| Ethnicity | | | | |
| Hispanic | 327 (8.4) | 31 (6.5) | 296 (8.7) | NS |
| Non-Hispanic | 3,556 (91.6) | 448 (93.5) | 3,108 (91.3) | 0.006 |

*Values are no. (%) except as indicated. CDI, *Clostridioides difficile* infection; IQR, interquartile range; NS, not significant.

patient-level risk factors nullified the significance of age and sex in predicting RCDI. Significant predictors of RCDI in the final model were year of incident CDI, White race, a history of malignancy, admission for incident CDI care, and nitrofurantoin use before incident CDI. Nitrofurantoin is prescribed for conditions such as urinary tract infection, more commonly used among older populations (*29*,*30*), and may be in part a marker for older persons with a longer pre-CDI history of antibiotic use than we measured. In addition, the finding of malignancy as the main underlying diagnosis associated with RCDI could reflect an ongoing need for antibiotic therapy, cytotoxic chemotherapy, or both, which could increase the risk for RCDI (*14*). We can draw parallels between the significant risk factors for RCDI from this study and some known factors that lead to severe COVID-19 disease: older age (*31*,*32*) and a history of malignancy (*33*). Taken together, those factors could, at least in part, explain the increase in RCDI in 2020,

**Table 2.** Clinical characteristics of persons with incident CDI, stratified by occurrence of recurrent CDI, New Haven County, Connecticut, USA, 2015–2020*

| Characteristic | Total | Recurrent CDI, n = 515 | No recurrent CDI, n = 3,786 | p value |
|---|---|---|---|---|
| Epidemiologic class | | | | |
| HCFO | 610 (14.2) | 83 (16.1) | 527 (13.9) | NS |
| CO-HCFA | 1,234 (28.7) | 174 (33.8) | 1,060 (28.0) | 0.006 |
| CA | 2,457 (57.1) | 258 (50.1) | 2,199 (58.1) | <0.001 |
| Medical history | | | | |
| Previous CDI | 837 (19.5) | 101 (19.6) | 736 (19.4) | NS |
| Immunocompromised | 1,397 (32.5) | 182 (35.3) | 1,215 (32.1) | NS |
| Cerebrovascular accident | 320 (7.4) | 48 (9.3) | 272 (7.2) | NS |
| Cognitive impairment or dementia | 337 (7.8) | 49 (9.5) | 288 (7.6) | NS |
| Malignancy | 903 (21.0) | 144 (28.0) | 759 (20.1) | <0.001 |
| HIV without AIDS | 32 (0.7) | 7 (1.4) | 25 (0.7) | NS |
| Diabetes mellitus | 1,024 (23.8) | 127 (24.7) | 897 (23.7) | NS |
| Chronic obstructive pulmonary disease | 790 (18.4) | 88 (17.1) | 702 (18.5) | NS |
| Chronic liver disease | 229 (5.3) | 27 (5.2) | 202 (5.3) | NS |
| Heart failure | 544 (12.7) | 67 (13.0) | 477 (12.6) | NS |
| Myocardial infarction | 261 (6.1) | 39 (7.6) | 222 (5.9) | NS |
| Peripheral vascular disease | 213 (5.0) | 33 (6.4) | 180 (4.8) | NS |
| Connective tissue disease | 184 (4.3) | 21 (4.1) | 163 (4.3) | NS |
| Gastrointestinal disease | 809 (18.8) | 88 (17.1) | 721 (19.0) | NS |
| Peptic ulcer disease | 71 (1.7) | 8 (1.6) | 63 (1.7) | NS |
| Morbid obesity | 149 (3.5) | 20 (3.9) | 129 (3.4) | NS |
| Medication history prior to incident CDI | | | | |
| Proton pump inhibitors | 1,487 (39.9) | 190 (41.0) | 1,297 (39.7) | NS |
| Histamine 2 receptor blockers | 598 (16.1) | 85 (18.5) | 513 (15.8) | NS |
| Antibiotics | 2,931 (68.2) | 375 (72.8) | 2,556 (67.5) | 0.015 |
| Penicillins | 1,033 (24.0) | 115 (22.3) | 918 (24.3) | NS |
| Cephalosporins | 1,274 (29.6) | 179 (34.8) | 1,095 (28.9) | 0.007 |
| Tetracyclines | 191 (4.4) | 32 (6.2) | 159 (4.2) | 0.037 |
| Nitroimidazole | 614 (14.3) | 88 (17.1) | 526 (13.9) | 0.052 |
| Nitrofurantoin | 99 (2.3) | 21 (4.1) | 78 (2.1) | 0.004 |
| Immunotherapeutic agents | 1,707 (39.7) | 190 (36.9) | 1,517 (40.1) | NS |
| Steroids | 811 (18.9) | 101 (19.6) | 710 (18.8) | NS |
| Chemotherapy | 334 (7.8) | 49 (9.5) | 285 (7.5) | NS |
| Clinical exposures prior to incident CDI | | | | |
| Admitted | 2,194 (51.1) | 264 (51.4) | 1,930 (51.0) | NS |
| CDI as reason for admission | 1,098 (50.1) | 143 (54.4) | 955 (49.5) | NS |
| Emergency department visit | 1,579 (37.7) | 216 (43.5) | 1,363 (36.9) | 0.005 |
| Dialysis | 191 (4.6) | 29 (5.8) | 162 (4.4) | NS |
| Surgery | 561 (13.4) | 77 (15.5) | 484 (13.1) | NS |
| Death | 163 (3.8) | 1 (0.2) | 162 (4.3) | <0.001 |
| Treatment of incident CDI | | | | |
| Total no. cases during 2018–2020 | 2,121 | 246 | 1,875 | |
| Received treatment | 1,890 (89.1) | 218 (88.6) | 1,672 (89.2) | NS |
| Vancomycin | 1,344 (63.4) | 162 (65.9) | 1,182 (63.0) | NS |
| Metronidazole | 479 (22.6) | 47 (19.1) | 432 (23.0) | NS |
| Fidaxomicin | 28 (1.3) | 3 (1.2) | 25 (1.3) | NS |
| Other antibiotic | 7 (0.3) | 1 (0.4) | 6 (0.3) | NS |
| Stool transplant | 9 (0.4) | 1 (0.4) | 8 (0.4) | NS |
| Probiotics | 383 (18.1) | 40 (16.2) | 343 (18.3) | NS |
| >1 treatment course duration | 458 (21.6) | 55 (22.4) | 403 (21.5) | NS |

*Values are no. (%) except as indicated. CA, community-associated; CDI, *Clostridioides difficile* infection; CO-HCFA, community-onset healthcare facility–associated; HCFO, healthcare facility–onset; NS, not significant.

**Table 3.** Characteristics of participants with recurrent CDI, stratified by epidemiologic class, New Haven County, Connecticut, USA, 2015–2020*

| Characteristic | Total | Epidemiologic class | | | p value |
|---|---|---|---|---|---|
| | | HCFO, n = 83 | CO-HCFA, n = 174 | CA, n = 258 | |
| Year of recurrent CDI | | | | | <0.001 |
| 2015 | 115 (22.3) | 17 (20.5) | 36 (20.7) | 62 (24.0) | |
| 2016 | 86 (16.7) | 6 (7.2) | 31 (17.8) | 49 (19.0) | |
| 2017 | 68 (13.2) | 9 (10.8) | 22 (12.6) | 37 (14.3) | |
| 2018 | 77 (15.0) | 10 (12.1) | 31 (17.8) | 36 (14.0) | |
| 2019 | 68 (13.2) | 5 (6.0) | 29 (16.7) | 34 (13.2) | |
| 2020 | 101 (19.6) | 36 (43.4) | 25 (14.4) | 40 (15.5) | |
| Age, y, median (IQR) | 70.0 (23.0) | 74.0 (20.0) | 71.0 (23.0) | 68.0 (26.0) | 0.002 |
| Sex | | | | | 0.083 |
| M | 175 (34.0) | 36 (43.4) | 61 (35.1) | 78 (30.2) | |
| F | 340 (66.0) | 47 (56.6) | 113 (64.9) | 180 (69.8) | |
| Race | | | | | <0.001 |
| White | 419 (81.4) | 70 (84.3) | 134 (77.0) | 215 (83.3) | |
| Black | 34 (6.6) | 5 (6.0) | 13 (7.5) | 16 (6.2) | |
| Asian, American Indian, or Pacific Islander | 1 (0.2) | 0 | 1 (0.6) | 0 | |
| Mixed race or unknown | 61 (11.8) | 8 (9.6) | 26 (14.9) | 27 (10.5) | |
| Ethnicity | | | | | 0.007 |
| Hispanic | 31 (6.5) | 2 (2.5) | 14 (8.7) | 15 (6.3) | |
| Non-Hispanic | 448 (93.5) | 77 (97.5) | 147 (91.3) | 224 (93.7) | |
| Medical history | | | | | |
| Previous CDI | 101 (19.6) | 19 (22.9) | 29 (16.7) | 53 (20.5) | 0.435 |
| Immunocompromised | 182 (35.3) | 47 (56.6) | 71 (40.1) | 64 (24.8) | <0.001 |
| Cerebrovascular accident | 48 (9.3) | 13 (15.7) | 19 (10.9) | 16 (6.2) | 0.024 |
| Cognitive impairment or dementia | 49 (9.5) | 17 (20.5) | 19 (10.9) | 13 (5.0) | <0.001 |
| Malignancy | 144 (28.0) | 22 (26.5) | 67 (38.5) | 55 (21.3) | <0.001 |
| Medication history | | | | | |
| Proton pump inhibitors | 190 (41.0) | 47 (58.0) | 74 (45.4) | 69 (31.5) | <0.001 |
| Histamine 2 receptor blockers | 85 (18.5) | 19 (23.5) | 37 (22.7) | 29 (13.4) | 0.031 |
| Antibiotics | 375 (72.8) | 73 (88.0) | 145 (83.3) | 157 (60.9) | <0.001 |
| Penicillins | 115 (22.3) | 28 (33.7) | 61 (35.1) | 26 (10.1) | <0.001 |
| Cephalosporins | 179 (34.8) | 56 (67.5) | 87 (50.0) | 36 (14.0) | <0.001 |
| Tetracyclines | 32 (6.2) | 7 (8.4) | 17 (9.8) | 8 (3.1) | 0.013 |
| Nitroimidazole | 88 (17.1) | 19 (22.9) | 45 (25.9) | 24 (9.3) | <0.001 |
| Nitrofurantoin | 21 (4.1) | 1 (1.2) | 10 (5.8) | 10 (3.9) | 0.012 |
| Immunotherapeutic agents | 190 (36.9) | 35 (42.2) | 68 (39.1) | 87 (33.7) | 0.292 |
| Clinical exposures | | | | | |
| Admitted | 264 (51.4) | 57 (68.7) | 113 (65.3) | 94 (36.4) | <0.001 |
| CDI as reason for admission | 143 (54.4) | 18 (31.6) | 69 (61.6) | 56 (59.6) | <0.001 |
| Emergency department visit | 216 (43.5) | 45 (54.9) | 102 (59.0) | 69 (28.5) | <0.001 |
| Dialysis | 29 (5.8) | 9 (11.0) | 14 (8.1) | 6 (2.5) | 0.005 |
| Surgery | 77 (15.5) | 22 (26.8) | 45 (26.0) | 10 (4.2) | <0.001 |

*Values are no. (%) except as indicated. CA, community-associated; CDI, *Clostridioides difficile* infection; CO-HCFA, community-onset healthcare facility–associated; HCFO, healthcare facility–onset; IQR, interquartile range.

in addition to antibiotic prescription in treatment of COVID-19 (*34*,*35*). Further understanding of the effect of COVID-19 on the incidence of CDI, which at this time is only an ecologic association, and other factors that may have influenced increased rates of RCDI during the pandemic are needed to determine whether COVID-19–specific interventions are needed to prevent RCDI in the pandemic era.

Although nitrofurantoin is known to have minimal effect on bowel flora, given that it concentrates in the urinary tract and has low serum concentration (*36*), this study shows a significant relationship between nitrofurantoin use and increased risk for RCDI. This observation could be attributable to the higher rates of prescription of multiple antibiotics to older populations (*37*,*38*). Other studies have found a tendency for inappropriate antibiotic use in LTCFs (*39*–*41*). However, after controlling for overall antibiotic use, nitrofurantoin use remained a significant risk factor for RCDI. Further studies into possible explanatory factors are needed, because currently available clinical factors do not completely explain increased risk for RCDI (*42*).

The first limitation of this study is that the surveillance system does not collect information on antibiotic or other medication use once a patient with incident CDI is admitted, other than whatever treatment regimen was initiated for treatment of the incident CDI infection. The collected information on medication use was limited to the 12 weeks before incident CDI diagnosis, which does not account for possible effects of antibiotics taken before that period. Nitrofurantoin

use, for example, could conceivably be a marker for patients with recurrent urinary tract infections who received multiple rounds of antibiotics in the past. Second, we were only able to look at the treatment regimen in a standardized way for the years 2018–2020, limiting our power to find significance, and then only for the initial treatment ordered, not changes to it. Third, because symptom information is not routinely collected for patients with recurrent cases, some of those cases could be misclassified if the reason for the patient's RCDI qualifying laboratory test were to assess test of cure or colonization status. In addition, the protocol for chart reviews used by HAIC allows for a limited random sampling of 1 in 10 HCFO cases, which could provide a potential point of bias given that information on CDI recurrence is unavailable for unsampled HCFO case-patients. Further, the review and modification of the CDI case report form over the years has helped improve reporting of patient-level characteristics of CDI cases. However, those changes have also produced variations in the case report form and the way information is collected, something particularly noticeable in the case report form change in 2019, which saw the inclusion of information such as route of medication for treatment of previous CDI and number of courses of treatment received, factors that could possibly be important predictors of recurrence. Last, we were unable to adjust for type of test; a previous study found that incident CDI case-patients identified by a common testing algorithm in which

**Table 4.** Factors associated with recurrent CDI identified in 3 models, New Haven County, Connecticut, USA, 2015–2020*

| Factor | OR (95% CI) | | |
|---|---|---|---|
| | Model 1* | Model 2† | Model 3‡ |
| Year of recurrent CDI | | | |
| 2016 | 0.73 (0.54–1.00)† | 0.68 (0.44–1.05) | 0.68 (0.44–1.06) |
| 2017 | 0.59 (0.42–0.83)† | 0.43 (0.26–0.72)‡ | 0.43 (0.26–0.73)§ |
| 2018 | 0.69 (0.50–0.96)† | 0.59 (0.37–0.95)‡ | 0.60 (0.37–0.97)§ |
| 2019 | 0.69 (0.49–0.97)† | 0.50 (0.30–0.84)‡ | 0.50 (0.30–0.84)§ |
| 2020 | 0.98 (0.72–1.32) | 0.72 (0.46–1.12) | 0.73 (0.46–1.16) |
| Age | 1.02 (1.01–1.02)† | 1.01 (1.00–1.02) | 1.01 (1.00–1.02) |
| Female sex | 1.20 (0.98–1.46) | 1.22 (0.92–1.63) | 1.22 (0.92–1.63) |
| Race or ethnicity | | | |
| Black | 0.61(0.42–0.89)† | 0.50 (0.31–0.83)‡ | 0.50 (0.30–0.83)§ |
| Asian/American Indian/Pacific Islander | 0.27 (0.04–1.98) | <0.01 (<0.01 to >999.99) | <0.01 (<0.01 to >999.99) |
| Mixed/Unknown race | 0.97 (0.54–1.75) | 1.36 (0.58–3.20) | 1.36 (0.58–3.19) |
| Hispanic | 0.90 (0.51–1.58) | 0.64 (0.28–1.50) | 0.65 (0.28–1.51) |
| Medication history | | | |
| Proton pump inhibitors | | 0.85 (0.64–1.13) | 0.85 (0.64–1.13) |
| Histamine 2 receptor blockers | | 0.98 (0.68–1.41) | 0.97 (0.67–1.39) |
| Antibiotics | | 1.21 (0.80–1.81) | 1.21 (0.81–1.81) |
| Penicillins | | 1.03 (0.74–1.44) | 1.02 (0.73–1.42) |
| Cephalosporins | | 1.13 (0.81–1.57) | 1.10 (0.79–1.54) |
| Tetracyclines | | 1.05 (0.60–1.85) | 1.05 (0.60–1.85) |
| Nitroimidazole | | 0.93 (0.64–1.35) | 0.93 (0.65–1.34) |
| Nitrofurantoin | | 2.38 (1.23–4.59)‡ | 2.37 (1.23–4.58)§ |
| Immunotherapeutic agents | | 0.86 (0.62–1.18) | 0.85 (0.62–1.17) |
| Clinical history | | | |
| Previous CDI | | 1.03 (0.74–1.44) | 1.03 (0.74–1.44) |
| Immunocompromised | | 1.20 (0.89–1.61) | 1.19 (0.88–1.60) |
| Cerebrovascular accident | | 0.91 (0.58–1.43) | 0.90 (0.57–1.41) |
| Cognitive Impairment or dementia | | 0.91 (0.58–1.42) | 0.91 (0.58–1.42) |
| Malignancy | | 1.52 (1.11–2.08)‡ | 1.51 (1.11–2.07)§ |
| Clinical exposures | | | |
| CDI as reason for admission | | 1.48 (1.10–2.01)‡ | 1.46 (1.07–12.01)§ |
| Emergency department visit | | 1.32 (1.00–1.76) | 1.28 (0.95–1.71) |
| Dialysis | | 1.45 (0.85–2.47) | 1.44 (0.85–2.46) |
| Surgery | | 1.14 (0.80–1.64) | 1.11 (0.77–1.59) |
| Epidemiologic class | | | |
| CO-HCFA | | | 1.10 (0.74–1.63) |
| CA | | | 0.93 (0.61–1.42) |

*Model 1 contains year of incident CDI diagnosis, age, sex, race, and ethnicity. Model 2 contains, in addition to model 1 variables, use of proton pump inhibitors, histamine 2 receptor blocker, antibiotics, penicillin, cephalosporin, tetracycline, nitroimidazole, nitroimidazoles, nitrofurans, immunotherapeutic agents, previous CDI, immunocompromised states, cerebrovascular accident, cognitive impairment or dementia, malignancy, admission because of CDI, emergency department visit, dialysis, and surgery. Model 3 contains, in addition to variables in model 2, the epidemiologic class of cases. CA, community-associated; CDI, *Clostridioides difficile* infection; CO-HCFA, community-onset healthcare facility–associated; OR, odds ratio.
†Statistically significant in the first model.
‡Statistically significant in the second model.
§Statistically significant in the final model.

confirmation was done by nucleic acid amplification test (NAAT) were less likely to have RCDI than case-patients identified through toxin testing (*43*), presumably because NAAT may be more likely to detect colonization than toxin testing. If testing of index CDI case-patients that used algorithms that were less likely to be falsely positive (identifying colonization) over time, then the increase in RCDI risk we observed from 2019 to 2020 might be partly attributable to that tendency. However, stratifying the risk for RCDI by tests that included NAAT versus those that did not made no difference in the magnitude or statistical significance of the increase.

Over the study period, a notable decline occurred in the incidence of RCDI, until 2020, when a sharp increase occurred. The initial reduction in RCDI incidence over time may reflect the effectiveness of measures for management of CDI, prevention of RCDI, or both. The increased risk for CDI recurrence in patients with a history of using nitrofurantoin, a drug commonly prescribed for urinary tract infections in older persons, and patients with malignancies reflects a particularly vulnerable population that requires targeted programs to prevent RCDI.

### Acknowledgments

We thank Alice Guh for her helpful review of an earlier draft of this manuscript.

This research article was supported by a cooperative agreement (no. NU50CK000488) from the Centers for Disease Control and Prevention.

## About the Author

Dr. Okafor is a recent graduate of the Yale School of Public Health and an administrative fellow with the Medical University of South Carolina Health System. Her primary research interests are disease outcomes and hospital health, including healthcare-associated infections.

### References

1. Centers for Disease Control and Prevention. *Clostridioides difficile* infection (CDI) tracking. 2022 [cited 2022 Dec 3]. https://www.cdc.gov/hai/eip/cdiff-tracking.html
2. Fu Y, Luo Y, Grinspan AM. Epidemiology of community-acquired and recurrent *Clostridioides difficile* infection. Therap Adv Gastroenterol. 2021;14:17562848211016248. https://doi.org/10.1177/17562848211016248
3. Guh AY, Mu Y, Winston LG, Johnston H, Olson D, Farley MM, et al.; Emerging Infections Program Clostridioides difficile Infection Working Group. Trends in U.S. burden of *Clostridioides difficile* infection and outcomes. N Engl J Med. 2020;382:1320–30. https://doi.org/10.1056/NEJMoa1910215
4. McDonald LC, Gerding DN, Johnson S, Bakken JS, Carroll KC, Coffin SE, et al. Clinical practice guidelines for *Clostridium difficile* infection in adults and children: 2017 update by the Infectious Diseases Society of America (IDSA) and Society for Healthcare Epidemiology of America (SHEA). Clin Infect Dis. 2018;66:e1–48. https://doi.org/10.1093/cid/cix1085
5. Thomas E, Bémer P, Eckert C, Guillouzouic A, Orain J, Corvec S, et al. *Clostridium difficile* infections: analysis of recurrence in an area with low prevalence of 027 strain. J Hosp Infect. 2016;93:109–12. https://doi.org/10.1016/j.jhin.2016.01.015
6. Khanna S, Montassier E, Schmidt B, Patel R, Knights D, Pardi DS, et al. Gut microbiome predictors of treatment response and recurrence in primary *Clostridium difficile* infection. Aliment Pharmacol Ther. 2016;44:715–27. https://doi.org/10.1111/apt.13750
7. Richardson C, Kim P, Lee C, Bersenas A, Weese JS. Comparison of *Clostridium difficile* isolates from individuals with recurrent and single episode of infection. Anaerobe. 2015;33:105–8. https://doi.org/10.1016/j.anaerobe.2015.03.003
8. Seekatz AM, Wolfrum E, DeWald CM, Putler RKB, Vendrov KC, Rao K, et al. Presence of multiple *Clostridium difficile* strains at primary infection is associated with development of recurrent disease. Anaerobe. 2018;53:74–81. https://doi.org/10.1016/j.anaerobe.2018.05.017
9. Martin JSH, Eyre DW, Fawley WN, Griffiths D, Davies K, Mawer DPC, et al. Patient and strain characteristics associated with *Clostridium difficile* transmission and adverse outcomes. Clin Infect Dis. 2018;67:1379–87. https://doi.org/10.1093/cid/ciy302
10. Kim J, Seo MR, Kang JO, Kim Y, Hong SP, Pai H. Clinical characteristics of relapses and re-infections in *Clostridium difficile* infection. Clin Microbiol Infect. 2014;20:1198–204. https://doi.org/10.1111/1469-0691.12704
11. Ma GK, Brensinger CM, Wu Q, Lewis JD. Increasing incidence of multiply recurrent *Clostridium difficile* infection in the United States: A Cohort Study. Ann Intern Med. 2017;167:152–8. https://doi.org/10.7326/M16-2733
12. Abdelfatah M, Nayfe R, Nijim A, Enriquez K, Ali E, Watkins RR, et al. Factors predicting recurrence of *Clostridium difficile* infection (CDI) in hospitalized patients: retrospective study of more than 2000 patients. J Investig Med. 2015;63:747–51. https://doi.org/10.1097/JIM.0000000000000188
13. Madoff SE, Urquiaga M, Alonso CD, Kelly CP. Prevention of recurrent *Clostridioides difficile* infection: a systematic review of randomized controlled trials. Anaerobe. 2020;61:102098. https://doi.org/10.1016/j.anaerobe.2019.102098
14. Kim JHS and YS. Recurrent *Clostridium difficile* infection: risk factors, treatment, and prevention. Gut Liver. 2019;13:16–24. https://doi.org/10.5009/gnl18071
15. Gómez S, Chaves F, Orellana MA. Clinical, epidemiological and microbiological characteristics of relapse and re-infection in *Clostridium difficile* infection. Anaerobe. 2017;48:147–51. https://doi.org/10.1016/j.anaerobe.2017.08.012
16. Haran JP, Bradley E, Howe E, Wu X, Tjia J. Medication exposure and risk of recurrent *Clostridium difficile* infection in community-dwelling older people and nursing home residents. J Am Geriatr Soc. 2018;66:333–8. https://doi.org/10.1111/jgs.15176
17. Scaria E, Powell WR, Birstler J, Alagoz O, Shirley D, Kind AJH, et al. Neighborhood disadvantage and 30-day readmission risk following *Clostridioides difficile* infection hospitalization. BMC Infect Dis. 2020;20:762. https://doi.org/10.1186/s12879-020-05481-x

18. Jeffery MM, D'Onofrio G, Paek H, Platts-Mills TF, Soares WE III, Hoppe JA, et al. Trends in emergency department visits and hospital admissions in health care systems in 5 states in the first months of the COVID-19 pandemic in the US. JAMA Intern Med. 2020;180:1328–33. https://doi.org/10.1001/jamainternmed.2020.3288
19. Shipe ME, Deppen SA, Farjah F, Grogan EL. Developing prediction models for clinical use using logistic regression: an overview. J Thorac Dis. 2019;11(Suppl 4):S574–84. https://doi.org/10.21037/jtd.2019.01.25
20. Guh AY, Mu Y, Baggs J, Winston LG, Bamberg W, Lyons C, et al. Trends in incidence of long-term-care facility onset *Clostridium difficile* infections in 10 US geographic locations during 2011–2015. Am J Infect Control. 2018;46:840–2. https://doi.org/10.1016/j.ajic.2017.11.026
21. Kazakova SV, Baggs J, McDonald LC, Yi SH, Hatfield KM, Guh A, et al. Association between antibiotic use and hospital-onset *Clostridioides difficile* infection in US acute care hospitals, 2006–2012: an ecologic analysis. Clin Infect Dis. 2020;70:11–8. https://doi.org/10.1093/cid/ciz169
22. Rizzo KR, Yi SH, Garcia EP, Zahn M, Epson E. Reduction in *Clostridium difficile* infection rates following a multifacility prevention initiative in Orange County, California: a controlled interrupted time series evaluation. Infect Control Hosp Epidemiol. 2019;40:872–9. https://doi.org/10.1017/ice.2019.135
23. Luc CM, Olson D, Banach DB, Clogher P, Hadler J. Evaluation of Connecticut medical providers' concordance with 2017 IDSA/SHEA *Clostridioides difficile* treatment guidelines in New Haven County, 2018–2019. Infect Control Hosp Epidemiol. 2021;42:549–56. https://doi.org/10.1017/ice.2020.1237
24. US Office of Management and Budget. HAIC CDI case report form (OMB: 0920–0978) [cited 2022 May 28]. https://omb.report/icr/202007-0920-014/ic/217334
25. Weiner-Lastinger LM, Pattabiraman V, Konnor RY, Patel PR, Wong E, Xu SY, et al. The impact of coronavirus disease 2019 (COVID-19) on healthcare-associated infections in 2020: a summary of data reported to the National Healthcare Safety Network. Infect Control Hosp Epidemiol. 2022;43:12–25. https://doi.org/10.1017/ice.2021.362
26. Scappaticci GB, Perissinotti AJ, Nagel JL, Bixby DL, Marini BL. Risk factors and impact of *Clostridium difficile* recurrence on haematology patients. J Antimicrob Chemother. 2017;72:1488–95. https://doi.org/10.1093/jac/dkx005
27. Kazakova SV, Baggs J, Yi SH, Reddy SC, Hatfield KM, Guh AY, et al. Associations of facility-level antibiotic use and hospital-onset *Clostridioides difficile* infection in US acute-care hospitals, 2012–2018. Infect Control Hosp Epidemiol. 2022;43:1067–9.
28. Lessa FC, Mu Y, Bamberg WM, Beldavs ZG, Dumyati GK, Dunn JR, et al. Burden of *Clostridium difficile* infection in the United States. N Engl J Med. 2015;372:825–34. https://doi.org/10.1056/NEJMoa1408913
29. Mouton CP, Bazaldua OV, Pierce B, Espino DV. Common infections in older adults. Am Fam Physician. 2001;63:257–68.
30. Cristina ML, Spagnolo AM, Giribone L, Demartini A, Sartini M. Epidemiology and prevention of healthcare-associated infections in geriatric patients: a narrative review. Int J Environ Res Public Health. 2021;18:5333. https://doi.org/10.3390/ijerph18105333
31. Pijls BG, Jolani S, Atherley A, Derckx RT, Dijkstra JIR, Franssen GHL, et al. Demographic risk factors for COVID-19 infection, severity, ICU admission and death: a meta-analysis of 59 studies. BMJ Open. 2021;11:e044640. https://doi.org/10.1136/bmjopen-2020-044640
32. Cummins L, Ebyarimpa I, Cheetham N, Tzortziou Brown V, Brennan K, Panovska-Griffiths J. Factors associated with COVID-19 related ospitalization, critical care admission and mortality using linked primary and secondary care data. Influenza Other Respir Viruses. 2021;15:577–88. https://doi.org/10.1111/irv.12864
33. Lee KA, Ma W, Sikavi DR, Drew DA, Nguyen LH, Bowyer RCE, et al.; COPE consortium. Cancer and risk of COVID-19 through a general community survey. Oncologist. 2021;26:e182–5. https://doi.org/10.1634/theoncologist.2020-0572
34. Gouin KA, Creasy S, Beckerson M, Wdowicki M, Hicks LA, Lind JN, et al. Trends in prescribing of antibiotics and drugs investigated for coronavirus disease 2019 (COVID-19) treatment in US nursing home residents during the COVID-19 pandemic. Clin Infect Dis. 2022;74:74–82. https://doi.org/10.1093/cid/ciab225
35. Knight GM, Glover RE, McQuaid CF, Olaru ID, Gallandat K, Leclerc QJ, et al. Antimicrobial resistance and COVID-19: intersections and implications. eLife. 2021;10:e64139.
36. Squadrito FJ, del Portal D. Nitrofurantoin. Treasure Island (FL): StatPearls Publishing; 2022 [cited 2022 Apr 16]. https://www.ncbi.nlm.nih.gov/books/NBK470526
37. Arizpe A, Reveles KR, Aitken SL. Regional variation in antibiotic prescribing among Medicare part D enrollees, 2013. BMC Infect Dis. 2016;16:744. https://doi.org/10.1186/s12879-016-2091-0
38. Cruz SP, Cebrino J. Prevalence and determinants of antibiotic consumption in the elderly during 2006–2017. Int J Environ Res Public Health. 2020;17:3243. https://doi.org/10.3390/ijerph17093243
39. Raban MZ, Gasparini C, Li L, Baysari MT, Westbrook JI. Effectiveness of interventions targeting antibiotic use in long-term aged care facilities: a systematic review and meta-analysis. BMJ Open. 2020;10:e028494. https://doi.org/10.1136/bmjopen-2018-028494
40. Raban MZ, Gates PJ, Gasparini C, Westbrook JI. Temporal and regional trends of antibiotic use in long-term aged care facilities across 39 countries, 1985–2019: systematic review and meta-analysis. PloS One. 2021;16:e0256501. https://doi.org/10.1371/journal.pone.0256501
41. Crayton E, Richardson M, Fuller C, Smith C, Liu S, Forbes G, et al. Interventions to improve appropriate antibiotic prescribing in long-term care facilities: a systematic review. BMC Geriatr. 2020;20:237. https://doi.org/10.1186/s12877-020-01564-1
42. van Rossen TM, van Dijk LJ, Heymans MW, Dekkers OM, Vandenbroucke-Grauls CMJE, van Beurden YH. External validation of two prediction tools for patients at risk for recurrent *Clostridioides difficile* infection. Therap Adv Gastroenterol. 2021;14:1756284820977385. https://doi.org/10.1177/1756284820977385
43. Guh AY, Hatfield KM, Winston LG, Martin B, Johnston H, Brousseau G, et al. Toxin enzyme immunoassays detect *Clostridioides difficile* infection with greater severity and higher recurrence rates. Clin Infect Dis. 2019;69:1667–74. https://doi.org/10.1093/cid/ciz009


Address for correspondence: James Hadler, Yale School of Public Health, Connecticut Emerging Infections Program, 1 Church St, Fl 7, New Haven, CT 06510, USA; email: hadlerepi@gmail.com

# Phylogenetic Analysis of Transmission Dynamics of Dengue in Large and Small Population Centers, Northern Ecuador

Sully Márquez, Gwenyth Lee, Bernardo Gutiérrez, Shannon Bennett, Josefina Coloma,[1] Joseph N.S. Eisenberg,[1] Gabriel Trueba[1]

Although dengue is typically considered an urban disease, rural communities are also at high risk. To clarify dynamics of dengue virus (DENV) transmission in settings with characteristics generally considered rural (e.g., lower population density, remoteness), we conducted a phylogenetic analysis in 6 communities in northwestern Ecuador. DENV RNA was detected by PCR in 121/488 serum samples collected from febrile case-patients during 2019–2021. Phylogenetic analysis of 27 samples from Ecuador and other countries in South America confirmed that DENV-1 circulated during May 2019–March 2020 and DENV-2 circulated during December 2020–July 2021. Combining locality and isolation dates, we found strong evidence that DENV entered Ecuador through the northern province of Esmeraldas. Phylogenetic patterns suggest that, within this province, communities with larger populations and commercial centers were more often the source of DENV but that smaller, remote communities also play a role in regional transmission dynamics.

Dengue virus (DENV) is a vectorborne tropical disease transmitted by *Aedes aegypti* and *Ae. albopictus* mosquitoes. Globally, an estimated 390 million cases occur per year, and 3.9 billion persons are at risk for infection (*1*). Dengue is endemic to 100 countries; southeast Asia is the most severely affected region, followed by the western Pacific and the Americas (*1*).

Author affiliations: Universidad San Francisco de Quito, Quito, Ecuador (S. Márquez, B. Gutiérrez, G. Trueba); University of Michigan, Ann Arbor, Michigan, USA (G. Lee, J.N.S. Eisenberg); University of Oxford, Oxford, UK (B. Gutiérrez); Institute for Biodiversity Science and Sustainability, California Academy of Sciences, San Francisco, California, USA (S. Bennett); University of California, Berkeley, Berkeley, California, USA (J. Coloma)

DOI: https://doi.org/10.3201/eid2905.221226

Dengue is considered an urban disease because transmission is often reported in areas with high population density. However, human mobility and active commerce have increased in classically defined rural sectors where population density is generally lower, influencing DENV transmission. DENV transmission in rural sectors is often reported to occur at similar rates as urban areas (*2*–*4*). More remote rural areas can also serve as a source for emerging febrile diseases, often through cases introduced through cross-border movement. For instance, in Laos, surveillance of fevers in rural areas provided evidence that more DENV serotypes were circulating in rural areas than in urban ones (*5*). Those introductions highlight the need for highly coordinated and timely arbovirus surveillance at the local and national level to enable early warning of potential DENV outbreaks among neighboring countries (*6*,*7*). In Asia, cross-border surveillance systems and networks such as UNITEDengue have been established to share data on disease outbreaks to monitor and control the disease more effectively (*8*).

DENV has been endemic to South America since the 1980s and to Ecuador since 1988. Generally, only 1 serotype circulates episodically within a region in South America, but all serotypes have circulated and reemerged in cycles (*9*,*10*). During 2010–2019, explosive epidemics were reported in the Americas; cases peaked at 3.1 million in 2019 (*11*) After a period of low prevalence in 2020, likely because of underreporting caused by the COVID-19 pandemic (*12*) and limited human movement between regions, Ecuador reported an increase of DENV cases in 2021.

[1]These senior authors contributed equally to this article.

Esmeraldas Province is located in the northern coast of Ecuador and shares a border with the Nariño department of Colombia. Fifty seven percent of the population lives in poverty and lacks basic needs such as potable water and garbage collection services (C. Robbins, unpub. data, https://digitalrepository.trincoll.edu/cgi/viewcontent.cgi?article=1857&context=theses). In a previous study conducted in rural communities in Esmeraldas during 2013–2014, we detected circulation of all DENV serotypes, whereas in the city of Esmeraldas, the largest city in the province, we detected only 2 serotypes (DENV-1 and DENV-2) (*13*). Those findings suggest that rural communities can act as a source of DENV transmission. High human mobility and levels of commerce reported in towns along the Colombia border suggest that DENV cases found in rural communities in Ecuador were likely introduced from Colombia (C. Robbins, unpub. data).

On the basis of this previous evidence, the aim of this study was to extract DENV nucleotide sequences obtained from serum samples from active DENV cases collected during 2019–2021 in Esmeraldas Province. We investigated the phylogenetic relationship of those sequences to DENV nucleotide sequences from throughout Ecuador to learn more about the role of rural DENV transmission dynamics in northwestern Ecuador.

## Materials and Methods

### Study Site

The study was conducted as part of an ongoing arboviral surveillance study in Cantón Eloy Alfaro, Esmeraldas Province, northwestern Ecuador. In brief, we selected 6 communities according to their gradient of remoteness: 2 remote riverine communities with no road access (Santa María and Santo Domingo), 3 communities with road access (Colón Eloy, Timbiré, and Maldonado), and 1 commercial center (Borbón) (Figure 1).

### Sample Collection

We collected data during May 2019–December 2021 by using active fever surveillance at the individual level. Except in the town of Borbón, community residents >2 years of age were invited to participate in prospective active surveillance. In Borbón, we invited a random sample of 500 households located in the town center to participate. In total, 1,460 households and 5,957 participants provided ≥1 month of active surveillance data from the study period of May 2019–December 2021. A group of community members trained to identify cases (brigadistas) conducted home visits weekly during the rainy season (June–October) and every 2 weeks during the dry season (November–December). The surveillance protocol began


**Figure 1.** Locations of the 6 rural communities in Esmeraldas Province and the city of Esmeraldas for study of transmission dynamics of dengue in large and small population centers, northern Ecuador.

with brigadistas inquiring whether any household members had experienced fever, red eyes, or rash within the previous 7 days. When a symptomatic person was identified, the brigadista alerted the study nurse, who then followed up with a questionnaire asking about ≈21 symptoms associated with DENV and travel history. Participants experiencing diarrhea or upper respiratory symptoms were excluded. When a DENV-like illness was identified (fever plus rash, myalgia, arthralgia), a blood sample was immediately collected and a rapid diagnostic test performed (data not shown). Serum derived from the blood sample was stored in liquid nitrogen for transportation to the laboratory, where the samples were kept at −80°C until processing. The study was approved by the Bioethics committee at the Universidad San Francisco de Quito, the University of Michigan, and the Ecuadorian Ministry of Health.

### RNA Extraction, Reverse Transcription PCR, and Sequencing

We extracted viral RNA from 488 febrile serum samples by using the QIAamp Viral RNA Mini Kit (QIAGEN, https://www.giagen.com), according to manufacturer instructions. We used this RNA as a template for the triplex real time reverse transcription PCR (RT-PCR) Zika-Dengue-Chikungunya assay, which we performed to confirm infection and etiology (*14*). We serotyped 121 samples positive for dengue using a conventional RT-PCR with some modifications (*15*).

We considered 27 positive samples with a real-time PCR cycle threshold (Ct) value of <30 optimal for sequencing. We amplified a 20-μL aliquot of cDNA obtained using the Superscript IV protocol by multiplex PCR, combining 5 μL of 5X Q5 Reaction Buffer, 0.5 μL of 10 mM dNTPs, 0.25 μL of Q5 DNA polymerase, 15.25 μL nuclease-free water, and 1.5 μL primer pool A (10 μM). For DENV-1 and DENV-2, we added 1.5 μL primer pool B (10 μM) (*16*). We selected the samples that showed a 900 bp band in pool A and pool B mix for sequencing. Using 2.5 μl of PCR products from each pool diluted in 45 μl of PCR water, we prepared the cDNA MinION library by using a native barcoding kit (NB-114) with a ligation sequencing kit (LSK-109) following manufacturers' instructions and loaded it into the MinION flow cell (FLO-MIN 106) (Oxford Nanopore Technologies, https://nanoporetech.com). We performed demultiplexing and adaptor removal with Porechop version 0.2.3_seqan 2.1.1 (https://github.com/rrwick/Porechop) and assembled the sequencing reads with a de novo assembly approach using Spades version 3.13.0 (http://cab.spbu.ru/files/release3.13.0/manual.html). Next, we mapped the reads in Minimap2 version 2.17-R941 (https://github.com/lh3/minimap2) against reference genomes for DENV-1 (GenBank accession no. NC_001477.1) and DENV-2 (accession no. NC_001474.2). The consensus sequence was generated with Samtools version 1.7 (http://www.htslib.org/doc/1.7/samtools.html) and the serotype was confirmed using Genome Detective Arbovirus Typing software Tool version 1.137 (*17*) and BLAST (https://blast.ncbi.nlm.nih.gov/Blast.cgi).

### Phylogenetic Analysis

In total, we generated 9 DENV-1 and 13 DENV-2 genome sequences from our field site and used them for the phylogenetic analysis (22 samples). In addition, we sequenced 5 samples from the national surveillance system at the reference hospital of the city of Esmeraldas, the capital of the province (3 DENV-1 and 2 DENV-2) (accession nos. SRR1593089–SRR15793115). The hospital samples were selected for patients residing in Esmeraldas on the basis of the patient's clinical record. To augment the Ecuador data for phylogenetic analysis, we incorporated 22 sequences from GenBank, 21 representing El Oro Province (located in southern Ecuador) and 1 sample from Esmeraldas. To enable cross-country analysis, we included available GenBank sequences from Argentina, Brazil, Perú, Nicaragua, Belize, Venezuela, and Colombia. Before generating an alignment, we identified genomes from the National Center for Biotechnology Information by randomly selecting the results of a BLAST of our whole-genome sequences for each serotype separately. We generated alignments by using MAFFT on XSEDE version 7.471 (https://mafft.cbrc.jp/alignment/server), then visually inspected and refined them in Aliview version 1.28 (https://github.com/AliView/AliView).

We constructed a maximum-likelihood phylogenetic tree for each serotype by using RaxML-HPC Blackbox version 8.2.12 (https://cme.h-its.org/exelixis/web/software/raxml) under a general time-reversible substitution model with 1,000 bootstrap replicates and plotting the resulting tree in FigTree version 1.4.4 (http://tree.bio.ed.ac.uk/software/figtree). We explored the temporal signal of the datasets by performing a root-to-tip genetic distance analysis using TempEst version 1.5.3 (*18*) and rooted the trees using the $R^2$ method. To explore the temporal patterns of DENV spread, we constructed Bayesian time-calibrated trees by using BEAST version 1.10.4 under a Hasegawa-Kishino-Yano substitution model and an uncorrelated lognormal relaxed molecular clock (*19*). We used a Bayesian skyline tree prior (*20*) with 10

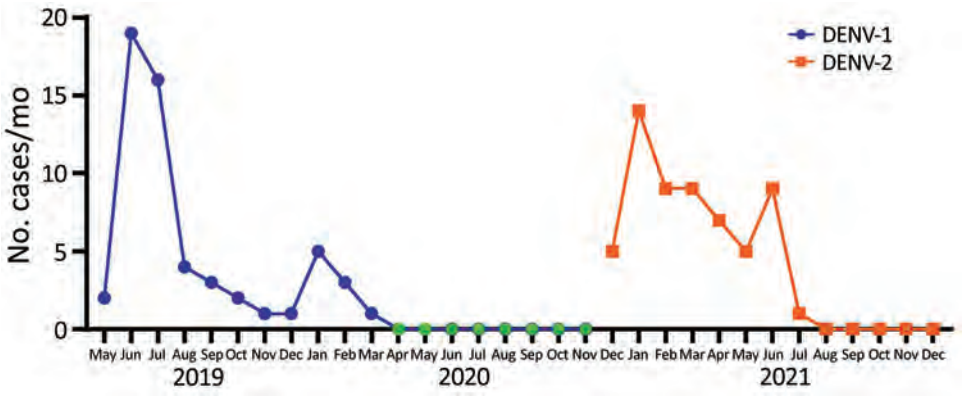


**Figure 2.** Number of febrile cases per month for DENV-1 (blue) and DENV-2 (orange) in study of transmission dynamics of dengue in large and small population centers, northern Ecuador, May 2019–December 2021. During April 2020–November 2020 (green), sampling was not conducted because of COVID-19 lockdown in Ecuador. DENV, dengue virus.

groups and a piece-wise constant reconstruction. We ran Markov chain Monte Carlo chains for 100 million steps and logged trees every 1,000 steps; we discarded the first 10% of the trees as burn-in by using TreeAnnotator version 1.10.4 (https://beast.community/treeannotator). We assessed adequate mixing and convergence of model parameters, defined by effective sample sizes of >200, in Tracer version 1.7.1 (*21*) and summarized maximum clade credibility (MCC) trees for each run using TreeAnnotator version 1.10.4, summarizing node ages as median heights.

## Results

### Samples Collected and DENV Serotypes Identified

During May 2019–December 2021, we collected 488 serum samples from febrile patients during the household-based active fever surveillance study: 187 samples from remote riverine communities with no road access (146 from Santa María patients and 41 from Santo Domingo); 181 samples from communities with road access (61 from Colon Eloy, 78 from Maldonado, and 42 from Timbiré), and 120 samples from the commercial center, Borbón. Of the 488 samples, 121 were PCR-positive for DENV. A percentage of the samples were positive for chikungunya virus, as reported elsewhere (*22*). Common symptoms among patients were fever, headache, muscle aches, joint aches, chills, backache, and stomachache. Cases confirmed in June 2019 (19 cases) and July 2019 (16 cases) were all identified as DENV-1, whereas cases detected in January and March 2021 (12 cases) were all identified as DENV-2 (Figure 2). We did not obtain any samples during April 2020–November 2020 because of COVID-19 pandemic lockdown restrictions in Ecuador.

### Phylogenetic Analysis of DENV-1 Serotype in Ecuador

The MCC tree for DENV-1 generated in BEAST software (http://beast.community) using whole-genome sequencing indicated at least 2 instances of viral variant exchange (viral exchanges) between countries. Those viral exchanges, inferred from the genetic similarities highlighted in the phylogeny, suggest that the strains were introduced into Ecuador. In one instance, a single Ecuador sequence collected in 2014 from Esmeraldas province (Figure 3, lower portion of clade I) shares a common ancestor with a sequence obtained in 2010 in Argentina. The theoretical most recent common ancestor of those 2 sequences was estimated to date back to 2006 and shared a common ancestor with viral sequences from Venezuela comprising the bulk of clade I (Figure 3). No additional sequences from this clade were detected in Ecuador, suggesting limited transmission after this potential introduction. The other DENV-1 viral exchange occurred no later than 2008 and was associated with the bulk of subsequent DENV-1 sequences from Ecuador. Those sequences formed 2 clusters, 1 from Esmeraldas Province and 1 primarily from El Oro Province that also included a sequence from Esmeraldas province (Figure 3, top portion of clade II and clade III). El Oro is located 600 km south of Esmeraldas Province (Figure 4). The introduction of those viruses into the rural communities of Esmeraldas Province is estimated to have occurred no later than 2012. Persistence of clade II lineage in Ecuador over time without the presence of other sequences from other countries suggests that Ecuador has sustained transmission that is continuing to evolve independent of external viral introductions.

### Phylogenetic Analysis of DENV-2 Serotype in Ecuador

The MCC tree for DENV-2 whole-genome sequencing (along with some partial genomes) also suggests ≥2 exchanges of distinct viruses among Ecuador, Colombia, and Venezuela. In one instance, a cluster composed of 20 sequences collected in 2014–2015 from Machala, a city in El Oro Province, shares a most recent common ancestor dating back to 2007

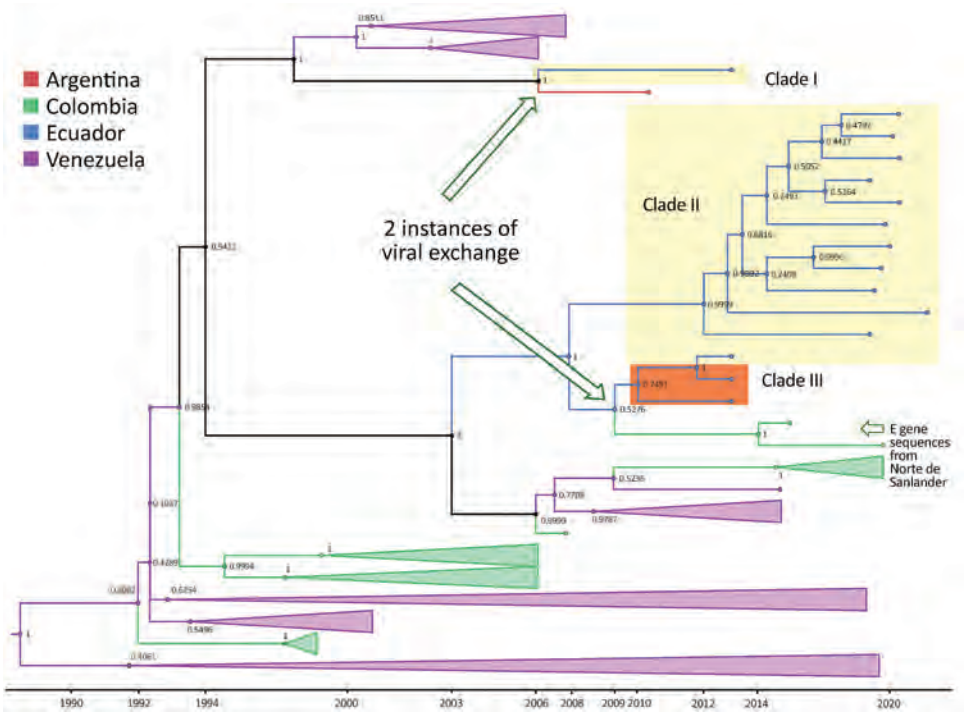


**Figure 3.** Maximum-clade credibility tree for dengue virus serotype 1 in study of transmission dynamics of dengue in large and small population centers, northern Ecuador. Tree was constructed using whole-genome sequences from Ecuador (blue), Colombia (green), Venezuela (purple), and Argentina (red) generated in BEAST software (https://beast.community). Within Ecuador, Esmeraldas Province samples are within the yellow rectangles and El Oro Province samples are within the orange rectangle, combined with E gene sequences from Norte de Santander department, Colombia. Posterior probabilities are shown in internal nodes. E, envelope.

with sequences from Colombia (Figure 5, clade II). The closest related sequence to this Ecuador clade is a Colombia envelope gene sequence from Valle del Cauca collected in 2013. In addition, 2 envelope gene sequences from Colombia (Putumayo) sampled in 2013 clustered within the Ecuador clade II. The other instance of viral exchange is suggested by 2 clusters, a cluster of 15 Ecuador sequences collected from 2020–2021 active surveillance of rural communities in Esmeraldas Province, which share a most recent common ancestor dating back to 2013, and a cluster of sequences from Colombia (Figure 5, clade I). The sequences from Machala arrived in Ecuador earlier than those from Esmeraldas Province, possibly because the Machala study predates the Esmeraldas study (Figure 5).


**Figure 4.** Location of El Oro Provinces in Ecuador, Nariño and Putumayo departments in Colombia, and Venezuela in relationship to Esmeraldas Province in study of transmission dynamics of dengue in large and small population centers, northern Ecuador.

### Phylogenetic Analysis of DENV-1 Serotype from Esmeraldas Province

Focusing on the DENV-1 serotype from our study in Esmeraldas Province (Figure 3, clade II), we labeled sequences on the basis of their gradient of remoteness: remote communities with no road access (Santa María and Santo Domingo), communities with road access (Colon Eloy, Timbiré, and Maldonado), the commercial center (Borbón), and the large population center of Esmeraldas Province (Esmeraldas city) (Figure 6). This DENV-1 subclade tree does not show distinct clustering by gradient of remoteness, although it does support the hypothesis that the cities of Esmeraldas and Borbón are sources of the viruses circulating in the smaller communities in our study site. A sequence from the city of Esmeraldas collected in 2019 (root position posterior node probability 0.9999) and a sequence from the Borbón hospital collected in 2021 (root position posterior node probability 0.9092) shared a most recent common ancestor dating back to 2012 (Figure 6). The descendants of those 2 ancestral sequences are found in remote communities and communities with road access; however, an Esmeraldas city sequence collected in 2019 derived within this cluster is suggestive of a subsequent exchange back into the large population center.

### Phylogenetic Analysis of DENV-2 Serotype from Esmeraldas Province

The DENV-2 Ecuador lineage from Esmeraldas Province demonstrates clustering by community (Figure 7, clade I). We also found strong support (0.9378) for the commercial center (Hospital of Borbón) and for those communities with road access (Colon Eloy and Timbire) being intermediate sources (0.992) of DENV-2 strains moving between the city of Esmeraldas and 2 remote communities (Santa Maria and Santo Domingo). The most recent common ancestor dates back to 2018 for a subset of the remote samples. Although much of the data support viral movement from cities and commercial centers to more remote communities, our phylogeny also supports movement from a remote community (Santo Domingo) to the commercial center of the region (Borbón) (Figure 7).

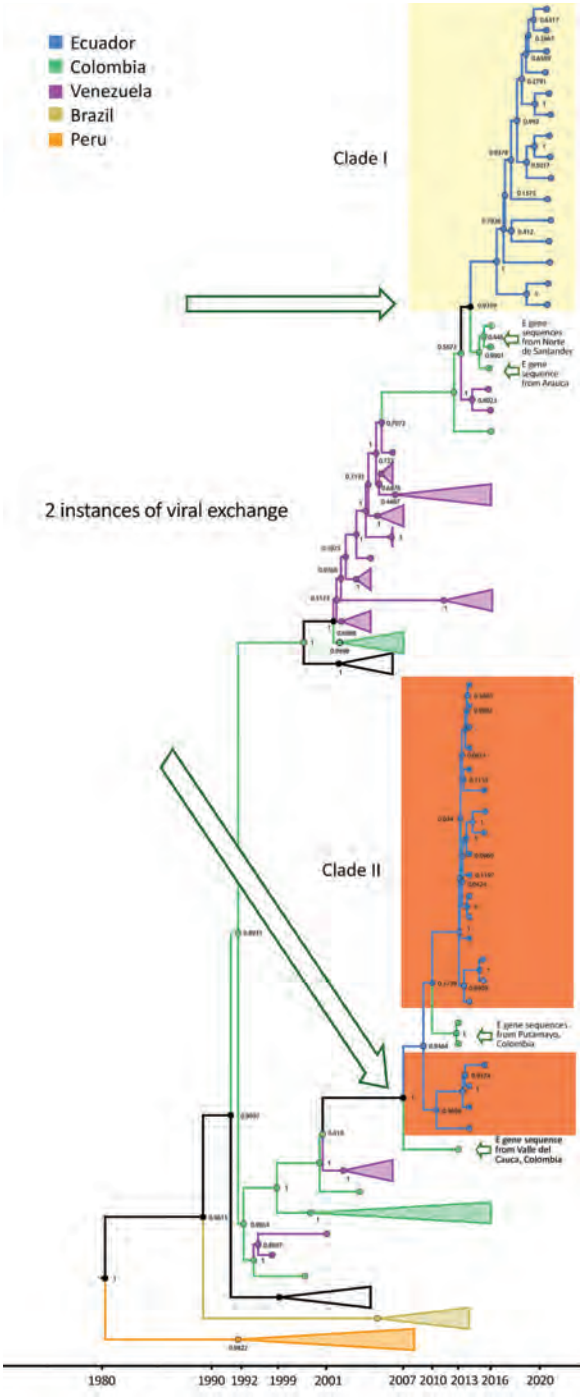


**Figure 5.** Maximum-clade credibility tree for dengue virus serotype 2 in study of transmission dynamics of dengue in large and small population centers, northern Ecuador. Tree was constructed using whole-genome sequences from Ecuador (blue), Colombia (green), and Venezuela (purple), combined with envelope gene sequences from Colombia departments (Nariño, Valle del Cauca, Putumayo, and Norte de Santander), and generated in BEAST software (https://beast.community). Within Ecuador, samples from Esmeraldas Province are within the yellow shaded area, and El Oro Province samples are within the orange shaded area. Posterior probabilities are shown in internal nodes.

## Discussion

Human mobility is one of the main determinants of DENV transmission (*23*) because the flight range of *Aedes* mosquitoes is minimal (*24*). The social dynamics of the region combined with our results suggest that Esmeraldas Province is an entry point for DENV strains arriving in Ecuador from Colombia. Legal and illegal commerce (mostly by sea) between Esmeraldas Province and Colombia is robust (*25*,*26*) and occurs

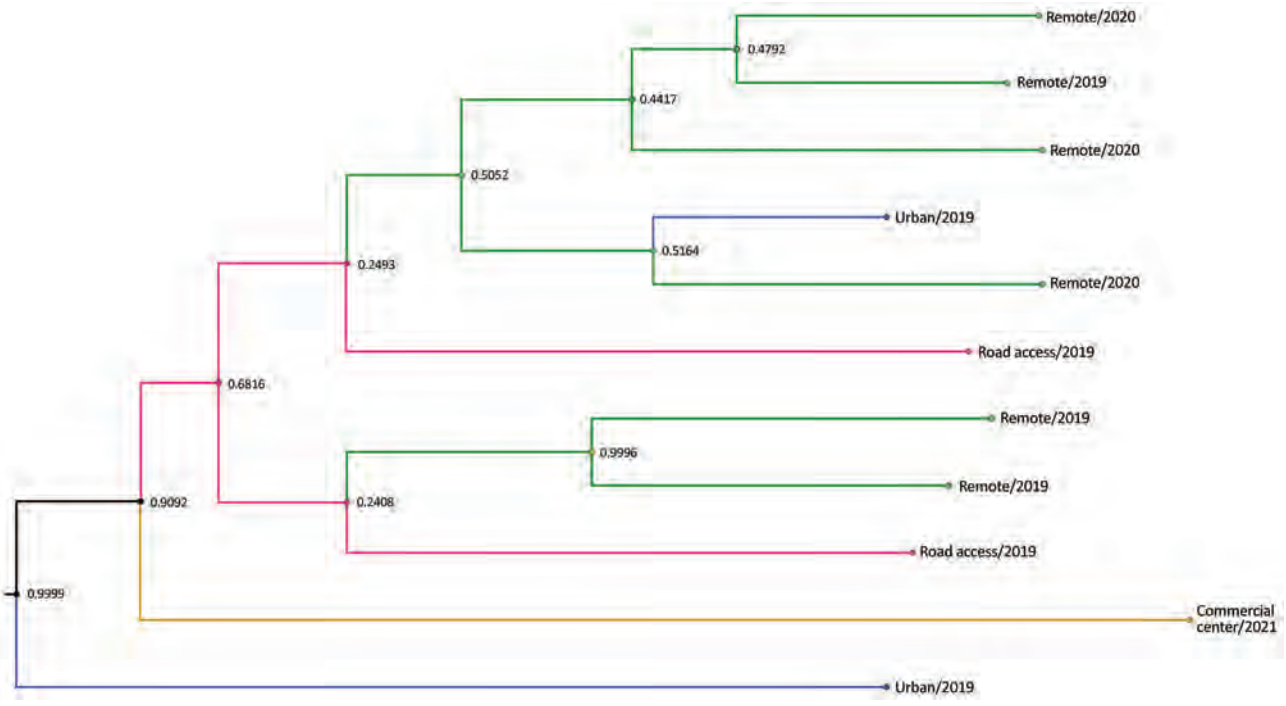


**Figure 6.** Subclade tree of dengue virus serotype 1 from rural communities of Esmeraldas Province in study of transmission dynamics of dengue in large and small population centers, northern Ecuador. Gradient of remoteness is classified as remote communities with no road access (green), communities with road access (pink), commercial center (yellow), and urban (blue). Subclade nodes are labeled with posterior probabilities generated in BEAST software (https://beast.community).

primarily in small, mostly rural communities with weak customs controls that favor informal and illegal commerce and irregular human migration.

Our data suggest that DENV-1 entered Ecuador no later than 2009 and moved to at least 2 Coastal provinces in Ecuador (Esmeraldas and El Oro). Sequences found in those provinces were most closely related to nucleotide sequences from Colombia, but they also showed similarity to sequences from Venezuela (Figure 3). Another DENV-1 sequence shares a theoretical most recent common ancestor from 2006 with an Argentina sequence and also shares high similarity with sequences from Venezuela (Figure 3). The first DENV-2 introduction might have occurred earlier than 2009, and the virus circulated in Ecuador until 2015. This DENV-2 strain was most closely related to Colombia strains circulating until 2013 (Figure 5). The second introduction probably occurred no later than 2013, resulting in an Ecuador lineage that persisted at least until 2021. Those DENV-2 sequences showed high similarity to both Colombia and Venezuela sequences.

The perspective that large tropical cities are the primary source of DENV (and other *Ae. aegypti* mosquito–transmitted viruses) has resulted in establishment of surveillance centers in large urban centers, but in Ecuador, social (and commercial) dynamics suggest that DENV is also entering through small rural community centers and subsequently disseminating to the cities. Although most of our data suggest that DENV is brought to remote communities from urban centers, we also found instances of DENV movement from remote communities to larger commercial centers (e.g., Esmeraldas and Borbon). Smaller communities with road access probably provide a bridge between more remote communities and larger commercial centers, such as Esmeraldas and Borbón, thereby serving as intermediate sources. Large population centers, such as Esmeraldas, are hubs for public transportation and therefore may become the epicenter of viral spread (*27*–*30*). Further studies are needed to understand how a heterogeneous landscape (including biological, social, and environmental factors) among communities in the region drive epidemic dynamics (*31*).

One reason that DENV transmission has remained endemic to regions such as Ecuador (in contrast to the diminished transmission of Zika and chikungunya viruses) is that there is continual serotype and lineage replacement to which cross immunity is only partial (*31*,*32*). For example, the Ministry of Health reported a 2.8-fold increase in the number of dengue cases from 2014 to 2015 (15,031 to 42,459 cases) (*32*,*33*). This increase was likely caused by introduction of a new lineage of

DENV-2 from Colombia to Ecuador, leading to the replacement of the previously dominant lineage that had been circulating since 2012 (Figure 5). The replacement of lineages has been reported in several studies associated with outbreaks linked to the introduction of novel lineages (*34*,*35*) and has long been considered a part of DENV transmission dynamics in endemic and hyperendemic regions (*25*,*26*,*36*). Those replacements might be fueled by viruses displaying novel antigenic variations for which the local population lacks immunity (*37*) or by viral variants with higher fitness (*38*). Another reason for the observed increases might be that cases reported by the Ministry of Health are other *Ae. aegypti* mosquito–transmitted arboviruses, such as chikungunya virus (*22*).

Several surveillance gaps should be considered when interpreting our data, including minimal historical specimens, lower resolution in rural sites than in urban sites, and limited country-specific data from countries in South America (including Ecuador). Although those gaps are reflective of working in a resource-limited setting, our data also reflect a unique contribution to dengue transmission dynamics in a resource-limited setting. Additional gaps in our data are a result of the COVID-19 pandemic, which might have resulted in our missing DENV cases and potential DENV introductions. Ecuador's countrywide state of emergency (March 16–April 24, 2020) and subsequent restrictions forced us to stop or sharply curtail our active household-based surveillance study (Figure 2, period of no surveillance shown in green). This state of emergency similarly affected the government's passive surveillance program.

We believe our conclusions are robust for several reasons. First, we are using complete genome sequences. Second, we obtained posterior probabilities by using a Bayesian Skyline analysis that provides us with a level of confidence for our phylogenetic relationships. Third, our results are biologically plausible and are supported by the social dynamics we observed.

For example, evidence is ample that Colombian viruses are ancestral to and a potential source of Ecuador DENV (Figures 3, 5). Colombia has numerous, very active Caribbean ports that likely serve as entry points to South America for the virus (*39*,*40*; B. Gutierrez, University of Oxford, pers. comm., 2023 Feb 14). In contrast to previous reports that suggest migration from Venezuela drives DENV lineage introduction into Ecuador (*39*), we believe its role is minimal. Ecuador does not share a border with Venezuela, and 75% of immigrants from Venezuela travel through Colombia (a 5-day journey). In addition, the main border crossing point in the highlands (Rumichaca, Ecuador) (*41*) is a region with no *Ae. aegypti* mosquito activity. A recent

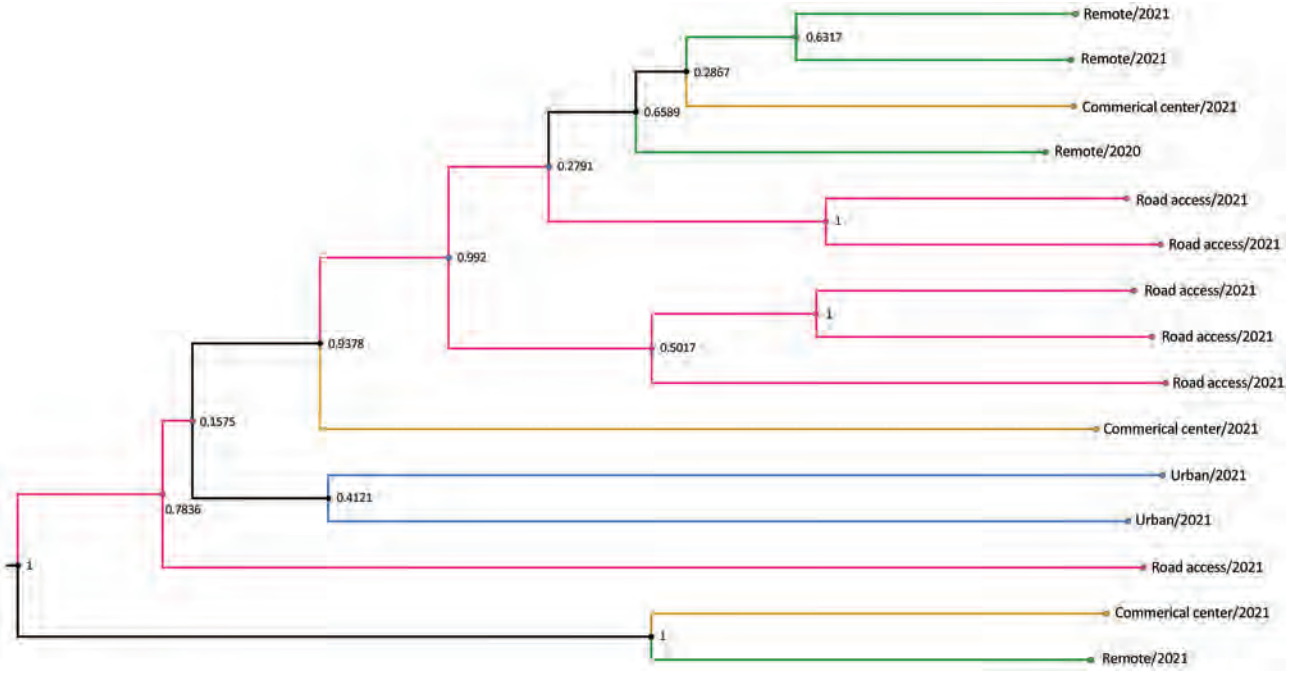


**Figure 7.** Subclade tree of dengue virus serotype 2 from rural communities of Esmeraldas Province in study of transmission dynamics of dengue in large and small population centers, northern Ecuador. Gradient of remoteness is classified as remote communities with no road access (green), communities with road access (pink), commercial center (yellow), and urban (blue). Subclade nodes are labeled with posterior probabilities generated in BEAST software (https://beast.community).

report, however, shows that migrants from Venezuela play a vital role in the introduction of DENV to Colombia (*42*), so further introductions to Ecuador through the Colombia border are likely.

Although our findings are consistent with what is known about the social dynamics of the study region, samples collected through community-based surveillance studies and previously reported strains were opportunistically gathered, usually from clinical settings. DENV cases are likely underestimated in Ecuador. Viral genomic characterization from countries such as Colombia and Venezuela are similarly limited, further adding uncertainty to our capacity to estimate the precise source and direction of exchanges.

Cases in smaller population centers are increasingly recognized as playing a vital role in broader DENV transmission dynamics (*43*). Our phylogenetic analyses in Ecuador shed light on those dynamics. Esmeraldas Province might be a key site from which DENV is introduced, amplified through local transmission, and then spread throughout Ecuador by human travel and movement of infected mosquitoes. Our results underline the need for coordinated efforts in DENV strain monitoring and control across national borders. Ministries of Health should intensify dengue surveillance in neglected remote regions, especially along national borders. Surveillance can also elucidate how DENV diffuses and becomes endemic, which requires an understanding of how large population centers affect viral dynamics regionally, and whether smaller, more remote communities represent a silent reservoir of ongoing dengue circulation.

### Acknowledgments

We thank Belén Prado for providing the pipeline for dengue genome assembly, obtaining the final consensus sequences, and submitted sequences to GenBank.

We also thank Yuri Villalobos for his help in creating the map for locations of the 6 rural communities in Esmeraldas Province.

This study was funded by the National Institute of Allergy and Infectious Diseases, National Institute of Health, R01 AI132372-02, entitled: "Zika and Dengue Co-circulation Under Environmental Change and Urbanization," 1U01AI151788 entitled "American and Asian Centers for Arboviral Research and Enhanced Surveillance-A2CARES-CREID" and Sustainable Sciences Institute.

## About the Author

Dr. Márquez is a graduate student at the Instituto de Microbiología in Universidad San Francisco de Quito. Her primary research interest is virology.

### References

1. World Health Organization. Dengue and severe dengue [cited 2022 Apr 11]. https://www.who.int/news-room/fact-sheets/detail/dengue-and-severe-dengue
2. Gómez-Dantés H, Willoquet JR. Dengue in the Americas: challenges for prevention and control. Cad Saude Publica. 2009;25(Suppl 1):S19–31. https://doi.org/10.1590/S0102-311X2009001300003
3. Vong S, Khieu V, Glass O, Ly S, Duong V, Huy R, et al. Dengue incidence in urban and rural Cambodia: results from population-based active fever surveillance, 2006-2008. PLoS Negl Trop Dis. 2010;4:e903. https://doi.org/10.1371/journal.pntd.0000903
4. Chew CH, Woon YL, Amin F, Adnan TH, Abdul Wahab AH, Ahmad ZE, et al. Rural-urban comparisons of dengue seroprevalence in Malaysia. BMC Public Health. 2016;16:824. https://doi.org/10.1186/s12889-016-3496-9
5. Mayxay M, Sengvilaipaseuth O, Chanthongthip A, Dubot-Pérès A, Rolain JM, Parola P, et al. Causes of fever in rural southern Laos. Am J Trop Med Hyg. 2015;93:517–20. https://doi.org/10.4269/ajtmh.14-0772
6. Lawpoolsri S, Kaewkungwal J, Khamsiriwatchara A, Sovann L, Sreng B, Phommasack B, et al. Data quality and timeliness of outbreak reporting system among countries in Greater Mekong subregion: challenges for international data sharing. PLoS Negl Trop Dis. 2018;12:e0006425. https://doi.org/10.1371/journal.pntd.0006425
7. Ng LC, Chem YK, Koo C, Mudin RNB, Amin FM, Lee KS, et al. 2013 dengue outbreaks in Singapore and Malaysia caused by different viral strains. Am J Trop Med Hyg. 2015;92:1150–5. https://doi.org/10.4269/ajtmh.14-0588
8. National Environmental Agency. Surveillance and Epidemiology Programme [cited 2022 Jun 10]. https://www.nea.gov.sg/corporate-functions/resources/research/surveillance-and-epidemiology-programme
9. Real J, Regato M, Burgos V, Jurado E. Evolution of dengue virus in Ecuador 2000–2015 [in Spanish]. An Fac Med (Perú). 2017;78:29–35.
10. Cifuentes SG, Trostle J, Trueba G, Milbrath M, Baldeón ME, Coloma J, et al. Transition in the cause of fever from malaria to dengue, Northwestern Ecuador, 1990-2011. Emerg Infect Dis. 2013;19:1642–5. https://doi.org/10.3201/eid1910.130137
11. World Health Organization. Geographical expansion of cases of dengue and chikungunya beyond the historical areas of transmission in the Region of the Americas [cited 2023 Apr 3]. https://www.who.int/emergencies/disease-outbreak-news/item/2023-DON448
12. Navarro JC, Arrivillaga-Henríquez J, Salazar-Loor J, Rodriguez-Morales AJ. COVID-19 and dengue, co-epidemics in Ecuador and other countries in Latin America: Pushing strained health care systems over the edge. Travel Med Infect Dis. 2020;37:101656. https://doi.org/10.1016/j.tmaid.2020.101656
13. Márquez S, Carrera J, Espín E, Cifuentes S, Trueba G, Coloma J, et al. Dengue serotype differences in urban and semi-rural communities in Ecuador. ACI Avances en Ciencias e Ingenierías. 2018 [cited 2022 Jan 12]. https://revistas.usfq.edu.ec/index.php/avances/article/view/959
14. Waggoner JJ, Gresh L, Mohamed-Hadley A, Ballesteros G, Davila MJV, Tellez Y, et al. Single-reaction multiplex reverse transcription PCR for detection of Zika, chikungunya, and dengue viruses. Emerg Infect Dis. 2016;22:1295–7. https://doi.org/10.3201/eid2207.160326
15. Harris E, Roberts TG, Smith L, Selle J, Kramer LD, Valle S, et al. Typing of dengue viruses in clinical specimens and mosquitoes by single-tube multiplex reverse transcriptase

PCR. J Clin Microbiol. 1998;36:2634–9. https://doi.org/10.1128/JCM.36.9.2634-2639.1998
16. Quick J, Grubaugh ND, Pullan ST, Claro IM, Smith AD, Gangavarapu K, et al. Multiplex PCR method for MinION and Illumina sequencing of Zika and other virus genomes directly from clinical samples. Nat Protoc. 2017;12:1261–76. https://doi.org/10.1038/nprot.2017.066
17. Cleemput S, Dumon W, Fonseca V, Abdool Karim W, Giovanetti M, Alcantara LC, et al. Genome Detective Coronavirus Typing Tool for rapid identification and characterization of novel coronavirus genomes. Bioinformatics. 2020;36:3552–5. https://doi.org/10.1093/bioinformatics/btaa145
18. Rambaut A, Lam TT, Max Carvalho L, Pybus OG. Exploring the temporal structure of heterochronous sequences using TempEst (formerly Path-O-Gen). Virus Evol. 2016;2:vew007. https://doi.org/10.1093/ve/vew007
19. Drummond AJ, Ho SYW, Phillips MJ, Rambaut A. Relaxed phylogenetics and dating with confidence. PLoS Biol. 2006;4:e88. https://doi.org/10.1371/journal.pbio.0040088
20. Drummond AJ, Rambaut A, Shapiro B, Pybus OG. Bayesian coalescent inference of past population dynamics from molecular sequences. Mol Biol Evol. 2005;22:1185–92. https://doi.org/10.1093/molbev/msi103
21. Rambaut A, Drummond AJ, Xie D, Baele G, Suchard MA. Posterior summarization in Bayesian phylogenetics using Tracer 1.7. Syst Biol. 2018;67:901–4. https://doi.org/10.1093/sysbio/syy032
22. Márquez S, Lee GO, Andrade P, Zuniga J, Trueba G, Eisenberg JNS, et al. A chikungunya outbreak in a dengue-endemic region in rural northern coastal Ecuador. Am J Trop Med Hyg. 2022;107:1226–33. https://doi.org/10.4269/ajtmh.22-0296
23. Allicock OM, Sahadeo N, Lemey P, Auguste AJ, Suchard MA, Rambaut A, et al. Determinants of dengue virus dispersal in the Americas. Virus Evol. 2020;6:veaa074.
24. Vavassori L, Saddler A, Müller P. Active dispersal of Aedes albopictus: a mark-release-recapture study using self-marking units. Parasit Vectors. 2019;12:583. https://doi.org/10.1186/s13071-019-3837-5
25. Zhang C, Mammen MP Jr, Chinnawirotpisan P, Klungthong C, Rodpradit P, Monkongdee P, et al. Clade replacements in dengue virus serotypes 1 and 3 are associated with changing serotype prevalence. J Virol. 2005;79:15123–30. https://doi.org/10.1128/JVI.79.24.15123-15130.2005
26. Carrillo-Valenzo E, Danis-Lozano R, Velasco-Hernández JX, Sánchez-Burgos G, Alpuche C, López I, et al. Evolution of dengue virus in Mexico is characterized by frequent lineage replacement. Arch Virol. 2010;155:1401–12. https://doi.org/10.1007/s00705-010-0721-1
27. Gubler DJ. Dengue, urbanization and globalization: the unholy trinity of the 21(st) century. Trop Med Health. 2011;39(Suppl):3–11. https://doi.org/10.2149/tmh.2011-S05
28. Lana RM, Gomes MFDC, Lima TFM, Honório NA, Codeço CT. The introduction of dengue follows transportation infrastructure changes in the state of Acre, Brazil: a network-based analysis. PLoS Negl Trop Dis. 2017;11:e0006070. https://doi.org/10.1371/journal.pntd.0006070
29. Sanna M, Hsieh YH. Ascertaining the impact of public rapid transit system on spread of dengue in urban settings. Sci Total Environ. 2017;598:1151–9. https://doi.org/10.1016/j.scitotenv.2017.04.050
30. Ren H, Wu W, Li T, Yang Z. Urban villages as transfer stations for dengue fever epidemic: A case study in the Guangzhou, China. PLoS Negl Trop Dis. 2019;13:e0007350. https://doi.org/10.1371/journal.pntd.0007350
31. Okano JT, Sharp K, Valdano E, Palk L, Blower S. HIV transmission and source-sink dynamics in sub-Saharan Africa. Lancet HIV. 2020;7:e209–14. https://doi.org/10.1016/S2352-3018(19)30407-2
32. Ecuadorian Ministry of Public Health. Weekly epidemiological gazette Nº 47. 2014 [cited 2022 Apr 13]. http://www.salud.gob.ec/wp-content/uploads/downloads/2014/12/Gaceta-N-47_opt.pdf
33. Ecuadorian Ministry of Public Health. Vector gazette N°52, 2019. 2019 [cited 2022 Apr 13]. https://www.salud.gob.ec/wp-content/uploads/2020/02/GACETA-VECTORES-SE-52.pdf
34. de Jesus JG, Dutra KR, Sales FCDS, Claro IM, Terzian AC, Candido DDS, et al. Genomic detection of a virus lineage replacement event of dengue virus serotype 2 in Brazil, 2019. Mem Inst Oswaldo Cruz. 2020;115:e190423–190423. https://doi.org/10.1590/0074-02760190423
35. Suzuki K, Phadungsombat J, Nakayama EE, Saito A, Egawa A, Sato T, et al. Genotype replacement of dengue virus type 3 and clade replacement of dengue virus type 2 genotype Cosmopolitan in Dhaka, Bangladesh in 2017. Infect Genet Evol. 2019;75:103977. https://doi.org/10.1016/j.meegid.2019.103977
36. Holmes EC, Twiddy SS. The origin, emergence and evolutionary genetics of dengue virus. Infect Genet Evol. 2003;3:19–28. https://doi.org/10.1016/S1567-1348(03)00004-2
37. Martinez DR, Yount B, Nivarthi U, Munt JE, Delacruz MJ, Whitehead SS, et al. Antigenic variation of the dengue virus 2 genotypes impacts the neutralization activity of human antibodies in vaccinees. Cell Rep. 2020;33:108226. https://doi.org/10.1016/j.celrep.2020.108226
38. Ko HY, Li YT, Chao DY, Chang YC, Li ZT, Wang M, et al. Inter- and intra-host sequence diversity reveal the emergence of viral variants during an overwintering epidemic caused by dengue virus serotype 2 in southern Taiwan. PLoS Negl Trop Dis. 2018;12:e0006827. https://doi.org/10.1371/journal.pntd.0006827
39. Maljkovic Berry I, Rutvisuttinunt W, Sippy R, Beltran-Ayala E, Figueroa K, Ryan S, et al. The origins of dengue and chikungunya viruses in Ecuador following increased migration from Venezuela and Colombia. BMC Evol Biol. 2020;20:31. https://doi.org/10.1186/s12862-020-1596-8
40. Campos TL, Durães-Carvalho R, Rezende AM, de Carvalho OV, Kohl A, Wallau GL, et al. Revisiting key entry routes of human epidemic arboviruses into the mainland Americas through large-scale phylogenomics. Int J Genomics. 2018;2018:6941735. https://doi.org/10.1155/2018/6941735
41. Blouin C. After the arrival: realities of Venezuelan migration. Lima: Pontificial Catholic University of Peru, Institute of Democracy and Human Rights (IDEHPUCP); 2019.
42. Carrillo-Hernandez MY, Ruiz-Saenz J, Jaimes-Villamizar L, Robledo-Restrepo SM, Martinez-Gutierrez M. Phylogenetic and evolutionary analysis of dengue virus serotypes circulating at the Colombian–Venezuelan border during 2015–2016 and 2018–2019. PLoS One. 2021;16:e0252379. https://doi.org/10.1371/journal.pone.0252379
43. xGuo C, Zhou Z, Wen Z, Liu Y, Zeng C, Xiao D, et al. Global epidemiology of dengue outbreaks in 1990-2015: a systematic review and meta-analysis. Front Cell Infect Microbiol. 2017;7:317. https://doi.org/10.3389/fcimb.2017.00317

Address for correspondence: Sully Márquez, Universidad San Francisco de Quito, Diego de Robles y Pampite, Quito 170901, Ecuador; email: smarqueza@usfq.edu.ec

# Emergence of Erythromycin-Resistant Invasive Group A *Streptococcus*, West Virginia, USA, 2020–2021

Lillie M. Powell, Soo Jeon Choi, Chloe E. Chipman, Megan E. Grund, P. Rocco LaSala,[1] Slawomir Lukomski[1]


In support of improving patient care, this activity has been planned and implemented by Medscape, LLC and *Emerging Infectious Diseases*. Medscape, LLC is jointly accredited with commendation by the Accreditation Council for Continuing Medical Education (ACCME), the Accreditation Council for Pharmacy Education (ACPE), and the American Nurses Credentialing Center (ANCC), to provide continuing education for the healthcare team.

Medscape, LLC designates this Journal-based CME activity for a maximum of 1.0 *AMA PRA Category 1 Credit(s)*™. Physicians should claim only the credit commensurate with the extent of their participation in the activity.

Successful completion of this CME activity, which includes participation in the evaluation component, enables the participant to earn up to 1.0 MOC points in the American Board of Internal Medicine's (ABIM) Maintenance of Certification (MOC) program. Participants will earn MOC points equivalent to the amount of CME credits claimed for the activity. It is the CME activity provider's responsibility to submit participant completion information to ACCME for the purpose of granting ABIM MOC credit.

All other clinicians completing this activity will be issued a certificate of participation. To participate in this journal CME activity: (1) review the learning objectives and author disclosures; (2) study the education content; (3) take the post-test with a 75% minimum passing score and complete the evaluation at https://www.medscape.org/journal/eid; and (4) view/print certificate. For CME questions, see page 1089.

**Release date: April 14, 2023; Expiration date: April 14, 2024**

**Learning Objectives**

Upon completion of this activity, participants will be able to:

- Assess the clinicoepidemiology of invasive group A *Streptococcus pyogenes* infections, based on a study of 76 invasive group A *Streptococcus pyogenes* isolates from 66 patients identified at J.W. Ruby Memorial Hospital in West Virginia from 2020 to 2021
- Evaluate the specific phenotypic and genotypic antimicrobial resistance traits of available isolates from invasive group A *Streptococcus pyogenes* infections, based on a study at J.W. Ruby Memorial Hospital in West Virginia from 2020 to 2021
- Determine the clinical and public health implications of the clinicoepidemiology of invasive group A *Streptococcus pyogenes* infections and specific phenotypic and genotypic antimicrobial resistance traits of corresponding available isolates, based on a study at J.W. Ruby Memorial Hospital in West Virginia from 2020 to 2021

**CME Editor**

**Jill Russell, BA,** Technical Writer/Editor, Emerging Infectious Diseases. *Disclosure: Jill Russell, BA, has no relevant financial relationships.*

**CME Author**

**Laurie Barclay, MD,** freelance writer and reviewer, Medscape, LLC. *Disclosure: Laurie Barclay, MD, has no relevant financial relationships.*

**Authors**

***Lillie M. Powell, BS; Soo Jeon Choi, MS; Chloe E. Chipman; Megan E. Grund, BS; P. Rocco LaSala, MD;*** and ***Slawomir Lukomski, PhD.***

Author affiliation: West Virginia University, Morgantown, West Virginia, USA

DOI: https://doi.org/10.3201/eid2905.221421

[1]These senior authors contributed equally to this article.

Clindamycin and β-lactam antibiotics have been mainstays for treating invasive group A *Streptococcus* (iGAS) infection, yet such regimens might be limited for strains displaying $MLS_B$ phenotypes. We investigated 76 iGAS isolates from 66 patients in West Virginia, USA, during 2020–2021. We performed *emm* typing using Centers for Disease Control and Prevention guidelines and assessed resistance both genotypically and phenotypically. Median patient age was 42 (range 23–86) years. We found 76% of isolates were simultaneously resistant to erythromycin and clindamycin, including all *emm92* and *emm11* isolates. Macrolide resistance was conferred by the plasmid-borne *ermT* gene in all *emm92* isolates and by chromosomally encoded *ermA*, *ermB*, and a single *mefA* in other *emm* types. Macrolide-resistant iGAS isolates were typically resistant to tetracycline and aminoglycosides. Vulnerability to infection was associated with socioeconomic status. Our results show a predominance of macrolide-resistant isolates and a shift in *emm* type distribution compared with historical reports.

*Streptococcus pyogenes,* also known as group A *Streptococcus* (GAS), is a ubiquitous pathogen that produces an array of human disease, including focal infections (e.g., pharyngitis, pyoderma) with or without localized suppurative complications; invasive soft tissue infections (e.g., myositis, necrotizing fasciitis); and systemic, often fatal, infections (e.g., bacteremia, toxic shock syndrome). In addition, 2 postinfectious complications (glomerulonephritis and rheumatic heart disease) attributable to GAS have been well described (*1*–*3*). Although GAS remains susceptible to penicillin, treatment with alternative or combination therapies, such as macrolides, clindamycin, and other second-line antimicrobial medications, is common because of patient β-lactam allergies, dosing convenience, infection severity, and patient acuity (*4*). In contrast to its predictable β-lactam susceptibility, GAS resistance to other classes of antimicrobial drugs has been increasingly reported (*5*–*7*). In the face of ongoing dissemination of the $MLS_B$ (macrolide, lincosamide, and streptogramin B) resistance phenotypes among GAS isolates, the Centers for Disease Control and Prevention (CDC) has labeled macrolide-resistant GAS an emerging threat of concern (*8*).

As 1 component of its Active Bacterial Core surveillance (ABCs) system, the CDC Emerging Infections Program, part of the National Center for Emerging and Zoonotic Infectious Diseases, Division of Preparedness and Emerging Infections, provides ongoing population-based assessments of GAS infections from 10 sites in the United States. Annual reports produced by the program estimate the incidence of invasive GAS (iGAS) infections within the United States doubled from 2009 to 2019; total numbers of infections increased from ≈11,000 cases (3.6 cases/100,000 population) to >25,000 cases (7.6 cases/100,000 population) (*9*,*10*). Concomitant with this change, substantial increases in the proportion of iGAS isolates resistant to erythromycin and clindamycin have been reported; overall resistance rates climbed from <10% in 2010 to near 25% by 2017 (*11*). Populations at risk for such macrolide-resistant iGAS infections have been predominantly persons 18–64 years of age; incidence is high among persons with a history of intravenous drug use (IVDU) and persons experiencing homelessness (*11*,*12*).

West Virginia, USA, has seen a noticeable increase in annual rates of iGAS erythromycin resistance; at West Virginia University Medicine System (WVUMed) hospitals in Morgantown, rates increased from 37% in 2019 to 54% in 2020 and 87% in 2021. The state also has an extremely high per capita rate of drug overdose (*13*). On the basis of all those considerations, we conducted a study to review clinicoepidemiology of iGAS infections within the region and to characterize specific phenotypic and genotypic antimicrobial resistance traits of corresponding available isolates.

## Materials And Methods

### Study Setting

The clinical laboratory at J.W. Ruby Memorial Hospital in Morgantown serves as the primary reference facility for all 19 WVUMed hospitals located throughout West Virginia, as well as facilities in western Maryland, southwestern Pennsylvania, and eastern Ohio. The WVUMed system serves an estimated patient population of 1.2 million. Most microbiological testing at J.W. Ruby Memorial Hospital and surrounding WVUMed outpatient clinics is performed by the Ruby clinical laboratory, as is referral antimicrobial susceptibility testing of many *Streptococcus* spp. isolates. The clinical laboratory routinely banks invasive isolates at −80°C for 1–2 years. Noninvasive isolates, including those recovered from pharyngitis cases, are not routinely held >7 days after specimen submission.

The strain collection for this study included all viable primary and referred iGAS isolates available from the freezer bank, which spanned the period January 2020–June 2021. After approval by the hospital's Institutional Review Board (protocol no. 2202533507), we reviewed patient records to capture demographic and clinical information, such as patient age, sex, residence status, history of IVDU, intensive care unit admission requirement, number of surgical interventions,

antimicrobial regimen, and clinical outcome (Appendix Table 1, https://wwwnc.cdc.gov/EID/article/29/5/22-1421-App1.pdf), for all isolates successfully retrieved. We included 2–4 replicate isolates recovered serially from 8 patients and tested them separately as a quality control measure. In all instances, intrapatient phenotypic and genotypic results were consistent, so isolates are reported per patient throughout.

#### Chromosomal and Plasmid DNA Isolation

We isolated genomic DNA from a 10-μL loopful of bacteria grown in Todd Hewitt broth by using the DNA extraction procedure, as described previously (*14*). We isolated plasmid DNA by using Gene JET Plasmid Miniprep Kit (ThermoFisher Scientific) with an additional cell-digestion step (1 mg/mL lysozyme and 0.5 U/μL mutanolysin) at 37°C for 1 hour. We analyzed plasmid DNA, uncut and digested with *Swa*I, on a 0.8% agarose gel for confirmation of plasmid pRW35 size in *emm92* isolates (*15*).

#### Identification of Resistance Genes *erm/mef* and *emm* Typing

We used plasmid DNA as a PCR template with the *ermT*-specific primers, whereas we used genomic DNA as the PCR template with primers detecting *ermA(TR)*, *ermB(AM)*, and *mefA* genes (Appendix Table 2). We obtained control GAS strains harboring the corresponding *erm* and *mef* genes from the CDC *Streptococcus* Laboratory (https://www.cdc.gov/streplab/index.html). We used genomic DNA to determine isolate *emm* type by Sanger sequencing of amplicons generated with primers *emm*1b and *emm*2 (*16*), followed by BLAST search (https://blast.ncbi.nlm.nih.gov/Blast.cgi) on the CDC *Streptococcus* Laboratory.

#### Antimicrobial Susceptibility Testing

We performed erythromycin, clindamycin, and tetracycline susceptibility testing in the clinical microbiology laboratory by using methods described by the Clinical Laboratory Standards Institute (CLSI) (*17*). All automated testing used Vitek 2 ST-02 cards (bioMériuex) and was performed upon isolate recovery for clinical management purposes. All valid results were reported to and retrieved from patient electronic health records (Epic). All historic testing met ongoing quality control criteria as outlined in the laboratory Quality Management Plan and Individualized Quality Control Plan as required for laboratory accreditation. Subsequently, we performed disc diffusion and D-testing over multiple days using thawed isolates from the freezer bank. After 2 serial propagations on sheep blood agar, we inoculated swabs of 0.5 MacFarland suspensions for confluent growth on cation-adjusted Mueller Hinton agar with 5% sheep blood (BD) using discs containing conventional drug masses. Quality control organisms, including ATCC BAA-977, ATCC BAA-976, and ATCC 49619, were tested in parallel each day of use. We incubated plates at 35°C in 5% $CO_2$ environment for 20–24 h before measuring zones of inhibition with a manual caliper in reflected light. We interpreted zone diameters by using CLSI clinical breakpoints (*17*) and interpreted any degree of clindamycin zone flattening in proximity to erythromycin disc as a positive D-test result.

Susceptibility testing against aminoglycosides (gentamicin, kanamycin, and streptomycin) was performed by agar dilution on Mueller Hinton media (BD) prepared in the research laboratory. A saline suspension of each isolate at an absorbance of 1 Klett unit was prepared and a 10-μL drop (≈$10^4$ CFU) was plated in singlicate onto agar medium containing arbitrarily selected concentrations ranging from 50 to 500 μg/mL, as described (*5*). Plates were incubated at 37°C in 5% $CO_2$ overnight, followed by observation of growth results.

## Results

#### Patients

We included 76 GAS isolates collected during January 2020–June 2021 from 66 patients with invasive infections (Figure 1; Appendix Table 1). Median patient age was 42 (mean 45, range 23–86) years; 59% were men. On the basis of addresses listed in medical records, geographic distribution of all 56 in-state patients spanned 20 of the 55 West Virginia counties; 3 northern counties (Harrison, Marion, and Monongalia) accounted for the highest proportion (53%), likely because of larger populations and proximity to the main WVUMed campus in Morgantown. Most out-of-state patients were also within the WVUMed catchment area in neighboring counties in Maryland (n = 4) and Pennsylvania (n = 5) (Figure 1), although 1 patient was visiting from the Midwest United States. For 9 patients, details of housing status in their medical records were insufficient; among the remaining patients, 9 (16%) were reported by a case worker to be experiencing homelessness at the time of culture, despite having an address on file in their medical records. For 64 patients whose social history was sufficiently documented, 39 (61%) reported recent or remote IVDU.

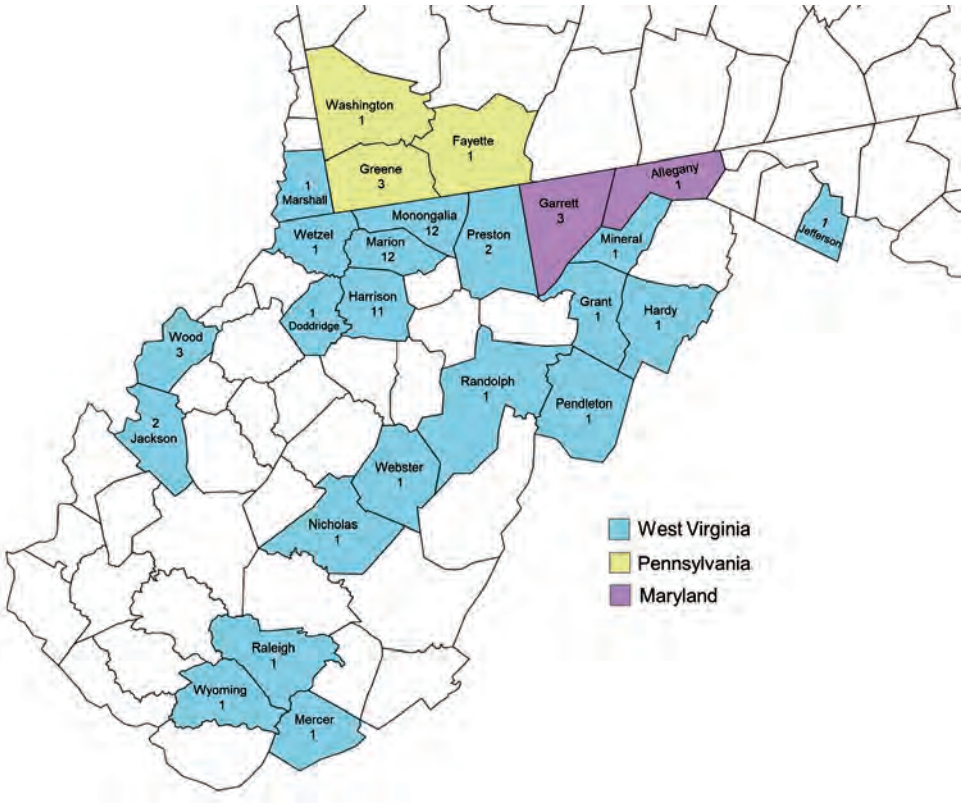


**Figure 1.** Geographic distribution of patients with invasive group A *Streptococcus* infection in West Virginia, USA, 2020–2021. A total of 56 iGAS isolates were collected from patients in 20 counties. Residence status for 9 patients was undocumented, and 9 patients were listed as homeless; in those cases, we used the county of residence for the billing address. Nine isolates were from neighboring counties in Pennsylvania and Maryland. The predominant *emm* type in the 3 West Virginia counties containing the most isolates was *emm92* (10 isolates in Harrison County, 6 in Marion County, and 8 in Monongalia County) (Appendix Table 3, https://wwwnc.cdc.gov/EID/article/29/5/22-1421-App1.pdf).

Assessing infection source for all 66 patients collectively revealed 38 (59%) with skin and soft tissue infections (SSTI) of the extremities: 8 (12%) with infections of deep neck structures; 6 (9%) with endovascular sources; 4 (6%) with SSTI of the gluteal, perianal, sacral, or inguinal region; 4 (6%) with respiratory sources; 1 (2%) with ocular source; and 4 (6%) with bloodstream infections of unknown origin (Figure 2). For an additional patient with a history of IVDU who had thrombophlebitis, bacteremia, and multiple SSTIs of the extremities and gluteal region, the primary source could not be discerned. A total of 35 (53%) patients required surgical intervention: single-stage debridement/washout (n = 24), fasciotomy with 2–13 serial debridements (n = 7), below-the-knee amputation revision (n = 1), tricuspid valve replacement (n = 1), thoracotomy with pleural decortication (n = 1), and vascular thrombectomy (n = 1) (Appendix Table 1). Of the remaining nonsurgical patients, 8 underwent incision-drainage procedures or chest tube placement at bedside. Overall, 18 (27%) patients required admission to the intensive care unit for ≥24 hours and at least 5 (7.5%) died as a result of iGAS infection, although records of follow-up care were incomplete for a substantial portion of patients.

Antimicrobial therapy varied considerably by patient acuity, duration of hospitalization, intravenous catheter availability, and degree of initial treatment response. A total of 51 patients (77%) received ≥1 dose of intravenous vancomycin or daptomycin during hospitalization, whereas β-lactams (amoxicillin/clavulanate, cephems, penicillin, or a combination) or clindamycin were used exclusively for 10 patients (15%). Another 3 patients who were not admitted to the hospital received no antimicrobial therapy. In total, the acuity of infection for 9 patients did not require hospital admission. Another 10 patients left the hospital against medical advice before being admitted or completing treatment, 9 of whom had histories of IVDU. All these patients received prescriptions for oral clindamycin or amoxicillin/clavulanate at discharge. Among the remaining 47 patients, median hospital length of stay was 7 (mean 14, range 1–60) days.

### *emm* Types

Although surveillance across the United States by ABCs has demonstrated an increase in iGAS, categorization of iGAS isolates in West Virginia was lacking. The M protein type of each isolate was determined by Sanger sequencing of the 5′ end of the *emm*-gene PCR product (Appendix Table 2), as described (*16*). Analysis showed the collection was predominated by isolates of 1 *emm* type; of the 66 unique patient isolates,

35 (53.0%) were *emm92* followed in decreasing proportion by *emm* types *emm11* (n = 8, 12.1%) and *emm89* (n = 5, 7.7%). (Table 1; Figure 3, panel A). Temporal analysis of isolate *emm* type recovery by 3-month periods showed an overall increase in isolates during April–June in 2020 and 2021; a substantial proportion of the isolates from all quarters were *emm* type 92. Although the presence of *emm11* and *emm89* isolates was relatively stable over time, the presence of *emm92* trended upward. Of note, the collection contained only 2 *emm1* isolates, 1 each of *emm12* and *emm28*, and no *emm3* isolates, which historically have been correlated with a high incidence of iGAS infections (Figure 3, panel A) (*1*,*18*,*19*). Although the data from this 1.5-year study period in West Virginia is less robust than ABCs national data, the findings do corroborate a continual shift in *emm* types responsible for iGAS disease, particularly among homeless populations and persons with a history of IVDU (*11*,*12*).

### $MLS_B$ Susceptibility and Resistance Profiles

Next, we assessed antimicrobial resistance among isolates in our iGAS collection. In aggregate, 76% (50/66) of isolates were resistant to erythromycin (Table 1), which is considerably higher than the percentage reported in a larger collection (*11*). Aside from *emm77*, which included 1 erythromycin-resistant isolate and 1 erythromycin-susceptible isolate, all other *emm* types exclusively harbored either erythromycin-resistant or erythromycin-susceptible phenotypes (Table 1; Figure 3, panel B). We used disc diffusion and D-testing to assess clindamycin susceptibility and to determine whether resistance was constitutive or inducible (Figure 3, panel C). Clindamycin susceptibility mirrored that of erythromycin; 16 erythromycin-susceptible isolates also demonstrated clindamycin susceptibility. Of the 50 erythromycin-resistant isolates, 40 exhibited inducible clindamycin resistance (i.e., not detectable without erythromycin induction), 9 demonstrated constitutive clindamycin resistance, and 1 isolate (*emm*22) was clindamycin susceptible without evidence of inhibition zone flattening. Similar to erythromycin, most *emm* types were uniformly susceptible or resistant to clindamycin except for 2 *emm77* (1 susceptible and 1 inducible-resistant isolate) (Table 1; Figure 3, panel C). Phenotypic heterogeneity was also noted

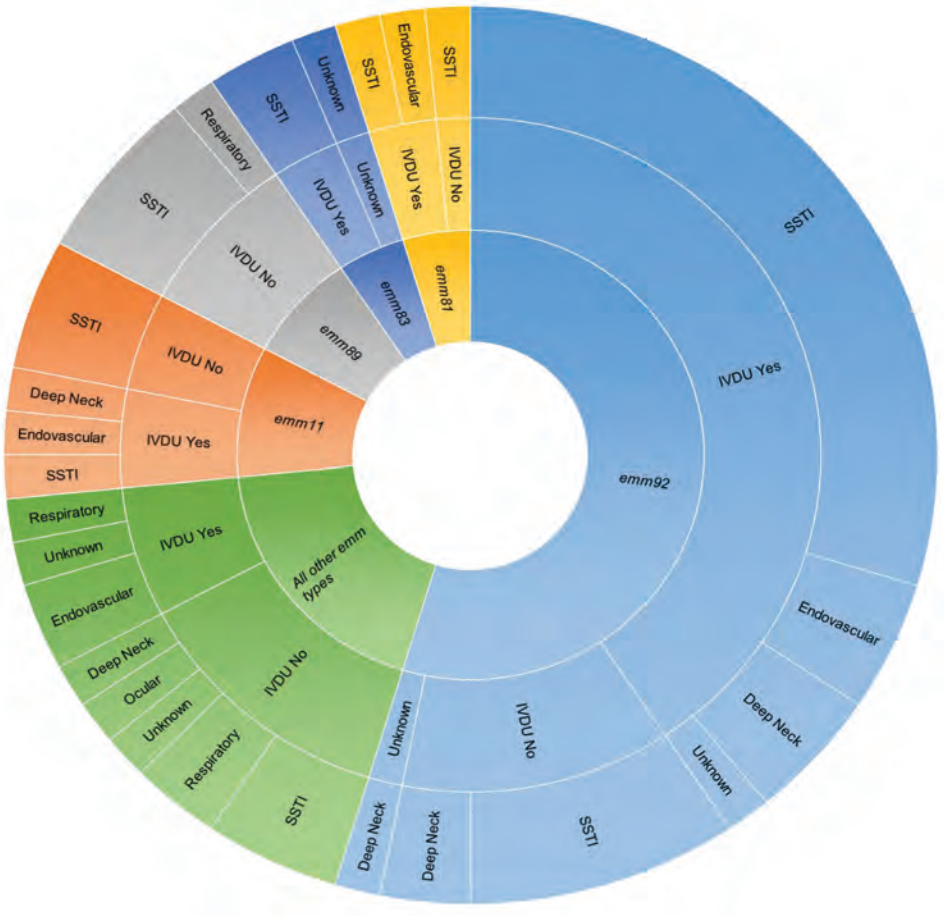


**Figure 2.** Assessment of *emm* type, infection source, and IVDU history of patients with invasive group A *Streptococcus* infection in this study, West Virginia, USA, 2020–2021. Anatomic source of infection and the status of patient IVDU history is shown corresponding to *emm* type. Size of the colored sections indicates the relative number of isolates per *emm* type. IVDU, intravenous drug use; SSTI, skin and soft tissue infection.

**Table 1.** Phenotypic antimicrobial susceptibility results in invasive group A *Streptococcus* isolates, by *emm* type and resistance determinant, West Virginia, USA, 2020–2021*

| | | No. (%) | | | | | | | | | | | | | |
|---|---|---|---|---|---|---|---|---|---|---|---|---|---|---|---|
| | Geno, | Erythromycin | | Clindamycin | | | Tetracycline | | Kanamycin | | Streptomycin | | Gentamicin | |
| *emm* type | no. | S | R | S | $iMLS_B$ | $cMLS_B$ | S | R | S | R | S | R | S | R |
| *emm92* | *ermT*, 35 | 0 | 35 (100) | 0 | 31 (89) | 4 (11) | 0 | 35 (100) | 0 | 35 (100) | 0 | 35 (100) | 35 (100) | 0 |
| *emm11* | *ermA*, 2 | 0 | 2 (100) | 0 | 2 (100) | 0 | 0 | 2 (100) | 0 | 2 (100) | 2 (100) | 0 | 2 (100) | 0 |
| | *ermB*, 6 | 0 | 6 (100) | 0 | 3 (50) | 3 (50) | | 6 (100) | 2 (33) | 4 (67) | 0 | 6 (100) | 6 (100) | 0 |
| *emm77* | *ermA*, 1 | 0 | 1 (100) | 0 | 1 (100) | 0 | 0 | 1 (100) | 0 | 1 (100) | 1 (100) | 0 | 1 (100) | 0 |
| | ND, 1 | 1 (100) | 0 | 1 (100) | 0 | 0 | 1 (100) | 0 | 0 | 1 (100) | 1 (100) | 0 | 1 (100) | 0 |
| *emm83* | *ermA*, 3 | 0 | 3 (100) | 0 | 3 (100) | 0 | 0 | 3 (100) | 0 | 3 (100) | 2 (67) | 1 (33) | 3 (100) | 0 |
| *emm197* | *ermA*, 1 | 0 | 1 (100) | 0 | 0 | 1 (100) | 0 | 1 (100) | 1 (100) | 0 | 1 (100) | 0 | 1 (100) | 0 |
| *emm82* | *ermB*, 1 | 0 | 1 (100) | 0 | 0 | 1 (100) | 0 | 1 (100) | 1 (100) | 0 | 1 (100) | 0 | 1 (100) | 0 |
| *emm22* | *mefA*, 1 | 0 | 1 (100) | 1 (100) | 0 | 0 | 0 | 1 (100) | 1 (100) | 0 | 1 (100) | 0 | 1 (100) | 0 |
| *emm89* | ND, 5 | 5 (100) | 0 | 5 (100) | 0 | 0 | 5 (100) | 0 | NT | | NT | | 5 (100) | 0 |
| *emm*† | ND, 10 | 10 (100) | 0 | 10 (100) | 0 | 0 | 9 (90) | 1 (10) | 2 (20) | 8 (80) | 9 (90) | 1 (10) | 10 (100) | 0 |
| Total = 66 | | 16 (24) | 50 (76) | 17 (25) | 40 (61) | 9 (14) | 15 (23) | 51 (77) | 7 (11) | 54 (89) | 24 (39) | 37 (61) | 66 (100) | 0 |

*Geno, genotype; ND, resistance gene not detected; NT, not tested; R, resistant; S, susceptible.
†One *emm11* isolate was not inducible by D-test but showed intermediate clindamycin resistance; other *emm* types with no *erm: emm1* (2), *emm2* (1), *emm12* (1), *emm28* (1), *emm75* (1), *emm81* (3), *emm87* (1).

among *emm*92 isolates (of which 4 exhibited constitutive clindamycin resistance and 31 exhibited inducible clindamycin resistance), as well as among *emm*11 isolates (of which 5 isolates produced inducible and 3 produced constitutive phenotypes) (Table 1).

### Detection of Erythromycin-Resistance Determinants

We tested isolates for common erythromycin resistance genes by PCR amplification to detect the presence of the methyl transferase genes *ermA*, *ermB*, *and ermT*, as well as *mefA*, a gene-encoding protein associated with an efflux pump (Appendix Table 2). On the basis of a previous ABCs report that *ermT* in *emm92* GAS was carried on the pRW35 plasmid (*15*), extrachromosomal DNA was isolated from resistant isolates of various *emm* types, yet only *emm92* isolates harbored plasmid DNA (Figure 4, panel A). Restriction digestion targeting a conserved *Swa*I site confirmed a ≈4.9-kb size of this pRW35-like plasmid (data not shown). All 35 *emm92* isolates were resistant to erythromycin (Table 1) and contained *ermT* detected by PCR (Figure 4, panel B).

Chromosomal DNA was used for the detection of *ermA/B* (Figure 4, panels C, D) and *mef* (data not shown) genes. Erythromycin-resistance genes identified in *emm11* isolates varied; 6 carried *ermB* and 2 harbored *ermA* (Table 1). Of the remaining 7 erythromycin-resistant isolates of various *emm* types, *ermA* was detected in 5, *ermB* in 1, and *mefA* in 1. Collectively, 86% of *ermA*-containing isolates (6 of 7) showed inducible clindamycin resistance, whereas isolates containing *ermB* had a more evenly split phenotype for clindamycin resistance (3 $iMLS_B$ vs. 4 $cMLS_B$) (Table 1). The *mefA* gene, which encodes a component of the *mefA-msrD* efflux pump, was detected in a single *emm*22 isolate and corresponded to the erythromycin-resistant, clindamycin-susceptible phenotype referred to as the M phenotype (*20*).

### Additional Susceptibility and Proposed Resistance Determinants

Isolates also underwent susceptibility testing for tetracycline by disc diffusion, as well as for the aminoglycosides (gentamicin, streptomycin, and kanamycin) by agar dilution method using concentration ranges as previously described (*5*). In aggregate, 76% of isolates were resistant to both tetracycline and erythromycin, whereas the single *emm87* isolate was erythromycin sensitive but tetracycline resistant. For aminoglycosides, all 66 isolates were susceptible to gentamicin using CLSI *Staphylococcus aureus* breakpoints, whereas we observed presumed resistance to kanamycin (MIC ≥500 μg/mL) in 89% of tested isolates and resistance to streptomycin (MIC ≥500 μg/mL) in 61% of isolates. In addition to their universal plasmid-encoded $MLS_B$

phenotype, all *emm92* strains in this collection were uniformly resistant to tetracycline, kanamycin, and streptomycin, presumably encoded by the ICESpyM92 mobile element (Table 2) (*5*). The remaining isolates of various *emm* types with $MLS_B$ phenotype demonstrated resistance to either kanamycin or tetracycline.

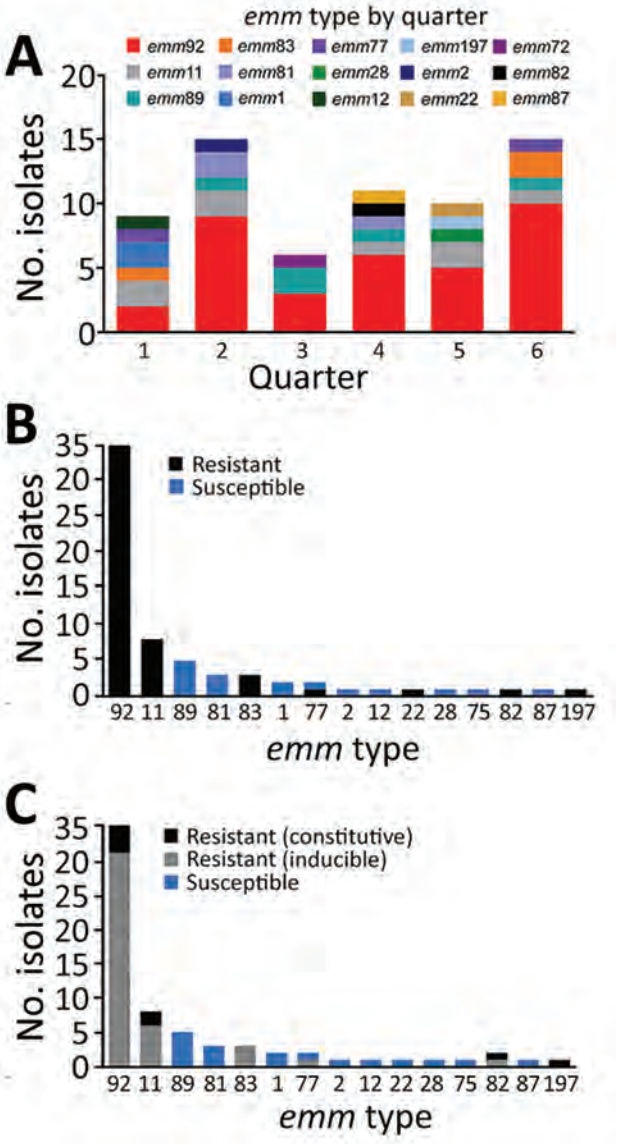


**Figure 3.** *emm* type distribution and $MLS_B$ resistance among invasive group A *Streptococcus* isolates, West Virginia, USA, 2020–2021. A) Temporal analysis of isolate *emm* type by 3-month periods. Specimens harboring isolates were collected during January 2020–June 2021, represented by consecutive quarters numbered 1–6. Graph indicates trend of *emm92* isolates predominating each quarter over the study period. B, C) $MLS_B$ susceptibility and resistance profiles. The number of isolates resistant to erythromycin (B) and clindamycin (C) by *emm* type was determined on the basis of antimicrobial susceptibility testing. Isolates were deemed nonsusceptible to clindamycin if they had either an inducible or constitutive resistance phenotype and deemed susceptible in the absence of growth as determined by D-test.

## Discussion

This study represents a comprehensive characterization of iGAS isolates from West Virginia, a geographic area beyond ABC surveillance, on the basis of the relationship between *emm* type and macrolide resistance. The results confirm a very high rate of erythromycin resistance (76%) across 7 different *emm* types producing invasive infections, most of which displayed $MLS_B$ phenotype and were concomitantly resistant to clindamycin. A relationship between *emm* type and erythromycin-resistance mechanisms in this collection also became apparent. We observed that type *emm92* represented 53% of patient isolates and *emm11* 12% of patient isolates, but together those types accounted for 86% of erythromycin-resistant strains. The third most prevalent *emm* type was *emm89,* although all isolates were susceptible to erythromycin. These findings corroborate 2010–2019 nationwide data from ABCs, which demonstrated an increasing incidence of iGAS infections caused by *emm92*, *emm11*, and *emm89* types affecting the adult US population (*11*,*22*–*24*). By contrast, *emm92* iGAS infections have been reported only sporadically and at much lower frequencies globally (*25*,*26*), suggesting that expansion and dissemination of this organism might thus far be limited to the United States. Nonetheless, all 3 *emm* types are represented in the 30-valent M protein–based vaccine, signifying their role in GAS disease (*27*).

All *emm92* strains in this study harbored the pRW35-like plasmid containing the *ermT* gene, which confers resistance to erythromycin. Plasmids harboring the conserved *ermT* gene have been found in several medically relevant bacteria, including *S. pyogenes*, *S. agalactiae*, methicillin-resistant strains of *Staphylococcus aureus*, *S. gallolyticus* subspecies *pasteurianus*, and *S. suis*, which suggests horizontal gene transfer (*15*,*28*–*30*). The practice of using animal feed containing tylosin, a macrolide additive, has been suggested as a contributing factor in the spread of *ermT* across different species (*30*). The second most commonly identified *emm* type was *emm11*, in which resistance was enabled by either the *ermA* or *ermB* gene. In contrast to *emm92*, infections caused by the *emm11* strains displaying $MLS_B$ phenotype have been broadly reported around the world (*4*,*31*–*34*), including fluoroquinolone-resistant isolates in China (*35*). We observed 5 iGAS infections related to *emm89.* Acapsular *emm89* strains emerged as a key cause of iGAS infections worldwide (*34*,*36*–*38*). Those strains also contain a mutation in the *nga* promoter leading to higher expression of cytotoxins NADase and streptolysin O (*36*,*39*).

We also tested resistance to tetracycline, kanamycin, streptomycin, and gentamicin. No strains

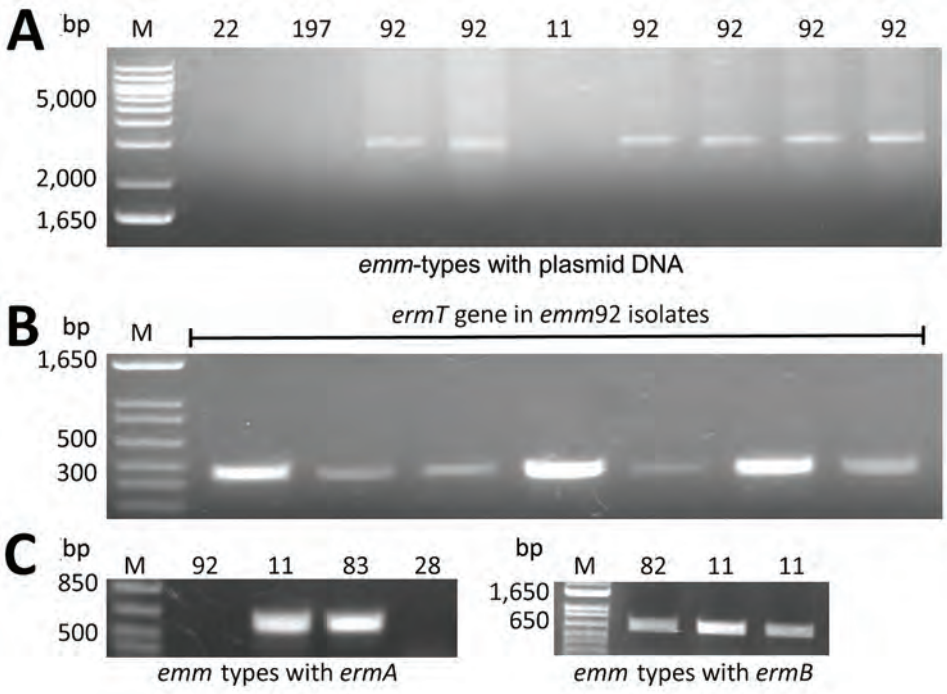


**Figure 4.** Detection of the methyl transferase genes *ermA, ermB, and ermT* in invasive group A *Streptococcus* (iGAS) isolates, West Virginia, USA, 2020–2021. A) Distribution of the pRW35-like plasmid among iGAS isolates. Presence of pRW35-like plasmid DNA was detected only in iGAS *emm92*-type isolates (representative samples are shown). B) PCR detection of the *ermT*-gene. The *ermT*-specific amplicon of 452 bp was detected in *emm92* isolates using plasmid DNA as a template. C, D) Detection of the *ermA* and *ermB* genes. Chromosomal DNA was used as a template to detect the 612-bp-*ermA* (C) and 663-bp-*ermB* (D) amplicons present in several different *emm* types. A 347-bp-*mefA* amplicon was detected in a single *emm22* isolate (data not shown).

were resistant to gentamicin, but all *emm92* strains demonstrated resistance to kanamycin, streptomycin, and tetracycline. Sanson et al. (*5*) used whole-genome sequencing to demonstrate that *emm92* isolates contain the ICESpyM92 element carrying the *tet(M)*, *ant (6)-Ia*, and *aph-(3')-III* genes, which accounts for resistance to tetracycline and the 2 aminoglycosides (also observed in this study) and has subsequently been linked to increased virulence of *emm92* strains (*40*). Further, that research showed that *emm11* isolates harboring *ermB* and exhibiting resistance to tetracycline and kanamycin contained a Tn6003-like transposon carrying the *aph (3')-III* gene, whereas those harboring *ermB* and tetracycline resistance alone carried Tn6002 (*5*). All 6 *emm11* isolates with *ermB* from this study displayed 1 of these 2 phenotypes. Other studies have reported ICESp2905 as the cause of resistance to tetracycline, erythromycin, and kanamycin in *emm11* isolates containing the *ermA* gene (*21*,*41*), which reflects the phenotypic pattern of 2 such isolates observed in this collection. Our collection contained 1 *emm22* isolate displaying M phenotype encoded by *mefA*, which could be carried on the transposon Tn1207.3 (*5*,*42*). Overall, these results suggest that many iGAS strains in West Virginia, especially *emm92* strains, are resistant to multiple classes of antimicrobial drugs, in addition to macrolides.

This study corroborates earlier reports noting the emergence of macrolide-resistant *emm92* iGAS nationally (*5*,*11*,*22*,*43*–*45*). We observed *emm92* as the predominant M type in every quarter, although an overall decrease in incidence was noted during July–September 2020. Quarantine related to the COVID-19 pandemic might in part explain this decrease, although periodic seasonality in disease incidence might also be a contributing factor. Nationwide data from 2010–2017 identified *emm92*, *emm49*, and *emm82* as predominant iGAS types among patients with a history of IVDU and in those experiencing homelessness (*22*), but 2020–2021 West Virginia data identified *emm92*, *emm11*, and *emm89* as the top

**Table 2.** Proposed aminoglycoside and tetracycline resistance determinants in group A *Streptococcus* isolates, West Virginia, USA, 2020–2021

| *emm* type | Kanamycin resistance | Streptomycin resistance | Tetracycline resistance | Determinant | Resistance element | Reference |
|---|---|---|---|---|---|---|
| *emm92* | + | + | + | ICESpyM92, Tn916 pRW35 | *Tet(M), ant (6)-Ia, aph-(3')-III ermT* | (*5*) (*15*) |
| *emm11* | + | – | + | Tn6003-like | *Tet(M), ermB, aph(3')-III* | (*5*) |
| | – | – | + | Tn6002 | *Tet(M), ermB* | (*5*) |
| | + | – | + | ICESp2905 | *Tet(O), ermA, aph-(3')-III* | (*21*) |
| *emm197* | – | – | + | ICESp2905 | *Tet(O), ermA* | (*21*) |
| *emm22* | – | – | + | Tn1207.1-like | *Tet(O), mefA,* | (*20*) |

3 iGAS types. In addition, CDC surveillance detected considerable numbers of historically classical iGAS *emm* types (e.g., *emm1*, *emm12*, *emm28*, and *emm3*), whereas our collection did not. Our results signify an area deserving of future investigation because of the emerging dominance of the *emm92* type in iGAS infections across the United States.

Drug abuse has become a serious epidemic in West Virginia; rates of overdose deaths have risen starting in 1999 (*46*). Patient data from this cohort corroborate that IVDU is a risk factor for resistant iGAS infections; 60.6% of affected patients reported IVDU, compared with 8.7% reported by the ABCs program. Recent studies have documented increases in drug use and overdose indicators during the COVID-19 pandemic, including higher rates of emergency department visits, emergency medical service dispatches, urine drug screen positivity, and death (*47*,*48*). Similarly, a study from Ontario, Canada, focusing on IVDU noted a 2-fold higher rate of IVDU-related SSTI than for the prepandemic era (*49*). At J.W. Ruby Memorial Hospital, overall GAS isolate recovery (calculated as total unique patient isolates per total aerobic cultures performed) declined during the pandemic, decreasing from 0.83% (890/107,150) in 2018–2019 to 0.54% (520/96,380) in 2020–2021, yet the percentage, rate, and absolute number of iGAS isolates among these totals increased substantially, from 159/892 (18%) isolates in 2018–2019 to 252/518 (49%) isolates in 2020–2021. Whether or to what extent increased IVDU during our study period affected strain diversity or resistance rates is unknown.

Homelessness among persons in West Virginia is also increasing. As of January 2020, an estimated 1,341 persons in the state experienced homelessness on any given day (*50*). In our study cohort, homelessness was reported by 13.6% of patients who had adequate documentation; 88.8% of those had a history of IVDU. In comparison, a study encompassing the 10 nationwide ABCs sites during 2010–2017 reported homelessness in 5.8% of patients and both risk factors in 6.1% of persons (*22*).

The first limitation of our study is that, although this collection of iGAS isolates was derived from a broad geographic area of the state, it did not include all invasive strains for the periods represented. Much of southern West Virginia is beyond the WVUMed catchment area, and isolates from some WVUMed hospitals and other health systems would not have been captured. Further, because our hospital laboratory only banks invasive strains, we were unable to compare genotypic or phenotypic features of pharyngitis strains. Resistance determinants for tetracycline and aminoglycosides were not defined here. We also did not explore reasons for variable inducible/constitutive phenotype within *emm* types harboring same *erm* determinant, although research is ongoing.

In conclusion, we describe the clinicoepidemiology of iGAS infections in West Virginia over a 1.5-year period, identifying prevalent *emm* types and associated patient risk factors. Our findings indicate a particular vulnerability to iGAS infections associated with socioeconomic status, which clearly affected this study population (*46*). Further studies of *emm92* iGAS isolates and categorization of resistance will be key to improve treatments and guidelines for preventing resistance. Providing greater information and access to supplies for preventing iGAS infections in those most at risk might help reduce the spread of resistant iGAS strains in the United States.

This article was preprinted at https://www.biorxiv.org/content/10.1101/2022.08.08.503263v1.

**Acknowledgments**

We thank the Centers for Disease Control and Prevention Emerging Infection Program laboratory for providing control group A *Streptococcus* strains.

S.L. and M.E.G. acknowledge funding from a grant awarded as a result of Broad Agency Announcement (BAA) HDTRA1-14-24-FRCWMD-Research and Development Enterprise, Basic and Applied Sciences Directorate, Basic Research for Combating Weapons of Mass Destruction (C-WMD), under contract #HDTRA1035955001, and in part by the Vaccine Development center at WVU-HSC, Research Challenge Grant no.HEPC.dsr.18.6 from the Division of Science and Research, WV Higher Education Policy Commission, and by the Transition Grant Support; Office of Research and Graduate Education, WVU Health Sciences Center (to S.L.). L.M.P. and C.E.C. were supported by the Department of Microbiology, Immunology and Cell Biology Research Internship for Undergraduates in the Immunology and Medical Microbiology degree program.

## About the Author

Miss Powell is a doctoral student enrolled in the Immunology and Microbial Pathogenesis program at West Virginia University School of Medicine. Her research is focused on the mechanisms of pathogenesis and antimicrobial resistance of group A Streptococcus. She is a member of Dr. Lukomski's laboratory in the Department of Microbiology, Immunology, and Cell Biology.

## References


1. Stevens DL. Invasive group A S*treptococcus* infections. Clin Infect Dis. 1992;14:2–11. https://doi.org/10.1093/clinids/14.1.2
2. Carapetis JR, Beaton A, Cunningham MW, Guilherme L, Karthikeyan G, Mayosi BM, et al. Acute rheumatic fever and rheumatic heart disease. Nat Rev Dis Primers. 2016;2:15084. https://doi.org/10.1038/nrdp.2015.84
3. Walker MJ, Barnett TC, McArthur JD, Cole JN, Gillen CM, Henningham A, et al. Disease manifestations and pathogenic mechanisms of group A *Streptococcus*. Clin Microbiol Rev. 2014;27:264–301. https://doi.org/10.1128/CMR.00101-13
4. Silva-Costa C, Friães A, Ramirez M, Melo-Cristino J. Macrolide-resistant *Streptococcus pyogenes*: prevalence and treatment strategies. Expert Rev Anti Infect Ther. 2015; 13:615–28. https://doi.org/10.1586/14787210.2015.1023292
5. Sanson MA, Macias OR, Shah BJ, Hanson B, Vega LA, Alamarat Z, et al. Unexpected relationships between frequency of antimicrobial resistance, disease phenotype and *emm* type in group A *Streptococcus*. Microb Genom. 2019;5:e000316. https://doi.org/10.1099/mgen.0.000316
6. Mingoia M, Morici E, Morroni G, Giovanetti E, Del Grosso M, Pantosti A, et al. Tn5253 family integrative and conjugative elements carrying *mef(I)* and *catQ* determinants in *Streptococcus pneumoniae* and *Streptococcus pyogenes*. Antimicrob Agents Chemother. 2014;58:5886–93. https://doi.org/10.1128/AAC.03638-14
7. Berbel D, Càmara J, García E, Tubau F, Guérin F, Giard JC, et al. A novel genomic island harbouring *lsa(E)* and *lnu(B)* genes and a defective prophage in a *Streptococcus pyogenes* isolate resistant to lincosamide, streptogramin A and pleuromutilin antibiotics. Int J Antimicrob Agents. 2019; 54:647–51. https://doi.org/10.1016/j.ijantimicag.2019.08.019
8. Centers for Disease Control and Prevention. Erythromycin-resistant group A *Streptococcus* [cited 2021 Nov 23]. https://www.cdc.gov/drugresistance/pdf/threats-report/gas-508.pdf
9. Centers for Disease Control and Prevention. Active Bacterial Core Surveillance (ABCs): Emerging Infections Program network, group A *Streptococcus*, 2010 [cited 2012 Jan 5]. https://www.cdc.gov/abcs/reports-findings/survreports/gas10.html
10. Centers for Disease Control and Prevention. Active Bacterial Core Surveillance Report: Emerging Infections Program network, group A *Streptococcus*, 2019 [cited 2022 Jun 16]. https://www.cdc.gov/abcs/downloads/GAS_Surveillance_Report_2019.pdf
11. Fay K, Onukwube J, Chochua S, Schaffner W, Cieslak P, Lynfield R, et al. Patterns of antibiotic nonsusceptibility among invasive group A *Streptococcus* infections—United States, 2006–2017. Clin Infect Dis. 2021;73:1957–64. https://doi.org/10.1093/cid/ciab575
12. Bruun T, Rath E, Madsen MB, Oppegaard O, Nekludov M, Arnell P, et al.; INFECT Study Group. Risk factors and predictors of mortality in streptococcal necrotizing soft-tissue infections: a multicenter prospective study. Clin Infect Dis. 2021;72:293–300. https://doi.org/10.1093/cid/ciaa027
13. Centers for Disease Control and Prevention. 2020 drug overdose death rates [cited 2022 Jul 27]. https://www.cdc.gov/drugoverdose/deaths/2020.html
14. Goldenberger D, Perschil I, Ritzler M, Altwegg M. A simple "universal" DNA extraction procedure using SDS and proteinase K is compatible with direct PCR amplification. PCR Methods Appl. 1995;4:368–70. https://doi.org/10.1101/gr.4.6.368
15. Woodbury RL, Klammer KA, Xiong Y, Bailiff T, Glennen A, Bartkus JM, et al.; Active Bacterial Core Surveillance Team. Plasmid-borne *erm(T)* from invasive, macrolide-resistant *Streptococcus pyogenes* strains. Antimicrob Agents Chemother. 2008;52:1140–3. https://doi.org/10.1128/AAC.01352-07
16. Beall B, Facklam R, Thompson T. Sequencing *emm*-specific PCR products for routine and accurate typing of group A streptococci. J Clin Microbiol. 1996;34:953–8. https://doi.org/10.1128/jcm.34.4.953-958.1996
17. Clinical and Laboratory Standards Institute. Performance standards for antimicrobial susceptibility testing. 31st ed. CLSI supplement M100. Wayne (PA): The Institute; 2021.
18. Musser JM, Hauser AR, Kim MH, Schlievert PM, Nelson K, Selander RK. *Streptococcus pyogenes* causing toxic-shock-like syndrome and other invasive diseases: clonal diversity and pyrogenic exotoxin expression. Proc Natl Acad Sci U S A. 1991;88:2668–72. https://doi.org/10.1073/pnas.88.7.2668
19. Jain I, Sarkar P, Danger JL, Medicielo J, Roshika R, Calfee G, et al. A mobile genetic element promotes the association between serotype M28 group A *Streptococcus* isolates and cases of puerperal sepsis. J Infect Dis. 2019;220:882–91. https://doi.org/10.1093/infdis/jiz195
20. Blackman Northwood J, Del Grosso M, Cossins LR, Coley MD, Creti R, Pantosti A, et al. Characterization of macrolide efflux pump *mef* subclasses detected in clinical isolates of *Streptococcus pyogenes* isolated between 1999 and 2005. Antimicrob Agents Chemother. 2009;53:1921–5. https://doi.org/10.1128/AAC.01065-08
21. Giovanetti E, Brenciani A, Lupidi R, Roberts MC, Varaldo PE. Presence of the *tet(O)* gene in erythromycin- and tetracycline-resistant strains of *Streptococcus pyogenes* and linkage with either the *mef(A)* or the *erm(A)* gene. Antimicrob Agents Chemother. 2003;47:2844–9. https://doi.org/10.1128/AAC.47.9.2844-2849.2003
22. Valenciano SJ, Onukwube J, Spiller MW, Thomas A, Como-Sabetti K, Schaffner W, et al. Invasive group A streptococcal infections among people who inject drugs and people experiencing homelessness in the United States, 2010–2017. Clin Infect Dis. 2021;73:e3718–26. https://doi.org/10.1093/cid/ciaa787
23. Chochua S, Metcalf BJ, Li Z, Rivers J, Mathis S, Jackson D, et al. Population and whole genome sequence based characterization of invasive group A streptococci recovered in the United States during 2015. MBio. 2017;8:e01422–17. https://doi.org/10.1128/mBio.01422-17
24. Li Y, Rivers J, Mathis S, Li Z, Velusamy S, Nanduri SA, et al. Genomic surveillance of *Streptococcus pyogenes* strains causing invasive disease, United States, 2016–2017. Front Microbiol. 2020;11:1547. https://doi.org/10.3389/fmicb.2020.01547
25. Le Hello S, Doloy A, Baumann F, Roques N, Coudene P, Rouchon B, et al. Clinical and microbial characteristics of invasive *Streptococcus pyogenes* disease in New Caledonia, a region in Oceania with a high incidence of acute rheumatic fever. [Erratum in: J Clin Microbiol. 2010;48:1993]. J Clin Microbiol. 2010;48:526–30. https://doi.org/10.1128/JCM.01205-09
26. Abraham T, Sistla S. Molecular epidemiology of macrolide resistant group A streptococci from Puducherry, India. J Infect Dev Ctries. 2017;11:679–83. https://doi.org/10.3855/jidc.9132
27. Dale JB, Penfound TA, Chiang EY, Walton WJ. New 30-valent M protein-based vaccine evokes cross-opsonic antibodies against non-vaccine serotypes of group A streptococci. Vaccine. 2011;29:8175–8. https://doi.org/10.1016/j.vaccine.2011.09.005

28. Palmieri C, Magi G, Creti R, Baldassarri L, Imperi M, Gherardi G, et al. Interspecies mobilization of an *ermT*-carrying plasmid of *Streptococcus dysgalactiae* subsp. *equisimilis* by a coresident ICE of the ICESa2603 family. J Antimicrob Chemother. 2013;68:23–6. https://doi.org/10.1093/jac/dks352
29. Kadlec K, Schwarz S. Identification of a plasmid-borne resistance gene cluster comprising the resistance genes *erm(T)*, *dfrK*, and *tet(L)* in a porcine methicillin-resistant *Staphylococcus aureus* ST398 strain. Antimicrob Agents Chemother. 2010;54:915–8. https://doi.org/10.1128/AAC.01091-09
30. DiPersio LP, DiPersio JR, Beach JA, Loudon AM, Fuchs AM. Identification and characterization of plasmid-borne *erm(T)* macrolide resistance in group B and group A *Streptococcus*. Diagn Microbiol Infect Dis. 2011;71:217–23. https://doi.org/10.1016/j.diagmicrobio.2011.07.010
31. Ksia S, Smaoui H, Hraoui M, Bouafsoun A, Boutiba-Ben Boubaker I, Kechrid A. Molecular characteristics of erythromycin-resistant *Streptococcus pyogenes* strains isolated from children patients in Tunis, Tunisia. Microb Drug Resist. 2017;23:633–9. https://doi.org/10.1089/mdr.2016.0129
32. Bocking N, Matsumoto CL, Loewen K, Teatero S, Marchand-Austin A, Gordon J, et al. High incidence of invasive group A streptococcal infections in remote indigenous communities in Northwestern Ontario, Canada. Open Forum Infect Dis. 2016;4:ofw243. https://doi.org/10.1093/ofid/ofw243
33. Meehan M, Murchan S, Gavin PJ, Drew RJ, Cunney R. Epidemiology of an upsurge of invasive group A streptococcal infections in Ireland, 2012–2015. J Infect. 2018;77:183–90. https://doi.org/10.1016/j.jinf.2018.05.010
34. Hasegawa T, Hata N, Matsui H, Isaka M, Tatsuno I. Characterisation of clinically isolated *Streptococcus pyogenes* from balanoposthitis patients, with special emphasis on *emm89* isolates. J Med Microbiol. 2017;66:511–6. https://doi.org/10.1099/jmm.0.000460
35. Shen Y, Cai J, Davies MR, Zhang C, Gao K, Qiao D, et al. Identification and characterization of fluoroquinolone non-susceptible S*treptococcus pyogenes* clones harboring tetracycline and macrolide resistance in Shanghai, China. Front Microbiol. 2018;9:542. https://doi.org/10.3389/fmicb.2018.00542
36. Zhu L, Olsen RJ, Nasser W, de la Riva Morales I, Musser JM. Trading capsule for increased cytotoxin production: contribution to virulence of a newly emerged clade of *emm89 Streptococcus pyogenes*. MBio. 2015;6:e01378–15. https://doi.org/10.1128/mBio.01378-15
37. Turner CE, Abbott J, Lamagni T, Holden MT, David S, Jones MD, et al. Emergence of a new highly successful acapsular group A *Streptococcus* clade of genotype *emm89* in the United Kingdom. MBio. 2015;6:e00622. https://doi.org/10.1128/mBio.00622-15
38. Wajima T, Chiba N, Morozumi M, Shouji M, Sunaoshi K, Sugita K, et al.; GAS Surveillance Study Group. Prevalence of macrolide resistance among group A streptococci isolated from pharyngotonsillitis. Microb Drug Resist. 2014;20:431–5. https://doi.org/10.1089/mdr.2013.0213
39. Turner CE, Holden MTG, Blane B, Horner C, Peacock SJ, Sriskandan S. The emergence of successful S*treptococcus pyogenes* lineages through convergent pathways of capsule loss and recombination directing high toxin expression. MBio. 2019;10:e02521–19. https://doi.org/10.1128/mBio.02521-19
40. Vega LA, Sanson MA, Cubria MB, Regmi S, Shah BJ, Shelburne SA, et al. The integrative conjugative element ICESpyM92 contributes to pathogenicity of emergent antimicrobial-resistant *emm92* group A *Streptococcus*. Infect Immun. 2022;90:e0008022. https://doi.org/10.1128/iai.00080-22
41. Partridge SR, Kwong SM, Firth N, Jensen SO. Mobile genetic elements associated with antimicrobial resistance. Clin Microbiol Rev. 2018;31:e00088–17. https://doi.org/10.1128/CMR.00088-17
42. Chancey ST, Bai X, Kumar N, Drabek EF, Daugherty SC, Colon T, et al. Transcriptional attenuation controls macrolide inducible efflux and resistance in *Streptococcus pneumoniae* and in other Gram-positive bacteria containing *mef/mel(msr(D))* elements. PLoS One. 2015;10:e0116254. https://doi.org/10.1371/journal.pone.0116254
43. Metcalf B, Nanduri S, Chochua S, Li Y, Fleming-Dutra K, McGee L, et al. Cluster transmission drives invasive group A *Streptococcus* disease within the United States and is focused on communities experiencing disadvantage. J Infect Dis. 2022;226:546–53. https://doi.org/10.1093/infdis/jiac162
44. Li Y, Rivers J, Mathis S, Li Z, McGee L, Chochua S, et al. Continued increase of erythromycin- and clindamycin-nonsusceptibility among invasive group A streptococci driven by genomic clusters, USA, 2018–2019. Clin Infect Dis. 2022. https://doi.org/10.1093/cid/ciac468
45. Chochua S, Metcalf B, Li Z, Mathis S, Tran T, Rivers J, et al. Invasive group A streptococcal penicillin binding protein 2× variants associated with reduced susceptibility to β-lactam antibiotics in the United States, 2015–2021. Antimicrob Agents Chemother. 2022;66:e0080222. https://doi.org/10.1128/aac.00802-22
46. National Institute on Drug Abuse. West Virginia: opioid-involved deaths and related harms. 2020 [cited 2022 May 5]. https://nida.nih.gov/drug-topics/opioids/opioid-summaries-by-state/west-virginia-opioid-involved-deaths-related-harms
47. Imtiaz S, Nafeh F, Russell C, Ali F, Elton-Marshall T, Rehm J. The impact of the novel coronavirus disease (COVID-19) pandemic on drug overdose-related deaths in the United States and Canada: a systematic review of observational studies and analysis of public health surveillance data. Subst Abuse Treat Prev Policy. 2021;16:87. https://doi.org/10.1186/s13011-021-00423-5
48. Simha S, Ahmed Y, Brummett CM, Waljee JF, Englesbe MJ, Bicket MC. Impact of the COVID-19 pandemic on opioid overdose and other adverse events in the USA and Canada: a systematic review. Reg Anesth Pain Med. 2023;48:37–43. https://doi.org/10.1136/rapm-2022-103591
49. McRae M, Sardiwalla Y, Nachmani O, Price E, Huynh M, Coroneos C. Upper extremity infection related to intravenous drug use: considering the true cost of the COVID-19 pandemic and lockdown. Hand (N Y). 2022 Feb 22 [Epub ahead of print]. https://doi.org/10.1177/15589447221077377
50. United States Interagency Council on Homelessness. West Virginia homelessness statistics. 2020 [cited 2022 May 5]. https://www.usich.gov/homelessness-statistics/wv


Address for correspondence: Slawomir Lukomski, West Virginia University, 2095 Health Sciences North, Morgantown, WV 26506, USA; email: slukomski@hsc.wvu.edu

# Environmental, Occupational, and Demographic Risk Factors for Clinical Scrub Typhus, Bhutan

Tandin Zangpo, Yoenten Phuentshok, Kezang Dorji, Chencho Dorjee, Sithar Dorjee, Peter Jolly, Roger Morris, Nelly Marquetoux, Joanna McKenzie

Underdiagnosis and underreporting of scrub typhus has increasingly affected public health in Bhutan since its initial detection in 2008. Identifying scrub typhus risk factors would support early diagnosis and treatment for this nonspecific febrile disease, reducing the incidence of potentially fatal complications. We conducted a hospital-based, case–control study during October–December 2015 in 11 scrub typhus–prone districts. We identified harvesting cardamom as the major risk factor (odds ratio 1,519; p<0.001); other factors were traditional housing, largely caused by an outside toilet location, as well as owning a goat and frequently sitting on grass. Harvesting vegetables, herding cattle in the forest, and female sex were protective. Age had a nonlinear effect; children and the elderly were more likely to seek treatment for clinical scrub typhus. This study has informed public health policies and awareness programs for healthcare workers through development of National Guidelines for Prevention, Treatment and Control of Scrub Typhus in Bhutan.

Scrub typhus, or tsutsugamushi disease, is a vectorborne zoonotic disease caused by *Orientia tsutsugamushi*, which is endemic to the tsutsugamushi triangle, centered in Southeast and Pacific Asia (*1*). Trombiculid mites of the genus *Leptotrombidium* are reservoir and vector for *O. tsutsugamushi* (*2*). The infective larvae, called chiggers, transmit the pathogen to humans as incidental hosts. Rodents are maintenance hosts for mites; high numbers increase mite abundance and risk for scrub typhus where the pathogen is present (*2*).

The resurgence and reemergence of scrub typhus in disease-endemic areas (*3*,*4*) places >1 billion persons at risk for this disease globally; an estimated 1 million new cases of scrub typhus occur each year (*4*–*6*). Scrub typhus manifests as a nonspecific febrile illness that is difficult to diagnose. Early treatment using doxycycline or chloramphenicol usually results in rapid remission, but delays in diagnosis and treatment are associated with potentially fatal complications (*7*–*9*). A median case-fatality rate of 6% in untreated patients has been reported, and death rates can be up to 70% (*4*).

In Bhutan, scrub typhus was first detected in 2008 among a cluster of pyrexia of unknown origin cases reporting to Gedu Hospital in Chukha District (*10*). The disease became reportable in 2010, and annual reports have regularly increased, particularly those from southern subtropical regions. A descriptive study showed that scrub typhus is a major cause of febrile illness in Bhutan, albeit underdiagnosed and underreported, presumably because of lack of healthcare worker awareness of the disease and differential diagnostic challenges (*11*). Scrub typhus was most commonly diagnosed in rural, elderly persons and students in southern districts of Bhutan; the highest incidence was in summer and autumn, during July–November (*11*). The high-incidence period aligns with the monsoon season, presumably associated with a higher density of chiggers (*2*) and a higher risk for exposure through intensive agricultural activities. Further epidemiologic studies are required to provide robust evidence of risk factors for scrub typhus in Bhutan, which would support public health action to prevent and control the disease.

The objective of our study was to identify risk factors for clinical scrub typhus in patients seeking

Author affiliations: Khesar Gyalpo University of Medical Sciences of Bhutan, Thimphu, Bhutan (T. Zangpo, Y. Phuentshok, K. Dorji, C. Dorjee, S. Dorjee); Massey University, Palmerston North, New Zealand (T. Zangpo, Y. Phuentshok, K. Dorji, P. Jolly, N. Marquetoux, J. McKenzie); Ministry of Health, Thimphu (T. Zangpo, K. Dorji); World Organisation for Animal Health, Paris, France (Y. Phuentshok); Morvet Ltd, Masterton, New Zealand (R. Morris)

DOI: https://doi.org/10/3201/eid2905.221430

treatment at healthcare centers in scrub typhus–endemic areas of Bhutan. Results from this study were intended to inform public health policies and contribute to raising awareness about scrub typhus among clinicians and populations at risk.

## Materials and Methods

We conducted a hospital-based, case–control study during October–December 2015, coinciding with autumn and the later months of the high-risk period for scrub typhus in Bhutan. The study was conducted in 11 of 20 districts in Bhutan that had reported the highest numbers of scrub typhus cases in the 5 years after scrub typhus was made a reportable disease in 2010. Study districts were located in the southern and central regions, at altitudes ranging from 173 m to 1,576 m above sea level. All 18 healthcare centers in those districts participated in the study, including 15 hospitals (secondary and tertiary healthcare centers) and 3 basic health units (primary healthcare centers) (Figure 1).

We recruited case-patients and controls from patients ≥1 year of age who came to the outpatient departments of the 18 healthcare centers. For each case-patient, we enrolled 3 controls from the same healthcare center, 2 matched by village and 1 unmatched. Matching controlled for the confounding effect of village-level risk factors, enabling investigation of occupational, recreational and household-related exposures of persons. Unmatched controls enabled investigation of individual exposures and spatially correlated variables such as urban/rural and possibly occupation (*12*).

Provisional case-patient definition was a patient consulting the outpatient department during the study period who met 3 criteria. Those criteria were febrile illness (axillary temperature >37.5°C) with ≥1 of the following signs/symptoms: eschar, rashes, headache, cough, general malaise, myalgia, or lymphadenopathy; having a positive test result on the ST Rapid Diagnostic Tsutsugamushi Test (RDT; Bioline, https://www.bioline.com) at the hospital on the visit day; and residing in the study district for the previous month or longer. Confirmed case-patient definition was a provisional patient who had a positive test result for a subsequent serum ELISA (Scrub Typhus Detect IgM ELISA System; InBios, https://inbios.com) conducted at the Royal Center for Disease Control in Thimphu, Bhutan.

Provisional controls were enrolled from patients who visited the same outpatient department on the same day or in the next few days (maximum 1 week) after recruitment of the provisional case and who met 2 criteria: no history of febrile illness or any of the signs/symptoms described for case eligibility in the previous month and a negative test result for the scrub typhus RDT on the visit day. Two provisional matched controls were selected for each provisional case-patient on the basis of their residing in the same village. One provisional unmatched control was selected for each provisional case-patient from patients visiting the same outpatient department who resided anywhere in the study districts, excluding the case-patient's village. Confirmed controls were provisional controls who had a negative result for subsequent serum ELISA.

Excluding provisional case-patients after a negative result for the ELISA resulted in excluding their provisional unmatched and matched controls. In a similar fashion, after excluding provisional controls based on a positive ELISA result, any case-patients who no longer had ≥1 matched control were also excluded.

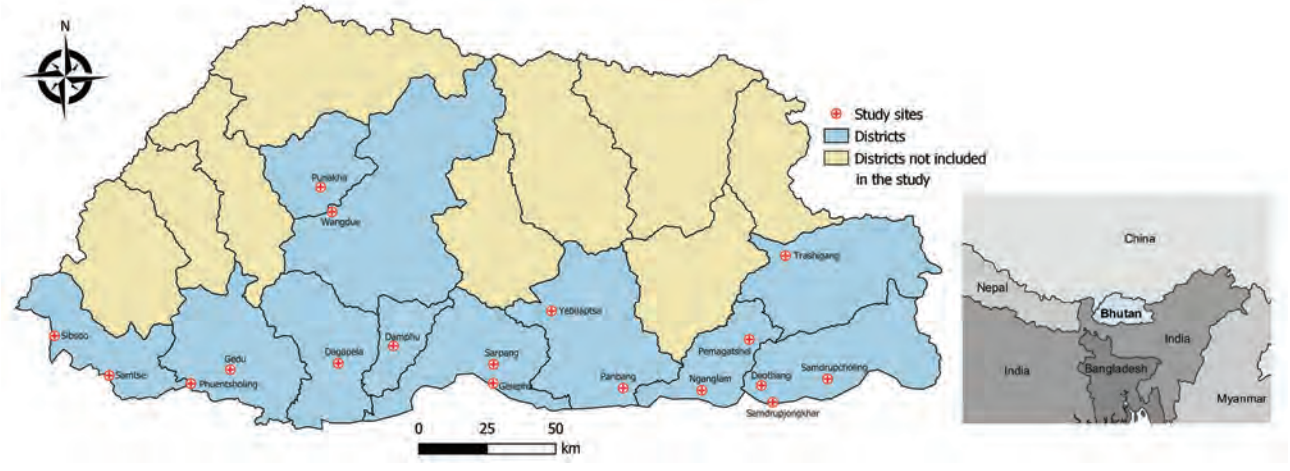


**Figure 1.** Location of 18 healthcare centers in 11 districts that had high reporting rates for scrub typhus that were included in the case–control study conducted in Bhutan, 2015.

The sample size was estimated at the design stage based on the magnitude of association of known risk factors from disease-endemic regions reported in the literature. A similar case–control study in China identified various exposures to crops, grasslands, and outdoors activities as risk factors for scrub typhus (*13*). The average odds ratio (OR) of all significant risk factors in that study was 2.5. For our study, assuming a 10% prevalence of exposure for the target population and aiming to detect an OR ≥2.5 with 95% confidence and 80% power, we required a sample size of 92 case-patients and 276 controls. We increased this number by 10% to include nonresponse or missing information and aimed to enroll ≥100 case-patients and 300 controls.

Blood samples from provisional case-patients and controls were obtained by trained laboratory technicians. The RDT was performed on serum samples at the healthcare center on the same day as sample collection. The SD Bioline Tsutsugamushi Test is a commercial point-of-care rapid diagnostic test that detects IgG, IgM, and IgA against *O. tsutsugamushi* (*14*) and is used in all hospitals in Bhutan to support clinicians' differential diagnosis and timely treatment for scrub typhus. Aliquots of serum samples were frozen at −4°C to −8°C and transported to the Royal Center for Disease Control for ELISA testing (InBios Scrub Typhus Detect IgM ELISA System). For the ELISA, we used an optical density (OD) ≥0.54 as the cutoff for positivity, based on regional cutoff values for OD readings in scrub typhus studies conducted in Thailand and India (*15*–*17*).

We trained healthcare workers from participating healthcare centers to enroll study participants and administer questionnaires. We used a structured, standardized, pretested questionnaire with closed questions in English to interview provisional case-patients and controls at the time of recruitment. We collected information on demographic characteristics, house details, animal ownership, environmental and occupational exposures. Given a scrub typhus incubation period of 21 days, questions were related to a potential exposure period of 1 month before recruitment.

We conducted descriptive analysis of demographic variables of confirmed case-patients and controls. We analyzed data for case-patients and matched controls by using conditional logistic regression and data for case-patients and unmatched controls by using standard logistic regression. We omitted variables with >10% missing information, as well as categorical variables with responses to only 1 level. We conducted initial univariable analysis for each dataset. We considered variables that had a $\chi^2$ p value for the likelihood ratio test (variance comparison with the null model) ≤0.2 in univariable analyses for multivariable analyses. Variables that contained too few responses were recategorized. For multivariable analysis, we used backward and forward variable selection and compared models by using the likelihood-ratio test ($\chi^2$ test, 5% significance level).

We explored collinearity between related variables. For correlated variables, we selected the variable with the most significant contribution to the model based on the likelihood ratio test to avoid multicollinearity in the final model. We tested 2-way interactions between significant variables. We tested linearity of continuous variables (e.g., age) by using polynomials and retained the best fitting model for each analysis to estimate adjusted ORs for scrub typhus risk factors. We performed data management and analyses in R software (The R Project for Statistical Computing, https://www.r-project.org).

Inclusion in the study was based upon patients' written consent. We coded samples to protect patient identity. There was no interruption of laboratory and treatment services because of this study. Our study was approved by the Research Ethics Board of Health, Ministry of Health, Bhutan.

## Results

We recruited 128 provisional scrub typhus case-patients and 381 provisional controls at the 18 healthcare centers during the 3-month study period. After confirmatory ELISA testing, we retained 78 confirmed case-patients and 139 confirmed matched controls for conditional analysis and 66 confirmed case-patients and unmatched controls for unconditional analysis (Figure 2). Of the 128 RDT-positive provisional case-patients, ELISA results were available for 123, of which 79 (64%) were confirmed ELISA-positive (OD ≥0.54) case-patients. Of the 237 RDT-negative provisional controls who were associated with case-patients retained for the analysis, ELISA results were available for 230, of which 205 (89%) were confirmed ELISA-negative (OD<0.54) controls.

Most (52%) study participants were farmers, equally represented in case-patients and controls (Table 1). The next most common categories were children and housewives, with a higher proportion of children as case-patients and a higher proportion of housewives as controls. There were more female (59%) than male participants. The median age was 28 years for case-patients and 35 years for controls. The age distribution for case-patients and controls was different; the middle-age category was overrepresented among controls (Figure 3).

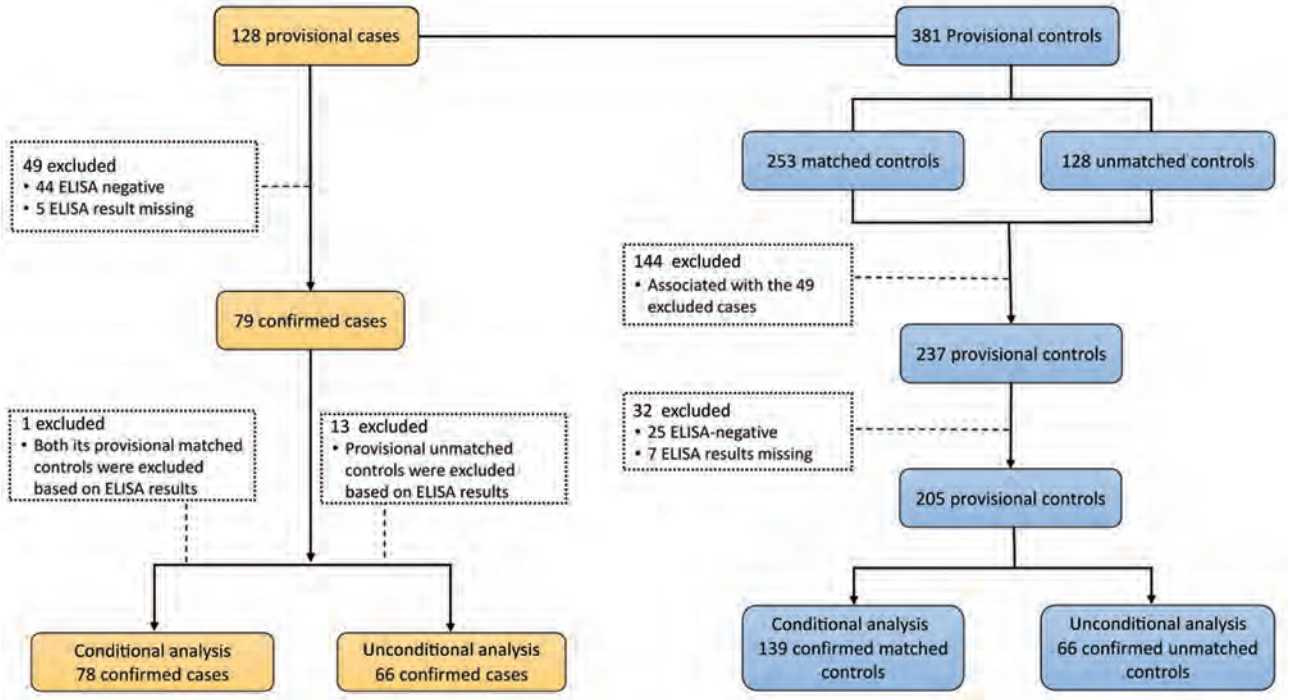


**Figure 2.** Selection process for provisional cases and controls for conditional and unconditional analyses based on confirmatory ELISA results, Bhutan, 2015.

We compiled results for conditional (Table 2) and unconditional (Table 3) univariable analyses and significant variables in the best-fitting conditional (Table 4) and unconditional (Table 5) multivariable models. Harvesting cardamom in the previous month was the major risk factor for clinical scrub typhus: OR 1,519 (95% CI 26.23–8,805.98) in conditional analysis (Table 4) and a smaller OR of 5.98 (95% CI 0.86–41.46) in unconditional analysis (Table 5). Traditional housing had a high OR of 472.3 (95% CI 17.28–12,900) in conditional analysis, and an additional independent risk was associated with having no shower in the house. A closely related variable, toilet outside the house, had a significant OR of 10.65 (95% CI 2.37–47.84) in unconditional analysis. Sitting or sleeping on the grass ≥10 times in the previous month had a high OR in both analyses. We found a significant, independent quadratic effect of age in both models, with a higher predicted probability of clinical scrub typhus for children and older persons after controlling for the effect of other variables (Figure 4).

Conditional analysis showed that possessing a goat was a major risk factor for scrub typhus (OR 36.52, 95% CI 3.59–371.91) but that herding cattle in the forest was strongly protective (OR 0.06, 95% CI 0.01–0.52). Being female and harvesting vegetables were also protective. Unconditional analysis showed that storing wood logs against the house and clearing bush had a higher risk for scrub typhus. Persons who sometimes worked outdoors with bare hands also had a higher risk compared with persons who never worked outdoors with bare hands.

**Table 1.** Distribution of occupation and sex for confirmed case-patients and controls in a study of risk factors for clinical scrub typhus in disease-endemic areas, Bhutan, 2015

| Variable | No. (%) controls | No. (%) case-patients | Total |
|---|---|---|---|
| Occupation | | | |
| Farmer | 108 (53) | 39 (50) | 147 |
| Housewife | 34 (17) | 4 (5) | 38 |
| Preschool/student | 20 (10) | 23 (29) | 43 |
| Civil servant/military | 19 (9) | 2 (3) | 21 |
| Corporate/private sector | 12 (6) | 4 (5) | 16 |
| Construction worker | 9 (4) | 2 (3) | 11 |
| Monk/nun | 3 (1) | 4 (5) | 7 |
| Sex | | | |
| F | 126 (61) | 40 (51) | 166 |
| M | 79 (39) | 38 (49) | 117 |

## Discussion

This study identified major occupational, recreational, household-related, animal ownership, and demographic risk factors for scrub typhus among ill patients who sought treatment during the latter months of the high-incidence period in Bhutan during 2015. Clinical diagnosis of scrub typus is challenging because of its nonspecific clinical manifestations. Furthermore, previous infections, cross-reactivity, and low accuracy of routine diagnostic tests are likely to complicate the diagnosis of scrub typhus (*18*). Thus, identifying risk factors for this disease is a valuable aid for accurate clinical diagnosis and instigation of early treatment, reducing the risk for potentially fatal complications.

Harvesting cardamom was the highest risk factor for scrub typhus, which had a conditional OR of 1,519.00 (95% CI 26.23–88,005.98) (Table 4). Cardamom is a short, bushy plant that might provide favorable mite habitat. It is grown throughout the southern districts of Bhutan, preferring shaded conditions on hilly terrain with moist soils (*19*). Cardamom harvest occurs during August–September in low and middle altitudes and November–December in high altitudes, coinciding with the scrub typhus risk period (*11*) and with our study period (October–December). Hilly terrain and autumn harvest also appeared as major risk factors for scrub typhus in China (*13*) and Japan (*20*). Growing cardamom is a lucrative business; its cultivation has been increasing in Bhutan since 2013 (*19*), which is likely to have contributed to the increasing incidence of scrub typhus. Cardamom is also cultivated in nearby countries (India [*21*] and Nepal [*22*]), where it might also contribute to increased incidence of scrub typhus (*23*,*24*).

Harvesting vegetables was negatively associated with scrub typhus in our study, contrasting with findings of a study in China conducted during the same time of year in which working in vegetable fields increased the risk for scrub typhus (*13*). A possible explanation is that vegetable species or growing environment differed between the 2 countries. In our study, vegetables harvested included broccoli, tomatoes, and onions, which might have been grown in an environment with minimal mite habitat, thus reducing the risk for scrub typhus.

Traditional housing was another strong risk factor in conditional analysis (OR 472.30, 95% CI 17.28–12,900.00). This variable was correlated with having an outside toilet; however, it captured more of the variability in scrub typhus risk than toilet location and was retained in the final model. In contrast, in unconditional analysis, having an outside toilet

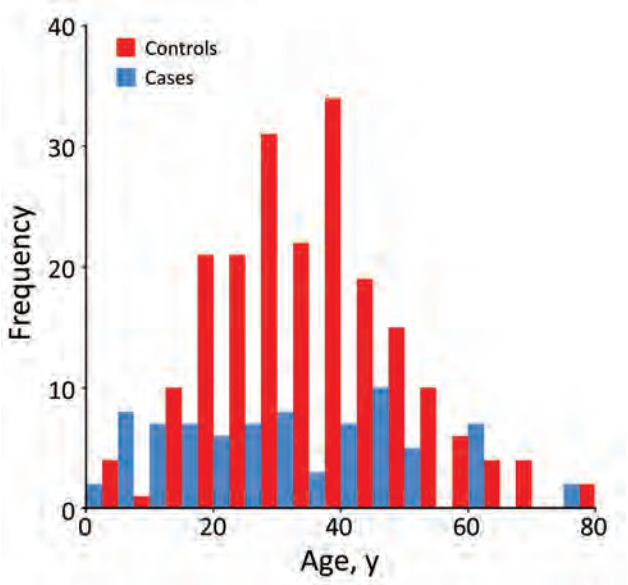


**Figure 3.** Age distribution of confirmed cases and controls included in a study of risk factors for clinical scrub typhus in disease-endemic areas of Bhutan, 2015.

explained more variability in scrub typhus risk than traditional house type. Having an outside toilet, regardless of whether the toilet was modern or traditional type, might directly increase exposure to mites from surrounding bushes, or it might be a proxy for other factors associated with traditional housing. Having no shower in the house was a major risk factor in conditional analysis, independent of house type. This result might be related to a finding from a study in India that bathing after work and changing clothes before sleep were protective measures (*25*). Traditional housing also might be more prone to rodent infestation than modern housing, which might increase the abundance of infected mites in the living area (*2*). Keeping wood logs against the house was a major risk factor in unconditional analysis, consistent with findings from a study in India (*25*) and possibly reflecting exposure while collecting wood or representing a suitable environment for rodents. Related findings from other studies include house yards without cement flooring (*13*) and poor sanitary conditions (*26*).

Frequently sitting or sleeping on grass was strongly associated with scrub typhus in both analyses, consistent with findings of previous studies (*2*). Owning a goat was a major risk factor identified in conditional analysis, but herding cattle in the forest was associated with a reduced risk. Other studies have found evidence of both scrub typhus seropositivity (*27*) and chigger infestation of goats (*28*). Thus, the association with owning a goat might be related to exposure to infected mites carried by goats or in

the goats' feeding environment. Given that goats are browsers and cattle are grazers, goat herders might have been more exposed to low-lying bushes, the preferred habitat of trombiculid mites, whereas cattle herders might have been more exposed to grassy patches in the forest that were clear of bushes, thus reducing their risk for scrub typhus.

Although wearing gumboots at work was associated with a reduced risk for scrub typhus in India (*25*), conditional analysis in our study found that sometimes wearing footwear outdoors was associated with a higher risk for scrub typhus than never wearing footwear outdoors. This paradoxical outcome might have been influenced by formulation

**Table 2.** Variables that had a $\chi^2$ p value ≤0.2 in conditional univariable analysis that were considered for the final multivariable model in a study of risk factors for clinical scrub typhus, Bhutan, 2015

| Variable* | Odds ratio | Wald p value | $\chi^2$ p value | Multivariable model |
|---|---|---|---|---|
| Demographic variables | | | | |
| Age (continuous) | 0.98 | 0.020 | 0.016 | † |
| Female sex (reference: male) | 0.59 | 0.059 | 0.057 | |
| Occupation (reference: farmer) | | | <0.001 | |
| Housewife | 0.32 | 0.086 | | |
| Civil servant/military | 0.31 | 0.209 | | |
| Corporate/private business | 0.86 | 0.848 | | |
| Preschool/student | 4.79 | 0.002 | | |
| Monk/nun | 6.09 | 0.145 | | |
| Construction worker | 0.26 | 0.235 | | |
| Rural residence (reference: urban) | 4.00 | 0.092 | 0.063 | |
| House-related variables | | | | |
| Traditional house (reference: modern) | 3.03 | 0.006 | 0.004 | † |
| Shower located outside (reference: inside) | 2.35 | 0.007 | 0.007 | † |
| Toilet located outside (reference: inside) | 5.21 | 0.032 | 0.011 | |
| Flooring of mud/clay (reference: no) | 2.08 | 0.079 | 0.075 | |
| Water supply from a stream (reference: no) | 4.59 | 0.070 | 0.053 | |
| Water supply community pipe (reference: no) | 0.54 | 0.150 | 0.149 | |
| Water supply private pipe (reference: no) | 1.77 | 0.162 | 0.159 | |
| Saw rodents in house (reference: no) | 3.02 | 0.017 | 0.009 | |
| Animal ownership | | | | |
| Possessed a cat (reference: no) | 1.53 | 0.171 | 0.168 | |
| Possessed poultry (reference: no) | 1.78 | 0.081 | 0.077 | |
| Possessed a goat (reference: no) | 2.77 | 0.023 | 0.019 | † |
| Protective measures | | | | |
| Wore footwear outdoors (reference: never) | | | 0.060 | † |
| Sometimes (occasionally and most of the time) | 5.55 | 0.047 | | |
| Always | 3.17 | 0.159 | | |
| Used insect repellent on clothes occasionally (reference: never) | 0.22 | 0.179 | 0.128 | |
| Bitten by ticks or fleas (reference: no) | 1.57 | 0.165 | 0.163 | |
| Cultivation-related exposures | | | | |
| Harvested cardamom (reference: no) | 4.15 | 0.007 | 0.004 | † |
| Harvested vegetables (reference: no) | 0.27 | 0.004 | 0.002 | † |
| Worked in vegetable garden (reference: no) | 0.42 | 0.009 | 0.006 | |
| Worked in mixed crop fields (reference: no) | 0.26 | 0.096 | 0.066 | |
| Worked in rice paddy (reference: no) | 1.79 | 0.194 | 0.189 | |
| Worked in an orchard (reference: no) | 2.15 | 0.124 | 0.120 | |
| Forest-related exposures | | | | |
| Household children <12 y of age played in the bush (reference: never) | | | 0.045 | |
| Occasionally | 8.04 | 0.214 | | |
| Daily | 4.07 | 0.302 | | |
| Did not have children <12 y of age | 1.28 | 0.842 | | |
| Collected forest products (reference: no) | 2.39 | 0.086 | 0.086 | |
| Visited forest for any reason (reference: no) | 1.71 | 0.096 | 0.089 | |
| Undertook reafforestation work (reference: no) | 2.64 | 0.122 | 0.110 | |
| Cleared scrub for others as a job (reference: no) | 1.63 | 0.125 | 0.123 | |
| Herded cattle in the forest (reference: no) | 0.47 | 0.080 | 0.068 | † |
| Other outdoor exposures | | | | |
| Sat or slept on grass (reference: never) | | | 0.053 | † |
| 1–5 times | 1.69 | 0.185 | | |
| 6–10 times | 2.74 | 0.066 | | |
| >10 times | 3.29 | 0.011 | | |

*Exposure variables related to a period of 1 mo before patients' recruitment at healthcare center.
†Significant (p≤0.05) in the multivariable model.

**Table 3.** Variables that had a $\chi^2$ p value ≤0.2 in unconditional univariable analysis that were considered for the final multivariable model in a study of risk factors for clinical scrub typhus, Bhutan, 2015

| Variable* | Odds ratio | Wald p value | $\chi^2$ p value | Multivariable model |
|---|---|---|---|---|
| Demographic variables | | | | |
| Age (continuous) | 0.98 | 0.032 | 0.028 | † |
| Occupation (reference: farmer) | | | 0.036 | |
| Housewife | 0.31 | 0.066 | | |
| Civil servant/military | 0.19 | 0.043 | | |
| Corporate/private business | 0.64 | 0.582 | | |
| Preschool/student | 1.48 | 0.387 | | |
| Other (monk/nun, construction) | 2.57 | 0.424 | | |
| Rural location (reference: urban) | 7.23 | <0.001 | <0.001 | |
| House-related variables | | | | |
| Traditional house (reference: modern) | 3.75 | 0.001 | <0.001 | |
| 2–3 floors in house (reference: 1 floor) | 0.40 | 0.017 | 0.015 | |
| Traditional toilet‡ (reference: modern) | 2.18 | 0.046 | 0.043 | † |
| Toilet located outside house§ (reference: inside) | 11.23 | <0.001 | <0.001 | |
| Toilet type (reference: modern inside) | | | <0.001 | |
| Modern outside | 11.57 | 0.002 | | |
| Traditional outside | 16.20 | <0.001 | | |
| Kept piles of wood (firewood, logs/timber, brush, and twigs) against the house wall (reference: no) | 1.88 | 0.078 | 0.076 | |
| Kept firewood against house wall (reference: no) | 1.85 | 0.100 | 0.098 | † |
| Kept logs/timber against house wall (reference: no) | 2.07 | 0.151 | 0.143 | |
| Kept wood in the yard (reference: no) | 0.48 | 0.047 | 0.045 | |
| Animal ownership | | | | |
| Possessed cattle (reference: no) | 0.44 | 0.023 | 0.021 | |
| Possessed poultry (reference: no) | 0.48 | 0.037 | 0.035 | |
| Protective measures | | | | |
| Worked outdoors in short sleeves (reference: never) | | | 0.035 | |
| Occasionally | 0.94 | 0.912 | | |
| Most of the time | 0.59 | 0.299 | | |
| Always | 2.71 | 0.091 | | |
| Worked in garden/fields with bare hands (reference: never) | | | 0.108 | † |
| Occasionally | 3.26 | 0.040 | | |
| Most of the time | 1.47 | 0.575 | | |
| Always | 0.95 | 0.911 | | |
| Changed working clothes to sleep (reference: never) | | | 0.119 | |
| Occasionally | 0.62 | 0.536 | | |
| Most of the time | 0.25 | 0.080 | | |
| Always | 0.60 | 0.499 | | |
| Frequency of showers (reference: never and weekly) | | | 0.120 | |
| 2–3 times/week | 0.47 | 0.069 | | |
| Every day | 0.48 | 0.104 | | |
| Cultivation-related exposures | | | | |
| Harvested cardamom (reference: no) | 7.11 | 0.013 | 0.003 | † |
| Worked in an orchard (reference: no) | 1.86 | 0.180 | 0.174 | |
| Cleared bushes for others as a job (reference: no) | 2.13 | 0.056 | 0.053 | † |
| Forest-related variables | | | | |
| Visited forest (Reference: no) | 2.26 | 0.023 | 0.022 | |
| Collected timber in the forest (reference: no) | 4.19 | 0.205 | 0.157 | |
| Collected nonwood products in forest (reference: no) | 2.90 | 0.129 | 0.109 | |
| Other outdoor exposures | | | | |
| Sat or slept on grass (reference: never) | | | 0.059 | † |
| 1– 6 times | 1.43 | 0.436 | | |
| 7–10 times | 1.67 | 0.392 | | |
| >10 times | 3.47 | 0.009 | | |

*Exposure variables related to a period of 1 mo before patients' recruitment at healthcare center.
†Significant (p≤0.05) in the multivariable model.
‡Traditional toilets are a pit latrine with wattle and daub walls or planks without continuous water supply. Modern toilets have an Indian or western pot type toilet with concrete or tiled walls and floor with a continuous water supply. Toilet type was considered regardless of location inside or outside the house.
§Considered location only, regardless of modern or traditional toilet type.

of the question (i.e., the reference category included persons who never worked outdoors, as well as persons who never wore footwear outdoors). Whereas the study from India (*25*) found no protective effect of wearing gloves while working outdoors, unconditional analysis in our study found that sometimes working outdoors with bare hands was associated with a higher risk than never working outdoors with

**Table 4.** Significant variables in best-fitting model for conditional multivariable analysis of laboratory-confirmed clinical case-patients who had scrub typhus and matched controls, Bhutan, 2015*

| Variable† | OR (95% CI) | p value |
|---|---|---|
| Age (order 1 term) | NA | 0.001 |
| Age (quadratic age) | NA | 0.007 |
| Female (reference: male) | 0.19 (0.05–0.67) | 0.010 |
| Traditional house type‡ (reference: modern) | 472.30 (17.28–12,900.00) | <0.001 |
| Shower located outside house (reference: inside) | 6.21 (1.28–30.00) | 0.023 |
| Sat or slept on grass (reference: never) | | |
| 1–10 times | 1.81 (0.51–6.5) | 0.360 |
| >10 times | 16.38 (1.68–160.05) | 0.016 |
| Wore footwear outdoors (reference: never) | | |
| Sometimes | 9.25 (1.09–78.37) | 0.041 |
| Always | 0.88 (0.12–6.31) | 0.898 |
| Herded cattle in the forest (reference: no) | 0.06 (0.01–0.52) | 0.010 |
| Possessed a goat (reference: no) | 36.52 (3.59–371.91) | 0.002 |
| Harvested vegetables (reference: no) | 0.03 (0.00–0.28) | 0.002 |
| Harvested cardamom (reference: no) | 1,519.00 (26.23–88,005.98) | <0.001 |

*NA, not applicable; OR, odds ratio.
†Exposure variables related to a period of 1 mo before patients' recruitment at healthcare center.
‡Traditional Bhutanese houses are commonly 2-storied structures made from wood and earthen material, namely wattle and daub interior walls, with stone and earth retaining walls and wooden plank roofing. Modern houses are generally multistoried structures made of concrete materials, such as bricks, cement, and iron rods with minimal use of wooden frames for windows and flooring with zinc sheet roofing.

bare hands. However, this result might not reflect a real protective effect of covering hands because it might also have been influenced by the reference category including persons who never worked outdoors and persons who never worked outdoors with bare hands.

In both analyses, we found a significant nonlinear effect of age; the risk for scrub typhus was higher for young children and the elderly, suggesting an increased exposure to infected mites in these age groups through age-related behaviors, or, alternatively, that the young or elderly are more susceptible to developing clinical scrub typhus. A study in India highlighted the usefulness of including scrub typhus in the differential diagnosis of pyrexia of unknown origin in children unresponsive to treatment with common antimicrobial drugs (*9*). The conditional analysis also indicated that female study participants had a lower risk for scrub typhus, consistent with a sex effect observed in China (*13*). This finding might reflect less frequent involvement in outdoor activities compared with men and boys, reducing risk for exposure to mites.

The findings of this study are relevant for patients who have clinical scrub typhus and visited a healthcare center during the later months (October–December) of the risk period for this disease. Thus, these persons might underrepresent the strength of risk or the full extent of risk factors associated with *O. tsutsugamushi* infection throughout the July–November risk period. Also, our study did not include infected persons who did not visit a healthcare center (*2*).

The RDT used to recruit case-patients who had scrub typhus has been reported to have a low sensitivity of 38% (95% CI 28%–49%) (*14*). This test detects IgG, IgM, and IgA against *O. tsutsugamushi* , so it might detect historical as well as active scrub typhus cases (*14*), resulting in persons who have historical infections to be included as provisional case-patients. The in-series ELISA targeting IgM would have increased

**Table 5.** Significant variables in best-fitting model for unconditional multivariable analysis of laboratory-confirmed clinical case-patients who had scrub typhus and matched controls, Bhutan, 2015*

| Variable† | OR (95% CI) | p value |
|---|---|---|
| Age (order 1 term) | NA | 0.001 |
| Age (quadratic term) | NA | 0.023 |
| Toilet outside the house (reference: toilet inside) | 10.65 (2.37–47.84) | 0.002 |
| Kept logs of wood against the wall (reference: no) | 4.17 (1.18–14.71) | 0.027 |
| Sat or slept on grass (reference: never) | | |
| 1–10 times | 2.08 (0.69–6.31) | 0.195 |
| >10 times | 6.06 (1.56–23.59) | 0.009 |
| Cleared bushes for others as a job (reference: no) | 4.71 (1.61–13.82) | 0.005 |
| Worked outdoors (garden/fields) with bare hands (reference: never) | | |
| Sometimes | 4.18 (1.03–17.01) | 0.045 |
| Always | 0.87 (0.26–2.90) | 0.824 |
| Harvested cardamom (reference: no) | 5.98 (0.86–41.46) | 0.070 |

*NA, not applicable; OR, odds ratio.
†Exposure variables related to a period of 1 mo before patients' recruitment at healthcare center.

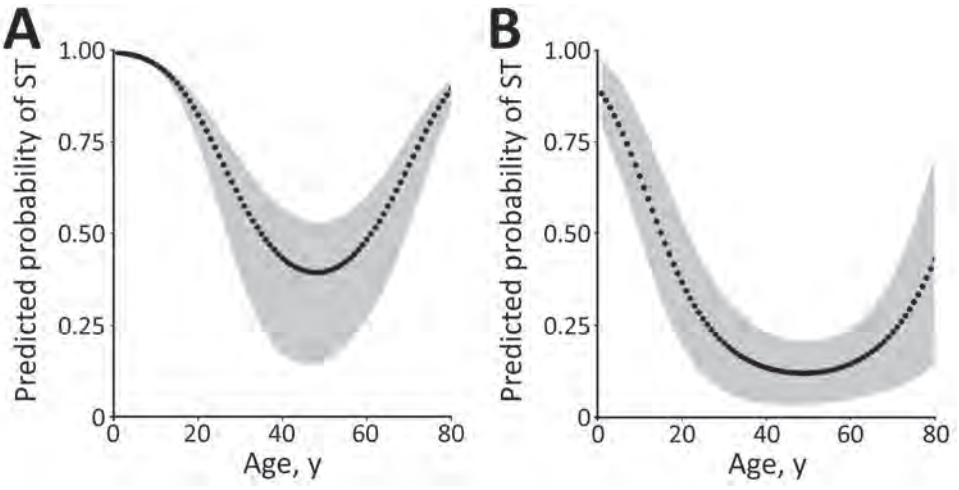


**Figure 4.** Effect of age on the probability of presenting to hospitals with a clinical case of ST in a group of matched cases and controls (A) and a second group of unmatched cases and controls (B), Bhutan, 2015. Gray areas indicate 95% CI.
ST, scrub typhus.

the classification accuracy of the case-patient and control groups, given the high sensitivity (99.9%, 95% CI 90.4–100.0) and specificity (99.1%, 95% CI 96.8%–99.8%) reported for that test (*14*). Any remaining misclassification in case-patient or control groups would contribute to biasing the results toward the null, but that did not preclude the study from identifying major risk factors.

In this study, we compared case-patients with a group of controls matched by village and a group of unmatched controls. Matching increased the probability that case-patients and controls had the same potential exposure to infected chiggers in the vicinity of their residential environment, enabling investigation of individual and household-related risk factors. The unmatched controls enabled an investigation of variables that might be spatially correlated, such as rural versus urban location and possibly occupation. Although conditional and unconditional analyses identified age, traditional house type or toilet location, harvesting cardamom, and sitting on the grass as risk factors, conditional analysis produced much larger ORs for most variables and identified additional risk factors: owning a goat, being female, harvesting vegetables, and herding cattle in the forest. Distribution and density of mites is known to vary throughout an area (*2*), which might have affected the power of the unmatched analysis. Case-patients and unmatched controls might not have had the same exposure to infected mites; thus, unmatched controls might have had similar recreational and occupational factors as case-patients but in environments where there were no infected mites.

This study has contributed major public health benefits by providing strong evidence for occupational, environmental, and demographic risk factors that can support early diagnosis and treatment for scrub typhus, reducing the incidence of complications and deaths. Many health workers were not aware of scrub typhus, and study findings contributed to public health policy and awareness raising among clinicians, particularly in areas with a high disk for this disease.

Recommendations from this study were made to the Department of Public Health and contributed to new National Guidelines for Prevention, Treatment and Control of Scrub Typhus in Bhutan. The findings of this study could also be useful for improving awareness, and early diagnosis and treatment in nearby countries in regions where scrub typhus is also an emerging disease of concern.

### Acknowledgments

We thank study participants for their cooperation, district health workers involved in disease reporting, enrolling study participants and questionnaire administration, and the laboratory officers of Royal Center for Disease Control for conducting confirmatory tests on study samples.

This study was supported by the European Union through the One Health Program in Asia (EuropeAid/133708/C/ACT/Multi; Contract DCI-ASIE/2013/331-217). The program was implemented by Massey University in collaboration with Khesar Gyalpo University of Medical Sciences of Bhutan and the Royal University of Bhutan.

### About the Author

Dr. Zangpo is a medical officer on special assignment at the National TB Control Program and National HIV/AIDS Control Program, in the Communicable Diseases Division, Department of Public Health, Ministry of Health, Thimphu, Bhutan. His primary research interests are One Health, zoonoses, emerging and reemerging infectious diseases, tuberculosis, malaria, neglected tropical diseases, and public health emergencies and responses.

## References


1. Yang HH, Huang IT, Lin CH, Chen TY, Chen LK. New genotypes of *Orientia tsutsugamushi* isolated from humans in eastern Taiwan. PLoS One. 2012;7:e46997. https://doi.org/10.1371/journal.pone.0046997
2. Elliott I, Pearson I, Dahal P, Thomas NV, Roberts T, Newton PN. Scrub typhus ecology: a systematic review of *Orientia* in vectors and hosts. Parasit Vectors. 2019;12:513. https://doi.org/10.1186/s13071-019-3751-x
3. Wei Y, Huang Y, Luo L, Xiao X, Liu L, Yang Z. Rapid increase of scrub typhus: an epidemiology and spatial-temporal cluster analysis in Guangzhou City, southern China, 2006–2012. PLoS One. 2014;9:e101976. https://doi.org/10.1371/journal.pone.0101976
4. Xu G, Walker DH, Jupiter D, Melby PC, Arcari CM. A review of the global epidemiology of scrub typhus. PLoS Negl Trop Dis.2017;11:e0006062. https://doi.org/10.1371/journal.pntd.0006062
5. Maude RR, Maude RJ, Ghose A, Amin MR, Islam MB, Ali M, et al. Serosurveillance of *Orientia tsutsugamushi* and *Rickettsia typhi* in Bangladesh. Am J Trop Med Hyg. 2014;91:580–3. https://doi.org/10.4269/ajtmh.13-0570
6. Zhang L, Zhao Z, Bi Z, Kou Z, Zhang M, Yang L, et al. Risk factors associated with severe scrub typhus in Shandong, northern China. Int J Infect Dis. 2014;29:203–7. https://doi.org/10.1016/j.ijid.2014.09.019
7. Sethi S, Prasad A, Biswal M, Hallur VK, Mewara A, Gupta N, et al. Outbreak of scrub typhus in north India: a re-emerging epidemic. Trop Doct. 2014;44:156–9. https://doi.org/10.1177/0049475514523761
8. Sinha P, Gupta S, Dawra R, Rijhawan P. Recent outbreak of scrub typhus in north western part of India. Indian J Med Microbiol. 2014;32:247–50. https://doi.org/10.4103/0255-0857.136552
9. Yadav D, Chopra A, Dutta AK, Kumar S, Kumar V. Scrub typhus: an uncommon cause of pyrexia without focus. J Nepal Paediatr Soc. 2013;33:234–5. https://doi.org/10.3126/jnps.v33i3.8172
10. Dorji T, Wangchuk S, Lhazeen K. Clinical characteristics of scrub typhus in Gedu and Mongar (Bhutan); 2010 [cited 2018 Apr 4]. http://www.rcdc.gov.bt/web/wp-content/uploads/2012/07/Scrub-Typhus-in-Gedu-and-Mongar.pdf
11. Dorji K, Phuentshok Y, Zangpo T, Dorjee S, Dorjee C, Jolly P, et al. Clinical and epidemiological patterns of scrub typhus, an emerging disease in Bhutan. Trop Med Infect Dis. 2019;4:56. https://doi.org/10.3390/tropicalmed4020056
12. le Cessie S, Nagelkerke N, Rosendaal FR, van Stralen KJ, Pomp ER, van Houwelingen HC. Combining matched and unmatched control groups in case-control studies. Am J Epidemiol.2008; 168:1204–10. https://doi.org/10.1093/aje/kwn236
13. Lyu Y, Tian L, Zhang L, Dou X, Wang X, Li W, et al. A case–control study of risk factors associated with scrub typhus infection in Beijing, China. PLoS One. 2013;8:e63668. https://doi.org/10.1371/journal.pone.0063668
14. Pote K, Narang R, Deshmukh P. Diagnostic performance of serological tests to detect antibodies against acute scrub typhus infection in central India. Indian J Med Microbiol. 2018;36:108–12. https://doi.org/10.4103/ijmm.IJMM_17_405
15. Blacksell SD, Tanganuchitcharnchai A, Nawtaisong P, Kantipong P, Laongnualpanich A, Day NP, et al. Diagnostic accuracy of the InBios Scrub Typhus Detect Enzyme-Linked Immunoassay for the detection of IgM antibodies in northern Thailand. Clin Vaccine Immunol. 2015;23:148–54. https://doi.org/10.1128/CVI.00553-15
16. Gupta N, Chaudhry R, Thakur CK. Determination of cutoff of ELISA and immunofluorescence assay for scrub typhus. J Glob Infect Dis. 2016;8:97–9. https://doi.org/10.4103/0974-777X.188584
17. Rahi M, Gupte MD, Bhargava A, Varghese GM, Arora R. DHR-ICMR Guidelines for diagnosis and management of rickettsial diseases in India. Indian J Med Res. 2015;141:417–22. https://doi.org/10.4103/0971-5916.159279
18. Mørch K, Manoharan A, Chandy S, Chacko N, Alvarez-Uria G, Patil S, et al. Acute undifferentiated fever in India: a multicentre study of aetiology and diagnostic accuracy. BMC Infect Dis. 2017;17:665. https://doi.org/10.1186/s12879-017-2764-3
19. Pulami TM. Value chain development and technology of large cardamom and ginger in Bhutan. In: Pandey PR, Pandey IR, editors. Challenges and opportunities in value chain of spices in south Asia. Dhaka (Bangladesh): SAARC Agriculture Centre, Indian Institute of Spices Research; 2017. p. 38–55.
20. Ogawa M, Hagiwara T, Kishimoto T, Shiga S, Yoshida Y, Furuya Y, et al. Scrub typhus in Japan: epidemiology and clinical features of cases reported in 1998. Am J Trop Med Hyg. 2002;67:162–5. https://doi.org/10.4269/ajtmh.2002.67.162
21. Thomas L, Bhat A, Cheriyan H, Nirmal Babu K. Value chain development and technology practices of spices crop in India (cardamom, ginger, turmeric, black pepper and cinnamon). In: Pandey PR, Pandey IR, editors. Challenges and opportunities in value chain of spices in south Asia. Dhaka (Bangladesh): SAARC Agriculture Centre, Indian Institute of Spices Research; 2017. p. 56–115.
22. Ansari A. Value chain development and technology practices of spice crop (cardamom (small and large), ginger, turmeric, black pepper, and cinnamon) in Nepal. In: Pandey PR, Pandey IR, editors. Challenges and opportunities in value chain of spices in south Asia. Dhaka (Bangladesh): SAARC Agriculture Centre, Indian Institute of Spices Research; 2017. p. 116–135.
23. Mina SS, Kumar V, Chhapola V. Emerging infections in children in north India: scrub typhus. J Pediatr Infect Dis. 2017;12:114–8. https://doi.org/10.1055/s-0037-1599835
24. Upadhyaya BP, Shakya G, Adhikari S, Rijal N, Acharya J, Maharjan L, et al. Scrub typhus: an emerging neglected tropical disease in Nepal. J Nepal Health Res Counc. 2016;14:122–7.
25. Sharma PK, Ramakrishnan R, Hutin YJ, Barui AK, Manickam P, Kakkar M, et al. Scrub typhus in Darjeeling, India: opportunities for simple, practical prevention measures. Trans R Soc Trop Med Hyg. 2009;103:1153–8. https://doi.org/10.1016/j.trstmh.2009.02.006
26. Vallée J, Thaojaikong T, Moore CE, Phetsouvanh R, Richards AL, Souris M, et al. Contrasting spatial distribution and risk factors for past infection with scrub typhus and murine typhus in Vientiane City, Lao PDR. PLoS Negl Trop Dis. 2010; 4:e909. https://doi.org/10.1371/journal.pntd.0000909
27. Thiga JW, Mutai BK, Eyako WK, Ng'ang'a Z, Jiang J, Richards AL, et al. High seroprevalence of antibodies against spotted fever and scrub typhus bacteria in patients with febrile illness, Kenya. Emerg Infect Dis. 2015;21:688–91. https://doi.org/10.3201/eid2104.141387
28. Faccini JL, Santos AC, Santos SB, Jacinavicius FC, Bassini-Silva R, Barros-Battesti DM. Trombiculiasis in domestic goats and humans in the state of Maranhão, Brazil. Rev Bras Parasitol Vet. 2017;26:104–9. https://doi.org/10.1590/s1984-29612016088


Address for correspondence: Tandin Zangpo, Communicable Disease Division, Department of Public Health, Ministry of Health, Thimphu, Bhutan; email: tzangpo@health.gov.bt

# Misdiagnosis of *Clostridioides difficile* Infections by Standard-of-Care Specimen Collection and Testing among Hospitalized Adults, Louisville, Kentucky, USA, 2019–2020[1]

Julio A. Ramirez,[2] Frederick J. Angulo, Ruth M. Carrico,[2] Stephen Furmanek,[2] Senén Peña Oliva, Joann M. Zamparo, Elisa Gonzalez, Pingping Zhang, Leslie A. Wolf Parrish, Subathra Marimuthu, Michael W. Pride, Sharon Gray, Cátia S. Matos Ferreira,[3] Forest W. Arnold, Raul E. Istúriz, Nadia Minarovic, Jennifer C. Moïsi, Luis Jodar

Although *Clostridioides difficile* infection (CDI) incidence is high in the United States, standard-of-care (SOC) stool collection and testing practices might result in incidence overestimation or underestimation. We conducted diarrhea surveillance among inpatients ≥50 years of age in Louisville, Kentucky, USA, during October 14, 2019–October 13, 2020; concurrent SOC stool collection and CDI testing occurred independently. A study CDI case was nucleic acid amplification test–/cytotoxicity neutralization assay–positive or nucleic acid amplification test–positive stool in a patient with pseudomembranous colitis. Study incidence was adjusted for hospitalization share and specimen collection rate and, in a sensitivity analysis, for diarrhea cases without study testing. SOC hospitalized CDI incidence was 121/100,000 population/year; study incidence was 154/100,000 population/year and, in sensitivity analysis, 202/100,000 population/year. Of 75 SOC CDI cases, 12 (16.0%) were not study diagnosed; of 109 study CDI cases, 44 (40.4%) were not SOC diagnosed. CDI incidence estimates based on SOC CDI testing are probably underestimated.

*Clostridioides difficile* infection (CDI) is a major cause of illness and death worldwide (*1*,*2*). The Centers for Disease Control and Prevention (CDC) classifies CDI as an urgent public health threat (*3*). In the CDC Emerging Infections Program (EIP), the CDI incidence in persons ≥50 years of age was 255/100,000 population in 2019, and the hospitalized CDI incidence in this age group was 140/100,000 population (*4*).

CDI incidence estimates derived from public health surveillance rely on standard-of-care (SOC) stool specimen collection and CDI testing practices. Laboratory testing using only a PCR nucleic acid amplification test (NAAT), which tests for the presence of the toxin gene without testing for the presence of free toxin, might misdiagnose a patient with *C. difficile* carriage as a CDI case-patient and thereby result in overestimation of the CDI incidence (*5*,*6*). NAAT-alone testing is commonly used by the laboratories in the EIP surveillance sites (*4*); 47% of CDI cases identified in 2017 were diagnosed by a laboratory that used NAAT-alone testing (*7*). Conversely, SOC practices might fail to collect or appropriately test a stool specimen from a person with diarrhea and thereby underdiagnose CDI, which will result in underestimation of CDI incidence (*8*–*11*).

Author affiliations: University of Louisville, Louisville, Kentucky, USA (J.A. Ramirez, R.M. Carrico, S. Furmanek, S. Peña Oliva, L.A. Wolf Parrish, S. Marimuthu, F.W. Arnold); Pfizer Vaccines, Collegeville, Pennsylvania, USA (F.J. Angulo, J.M. Zamparo, E. Gonzalez, P. Zhang, S. Gray, C.S. Matos Ferreira, R.E. Istúriz, N. Minarovic, J.C. Moïsi, L. Jodar); Pfizer, Pearl River, New York, USA (M.W. Pride)

DOI: https://doi.org/10.3201/eid2905.221618

[1]Study results were presented at the annual Anaerobe 2022 Congress, July 28–31, 2022, Seattle, Washington, USA.

[2]Current affiliation: Norton Healthcare, Louisville, Kentucky, USA.

[3]Current affiliation: AstraZeneca Pharmaceuticals, Wilmington, Delaware, USA.

Incidence estimates are essential for evaluating the need for public health interventions aimed at reducing the CDI burden. We conducted a population-based study to determine CDI incidence and to evaluate the potential effect of misdiagnosis caused by SOC specimen collection and testing practices on CDI incidence estimates in Louisville, Kentucky, USA.

## Methods

### Study Design, Population, and Setting

Study staff conducted daily, prospective, active surveillance for incident diarrhea cases (≥3 stools with Bristol scale ≥5 in previous 24 hours) among eligible inpatients (Louisville residents ≥50 years of age) by visiting inpatients, reviewing medical charts, and meeting with nursing staff. Surveillance was conducted on all 119 wards (including 26 intensive care units [ICUs]) at 8 of 9 Louisville adult hospitals from October 14, 2019, through October 13, 2020, with a surveillance pause during April 12, 2020–August 16, 2020 because of hospital restrictions enacted in response to COVID-19. Participating hospitals had 84.4% (2,596/3,077) of the Louisville adult hospital beds. Population demographics of Louisville and the United States are similar (*12*).

### Study and SOC-Related Procedures

All eligible inpatients with incident diarrhea were invited to participate in the study. After written informed consent was obtained, a study stool specimen was collected by study staff from inpatients with diarrhea and screened by using C. Diff Quik Chek Complete , a rapid, membrane, enzyme-linked immunosorbent assay (Alere Techlab, https://www.techlab.com) (*13*). Before the COVID-19 pause, study stool specimens that were glutamate dehydrogenase (GDH)–positive or GDH-negative/toxin-positive were sent to the Pfizer laboratory in Pearl River, New York, USA, for NAAT and, if NAAT positive, for automated cell cytotoxicity neutralization assay (CCNA) testing. CCNA testing at the Pfizer laboratory has been validated to provide specific, sensitive, and reproducible results to support CDI clinical and epidemiology studies (*14*).

After the pause, all study specimens were tested by Quik Chek and sent to the Pfizer laboratory for NAAT and CCNA testing. Shipped specimens were frozen on dry ice (replenished daily) and stored, upon receipt, in −80°C freezers. Throughout the study, patients with GDH-positive or GDH-negative/toxin-positive specimens were followed up by study staff for 90 days to determine outcomes, and SOC stool specimen collection by hospital staff occurred in parallel and independent of study procedures. For SOC CDI testing at the 8 participating hospitals, 2 used Quik Chek only, 5 used Quik Chek with NAAT of Quik Chek discordant specimens (but during the study, 1 changed to NAAT-alone testing and 1 to NAAT with toxin enzyme-linked immunosorbent assay testing of NAAT-positive), and 1 used NAAT-alone testing. Actual SOC test results (i.e., NAAT-positive or NAAT-negative) were provided to clinicians. For our analysis, we defined NAAT-positive/toxin-negative as SOC *C. difficile* carriage.

### Study Case Definition and Classification

A study CDI case-patient was a patient who had a NAAT-positive/CCNA-positive specimen or a patient who had a NAAT-positive specimen and pseudomembranous colitis (PMC). A CDI recurrent case was the occurrence of diarrhea ≤56 days after resolution of a previous case of diarrhea. A primary CDI case was a nonrecurrent CDI case. CDI in hospitalized case-patients was classified as hospital-onset (i.e., positive stool specimen collected >3 days after admission), community-onset (i.e., positive stool specimen collected in an outpatient setting or ≤3 days after admission), healthcare-associated (i.e., positive stool specimen in a person with hospital-onset or in a person with community-onset with a documented overnight stay in the 12 weeks before stool specimen collection), or community-associated (i.e., positive stool specimen in a person with community-onset with no documented overnight stay before the current admission in the 12 weeks before stool specimen collection) (*15*).

### Comparisons among Study and SOC Inpatients with Diarrhea

We reviewed medical records to compare the characteristics of inpatients with diarrhea who were enrolled and not enrolled in the study and to compare the characteristics of enrolled inpatients with diarrhea who had and did not have a study CDI test. We used $\chi^2$ tests (for categorical or binary variables) and t-tests (for continuous variables) to evaluate differences between the groups by using SAS Studio 3.71 (https://www.sas.com).

We compared laboratory results of study and SOC specimens collected from inpatients with diarrhea to determine the frequency of discordant results indicating SOC laboratory testing CDI overdiagnosis or underdiagnosis compared with study testing. We used laboratory results of specimens from inpatients with diarrhea who had a study specimen tested but did not have a SOC specimen collected to determine

the frequency of SOC CDI underdiagnosis caused by lack of SOC specimen collection. We compared laboratory results of specimens collected after the pause from inpatients with diarrhea who had a study specimen screened by GDH and tested by NAAT to determine the negative predictive value (NPV) of the GDH test compared with the NAAT.

### Estimation of Population-Based Hospitalized CDI Incidence

We estimated population-based hospitalized CDI incidence among Louisville residents ≥50 years of age (n = 276,456), ≥65 years of age (n = 127,864), and ≥75 years of age (n = 51,509) after adjusting the number of study CDI cases for the percentage of Louisville adult hospital beds that were present in the nonparticipating hospital (multiplying by the inverse of the percentage of Louisville beds in participating hospitals [84.4%]) and for the percentage of inpatients with diarrhea who did not have a study specimen collected (multiplying by the inverse of percentage of participants with specimen collected [67.9%]). In a sensitivity analysis, we adjusted further the number of study CDI cases for specimens that were NAAT positive but with quantity not sufficient (QNS) for CCNA testing (multiplying by the inverse of the percentage of NAAT positive with CCNA testing [93.3%]) and, using the NPV of the GDH test compared with NAAT, for specimens that were not tested by NAAT (multiplying by the inverse of NPV [93.8%]).

### Ethics

This study was approved by the institutional review boards at each hospital. It was also conducted in accordance with the study protocol.

## Results

### Study and SOC Incident CDI Cases

Study staff identified 1,541 incident diarrhea cases among 85,719 patient-days before the COVID-19 pause (Figure 1). SOC specimens were collected from 680 inpatients with diarrhea, for a SOC CDI testing density of 79.3/10,000 patient-days. Study specimens were collected from 1,047 (67.9%) inpatients with diarrhea, for a study CDI testing density of 122.1/10,000 patient-days; the study enrollment rate was 83.3% (1,283/1,541) and the specimen collection rate among enrolled participants was 81.6% (1,047/1,283) (Table 1). Patient transfer or discharge was the main reason that a specimen was not collected from all enrolled participants. Study staff identified 319 incident diarrhea cases among 27,373 patient-days after the COVID-19 pause. After the pause, study specimens were collected from 144 inpatients with diarrhea for a study CDI testing density of 52.6/10,000 patient-days; the study enrollment rate was 59.6% (190/319), and the specimen collection rate was 75.8% (144/190) (Figure 2).

Before the pause, 222 specimens were sent to the Pfizer laboratory after Quik Chek testing (74 GDH-positive/toxin-positive, 146 GDH-positive/toxin-negative, and 2 GDH-negative/toxin-positive); 163 (74.8%) were NAAT-positive. Of the NAAT-positive specimens, 103 (63.2%) were CCNA-positive, 49 (30.1%) were CCNA-negative, and 11 (6.7%) were QNS for CCNA testing. Of 103 NAAT-positive/CCNA-positive cases, 99 (96.1%) were primary CDI cases, and of the 49 NAAT-positive/CCNA-negative cases, 10 (20.4%) were primary CDI cases (7 had PMC and 3 had a specimen collected during the 90-day follow-up period that was NAAT-positive/CCNA-positive), for a total of 109 study-identified primary CDI cases. Before the pause, SOC testing identified 128 CDI cases, of which 126 were primary CDI cases (15 were identified by NAAT alone). After the pause, study testing identified 10 primary CDI cases, and SOC testing identified 22 primary CDI cases.

### CDI Misdiagnosis by SOC

An SOC specimen and a study specimen were collected and tested from 145 cases before the pause, of which 7 were recurrent CDI cases, yielding 138 for the evaluation of SOC misdiagnosis; of those cases, 75 (54.3%) were SOC primary CDI cases and 79 (57.2%) were study primary CDI cases (Table 2). Of 75 SOC primary CDI cases, 12 (16.0%) were not study-diagnosed as CDI cases; 6 NAAT-positive/CCNA-negative (SOC testing: 3 GDH-positive/toxin-positive/NAAT-positive and 3 NAAT-positive/toxin-positive) and 6 NAAT-negative (SOC testing: 3 GDH-positive/toxin-positive/NAAT-positive and 3 GDH-positive/toxin-positive). Of 79 study primary CDI cases, 16 (20.3%) were not SOC-diagnosed as CDI cases; SOC test results for those 16 were 13 NAAT-positive/toxin-negative, 2 NAAT-negative, and 1 GDH-negative/toxin-negative. In addition, 70 case-patients before the pause had a study specimen tested but without a SOC specimen collected; of those, 28 were study primary CDI case-patients. Therefore, 44 study-diagnosed primary CDI cases were not SOC diagnosed: 16 (36.4%) SOC-undiagnosed after SOC testing and 28 (63.6%) SOC-undiagnosed because of lack of specimen collection. Of 28 study-diagnosed CDI case-patients who were not SOC diagnosed because of lack of specimen collection, 11 (39.3%) were taking laxatives.

### Characteristics of Inpatients with Study-Diagnosed and SOC-Diagnosed CDI

The median age of the 109 study inpatients with primary CDI identified before the pause was 72 (range 50–98) years. A total of 63 (57.8%) were women. Based on the diarrhea onset date, 23 (21.1%) were community-onset and community associated and 86 (78.9%) were healthcare associated; of the healthcare-associated cases, 55 (64.0%) were community-onset and 31 (36.0%) were hospital-onset. Of the 109 study patients with primary CDI, 18 (16.5%) had PMC, 36 (33.0%) were admitted to an ICU, and 21 (19.3%) died within 90 days of CDI diagnosis. The median patient age among the CDI cases who died was 78 (range 56–95) years.

Characteristics of 44 study-diagnosed but SOC-undiagnosed inpatients who had primary CDI before the pause and the 126 SOC-diagnosed inpatients who had primary CDI before the pause were similar except that the SOC-undiagnosed inpatients who had CDI were more likely to be hospital-onset CDI case-patients and less likely to have

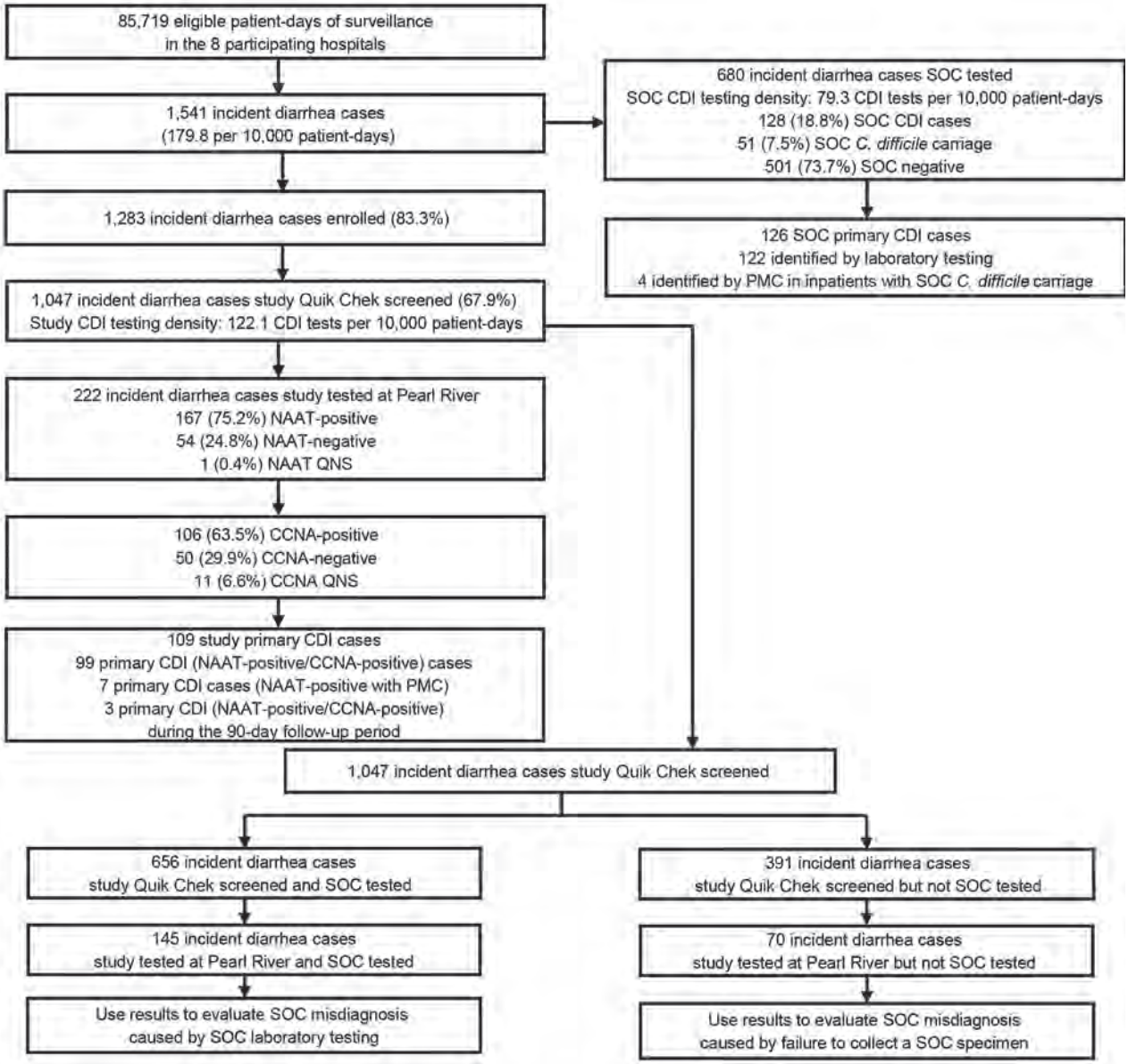


**Figure 1.** Incident diarrhea cases and testing of stool specimens among inpatients ≥50 years of age in Louisville, Kentucky, USA, before the COVID-19 pause in study of misdiagnosis of CDI by SOC specimen collection and testing among hospitalized adults, October 14, 2019–April 11, 2020. CCNA, cell culture cytotoxicity neutralization assay; CDI, *Clostridioides difficile* infection; NAAT, nucleic acid amplification test; PMC, pseudomembranous colitis; QNS, quantity not sufficient; Quik Chek, C. Diff Quik Chek Complete (Alere Techlab, https://www.techlab.com); SOC, standard-of-care.

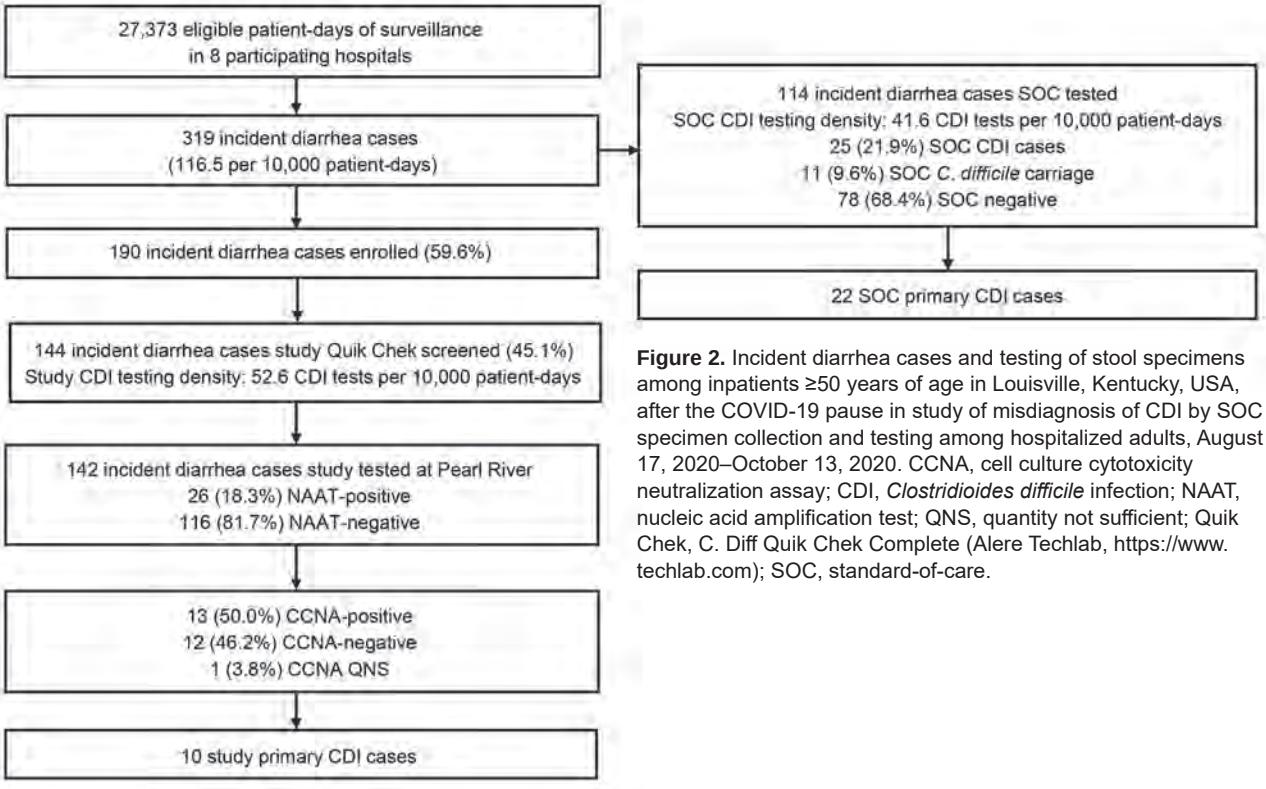


**Figure 2.** Incident diarrhea cases and testing of stool specimens among inpatients ≥50 years of age in Louisville, Kentucky, USA, after the COVID-19 pause in study of misdiagnosis of CDI by SOC specimen collection and testing among hospitalized adults, August 17, 2020–October 13, 2020. CCNA, cell culture cytotoxicity neutralization assay; CDI, *Clostridioides difficile* infection; NAAT, nucleic acid amplification test; QNS, quantity not sufficient; Quik Chek, C. Diff Quik Chek Complete (Alere Techlab, https://www.techlab.com); SOC, standard-of-care.

PMC (Table 3). Of the 19 study-diagnosed but SOC-undiagnosed hospital-onset CDI cases, 16 (84%) were SOC-undiagnosed because an SOC specimen was not collected. On the basis of the 109 study-diagnosed primary CDI cases before the pause, SOC practices underdiagnosed 40.4% (44/109) of the study-diagnosed primary CDI cases. Because SOC overdiagnosed 16.0% of the study-diagnosed primary CDI cases and underdiagnosed 40.4% of study-diagnosed primary CDI cases, SOC testing identified 24.4% fewer primary CDI cases than did the study.

After the pause, study specimens from 142 cases were screened by Quik Chek and tested by NAAT; of the 113 GDH-negative/toxin-negative specimens, 106 (93.8%) were NAAT-negative. Therefore, the NPV of the Quik Chek GDH test compared with NAAT was 93.8%, indicating that an estimated 6.2% of NAAT-positive specimens might have been missed because of the screening used during the pre–COVID-19 period.

**Table 1.** Hospital-based incidence of diarrhea, enrollment rates, stool collection rate, and CDI testing density in participating hospitals before the COVID-19 pause in study of misdiagnosis of CDI by SOC specimen collection and testing among hospitalized adults, Louisville, Kentucky, USA, October 14, 2019–April 11, 2020*

| Hospital† | No. adult hospital beds | Surveillance initiation date, 2019 | No. eligible patient-days of surveillance | No. incident diarrhea cases identified | Diarrhea incidence‡ | No. (%) incident diarrhea cases enrolled | No. (%) study stool specimens collected from enrolled cases | Study CDI stool specimen testing rate, % | Study CDI testing density§ |
|---|---|---|---|---|---|---|---|---|---|
| A | 671 | Oct 14 | 19,166 | 195 | 101.7 | 163 (83.6) | 123 (75.5) | 63.1 | 64.2 |
| B | 377 | Oct 14 | 16,252 | 328 | 201.8 | 282 (86.0) | 259 (91.8) | 79.0 | 159.4 |
| C | 367 | Oct 14 | 11,658 | 247 | 211.9 | 208 (84.2) | 183 (88.0) | 74.1 | 157.0 |
| D | 348 | Oct 14 | 8,723 | 143 | 163.9 | 122 (85.3) | 98 (80.3) | 68.5 | 112.3 |
| E | 336 | Nov 4 | 11817 | 281 | 237.8 | 218 (77.6) | 133 (61.0) | 47.3 | 112.5 |
| F | 200 | Dec 23 | 4,256 | 41 | 96.3 | 32 (78.0) | 21 (65.6) | 51.2 | 49.3 |
| G | 170 | Nov 4 | 5,754 | 146 | 253.7 | 120 (82.2) | 98 (81.7) | 67.1 | 170.3 |
| H | 127 | Oct 14 | 8,093 | 160 | 197.7 | 138 (86.3) | 132 (95.7) | 82.5 | 163.1 |
| Total | 2,596 | Oct 14–Dec 23 | 85,719 | 1,541 | 179.8 | 1,283 (83.3) | 1,047 (81.6) | 67.9 | 122.1 |

*CDI, *Clostridioides difficile* infection; SOC, standard-of-care.
†Participating hospitals are listed in descending order of the number of adult hospital beds.
‡Cases per 10,000 patient-days.
§Tests per 10,000 patient-days.

**Table 2.** SOC misdiagnosis caused by SOC laboratory testing after excluding recurrent CDI cases in study of misdiagnosis of CDI by SOC specimen collection and testing among hospitalized adults, Louisville, Kentucky, USA, October 14, 2019–April 11, 2020*

| SOC CDI test results | No. study primary CDI cases | No. not study primary CDI cases | Total |
|---|---|---|---|
| SOC primary CDI cases | 63 | 12 | 75 |
| SOC *C. difficile* carriage | 13 | 17 | 30 |
| Not SOC primary CDI cases | 3 | 30 | 33 |
| Total | 79 | 59 | 138 |

*CDI, *Clostridioides difficile* infection; SOC, standard-of-care.

### Comparisons among Study and SOC Inpatients with Diarrhea

A review of the medical records of inpatients with diarrhea before the pause (Table 4) indicated that patients who were enrolled and those not enrolled had similar demographics and medical histories, except enrolled patients were more likely to be women and less likely to die in the 90 days after diarrhea onset. Among diarrhea case-patients who were enrolled (Table 5), patients with and without a stool specimen collected for CDI testing had similar demographics and medical histories, except that those who had a stool specimen collected were less likely to be Black and more likely to have taken antimicrobial drugs in the previous 3 months.

### Population-Based Hospitalized CDI Incidence

The study incidence was 154 hospitalized CDI cases/100,000 population/year and the SOC incidence was 121 hospitalized CDI cases/100,000 population/year for persons ≥50 years of age before the pause. The study hospitalized CDI incidence was 226/100,000 population/year for persons ≥65 years of age and 334/100,000 population/year for persons ≥75 years of age. In the sensitivity analysis adjusted for CCNA QNS and for stool specimens that were not NAAT/CCNA tested because of the GDH screen, the study incidence was 202 hospitalized CDI cases/100,000 population/year for persons ≥50 years of age, 296 hospitalized CDI cases/100,000 population/year for persons ≥65 years of age, and 438 hospitalized CDI cases/100,000 population/year for persons ≥75 years of age.

## Discussion

In a comprehensive population-based surveillance study of diarrhea among hospitalized patients in the United States, including a high stool specimen CDI testing density and rigorous laboratory testing, we identified high incidence of CDI among hospitalized persons

**Table 3.** Comparison between SOC-diagnosed primary CDI cases (n = 126) and study-diagnosed but not SOC-diagnosed primary CDI cases (n = 44) in study of misdiagnosis of CDI by SOC specimen collection and testing among hospitalized adults, Louisville, Kentucky, USA, October 14, 2019–April 11, 2020*

| Characteristic | SOC-diagnosed primary CDI cases, n =126 | Study-diagnosed but not SOC-diagnosed primary CDI cases, n = 44† | p value |
|---|---|---|---|
| Demographics | | | |
| Median age, y, (IQR) | 73 (61–81) | 67 (59–76) | 0.13 |
| Female sex | 74 (58.7) | 27 (61.4) | 0.76 |
| Signs and symptoms | | | |
| Fever | 11 (9.1) | 6 (13.6) | 0.40 |
| Nausea | 38 (34.5) | 11 (25.5) | 0.29 |
| Abdominal cramping | 19 (19.2) | 5 (12.8) | 0.37 |
| Dehydration | 13 (12.5) | 2 (5.3) | 0.21 |
| Location of diarrhea onset | | | |
| Hospital-onset‡ | 22 (17.5) | 19 (43.2) | <0.01 |
| Medical history | | | |
| Dementia | 14 (11.1) | 4 (9.1) | 0.71 |
| Cancer | 42 (33.3) | 11 (25.0) | 0.30 |
| Congestive heart disease | 41 (32.5) | 23 (52.3) | 0.02 |
| Pneumonia | 33 (26.2) | 13 (29.5) | 0.67 |
| Inflammatory bowel disease | 17 (13.5) | 3 (6.8) | 0.24 |
| Diabetes | 47 (37.3) | 21 (47.7) | 0.22 |
| Medical course | | | |
| Recurrence | 4 (3.2) | 0 (0) | 0.23 |
| PMC | 26 (20.8) | 0 (0) | <0.01 |
| Transferred to ICU | 36 (28.6) | 18 (40.9) | 0.13 |
| Death at 90 days | 20 (15.9) | 7 (15.9) | 1.00 |

*Values are no. (%) except as indicated. CDI, *Clostridioides difficile* infection; ICU, intensive care unit; IQR, interquartile range; PMC, pseudomembranous colitis; SOC, standard-of-care.
†Includes 28 study-diagnosed primary CDI cases that did not have SOC testing and 16 study-diagnosed primary CDI cases that had SOC testing but were not SOC-diagnosed primary CDI cases.
‡Defined as onset of diarrhea ≥3 days after hospital admission.

**Table 4.** Comparison between enrolled and nonenrolled incident diarrhea cases before the COVID-19 pause (n = 1,490) in study of misdiagnosis of CDI by SOC specimen collection and testing among hospitalized adults, Louisville, Kentucky, USA, October 14, 2019–April 11, 2020*

| Characteristic | Enrolled, n = 1,249 | Nonenrolled, n = 241 | p value |
|---|---|---|---|
| Demographics | | | |
| Median age, y | 68 | 68 | NA |
| Female sex | 737 (59) | 119 (49) | <0.01 |
| Black | 297 (24) | 62 (26) | 0.52 |
| Medical history | | | |
| Heart disease | 638 (51) | 131 (54) | 0.35 |
| Cancer | 371 (30) | 57 (24) | 0.06 |
| Stroke | 235 (19) | 41 (17) | 0.51 |
| Dementia | 85 (7) | 27 (11) | 0.02 |
| Antimicrobial drug use in past 2 weeks | 370 (30) | 74 (31) | 0.74 |
| Admission diagnosis | | | |
| Heart disease | 131 (10) | 26 (11) | 0.89 |
| Respiratory disease | 105 (8) | 21 (9) | 0.88 |
| Pneumonia | 95 (8) | 20 (8) | 0.71 |
| Nervous system disease | 61 (5) | 21 (9) | 0.02 |
| Medical course | | | |
| Transferred to ICU | 297 (24) | 73 (30) | 0.03 |
| Death in 90 days | 152 (12) | 53 (22) | <0.01 |

*Values are no. (%) except as indicated. Surveillance ascertained 1,541 incident diarrhea cases. Medical record review was conducted at 7 of 8 participating hospitals. Hospital F, where 41 incident diarrhea cases were ascertained, did not participate in medical record review. Data from 10 medical records at hospitals A–E, G, and H were not available for this analysis. Data are presented in descending order, where applicable, of Enrolled column. CDI, *Clostridioides difficile* infection; ICU intensive care unit; NA, not applicable; SOC, standard-of-care.

≥50 years of age, with frequent severe clinical consequences. Among inpatients hospitalized with primary CDI identified before the COVID-19 pandemic, almost one fifth had PMC, one third were admitted to an ICU, and one fifth died in the 90 days after diagnosis. When adjusted for the diarrhea case-patients without a study CDI test result, the incidence was 202 hospitalized primary CDI cases per 100,000 persons ≥50 years of age per year, which is 44% higher than the incidence of 140 hospitalized CDI cases per 100,000 persons ≥50 years of age per year that were reported in the CDC EIP CDI surveillance system in 2019 (*4*). The study also found 24.4% more hospitalized primary CDI case-patients than were found by independent SOC CDI testing of the same diarrhea cases.

Public health surveillance systems, including EIP surveillance, rely on SOC CDI stool collection and testing practices. However, results from this study indicate that public health surveillance systems probably underestimate the incidence of hospitalized patients who have CDI. There are 112 million persons ≥50 years of age in the United States, and results from

**Table 5.** Comparison between inpatients who had a stool specimen collected for CDI testing and inpatients who did not among incident diarrhea cases enrolled before COVID-19 pause (n = 1,283) in study of misdiagnosis of CDI by SOC specimen collection and testing among hospitalized adults, Louisville, Kentucky, USA, October 14, 2019–April 11, 2020*

| Characteristic | Study stool specimen collected, n = 1,047 | Study stool specimen not collected, n = 236 | p value |
|---|---|---|---|
| Demographics | | | |
| Median age, y (IQR) | 68 (61–78) | 67.5 (60–77) | 0.46 |
| Female sex | 595 (56.8) | 146 (61.9) | 0.16 |
| Black | 218 (21.5) | 81 (34.8) | <0.01 |
| Hispanic | 18 (1.8) | 2 (0.9) | 0.33 |
| Signs and symptoms | | | |
| Abdominal pain | 283 (28.7) | 53 (23.8) | 0.14 |
| Fever | 109 (10.7) | 18 (7.8) | 0.18 |
| Blood or pus in stool | 90 (9.3) | 20 (9.0) | 0.91 |
| Medical history | | | |
| Overnight stay in healthcare facility in previous 12 weeks | 615 (60) | 150 (63.8) | 0.39 |
| Diabetes | 432 (41.5) | 91 (38.9) | 0.46 |
| Antimicrobial drug use in previous 3 months | 387 (39.2) | 63 (26.9) | < 0.01 |
| Cancer | 313 (30.2) | 59 (25.1) | 0.12 |
| Congestive heart disease | 305 (29.3) | 64 (27.2) | 0.53 |
| CDI in past 5 years | 66 (7.5) | 18 (8.1) | 0.76 |
| Dementia | 76 (7.3) | 14 (5.9) | 0.46 |
| Inflammatory bowel disease | 65 (6.3) | 10 (4.3) | 0.26 |
| Hemiplegia/quadriplegia | 54 (5.2) | 8 (3.4) | 0.25 |

*Values are no. (%) except as indicated. Data are presented in descending order of Study stool specimen collected column. Values of missing or unknown were excluded from percentage and p value calculations. CDI, *Clostridioides difficile* infection; IQR, interquartile range; SOC, standard-of-care.

our study indicate that at least 226,000 persons in that age group are hospitalized with CDI each year in the United States, rather than the 160,000 estimated by EIP surveillance (*4*).

The effect of SOC specimen collection and testing practices on CDI incidence has been frequently discussed (*5*,*6*,*8*–*11*). SOC testing can result in overdiagnosis of CDI and overestimation of CDI incidence, if SOC testing practices misidentify *C. difficile* carriage as CDI. Concerns have been raised about use of NAAT alone for CDI diagnosis because a NAAT-positive specimen only indicates the presence of toxigenic *C. difficile* and does not identify the presence of toxin (*5*,*6*). Those concerns have led to guidance in Europe to use 2-step testing with the first step determining the presence of toxin, the toxin gene, or *C. difficile* and positive specimens tested in the second step so that results of the 2 steps confirm the presence of *C. difficile* and the presence of free toxin (*16*,*17*).

NAAT alone is commonly used in clinical laboratories in the United States (*4*,*7*), where the guidance supports use of NAAT alone if there are institutional criteria for patient stool submission (*18*). The frequent use of NAAT alone in the United States means that CDI incidence could be overestimated. However, results from this study indicate that SOC CDI testing practices, when compared with comprehensive and rigorous NAAT and CCNA testing, result in CDI overdiagnosis less frequently than CDI underdiagnosis. Therefore, CDI overdiagnosis caused by SOC practices is unlikely to result in overestimation of CDI incidence in public health surveillance in the United States.

SOC CDI underdiagnosis can result from either misdiagnosis by laboratory testing or lack of specimen collection. Of the instances of SOC CDI underdiagnosis in our study, 36.4% occurred when study testing diagnosed CDI but SOC testing did not, and 63.6% occurred when SOC did not collect a specimen. Perhaps not surprisingly, because guidelines recommend against CDI testing of patients who had received a laxative within the preceding 48 hours (*18*), a high percentage (39.3%) of the study-diagnosed CDI case-patients who were not SOC-diagnosed because of lack of specimen collection were receiving laxatives. We found that SOC-diagnosed CDI cases were less likely to be hospital-onset cases than study-diagnosed (but SOC-undiagnosed) cases, perhaps reflecting less willingness to diagnosed hospital-onset CDI, which might be associated with penalties for having an increased incidence of hospital-onset CDI cases.

We also found that a higher percentage of study-identified primary CDI cases were healthcare-associated cases (78.9%) than as reported in EIP surveillance (48%) during 2019 (*4*), a difference that is, in part, related to the higher percentage of hospital-onset cases in our study. Other investigators have reported on CDI underdiagnosis from not collecting specimens and the resulting effect on CDI incidence estimates (*8*–*11*). Because clinical judgment can identify patients with diarrhea who are more likely to have CDI, clinical judgment should be the most essential factor in deciding when to collect a specimen from a patient with diarrhea. The objective of this study was not to suggest when CDI testing is appropriate but to illuminate that CDI underdiagnosis probably results in underestimation of the CDI incidence in public health surveillance in the United States.

The strength of this study was that we conducted active surveillance for incident diarrhea cases and collected specimens from inpatients with diarrhea, in parallel with (and independent of) SOC specimen collection and testing. Surveillance, patient informed consent, and study specimen collection were conducted by designated study staff, independent of hospital staff, to reduce the influence on SOC practices. The extent to which the study influenced SOC practices is unknown, but the study might have increased awareness of CDI and increased SOC CDI testing. Use of the independent study staff resulted in high enrollment and specimen collection rates, which resulted in a small percentage of inpatients with diarrhea not having a study specimen collected for CDI testing. Another strength of this population-based study was that it was conducted in Louisville, Kentucky, which has been shown to be representative of the United States (*12*).

Surveillance for the study was interrupted after 6 months because of hospital-enacted COVID-19 restrictions. After a 4-month pause, surveillance was reinstated, but access to patients remained restricted, which resulted in a decrease in the study enrollment rate. After reinstatement of surveillance, most of the hospitalized patients were admitted for treatment of COVID-19, resulting in a different inpatient population than that for the prepandemic period. Therefore, we restricted our analysis estimating the population-based hospitalized CDI incidence and the extent of SOC CDI misdiagnosis to the data collected before the COVID-19 pause. The only data collected after the pause that were used in the incidence estimates were for the determination of the NPV of the GDH test compared with the NAAT, an evaluation that was unlikely to be affected by differences in the inpatient populations.

Limitations of this study include that, despite the intense active surveillance, incident diarrhea cases

might have been undetected, and the incidence estimates are based only on 6 months of surveillance. Although minor seasonal variation of hospitalized CDI incidence has been reported in the United States (*19*), there was limited variation in the monthly CDI incidence during this study (data not shown). A study limitation is that, when assessing CDI misdiagnosis by SOC testing, study and SOC specimen collection were independent, and therefore the same specimen was not tested by both methods; this limitation is most evident with SOC overdiagnosed cases, some of which might have been CDI cases. Another study limitation is that a specimen was not available for study CDI testing from all inpatients with diarrhea for various reasons.

Furthermore, insufficient stool was available for CCNA testing for some of the study specimens collected. Another reason was that the NPV of the GDH screening test indicates that the GDH test probably identified a small number of primary CDI cases incorrectly as GDH-negative. Because a comparison of the medical records of the diarrhea case-patients with and without study CDI testing demonstrated few differences, we conducted a sensitivity analysis to evaluate the effect of not conducting CDI testing for all inpatients with diarrhea, adjusting the incidence estimates for inpatients with diarrhea who did not have a study CDI test. Finally, there is no recognized standard laboratory test for CDI diagnosis. Although we used a validated automated CCNA test, study laboratory testing might have missed CDI cases (*20*), emphasizing that the diagnosis of CDI should not be based on laboratory results alone.

In conclusion, we identified a high population-based incidence of hospitalized CDI case-patients that had frequent severe clinical consequences in Louisville, Kentucky, which, when generalized nationwide, demonstrates that the hospitalized CDI burden is high in the United States. Furthermore, the hospitalized CDI burden in the United States is probably higher than is currently reported in public health surveillance systems because of CDI underdiagnosis by SOC specimen collection and testing practices. This high burden in the United States indicates that additional interventions are needed for the prevention of CDI.

CLOUD Study Working Group, University of Louisville,: Adnan M. Qureshi, Ahmed A.M.F Abdelhaleem, Ahmed A.A.A. Eladely, Ahmed E.A.M Omran, Ahmed G.S.A. Ali, Javed Ahmad, Ahsan M. Khan, Amr A.A. Aboelnasr, Anupama Raghuram, Arashpreet K. Chhina, Arpan Chawala, Arshdeep S. Batth, Ashraf Rjob, Athar I.A.A. Eysa, Ayesha Shameen, Balachandran R. Vaidyanath, Balaji Sekeran, Basel H.M. Alhaddad, Bidoh J. Karki, Chet N. Dhakal, Dana Mantash, Daniya Sheikh, Dawn Balcom, Danial A. Malik, Lakshmi P.D. Cherukuwada, Deepti Deepti, Devika Gopan, Duremala, Evelyn E. Gonzalez, Farah M.S. Daas, Hammad Tanzeem, Harideep Samanapally, Ahmed Iqbal, Isabel C. Rozema, Javaria Answer, Joanna J. Ekabua, Khaled J.A.K. Alweis, Leslie A. Beavin, Lucia B. P. Sanchez, Mahmoud Abdelsamia, Manish KC, Marjan Haider, Maryta N. Sztukowska, Meredith N. Cahill, Mohamed M.A. Abdelmabi, Muhammad H. Khan, Mohammed K. Abdulaziz, Muhammad A. Tariq, Mutasem Abuhalaweh, Nishita Tripathi, Pavani Nathala, Prashant Tripathi, Rachel A. Sheppard, Rafik Elbeblawy, Raghava S. Ambadapoodi, Rehab S.S. Mohamed, Rishav Sinha, Ritika Gadodia, Rupa Garikipati, Salman M.E. Elgharbawi, Satya R. Durugu, Shivam Gulati, Simra Kiran, Steven M. Gootee, Subathra Marimuthu, Usman A. Akbar, Vidyulata Salunkhe, and Zahid Imran.

**Acknowledgments**

We thank members of the CLOUD Study Working Group for their contributions, Kimbal D. Ford for support, Melissa Furtado for medical writing support, and Varkha Agrawal for editorial support.

This study was supported by Pfizer Inc., which was involved in the study design, data collection, data analysis, data interpretation, and writing of the article. All authors had full access to the study data and approved the decision to submit for publication. Upon request, and subject to review, Pfizer will provide the data that support the findings of this study. Subject to certain criteria, conditions and exceptions, Pfizer may also provide access to the related individual de-identified participant data. For more information, see https://www.pfizer.com/science/clinical-trials/trial-data-and-results.

J.A.R. has a grant from Pfizer Inc. to the University of Louisville Research Foundation for the epidemiologic study. F.J.A., J.M.Z. E.G., P.Z., M.W.P., S.G., R.E.I., J.C.M, and L.J. hold stock and stock options in Pfizer Inc. R.M.C. has grants or contracts from Pfizer Inc. for *C. difficile* research and honoraria from Pfizer Inc. for content development and presentation regarding *C. difficile* to professional organization. L.A.W.P. and S.M. declare support from Pfizer Inc. for this study (i.e., kits for performing Quik Chek rapid tests, supplies for aliquoting stool samples, sample forms, and barcoding labels and scanners); contract from Pfizer Inc. to support the project; and receipt of equipment (i.e., 1 biologic safety cabinet, 1 refrigerator, 1 incubator, 1 anaerobic chamber, and 1 freezer). C.S.M.F. declares support from Pfizer Inc. for this manuscript and stock

options from AstraZeneca, PLC. F.W.A. declares institutional payment from Pfizer Inc. for this manuscript and grants or contracts from the US Health Resources and Services Administration for the Ryan White HIV clinic, Janssen for COVID-19 vaccine study, and Gilead for rapid start antiretroviral therapy study. The other co-authors declare no conflicts of interest.

## About the Author

Dr. Ramirez is chief scientific officer for the Norton Infectious Diseases Institute at Norton Healthcare in Louisville, KY, and emeritus professor of medicine, Division of Infectious Diseases, University of Louisville. His primary research interests include respiratory tract infections, with a focus on community-acquired pneumonia and emerging respiratory pathogens.

## References


1. Lessa FC, Mu Y, Bamberg WM, Beldavs ZG, Dumyati GK, Dunn JR, et al. Burden of *Clostridium difficile* infection in the United States. N Engl J Med. 2015;372:825–34. https://doi.org/10.1056/NEJMoa1408913
2. Balsells E, Shi T, Leese C, Lyell I, Burrows J, Wiuff C, et al. Global burden of *Clostridium difficile* infections: a systematic review and meta-analysis. J Glob Health. 2019;9:010407. 10.7189/jogh.09.010407 https://doi.org/10.7189/jogh.09.010407
3. Centers for Disease Control and Prevention. Antibiotic resistance threats in the United States, 2019 [cited 2023 Jan 13]. https://doi.org/10.15620/cdc:82532
4. Centers for Disease Control and Prevention. Emerging Infections Program, Healthcare Associated Infections Community interface surveillance report, *Clostridioides difficile* infection (CDI), 2019 [cited 2023 Jan 13]. https://www.cdc.gov/hai/eip/pdf/cdiff/2019-CDI-Report-H.pdf
5. Polage CR, Gyorke CE, Kennedy MA, Leslie JL, Chin DL, Wang S, et al. Overdiagnosis of *Clostridium difficile* infection in the molecular test era. JAMA Intern Med. 2015;175:1792–801. https://doi.org/10.1001/jamainternmed.2015.4114
6. Longtin Y, Trottier S, Brochu G, Paquet-Bolduc B, Garenc C, Loungnarath V, et al. Impact of the type of diagnostic assay on *Clostridium difficile* infection and complication rates in a mandatory reporting program. Clin Infect Dis. 2013;56:67–73. https://doi.org/10.1093/cid/cis840
7. Centers for Disease Control and Prevention. Annual report for the Emerging Infections Program for *Clostridioides* difficile infection, 2017 [cited 2023 Jan 13]. https://www.cdc.gov/hai/eip/Annual-CDI-Report-2017.html
8. Davies KA, Longshaw CM, Davis GL, Bouza E, Barbut F, Barna Z, et al. Underdiagnosis of *Clostridium difficile* across Europe: the European, multicentre, prospective, biannual, point-prevalence study of *Clostridium difficile* infection in hospitalised patients with diarrhoea (EUCLID). Lancet Infect Dis. 2014;14:1208–19. https://doi.org/10.1016/S1473-3099(14)70991-0
9. Reigadas E, Alcalá L, Marín M, Burillo A, Muñoz P, Bouza E. Missed diagnosis of *Clostridium difficile* infection; a prospective evaluation of unselected stool samples. J Infect. 2015;70:264–72. https://doi.org/10.1016/j.jinf.2014.10.013
10. Effelsberg N, Buchholz M, Kampmeier S, Lücke A, Schwierzeck V, Angulo FJ, et al. Frequency of diarrhea, stool specimen collection and testing, and detection of *Clostridioides difficile* infection among hospitalized adults in the Muenster/Coesfeld area, Germany. Curr Microbiol. 2022;80:37. https://doi.org/10.1007/s00284-022-03143-6
11. Fridkin SK, Onwubiko UN, Dube W, Robichaux C, Traenkner J, Goodenough D, et al. Determinates of *Clostridioides difficile* infection (CDI) testing practices among inpatients with diarrhea at selected acute-care hospitals in Rochester, New York, and Atlanta, Georgia, 2020–2021. Infect Control Hosp Epidemiol. 2022;Sep 14:1–8. https://doi.org/10.1017/ice.2022.205
12. Furmanek SP, Glick C, Chandler T, Tella MA, Mattingly WA, Ramirez JA, et al. The City of Louisville encapsulates the United States demographics. Univ Louisville J Respir Infect. 2020;2:4. https://doi.org/10.18297/jri/vol4/iss2/4
13. Sharp SE, Ruden LO, Pohl JC, Hatcher PA, Jayne LM, Ivie WM. Evaluation of the C.Diff Quik Chek Complete Assay, a new glutamate dehydrogenase and A/B toxin combination lateral flow assay for use in rapid, simple diagnosis of *Clostridium difficile* disease. J Clin Microbiol. 2010;48:2082–6. https://doi.org/10.1128/JCM.00129-10
14. Elfassy A, Kalina WV, French R, Nguyen H, Tan C, Sebastian S, et al. Development and clinical validation of an automated cell cytotoxicity neutralization assay for detecting *Clostridioides difficile* toxins in clinically relevant stools samples. Anaerobe. 2021;71:102415. https://doi.org/10.1016/j.anaerobe.2021.102415
15. Centers for Disease Control and Prevention. Epidemiologic classification of CDI cases [cited 2023 Jan 13]. https://www.cdc.gov/hai/eip/cdiff-tracking.html
16. Crobach MJ, Dekkers OM, Wilcox MH, Kuijper EJ. European Society of Clinical Microbiology and Infectious Diseases (ESCMID): data review and recommendations for diagnosing *Clostridium difficile*-infection (CDI). Clin Microbiol Infect. 2009;15:1053–66. https://doi.org/10.1111/j.1469-0691.2009.03098.x
17. Crobach MJ, Planche T, Eckert C, Barbut F, Terveer EM, Dekkers OM, et al. European Society of Clinical Microbiology and Infectious Diseases: update of the diagnostic guidance document for *Clostridium difficile* infection. Clin Microbiol Infect. 2016;22(Suppl 4):S63–81.
18. McDonald LC, Gerding DN, Johnson S, Bakken JS, Carroll KC, Coffin SE, et al. Clinical practice guidelines for *Clostridium difficile* infection in adults and children: 2017 update by the Infectious Diseases Society of America (IDSA) and Society for Healthcare Epidemiology of America (SHEA). Clin Infect Dis. 2018;66:e1–48. https://doi.org/10.1093/cid/cix1085
19. Argamany JR, Aitken SL, Lee GC, Boyd NK, Reveles KR. Regional and seasonal variation in *Clostridium difficile* infections among hospitalized patients in the United States, 2001–2010. Am J Infect Control. 2015;43:435–40. https://doi.org/10.1016/j.ajic.2014.11.018
20. Schweitzer L, Gervais P, Paquet-Bolduc B, Loo VG, Longtin Y. Detection of free toxin B in the stool of asymptomatic *Clostridioides difficile* carriers by the cell cytotoxicity neutralization assay. Open Forum Infect Dis. 2021;8:b209. https://doi.org/10.1093/ofid/ofab209


Address for correspondence: Frederick J. Angulo, Medical Development and Scientific/Clinical Affairs, Pfizer Vaccines, 500 Arcola Rd, Collegeville, PA 19426, USA; email: frederick.j.angulo@pfizer.com

# SARS-CoV-2 Seroprevalence Compared with Confirmed COVID-19 Cases among Children, Colorado, USA, May–July 2021

Shannon C. O'Brien, Lyndsey D. Cole, Bernadette A. Albanese, Allison Mahon, Vijaya Knight, Nathan Williams, Rachel Severson, Alexis Burakoff, Nisha B. Alden, Samuel R. Dominguez

To compare SARS-CoV-2 antibody seroprevalence among children with seropositive confirmed COVID-19 case counts (case ascertainment by molecular amplification) in Colorado, USA, we conducted a cross-sectional serosurvey during May–July 2021. For a convenience sample of 829 Colorado children, SARS-CoV-2 seroprevalence was 36.7%, compared with prevalence of 6.5% according to individually matched COVID-19 test results reported to public health. Compared with non-Hispanic White children, seroprevalence was higher among Hispanic, non-Hispanic Black, and non-Hispanic other race children, and case ascertainment was significantly lower among Hispanic and non-Hispanic Black children. This serosurvey accurately estimated SARS-CoV-2 prevalence among children compared with confirmed COVID-19 case counts and revealed substantial racial/ethnic disparities in infections and case ascertainment. Continued efforts to address racial and ethnic differences in disease burden and to overcome potential barriers to case ascertainment, including access to testing, may help mitigate these ongoing disparities.

Since identification of SARS-CoV-2 and the ensuing pandemic, epidemiologic studies have shown that COVID-19 outcomes are less severe among children than adults (*1*–*8*). Conclusions drawn from published studies on COVID-19 prevalence in the pediatric population have varied (*5*,*9*–*16*), possibly because of differences in mitigation measures, community transmission rates, and case ascertainment practices. Noted trends in the prevalence of SARS-CoV-2 infection among children can be affected by population-level decisions, such as viral test prioritization and distribution as well as individual-level test-seeking behavior, because the disease in many children is asymptomatic or only mildly symptomatic. In addition, societal effects, such as loss of work for parents and caregivers and missed school days if a child tests positive, may also affect test-seeking behavior. Those factors can lower case ascertainment when relying on reported viral testing as the primary source of surveillance data, resulting in underestimation of disease burden and transmission in the pediatric population, and may lead to an overestimation of disease severity (*17*).

The issue of underestimation by disease surveillance systems that rely heavily on diagnostic testing and reporting is not specific to SARS-CoV-2. Strategies to improve the accuracy of disease prevalence estimates exist, including use of mathematical modeling. However, modeling based on more consistently reported outcome-based metrics, such as hospitalizations, can be limited in the ability to describe disease prevalence in some subpopulations, especially when measured outcomes are rare, as with SARS-CoV-2 hospitalizations among children. Thus, other modalities are needed to refine information about SARS-CoV-2 prevalence among children.

True prevalence of pediatric SARS-CoV-2 infection may be more accurately measured by using laboratory assays to detect SARS-CoV-2 IgG, compared with surveillance systems that rely on viral testing (*17*,*18*). Few published serosurveys in the United States include enough children to adequately describe SARS-CoV-2 infection in the pediatric population

Author affiliations: Colorado Department of Public Health and Environment, Denver, Colorado, USA (S.C. O'Brien, N. Williams, R. Severson, A. Burakoff, N.B. Alden); Children's Hospital Colorado, Aurora, Colorado, USA (L.D. Cole, A. Mahon, V. Knight, S.R. Dominguez); Tri-County Health Department, Greenwood Village, Colorado, USA (B.A. Albanese)

DOI: https://doi.org/10.3201/eid2905.221541

[1]Preliminary results from this study were presented at the Council of State and Territorial Epidemiologists Conference; Louisville, Kentucky, USA; June 19–23, 2022.

by subgroups. In addition, available state-level modeling data were not designed for subpopulation analysis within the pediatric population because of relatively low rates of pediatric hospitalization, limiting applicability to prevalence comparisons.

We conducted a cross-sectional serosurvey to determine SARS-CoV-2 seroprevalence, seropositive case ascertainment, and age and racial/ethnic group differences during May–July 2021 in a convenience sample of children in Colorado, USA. The Colorado Department of Public Health and Environment (CDPHE) Communicable Disease Branch determined this activity to be consistent with enhanced disease surveillance activities, not human subjects research. Institutional review board approval was provided by the Colorado Multiple Institutional Review Board. Informed consent was waived.

## Methods

### Study Design and Conduct

Our cross-sectional serosurvey tested residual serum from a convenience sample of Colorado children 1–17 years of age from whom blood was collected during May 12–July 13, 2021, as part of care in nonsubspecialty outpatient clinics, urgent care centers, and emergency departments within the largest pediatric healthcare system in Colorado. We extracted age, sex, race, ethnicity, and specimen collection date from the electronic medical record. We assigned racial/ethnic group according to self-report as Hispanic/any race, non-Hispanic White, non-Hispanic Black, non-Hispanic other, and unknown. The non-Hispanic other group includes Asian, American Indian or Alaskan Native, Native Hawaiian or other Pacific Islander, ≥1 race, or other race. The unknown group includes persons for whom race and ethnicity data were not reported. For children included in the study, names and dates of birth were matched to the Colorado Immunization Information System to establish SARS-CoV-2 vaccination status and to the Colorado COVID-19 surveillance system to obtain SARS-CoV-2 molecular amplification test results reported to the CDPHE. Children for whom molecular amplification tests were positive were considered to have confirmed cases of COVID-19, per the Council of State and Territorial Epidemiologists surveillance case definition.

### Eligibility Criteria and Study Procedure

Residual serum specimens from children 1–17 years of age at the time of blood collection were eligible for inclusion. To improve generalizability, we excluded specimens from subspecialty outpatient clinics (e.g., oncology, cardiology). We selected eligible children sequentially. After selecting approximately half of the 1,000 planned specimens, we oversampled from the 1–4-year age group and non-Hispanic Black children to improve representativeness for subgroup analysis. To improve the sensitivity of positive serology results as a proxy for previous SARS-CoV-2 infection and to avoid misclassification error among previously vaccinated children not previously infected (Appendix Table 1, https://wwwnc.cdc.gov/EID/article/29/5/22-1541-App1.pdf), we excluded from final analysis children who had received ≥1 SARS-CoV-2 vaccine dose on any date before the serum specimen collection date. We also excluded non-Colorado residents from the final analysis.

### Laboratory Analysis

We tested residual serum specimens for SARS-CoV-2 nucleocapsid and spike IgG. We analyzed nucleocapsid antibodies by using the automated Abbott Alinity chemiluminescent microparticle immunoassay (Abbott, https://www.abbott.com). We determined the presence or absence of nucleocapsid antibodies by comparing the relative light units of the specimen (S) to a calibrator (C) and expressed results as an S/C index. We reported specimens with an S/C index <0.8 as negative, ≥1.4 as positive, and >0.8 to 1.3 as borderline for nucleocapsid antibodies. For purposes of this study, borderline results were considered negative.

We analyzed spike antibodies by using the qualitative Euroimmun ELISA Kit EI 2606–9601 (Euroimmun, https://www.euroimmun.com), which uses the S1 domain of the SARS-CoV-2 spike protein. We added specimens diluted 1:101 with dilution buffer, positive and negative controls, and kit-specific calibrator to SARS-CoV-2 S1 antigen precoated wells. We performed the ELISA according to the manufacturer's specifications and read the final color development at optical density 450 nm ($OD_{450}$). We interpreted results based on the ratio of the specimen $OD_{450}$ to the calibrator $OD_{450}$; specimens with a ratio of <0.8 were reported as negative, ≥1.1 as positive, and >0.8 to <1.1 as borderline for spike antibodies. For purposes of this study, we considered borderline results negative.

We established sensitivity and specificity of the Abbott and Euroimmun assays by using serum specimens with SARS-CoV-2 positivity confirmed by PCR and prepandemic specimens that had been collected before November 2019. According to our data, sensitivity of the Euroimmun assay was 92% and specificity 97%. We verified the manufacturer-stated sensitivity of the Abbott Alinity of 96.7% and specificity of 99% (*19*).

Reported viral tests used in the analysis included any molecular amplification test before the serum specimen collection date for each person. All viral test samples were collected, interpreted, and reported outside the context of this study.

### Statistical Analyses

We calculated descriptive characteristics, including counts and proportions with 95% CIs. We calculated SARS-CoV-2 seroprevalence by dividing the number of specimens positive for nucleocapsid IgG, spike IgG, or both by the total number of specimens tested among the sample of unvaccinated children (Appendix Table 2). We selected this method of calculating seroprevalence because it provides the most sensitive estimate of previous infection. To calculate sample prevalence of SARS-CoV-2 infection determined by confirmed cases reported to public health, we divided the number of persons with ≥1 positive molecular amplification test result preceding the serum specimen collection date by the total number of serum specimens tested. We included children with ≥1 previous positive molecular amplification test result only once. We calculated seropositive case ascertainment as the number of seropositive persons identified as confirmed cases reported to public health divided by the number of seropositive persons. We calculated multiplication factors, or the number of infections estimated per reported case, as the inverse of case ascertainment and prevalence ratios by racial/ethnic and age groups for serology results and case ascertainment. We analyzed differences in time between first positive viral test sample collection and serology sample collection stratified by serology test results by using Wilcoxon/Mann-Whitney testing. We conducted statistical analyses by using R version 4.1.1 (The R Foundation for Statistical Computing, https://www.r-project.org) and set statistical significance at $p<0.05$.

## Results

### Descriptive Characteristics

We collected 940 unique residual serum specimens for the study. We excluded 78 from children who had received ≥1 SARS-CoV-2 vaccine doses before specimen collection and 33 from children identified as non-Colorado residents. Among the 829 children included, 422 (50.9%) were female, and the median age was 9 (range 1–17) years (Table 1).

### SARS-CoV-2 Seroprevalence

Overall SARS-CoV-2 seroprevalence was 36.7% (95% CI 33.4%–40.1%) (Table 2). Seroprevalence across racial/ethnic groups was highest among Hispanic children at 49.8% (95% CI 43.9%–55.8%), followed by non-Hispanic Black at 37.7%, (95% CI 28.5%–47.7%) and non-Hispanic other race children at 35.4% (95% CI 26.0%–45.6%). Seroprevalence ratios showed higher seroprevalence for Hispanic (2.01 [95% CI 1.59–2.53]), non-Hispanic Black (1.52 [95% CI 1.11–2.08]), and non-Hispanic other race children (1.42 [95% CI 1.02–1.99]) than for non-Hispanic White children (referent group). Seroprevalence across age groups was 39.0% (95% CI 32.9%–45.3%) for children 1–4 years of age, 32.3% (95% CI 27.0%–38.0%) for children 5–11 years of age, and 39.2% (95% CI 33.4%–45.2%) for children 12–17 years of age. We found no statistically significant difference between age groups.

### Sample SARS-CoV-2 Prevalence Determined by Confirmed Case Counts

Overall sample SARS-CoV-2 prevalence, determined by confirmed case counts reported to public health, was 6.5% (95% CI 4.9%–8.4%) (Appendix Table 3). Across racial/ethnic groups, SARS-CoV-2 prevalence by confirmed case counts was 7.6% (95% CI 4.8%–11.3%) for non-Hispanic White, 6.6% (95% CI 4.0%–10.2%) for Hispanic, and 3.8% (95% CI 1.0%–9.4%) for non-Hispanic Black children. Across age groups, SARS-CoV-2 prevalence by confirmed case counts was 5.1% (95% CI 2.8%–8.6%) for children 1–4 years of age, 7.4% (95% CI 4.7%–11.0%) for children 5–11 years of age, and 6.8% (95% CI 4.2%–10.5%) for children 12–17 years of age.

### Seropositive Case Ascertainment and Multiplication Factors

Seropositive case ascertainment in the overall study population was 16% with a multiplication factor of 6 (Table 3). Seropositive case ascertainment was highest among non-Hispanic White children (26.4% with multiplication factor of 4), followed by Hispanic (13.3%, multiplication factor of 8) and non-Hispanic Black children (7.5%, multiplication factor of 13). Seropositive case ascertainment prevalence ratios showed lower seropositive case ascertainment for Hispanic (0.50 [95% CI 0.28–0.89]) and non-Hispanic Black (0.28 [95% CI 0.09–0.90]) children than for non-Hispanic White children. Seropositive case ascertainment across age groups ranged from a high of 21.9% for the 5–11-year age group to a low of 13.1% for the 1–4-year age group. Case ascertainment prevalence ratios across age groups did not differ statistically.

### Spike Versus Nucleocapsid IgG Results

Of the 54 children with a previous reported positive SARS-CoV-2 viral test result, 36 (66.7%) were seropositive for both spike and nucleocapsid IgG, 13 (24.1%)

**Table 1**. Descriptive characteristics of children included in seroprevalence and case ascertainment analyses, Colorado, USA, May 12–July 13, 2021*

| Characteristic | No. (%) | Median age (IQR) |
|---|---|---|
| Total population | 829 | 9 y (3–14) |
| Female sex | 422 (50.9) | NA |
| Male sex | 405 (48.9) | NA |
| Racial/ethnic group | | |
| Non-Hispanic White | 290 (35.0) | 8 (3.8–12) |
| Hispanic all races | 287 (34.6) | 10 (4–14) |
| Non-Hispanic Black | 106 (12.8) | 10.5 (3–14) |
| Non-Hispanic other† | 99 (11.9) | 8 (3–12) |
| Unknown‡ | 47 (5.7) | 7 (2–13) |
| Age group, y | | |
| 1–4 | 254 (30.6) | NA |
| 5–11 | 297 (35.8) | NA |
| 12–17 | 278 (33.5) | NA |

*IQR, interquartile range; NA, not applicable.
†Includes persons self-reported as not Hispanic or Latino and Asian, American Indian or Alaskan Native, Native Hawaiian or other Pacific Islander, >1 race, or other race.
‡Includes persons for whom race and ethnicity data were not reported.

for spike IgG only, 4 (7.4%) for spike and nucleocapsid IgG, and 1 (1.9%) for nucleocapsid IgG only. The average interval between the time of the first positive SARS-CoV-2 viral test specimen collection and serum specimen collection was 116 days for those seropositive for spike and nucleocapsid IgG and 191 days for those seropositive for spike IgG only (p = 0.005) (Figure 1).

## Discussion

In this convenience sample of residual serum collected from Colorado children 1–17 years of age during spring/summer 2021, seroprevalence of SARS-CoV-2 IgG was 36.7%. Our results show higher seroprevalence than that found from rounds 20 and 21 of the nationwide antibody seroprevalence survey (https://covid.cdc.gov/covid-data-tracker/#national-lab), the only contemporaneous rounds with an estimate for seroprevalence among children, which estimated seroprevalence of 13.4% (95% CI 6.2%–23.8%) for round 20 and 17.5% (95% CI 12.4%–22.8%) for round 21 (*20*). A few factors may explain those differences: the nationwide surveys were conducted just before and during the first few weeks of our study, the nationwide survey used a different nucleocapsid assay and did not test for spike antibodies, and the relatively small pediatric populations in these convenience samples may demographically differ from those in our sample. In addition, although adjusted rates, such as those calculated in the nationwide survey, are comparable to other similarly adjusted rates across different populations, they may not be comparable to unadjusted rates such as those in our study. However, results for round 25, conducted a few months after the conclusion of our sample selection, was much more consistent with our results: seroprevalence of 40.1% (95% CI 33.7%–46.6%).

Among our study cohort, SARS-CoV-2 prevalence determined by positive molecular amplification testing was only 6.5% and seropositive case ascertainment was 16%. This finding indicates a potential underestimation of cases among this pediatric population by 84% when relying solely on confirmed case counts, either because of underascertainment or underreporting. If the unadjusted study results were generalized to the larger Colorado pediatric population, confirmed case counts statewide could require a multiplication factor of 6 to more accurately reflect the prevalence of SARS-CoV-2 infection among children. This result is consistent with findings from other states that showed multiplication factors from 4.7 to 8.9 during a similar time frame (*21*). Our results may represent opportunities to improve individual-level awareness of SARS-CoV-2 infection and increase mitigation measures, including isolation and quarantine. On a population level, our results can be used to corroborate modeled SARS-CoV-2 prevalence estimates based on hospitalization rates.

In addition, we found statistically significant differences in seroprevalence and seropositive case

**Table 2.** SARS-CoV-2 serology results, seroprevalence, and seroprevalence ratios by racial/ethnic and age group, Colorado, USA, May 12-July 13, 2021*

| Group | Serology results, no. | | Seroprevalence, % (95% CI) | Seroprevalence ratio (95% CI) |
|---|---|---|---|---|
| | Seronegative | Seropositive† | | |
| Total | 525 | 304 | 36.7 (33.4–40.1) | NA |
| Race/ethnicity | | | | |
| Non-Hispanic White | 218 | 72 | 24.8 (20.0–30.2) | Referent |
| Hispanic all races | 144 | 143 | 49.8 (43.9–55.8) | 2.01 (1.59–2.53)‡ |
| Non-Hispanic Black | 66 | 40 | 37.7 (28.5–47.7) | 1.52 (1.11–2.08)‡ |
| Non-Hispanic other | 64 | 35 | 35.4 (26.0–45.6) | 1.42 (1.02–1.99)‡ |
| Unknown | 33 | 14 | 29.8 (17.3–44.9) | 1.20 (0.74–1.94) |
| Age, y | | | | |
| 1–4 | 155 | 99 | 39.0 (32.9–45.3) | Referent |
| 5–11 | 201 | 96 | 32.3 (27.0–38.0) | 0.83 (0.66–1.04) |
| 12–17 | 169 | 109 | 39.2 (33.4–45.2) | 1.01 (0.81–1.24) |

*NA, not applicable.
†Seropositivity determined by presence of spike and/or nucleocapsid IgG.
‡Significant at p<0.05.

**Table 3.** Previously reported positive SARS-CoV-2 viral diagnostic testing, seropositive case ascertainment, and multiplication factors by racial/ethnic and age group among seropositive children, Colorado, May 12–July 13, 2021*

| Group | Previous positive result | Case ascertainment, % (95% CI)† | Case ascertainment prevalence ratio (95% CI) | Multiplication factor‡ |
|---|---|---|---|---|
| Total | 50 | 16.4 (12.5–21.1) | NA | 6 |
| Race/ethnicity | | | | |
| Non-Hispanic White | 19 | 26.4 (16.7–38.1) | Referent | 4 |
| Hispanic all races | 19 | 13.3 (8.2–20.0) | 0.50 (0.28–0.89§ | 8 |
| Non-Hispanic Black | 3 | 7.5 (1.6–20.4) | 0.28 (0.09–0.90)§ | 13 |
| Non-Hispanic other | 6 | 17.1 (6.6–33.7) | 0.65 (0.28–1.48) | 6 |
| Unknown | 3 | 21.4 (4.7–50.8) | 0.81 (0.28–2.38) | 5 |
| Age, y | | | | |
| 1–4 | 13 | 13.1 (7.2–21.4) | Referent | 8 |
| 5–11 | 21 | 21.9 (14.1–31.5) | 1.67 (0.89–3.13) | 5 |
| 12–17 | 16 | 14.7 (8.6–22.7) | 1.12 (0.57–2.21) | 7 |

*NA, not applicable.
†Case ascertainment calculated as the number of previous positive tests among seropositive children divided by the total number of seropositive children.
‡Multiplication factor calculated as the number of seropositive cases divided by the number of previous positive tests, also known as the inverse of case ascertainment.
§Statistically significant at p<0.05.

ascertainment across racial/ethnic groups. Compared with non-Hispanic White children, seroprevalence was significantly higher among Hispanic and non-Hispanic Black children, indicating higher rates of previous SARS-CoV-2 infection, consistent with results of several published studies on molecular test positivity and seroprevalence studies in adults (*11*,*22*–*27*). Our study also found that seropositive case ascertainment was lower among Hispanic and non-Hispanic Black children than among non-Hispanic White children; cases were detected in Hispanic children half as often as in non-Hispanic White children, and cases in non-Hispanic Black children were detected less than one third as often as in non-Hispanic White children. This disparity is supported by studies showing reduced rates of testing in many racial/ethnic minority groups (*22*,*27*). Our results show that reliance on reported case counts would lead to the erroneous assumption that rates of SARS-CoV-2 infection in the study period were highest among non-Hispanic White children. Those results further demonstrate the value of complementary surveillance mechanisms such as serologic and wastewater testing that can avoid testing and reporting biases.

Seroprevalence measured in our study reflects infections among children occurring during the 2020–21 school year and early summer before the peaks of the Delta and Omicron variants in Colorado. During that period, several school-based SARS-CoV-2 mitigation measures were mandatory in Colorado (e.g., masking and classroom cohorting), and in-person learning was interspersed with remote learning for intermittent school closures or hybrid learning models. Despite those measures and questions of whether children were at lower risk for infection with and transmission of SARS-CoV-2, compared with reported viral test results, our study shows that SARS-CoV-2 prevalence among children was higher. Those findings may have broad implications for estimating the severity of SARS-CoV-2 among children, levels of potential immunity, and the effectiveness of various mitigation measures in the pediatric population, and they may help guide future public health recommendations.

Our study did not evaluate causal mechanisms for the observed racial/ethnic disparities in previous SARS-CoV-2 infection or seropositive case ascertainment. However, those findings could be explained by the existing literature, which suggests differences in risk for exposure to SARS-CoV-2 because of occupation or living setting, test-seeking behavior, underlying health and healthcare disparities, or differential barriers to viral testing (*22*,*28*). Despite extensive efforts at the federal, state, and local levels to improve access to free SARS-CoV-2 testing throughout Colorado during the study period, some barriers to access (e.g., time and transportation) may persist in some communities. In addition, differences in individual factors (e.g., perceived vulnerability and variability in access to childcare) could guide testing-seeking behaviors. The discrepancy between the number of seropositive children with any prior test (162, 53.3%;

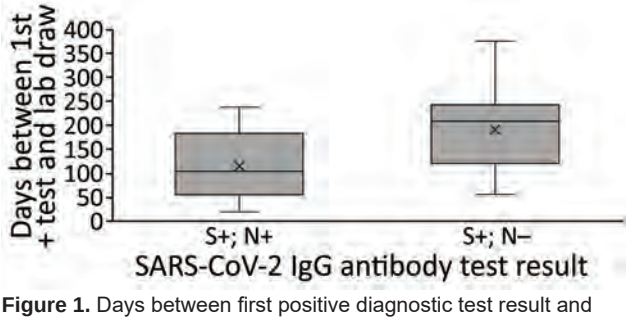


**Figure 1.** Days between first positive diagnostic test result and sample collection for serology testing for SARS-CoV-2 IgG, Colorado, USA, May 12–July 13, 2021. N, nucleocapsid; S, spike.

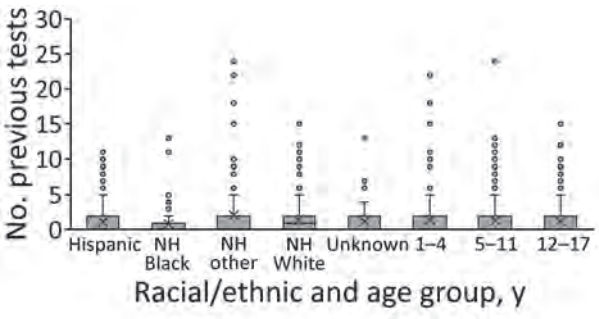


**Figure 2.** Boxplots showing number of previous tests, by racial/ethnic and age groups, among 829 children included in seroprevalence and case ascertainment analyses, Colorado, USA, May 12–July 13, 2021. NH, non-Hispanic.

Appendix Table 3) and the number with previous positive test results (50, 16.4%) suggests that timing of viral testing or changes in access over time may also complicate case identification efforts. That 53% of seropositive persons had been previously tested but only 16% ever received a positive test result suggests that access to testing is necessary but not sufficient for identifying cases. The overall number of previous tests was skewed toward zero across all racial/ethnic and age groups; however, each group had outliers with high numbers of prior testing (Figure 2). The only group with a median number of tests >0 was non-Hispanic White children. To improve case finding within this population, greater knowledge of drivers for and access to viral testing is needed. Among children, for whom cases are often asymptomatic or mildly symptomatic, pursuing regular screening and postexposure testing may be needed to improve case ascertainment or better incorporate pediatric specimens in serosurveys to provide more information about disease prevalence. These considerations may also apply to other populations with largely asymptomatic illness, possible future SARS-CoV-2 variants that may cause fewer symptoms, or emergence of novel respiratory viruses with similar symptoms in children.

Results from this study are also consistent with literature suggesting that the SARS-CoV-2 spike IgG response may be more durable than the nucleocapsid IgG response because children who were spike IgG positive but nucleocapsid IgG negative were further from their positive test result at the time of serum sampling (*29*–*34*). As with any laboratory test, knowledge of the test characteristics, including seroreversion over time in the case of serology tests, is relevant for study design and interpreting results. The differential kinetics of IgG response after SARS-CoV-2 infection require further study, should inform serosurveillance efforts, and may complicate the ability to estimate SARS-CoV-2 prevalence among vaccinated populations.

Among the limitations of this study, the use of reported COVID-19 PCR and other molecular viral testing may miss some positive results from viral tests, such as antigen tests and testing performed out of state. However, during the study period, antigen tests were not widely available in Colorado, and molecular tests were the recommended test for schools. Free testing services provided by the state throughout Colorado used PCR testing, as did other large testing providers serving schools during the study period. Similarly, use of the Colorado Immunization Information System to determine vaccination status might lead to misclassification of some children as unvaccinated, although the time between specimen collection and data analysis should greatly limit the potential for missing vaccine data.

Second, unadjusted results from the study convenience sample may not be generalizable to other pediatric populations. Exclusion of previously vaccinated children could introduce some bias because only certain age groups were eligible for vaccination and vaccinated children may differ in relevant ways from their unvaccinated peers. Specifically, half of excluded vaccinees were non-Hispanic White children, and all were 12–17 years of age. However, we believe that exclusion of this group (Appendix Table 1) is likely to bias the sample toward the null and may lead to underestimation of the disparities noted. Although residence was not included in the study, this convenience sample may overrepresent children from the Denver-metro area, who account for a larger percentage of the patient population in this healthcare system, reducing generalizability. Because specimens were selected from children within a large pediatric healthcare system, this study cohort may represent children with greater access to care and families who are more likely to seek care, which could be associated with fewer barriers to testing. This population may also have a greater number of underlying health conditions, although our study sought to limit some of this bias by excluding children from subspecialty care clinics, which could lead to higher case ascertainment in this than in other populations. Similarly, SARS-CoV-2 positivity may be higher in the study cohort because symptomatic children seeking care and for whom providers ordered serum-based laboratory tests may be overrepresented, which could lead to higher seroprevalence.

Third, because of low numbers of members of certain racial/ethnic groups, including children in the non-Hispanic Asian, American Indian or

Alaskan Native, Native Hawaiian or other Pacific Islander, >1 race, or other race categories, we were unable to analyze completely disaggregated racial/ethnic groups. This limitation is notable because there are known health disparities in some of the aggregated racial/ethnic groups, and a sample powered for analysis of these groups may identify similar disparities in SARS-CoV-2 serologic results and case ascertainment.

Last, seroconversion is an imperfect proxy for measuring disease prevalence because not all persons seroconvert after SARS-CoV-2 infection, and some literature suggests that rates of seroconversion may be lower or that antibody waning after infection may be more rapid for children or those with asymptomatic or mild illness (*34*–*38*). However, because some data on this issue are conflicting, the potential effect on our results is unclear (*39*). Similarly, the exact test characteristics over time for the assays used are not well known.

Strengths of the study include our ability to individually match serologic results to associated vaccination and reported test results, which enabled us to make direct comparisons and avoids ecological fallacy, which can arise when inferring information about individuals based on results from population-based data. Also, oversampling of children 1–4 years of age and Black children improved the representativeness of our sample across subgroups, which enabled a more nuanced analysis of racial/ethnic differences in serologic results and case ascertainment.

In conclusion, before the Delta variant peak, we found evidence of previous SARS-CoV-2 infection in more than one third of Colorado children 1–17 years of age based on seroprevalence, despite far fewer confirmed cases in this study population. Repeating this analysis after the Delta and Omicron variant peaks would be prudent. Racial/ethnic disparities identified in this pediatric population are consistent with trends identified among adults; higher seroprevalence, lower rates of reported viral testing, and lower seropositive case ascertainment were found among Hispanic and Non-Hispanic Black children than among non-Hispanic White children. Continued efforts to address racial/ethnic differences in illness burden and potential barriers to viral testing in pediatric populations are warranted.

### Acknowledgments

We thank Gillian Andersen, Alice Campbell, Leah Huey, Patricia A. Merkel, and Amanda Pierce for assistance with specimen procurement and testing at the Children's Hospital of Colorado laboratory.

### About the Author

Dr. O'Brien is a preventive medicine physician and medical epidemiologist working for the CDPHE in Denver. Her research interests focus on issues at the intersection of public health and clinical medicine, including cancer prevention, communicable disease response, and immunization.

### References

1. Bialek S, Gierke R, Hughes M, McNamara LA, Pilishvili T, Skoff T; CDC COVID-19 Response Team. Coronavirus disease 2019 in children—United States, February 12–April 2, 2020. MMWR Morb Mortal Wkly Rep. 2020;69:422–6. https://doi.org/10.15585/mmwr.mm6914e4
2. Dong Y, Mo X, Hu Y, Qi X, Jiang F, Jiang Z, et al. Epidemiology of COVID-19 among children in China. Pediatrics. 2020;145:e20200702. https://doi.org/10.1542/peds.2020-0702
3. Gaythorpe KAM, Bhatia S, Mangal T, Unwin HJT, Imai N, Cuomo-Dannenburg G, et al. Children's role in the COVID-19 pandemic: a systematic review of early surveillance data on susceptibility, severity, and transmissibility. Sci Rep. 2021;11:13903. https://doi.org/10.1038/s41598-021-92500-9
4. Mehta NS, Mytton OT, Mullins EWS, Fowler TA, Falconer CL, Murphy OB, et al. SARS-CoV-2 (COVID-19): what do we know about children? A systematic review. Clin Infect Dis. 2020;71:2469–79. https://doi.org/10.1093/cid/ciaa556
5. Molteni E, Sudre CH, Canas LS, Bhopal SS, Hughes RC, Antonelli M, et al. Illness duration and symptom profile in symptomatic UK school-aged children tested for SARS-CoV-2. Lancet Child Adolesc Health. 2021;5:708–18. https://doi.org/10.1016/S2352-4642(21)00198-X
6. Rankin DA, Talj R, Howard LM, Halasa NB. Epidemiologic trends and characteristics of SARS-CoV-2 infections among children in the United States. Curr Opin Pediatr. 2021;33:114–21. https://doi.org/10.1097/MOP.0000000000000971
7. Williams PCM, Howard-Jones AR, Hsu P, Palasanthiran P, Gray PE, McMullan BJ, et al. SARS-CoV-2 in children: spectrum of disease, transmission and immunopathological underpinnings. Pathology. 2020;52:801–8. https://doi.org/10.1016/j.pathol.2020.08.001
8. Zimmermann P, Curtis N. COVID-19 in children, pregnancy and neonates: a review of epidemiologic and clinical features. Pediatr Infect Dis J. 2020;39:469–77. https://doi.org/10.1097/INF.0000000000002700
9. Comar M, Benvenuto S, Lazzerini M, Fedele G, Barbi E, Amaddeo A, et al. Prevalence of SARS-CoV-2 infection in Italian pediatric population: a regional seroepidemiological study. Ital J Pediatr. 2021;47:131. https://doi.org/10.1186/s13052-021-01074-9
10. Espenhain L, Tribler S, Sværke Jørgensen C, Holm Hansen C, Wolff Sönksen U, Ethelberg S. Prevalence of SARS-CoV-2 antibodies in Denmark: nationwide, population-based seroepidemiological study. Eur J Epidemiol. 2021;36:715–25. https://doi.org/10.1007/s10654-021-00796-8
11. Hobbs CV, Drobeniuc J, Kittle T, Williams J, Byers P, Satheshkumar PS, et al.; CDC COVID-19 Response Team. Estimated SARS-CoV-2 seroprevalence among persons aged <18 years—Mississippi, May–September 2020. MMWR Morb Mortal Wkly Rep. 2021;70:312–5. https://doi.org/10.15585/mmwr.mm7009a4
12. Keuning MW, Grobben M, de Groen AC, Berman-de Jong EP, Bijlsma MW, Cohen S, et al. Saliva SARS-CoV-2 antibody prevalence in children. Microbiol Spectr. 2021;9:e0073121. https://doi.org/10.1128/Spectrum.00731-21

13. Rytter MJH, Nygaard U, Mandic IN, Glenthøj JP, Schmidt LS, Cortes D, et al. Prevalence of SARS-CoV-2 antibodies in Danish children and adults. Pediatr Infect Dis J. 2021;40: e157–9. https://doi.org/10.1097/INF.0000000000003048
14. Thamm R, Buttmann-Schweiger N, Fiebig J, Poethko-Müller C, Prütz F, Sarganas G, et al. Seroprevalence of SARS-CoV-2 among children and adolescents in Germany—an overview [in German]. Bundesgesundheitsblatt Gesundheitsforschung Gesundheitsschutz. 2021;64:1483–91.
15. Tönshoff B, Müller B, Elling R, Renk H, Meissner P, Hengel H, et al. Prevalence of SARS-CoV-2 infection in children and their parents in southwest Germany. JAMA Pediatr. 2021;175:586–93. https://doi.org/10.1001/jamapediatrics.2021.0001
16. Zinszer K, McKinnon B, Bourque N, Pierce L, Saucier A, Otis A, et al. Seroprevalence of SARS-CoV-2 antibodies among children in school and day care in Montreal, Canada. JAMA Netw Open. 2021;4:e2135975. https://doi.org/10.1001/jamanetworkopen.2021.35975
17. Gibbons CL, Mangen MJ, Plass D, Havelaar AH, Brooke RJ, Kramarz P, et al.; Burden of Communicable Diseases in Europe (BCoDE) Consortium. Measuring underreporting and under-ascertainment in infectious disease datasets: a comparison of methods. BMC Public Health. 2014;14:147. https://doi.org/10.1186/1471-2458-14-147
18. Centers for Disease Control and Prevention. COVID-19 serology surveillance strategy [cited 2022 Jan 30]. https://www.cdc.gov/coronavirus/2019-ncov/covid-data/serology-surveillance/index.html
19. Tacker DH, Bashleben C, Long TC, Theel ES, Knight V, Kadkhoda K, et al. Interlaboratory agreement of severe acute respiratory syndrome coronavirus 2 (SARS-CoV-2) serologic assays in the expedited College of American Pathologists Proficiency Testing Program. Arch Pathol Lab Med. 2021;145:536–42. https://doi.org/10.5858/arpa.2020-0811-SA
20. Centers for Disease Control and Prevention. COVID data tracker [cited 2023 Mar 3]. https://covid.cdc.gov/covid-data-tracker
21. Couture A, Lyons BC, Mehrotra ML, Sosa L, Ezike N, Ahmed FS, et al. Severe acute respiratory syndrome coronavirus 2 seroprevalence and reported coronavirus disease 2019 cases in US children. Open Forum Infect Dis. 2022;9:ofac044. https://doi.org/10.1093/ofid/ofac044
22. Brandt K, Goel V, Keeler C, Bell GJ, Aiello AE, Corbie-Smith G, et al. SARS-CoV-2 testing in North Carolina: racial, ethnic, and geographic disparities. Health Place. 2021;69:102576. https://doi.org/10.1016/j.healthplace.2021.102576
23. Goyal MK, Simpson JN, Boyle MD, Badolato GM, Delaney M, McCarter R, et al. Racial and/or ethnic and socioeconomic disparities of SARS-CoV-2 infection among children. Pediatrics. 2020;146:e2020009951. https://doi.org/10.1542/peds.2020-009951
24. Inagaki K, Garg P, Hobbs CV. SARS-CoV-2 positivity rates among children of racial and ethnic minority groups in Mississippi. Pediatrics. 2021;147:e2020024349. https://doi.org/10.1542/peds.2020-024349
25. Jones JM, Stone M, Sulaeman H, Fink RV, Dave H, Levy ME, et al. Estimated US infection- and vaccine-induced SARS-CoV-2 seroprevalence based on blood donations, July 2020-May 2021. JAMA. 2021;326:1400–9. https://doi.org/10.1001/jama.2021.15161
26. Kugeler KJ, Podewils LJ, Alden NB, Burket TL, Kawasaki B, Biggerstaff BJ, et al. Assessment of SARS-CoV-2 seroprevalence by community survey and residual specimens, Denver, Colorado, July-August 2020. Public Health Rep. 2022; 137:128–36. https://doi.org/10.1177/00333549211055137
27. Saatci D, Ranger TA, Garriga C, Clift AK, Zaccardi F, Tan PS, et al. Association between race and COVID-19 outcomes among 2.6 million children in England. JAMA Pediatr. 2021;175:928–38. https://doi.org/10.1001/jamapediatrics.2021.1685
28. Smitherman LC, Golden WC, Walton JR. Health disparities and their effects on children and their caregivers during the coronavirus disease 2019 pandemic. Pediatr Clin North Am. 2021;68:1133–45. https://doi.org/10.1016/j.pcl.2021.05.013
29. Fenwick C, Croxatto A, Coste AT, Pojer F, André C, Pellaton C, et al. Changes in SARS-CoV-2 spike versus nucleoprotein antibody responses impact the estimates of infections in population-based seroprevalence studies. J Virol. 2021;95:e01828–20. https://doi.org/10.1128/JVI.01828-20
30. Gallais F, Gantner P, Bruel T, Velay A, Planas D, Wendling MJ, et al. Evolution of antibody responses up to 13 months after SARS-CoV-2 infection and risk of reinfection. BioMedicine. 2021;71:103561. https://doi.org/10.1016/j.ebiom.2021.103561
31. Ortega N, Ribes M, Vidal M, Rubio R, Aguilar R, Williams S, et al. Seven-month kinetics of SARS-CoV-2 antibodies and role of pre-existing antibodies to human coronaviruses. Nat Commun. 2021;12:4740. https://doi.org/10.1038/s41467-021-24979-9
32. Spencer EA, Klang E, Dolinger M, Pittman N, Dubinsky MC. Seroconversion following SARS-CoV-2 infection or vaccination in pediatric IBD patients. Inflamm Bowel Dis. 2021;27:1862–4. https://doi.org/10.1093/ibd/izab194
33. Van Elslande J, Gruwier L, Godderis L, Vermeersch P. Estimated half-life of SARS-CoV-2 spike antibodies more than double the half-life of nucleocapsid antibodies in healthcare workers. Clin Infect Dis. 2021;73:2366–8. https://doi.org/10.1093/cid/ciab219
34. Weisberg SP, Connors TJ, Zhu Y, Baldwin MR, Lin WH, Wontakal S, et al. Distinct antibody responses to SARS-CoV-2 in children and adults across the COVID-19 clinical spectrum. Nat Immunol. 2021;22:25–31. https://doi.org/10.1038/s41590-020-00826-9
35. Dobaño C, Ramírez-Morros A, Alonso S, Rubio R, Ruiz-Olalla G, Vidal-Alaball J, et al. Sustained seropositivity up to 20.5 months after COVID-19. BMC Med. 2022;20:379. https://doi.org/10.1186/s12916-022-02570-3
36. Liu W, Russell RM, Bibollet-Ruche F, Skelly AN, Sherrill-Mix S, Freeman DA, et al. Predictors of nonseroconversion after SARS-CoV-2 infection. Emerg Infect Dis. 2021;27:2454–8. https://doi.org/10.3201/eid2709.211042
37. Peluso MJ, Takahashi S, Hakim J, Kelly JD, Torres L, Iyer NS, et al. SARS-CoV-2 antibody magnitude and detectability are driven by disease severity, timing, and assay. Sci Adv. 2021;7:eabh3409. https://doi.org/10.1126/sciadv.abh3409
38. Toh ZQ, Anderson J, Mazarakis N, Neeland M, Higgins RA, Rautenbacher K, et al. Comparison of seroconversion in children and adults with mild COVID-19. JAMA Netw Open. 2022;5:e221313. https://doi.org/10.1001/jamanetworkopen.2022.1313
39. Yung CF, Saffari SE, Mah SYY, Tan NWH, Chia WN, Thoon KC, et al. Analysis of neutralizing antibody levels in children and adolescents up to 16 months after SARS-CoV-2 infection. JAMA Pediatr. 2022;176:1142–3. https://doi.org/10.1001/jamapediatrics.2022.3072

Address for correspondence: Shannon C. O'Brien, Colorado Department of Public Health and Environment, 4300 Cherry Creek S Dr, Denver, CO 80246, USA; email: shannon.obrien@state.co.us

# Disparities in Implementing COVID-19 Prevention Strategies in Public Schools, United States, 2021–22 School Year

Sanjana Pampati, Catherine N. Rasberry, Zach Timpe, Luke McConnell, Shamia Moore, Patricia Spencer, Sarah Lee, Colleen Crittenden Murray, Susan Hocevar Adkins, Sarah Conklin, Xiaoyi Deng, Ronaldo Iachan, Tasneem Tripathi, Lisa C. Barrios

During the COVID-19 pandemic, US schools have been encouraged to take a layered approach to prevention, incorporating multiple strategies to curb transmission of SARS-CoV-2. Using survey data representative of US public K–12 schools (N = 437), we determined prevalence estimates of COVID-19 prevention strategies early in the 2021–22 school year and describe disparities in implementing strategies by school characteristics. Prevalence of prevention strategies ranged from 9.3% (offered COVID-19 screening testing to students and staff) to 95.1% (had a school-based system to report COVID-19 outcomes). Schools with a full-time school nurse or school-based health center had significantly higher odds of implementing several strategies, including those related to COVID-19 vaccination. We identified additional disparities in prevalence of strategies by locale, school level, and poverty. Advancing school health workforce and infrastructure, ensuring schools use available COVID-19 funding effectively, and promoting efforts in schools with the lowest prevalence of infection prevention strategies are needed for pandemic preparedness.

To prevent transmission of SARS-CoV-2, the virus that causes COVID-19, in school settings and maintain in-person learning during the 2021–22 school year, US schools implemented a range of COVID-19 prevention strategies (*1*–*4*). Since the pandemic began, the Centers for Disease Control and Prevention (CDC) has provided guidance for schools on strategies for COVID-19 prevention (*5*). This guidance evolved as new scientific evidence emerged but has consistently emphasized layering multiple prevention strategies. CDC updated guidance for COVID-19 prevention in schools in May 2022 (*5*); recommended core prevention strategies for schools included staying home when sick; optimizing ventilation; practicing proper hand hygiene and respiratory etiquette; performing cleaning and disinfection; and encouraging families, staff, and students to stay up to date on vaccines. Those core prevention strategies are important in preventing the spread of multiple infectious diseases. On the basis of local COVID-19 context, additional prevention strategies included mask requirements, COVID-19 screening and diagnostic testing, cohorting, ventilation improvements, case investigation and contact tracing, and quarantining. Many of the same strategies included in CDC guidance from May 2022 were also included in CDC guidance from August 2021 (*6*), when we conducted our study, and in COVID-19 guidance for safe schools from the American Academy of Pediatrics (AAP) in July 2021 (*7*), which included promoting vaccines, improving ventilation, testing, and cleaning.

Recommended infection prevention strategies varied in terms of expertise, staffing, infrastructure, and financial costs required for implementation. Delivery of specific health services in school settings (e.g., vaccines and tests) might require personnel with medical and public health expertise and existing infrastructure for offering services. For example, implementation studies of school-based influenza vaccination programs have underscored the importance of dedicated staff and program infrastructure for securing supplies and necessary funding, disseminating materials (e.g., consent forms), communicating about the program to students and families, and managing logistics (*8*). Numerous

Author affiliations: Centers for Disease Control and Prevention, Atlanta, Georgia, USA (S. Pampati, C.N. Rasberry, S. Lee, S. Hocevar Adkins, L.C. Barrios); ICF, Atlanta (Z. Timpe, L. McConnell, C. Crittenden Murray, S. Conklin, X. Deng, R. Iachan, T. Tripathi); Oak Ridge Institute for Science and Education, Oak Ridge, Tennessee, USA (S. Moore, P. Spencer)

DOI: https://doi.org/10.3201/eid2905.221533

other studies on school-based delivery of vaccines and COVID-19 tests also highlight the value of workforce capacity and infrastructure (*9*–*14*). Furthermore, staff shortages and gaps in expertise within schools might interplay with urban–rural disparities. One study in New Mexico found that nurses in rural schools were more likely to serve multiple campuses, more likely to have fewer years of formal education, and less likely to have continuing education in specific health topics (e.g., anaphylaxis) (*15*). Infection prevention strategies unrelated to health services might also vary by school characteristics. Ventilation improvement strategies, particularly more costly strategies such as upgrading heating, ventilation, and air conditioning (HVAC) systems, might vary by school poverty level. Household studies have found indoor environmental exposures are more concentrated in low-income households, partially because of inadequate ventilation and low air exchange rates (*16*). Evidence on disparities in infection prevention strategies has primarily focused on a single state or school district and a single prevention strategy or a narrow set of prevention strategies. Little is known about how implementing a comprehensive set of infection prevention strategies varies across kindergarten through 12th grade (K–12) schools in the United States by school characteristics. Such findings can guide interventions to improve schools' ability to prevent transmission of infectious diseases, identify schools to prioritize in resource allocation and capacity building to reduce disparities, and contribute to current and future emergency preparedness.

Accordingly, our study aimed to describe implementing infection prevention strategies relating to vaccines, ventilation, cleaning and disinfection, mask requirements, COVID-19 screening and diagnostic testing, cohorting, case investigation, contact tracing, and quarantining among a nationally representative sample of K–12 public schools early in the 2021–22 school year. The study period coincided with the surge of the of the SARS-CoV-2 Delta variant and was one of high community transmission nationwide, necessitating that all US schools incorporate layered COVID-19 prevention strategies. Further, we characterize disparities in implementation by school level, poverty, urban or rural classification, and presence of health personnel and infrastructure.

## Methods

### Data

The National School COVID-19 Prevention Study (NSCPS) was initiated to better understand implementation and effectiveness of infection prevention strategies in K–12 school settings (*17*,*18*). NSCPS is a population-based, longitudinal study designed to be representative of K–12 public schools in the United States. The study used a single-stage, stratified random sample of K–12 public schools based on strata defined by region (Northeast, South, Midwest, or West), school level (elementary, middle, or high), and National Center for Education Statistics (NCES) locale (city, town, suburb, or rural). School locale was categorized on the basis of the NCES locale classification scheme, derived from the US Census Bureau's standard urban and rural definitions, which are based on population size and proximity to populated areas (*19*). The allocation was nearly proportional to ensure approximately equal probabilities for schools, which is an efficient design for a survey in which schools (rather than students) are the unit of analysis.

The sampling frame for this study consisted of public K–12 schools. We excluded the following school types: private schools, alternative schools, schools providing special services to a pull-out population enrolled at another eligible school, schools run by the US Department of Defense, and schools with <30 students. We followed the cohort of schools for 5 waves of data collection from June 2021 through May 2022. For each wave, a school-level designee was invited to complete a survey on COVID-19 prevention strategies and COVID-19–related outcomes.

We report data from a cross-sectional analysis of wave 2, the first wave of the 2021–22 school year. The wave 2 survey was administered during October 5–November 19, 2021, and included 81 survey questions primarily assessing the implementation of COVID-19 prevention strategies. A draft version of the survey was pilot-tested with a small number of school principals (n = 8), whose feedback was incorporated in the final survey. Each participant was given a unique link to complete the survey online. Of the 1,602 schools invited to participate, 437 (27%) completed the survey. The primary survey respondents were principals (n = 340, unweighted) and school nurses (n = 39, unweighted). Respondents were offered an electronic gift card valued at $50 for their time and effort. This study was approved by the Institutional Review Board of ICF, a research and evaluation consulting firm, in accordance with CDC's policies.

### Measures

We examined 21 school-level prevention strategies (e.g., promoting vaccination) assessed through the survey questions (Appendix Table 1, https://wwwnc.cdc.gov/EID/article/29/5/22-1533-App1.pdf). We obtained 2 school-level characteristics

from the survey: having a school-based health center (SBHC) and having a full-time school nurse. We categorized school level as elementary (any grade from kindergarten through grade 4), middle (any grade 7 or 8), or high (any grade from 10 through 12). We did not use grades 5, 6, and 9 to categorize school level, and we considered schools categorized as multiple school levels (e.g., kindergarten through grade 8) to be separate schools for sampling purposes. We linked NSCPS surveys with the MDR database, which provides information about individual US schools (*20*). We used the percentage of students eligible for free or reduced-price meals during the 2019–20 school year as a proxy for school-level poverty (*21*,*22*). High-poverty schools had ≥76% of students eligible for free or reduced-price meals, mid-poverty schools had 26%–75% eligible, and low-poverty schools had ≤25% eligible (*23*). We categorized school locale according to the NCES locale classification scheme (town, suburb, rural, or city) (*19*). To capture local COVID-19 dynamics preceding survey administration, we pulled from CDC's county-level community transmission level data the total number of new cases per 100,000 persons within the previous 7 days in each school's county on September 23, 2021 (i.e., 2 weeks before the survey opened).

### Statistical Analyses

We accounted for survey nonresponse by creating survey weights. Examined school characteristics were not significantly associated with participation except for school affluence level, a measure in MDR's database summarizing the socioeconomic status of a school derived through a proprietary algorithm (*20*). Schools that were low or below average in affluence were more likely to participate than schools that were average, above average, or high in affluence; thus, we used school affluence to develop nonresponse adjustment classes (Appendix Table 2). We calculated the weighted prevalence of each prevention strategy and 95% CIs for the overall sample. We also calculated unweighted numbers, weighted prevalence, and 95% CIs of strategies by school-level characteristics and used $\chi^2$ tests to identify differences. We ran separate weighted logistic regression models with each COVID-19 prevention strategy as the dependent variable and school-level characteristics (i.e., school level, NCES locale, school poverty, having a full-time school nurse, and having an SBHC) as the independent variables, controlling for new cases per 100,000 persons in the previous 7 days in the county. We selected independent and control variables on the basis of a review of literature on factors influencing implementation of infection prevention strategies in schools; selected controls satisfied criteria for confounder selection (*24*). We calculated adjusted odds ratios (aORs) and defined differences with p values <0.05 as statistically significant. We conducted analyses in R 4.1.2 (The R Foundation for Statistical Computing, https://www.r-project.org) by using the survey package (*25*).

## Results

Participating schools were heterogenous in terms of school level, urban status, size, and the racial composition (Appendix Table 2). Most schools reported having had a school-based system to report COVID-19 outcomes (95.1% [95% CI 92.5%–96.8%]), had a COVID-19 isolation space in school (92.5% [95% CI 89.4%–94.7%]), quarantined students identified as close contacts (83.5% [95% CI 79.3%–87.0%]), adhered to at least daily or between-use cleaning schedules (79.7% [95% CI 75.5%–83.4%]), inspected and validated existing HVAC systems (74.6% [95% CI 69.8%–78.8%]), and maintained a physical distance of ≥3 feet in classrooms (74.3% [95% CI 69.8%–78.4%]) (Table, https://wwwnc.cdc.gov/EID/article/29/5/22-1533-T1.htm). In addition, more than two thirds of schools offered COVID-19 diagnostic testing to students and staff (68.7% [95% CI 63.8%–73.3%]) and opened windows when safe to do so (66.8% [95% CI 62.2%–71.1%]). Approximately two thirds of schools required masks for students and staff (66.4% [95% CI 61.9%–70.6%]). Less than one third of schools reported having offered COVID-19 screening testing to students and staff (9.3% [95% CI 6.9%–12.5%]), installed or used high-efficiency particulate air (HEPA) filtration systems in classrooms (27.3% [95% CI 23.3%–31.7%]), and provided COVID-19 vaccines on-campus to staff, students, or their families (30.9% [95% CI 26.5%–35.8%]).

### School-Level Mask Requirements, Ventilation Improvements, and Cleaning Procedures

Bivariate analysis indicated that, among 7 strategies related to school-level mask requirements, ventilation improvements, and cleaning procedures, none varied by school level, 2 varied by NCES locale, 4 varied by school poverty, and 1 varied by whether the school had a full-time school nurse and SBHC (Appendix Table 3). After adjustment for all examined school-level characteristics and the county COVID-19 case rate, mid-poverty schools had lower odds of having inspected and validated existing HVAC systems (aOR 0.37 [95% CI 0.16–0.84]), used HEPA filtration systems in classrooms (aOR 0.52 [95% CI 0.28–0.96]), and opened

windows when safe to do so (aOR 0.48 [95% CI 0.24–0.95]) than did low-poverty schools (Appendix Table 4). Rural schools had lower odds of having installed or used HEPA filtration systems in classrooms (aOR 0.36 [95% CI 0.17–0.76]) than did city schools. However, rural schools had higher odds of having opened doors (aOR 2.08 [95% CI 1.03–4.17]) and opened windows (aOR 4.51 [95% CI 2.11–9.60]) when safe to do so compared with city schools. Town schools had lower odds of having required masks for students and staff (aOR 0.38 [95% CI 0.17–0.85]) than did city schools. Schools with a full-time school nurse had lower odds of having opened doors when safe to do so (aOR 0.57 [95% CI 0.34–0.96]) than did schools without.

### Physical Distancing, Isolation Space, COVID-19 Testing and Screening, Contact Tracing, and Quarantine Protocols

Bivariate analysis indicated that, among 7 strategies relating to physical distancing, isolation space, COVID-19 testing and screening, contact tracing, and quarantine protocols, none varied by school level, NCES locale, school poverty, or having an SBHC, and 2 varied by having a full-time school nurse (Appendix Table 5). After adjustment for all examined school-level characteristics and the county COVID-19 case rate, schools that had a full-time school nurse had higher odds of having quarantined students identified as close contacts (aOR 2.02 [95% CI 1.05–3.91]) than did schools without (Appendix Table 6).

### Promoting and Tracking Vaccination of Students and Staff

Bivariate analysis indicated that, among 7 strategies relating to efforts to promote and track vaccination of students and staff, 3 varied by school level, 2 varied by NCES locale, 3 varied by school poverty, 3 varied by having a full-time school nurse, and 4 varied by having an SBHC (Appendix Table 7). After adjustment for all examined school-level characteristics and the county COVID-19 case rate, compared with high schools, elementary schools had lower odds of having provided information on COVID-19 vaccines to parents (aOR 0.49 [95% CI 0.25–0.97]); provided information on COVID-19 vaccines to students (aOR 0.15 [95% CI 0.08–0.29]); provided COVID-19 vaccines on-campus to staff, students, or their families (aOR 0.47 [95% CI 0.26–0.87]); and tracked vaccination status of students (aOR 0.45 [95% CI 0.24–0.83]) (Appendix Table 8). Compared with high schools, middle schools had lower odds of having provided information on COVID-19 vaccines to students (aOR 0.39 [95% CI 0.20–0.79]); provided COVID-19 vaccines through school district events to staff, students, or their families (aOR 0.44 [95% CI 0.21–0.92]); and tracked vaccination status of staff (aOR 0.44 [95% CI 0.20–0.95]). High-poverty schools had higher odds of having provided information on COVID-19 vaccines to students (aOR 3.88 [95% CI 1.81–8.30]) and provided COVID-19 vaccines through school district events to staff, students, or their families (aOR 2.47 [95% CI 1.23–4.98]) compared with low-poverty schools. Mid-poverty schools had higher odds of having provided parents or students with information about catching up on missed healthcare (e.g., routine vaccines (aOR 1.91 [95% CI 1.06–3.44]) compared with low-poverty schools. Rural schools had lower odds of having provided COVID-19 vaccines through school district events to staff, students, or their families (aOR 0.45 [95% CI 0.23–0.88]) and tracked vaccination status of staff (aOR 0.45 [95% CI 0.23–0.90]) than city schools. Town schools had higher odds of having tracked the vaccination status of students (aOR 3.09 [95% CI 1.36–7.01]) than city schools. Schools that had a full-time school nurse had higher odds of having tracked the vaccination status of students (aOR 1.80 [95% CI 1.07–3.03]) than those that did not. Schools that had an SBHC had higher odds of having provided COVID-19 vaccines on campus to staff, students, or their families (aOR 2.00 [95% CI 1.03–3.89]) and of having provided COVID-19 vaccines through school district events to staff, students, or their families (aOR 2.25 [95% CI 1.18–4.30]) than those that did not.

## Discussion

At the time of our study, guidance from CDC and AAP recommended a layered approach to COVID-19 prevention in schools, incorporating multiple strategies to curb transmission of SARS-CoV-2 and protect students, staff, and families while maintaining in-person learning (*6*,*7*). These approaches were used to varying degrees by schools, as affirmed by our findings. This heterogeneity might be partially attributable to school-level inequities predating the COVID-19 pandemic (e.g., in terms of financial resources, available staff, and school infrastructure) that affect schools' ability to implement the recommended infection prevention strategies. The findings reflect not only school-based responses to the pandemic but also the expertise and resources required to implement infection prevention and control in schools more broadly.

In general, strategies that were less resource-intensive had greater uptake than those that were more resource-intensive. For example, most schools reported requiring masks for students and staff. In contrast, prevalence was lower for providing

COVID-19 screening testing to students and staff or providing COVID-19 vaccines on-campus to staff, students, or their families. Numerous methods to support school-based vaccination and COVID-19 testing have been documented (e.g., partnerships with local health departments, workforce capacity, and communication with parents and students), as have challenges (e.g., staffing shortages, availability of testing supplies, lack of perceived community support, difficulty reporting test results and obtaining consent forms, and low participation) (*9*–*14*). Identifying additional sources of support at school, school district, community, health department, state, and federal levels might strengthen schools' capacity to respond to public health emergencies.

Several strategies that are recommended regardless of local COVID-19 community levels, according to updates to CDC guidance released in May 2022 (*5*), such as promoting routine vaccines, had low uptake. Differences in COVID-19 vaccination promotion by school level were likely because vaccines were not approved or widely available for most elementary school–aged children at the time. Only half of schools provided parents or students with information about catching up on missed healthcare (e.g., routine vaccines), which is concerning given recent declines in childhood vaccination coverage (*26*–*28*). Schools can play an important role in educating about, linking to, or directly offering vaccines in accordance with local or state policies, including COVID-19 and routine pediatric vaccines, and CDC has resources for schools and community partners to support such efforts (*29*).

Schools with health infrastructure and personnel (i.e., having an SBHC or full-time nurse) were more likely to have certain prevention strategies in place even after adjustment for other school- and county-level characteristics. Schools with an SBHC might be better equipped to respond to public health emergencies and provide certain health services (e.g., vaccines). The National Association of School Nurses and AAP recommend that every school have a full-time school nurse (*30*,*31*). Nurses undergo training in infection prevention and control, serve as liaisons with local health officials, and are well-positioned to develop comprehensive emergency response procedures (*32*,*33*). Our finding that schools with a full-time school nurse were more likely to have several prevention strategies extends a robust body of research that has linked school nurses to health-promoting practices and programs in schools and positive student health- and service-related outcomes (*30*,*34*). In our study, 60.4% of schools had a full-time school nurse, and only 17.3% had an SBHC. The White House's 2022 National COVID-19 Preparedness Plan explicitly acknowledges investing in the expansion of nurses in schools as a priority (*35*). Such investments in the school nurse workforce, as well as in expanding the health infrastructure of schools, could provide immediate benefits for COVID-19 prevention in schools and also lead to long-term gains in emergency preparedness for schools, as well as positive downstream effects for other student health-related outcomes.

Since March 2020, the federal government has approved billions of dollars in funding to cover pandemic-related costs for K–12 schools through the US Department of Education's Elementary and Secondary Schools Emergency Relief Fund (*36*), the Governor's Emergency Education Relief Fund (*37*), the US Department of Health and Humans Services' Head Start and Child Care American Rescue Plan funds (*38*), and the Epidemiology and Laboratory Capacity for Prevention and Control of Emerging Infectious Diseases Reopening Schools supplement (*39*). Mid-poverty schools had the lowest prevalence of several prevention strategies, including higher-cost strategies to improve ventilation (e.g., HEPA filtration systems in classrooms), compared with low-poverty and high-poverty schools, as noted in a previous NSCPS publication (*17*). One possible hypothesis explaining this pattern is high-poverty schools might have more experience applying for federal funding and might be prioritized by state and local education agencies for these funds. A recent survey found school districts with a higher percentage of free or reduced-price meal eligibility were more likely to use federal COVID-19 funds for ventilation improvements (*40*). Low-poverty schools might have more existing operational and discretionary funds to rely on for implementation of prevention strategies. Taken together, although all schools might benefit from additional support in implementing prevention strategies, mid-poverty schools, in particular, could require more strategic efforts.

One limitation of our study is that the survey assessed presence of prevention strategies but not nuances related to compliance, participation, and fidelity. Second, the reporting of certain prevention strategies might be subject to social-desirability biases, leading to respondents overreporting that certain strategies were in place. Third, the response rate for our survey was low (27%); however, most school-level characteristics were not associated with survey participation based on our nonresponse analysis (Appendix Table 2), and nonresponse weight adjustments were incorporated. Fourth, because of a limited sample, the presence of unmeasured confounders,

and minimal clustering at certain levels (e.g., school district level), we were limited in the number and type of controls we could use. For example, state policies (e.g., mask mandates) may have affected schools' ability to implement specific prevention strategies (e.g., mask requirements). Future studies may benefit from examining various levels of influence (e.g., national, state, and school district), as well as their interplay with school characteristics, on schools' implementation of infection prevention strategies.

Despite those limitations, our study expands understanding of COVID-19 prevention strategies used by schools during the 2021–22 school year, by using data from a population-based sample drawn to be representative of K–12 public schools in the United States. Our study documents strategy implementation at the school level, as opposed to the school district level. Although COVID-19 prevention policies are likely set at the school district level, variation exists in what schools implement, and measuring implementation at the school-level can better capture what occurred in practice. Because survey administration coincided with the surge of the SARS-CoV-2 Delta variant, the period examined represents one of high community transmission nationally, which necessitated layered prevention strategies in all schools. Moving forward, schools might consider adapting to their local context and monitoring COVID-19 community levels to guide implementation of prevention strategies (*41*). Our findings show variation in the prevalence of strategy implementation, including lower implementation of several strategies that can be more resource-intensive, particularly among mid-poverty schools, and increased implementation for several key strategies among schools with expanded health infrastructure (e.g., having a full-time school nurse, SBHC, or both). Our findings suggest a need to enhance efforts to ensure schools can take advantage of available federal funding for COVID-19 prevention. Advancing the school health workforce and infrastructure across US schools could provide stronger support for pandemic preparedness.

### Acknowledgments

We thank the school staff for their participation in the study and their willingness to provide insights on COVID-19 prevention. In addition, we acknowledge James Demery, Cherrelle Dorleans, Brandee Hicks, Adrian King, Erica McCoy, Leah Powell, Lynnea Roberts, India Rose, April Carswell, Syreeta Skelton-Wilson, Carmen Ashley, Lorin Boyce, Nancy Brener, Michelle Carman-McClanahan, Marci Hertz, Neha Kanade Cramer, Dana Keener Mast, Catherine Lesesne, Seraphine Pitt Barnes, Leah Robin, Lucas Godoy Garraza, Nicole Gonzalez, and Christine Walrath for their efforts related to the National School COVID-19 Prevention Study.

This study is funded, in part, by a task order (no. 75D30121F10577) directed from CDC to ICF.

### About the Author

Ms. Pampati is a health scientist in the Division of Adolescent and School Health, National Center for HIV/AIDS, Viral Hepatitis, STD, and TB Prevention, CDC. Her works aims to advance the evidence base for effective programs and policies that reduce illness and death from COVID-19, HIV, and sexually transmitted infections among child and adolescent populations.

### References

1. Lessler J, Grabowski MK, Grantz KH, Badillo-Goicoechea E, Metcalf CJE, Lupton-Smith C, et al. Household COVID-19 risk and in-person schooling. Science. 2021;372:1092–7. https://doi.org/10.1126/science.abh2939
2. US Department of Education Institute of Education Sciences. 2022 School Pulse Panel. 2022 [cited 2022 Jun 30]. https://ies.ed.gov/schoolsurvey/spp
3. Wiens KE, Smith CP, Badillo-Goicoechea E, Grantz KH, Grabowski MK, Azman AS, et al. In-person schooling and associated COVID-19 risk in the United States over spring semester 2021. Sci Adv. 2022;8:eabm9128. https://doi.org/10.1126/sciadv.abm9128
4. Krishnaratne S, Pfadenhauer LM, Coenen M, Geffert K, Jung-Sievers C, Klinger C, et al. Measures implemented in the school setting to contain the COVID–19 pandemic: a rapid scoping review. Cochrane Database Syst Rev. 2020;12(12):CD013812.
5. Centers for Disease Control and Prevention. Operational guidance for K-12 schools and early care and education programs to support safe in-person learning (May 2022 update). 2022 [cited 2023 Jan 24]. https:/www.cdc.gov/coronavirus/2019-ncov/community/schools-childcare/k-12-childcare-guidance.html
6. Centers for Disease Control and Prevention. Guidance for COVID-19 prevention in K-12 schools (August 2021 update). 2021 [cited 2023 Jan 24]. https://web.archive.org/web/20211021081927/http:/cdc.gov/coronavirus/2019-ncov/community/schools-childcare/k-12-guidance.html
7. American Academy of Pediatrics. COVID-19 guidance for safe schools and promotion of in-person learning. 2021 [cited 2023 Jan 22]. https://web.archive.org/web/20210819180640/https://www.aap.org/en/pages/2019-novel-coronavirus-covid-19-infections/clinical-guidance/covid-19-planning-considerations-return-to-in-person-education-in-schools
8. Tran CH, McElrath J, Hughes P, Ryan K, Munden J, Castleman JB, et al. Implementing a community-supported school-based influenza immunization program. Biosecur Bioterror. 2010;8:331–41. https://doi.org/10.1089/bsp.2010.0029
9. Neatherlin J, Thomas ES, Barrios LC. Test-to-stay programs in schools are effective, but are they equitable? Pediatrics. 2022;149:e2021055930. https://doi.org/10.1542/peds.2021-055930

10. Schechter-Perkins EM, Doron S, Johnston R, Hay J, Berlin D, Ciaranello A, et al. A test-to-stay modified quarantine program for COVID-19 in schools. Pediatrics. 2022;149:e2021055727. https://doi.org/10.1542/peds.2021-055727
11. Lanier WA, Babitz KD, Collingwood A, Graul MF, Dickson S, Cunningham L, et al. COVID-19 testing to sustain in-person instruction and extracurricular activities in high schools—Utah, November 2020–March 2021. MMWR Morb Mortal Wkly Rep. 2021;70:785–91. https://doi.org/10.15585/mmwr.mm7021e2
12. Haroz EE, Kalb LG, Newland JG, Goldman JL, Mast DK, Ko LK, et al. Implementation of school-based COVID-19 testing programs in underserved populations. Pediatrics. 2022;149(12 Suppl 2):e2021054268G.
13. Batista Ferrer H, Trotter CL, Hickman M, Audrey S. Barriers and facilitators to uptake of the school-based HPV vaccination programme in an ethnically diverse group of young women. J Public Health (Oxf). 2016;38:569–77. https://doi.org/10.1093/pubmed/fdv073
14. Perman S, Turner S, Ramsay AI, Baim-Lance A, Utley M, Fulop NJ. School-based vaccination programmes: a systematic review of the evidence on organisation and delivery in high income countries. BMC Public Health. 2017;17:252. https://doi.org/10.1186/s12889-017-4168-0
15. Ramos MM, Fullerton L, Sapien R, Greenberg C, Bauer-Creegan J. Rural-urban disparities in school nursing: implications for continuing education and rural school health. J Rural Health. 2014;30:265–74. https://doi.org/10.1111/jrh.12058
16. Adamkiewicz G, Zota AR, Fabian MP, Chahine T, Julien R, Spengler JD, et al. Moving environmental justice indoors: understanding structural influences on residential exposure patterns in low-income communities. Am J Public Health. 2011;101(Suppl 1):S238–45. https://doi.org/10.2105/AJPH.2011.300119
17. Pampati S, Rasberry CN, McConnell L, Timpe Z, Lee S, Spencer P, et al. Ventilation improvement strategies among K-12 public schools—the National School COVID-19 Prevention Study, United States, February 14–March 27, 2022. MMWR Morb Mortal Wkly Rep. 2022;71:770–5. https://doi.org/10.15585/mmwr.mm7123e2
18. Centers for Disease Control and Prevention. National School COVID-19 Prevention Study (NSCPS). 2021 [cited 2022 Jun 16]. https://www.cdc.gov/healthyyouth/data/nscps/index.htm
19. National Center for Education Statistics. Locale classifications [cited 2022 Apr 4]. https://nces.ed.gov/programs/edge/Geographic/LocaleBoundaries
20. MDR. Education data [cited 2022 Jun 30]. https://mdreducation.com/data-and-analytics
21. Jones SE, Underwood JM, Pampati S, Le VD, DeGue S, Demissie Z, et al. School-level poverty and persistent feelings of sadness or hopelessness, suicidality, and experiences with violence victimization among public high school students. J Health Care Poor Underserved. 2020;31:1248–63. https://doi.org/10.1353/hpu.2020.0092
22. Underwood JM, Pampati S, Everett Jones S, Bryan LN, Demissie Z, Cavalier Y, et al. School-level poverty and rurality associated with differences in sexual risk behaviors among U.S. public high school students. J Adolesc Health. 2021;69:964–9. https://doi.org/10.1016/j.jadohealth.2021.06.005
23. Snyder T, Musu-Gillette L. Free or reduced price lunch: a proxy for poverty. NCES Blog. 2015 Apr 16 [cited 2022 Apr 4]. https://nces.ed.gov/blogs/nces/post/free-or-reduced-price-lunch-a-proxy-for-poverty
24. VanderWeele TJ. Principles of confounder selection. Eur J Epidemiol. 2019;34:211–9. https://doi.org/10.1007/s10654-019-00494-6
25. Lumley T. Package 'survey'. 2022 Oct 14 [cited 2022 Aug 18]. https://cran.r-project.org/web/packages/survey/survey.pdf
26. Santoli JM, Lindley MC, DeSilva MB, Kharbanda EO, Daley MF, Galloway L, et al. Effects of the COVID-19 pandemic on routine pediatric vaccine ordering and administration—United States, 2020. MMWR Morb Mortal Wkly Rep. 2020;69:591–3. https://doi.org/10.15585/mmwr.mm6919e2
27. Bramer CA, Kimmins LM, Swanson R, Kuo J, Vranesich P, Jacques-Carroll LA, et al. Decline in child vaccination coverage during the COVID-19 pandemic—Michigan Care Improvement Registry, May 2016–May 2020. Am J Transplant. 2020;20:1930–1. https://doi.org/10.1111/ajt.16112
28. Seither R, Calhoun K, Yusuf OB, Dramann D, Mugerwa-Kasujja A, Knighton CL, et al. Vaccination coverage with selected vaccines and exemption rates among children in kindergarten—United States, 2021–22 school year. MMWR Morb Mortal Wkly Rep. 2023;72:26–32. https://doi.org/10.15585/mmwr.mm7202a2
29. Centers for Disease Control and Prevention. How schools can support COVID-19 vaccination. 2022 [cited 2022 Jun 16]. https://www.cdc.gov/vaccines/covid-19/planning/school-located-clinics/how-schools-can-support.html
30. Holmes BW, Sheetz A, Allison M, Ancona R, Attisha E, Beers N, et al.; Council On School Health. Role of the school nurse in providing school health services. Pediatrics. 2016;137:e20160852. https://doi.org/10.1542/peds.2016-0852
31. National Association of School Nurses. Student access to school nursing services. 2022 [cited 2022 Jun 16]. https://www.nasn.org/nasn-resources/professional- practice-documents/position-statements/ps-access-to-services
32. COVID Collaborative. Roadmap to healthy schools: building organizational capacity for infection prevention and control (IPC). 2021 Apr [cited 2022 Jun 16]. https://bestpractices-clearinghouse.ed.gov/docs/ResourcesLibrary_PDF/ED12-491a.pdf
33. National Association of School Nurses. Emergency preparedness and response in the school setting–the role of the school nurse. 2019 [cited 2022 Jun 16]. https://www.nasn.org/nasn-resources/professional-practice-documents/position-statements/ps-emergency-preparedness
34. Best NC, Oppewal S, Travers D. Exploring school nurse interventions and health and education outcomes: an integrative review. J Sch Nurs. 2018;34:14–27. https://doi.org/10.1177/1059840517745359
35. The White House. National COVID-19 Preparedness Plan. 2022 [cited 2022 Apr 20]. https://www.whitehouse.gov/wp-content/uploads/2022/03/NAT-COVID-19-PREPAREDNESS-PLAN.pdf
36. US Department of Education. Elementary and Secondary School Emergency Relief Fund [cited 2022 Jul 18]. https://oese.ed.gov/offices/education-stabilization-fund/elementary-secondary-school-emergency-relief-fund
37. US Department of Education. Governor's Emergency Education Relief Fund [cited 2022 Jul 18]. https://oese.ed.gov/offices/education-stabilization-fund/governors-emergency-education-relief-fund
38. US Department of Health and Human Services. FY 2021 American Rescue Plan funding increase for Head Start programs [cited 2022 Jul 18]. https://eclkc.ohs.acf.hhs.gov/policy/pi/acf-pi-hs-21-03
39. Centers for Disease Control and Prevention. ELC reopening schools: support for COVID-19 screening testing

to reopen and keep schools operating safely [cited 2022 Jul 18]. https://www.cdc.gov/ncezid/dpei/elc/covid-response/index.html

40. US Green Building Council. Managing air quality during the pandemic: how K-12 school addressed air quality in the second year of COVID-19. 2022 May 6 [cited 2022 May 17]. https://www.usgbc.org/resources/managing-air-quality-during-pandemic-how-k-12-schools-addressed-air-quality-second-year

41. Centers for Disease Control and Prevention. COVID-19 community levels. 2022 [cited 2022 May 17]. https://www.cdc.gov/coronavirus/2019-ncov/science/community-levels.html

Address for corresponding: Sanjana Pampati, Centers for Disease Control and Prevention,1600 Clifton Rd NE, Mailstop US8-1, Atlanta, GA 30329-4027, USA; email: mix2@cdc.gov

# *Leishmania donovani* Transmission Cycle Associated with Human Infection, *Phlebotomus alexandri* Sand Flies, and Hare Blood Meals, Israel[1]

Liora Studentsky, Laor Orshan, Fouad Akad, Irina Ben Avi, Debora Diaz, Shirly Elbaz, Orly Sagi, Gal Zagron, Lea Valinsky, Maya Davidovich-Cohen, Gad Baneth

Cutaneous leishmaniasis caused by *Leishmania major* or *L. tropica* and visceral leishmaniasis caused by *L. infantum* have been reported in Israel. We collected *Phlebotomus* spp. sand flies in the Negev desert of southern Israel to identify circulating *Leishmania* spp. Of 22,636 trapped sand flies, 80% were *P. alexandri*. We sequenced *Leishmania*-specific internal transcribed spacer 1 fragments and *K26* genes. Of 5,019 *Phlebotomus* female sand flies, 2.5% were *Leishmania* DNA–positive; 92% of infections were *L. donovani*. Phylogenetic analyses showed separate clustering of *L. donovani* and *L. infantum*. *P. alexandri* flies positive for *L. donovani* harbored blood meals from European hares. *Leishmania* DNA isolated from a patient with cutaneous leishmaniasis who lived in the survey area was identical to *L. donovani* from *P. alexandri* flies. We report circulation of *L. donovani*, a cause of visceral leishmaniasis, in southern Israel. Prompt diagnosis and *Leishmania* spp. identification are critical to prevent leishmaniasis progression.

Zoonotic leishmaniasis is endemic to Israel. *Leishmania tropica*, *L. major*, and *L. infantum* infect humans in different areas of Israel and circulate through distinct zoonotic transmission cycles (*1*). Cutaneous leishmaniasis (CL) is caused by *L. major*, which is transmitted by *Phlebotomus papatasi* sand flies, and *L. tropica*, which is transmitted by *P. sergenti* and *P. arabicus* sand flies. Canine leishmaniasis and human visceral leishmaniasis (VL) are caused by *L. infantum* in Israel, and the putative vectors are *P. perfiliewi*, *P. syriacus*, and *P. tobbi* sand flies (*1*–*9*). Reservoirs for *L. major* are sand rats (*Psammomys obesus*), gerbils (*Gerbillus dasyurus*), jirds (*Meriones crassus* and *M. tristrami*), and possibly also voles (*10*–*13*), whereas rock hyraxes (*Procavia capensis*) are considered the animal reservoir for *L. tropica* in Israel (*14*). Domestic dogs (*Canis lupus familiaris*), jackals (*C. aureus*), foxes (*Vulpes vulpes*), and wolves (*C. lupus*) are recognized reservoir hosts for *L. infantum* (*15*).

A substantial increase in CL incidence has been recorded since 2002, and endemic transmission has occurred in areas of Israel where it was previously unknown (*6*,*16*,*17*). Although not life-threatening, CL is a considerable public health problem in Israel; CL is diagnosed in hundreds of new patients annually. During 2001–2018, CL incidence rates increased 7-fold, from 0.4 to 2.9/100,000 population; a peak was observed in 2012, when the mean annual incidence increased to 4.4/100,000 population (*18*,*19*). Our study combines results from sand fly surveys, *Phlebotomus* spp. blood meal analysis, and human patient clinical data from the mountainous area of central Negev in southern Israel during the summer months of 2018–2020. We found a fourth leishmaniasis transmission cycle associated with human illness.

Author affiliations: Ministry of Health Central Laboratories for Public Health, Jerusalem, Israel (L. Studentsky, L. Orshan, I. Ben Avi, D. Diaz, S. Elbaz, M. Davidovich-Cohen); The Hebrew University of Jerusalem, Rehovot, Israel (L. Studentsky, G. Baneth); Ministry of Health National Laboratory for Public Health, Tel Aviv, Israel (F. Akad); Soroka University Medical Center, Beer-Sheba, Israel (O. Sagi); Israeli Ministry of Environmental Protection, Jerusalem (G. Zagron); Maccabi Healthcare Services, Tel Aviv (L. Valinsky)

DOI: https://doi.org/10.3201/eid2905.221657

[1]Data from this study were presented at the Israeli Society for Parasitology, Protozoology and Tropical Diseases Annual Meeting; March 21, 2022; Kfar Hamaccabiah, Ramat Gan, Israel.

## Materials and Methods

### Study Area and Sand Fly Trapping

We conducted our study in the mountainous desert area of central Negev in southern Israel (Figure 1). In this region, elevations range from 50 to 1,037 m above sea level, large differences occur between peak daytime and nighttime temperatures, and annual average precipitation is 30–150 mm (*20*,*21*). We collected sand flies outdoors in August 2018, September 2019, and August 2020 by using modified traps from the US Centers for Disease Control and Prevention. The traps operated without light and were powered by 2 AA (1.2V) rechargeable batteries and baited with ≈1 kg dry ice. We placed traps in an updraft vertical position overnight; openings were ≈10 cm above the ground, and collection cups hung above the motor and fan (*22*,*23*).

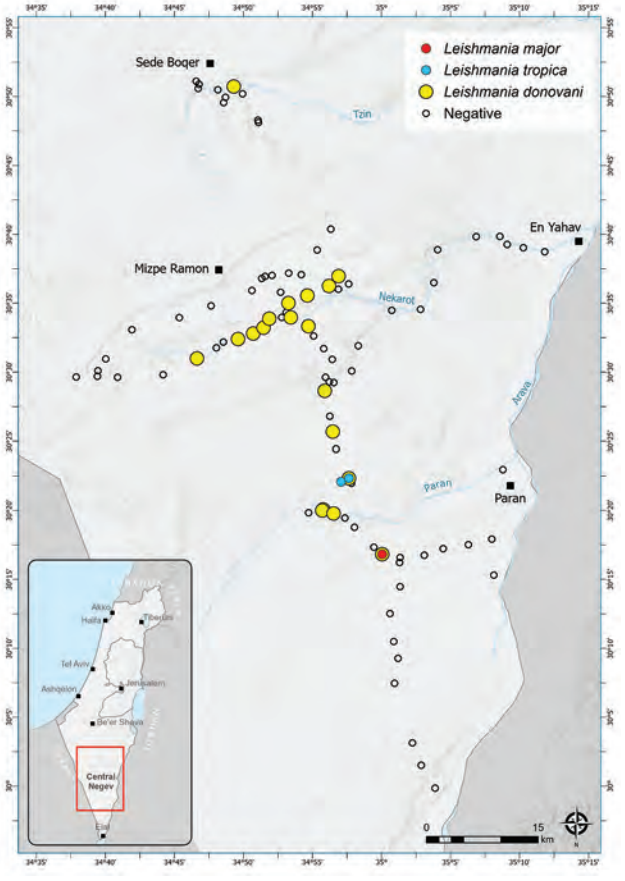


**Figure 1.** Locations of *Phlebotomus* spp. sand fly collection sites within the central Negev region of Israel in study of *Leishmania donovani* transmission cycle associated with human infection, *Phlebotomus alexandri* sand flies, and hare blood meals. We collected sand flies outdoors in August 2018, September 2019, and August 2020 by using modified traps from the US Centers for Disease Control and Prevention. The traps operated without light and were powered by 2 AA (1.2V) rechargeable batteries and baited with ≈1 kg dry ice. Traps were placed in an updraft vertical position overnight; openings were ≈10 cm above the ground, and collection cups hung above the motor and fan. Different colored circles indicate sites where specific *Leishmania* spp. infections were identified in trapped *Phlebotomus* sand flies. Empty circles indicate sites where sand flies were negative for *Leishmania* spp. Inset shows location of the survey area in Israel (red box).

### Identification and Sample Preparation

We transferred live sand fly catches to the laboratory, which we then chilled and processed. We counted dead sand flies and sorted by sex, identifying all male flies at the species level by using specific morphologic keys for genitalia (*24*,*25*). We kept all engorged females and ≤10–15 unfed females from each trap individually. If the number of female sand flies in the trap was >15, we pooled those flies with others in groups of 20 specimens each. We noted the blood meal size and freshness for each engorged female (*26*). We stored all female fly specimens in collection microtubes at −80°C until DNA extraction.

### Molecular Analysis by Real-Time PCR, HRM Assay, and Sequencing

We extracted total DNA from sand fly samples by using the QIAsymphony DSP DNA Mini Kit and QIAsymphony SP robot (QIAGEN, https://www.qiagen.com). We homogenized the samples for 5 min in 50 µL lysis buffer and stainless steel beads by using a TissueLyser II instrument (QIAGEN). The lysis buffer contained DNase- and proteinase-free RNaseA (ThermoFisher Scientific, https://www.thermofisher.com), proteinase K, and ATL tissue lysis buffer (QIAGEN). After homogenization, we added 200 µL lysis buffer to each samples and incubated at 56°C for 2 h. We performed centrifugation and transferred the samples directly to the robot. We extracted DNA in accordance with the manufacturer's instructions and eluted the DNA in 100 µL of elution buffer.

We performed all real-time PCR reactions by using a Roche LightCycler 96 (Roche, https://www.roche.com) and AccuMelt HRM SuperMix (Quantabio, https://www.quantabio.com). We analyzed all female sand flies for *Leishmania* spp. infection and single and engorged female flies to determine *Phlebotomus* sand fly species and blood meal source. We performed high-resolution melting (HRM) assays at the final step of each real-time PCR. We performed amplicon dissociation analysis by capturing fluorescence signals in 0.1°C/s increments and holding for 60 s in each range of the melting curve (60°C–85°C for sand fly species and blood meal detection assays or ≤95°C for *Leishmania* PCR). Sanger sequencing was

performed at the Center for Genomic Technologies at Hebrew University of Jerusalem.

We screened all female sand flies for *Leishmania* DNA and identified parasite species by amplifying an internal transcribed spacer (ITS) 1 rRNA fragment with ITS1–219 PCR primers (Appendix Table 1, https://wwwnc.cdc.gov/EID/article/29/5/22-1657-App1.pdf) and by using the HRM assay (*27*). For PCR controls, we extracted DNA from parasite promastigote cultures of international reference strains: *L. major* (MHOM/PS/1967/JerichoII), *L. tropica* (MHOM/IL/1990/P283), *L. infantum* (MHOM/SD/62/2S), *L. donovani* (MHOM/SD/1962/1S-CLD2), and *L. aethiopica* (MHOM/ET/1972/L102). High purity water for molecular biology (Bio-Lab, http://www.biolab-chemicals.com) was used as a negative control.

We included DNA isolated from skin lesions from 4 patients who had leishmaniasis diagnosed at the parasitology laboratory at Soroka Medical Center, Beer-Sheba, Israel; leishmaniasis was caused by *L. donovani/L. infantum* complex in those patients (Table 1). Leishmaniasis was diagnosed at the hospital by using multiplex real-time PCR with 5 probes for the ITS region of *Leishmania* sp. (*28*,*29*). We analyzed the samples further at the Ministry of Health by using real-time PCR–HRM amplification of the ITS1 fragment and ITS region and then sequencing.

We amplified the entire 1,020-bp ribosomal ITS region from *Leishmania*-positive field, clinical, and control samples by using PCR primers LITSR and LITSV (Appendix Table 1). If the entire ITS region was not successfully amplified with LITSR and LITSV primers, we used an internal pair of primers, L5.8S and L5.8SR, to amplify ITS1 and ITS2 separately (*30*). We performed ITS1 amplicon sequencing for 12 of the positive samples, and the entire ITS region was sequenced from 6 unfed and 3 engorged females, 3 pooled *Phlebotomus* spp. samples, all 4 human samples, and 4 *Leishmania*-positive controls. We amplified the repeat region of the *L. donovani* and *L. infantum HASPB* (known as *K26*) gene for additional separation of *L. donovani* complex–positive samples by using primers K26F and K26R (*31*).

To identify *Phlebotomus* spp., we amplified a 368–393-bp fragment of the cytochrome b gene by using a universal primer set designed for this study (cytb-F and cytb-R; Appendix Table 1). The specificity of the designed primers was tested against DNA sequences from hematophagous arthropods, including sand flies, mosquitoes, and ticks. Male sand flies identified at the species level by using morphologic characteristics were used as positive controls and molecular biology grade water was used as a negative control. We analyzed all individual samples, and 1 third of samples from each melting curve pattern were sequenced.

We identified blood meal sources in *Phlebotomus* sand fly specimens by amplifying a 500-bp segment of host 12S and 16S mitochondrial rRNA genes by using modified vertebrate universal primers N12–16F and N12–16R (*32*). We included negative (water) and positive (100 ng of human DNA) controls in each PCR. We sequenced 50 samples that represented all HRM curve patterns and all female sand flies containing blood meals that had a melting curve of a rare host (<5 samples).

We used DNA from *Leishmania* reference strains, male sand fly specimens identified by morphologic characteristics, and human blood as templates for real-time PCR and HRM curve standardization. Each species produced a unique melting curve that was easily distinguishable from other species and consistent with observed nucleotide differences (Appendix Figures 1–3). We compared normalized HRM curves of field samples with the positive control included in each PCR, which enabled species determination (*27*). We validated species identification by sequencing 1 third of the samples; complete matches were observed for speciation by HRM curve analysis and DNA sequencing.

We aligned and corrected nucleotide sequences by using BioNumerics version 8.0 software (Applied Maths, https://www.applied-maths.com) and

**Table 1.** Human clinical samples from Soroka Medical Center in study of *Leishmania donovani* transmission cycle associated with human infection, *Phlebotomus alexandri* sand flies, and hare blood meals, Israel*

| Patient no. | Diagnosis | Age, y/sex | Clinical description | Residence | Infecting *Leishmania* sp.† |
|---|---|---|---|---|---|
| 1 | VL | 47/M | Splenomegaly | Northern Israel | *L. infantum* (100% identity with *L. infantum*, GenBank accession no. KU680954) |
| 2 | VL | 4/F | Splenomegaly, hepatomegaly | Hebron | *L. infantum* (99.19% identity with *L. infantum*, GenBank accession no. MN503527) |
| 3 | CL | 69/F | Skin ulcer | Negev | *L. infantum* (99.87% identity with *L. infantum*, GenBank accession no. KU680954) |
| 4 | CL | 51/M | Skin ulcer | Arava | *L. donovani* (99.75% identity with *L. donovani*, GenBank accession no. LC459330) |

*CL, cutaneous leishmaniasis; VL, visceral leishmaniasis.
†*Leishmania* spp. were identified by PCR high resolution melting curves and Sanger sequencing.

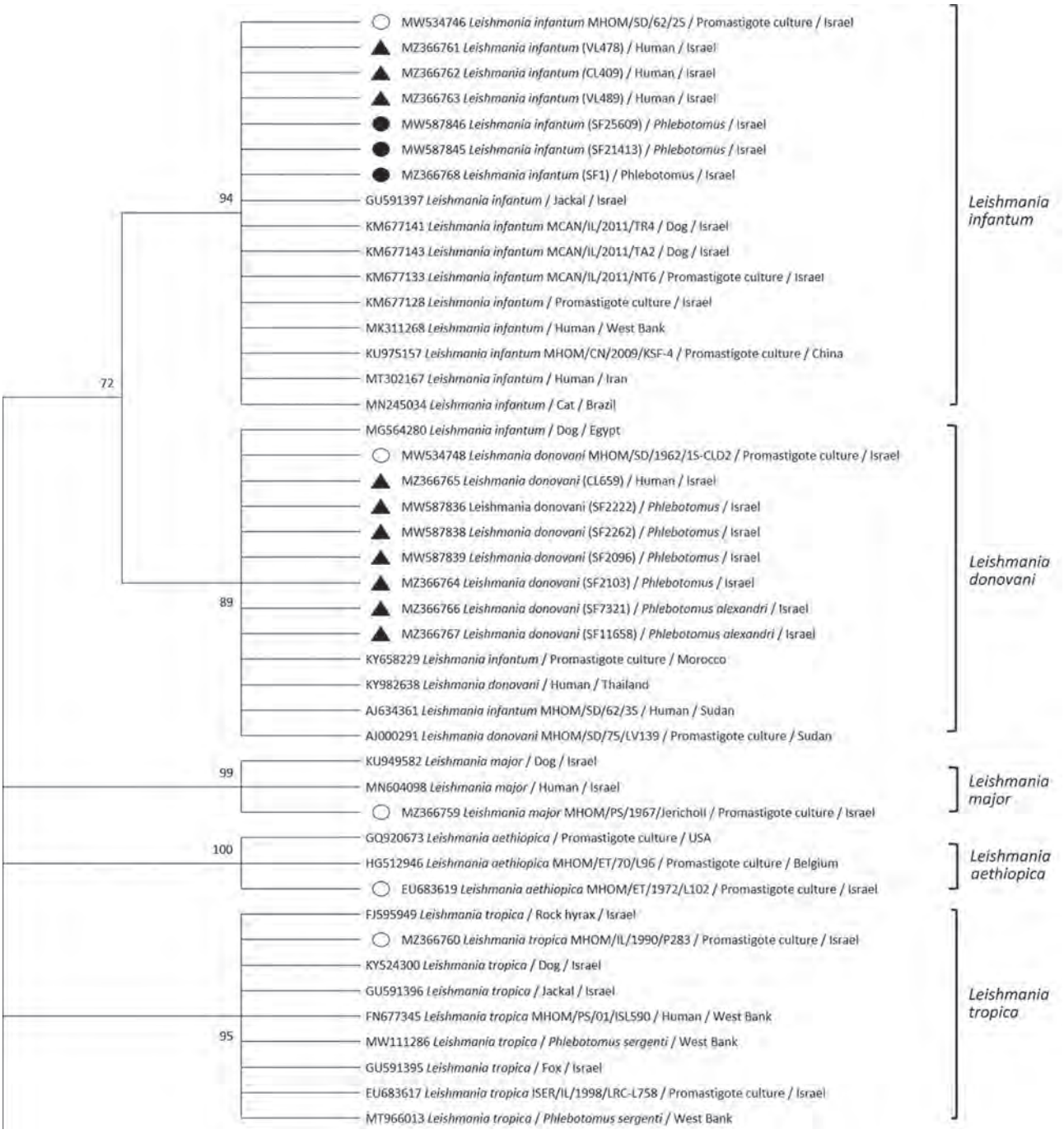


**Figure 2.** Phylogenetic analysis of *Leishmania* internal transcribed spacer 1 rRNA fragments in study of *Leishmania donovani* transmission cycle associated with human infection, *Phlebotomus alexandri* sand flies, and hare blood meals, Israel. *Leishmania*-specific internal transcribed spacer 1 rRNA fragments (201 bp) were amplified by PCR from *P. alexandri* sand flies, pooled female *Phlebotomus* spp. flies, and patient samples and then sequenced. Tree was constructed by using the maximum-likelihood method and Tamura 3-parameter model, estimated by using the Aikaike information criterion (*33*). Dendogram includes sequences from *L. donovani* and *L. infantum* isolated from sand flies and clinical samples in this study compared with *Leishmania* spp. reference controls and GenBank sequences from Israel and other countries. Tree shows substantial separate clustering of *L. infantum* (boostrap 94%) and *L. donovani* (bootstrap 89%) sequences. Empty circles are *Leishmania* international reference strains, black triangles are the 10 sequences from our study deposited in GenBank, and black circles are additional *L. infantum*–positive sand flies samples from Israel. Available GenBank sequences for *L. major, L. tropica*, *L. infantum*, and *L. donovani* from Israel and other countries are also included. GenBank accession numbers, *Leishmania* spp., isolate source, and country are indicated. Only bootstrap values >70% are shown. Not to scale.

compared sequences against the GenBank database by using BLASTN (http://blast.ncbi.nlm.nih.gov). We identified *Leishmania* spp., blood meal sources, and sand fly species on the basis of >98% identity with sequences obtained during the BLAST search. We submitted sequences of the ITS1 fragments and entire ITS and *K26* regions obtained in this study to GenBank (Appendix Table 2).

We constructed phylogenetic trees on the basis of marker gene sequences in this study and relevant

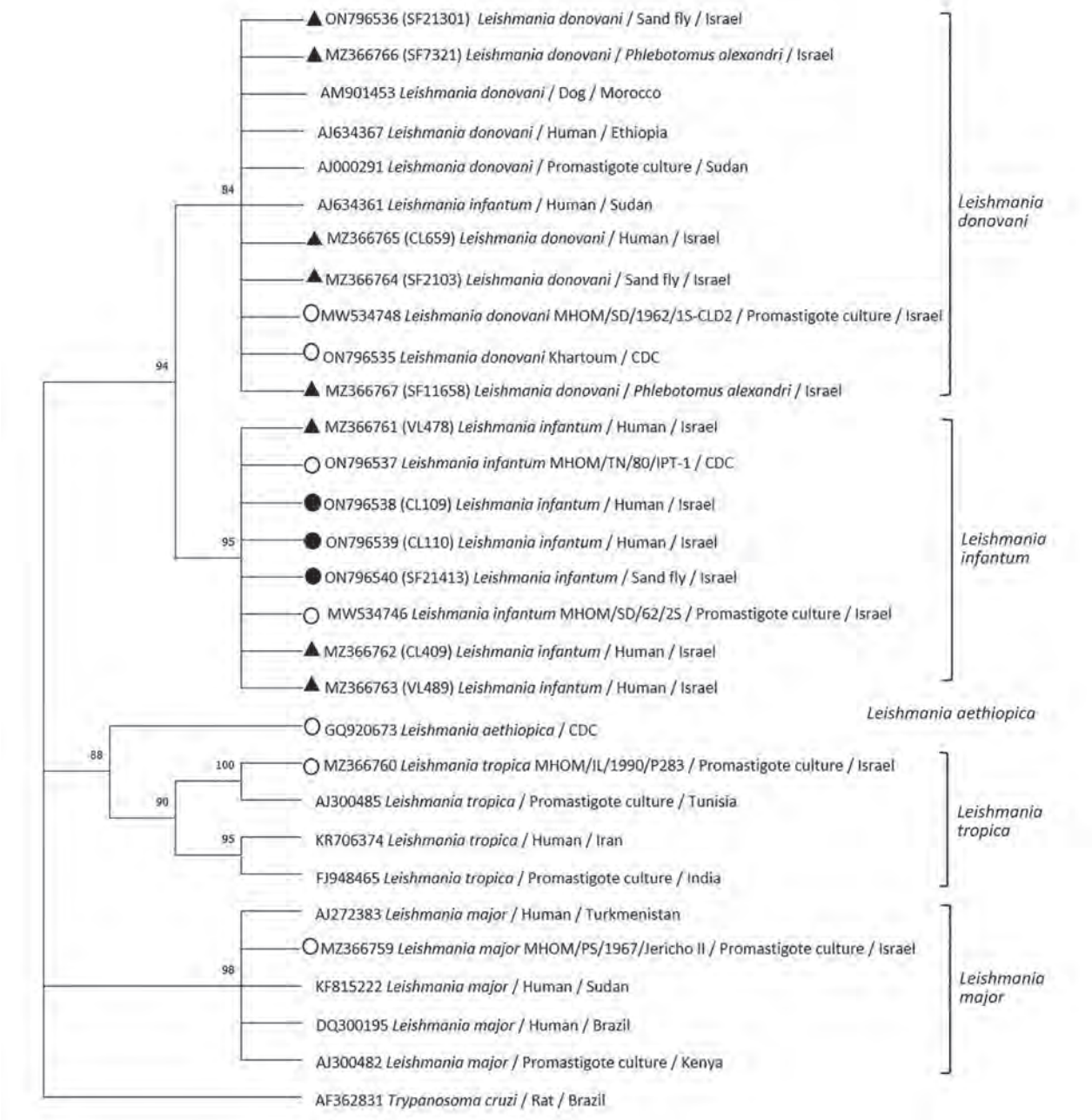


**Figure 3.** Phylogenetic analysis of entire *Leishmania* internal transcribed spacer region in study of *Leishmania donovani* transmission cycle associated with human infection, *Phlebotomus alexandri* sand flies, and hare blood meals, Israel. *Leishmania*-specific internal transcribed spacer region (988 bp) was amplified by PCR from *P. alexandri* sand flies, pooled female *Phlebotomus* spp. flies, and patient samples and then sequenced. Tree was constructed by using by using the maximum-likelihood method and Tamura 3-parameter model of all relevant *Leishmania* spp. and *Trypanosoma cruzi* as an outgroup. Sand fly and clinical samples from this study (black triangles), *L. infantum* isolates from Israel (black circles), *Leishmania* international reference strains (empty circles), and available GenBank *Leishmania* sequences are shown. GenBank accession numbers, isolate source, and country of origin are shown for each sequence. Only bootstrap values >70% are shown next to branches. Not to scale.

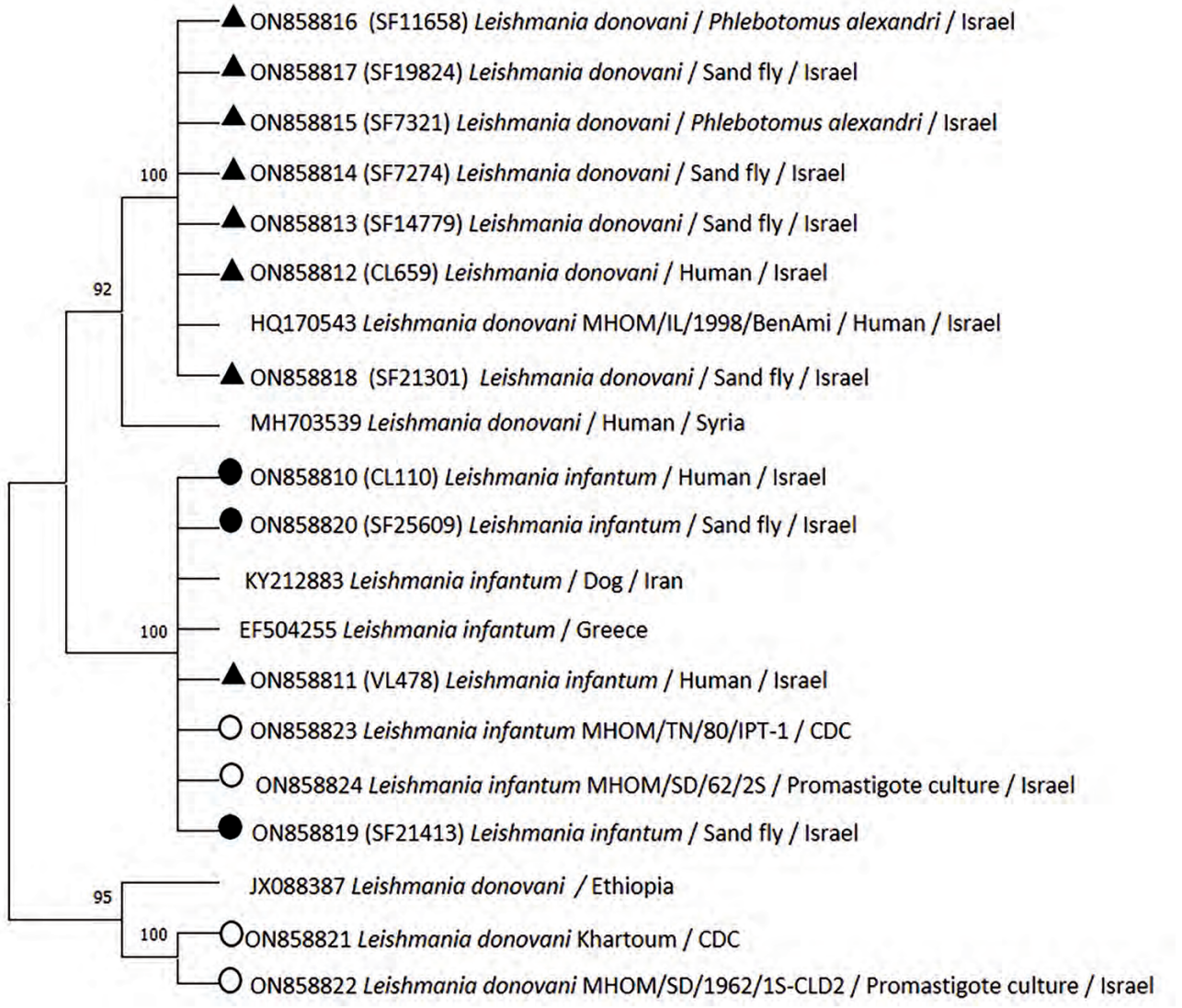


**Figure 4.** Phylogenetic analysis of *Leishmania K26* gene in study of *Leishmania donovani* transmission cycle associated with human infection, *Phlebotomus alexandri* sand flies, and hare blood meals, Israel. *Leishmania*-specific *K26* gene fragment (348 bp) was amplified by PCR from *P. alexandri* flies, pooled female *Phlebotomus* spp. flies, and patient samples and then sequenced. Tree was constructed by using the maximum-likelihood method and Hasegawa-Kishino-Yano model. *K26* phylogenetic analysis shows separation between *L. infantum* and *L. donovani*. Sand fly and clinical samples from this study (black triangles), *L. infantum* isolates from Israel (black circles), *Leishmania* international reference strains (empty circles), and available GenBank *Leishmania* sequences are shown. GenBank accession number, isolate source, and country of origin are shown for each sequence. Only bootstrap values >70% are shown next to branches. Not to scale.

sequences of other *Leishmania* spp. deposited in GenBank. We used MEGA X software (33) to infer phylogenetic trees after nucleotide sequence alignment was performed by using ClustalW software (http://www.clustal.org) and maximum-likelihood and neighbor-joining algorithms. We used 1,000 bootstrap replicates to determine percentages of replicate trees. We constructed a phylogenetic tree composed of 45 analyzed partial sequences of the ITS1 locus, including sequences of *Leishmania* spp. from Israel and other countries deposited in GenBank and *Trypanosoma cruzi* as an outgroup (Figure 2). We constructed a second tree that included 30 nearly complete ITS sequences of all relevant *Leishmania* spp. and *T. cruzi* as an outgroup (Figure 3) and an additional phylogenetic tree that included 20 *K26* gene sequences of *L. donovani* complex–positive samples (Figure 4).

## Results

We collected 22,636 *Phlebotomus* spp. sand fly specimens (15,720 female and 6,916 male; sex ratio 2.3) during 7 trapping nights by using 118 traps placed

**Table 2.** Number of female and male *Phlebotomus* spp. collected during 2018–2020 in central Negev in study of *Leishmania donovani* transmission cycle associated with human infection, *Phlebotomus alexandri* sand flies, and hare blood meals, Israel

| | 2018 | | 2019 | | 2020 | | |
|---|---|---|---|---|---|---|---|
| Phlebotomus spp. | F | M | F | M | F | M | Total no. (%) |
| *P. alexandri* | 129 | 1,452 | 70 | 126 | 431 | 4,039 | 6,247 (80.0) |
| *P. kazeruni* | 38 | 837 | 22 | 11 | 78 | 142 | 1,128 (14.5) |
| *P. sergenti* | 5 | 109 | 26 | 9 | 34 | 56 | 239 (3.1) |
| *P. papatasi* | 25 | 97 | 8 | 8 | 8 | 27 | 173 (2.2) |
| *P. syriacus* | 0 | 0 | 3 | 0 | 17 | 3 | 23 (0.3) |
| Not identified* | 8,344 | 0 | 265 | 0 | 6,217 | 0 | 14,826 |
| Total | 8,541 | 2,495 | 394 | 154 | 6,785 | 4,267 | 22,636 |

*Sand flies were pooled before molecular testing in batches of 20 speciments each.

at 94 sites. After identifying all male and 894 (6%) female flies, we found the catches consisted of 5 species. The most abundant sand fly species were *P. alexandri* (80%), *P. kazeruni* (14.4%), *P. sergenti* (3.1%), *P. papatasi* (2.2%), and *P. syriacus* (0.3%) (Table 2).

Among the 4,140 unfed female sand flies tested in 210 pools,we found 41 pools were positive for *Leishmania* spp. In addition, 6/688 single female flies and 4/206 engorged female flies were positive for *Leishmania* spp. Of the 51 *Leishmania*-positive samples, the HRM curves of 47 (36 pools, 6 single females, and 3 engorged female flies) were similar to the HRM curve of the *L. donovani* control (Table 3; Appendix Figure 1). The HRM curves for 2 pooled fly samples from 2018 were identical to the HRM curve of the *L. tropica* control. One pooled fly sample and 1 engorged female fly collected in 2020 had an HRM curve identical to the *L. major* control. The ITS1–PCR sequences of 20 samples (11 pools and all 9 single and engorged females) that had HRM curves similar to the *L. donovani* control HRM curve were also 100% identical to the *L. donovani* control sequence.

Leishmaniasis was diagnosed in 4 human patients (Table 1). The ITS1 HRM curve and sequence from patient 4 with CL were similar to the *L. donovani* control and 47 *L. donovani*–positive *Phlebotomus* spp. samples. The ITS1 HRM and sequences from patients 1 and 2 with VL and patient 3 with CL were similar to the *L. infantum* control. Alignment of ITS1 sequences from *L. infantum* and *L. donovani* controls, 3 representative sand fly samples showing HRM identical to *L. donovani*, and the 4 patient samples showed clustering into 2 distinct groups. The first group comprised the *L. donovani* control, 3 sand fly samples, and patient 4. The second group comprised the *L. infantum* control and samples from patients 1, 2, and 3. The difference between the groups was at position 71–74 in ITS1; the *L. donovani* group had a 4-nt (ATAT) insertion that was missing in the *L. infantum*–positive samples. A comparison of ITS1 sequences with those in GenBank showed 100% query coverage and 99.65%–100% identity with GenBank sequences for *L. infantum* and *L. donovani* from various countries (data not shown).

We aligned DNA sequences from the entire ITS region obtained from *Leishmania*–positive *P. alexandri* samples from our study and the *L. infantum* and *L. donovani* controls (Appendix Figure 4). We found 2 additional regions containing polymorphic sites that distinguished between *L. infantum* and *L. donovani*: a 2-nt (GG) deletion at position 724–725 and 1-nt (G) insertion at position 817 in the *L. donovani* sequence.

We constructed a phylogenetic tree of ITS1 rRNA fragments of *Leishmania* sequences obtained from *P. alexandri* flies, pooled female *Phlebotomus* spp. flies, and

**Table 3.** Number of *Leishmania* spp. detected in sand fly samples by PCR during 2018–2020 in study of *Leishmania donovani* transmission cycle associated with human infection, *Phlebotomus alexandri* sand flies, and hare blood meals, Israel*

| Year | Total no. tested | *L. donovani* | *L. tropica* | *L. major* |
|---|---|---|---|---|
| 2018 | | | | |
| Females (no. pools) | 2,938 (148) | 24 | 2 | 0 |
| Single unfed females | 108 | 0 | 0 | 0 |
| Single engorged females | 89 | 0 | 0 | 0 |
| 2019 | | | | |
| Females (no. pools) | 262 (15) | 4 | 0 | 0 |
| Single unfed females | 121 | 3 | 0 | 0 |
| Single engorged females | 8 | 0 | 0 | 0 |
| 2020 | | | | |
| Females (no. pools) | 940 (47) | 10 | 0 | 1 |
| Single unfed females | 459 | 3 | 0 | 0 |
| Single engorged females | 109 | 3 | 0 | 1 |
| Total no. | 5,019 | 47 | 2 | 2 |

*All engorged females and ≤10–15 unfed females from each trap were maintained and analyzed individually. If the number of female sand flies in the trap was >15, they were pooled in batches of 20 specimens each.

**Table 4.** Number of female *Phlebotomus* spp. sand flies collected in the central Negev region engorged with different blood meals in study of *Leishmania donovani* transmission cycle associated with human infection, *Phlebotomus alexandri* sand flies, and hare blood meals, Israel

| Blood meal source | *Phlebotomus* spp. | | | | Total no. |
|---|---|---|---|---|---|
| | *P. alexandri* | *P. kazeruni* | *P. papatasi* | *P. sergenti* | |
| *Lepus europaeus* (hare) | 107 | 8 | 5 | 6 | 126 |
| *Equus hemionus* (onager) | 31 | 1 | 0 | 1 | 33 |
| *Gazella dorcas* (gazelle) | 10 | 0 | 4 | 2 | 16 |
| *Canis lupus familiaris* (dog) | 1 | 0 | 3 | 0 | 4 |
| *Homo sapiens* (human) | 1 | 0 | 0 | 0 | 1 |
| *Psammomys obesus* (fat sand rat) | 0 | 0 | 1 | 0 | 1 |
| *Vulpes vulpes* (fox) | 1 | 0 | 0 | 0 | 1 |
| Total no. | 151 | 9 | 13 | 9 | 182 |

patient samples from this study. We compared those sequences with *Leishmania* spp. controls and GenBank sequences from Israel and other countries. The tree showed substantial separate clustering of *L. infantum* (boostrap 94%) and *L. donovani* (bootstrap 89%) sequences (Figure 2). Phylogenetic analysis of the entire ITS region showed separate clustering of *L. infantum* (bootstrap 84%) and *L. donovani* (bootstrap 95%) sequences (Figure 3). *K26* phylogenetic analysis also showed separation between *L. infantum* and *L. donovani* (Figure 4).

We identified the blood meal source for 182/206 (88%) engorged female sand flies that represented the 4 most abundant sand fly species within the study area. We observed 7 types of HRM curves. We compared blood meal sequences with GenBank sequences and determined similarities between HRM curves. We identified European brown hare (*Lepus europaeus*) blood in 126 (69.2%) flies, onager (*Equus hemionus*) blood in 33 (18.3%) flies, gazelle (*Gazella dorcas*) blood in 16 (8.8%) flies, and domestic dog (*C. lupus familiaris*) blood in 4 (2.2%) flies; 1 female sand fly each contained blood from either a fat sand rat (*Psammomys obesus*), fox (*V. vulpes*), or human (Table 4). Hare blood was the dominant blood meal found in all 4 *Phlebotomus* spp. flies: *P. papatasi*, 38%; *P. sergenti*, 67%; *P. alexandri*, 71%; and *P. kazeruni*, 89%. The 12S–16S hare blood meal sequences were 99.8% similar to *L. europaeus* hares and only 95.3% similar to *L. capensis* hares.

Of the 47 *Phlebotomus* spp. sand fly samples with HRM curve patterns and sequences similar to the *L. donovani* control, 9 were single *P. alexandri* female sand flies, 3 of which were engorged with hare blood. Of the 2 *Phlebotomus* spp. samples positive for *L. major*, 1 was in a single engorged *P. papatasi* female sand fly that had an unsuccessful blood meal identification. The 2 identified *L. tropica* samples were from pooled female sand flies.

## Discussion

We found a fourth transmission cycle of leishmaniasis in the central Negev region of southern Israel. On the basis of molecular analysis of the ITS region and *K26* gene and phylogenetic analysis, we concluded that the parasite found in patient 4, who lives in the survey area, and in *P. alexandri* sand flies was *L. donovani* sensu stricto. We found that *L. infantum* was the cause of illness in the other 3 patients with leishmaniasis. A case report describing patient 4 was published in 2016; the authors concluded that the infecting parasite was likely *L. infantum* because of prevailing knowledge of endemic *Leishmania* transmission in Israel (*29*). An earlier study reported another patient from the Arava region of central Negev, close to where patient 4 lives, who had symptoms of both CL and VL (*34*). The cause of infection was identified as *L. donovani*; the authors noted that this infection was unusual because *L. donovani* was not known to circulate in Israel. The earlier study substantiates our findings of *L. donovani* in both sand flies and another human patient within the same geographic area. *L. infantum* was identified as the causative agent in the other 3 patients in our study and was also described in canines in Israel (*1*).

The high abundance of *P. alexandri* sand flies within the study area and the association with *L. donovani* infections suggest that the *P. alexandri* sand fly is the putative vector of *L. donovani* in Israel. *P. alexandri* flies have been associated with *L. donovani* sensu latu transmission in other parts of the Old World. Natural infection by *L. donovani* was found in field-collected *P. alexandri* sand fly specimens in China, and inoculation of hamsters with those parasites caused VL (*35*). Another study reported the susceptibility of *P. alexandri* to artificial infection with *L. donovani* isolated from human patients in China (*36*).

We found blood meals from European brown hares in ≈70% of engorged female *Phlebotomus* sand flies in our study. The high feeding rates on hares, presence of *L. donovani* in female *P. alexandri* sand flies engorged with hare blood and illnesses reported in humans infected with *L. donovani* suggest a zoonotic *L. donovani* transmission cycle in Israel. Those data

suggest that the hare could be a potential reservoir and *P. alexandri* flies could be the putative vector for *L. donovani*. The role of hares as a reservoir host for *L. donovani* requires further investigation; however, a related hare species, *Lepus granatensis*, was reported as a potential sylvatic reservoir for *L. infantum* in a leishmaniasis outbreak in Madrid, Spain (*37*,*38*). Furthermore, studies in Greece and Italy detected *L. donovani* complex infection in *L. europaeus* hares (*39*,*40*), providing support for hares as a potential reservoir for *L. donovani* in Israel. Dogs were identified as reservoirs for *L. donovani* in India, Sudan, and Ethiopia, and different rodent species have been identified as possible reservoirs of *Leishmania* spp. from the *L. donovani* complex (*41*–*48*). However, no *L. donovani* infections in canines and rodents have been reported in Israel; infections in sand fly blood meals found in our study do not implicate those hosts in the local life cycle of *L. donovani*.

In conclusion, we found circulation of *L. donovani* in the Negev region of southern Israel that was associated with cutaneous lesions in humans. We determined that *P. alexandri* was the putative sand fly vector and that hares were the main reservoir host of *L. donovani*. We found 2 distinct *Leishmania* spp. in the *L. donovani* complex in Israel. Previously, the few reported human cases of CL resulting from *L. donovani* infections were attributed to either *L. infantum* or nonautochthonous infections. Analysis of patient samples in our study indicates that, in addition to *L. major* and *L. tropica* (the known agents causing CL), *L. donovani* is also a cause of autochthonous CL in Israel. Our results suggest that CL in Israel can be caused by *L. donovani*, a primary cause of VL. Therefore, prompt diagnosis, identification of the *Leishmania* sp., and treatment with drugs intended for visceral leishmaniasis, such as pentavalent antimonials or liposomal amphotericin B (*49*), are critical to prevent disease progression and death among patients with leishmaniasis.

### Acknowledgments

We thank Simha Shilo, Anna Sarner, and Arik Levy for assisting with sand fly sorting; Aviv Rashti, Anat Berkowitz, Karin Cohen, and Alina Bazarski for assisting with human sample analysis; Itay Naveh and Dan Ish-Shalom for supporting and participating in the fieldwork; Heather Schnur for editorial remarks; Yaarit Nachum-Biala for sharing professional knowledge of phylogenetic tree construction; and Guy Nizry for helping with map creation.

This study was supported by internal funding from the Ministry of Health, Jerusalem, Israel.

### About the Author

Ms. Studentsky is a PhD student at the Koret School of Veterinary Medicine, The Hebrew University of Jerusalem, Israel, and works at the Medical Entomology Laboratory, Ministry of Health, Jerusalem. Her primary research interests focus on leishmaniasis, sand fly surveillance, and vector competence.

### References

1. Jaffe CL, Baneth G, Abdeen ZA, Schlein Y, Warburg A. Leishmaniasis in Israel and the Palestinian Authority. Trends Parasitol. 2004;20:328–32. https://doi.org/10.1016/j.pt.2004.05.001
2. Schlein Y, Warburg A, Schnur LF, Gunders AE. Leishmaniasis in the Jordan Valley II. Sandflies and transmission in the central endemic area. Trans R Soc Trop Med Hyg. 1982;76:582–6. https://doi.org/10.1016/0035-9203(82)90215-2
3. Schlein Y, Warburg A, Schnur LF, Le Blancq SM, Gunders AE. Leishmaniasis in Israel: reservoir hosts, sandfly vectors and leishmanial strains in the Negev, Central Arava and along the Dead Sea. Trans R Soc Trop Med Hyg. 1984;78:480–4. https://doi.org/10.1016/0035-9203(84)90067-1
4. Anis E, Leventhal A, Elkana Y, Wilamowski A, Pener H. Cutaneous leishmaniasis in Israel in the era of changing environment. Public Health Rev. 2001;29:37–47.
5. Jacobson RL, Eisenberger CL, Svobodova M, Baneth G, Sztern J, Carvalho J, et al. Outbreak of cutaneous leishmaniasis in northern Israel. J Infect Dis. 2003;188:1065–73. https://doi.org/10.1086/378204
6. Schnur LF, Nasereddin A, Eisenberger CL, Jaffe CL, El Fari M, Azmi K, et al. Multifarious characterization of *Leishmania tropica* from a Judean desert focus, exposing intraspecific diversity and incriminating *Phlebotomus sergenti* as its vector. Am J Trop Med Hyg. 2004;70:364–72. https://doi.org/10.4269/ajtmh.2004.70.364
7. Svobodova M, Votypka J, Peckova J, Dvorak V, Nasereddin A, Baneth G, et al. Distinct transmission cycles of *Leishmania tropica* in 2 adjacent foci, northern Israel. Emerg Infect Dis. 2006;12:1860–8. https://doi.org/10.3201/eid1212.060497
8. Jacobson RL. Leishmaniasis in an era of conflict in the Middle East. Vector Borne Zoonotic Dis. 2011;11:247–58. https://doi.org/10.1089/vbz.2010.0068
9. Ready PD. Biology of phlebotomine sand flies as vectors of disease agents. Annu Rev Entomol. 2013;58:227–50. https://doi.org/10.1146/annurev-ento-120811-153557
10. Gunders AE, Foner A, Montilio B. Identification of *Leishmania* species isolated from rodents in Israel. Nature. 1968;219:85–6. https://doi.org/10.1038/219085a0
11. Gunders AE, Lidror R, Montilo B, Amitai P. Isolation of *Leishmania* sp. from *Psammomys obesus* in Judea. Trans R Soc Trop Med Hyg. 1968;62:465. https://doi.org/10.1016/0035-9203(68)90129-6
12. Wasserberg G, Abramsky Z, Anders G, El-Fari M, Schoenian G, Schnur L, et al. The ecology of cutaneous leishmaniasis in Nizzana, Israel: infection patterns in the reservoir host, and epidemiological implications. Int J Parasitol. 2002;32:133–43. https://doi.org/10.1016/S0020-7519(01)00326-5
13. Faiman R, Abbasi I, Jaffe C, Motro Y, Nasereddin A, Schnur LF, et al. A newly emerged cutaneous leishmaniasis focus in northern Israel and two new reservoir hosts of

*Leishmania major*. PLoS Negl Trop Dis. 2013;7:e2058. https://doi.org/10.1371/journal.pntd.0002058
14. Talmi-Frank D, Jaffe CL, Nasereddin A, Warburg A, King R, Svobodova M, et al. *Leishmania tropica* in rock hyraxes (*Procavia capensis*) in a focus of human cutaneous leishmaniasis. Am J Trop Med Hyg. 2010;82:814–8. https://doi.org/10.4269/ajtmh.2010.09-0513
15. Ya'ari A, Jaffe CL, Garty BZ. Visceral leishmaniasis in Israel, 1960–2000. Isr Med Assoc J. 2004;6:205–8.
16. Singer SR, Abramson N, Shoob H, Zaken O, Zentner G, Stein-Zamir C. Ecoepidemiology of cutaneous leishmaniasis outbreak, Israel. Emerg Infect Dis. 2008;14:1424–6. https://doi.org/10.3201/eid1409.071100
17. Azmi K, Krayter L, Nasereddin A, Ereqat S, Schnur LF, Al-Jawabreh A, et al. Increased prevalence of human cutaneous leishmaniasis in Israel and the Palestinian Authority caused by the recent emergence of a population of genetically similar strains of *Leishmania tropica*. Infect Genet Evol. 2017;50:102–9. https://doi.org/10.1016/j.meegid.2016.07.035
18. Gandacu D, Glazer Y, Anis E, Karakis I, Warshavsky B, Slater P, et al. Resurgence of cutaneous leishmaniasis in Israel, 2001–2012. Emerg Infect Dis. 2014;20:1605–11. https://doi.org/10.3201/eid2010.140182
19. Israel Ministry of Health. Annual report of central laboratories, 2019 (Hebrew) [cited 2021 Jan 5]. https://www.health.gov.il/PublicationsFiles/LAB_JER2019.pdf
20. Nezer O, Bar-David S, Gueta T, Carmel Y. High-resolution species-distribution model based on systematic sampling and indirect observations. Biodivers Conserv. 2017;26:421–37. https://doi.org/10.1007/s10531-016-1251-2
21. Stern E, Gardus Y, Meir A, Krakover S, Tzoar H. Atlas of the Negev. Jerusalem (Israel): Keter Publishing House; 1986.
22. Orshan L, Szekely D, Khalfa Z, Bitton S. Distribution and seasonality of *Phlebotomus* sand flies in cutaneous leishmaniasis foci, Judean Desert, Israel. J Med Entomol. 2010;47:319–28. https://doi.org/10.1093/jmedent/47.3.319
23. Orshan L, Elbaz S, Ben-Ari Y, Akad F, Afik O, Ben-Avi I, et al. Distribution and dispersal of *Phlebotomus papatasi* (Diptera: Psychodidae) in a zoonotic cutaneous leishmaniasis focus, the northern Negev, Israel. PLoS Negl Trop Dis. 2016;10:e0004819. https://doi.org/10.1371/journal.pntd.0004819
24. Abonnenc E. Les Phlébotomes de la région éthiopienne (Diptera, Psychodidae). In: Memoires ORSTOM series. Paris: Office de la Recherche Scientifique et Technique; 1972
25. Lewis DJ. A taxonomic review of the genus *Phlebotomus* (Diptera: Psychodidae). Bull Br Mus Nat Hist. 1982;45:121–209.
26. Lukes J, Mauricio IL, Schönian G, Dujardin JC, Soteriadou K, Dedet JP, et al. Evolutionary and geographical history of the *Leishmania donovani* complex with a revision of current taxonomy. Proc Natl Acad Sci USA. 2007;104:9375–80. https://doi.org/10.1073/pnas.0703678104
27. Talmi-Frank D, Nasereddin A, Schnur LF, Schönian G, Töz SO, Jaffe CL, et al. Detection and identification of old world *Leishmania* by high resolution melt analysis. PLoS Negl Trop Dis. 2010;4:e581. https://doi.org/10.1371/journal.pntd.0000581
28. Sagi O, Berkowitz A, Codish S, Novack V, Rashti A, Akad F, et al. Sensitive molecular diagnostics for cutaneous leishmaniasis. Open Forum Infect Dis. 2017;4:ofx037. https://doi.org/10.1093/ofid/ofx037
29. Ben-Shimol S, Sagi O, Horev A, Avni YS, Ziv M, Riesenberg K. Cutaneous leishmaniasis caused by *Leishmania infantum* in southern Israel. Acta Parasitol. 2016;61:855–8. https://doi.org/10.1515/ap-2016-0118
30. el Tai NO, Osman OF, el Fari M, Presber W, Schönian G. Genetic heterogeneity of ribosomal internal transcribed spacer in clinical samples of *Leishmania donovani* spotted on filter paper as revealed by single-strand conformation polymorphisms and sequencing. Trans R Soc Trop Med Hyg. 2000;94:575–9. https://doi.org/10.1016/S0035-9203(00)90093-2
31. Haralambous C, Antoniou M, Pratlong F, Dedet JP, Soteriadou K. Development of a molecular assay specific for the *Leishmania donovani* complex that discriminates *L. donovani*/*Leishmania infantum* zymodemes: a useful tool for typing MON-1. Diagn Microbiol Infect Dis. 2008;60:33–42. https://doi.org/10.1016/j.diagmicrobio.2007.07.019
32. Valinsky L, Ettinger G, Bar-Gal GK, Orshan L. Molecular identification of bloodmeals from sand flies and mosquitoes collected in Israel. J Med Entomol. 2014;51:678–85. https://doi.org/10.1603/ME13125
33. Kumar S, Stecher G, Li M, Knyaz C, Tamura K. MEGA X: molecular evolutionary genetics analysis across computing platforms. Mol Biol Evol. 2018;35:1547–9. https://doi.org/10.1093/molbev/msy096
34. Ben-Ami R, Schnur LF, Golan Y, Jaffe CL, Mardi T, Zeltser D. Cutaneous involvement in a rare case of adult visceral leishmaniasis acquired in Israel. J Infect. 2002;44:181–4. https://doi.org/10.1053/jinf.2002.0953
35. Guan LR, Xu YX, Li BS, Dong J. The role of *Phlebotomus alexandri* Sinton, 1928 in the transmission of kala-azar. Bull World Health Organ. 1986;64:107–12.
36. Guan LR, Zhou ZB, Jin CF, Fu Q, Chai JJ. Phlebotomine sand flies (Diptera: Psychodidae) transmitting visceral leishmaniasis and their geographical distribution in China: a review. Infect Dis Poverty. 2016;5:15. https://doi.org/10.1186/s40249-016-0107-z
37. Molina R, Jiménez MI, Cruz I, Iriso A, Martín-Martín I, Sevillano O, et al. The hare (*Lepus granatensis*) as potential sylvatic reservoir of *Leishmania infantum* in Spain. Vet Parasitol. 2012;190:268–71. https://doi.org/10.1016/j.vetpar.2012.05.006
38. Sevá ADP, Martcheva M, Tuncer N, Fontana I, Carrillo E, Moreno J, et al. Efficacies of prevention and control measures applied during an outbreak in southwest Madrid, Spain. PLoS One. 2017;12:e0186372. https://doi.org/10.1371/journal.pone.0186372
39. Tsokana CN, Sokos C, Giannakopoulos A, Mamuris Z, Birtsas P, Papaspyropoulos K, et al. First evidence of *Leishmania* infection in European brown hare *(Lepus europaeus*) in Greece: GIS analysis and phylogenetic position within the *Leishmania* spp. Parasitol Res. 2016;115:313–21. https://doi.org/10.1007/s00436-015-4749-8
40. Rocchigiani G, Ebani VV, Nardoni S, Bertelloni F, Bascherini A, Leoni A, et al. Molecular survey on the occurrence of arthropod-borne pathogens in wild brown hares (*Lepus europaeus*) from Central Italy. Infect Genet Evol. 2018;59:142–7. https://doi.org/10.1016/j.meegid.2018.02.005
41. Jambulingam P, Pradeep Kumar N, Nandakumar S, Paily KP, Srinivasan R. Domestic dogs as reservoir hosts for *Leishmania donovani* in the southernmost Western Ghats in India. Acta Trop. 2017;171:64–7. https://doi.org/10.1016/j.actatropica.2017.03.006
42. Hassan MM, Osman OF, El-Raba'a FM, Schallig HD, Elnaiem DE. Role of the domestic dog as a reservoir host of *Leishmania donovani* in eastern Sudan. Parasit Vectors. 2009;2:26. https://doi.org/10.1186/1756-3305-2-26
43. Dereure J, El-Safi SH, Bucheton B, Boni M, Kheir MM, Davoust B, et al. Visceral leishmaniasis in eastern Sudan: parasite identification in humans and dogs; host-parasite

relationships. Microbes Infect. 2003;5:1103–8. https://doi.org/10.1016/j.micinf.2003.07.003
44. Bsrat A, Berhe M, Gadissa E, Taddele H, Tekle Y, Hagos Y, et al. Serological investigation of visceral *Leishmania* infection in human and its associated risk factors in Welkait District, Western Tigray, Ethiopia. Parasite Epidemiol Control. 2017;3:13–20. https://doi.org/10.1016/j.parepi.2017.10.004
45. Bashaye S, Nombela N, Argaw D, Mulugeta A, Herrero M, Nieto J, et al. Risk factors for visceral leishmaniasis in a new epidemic site in Amhara Region, Ethiopia. Am J Trop Med Hyg. 2009;81:34–9. https://doi.org/10.4269/ajtmh.2009.81.34
46. Kalayou S, Tadelle H, Bsrat A, Abebe N, Haileselassie M, Schallig HDFH. Serological evidence of *Leishmania donovani* infection in apparently healthy dogs using direct agglutination test (DAT) and rk39 dipstick tests in Kafta Humera, northwest Ethiopia. Transbound Emerg Dis. 2011;58:255–62. https://doi.org/10.1111/j.1865-1682.2011.01209.x
47. Magri A, Galuppi R, Fioravanti M, Caffara M. Survey on the presence of *Leishmania* sp. in peridomestic rodents from the Emilia-Romagna Region (northeastern Italy). Vet Res Commun. 2023;47:291–6. https://doi.org/10.1007/s11259-022-09925-4
48. Özbilgin A, Çavuş İ, Yıldırım A, Gündüz C. Do the rodents have a role in transmission of cutaneous leishmaniasis in Turkey? [in Turkish]. Mikrobiyol Bul. 2018;52:259–72. https://doi.org/10.5578/mb.66828
49. Frézard F, Aguiar MMG, Ferreira LAM, Ramos GS, Santos TT, Borges GSM, et al. Liposomal amphotericin B for treatment of leishmaniasis: from the identification of critical physicochemical attributes to the design of effective topical and oral formulations. Pharmaceutics. 2022;15:99. https://doi.org/10.3390/pharmaceutics15010099

Address for correspondence: Liora Studentsky, Laboratory of Medical Entomology, Ministry of Health, Elaiv Yaakov 9, Jerusalem 9546208, Israel; email: liora.studenetsky@moh.gov.il

# etymologia revisited

## *Dermatophilus congolensis*

[dur”mə-tof’ĭ-ləs con-gō-len’sis]

From the Greek *derma* (skin) + *philos* (loving), *Dermatophilus congolensis* is a Gram-positive, aerobic actinomycete, and facultatively anaerobic bacteria (Figure 1). *D. congolensis* infects the epidermis and produces exudative dermatitis termed dermatophilosis that was previously known as rain rot, rain scald, streptotrichosis, and mycotic dermatitis.

In 1915, René Van Saceghem (Figure 2), a Belgian military veterinarian stationed at a veterinary laboratory in the former Belgian Congo (thus, the species name *congolensis*), reported *D. congolensis* from exudative dermatitis in cattle. Local breeders and veterinarians had observed the disease since 1910, but the causal agent was not identified.

Dermatophilosis affects animals, mainly cattle, and more rarely humans. Outbreaks of *D. congolensis* infection have severe economic implications in the livestock and leather industries.

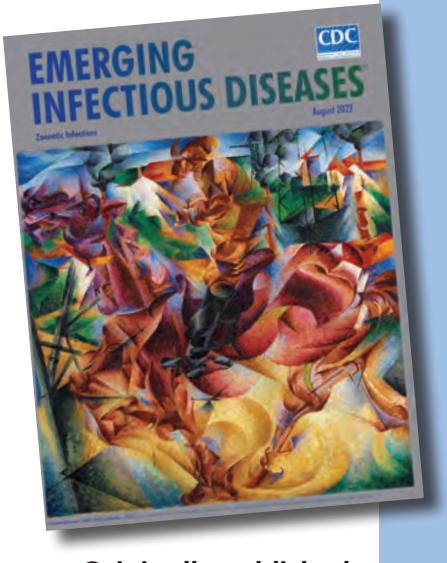


***Originally published in August 2022***

**References:**

1. Amor A, Enríquez A, Corcuera MT, Toro C, Herrero D, Baquero M. Is infection by *Dermatophilus congolensis* underdiagnosed? J Clin Microbiol. 2011;49:449–51.
2. Branford I, Johnson S, Chapwanya A, Zayas S, Boyen F, Mielcarska MB, et al. Comprehensive molecular dissection of *Dermatophilus congolensis* genome and first observation of tet(z) tetracycline resistance. Int J Mol Sci. 2021;22:7128.
3. Dorland’s illustrated medical dictionary. 32nd ed. Philadelphia: Elsevier Saunders; 2012.
4. Van Saceghem R. Contagious skin disease (contagious impetigo) [in French]. Bull Soc Pathol Exot. 1915;8:354–9.

***https//wwwnc.cdc.gov/eid/article/28/8/et-2808_article***

# Case–Control Study of Long COVID, Sapporo, Japan

Toshiaki Asakura,[1] Takashi Kimura,[1] Isaku Kurotori, Katabami Kenichi, Miyuki Hori, Mariko Hosogawa, Masayuki Saijo, Kaori Nakanishi, Hiroyasu Iso, Akiko Tamakoshi

We conducted a cross-sectional survey among SARS-CoV-2–positive persons and negative controls in Sapporo, Japan, to clarify symptoms of long COVID. We collected responses from 8,018 participants, 3,694 case-patients and 3,672 controls. We calculated symptom prevalence for case-patients at 2–3, 4–6, 7–9, 10–12, and 13–18 months after illness onset. We used logistic regression, adjusted for age and sex, to estimate the odds ratio (OR) for each symptom and control reference. We calculated symptom prevalence by stratifying for disease severity, age, and sex. At 4–18 months from illness onset, ORs for anosmia, ageusia, dyspnea, alopecia, and brain fog were consistently >1, whereas ORs for common cold–like, gastrointestinal, and dermatologic symptoms were <1. Time trend ORs increased for diminished ability to concentrate, brain fog, sleep disturbance, eye symptoms, and tinnitus. Clinicians should focus on systemic, respiratory, and neuropsychiatric symptoms among long COVID patients.

Several months after the COVID-19 pandemic began, patients coined the term long COVID to describe the fluctuated, progressive, persistent, and multiphasic symptoms caused by SARS-CoV-2 infection (*1*). This patient-derived notion was rapidly adopted, and many biomedical research studies were conducted using a variety of definitions and terms, such as post–COVID-19 syndrome and post-acute sequelae of SARS-CoV-2 infection (*2*).

The World Health Organization (WHO) conducted a Delphi process to create a consensus definition of post–COVID-19 condition for adult patients (*3*). The WHO consensus definition states that "post–COVID-19 condition occurs in individuals with a history of probable or confirmed SARS-CoV-2 infection, usually 3 months from the onset of COVID-19, with symptoms that last for at least 2 months and cannot be explained by an alternative diagnosis" (*3*). The WHO consensus definition also pointed out that common symptoms of post–COVID-19 condition were fatigue, shortness of breath, and cognitive dysfunction and that these symptoms affected everyday functioning among patients.

Although symptom prevalences among COVID-19 patients are reportedly high, demonstrating that such prevalences are specific to COVID-19 patients versus uninfected persons has been difficult, and only a few cohort studies have been conducted with controls (*4*,*5*). One national cohort study reported symptom prevalence among children and adolescents 3 months after SARS-CoV-2 test-positive date and among test-negative controls (*5*). The study showed that the number of symptom types in case-patients was higher 3 months after the test-positive date than at the time they received a PCR test. That study also showed that COVID-19 case-patients generally had more symptom types than the control group (*5*), emphasizing the need for controls to accurately assess long COVID. However, that study did not assess the 6-month or 12-month effects of SARS-CoV-2 infection on health and focused only on children. Another study used a small sample size and did not comprehensively investigate symptom characteristics (*4*). Another approach to set controls is by using electronic health records (*6*,*7*). The Centers for Disease Control and Prevention reported that COVID-19 potentially had long-term effects on multiple organs and caused a wide range of diseases (*6*). In a study in which patients with acute respiratory infection other than COVID-19 were set as controls, prevalence of neurologic complications was substantially higher among COVID-19 case-patients than controls (*7*). However, those studies did not have

Author affiliations: Hokkaido University, Sapporo, Japan (T. Asakura, T. Kimura, I. Kurotori, K. Kenichi, A. Tamakoshi); National Center for Global Health and Medicine, Tokyo, Japan (M. Hori, M. Hosogawa, H. Iso); Health and Welfare Bureau, Sapporo (M. Saijo, K. Nakanishi)

DOI: https://doi.org/10.3201/eid2905.221349

[1]These authors contributed equally to this article.

consistent symptomatic information and only assessed diagnosed diseases. Therefore, symptomatic characteristics of long COVID could not be explored by those approaches.

The complicated sequelae, long-term health effects, and health outcomes among adult COVID-19 patients remain unknown. To clarify the clinical features and long-lasting manifestations of SARS-CoV-2 infection, we conducted a large case–control cohort study in Sapporo, Japan, during the beginning of the first Omicron wave in February 2022. We analyzed cross-sectional baseline data to distinguish COVID-19–related long-term symptoms from non–COVID-19 symptoms by setting controls and using the WHO definition of post–COVID-19 condition (*3*).

## Methods

### Study Design and Participants

We collected cross-sectional data of COVID-19 patients and a control group in Sapporo, Japan, in a cohort study of long-term health effects of SARS-CoV-2 infection among adults. We randomly selected laboratory-confirmed COVID-19 case-patients and controls from among residents 20–64 years of age in Sapporo on February 1, 2022. We selected case-patients from the registry of the Sapporo Public Health Office, regardless of which SARS-CoV-2 variants were circulating at the time of their infections. Controls were persons who did not have a COVID-19 diagnosis as of February 1, 2022; we randomly sampled the control group to match the age and sex distribution of the general population of Sapporo. We mailed information about the study and the protocol to the selected possible participants, who then accessed and answered web-based questionnaires by using a URL provided (Appendix, https://wwwnc.cdc.gov/EID/article/29/5/22-1349-App1.pdf). We assessed the COVID-19 epidemiologic situation in Sapporo from daily cases, cumulative incidence, and vaccination coverage (Figure 1).

### Definition of Symptoms and Data Collection

To define case-patient symptoms, we used the WHO definition for post–COVID-19 condition (*3*), which considers a long COVID symptom as any symptom that developed after the initial illness onset, lasted for at least 2 months, and could not be explained by an alternative diagnosis. Using this definition, we asked case-patients about each symptom at the time they answered the questionnaire and at various timepoints after illness onset: 2–3, 4–6, 7–9, and 10–12 months. Although symptoms 2–3 months after illness onset were not exactly matched with the post–COVID-19 condition definition, we used the 2–3-month period as a proxy for relatively short-term influences of SARS-CoV-2 infection on the development and persistence of symptoms. We asked the control group about symptoms lasting for at least 2 months at the time they responded to the questionnaire. Of note, we only applied the WHO definition of long COVID symptoms to case-patients. All participants were asked about 31 symptom types, including COVID-19–related symptoms such as fatigue,

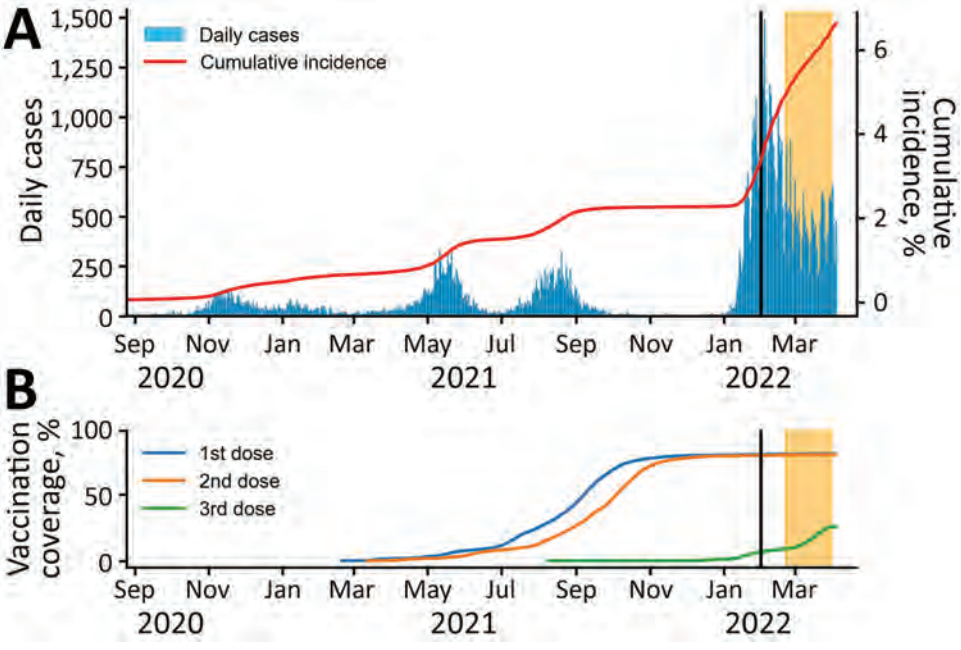


**Figure 1.** Daily COVID-19 cases, cumulative incidence, and vaccination rates during a case–control study of long COVID, Sapporo, Japan, August 2020–March 2022. A) Number of daily COVID-19 cases and cumulative incidence rates. B) Vaccination rates among the population of Sapporo. Date range represents timeframe in which participating case-patients might have been infected. Vertical black lines indicate February 1, 2022, the date potential participants were randomly identified. Yellow shading at right indicates the period of the survey in this study, February 21–March 31, 2022.

ageusia, and anosmia (*8*–*10*) and common symptoms like headache, constipation, and diarrhea.

We mapped the symptoms to the Human Phenotype Ontology (HPO) terminology for consistency of research on long COVID (*11*). However, we did not follow HPO for 3 symptom types: tingling, abnormal menstruation, and eye symptoms. Tingling could be mapped to paresthesia, but the HPO term also included pricking or numbness of the skin, which is a broader meaning than we used. We asked about abnormal menstruation but did not include more granular HPO terminology, such as amenorrhea, irregular menstruation, and dysmenorrhea. In contrast, we asked about eye symptoms using a broader meaning than the prepared terminologies in the HPO; for eye symptoms, we included ocular pain, pruritus, gritty eye, hyperemia, epiphora, and blurred vision.

We collected age and sex information through the questionnaires and collected unique identifiers for patient data that were linked with the COVID-19 registry database operated by the Sapporo Public Health Office. We extracted information on test-positive date and acute-phase COVID-19 severity from the registry data, which were updated on April 5, 2022. Official documentation from the Ministry of Health, Labour and Welfare in Japan described classification of the severity (*12*); severity levels of moderate and severe were registered when COVID-19 patients were hospitalized. The National Vaccine Record System also provided vaccination status of participants registered in the database as of April 5, 2022.

The Sapporo Public Health Office anonymized all data and we and used linkage keys to merge each dataset: our survey data, the COVID-19 registry from the Public Health Office, and the National Vaccine Registry. We made certain participants who received study information by mail could not be identified as COVID-19 cases by others. Participants received no compensation for answering the questionnaire. The study was approved by the ethical review board for Life Science and Medical Research, Hokkaido University Hospital, on February 10, 2022, under protocol code 021-0190.

### Statistical Analyses

Because some participants only answered for current symptoms, we mapped current symptoms to the appropriate time category based on the elapsed time from illness onset to response date. If onset date was missing, we imputed test-positive date subtracted by the mean incubation period for different SARS-CoV-2 variants: 7 days for wild-type, 5 days for Alpha variant, 4 days for Delta variant, and 3 days for Omicron (*13*). We assumed the wild-type SARS-CoV-2 variant for participants who tested positive through February 2021, Alpha variant for those who tested positive during March–June 2021, Delta variant for those who tested positive during July–December 2021, and Omicron variant for those who tested positive during January 2022. In addition, we created a 13–18-month category, which comprised only case-patients who had symptoms at the time of answering the questionnaire and whose illness onset was 13–18 months prior. We considered 1 month to be 30 days. In the questionnaire, we first asked whether the participant had symptoms lasting >2 months and then asked the timeframe in which they had each symptom they selected. For analysis of each symptom, we excluded participants who did not respond about the timeframe for each symptom.

We calculated symptom prevalences at each timepoint among case-patients and at the time of answering among controls. If the elapsed time from onset to answer date was shorter than each time category, we excluded those participants from the denominator. We used the Wilson score interval to calculate CIs (*14*). We also calculated stratified symptom prevalence of case-patients and controls stratified by illness severity, age, and sex. We applied logistic regression to calculate odds ratios of having symptoms among case-patients compared with controls and adjusted for age and sex. To assess co-occurrence of symptoms, we calculated co-occurrence matrices for symptoms and visualized their networks by using the Python package of NetworkX (https://networkx.org).

We performed all analyses in Python version 3.9 (Python Software Foundation, https://www.python.org). We used the following packages for analyses: pandas version 1.4.1 (https://pandas.pydata.org) for data cleaning, matplotlib version 3.5.1 (https://matplotlib.org) for data visualization, Statsmodels version 0.13.2 (*15*) for calculation of the Wilson score interval and adjusted odds ratios, and NetworkX version 2.7.1 (*16*) for visualization of co-occurrence matrices.

## Results

### Participant Demographics

We mailed study information to 26,781 possible case-patients and 21,434 possible controls. In all, 8,018 participants answered questionnaires. Case-patients included persons who were confirmed to be registered only once in Sapporo's registry database on SARS-CoV-2 infections (Figure 2). Forty-seven participants had COVID-19 confirmed after January 1, 2022; 52

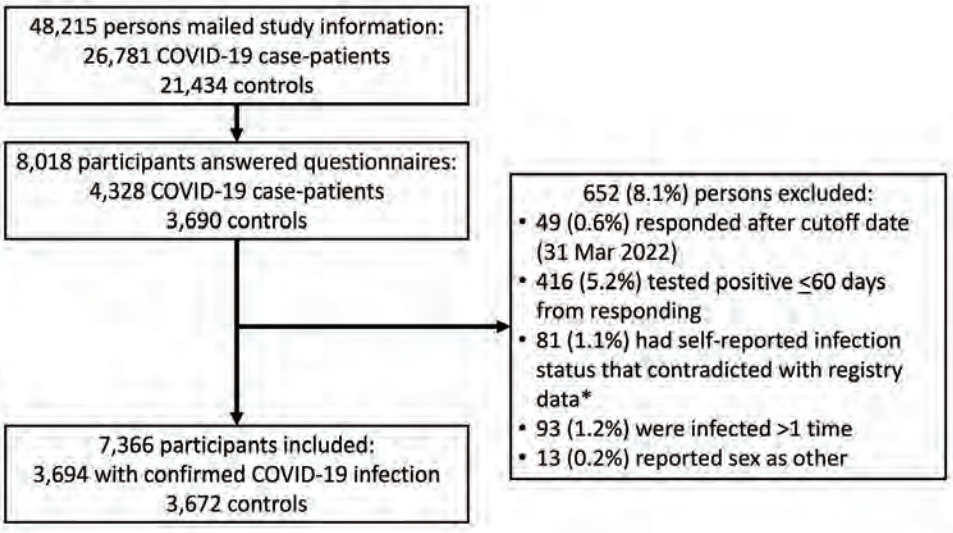


**Figure 2.** Flow chart of participant selection for a case–control study of long COVID, Sapporo, Japan. Controls were persons who self-reported as uninfected. *The Sapporo Public Health Office kept a registry of all the confirmed cases from the beginning of the COVID-19 epidemic.

participants originally selected for the control group on February 1 answered as cases and had infections confirmed before questionnaires were sent in March. We used self-reported answers for age and included 93 participants who were 65 years of age, despite our original cutoff of 64 years.

Among participants, a higher percentage of persons 20–29 years of age (16.5%, 608/3,694) were among cases than among controls (11.4%, 420/3,672), whereas fewer persons 50–65 years of age (35.3%, 1,303/3,694) were among cases than among controls (41.3%, 1,516/3,672) (Table 1). The National Vaccine Record System provided the number of COVID-19 vaccinations as of April 5, 2022; the percentage of case-patients receiving no vaccination was nearly double that of the control group (11.0% vs. 6.0%). Among case-patients, 30.2% (1,117/3,694) reported symptoms at elapsed timepoints of 7–9 months, 34.2% (1,264/3,694) at 10–12 months, and 30.6% (1,132/3,694) at ≥13 months. For severity, 10.0% (370/3,694) of case-patients had a moderate or severe COVID-19 clinical course.

### Symptom Types at Designated Timepoint from Onset

We calculated the number of symptom types observed at the designated timepoints for case-patients and at the time of questionnaire response for controls. We used 29 of 31 symptom types (Figure 3); we excluded erectile dysfunction and abnormal menstruation because those symptoms were sex-specific. Among case-patients, 31.1% (1,148/3,694) had ≥1 symptom at 2–3 months after illness onset, which is nearly the same percentage as reported symptoms at 13–18 months (30.5%, 305/1,001). When we focused on timepoints of 2–3 and 13–18 months, case-patients were likely to have more varieties of symptoms than controls; this tendency was more apparent in case-patient who had ≥5 symptom types.

### Prevalence of Each Symptom at Designated Timepoints

We calculated the prevalence and adjusted odds ratio (aOR) of each symptom at designated timepoints for cases and at the time of response for controls (Figure 4; Appendix Tables 1, 2). Among all symptoms

**Table 1.** Demographic of participants in a case–control study of long COVID, Sapporo, Japan*

| Characteristics | No. (%) | |
|---|---|---|
| | Cases, n = 3,694 | Controls, n = 3,672 |
| Age group, y | | |
| 20–29 | 608 (16.5) | 420 (11.4) |
| 30–39 | 772 (20.9) | 735 (20.0) |
| 40–49 | 1,011 (27.4) | 1,001 (27.3) |
| 50–65 | 1,303 (35.3) | 1,516 (41.3) |
| Sex | | |
| M | 1,528 (41.4) | 1,591 (43.3) |
| F | 2,166 (58.6) | 2,081 (56.7) |
| No. COVID-19 vaccines† | | |
| 0 | 407 (11.0) | 220 (6.0) |
| 1 | 65 (1.8) | 22 (0.6) |
| 2 | 2,233 (60.4) | 1,982 (54.0) |
| 3 | 989 (26.8) | 1,448 (39.4) |
| Time after illness onset, mo | | |
| 2–3‡ | 55 (1.5) | NA |
| 4–6 | 126 (3.4) | NA |
| 7–9 | 1,117 (30.2) | NA |
| 10–12 | 1,264 (34.2) | NA |
| 13–18 | 451 (12.2) | NA |
| ≥19 | 681 (18.4) | NA |
| Illness severity‡ | | |
| Asymptomatic | 115 (3.1) | NA |
| Mild | 2,952 (79.9) | NA |
| Moderate | 334 (9.0) | NA |
| Severe | 36 (1.0) | NA |
| Missing | 257 (7.0) | NA |

*NA, not applicable.
†As of April 5, 2022.
‡Severity during acute phase of infection.

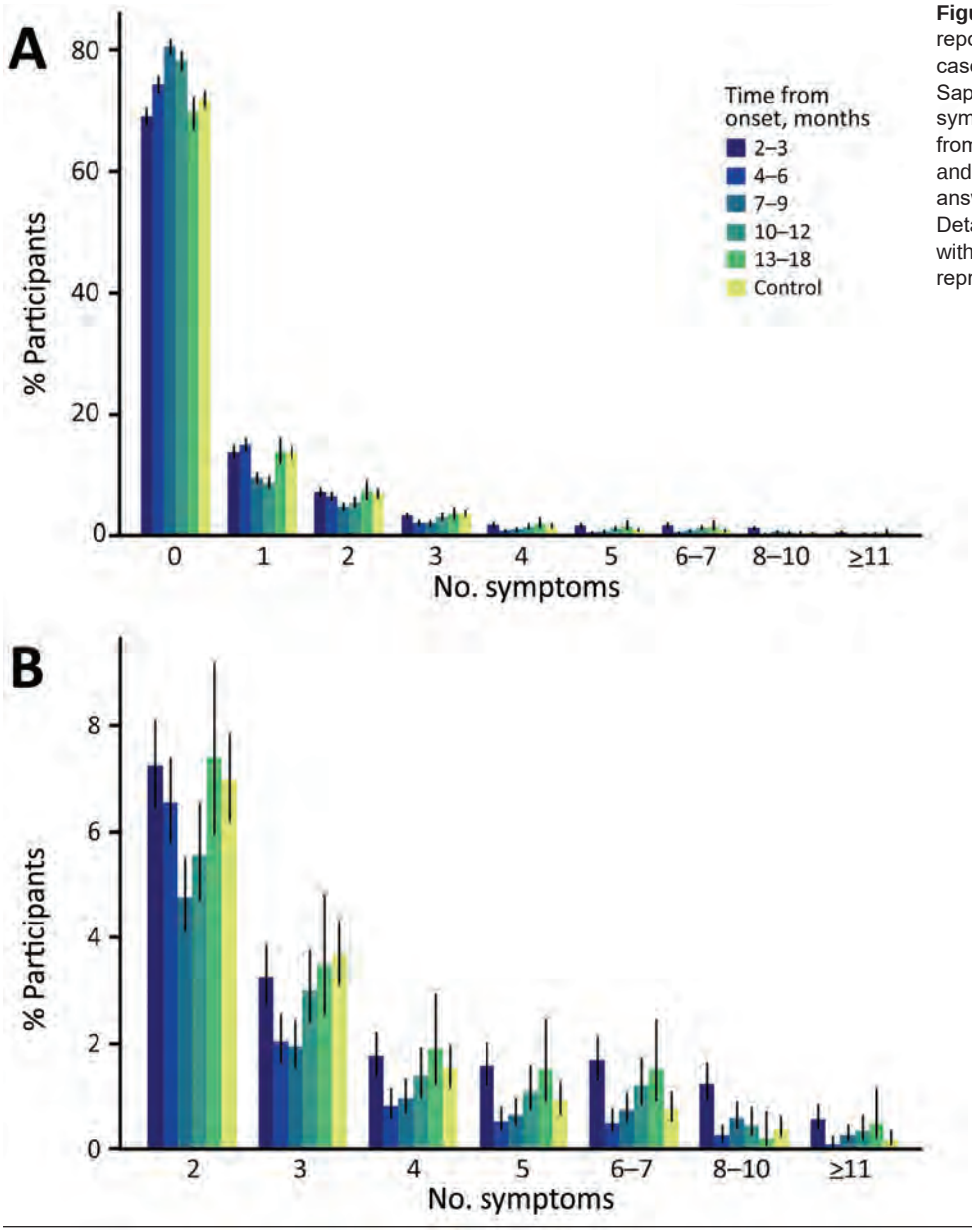


**Figure 3.** Percentage of symptoms reported among participants in a case–control study of long COVID, Sapporo, Japan. A) Number of symptoms at designated timepoints from onset among case-patients and among controls at the time of answering the questionnaire. B) Detail of percentage of participants with ≥2 symptom types. Error bars represent 95% CIs.

observed, fatigue accounted for the highest percentage, 11.55% (423/3,661), at 2–3 months after onset (aOR 2.36, 95% CI 1.97–2.81), and remained higher after 13 months (aOR 1.38, 95% CI 1.04–1.84).

Symptoms with an aOR >1 during all timepoints were anosmia, ageusia, dyspnea, and alopecia. Muscle weakness, chest pain, and brain fog had aORs >1 at 3 or 4 timepoints. Symptoms with explicitly higher aORs at 2–3 months than at other timepoints were fatigue, cough, fever, poor appetite, pharyngalgia, nausea or vomiting, and night sweats. We observed time trends of increasing aORs for diminished ability to concentrate, brain fog, sleep disturbance, tinnitus, and eye symptoms. Arthralgia or joint swelling, rhinorrhea, diarrhea, abnormal menstruation, skin rash, eye symptoms, and constipation had aORs <1 at all timepoints.

### Prevalences of Symptoms Stratified by Illness Severity, Age, and Sex

The prevalence of each symptom was more strongly related to disease severity than to age or sex (Appendix Figure 1). Prevalences for fatigue, dyspnea, alopecia, headache, diminished ability to concentrate, muscle weakness, chest pain, brain fog, myalgia, sleep disturbance, and nausea were higher among participants with moderate or severe COVID-19 cases than among those with asymptomatic and mild cases.

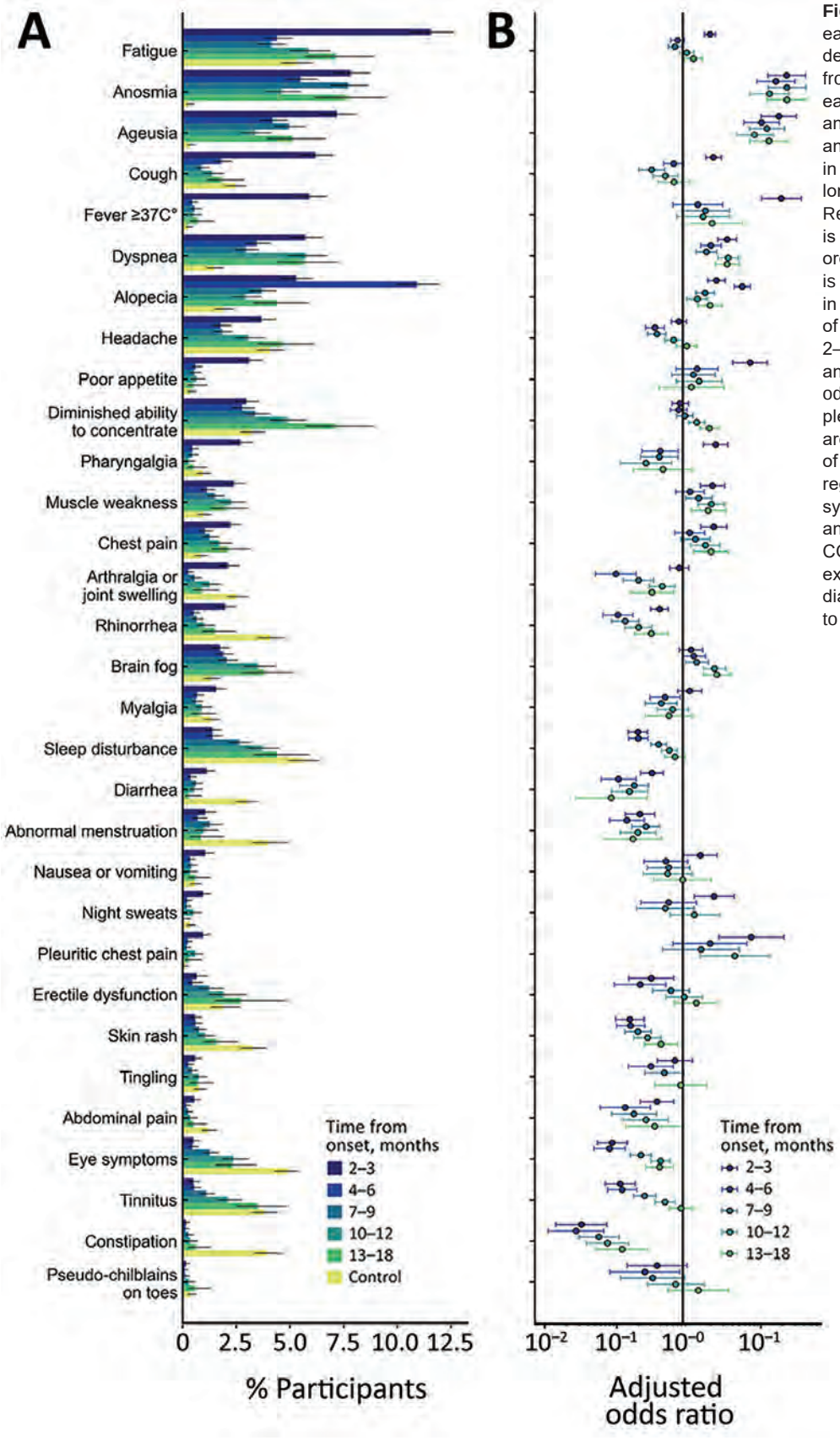


**Figure 4.** Prevalences of each symptom of cases at designated elapsed timepoints from onset including those of each symptom at the time of answering for controls (A), and adjusted odds ratios (B) in a case–control study of long COVID, Sapporo, Japan. Reference for the regression is based on controls. The order of symptoms described is listed in descending order in terms of the prevalence of symptoms of cases at 2–3 months after onset. Age and sex are adjusted. Some odds ratios for night sweats, pleuritic chest pain, and tingling are not displayed because of nonapplicability of the regression. The definition of symptoms, which developed and persisted after onset of COVID-19 and cannot be explained by an alternative diagnosis, is only applicable to cases.

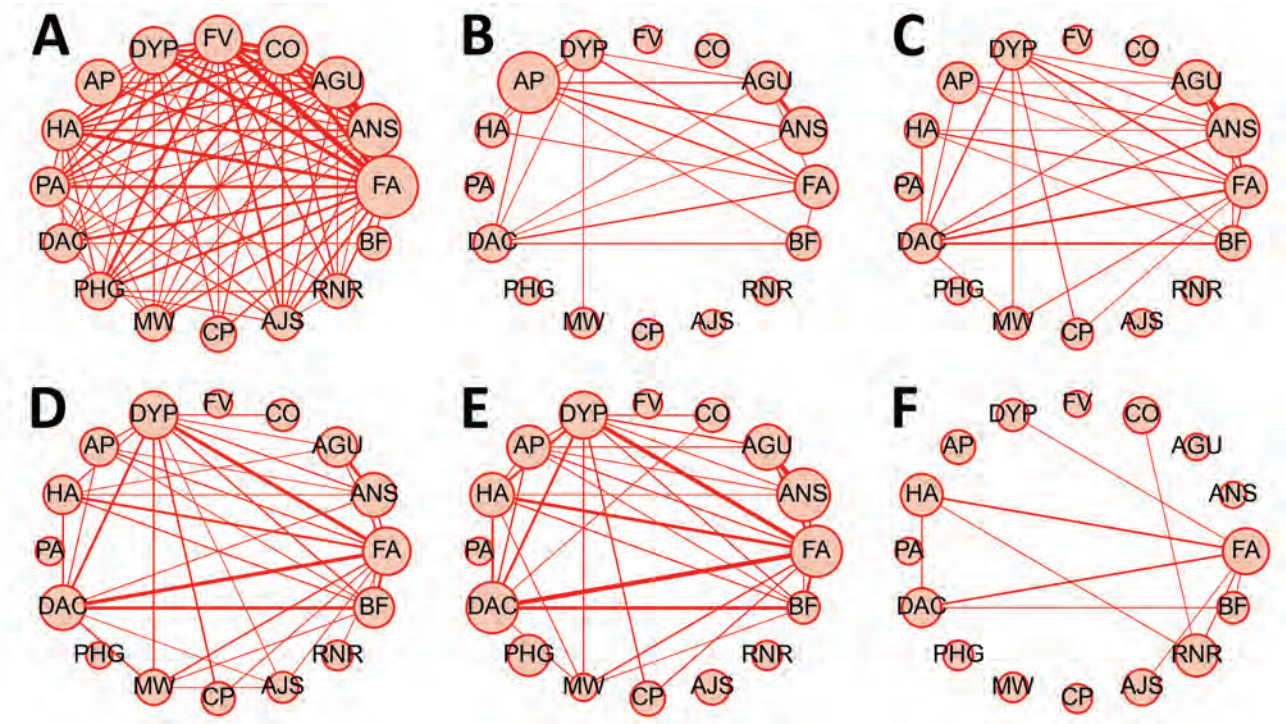


**Figure 5.** Co-occurrence network of symptoms among case-patients and controls in a case–control study of long COVID, Sapporo, Japan. A–E) Patients experiencing symptoms were queried at various timepoints after illness onset 2–3 mo (A), 4–6 mo (B), 7–9 mo (C), 10–12 mo (D), and 13–18 mo (E). F) Controls. Circle size and edge width are weighted based on number of occurrences; no edge indicates occurrence <0.5% of eligible participants. Counterclockwise order is based on the prevalence of each symptom at 2–3 months; we included the top 16 symptoms prevalent at 2–3 months from COVID-19 diagnosis. AGU, ageusia; AJS, arthralgia or joint swelling; ANS, anosmia; AP, alopecia; BF, brain fog; CO, cough; CP, chest pain; DAC, diminished ability to concentrate; DYP, dyspnea; FA, fatigue; FV, fever (temperature ≥37°C); HA, headache; MW, muscle weakness; PA, poor appetite; PHG, pharyngalgia; RNR, rhinorrhea.

Case-patients ≥40 years of age had a higher prevalences of fatigue, dyspnea, alopecia, and diminished ability to concentrate (Appendix Figures 2, 3). Prevalences of fatigue and diminished ability to concentrate were lower among case-patients 20–29 years of age than among controls at 4–12 months from onset. Case-patients 30–65 years of age had higher prevalences of alopecia than did case-patients <30 years of age or controls.

Women had higher prevalences of anosmia, ageusia, and alopecia (Appendix Figure 4). The prevalence of anosmia for women at 13–18 months was nearly triple that for men. We observed a similar trend in ageusia, and higher proportions of women in both the case and control groups had alopecia. Although we performed comparisons within each sex, the prevalences of alopecia for male and female case-patients were consistently higher than those for controls.

### Co-occurrence Network of Symptom Types

We visualized co-occurrence networks and heatmaps of symptoms at each timepoint (Figure 5; Appendix Figure 5). Symptom co-occurrence at 2–3 months was more densely connected among case-patients than among controls. Among case-patients, fatigue mainly co-occurred with 15 other symptoms at 2–3 months. Dyspnea mainly co-occurred with fatigue, alopecia, and diminished ability to concentrate and weakly occurred with ageusia, muscle weakness, and chest pain. Also, anosmia and ageusia frequently co-occurred at each timepoint. Fatigue, alopecia, and diminished ability to concentrate occurred simultaneously among controls. Brain fog was related to diminished ability to concentrate and fatigue, but those relationships were more apparent among case-patients at 13–18 months after onset than at other timepoints.

## Discussion

We conducted a large cross-sectional study on prevalences of and risks for COVID-19 sequelae over multiple timepoints among the general population in Sapporo, Japan. The study revealed COVID-19–related symptoms that remained long after illness

onset mainly were systemic, neuropsychiatric, or in the respiratory system (Table 2). Moreover, COVID-19 case-patients had a higher risk for ageusia, anosmia, muscle weakness, chest pain, poor appetite, and alopecia compared with controls. On the other hand, case-patients had the same or lower risk for several manifestations in musculoskeletal, gastrointestinal, and dermatologic systems compared with controls, suggesting weak or least likely long-term effects on these systems.

COVID-19 case-patients had a wider variety of symptom types at 2–3 months and 13–18 months than did controls; the difference in the number of symptom types was more apparent in COVID-19 case-patients who had ≥5 symptom types, which is consistent with a previous study (*5*). In addition, we analyzed the time trend of aORs and cluster characteristics between symptoms for cases compared with controls (Figures 4, 5) The odds ratios for neuropsychiatric symptoms (diminished ability to concentrate, brain fog, and sleep disturbance) increased over elapsed timepoints, even after 13 months. On the other hand, typical common cold–like symptoms (cough, pharyngalgia, and rhinorrhea) disappeared 4 months after onset, although those prevalences were higher at 2–3 months among cases compared with controls. We noted cluster characteristics of symptoms among cases, especially between fatigue, dyspnea, alopecia, diminished ability to concentrate, and brain fog, but we observed similar cluster characteristics among controls.

COVID-19 is a systemic disease with diverse manifestations, which complicates the exploration of long COVID. A previous study in which COVID-19 cases

**Table 2.** Summarized adjusted odds ratio for each symptom in a case–control study of long COVID, Sapporo, Japan*

| Symptoms | Adjusted odds ratio, by time after illness onset | | | | | Likeliness |
|---|---|---|---|---|---|---|
| | 2–3 mo | 4–6 mo | 7–9 mo | 10–12 mo | 13–18 mo | |
| Systemic | | | | | | |
| Fatigue | **>1.5** | <1 | <1 | ≥1 | **≥1** | Likely |
| Fever, temp. ≥37C° | **>1.5** | >1.5 | >1.5 | >1.5 | >1.5 | Likely |
| Headache | <1 | <0.66 | <0.66 | <1 | ≥1 | Less likely |
| Night sweats | **>1.5** | <0.66 | <0.66 | ≥1 | NA | Less likely |
| Respiratory | | | | | | |
| Cough | **>1.5** | <1 | <0.66 | <0.66 | <1 | Unlikely |
| Dyspnea | **>1.5** | **>1.5** | **>1.5** | **>1.5** | **>1.5** | Very likely |
| Pleuritic chest pain | **>1.5** | >1.5 | >1.5 | **>1.5** | NA | Very likely |
| Neuropsychiatric | | | | | | |
| Diminished ability to concentrate | <1 | <1 | ≥1 | **>1.5** | **>1.5** | Likely |
| Brain fog | ≥1 | ≥1 | **>1.5** | **>1.5** | **>1.5** | Very likely |
| Sleep disturbance | <0.66 | <0.66 | <0.66 | <0.66 | <1 | Unlikely |
| Otorhinolaryngological | | | | | | |
| Ageusia | **>1.5** | **>1.5** | **>1.5** | **>1.5** | **>1.5** | Very likely |
| Anosmia | **>1.5** | **>1.5** | **>1.5** | **>1.5** | **>1.5** | Very likely |
| Pharyngalgia | **>1.5** | <0.66 | <0.66 | <0.66 | <0.66 | Unlikely |
| Rhinorrhea | <0.66 | <0.66 | <0.66 | <0.66 | <0.66 | Unlikely |
| Tinnitus | <0.66 | <0.66 | <0.66 | <0.66 | <1 | Unlikely |
| Musculoskeletal | | | | | | |
| Muscle weakness | **>1.5** | ≥1 | **>1.5** | **>1.5** | **>1.5** | Very likely |
| Arthralgia or joint swelling | <1 | <0.66 | <0.66 | <0.66 | <0.66 | Unlikely |
| Myalgia | ≥1 | <0.66 | <0.66 | <1 | <0.66 | Unlikely |
| Cardiovascular | | | | | | |
| Chest pain | **>1.5** | ≥1 | ≥1 | **>1.5** | **>1.5** | Very likely |
| Gastrointestinal | | | | | | |
| Poor appetite | **>1.5** | >1.5 | ≥1 | >1.5 | ≥1 | Likely |
| Diarrhea | <0.66 | <0.66 | <0.66 | <0.66 | <0.66 | Unlikely |
| Nausea or vomiting | **>1.5** | <0.66 | <0.66 | <0.66 | <1 | Unlikely |
| Abdominal pain | <0.66 | <0.66 | <0.66 | <0.66 | <0.66 | Unlikely |
| Constipation | <0.66 | <0.66 | <0.66 | <0.66 | <0.66 | Unlikely |
| Dermatologic | | | | | | |
| Alopecia | **>1.5** | **>1.5** | **>1.5** | **>1.5** | **>1.5** | Very likely |
| Skin rash | <0.66 | <0.66 | <0.66 | <0.66 | <0.66 | Unlikely |
| Tingling | <1 | <0.66 | <0.66 | NA | <1 | Unlikely |
| Pseudo-chilblains on toes | <0.66 | <0.66 | <0.66 | <1 | >1.5 | Less likely |
| Other | | | | | | |
| Abnormal menstruation | <0.66 | <0.66 | <0.66 | <0.66 | <0.66 | Unlikely |
| Erectile dysfunction | <0.66 | <0.66 | <1 | ≥1 | >1.5 | Less likely |
| Eye symptoms | <0.66 | <0.66 | <0.66 | <0.66 | <0.66 | Unlikely |

*Reference for regression is based on controls. Bold text indicates 95% CI that does not contain 1. NA, not applicable.

were compared with matched controls by using electronic health records showed an increased risk for disease in an extensive range of organs and tissue types, including gastrointestinal organs, endocrine system, and renal organs, and the increased risks were observed even in analysis among a limited number of persons 18–64 years of age (*6*). Because that study used electronic health records for both cases and controls, results might be biased toward cases. In this study, we investigated general symptoms of COVID-19 cases and observed high odds ratios for systemic, respiratory, and neuropsychiatric symptoms. Potential mechanisms for differences in observed risks between the previous electronic health record–based studies and this study could be less severe hyperinflammatory status caused by infection (*17*). SARS-CoV-2 infection causes hyperinflammation, including cytokine storm, inducing production of endogenous chemical substances, and prothrombotic condition, which causes respiratory failure, pulmonary embolism, diarrhea, gastrointestinal hemorrhage, myocardial injury, and other systemic syndromes (*18*). However, cases with mild symptoms would not experience the severe hyperinflammatory status.

A prospective study on 15-year follow-up of patients with SARS (severe acute respiratory syndrome), a disease similar to COVID-19, showed long-term effects on pulmonary function, bone health, and lipid metabolism (*19*). Similar results were reported in an examination of SARS cases at 12 years after disease onset (*20*). Similarly, COVID-19 could affect long-term pulmonary function. Our study results showed prolonged effects on the respiratory system (dyspnea and pleuritic chest pain), even in mildly symptomatic cases, and a much higher prevalence of dyspnea and cough among severe cases, necessitating long-term and continuous monitoring of COVID-19 patients.

Other reports showed COVID-19 patients had high prevalences of neurologic complications several months after disease onset (*7*,*21*). Neuroinvasiveness and neurovirulence of SARS-CoV-2 are potential mechanisms of those neurologic complications (*22*). Our study demonstrated that mildly symptomatic cases had a high risk for neuropsychiatric symptoms, such as diminished ability to concentrate and brain fog. Those data suggest that immune-mediated damage, neurotropism, or neurovirulence properties of SARS-CoV-2 are involved in long-term effects. Those properties also could be related to autoimmune diseases and alopecia (*23*–*25*).

The prevalence of all symptoms reported in our study was lower than those reported through meta-analysis of cross-sectional studies (*10*,*26*). This difference might be a result of the difference in the definition of symptom. Our definition included conditions lasting at least 2 months, but other studies included only symptoms at the time of answering questions without asking how long symptoms had persisted. Furthermore, the difference in the definitions used between cases and controls in the current study caused the odds ratios of some symptoms to be <1.

The first limitation of our study is that the results could be affected by recall bias, which is indicated by U-shaped prevalences of 22 of 31 symptom types. This bias might be explained by the evidence that 30.6% of case-patients reported symptoms ≥13 months after illness onset, and from evidence that 38.2% of case-patients who reported having that symptom only at the time of responding to the questionnaire. Those biases could introduce an underestimation of the prevalence of symptoms in case-patients at each elapsed timepoint. Second, the data obtained in this study were collected by self-reporting method, and patients might not have been able to decide whether their symptoms were related to their COVID-19 diagnosis or another illness. Third, we did not include vaccination effects in this study. Several studies showed the effectiveness of vaccination against long COVID (*27*,*28*), but in our study only a small number of case-patients were vaccinated ≥2 times before COVID-19 diagnosis, suggesting that the results obtained in this study were not largely biased by vaccination effect. Fourth, we compared long-term symptoms of case-patients with those of controls sampled from the general population of Sapporo, and that comparison might be biased if persons with certain demographic characteristics were more likely to be infected. Therefore, prevalences of symptoms for case-patients might have been higher than those of controls because of the difference in demographic characteristics of the population, not because of having SARS-CoV-2 infection.

In conclusion, among symptomatic case-patients, fatigue, dyspnea, and neuropsychiatric symptoms were key characteristics of COVID-19 sequelae over time, but most common cold–like, gastrointestinal, and dermatologic symptoms disappeared several months after illness onset. Clinicians evaluating patients for potential long COVID should focus on systemic, respiratory, and neuropsychiatric symptoms associated with long-term sequelae of severe COVID-19 and on ageusia, anosmia, and alopecia for patients who had mildly symptomatic cases.

This work was supported by Japan Agency for Medical Research and Development (grant no. JP20fk0108471) and MHLW Special Research Program (grant no. JPMH-20CA2046). The sponsors of the study had no role in study design, data collection, data analyses, data interpretation, or writing of the manuscript.

### Acknowledgments

We thank Hidehiro Ozawa and Masami Iwama for preparing the in-house COVID-19 registry, and assistance in launching this study.

## About the Author

Dr. Asakura is an academic fellow in the Department of Public Health, Faculty of Medicine, Hokkaido University, Sapporo, Hokkaido, Japan. His research focuses on infectious disease epidemiology and mathematical modelling.

### References

1. Callard F, Perego E. How and why patients made long Covid. Soc Sci Med. 2021;268:113426. https://doi.org/10.1016/j.socscimed.2020.113426
2. Munblit D, O'Hara ME, Akrami A, Perego E, Olliaro P, Needham DM. Long COVID: aiming for a consensus. Lancet Respir Med. 2022;10:632–4. https://doi.org/10.1016/S2213-2600(22)00135-7
3. Soriano JB, Murthy S, Marshall JC, Relan P, Diaz JV; WHO Clinical Case Definition Working Group on Post-COVID-19 Condition. A clinical case definition of post-COVID-19 condition by a Delphi consensus. Lancet Infect Dis. 2022; 22:e102–7. https://doi.org/10.1016/S1473-3099(21)00703-9
4. Sandmann FG, Tessier E, Lacy J, Kall M, Van Leeuwen E, Charlett A, et al. Long-term health-related quality of life in non-hospitalized coronavirus disease 2019 (COVID-19) cases with confirmed severe acute respiratory syndrome coronavirus 2 (SARS-CoV-2) infection in England: longitudinal analysis and cross-sectional comparison with controls. Clin Infect Dis. 2022;75:e962–73. https://doi.org/10.1016/10.1093/cid/ciac151
5. Stephenson T, Pinto Pereira SM, Shafran R, de Stavola BL, Rojas N, McOwat K, et al.; CLoCk Consortium. Physical and mental health 3 months after SARS-CoV-2 infection (long COVID) among adolescents in England (CLoCk): a national matched cohort study. Lancet Child Adolesc Health. 2022;6:230–9. https://doi.org/10.1016/S2352-4642(22)00022-0
6. Bull-Otterson L, Baca S, Saydah S, Boehmer TK, Adjei S, Gray S, et al. Post–COVID conditions among adult COVID-19 survivors aged 18–64 and ≥65 years—United States, March 2020–November 2021. MMWR Morb Mortal Wkly Rep. 2022;71:713–7. https://doi.org/10.15585/mmwr.mm7121e1
7. Taquet M, Geddes JR, Husain M, Luciano S, Harrison PJ. 6-month neurological and psychiatric outcomes in 236 379 survivors of COVID-19: a retrospective cohort study using electronic health records. Lancet Psychiatry. 2021;8:416–27. https://doi.org/10.1016/S2215-0366(21)00084-5
8. Davis HE, Assaf GS, McCorkell L, Wei H, Low RJ, Re'em Y, et al. Characterizing long COVID in an international cohort: 7 months of symptoms and their impact. EClinicalMedicine. 2021;38:101019. https://doi.org/10.1016/j.eclinm.2021.101019
9. Fernández-de-las-Peñas C, Palacios-Ceña D, Gómez-Mayordomo V, Florencio LL, Cuadrado ML, Plaza-Manzano G, et al. Prevalence of post-COVID-19 symptoms in hospitalized and non-hospitalized COVID-19 survivors: a systematic review and meta-analysis. Eur J Intern Med. 2021;92:55–70. https://doi.org/10.1016/j.ejim.2021.06.009
10. Han Q, Zheng B, Daines L, Sheikh A. Long-term sequelae of COVID-19: A systematic review and meta-analysis of one-year follow-up studies on post-COVID symptoms. Pathogens. 2022;11:269. https://doi.org/10.3390/pathogens11020269
11. Köhler S, Gargano M, Matentzoglu N, Carmody LC, Lewis-Smith D, Vasilevsky NA, et al. The human phenotype ontology in 2021. Nucleic Acids Res. 2021;49(D1):D1207–17. https://doi.org/10.1093/nar/gkaa1043
12. Ministry of Health, Labour and Welfare, Japan. Clinical management of patients with COVID-19: a guide for front-line healthcare workers, version 7.2 [cited 2022 Jul 12]. https://www.mhlw.go.jp/content/000936655.pdf
13. Wu Y, Kang L, Guo Z, Liu J, Liu M, Liang W. Incubation period of COVID-19 caused by unique SARS-CoV-2 strains: a systematic review and meta-analysis. JAMA Netw Open. 2022;5:e2228008. https://doi.org/10.1001/jamanetworkopen.2022.28008
14. Wilson EB. Probable inference, the law of succession, and statistical inference. J Am Stat Assoc. 1927;22:209–12. https://doi.org/10.1080/01621459.1927.10502953
15. Seabold S, Perktold J. Statsmodels: econometric and statistical modeling with Python, 2010 [cited 2022 May 22]. https://conference.scipy.org/proceedings/scipy2010/seabold.html
16. Hagberg AA, Swart PJ, S Chult DA. Exploring network structure, dynamics, and function using Networkx [cited 2022 May 22]. https://www.osti.gov/servlets/purl/960616
17. Hojyo S, Uchida M, Tanaka K, Hasebe R, Tanaka Y, Murakami M, et al. How COVID-19 induces cytokine storm with high mortality. Inflamm Regen. 2020;40:37. https://doi.org/10.1186/s41232-020-00146-3
18. Kumar A, Narayan RK, Prasoon P, Kumari C, Kaur G, Kumar S, et al. COVID-19 mechanisms in the human body—what we know so far. Front Immunol. 2021;12:693938. https://doi.org/10.3389/fimmu.2021.693938
19. Zhang P, Li J, Liu H, Han N, Ju J, Kou Y, et al. Long-term bone and lung consequences associated with hospital-acquired severe acute respiratory syndrome: a 15-year follow-up from a prospective cohort study. Bone Res. 2020;8:8. https://doi.org/10.1038/s41413-020-0084-5
20. Wu Q, Zhou L, Sun X, Yan Z, Hu C, Wu J, et al. Altered lipid metabolism in recovered SARS patients twelve years after infection. Sci Rep. 2017;7:9110. https://doi.org/10.1038/s41598-017-09536-z
21. Blomberg B, Mohn KGI, Brokstad KA, Zhou F, Linchausen DW, Hansen BA, et al.; Bergen COVID-19 Research Group. Long COVID in a prospective cohort of home-isolated patients. Nat Med. 2021;27:1607–13. https://doi.org/10.1038/s41591-021-01433-3
22. Bauer L, Laksono BM, de Vrij FMS, Kushner SA, Harschnitz O, van Riel D. The neuroinvasiveness, neurotropism, and neurovirulence of SARS-CoV-2. Trends Neurosci. 2022;45:358–68. https://doi.org/10.1016/j.tins.2022.02.006
23. Silva Andrade B, Siqueira S, de Assis Soares WR, de Souza Rangel F, Santos NO, Dos Santos Freitas A, et al. Long-COVID and post-COVID health complications: an

up-to-date review on clinical conditions and their possible molecular mechanisms. Viruses. 2021;13:700. https://doi.org/10.3390/v13040700
24. Rossi A, Magri F, Michelini S, Sernicola A, Muscianese M, Caro G, et al. New onset of alopecia areata in a patient with SARS-CoV-2 infection: possible pathogenetic correlations? J Cosmet Dermatol. 2021;20:2004–5. https://doi.org/10.1111/jocd.14080
25. Menni C, Valdes AM, Polidori L, Antonelli M, Penamakuri S, Nogal A, et al. Symptom prevalence, duration, and risk of hospital admission in individuals infected with SARS-CoV-2 during periods of omicron and delta variant dominance: a prospective observational study from the ZOE COVID Study. Lancet. 2022;399:1618–24. https://doi.org/10.1016/S0140-6736(22)00327-0
26. Alkodaymi MS, Omrani OA, Fawzy NA, Shaar BA, Almamlouk R, Riaz M, et al. Prevalence of post-acute COVID-19 syndrome symptoms at different follow-up periods: a systematic review and meta-analysis. Clin Microbiol Infect. 2022;28:657–66. https://doi.org/10.1016/j.cmi.2022.01.014
27. Taquet M, Dercon Q, Harrison PJ. Six-month sequelae of post-vaccination SARS-CoV-2 infection: a retrospective cohort study of 10,024 breakthrough infections. Brain Behav Immun. 2022;103:154–62. https://doi.org/10.1016/j.bbi.2022.04.013
28. Pfaff ER, Girvin AT, Bennett TD, Bhatia A, Brooks IM, Deer RR, et al.; N3C Consortium. Identifying who has long COVID in the USA: a machine learning approach using N3C data. Lancet Digit Health. 2022;4:e532–41. https://doi.org/10.1016/S2589-7500(22)00048-6

Address for correspondence: Kimura Takashi, Hokkaido University, Kita 15, Nishi 7, Kita-ku, Sapporo 060-8638, Japan; email: kimura@med.hokudai.ac.jp

# Influence of Sex and Sex-Based Disparities on Prevalent Tuberculosis, Vietnam, 2017–2018

Hai Viet Nguyen, Daniella Brals, Edine Tiemersma, Robert Gasior, Nhung Viet Nguyen, Hoa Binh Nguyen, Hung Van Nguyen, Ngoc Anh Le Thi, Frank Cobelens

To assess sex disparities in tuberculosis in Vietnam, we conducted a nested, case–control study based on a 2017 tuberculosis prevalence survey. We defined the case group as all survey participants with laboratory–confirmed tuberculosis and the control group as a randomly selected group of participants with no tuberculosis. We used structural equation modeling to describe pathways from sex to tuberculosis according to an a priori conceptual framework. Our analysis included 1,319 participants, of whom 250 were case-patients. We found that sex was directly associated with tuberculosis prevalence (adjusted odds ratio for men compared with women 3.0 [95% CI 1.7–5.0]) and indirectly associated through other domains. The strong sex difference in tuberculosis prevalence is explained by a complex interplay of factors relating to behavioral and environmental risks, access to healthcare, and clinical manifestations. However, after controlling for all those factors, a direct sex effect remains that might be caused by biological factors.

Tuberculosis (TB) affects millions of persons worldwide. In most regions, the TB notification rate for men is higher than for women. According to the World Health Organization, the male-to-female (M:F) ratio of notified TB cases in 2020 was 1.7 globally; 56% of all TB cases were in men, 33% in women, and 11% in children (*1*). Several studies indicate that the high M:F ratio is mainly because cases in women are undernotified and because of bias in case reporting (*2*,*3*). However, a meta-analysis of 56 surveys of TB prevalence around the world showed a M:F ratio of 2.2, with the highest ratio in Southeast Asia (3.4, 95% CI 2.8–4.0) (*4*), suggesting that the sex variation in TB exists independently of reporting. Commonly proposed reasons behind this phenomenon include differences in how men and women seek and access TB care, how social roles affect contact with persons harboring *Mycobacterium tuberculosis* infection, and how certain male-dominated occupations (e.g., mining) can increase the risk for TB (*4*). Moreover, risk factors for TB, such as tobacco smoking and excessive alcohol consumption, are generally more frequent among men (*5*). Some studies have suggested biological differences in TB risk between men and women (*6*). The relative contributions of those factors in explaining the differences in TB risk between men and women are still under debate, and they may confound or obscure one another.

Vietnam, 1 of 30 countries that carries a high TB burden, conducted a national TB prevalence survey in 2017, coordinated by its National TB Program (*7*). That survey found a TB prevalence of 322 (95% CI 260–399) cases/100,000 adults nationally and a M:F ratio of 4.0. We conducted a nested, case–control study within this TB prevalence survey to assess the contribution of various factors that might have contributed to that ratio, including access to health care, exposure, socioeconomic status (SES), and possible biological factors. We acknowledge that other potentially underlying sex disparities could also have contributed.

## Methods

### Study Population

The second national TB prevalence survey in Vietnam was conducted during October 2017–February 2018, using multistage cluster sampling to select 87,207 eligible participants ≥15 years of age from 82 population clusters across the country (*7*). Using this

Author affiliations: Amsterdam University Medical Centers, University of Amsterdam, Amsterdam, the Netherlands (H.V. Nguyen, D. Brals, F. Cobelens); Vietnam National Tuberculosis Program, Hanoi, Vietnam (H.V. Nguyen, N.V. Nguyen, H.B. Nguyen, H.V. Nguyen, N.A. Le Thi); KNCV Tuberculosis Foundation, Den Haag, the Netherlands (E. Tiemersma); National Academies of Sciences, Engineering, and Medicine, Washington, DC, USA (R. Gasior).

DOI: http://doi.org/10.3201/eid2905.221476

survey, we designed a nested, case–control study (PEER study) in which the case group consisted of all participants with ≥1 positive TB test (Xpert MTB/Rif; Cepeheid, https://www.cepheid.com) conducted in the field. The control group consisted of persons who screened negative for TB or had an Xpert-negative result. We interviewed participants using an in-depth questionnaire to assess their TB-suggestive symptoms, access to health care, and TB-associated risk factors.

### Case Group Selection

We defined a case-patient as an eligible participant who had ≥1 positive Xpert result. To identify case-patients, we screened all survey participants for TB by a short questionnaire and chest radiograph. We defined presumptive TB cases as persons who had cough for ≥2 weeks (or cough of any duration for pregnant women), self-reported TB treatment in the 2 years preceding the survey, or chest radiograph with abnormalities consistent with TB; we asked those persons to provide a sputum sample. We collected the first sputum sample at the initial screening and examined it with Xpert either in the district laboratory or directly in the field. If the Xpert result was positive for M. *tuberculosis*, we asked the participants to provide an additional sputum sample the next day for confirmation, invited them to participate in the PEER study, and interviewed them after collecting consent on submission of the second sample.

### Control Group Selection

We defined a control as an eligible participant who was randomly selected for the PEER study, attended the screening event and screened negative for TB, or had a negative Xpert result. Before the TB screening event started, we conducted a house-to-house census in each cluster. All eligible adults received an invitation card with a unique PIN code. We randomly selected the PIN code of participants in each cluster to be recruited in the control group, regardless of the number of TB cases detected in each cluster. We invited those who attended the screening event to participate in the PEER study. Trained interviewers interviewed persons consenting to participate.

### Sample Size

On the basis of TB prevalence in Vietnam in 2007 and the assumed decline in TB burden (*8*,*9*), we expected to find 3 TB cases per cluster, resulting in 246 cases. Per case, aiming to achieve a final case-to-control ratio of 1:4, we randomly selected 5 controls to account for persons refusing participation and loss of controls because of Xpert-positive results. This process resulted in a control group sample size of 1,230 participants.

### Data Analysis

We used structural equation modeling (SEM) to describe pathways to prevalent TB through sex and gender-related exposures according to an a priori conceptual framework (Figure 1) (*10*). In addition to the main exposure, sex, we examined exposures grouped a priori into pre-conceived domains (i.e., SES, access to healthcare, TB behavioral and environmental risks, and clinical symptoms), reflecting factors likely to influence the risk for TB disease or affect TB disease detection (*11*–*14*). Because we analyzed prevalence of disease rather than incidence, and the relationship between prevalence and incidence (i.e., the duration of TB disease) is affected by disease detection, we added clinical symptoms and access to healthcare to our analysis to address this potential selection bias. For each preconceived domain, we performed confirmatory factor analysis where we estimated the domain score as a stand-alone latent variable using all relevant underlying variables collected from the in-depth questionnaire and household visits (Figure 1; Appendix Table 1). The clinical symptoms domain consisted of weight loss, fever, night sweats, and cough. The access to healthcare domain consisted of health insurance status, HIV status, previous chest radiograph, types of healthcare facilities visited due to reported symptoms, and distance from the nearest hospital. The behavioral and environmental risks domain consisted of working indoors or as a miner, being close contacts of TB patients, having diabetes, excessive drinking of alcoholic beverages, and tobacco smoking (including the amount of pack-years and passive smoking). The SES domain consisted of household assets, participants' occupations, marital status, and level of education.

We computed a predicted latent continuous variable for each domain. Using the xtile command in Stata (StataCorp LLC, https://www.stata.com), we categorized each latent domain variable into relatively equal tertiles that represent the highest to lowest values of the latent variables (*15*). For the clinical symptoms domain, the tertiles were least severe, moderately severe, and most severe; for the access to healthcare domain, they were good access, moderate access, and poor access; for the behavioral and environmental risk domain, they were low risk, moderate risk, and high risk; and for the SES domain, they were high, medium, and low.

To investigate the pathways from sex to TB, we included the domain tertile scores in a multivariable

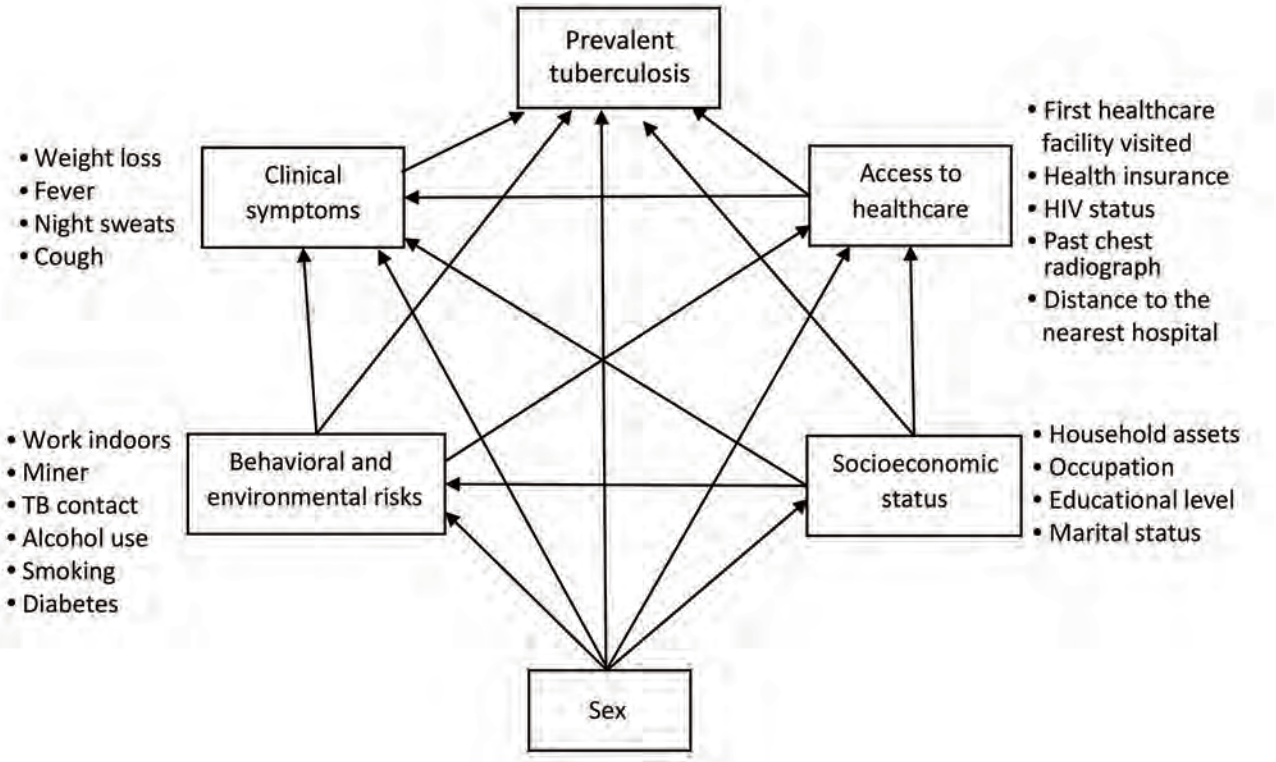


**Figure 1.** Conceptual framework of the structural equation model to describe pathways between tuberculosis prevalence, sex, and the associated domains for case–control analysis of tuberculosis prevalence, Vietnam, 2017–2018.

SEM according to the conceptual framework (Figure 1). We modeled TB within the SEM using the Bernoulli logit model, and we fit the predicted latent domain variables using ordinal logit models. We adjusted each outcome within the SEM for age, area (urban, remote, and rural), and region (North, Central, or South). In reporting, we distinguished direct pathways (from a domain to an outcome) and indirect pathways (from a domain to an outcome via another domain). We assessed goodness-of-fit by using bootstrapped area under the curve (1,000 replications). We employed Stata version 14.0 for statistical analyses.

We included the clinical symptoms domain in our conceptual framework because having symptoms increases the chance for TB patients to be identified through the survey process but also to be diagnosed with TB during routine care before the survey, thereby controlling for potential selection bias inherent in a prevalence survey. We acknowledged that doing so might obscure the effects of other domains by being on the causal pathway between sex and prevalent TB. In the TB prevalence survey, the final status of a TB case was decided by an expert panel, not just by the result of Xpert. We therefore performed sensitivity analyses in which the clinical domain was excluded (model 1), the definition of a TB case was replaced with the expert panel decision (model 2), and Xpert-positive TB cases with previous TB treatment history were excluded (model 3). We applied inverse probability weighting and poststratification weighting to adjust for differences in participation rate by age, sex, cluster, and the relative contribution of each participant, as described in our previous publication (*7*).

### Ethics Statement

This study was given scientific and ethical approval by the Institutional Review Board of the Vietnam National Lung Hospital, under approval letter number 62/17/CTHĐKH-ĐĐ. All participants signed an individual written informed consent. All of those in the case group were referred to their local district TB unit for appropriate treatment.

## Results

Of the 1,230 preselected controls, 107 did not attend the screening event or declined to participate, and 54 had a positive Xpert result that defined them as TB cases (Figure 2). There were 1,319 interviewed participants in total, of which 250 were cases and 1,069 were controls (Table 1); 694 (52.6%) participants were men and 625 (47.4%) women. Among the controls, 2 were

later reported to have positive culture results, classified as TB cases by the expert panel, and excluded from our analysis.

The distribution of men and women among the domains (Table 2) shows that men were more dominant in the most disadvantaged tertile of all domains, except for SES. Compared with women, men more often reported severe clinical symptoms (12.8% vs. 6.7%), poor access to healthcare (38.9% vs. 24.0%), and high behavioral and environmental risk (52.9% vs. 4.2%) (Table 1).

SEM results (Figure 3), full estimation results (Table 3), and the confirmatory factor analysis results (Appendix Table 1) indicate that sex was directly associated with prevalent TB (adjusted odds ratio [aOR] for men compared with women 3.0 [95% CI 1.7–5.0]). Sex was also associated indirectly with prevalent TB through behavioral and environmental risks, behavioral and environmental risks and clinical symptoms, and behavioral and environmental risks and access to healthcare. Clinical symptoms (aOR for moderate severity 5.0 [95% CI 2.8–8.7]; aOR for most severe 13.2 [95% CI 5.9–29.2]), access to healthcare (aOR for moderate access 2.5 [95% CI 1.4–4.4]; aOR for poor access 13.4 [95% CI 7.0–25.6]), and behavioral and environmental risks (aOR for moderate risk 2.1 [95% CI 1.1–3.9]; aOR for high risk 2.9 [95% CI 1.5–5.6]) were directly associated with TB as well. SES did not directly affect prevalent TB, only indirectly through access to healthcare, behavioral and environmental risks, and clinical symptoms (Figure 3, Table 3). When we stratified the SEM model by sex, we found a statistically significant association between prevalent TB and behavioral and environmental risks among men (aOR for moderate risk 3.5 [95% CI 1.5–8.2]; aOR for high risk 4.8 (95% CI 2.0–11.7]). That same association was not statistically significant among women (Appendix Figures 1 and 2).

Considering associations between domains and covariates, we found more severe clinical symptoms among participants who were >55 years of age, lived in northern Vietnam, had poor access to healthcare, were more exposed to harmful substances, or had lower SES. Poor access to healthcare was more frequently observed in participants living in rural areas and among those with high behavioral and environmental risks or lower SES. Behavioral and environmental risks were less frequently observed in women, younger participants (15–24 years of age), those living in northern locations, and those with high SES. The bootstrapped AUC result showed that our model

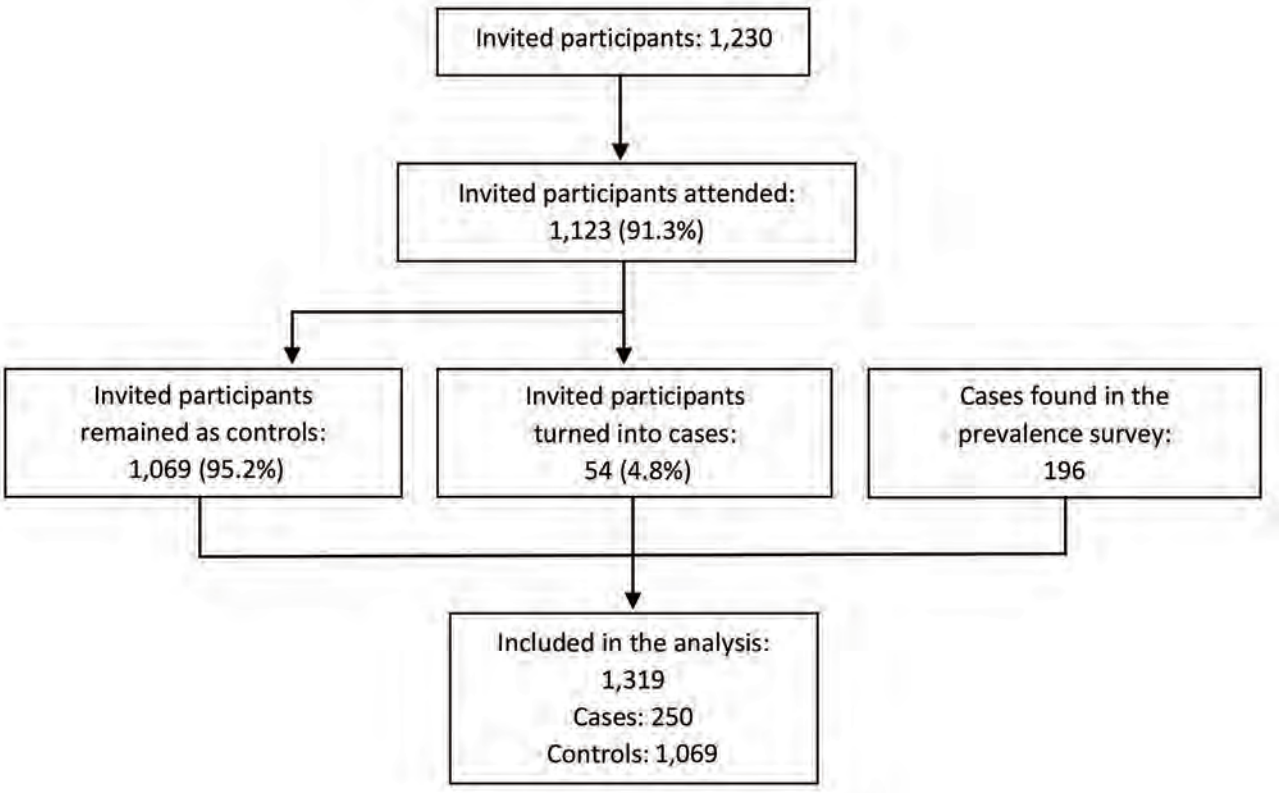


**Figure 2.** Summary of the data flow for case–control analysis of tuberculosis prevalence, Vietnam, 2017–2018.

**Table 1.** Characteristics of participants (N = 1,319) in case–control analysis of tuberculosis prevalence, Vietnam, 2017–2018

| Characteristics | Controls, no. (%) | Cases, no. (%) | Total, no. (%) |
|---|---|---|---|
| Sex | | | |
| M | 493 (46.1) | 201 (80.4) | 694 (52.6) |
| F | 576 (53.9) | 49 (19.6) | 625 (47.4) |
| Age groups, y | | | |
| 15–24 | 77 (7.2) | 7 (2.8) | 84 (6.4) |
| 25–34 | 193 (18.0) | 25 (10.0) | 218 (16.5) |
| 35–44 | 216 (20.2) | 33 (13.2) | 249 (18.9) |
| 45–54 | 239 (22.4) | 62 (24.8) | 301 (22.8) |
| 55–64 | 212 (19.8) | 61 (24.4) | 273 (20.7) |
| ≥65 | 132 (12.4) | 62 (24.8) | 194 (14.7) |
| Area | | | |
| Urban | 447 (41.8) | 96 (38.4) | 543 (41.2) |
| Remote | 255 (23.9) | 59 (23.6) | 314 (23.8) |
| Rural | 367 (34.3) | 95 (38.0) | 462 (35.0) |
| Region | | | |
| North | 438 (41.0) | 74 (29.6) | 512 (38.8) |
| Center | 190 (17.8) | 41 (16.4) | 231 (17.5) |
| South | 441 (41.2) | 135 (54.0) | 576 (43.7) |
| Clinical symptoms | | | |
| Least severe | 760 (71.1) | 71 (28.4) | 831 (63.0) |
| Moderately severe | 245 (22.9) | 112 (44.8) | 357 (27.1) |
| Most severe | 64 (6.0) | 67 (26.8) | 131 (9.9) |
| Access to healthcare | | | |
| Good | 451 (42.2) | 20 (8.0) | 471 (35.7) |
| Moderate | 379 (35.4) | 49 (19.6) | 428 (32.5) |
| Poor | 239 (22.4) | 181 (72.4) | 420 (31.8) |
| Behavioral and environmental risk | | | |
| Low | 461 (43.1) | 34 (13.6) | 495 (37.5) |
| Moderate | 358 (33.5) | 76 (30.4) | 431 (32.7) |
| High | 250 (23.4) | 140 (56.2) | 393 (29.8) |
| Socioeconomic status | | | |
| High | 389 (34.0) | 60 (24.0) | 609 (46.2) |
| Medium | 373 (33.2) | 65 (26.0) | 334 (25.3) |
| Low | 307 (32.8) | 125 (50.0) | 376 (28.5) |
| Total | 1,069 (100) | 250 (100) | 1,319 (100) |

could predict the TB status of persons living in Vietnam, assuming the input information is adequate, with a probability of 0.90 (95% CI 0.89–0.92, Table 3).

In the sensitivity analyses, when the clinical domain was excluded in model 1, there was no statistically significant difference in the direct effect of sex nor in the effect of access to healthcare, behavioral and environmental risks, and SES on prevalent TB compared with the primary SEM model (Appendix Table 2). We found no statistically significant difference between the main SEM model and sensitivity analysis in model 2, where the main outcome was replaced by TB status defined by the expert panel (Appendix Table 3). This was also the case for analysis model 3, where all Xpert-positive TB cases with a history of previous TB treatment were excluded from the analysis (Appendix Table 4).

## Discussion

In Vietnam, we witnessed an exceptionally large difference in TB prevalence in relation to sex, with behavioral and environmental risks as the biggest contributors to this disparity: sex determined behavioral and environmental risks leading to TB. Even after accounting for all known associated factors of prevalent TB collected in our data, we found that the odds of having TB were still 3 times higher for men than for women, and this difference remained in our sensitivity analyses. Although we cannot exclude unmeasured confounding, our data suggest that in addition to behavioral and environmental factors, access to healthcare, and symptom presentation, there may be biologic factors that render men more vulnerable to TB than women. Such biologic factors may contribute substantially to the M:F ratio for TB observed in Vietnam and globally.

The behavioral and environmental risks domain, while being strongly associated with sex, only exerted a modest effect on prevalent TB. Of note, in the sex-stratified SEM models, the behavioral and environmental risks domain had a statistically significant effect on prevalent TB among men, but not among women (Appendix Figures 1, 2). This domain consisted both of factors affecting the risk for MTB infection (working indoors, contact with TB patients) and of factors affecting the risk for TB disease progression (smoking, excessive

**Table 2.** Distribution of domains by sex among interviewed participants (N = 1,319) in case–control analysis of tuberculosis prevalence, Vietnam, 2017–2018

| Domains | Women, no. (%) | Men, no. (%) | Total, no. (%) | p value* |
|---|---|---|---|---|
| Clinical symptoms | | | | |
| Least | 439 (70.2) | 392 (56.5) | 831 (63.0) | <0.001 |
| Moderately | 144 (23.1) | 213 (30.7) | 357 (27.1) | |
| Most | 42 (6.7) | 89 (12.8) | 131 (9.9) | |
| Access to healthcare | | | | |
| Good | 256 (41.0) | 215 (31.0) | 471 (35.7) | <0.001 |
| Moderate | 219 (35.0) | 209 (30.1) | 428 (32.5) | |
| Poor | 150 (24.0) | 270 (38.9) | 420 (31.8) | |
| Behavioral and environmental risk | | | | |
| Low | 347 (55.5) | 148 (21.3) | 495 (37.5) | <0.001 |
| Moderate | 252 (40.3) | 182 (26.2) | 434 (32.9) | |
| High | 26 (4.2) | 364 (52.5) | 390 (29.6) | |
| Socioeconomic status | | | | |
| High | 202 (32.3) | 247 (35.6) | 449 (34.0) | 0.440 |
| Medium | 215 (34.4) | 223 (32.1) | 438 (33.2) | |
| Low | 208 (33.3) | 224 (32.3) | 432 (32.8) | |
| Total | 625 (100) | 694 (100) | 1,319 (100) | |

*By Pearson $\chi^2$ test to compare the differences between men and women.

drinking), because we believe that the exact pathophysiologic effect of these factors is unknown and may be multiple and interactive. For example, heavy drinkers may also socialize with more persons in poorly ventilated spaces, thus increasing their risk for MTB infection. In Vietnam, men smoke and drink excessively at an overwhelmingly higher rate compared with women, with a smoking rate of 45.3% vs 1.1% (*16*) and an excessive drinking rate of 44.2% vs 1.2% (*17*). This explains the tremendous influence of sex on the behavioral and environmental risks domain, even when the levels of working indoors and contact with TB patients were similar for both sexes. Also, behavioral and environmental risks were higher among the middle-aged compared with the youngest age group, which is consistent with findings of a survey of tobacco consumption in Vietnam in 2015 (*17*). The effect of this pathway on TB in the sex-stratified SEM models solidifies the evidence that smoking and drinking are major drivers of the difference in TB prevalence between men and women.

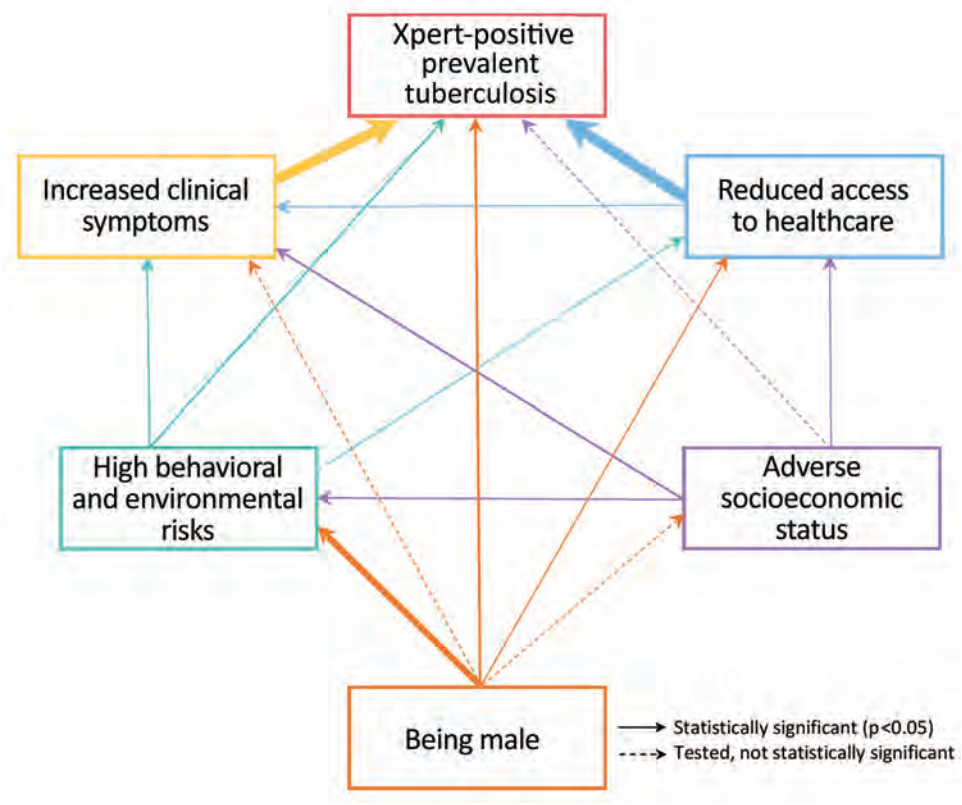


**Figure 3.** Structural equation model of the relationships between domains and Xpert-positive (Xpert MTB/Rif; Cepeheid, https://www.cepheid.com) tuberculosis prevalence for case–control analysis of tuberculosis prevalence, Vietnam, 2017–2018. For significant associations, the arrow thickness corresponds to the effect size. Each outcome was adjusted for age, area, and region. See Table 3 for the full estimation results. Model results were weighted using sampling and lost-to-follow-up weights. Bootstrapped area under the curve (1,000 replications) was 0.90 (95% CI 0.89–0.92).

Although access to healthcare appeared the strongest predictor of tuberculosis prevalence, we did not find a direct effect of sex on the access to healthcare domain, because men and women in Vietnam tend to have similar access to healthcare. This opposes the findings of other studies, where the gap in access to TB health services is stated to be the main reason behind sex-related differences in the TB burden (*2*,*18*). In Vietnam, a nationwide study in 2002 showed that women have longer TB diagnostic delays than men

**Table 3.** Structural equation model full estimation results of the relationships between sex, clinical symptoms, behavioral and environmental risks, access to healthcare, SES, and Xpert-positive prevalent tuberculosis, Vietnam, 2017–2018*

| | Xpert-postive prevalent TB | | Clinical symptoms | | Access to healthcare | | Behavioral and environmental risks | | Socioeconomic status | |
|---|---|---|---|---|---|---|---|---|---|---|
| Outcomes | aOR (95% CI) | p value | aOR (95% CI) | p value | aOR (95% CI) | p value | aOR (95% CI) | p value | aOR (95% CI) | p value |
| Male sex | 3.0 (1.7–5.0) | <0.001 | 1.2 (0.9–1.7) | 0.281 | 1.4 (1.1–1.7) | 0.005 | 7.7 (6.0–9.8) | <0.001 | 0.8 (0.6–1.0) | 0.172 |
| Age groups, y | | | | | | | | | | |
| 15–24 | Referent | | Referent | | Referent | | Referent | | Referent | |
| 25–34 | 1.1 (0.4–2.8) | 0.824 | 1.2 (0.5–2.4) | 0.706 | 1.1 (0.7–1.7) | 0.611 | 1.3 (0.7–2.2) | 0.395 | 1.3 (0.7–2.4) | 0.481 |
| 35–44 | 0.9 (0.4–2.3) | 0.874 | 1.1 (0.5–2.7) | 0.776 | 1.1 (0.8–1.7) | 0.562 | 1.9 (1.0–3.4) | 0.042 | 3.7 (2.1–6.3) | <0.001 |
| 45–54 | 1.1 (0.4–3.0) | 0.755 | 1.3 (0.6–3.0) | 0.459 | 1.1 (0.7–1.7) | 0.651 | 2.6 (1.5–4.5) | 0.001 | 5.0 (2.9–8.8) | <0.001 |
| 55–64 | 1.2 (0.4–3.4) | 0.767 | 1.8 (0.9–3.6) | 0.112 | 1.2 (0.8–2.0) | 0.372 | 1.7 (0.9–3.1) | 0.089 | 6.5 (3.6–11.5) | <0.001 |
| ≥65 | 1.9 (0.8–5.2) | 0.164 | 1.8 (0.8–4.1) | 0.173 | 1.3 (0.7–2.3) | 0.429 | 1.4 (0.7–2.7) | 0.315 | 15.8 (7.7–32.2) | <0.001 |
| Area | | | | | | | | | | |
| Urban | Referent | | Referent | | Referent | | Referent | | Referent | |
| Remote | 1.4 (0.8–2.5) | 0.212 | 0.9 (0.5–1.4) | 0.531 | 1.1 (0.6–2.1) | 0.801 | 1.0 (0.6–1.8) | 0.940 | 1.7 (0.9–2.9) | 0.067 |
| Rural | 1.6 (0.9–3.1) | 0.141 | 0.8 (0.5–1.4) | 0.440 | 1.3 (0.8–2.2) | 0.235 | 0.9 (0.6–1.4) | 0.620 | 0.6 (0.4–0.8) | 0.002 |
| Region | | | | | | | | | | |
| North | Referent | | Referent | | Referent | | Referent | | Referent | |
| Central | 1.0 (0.5–2.2) | 0.922 | 0.6 (0.4–0.9) | 0.039 | 0.9 (0.5–1.6) | 0.771 | 1.6 (0.8–3.2) | 0.148 | 4.0 (2.2–7.3) | <0.001 |
| South | 1.9 (1.1–3.7) | 0.030 | 0.4 (0.2–0.6) | <0.001 | 1.1 (0.6–2.0) | 0.684 | 1.7 (1.1–2.6) | 0.025 | 4.0 (2.7–6.0) | <0.001 |
| Clinical symptoms | | | | | | | | | | |
| Least severe | Referent | | | | † | | † | | † | |
| Moderate severe | 5.0 (2.8–8.7) | <0.001 | | | † | | † | | † | |
| Most severe | 13.2 (5.9–29.2) | <0.001 | | | † | | † | | † | |
| Access to healthcare | | | | | | | | | | |
| Good | Referent | | Referent | | | | † | | † | |
| Moderate | 2.5 (1.4–4.4) | 0.002 | 1.2 (0.8–1.9) | 0.343 | | | † | | † | |
| Poor | 13.4 (7.0–25.6) | <0.001 | 1.6 (1.1–2.4) | 0.016 | | | † | | † | |
| Behavioral and environmental risks | | | | | | | | | | |
| Low | Referent | | Referent | | Referent | | | | † | |
| Moderate | 2.1 (1.1–3.9) | 0.017 | 1.5 (1.1–2.2) | 0.015 | 1.2 (0.8–1.6) | 0.336 | | | † | |
| High | 2.9 (1.5–5.6) | 0.001 | 2.4 (1.6–3.6) | <0.001 | 1.5 (1.0–2.1) | 0.029 | | | † | |
| Socioeconomic status | | | | | | | | | | |
| High | Referent | | Referent | | Referent | | Referent | | | |
| Medium | 1.0 (0.6–1.7) | 0.992 | 1.2 (0.9–1.6) | 0.326 | 0.8 (0.6–1.1) | 0.172 | 1.4 (1.1–1.9) | 0.020 | | |
| Low | 1.2 (0.6–2.3) | 0.526 | 2.2 (1.4–3.5) | 0.001 | 1.4 (1.0–2.0) | 0.045 | 2.0 (1.4–2.8) | <0.001 | | |
| Bootstrapped AUC | 0.90 (0.89–0.92) | | | | | | | | | |

*aOR, adjusted odds ratio; AUC, area under the curve.
†Variable was not included as predictor for the respective outcome. Sex, age, area, and region were not an outcome in this structural equation model. Model results were weighted using sampling and lost-to-follow-up weights.

(5.6 weeks vs 4.4 weeks on average) (*19*), but results from a laboratory study in northern Vietnam suggested that women are more likely than men to have sputum smear examinations (*20*). Our study revealed no significant direct effect of sex on access to healthcare but did demonstrate an indirect effect through exposure. This finding is in line with studies indicating an association between heavy drinking and decreased healthcare utilization (*21*,*22*), because drinkers may be less likely to seek preventive care and primary healthcare than abstainers.

Before 1945, only 10% of the population of Vietnam was literate (*23*); thus, in our study, elderly persons most often had no schooling. We found no difference in SES between men and women, but elderly participants (≥60 years of age) reported a much lower SES than younger participants (15–24 years of age). The SES domain showed only a marginal direct association with TB, but significant indirect associations through the other 3 domains. Studies have shown that persons with low SES are more likely to be uninsured, seek healthcare less often, and have poor-quality healthcare, which may have led some participants to visit medical facilities with more severe clinical symptoms during the survey (*24*,*25*). Persons with low SES also are more likely to smoke and drink alcohol excessively (*26*), which suggest the need for welfare-focused interventions for TB control and prevention.

After controlling for all domains, we still found that men in Vietnam are 3 times more likely to have TB than women. Although other latent factors might have contributed to those odds (e.g., silicosis, nutritional status, illicit drug use, social contact patterns), our findings suggest that a direct biologic effect contributes to this sexual disparity. Although the contribution of some domains might be very specific to the setting of Vietnam, we expect that the residual biologic effect might be the same across settings. Further, we suspect that the M:F ratios observed in other surveys might be underestimated, given that confounders (e.g., with respect to access and exposure) were not addressed. Further research should focus on biologic aspects that might influence TB risk among men and women, for example, innate recognition of pathogens and antimicrobial immune responses. Recent mouse model data showed that estrogen in women boosts the potential of macrophages to kill bacteria that cause pneumonia (*27*). Compared with male mice, female mice also produced more IFNγ, an important cytokine that increases the antibacterial functions of macrophages (*28*). Data also suggest that testosterone is a mediator that inhibits the immune system by inhibiting such proinflammatory factors as TNF-α and nitric oxide and that male castration increases TNF-α secretion in mice (*29*,*30*). Aside from the influence of hormones, genetics might have a critical impact on improving women's susceptibility to infections like TB since the X chromosome expresses several immune-related genes and immune-associated microRNAs. Women therefore may benefit from having 2 X chromosomes (*31*).

Our SEM analysis included all known and commonly occurring associated factors of prevalent TB that were collected in the PEER questionnaire, but we acknowledge that there may be other factors that were not measured. There also might be selection bias among the case group, since this group consisted of participants with only one positive Xpert test, which may include false-positive Xpert results, causing a slight underestimation of the associations. The prevalence survey used BACTEC MGIT 960 liquid culture (Becton, Dickinson and Company, https://www.bd.com/en-us) to diagnose TB, but the turnaround time was too long to inform selection for the PEER study; therefore, 2 participants selected as controls for the study who had MTB-positive culture results had to be excluded from the analyses. In addition, 83 survey participants who were Xpert-negative but culture-positive were missed being selected to participate in the PEER study. There were also 38 cases who were likely to be Xpert false-positive due to their previous TB treatment history. In the sensitivity analysis that excluded these cases, the SEM model yielded similar results. Another limitation of this study is that gender was not explicitly taken into account in our analysis. Indeed, some factors such as access to care and risk behaviors are likely to be more closely associated with gender than with sex, making the delineation between the 2 concepts in our study not straightforward. Neyman bias might have occurred because of our choice of prevalent TB as the outcome. Using prevalence survey data offers the benefit of minimizing sex bias in reporting. However, prevalence reflects both incidence and duration of disease, and we could not distinguish TB patients with different duration of disease in our analysis. Selection bias also might have occurred in our study, because the proportion of Xpert-positive TB cases found among the preselected controls was much higher than the proportion of TB cases found in the overall TB prevalence survey population. The participation rate among the preselected controls was also higher than that of the TB prevalence survey population

(*7*). Like the TB prevalence survey, our analysis involved an undersampling in the youngest age group because the prevalence of TB among young persons in Vietnam was very low, which limited the allocation of participants in this age group (*7*).

In conclusion, we attribute the strong sex difference in TB prevalence found in Vietnam to a complex interplay of factors relating to behavioral and environmental risks, access to healthcare, and clinical manifestations. However, after controlling for all these factors, there remains a direct effect that is likely biological. Further insights from basic and clinical research are needed to explore this biologic difference. Aside from addressing other controllable factors, such as access to healthcare and behavioral and environmental risks, efforts to control TB should include effective strategies focused on men and reducing that specific disease burden.

### Acknowledgment

We thank the Board of Directors of the Vietnam National Tuberculosis Program, all staff who were involved in this study, and the participants who took part in this study.

This study was funded by the US National Academies of Science and the US Agency for International Development under the USAID Prime Award Number AID-OAA-A-11-00012. The funders have no role in the study design; in the collection, analysis, and interpretation of the data; in the writing of the report; and in the decision to submit the paper for publication.

### About the Author

Dr. Nguyen is a researcher at the Vietnam Integrated Centre for Tuberculosis and Respirology Research, Vietnam National Tuberculosis Program. He obtained his PhD using the findings from the second national TB prevalence survey in Vietnam at the University of Amsterdam in 2022. He is interested in research on TB epidemiology and whole genome sequencing technology.

### References

1. World Health Organization. Global tuberculosis report 2020. WHO Press. 2021:34 [cited 2021 Jul 17]. https://www.who.int/publications/i/item/9789240013131
2. Horton KC, Sumner T, Houben RMGJ, Corbett EL, White RG. A Bayesian approach to understanding sex differences in tuberculosis disease burden. Am J Epidemiol. 2018;187:2431–8. https://doi.org/10.1093/aje/kwy131
3. Thorson A, Diwan VK. Gender inequalities in tuberculosis: aspects of infection, notification rates, and compliance. Curr Opin Pulm Med. 2001;7:165–9. https://doi.org/10.1097/00063198-200105000-00009
4. Horton KC, MacPherson P, Houben RMGJ, White RG, Corbett EL. Sex differences in tuberculosis burden and notifications in low- and middle-income countries: a systematic review and meta-analysis. PLoS Med. 2016;13:e1002119-e. https://doi.org/10.1371/journal.pmed.1002119
5. Horton KC, Hoey AL, Béraud G, Corbett EL, White RG. Systematic review and meta-analysis of sex differences in social contact patterns and implications for tuberculosis transmission and control. Emerg Infect Dis. 2020;26:910–9. https://doi.org/10.3201/eid2605.190574
6. Hertz D, Schneider B. Sex differences in tuberculosis. Semin Immunopathol. 2019;41:225–37. https://doi.org/10.1007/s00281-018-0725-6
7. Nguyen HV, Tiemersma EW, Nguyen HB, Cobelens FGJ, Finlay A, Glaziou P, et al. The second national tuberculosis prevalence survey in Vietnam. PLoS One. 2020;15:e0232142. https://doi.org/10.1371/journal.pone.0232142
8. Hoa NB, Sy DN, Nhung NV, Tiemersma EW, Borgdorff MW, Cobelens FG. National survey of tuberculosis prevalence in Viet Nam. Bull World Health Organ. 2010;88:273–80. https://doi.org/10.2471/BLT.09.067801
9. World Health Organization. Global tuberculosis report 2015. WHO Press. 2016 [cited 2016 May 02]. https://apps.who.int/iris/handle/10665/191102
10. Stein CM, Morris NJ, Hall NB, Nock NL. Structural equation modeling. Methods Mol Biol. 2017;1666:557–80. https://doi.org/10.1007/978-1-4939-7274-6_28
11. Narasimhan P, Wood J, Macintyre CR, Mathai D. Risk factors for tuberculosis. Pulm Med. 2013;2013:1-. https://doi.org/10.1155/2013/828939
12. Lönnroth K, Williams BG, Stadlin S, Jaramillo E, Dye C. Alcohol use as a risk factor for tuberculosis—a systematic review. BMC Public Health. 2008;8:289. https://doi.org/10.1186/1471-2458-8-289
13. Mohidem NA, Hashim Z, Osman M, Shaharudin R, Muharam FM, Makeswaran P. Demographic, socio-economic and behavior as risk factors of tuberculosis in Malaysia: a systematic review of the literature. Rev Environ Health. 2018;33:407–21. https://doi.org/10.1515/reveh-2018-0026
14. Obsa MS, Daga WB, Wosene NG, Gebremedhin TD, Edosa DC, Dedecho AT, et al. Treatment seeking delay and associated factors among tuberculosis patients attending health facility in Ethiopia from 2000 to 2020: A systematic review and meta analysis. PLoS One. 2021;16:e0253746. https://doi.org/10.1371/journal.pone.0253746
15. Kaiser HF. A second generation little jiffy. Psychometrika. 1970;35:401–15. https://doi.org/10.1007/BF02291817
16. Van Minh H, Giang KB, Ngoc NB, Hai PT, Huyen DT, Khue LN, et al. Prevalence of tobacco smoking in Vietnam: findings from the Global Adult Tobacco Survey 2015. Int J Public Health. 2017;62(Suppl 1):121–9. https://doi.org/10.1007/s00038-017-0955-8
17. Tran QB, Hoang VM, Vu HL, Bui PL, Kim BG, Pham QN, et al. Risk factors for non-communicable diseases among adults in Vietnam: Findings from the Vietnam STEPS Survey 2015. J Glob Health Sci. 2020;2(1):e7. https://doi.org/10.35500/jghs.2020.2.e7
18. Mason PH, Snow K, Asugeni R, Massey PD, Viney K. Tuberculosis and gender in the Asia-Pacific region. Aust N Z J Public Health. 2017;41:227–9. https://doi.org/10.1111/1753-6405.12619
19. Huong NT, Vree M, Duong BD, Khanh VT, Loan VT, Co NV, et al. Delays in the diagnosis and treatment of tuberculosis patients in Vietnam: a cross-sectional study. BMC Public Health. 2007;7:110. https://doi.org/10.1186/1471-2458-7-110
20. Huong NT, Duong BD, Linh NN, Van LN, Co NV, Broekmans JF, et al. Evaluation of sputum smear microscopy

in the National Tuberculosis Control Programme in the north of Vietnam. Int J Tuberc Lung Dis. 2006;10:277-82.
21. Zarkin GA, Bray JW, Babor TF, Higgins-Biddle JC. Alcohol drinking patterns and health care utilization in a managed care organization. Health Serv Res. 2004;39:553–70. https://doi.org/10.1111/j.1475-6773.2004.00244.x
22. Cook WK, Cherpitel CJ. Access to health care and heavy drinking in patients with diabetes or hypertension: implications for alcohol interventions. Subst Use Misuse. 2012;47:726–33. https://doi.org/10.3109/10826084.2012.665558
23. Biddington R, Biddington J. Education for All: literacy in Vietnam 1975–1995. Compare. 1997;27:43–61. https://doi.org/10.1080/0305792970270104
24. Becker G, Newsom E. Socioeconomic status and dissatisfaction with health care among chronically ill African Americans. Am J Public Health. 2003;93:742–8. https://doi.org/10.2105/AJPH.93.5.742
25. Franks P, Clancy CM, Gold MR. Health insurance and mortality. Evidence from a national cohort. JAMA. 1993;270:737–41. https://doi.org/10.1001/jama.1993.03510060083037
26. Hall W. Socioeconomic status and susceptibility to alcohol-related harm. Lancet Public Health. 2017;2:e250–1. https://doi.org/10.1016/S2468-2667(17)30089-0
27. Yang Z, Huang YC, Koziel H, de Crom R, Ruetten H, Wohlfart P, et al. Female resistance to pneumonia identifies lung macrophage nitric oxide synthase-3 as a therapeutic target. eLife. 2014;3:e03711;3:e03711. https://doi.org/10.7554/eLife.03711
28. Gourdy P, Araujo LM, Zhu R, Garmy-Susini B, Diem S, Laurell H, et al. Relevance of sexual dimorphism to regulatory T cells: estradiol promotes IFN-gamma production by invariant natural killer T cells. Blood. 2005;105:2415–20. https://doi.org/10.1182/blood-2004-07-2819
29. Rettew JA, Huet-Hudson YM, Marriott I. Testosterone reduces macrophage expression in the mouse of toll-like receptor 4, a trigger for inflammation and innate immunity. Biol Reprod. 2008;78:432–7. https://doi.org/10.1095/biolreprod.107.063545
30. Bini EI, Mata Espinosa D, Marquina Castillo B, Barrios Payán J, Colucci D, Cruz AF, et al. The influence of sex steroid hormones in the immunopathology of experimental pulmonary tuberculosis. PLoS One. 2014;9:e93831. https://doi.org/10.1371/journal.pone.0093831
31. Dutta NK, Schneider BE. Are there sex-specific differences in response to adjunctive host-directed therapies for tuberculosis? Front Immunol. 2020;11:1465. https://doi.org/10.3389/fimmu.2020.01465

Address for correspondence: Hai Viet Nguyen, Vietnam National Tuberculosis Program, 463 Hoang Hoa Tham, Hanoi, Vietnam; email: nguyenviethai@bvptw.org

# etymologia revisited

## *Mycobacterium chimaera*

[mi'ko-bak-tēr'e-əm ki-mēr'ə]

Formerly an unnamed *Mycobacterium* sequevar within the *M. avium–M. intracellulare–M. scrofulaceum* group (MAIS), *M. chimaera* is an emerging opportunistic pathogen that can cause infections of heart valve prostheses, vascular grafts, and disseminated infections after open-heart surgery. Heater–cooler units used to regulate blood temperature during cardiopulmonary bypass have been implicated, although most isolates are respiratory. In 2004, Tortoli et al. proposed the name M. chimaera for strains that a reverse hybridization–based line probe assay suggested belonged to MAIS but were different from *M. avium, M. intracellulare*, or *M. scrofulaceum*. The new species name comes from the chimera, a mythological being made up of parts of 3 different animals.

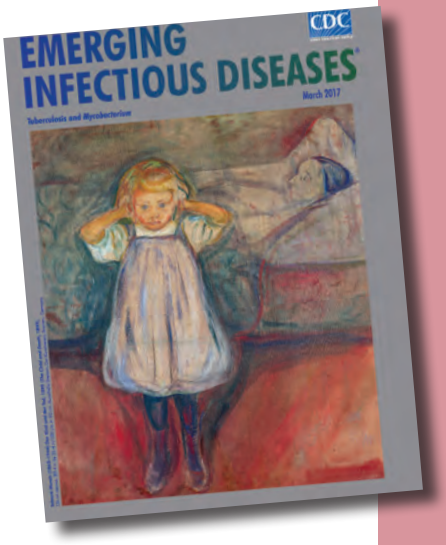


***Originally published in March 2017***

**References:**

1. Schreiber PW, Kuster SP, Hasse B, Bayard C, Rüegg C, Kohler P, et al. Reemergence of *Mycobacterium chimaera* in heater–cooler units despite intensified cleaning and disinfection protocol. Emerg Infect Dis. 2016;22:1830–3.
2. Struelens MJ, Plachouras D. *Mycobacterium chimaer*a infections associated with heater-cooler units (HCU): closing another loophole in patient safety. Euro Surveill. 2016;21:1–3.
3. Tortoli E, Rindi L, Garcia MJ, Chiaradonna P, Dei R, Garzelli C, et al. Proposal to elevate the genetic variant MAC-A, included in the *Mycobacterium avium* complex, to species rank as *Mycobacterium chimaera* sp. nov. Int J Syst Evol Microbiol. 2004;54:1277–85.

***https://wwwnc.cdc.gov/eid/article/23/3/et-2303_article***

# Use of High-Resolution Geospatial and Genomic Data to Characterize Recent Tuberculosis Transmission, Botswana

Chelsea R. Baker,[1] Ivan Barilar,[1] Leonardo S. de Araujo, Anne W. Rimoin, Daniel M. Parker, Rosanna Boyd, James L. Tobias, Patrick K. Moonan, Eleanor S. Click, Alyssa Finlay, John E. Oeltmann, Vladimir N. Minin, Chawangwa Modongo, Nicola M. Zetola,[2] Stefan Niemann,[2] Sanghyuk S. Shin[2]

Combining genomic and geospatial data can be useful for understanding *Mycobacterium tuberculosis* transmission in high-burden tuberculosis (TB) settings. We performed whole-genome sequencing on *M. tuberculosis* DNA extracted from sputum cultures from a population-based TB study conducted in Gaborone, Botswana, during 2012–2016. We determined spatial distribution of cases on the basis of shared genotypes among isolates. We considered clusters of isolates with ≤5 single-nucleotide polymorphisms identified by whole-genome sequencing to indicate recent transmission and clusters of ≥10 persons to be outbreaks. We obtained both molecular and geospatial data for 946/1,449 (65%) participants with culture-confirmed TB; 62 persons belonged to 5 outbreaks of 10–19 persons each. We detected geospatial clustering in just 2 of those 5 outbreaks, suggesting heterogeneous spatial patterns. Our findings indicate that targeted interventions applied in smaller geographic areas of high-burden TB identified using integrated genomic and geospatial data might help interrupt TB transmission during outbreaks.

Author affiliations: University of California, Irvine, California, USA (C.R. Baker, D.M. Parker, V.N. Minin, S.S. Shin); Forschungszentrum, Borstel, Germany (I. Barilar, L.S. de Araujo, S. Niemann); University of California, Los Angeles, California, USA (A.W. Rimoin); US Centers for Disease Control and Prevention, Gaborone, Botswana (R. Boyd, A. Finlay); US Centers for Disease Control and Prevention, Atlanta, Georgia, USA (J.L. Tobias, P.K. Moonan, R. Boyd, E.S. Click, A. Finlay, J.E. Oeltmann); Botswana–UPenn Partnership, Gaborone (C. Modongo, N.M. Zetola); Victus Global Botswana Organisation, Gaborone (C. Modongo, N.M. Zetola)

DOI: https://doi.org/10.3201/eid2905.220796

Tuberculosis (TB) remains among the leading causes of death from infectious diseases worldwide, killing 1.5 million persons in 2020 despite being preventable and curable (*1*). High-burden TB countries often contend with limited financial and labor resources and rely on generalized interventions that, although helpful, treat TB as a uniform epidemic (*2*–*4*). However, recent advances in molecular methods have shown that TB epidemics are composed of multiple simultaneous chains of transmission that could serve as distinct targets for intervention (*4*–*7*). Targeted interventions to interrupt transmission might be particularly effective for reducing TB in high-burden settings, where recent infections contribute substantially to disease incidence (*3*–*6*).

Genomic sequencing is a powerful tool for identifying discrete, but closely related, *Mycobacterium tuberculosis* strains, helping to reconstruct likely chains of recent transmission (*3*,*8*,*9*). Genomic and geospatial data can be integrated to investigate whether transmission chains fall within distinct geographic areas (*3*–*6*). For example, spatial clusters of closely related *M. tuberculosis* strains may indicate localized areas of ongoing transmission, which could be targeted for public health interventions, such as active case finding (*3*–*5*,*10*). A growing body of evidence suggests that geographically targeted interventions could be effective and cost-efficient in high-burden, low-resource settings and instrumental in accelerating progress toward eliminating TB (*4*,*11*–*13*).

[1]These first authors contributed equally to this article.

[2]These senior authors contributed equally to this article.

In the Kopanyo Study, a population-based study of TB transmission in Botswana during 2012–2016, localized transmission events were characterized by detecting spatial clustering of participants belonging to genotype-specific (genotypic) cluster groups identified by using MIRU-VNTR (mycobacterial interspersed repetitive unit–variable number tandem repeat) genotyping (*5*,*14*). The objectives of our analysis were to build on data from the original study by incorporating higher resolution genomic data from whole-genome sequencing (WGS) and to investigate the geographic distribution of distinct genotypic cluster groups representing potential recent transmission chains. The Kopanyo Study was approved by the US Centers for Disease Control and Prevention institutional review board (approval no. 6291), the Health Research and Development Committee of the Botswana Ministry of Health and Wellness, and institutional review boards of the University of Pennsylvania. We received written informed consent from all participants and mapped residential coordinates in sufficiently low resolution to prevent identification of participants.

## Methods

### Study Design and Setting

We analyzed data collected during August 2012–March 2016 for the Kopanyo Study among persons with TB in Botswana, a country in southern Africa with a high burden of TB and TB/HIV co-infection (*1*,*5*,*14*). Nationwide TB incidence when the study began was 305 cases/100,000 persons (*5*,*14*). This analysis included participants residing in greater Gaborone, including the capital city and its surrounding suburbs. During the 5 years before the study, TB incidence was 440–470 cases/100,000 persons in Gaborone, which had a total population of 354,380 (*5*,*14*).

Study participants included men and women of all ages with TB disease who were sequentially enrolled by date of diagnosis; those who had already received TB treatment for ≥14 days, prisoners, and patients who declined to participate were excluded (*5*,*14*). At least 1 sputum sample was collected from each participant for bacterial culture. Clinical and demographic data, including residential address, were collected through in-person interviews and medical record review (*5*,*14*). We obtained residential geocoordinates using global positioning system (GPS) devices during site visits or by geocoding addresses using Google Maps (https://www.google.com/maps), OpenStreetMap (https://www.openstreetmap.org), and ArcGIS (Esri, https://www.esri.com) (*5*,*14*).

### WGS

We conducted WGS on archived DNA samples from the original study with sufficient amounts of DNA (>0.05 ng/μL) for analysis. We initially prepared DNA by crude extraction from liquid culture samples as described elsewhere (*15*). We prepared libraries for sequencing using an Illumina Nextera XT kit (https://www.illumina.com) to obtain 2 × 150 bp fragments for paired-end sequencing using a Illumina NextSeq 500 platform (*16*,*17*). To assemble and analyze sequences, we used MTBseq pipeline (https://github.com/ngs-fzb/MTBseq_source), which incorporates several open-source programs, including Burrows-Wheeler Aligner (https://github.com/lh3/bwa), Samtools (http://www.htslib.org), and Genome Analysis Toolkit version 3 (https://github.com/broadinstitute/gatk/releases), to automate steps involved in sample-specific and comparative analyses (*16*,*17*). We mapped reads to the *M. tuberculosis* H37Rv reference genome (GenBank accession no. NC_000962.3) (*16*). We performed variant calling using default thresholds for coverage and quality (*16*). We identified phylogenetically informative single-nucleotide polymorphisms (SNPs) from existing literature (*16*). We annotated variants associated with antimicrobial resistance on the basis of a built-in list of known mutations (*16*,*17*) and generated summaries to predict resistance for each genotype. As an indicator of recent TB transmission, we used a cluster-detection algorithm to identify closely related strains within each lineage (lineages 1–4) based on a distance threshold of ≤5 pairwise SNPs to establish bacterial genetic relatedness (*8*). The single linkage cluster detection algorithm used to identify genotype-specific groups detects isolates within 5 SNPs from the next closest isolate, so not all members within a given group are necessarily within 5 SNPs of all other members (*16*).

### Spatial Analysis

Our main analysis included participants residing in greater Gaborone who had both WGS data and GPS coordinates available. We excluded 29 participants with evidence of possible mixed-strain infection (*18*), which was detected using a method based on a binomial test procedure described elsewhere (*19*). For our analysis, we focused mainly on participants in 5 outbreak groups, defined as groups of ≥10 persons infected with genotype-specific TB. To represent the underlying density of TB infection in the population, we included ungrouped participants (those not in an identified genotypic group of any size) as a comparison group.

We conducted a preliminary analysis comparing the geographic distribution of participants with and without WGS data available to rule out geographic sampling bias. We estimated the geographic median center point and standard deviational ellipse (directional distribution at 2 SD) for both sets of participants. The median center is a measure of central tendency that is robust to outliers and minimizes the distance from the central location to all other points being analyzed. The standard deviational ellipse encompasses most observed points along both geographic coordinates (latitude and longitude), providing a representation of geographic range and directional orientation. We then used those same methods to characterize the geographic distribution of participants belonging to each outbreak, as well as ungrouped participants. We used a Monte Carlo test of spatial segregation to measure geographic variation among the different outbreak groups (*20*).

We generated kernel density maps to visualize locations of potential spatial clusters. Estimating kernel density provides an estimate of spatial concentration in terms of points per unit area using a moving window method with a weighting scheme and generating a smoothed map that displays areas of greater density (*21*). We generated maps for each outbreak group and for ungrouped strains using a 1-km buffer window. For visual display, density is shown on a different scale for ungrouped (up to 35 persons/km$^2$) and grouped participants (up to 5 persons/km$^2$) because of differences in size of datasets.

To estimate spatial clustering among participants in each outbreak group, we used spatial K-function analysis, a method that measures whether points are located closer to one another on average than would be expected in a completely random spatial pattern (*21*). To account for potential clustering caused by underlying population density, we compared relative clustering in grouped and ungrouped participants by estimating the difference in K-functions over a range of distances (0–8,000 m) (*21*,*22*). We generated plots with distances indicated along the x axis and K-function estimates along the y axis and examined the shape and behavior of the observed K-function values for interpretation (*21*). We used 999 random permutations to obtain 95% CIs. We assessed the magnitude of lines above or below 0 on the y axis to compare degree of clustering among groups and lines falling outside the upper or lower confidence intervals to detect statistically significant differences.

We calculated pairwise SNP and geographic distances of participants by outbreak group to assess whether relationships between geographic and genetic difference varied by group and generated boxplots to display SNP distance summaries. We plotted geographic distance against SNP distance and tested for correlation using Spearman ρ. We investigated possible spatial-temporal trends by measuring the geographic distance between the first participant (based on dates documented during the original study) diagnosed with TB and subsequently diagnosed participants in each outbreak group. We plotted date of diagnosis against geographic distance to visualize possible patterns. In addition, we conducted a sensitivity analysis to assess geographic characteristics of genotypic groups obtained using a

**Table 1.** Characteristics of participants (N = 548) in study of high-resolution geospatial and genomic data to characterize recent tuberculosis transmission, by outbreak group (≤5 SNP), Gaborone, Botswana, 2012–2016*

| | Group and lineage | | | | | |
|---|---|---|---|---|---|---|
| | A, n = 19 | B, n = 12 | C, n = 11 | D, n = 10 | E, n = 10 | Ungrouped, |
| Category | 4.1.1.3 | 4.1.1.3 | 4.1.2.1 | 4.1.1.3 | 4.3.4.1 | n = 486 |
| Median age, y (IQR) | 29 (24–40) | 35 (28–40) | 33 (31–42) | 31.5 (30–37) | 39 (34–42) | 35 (28–42) |
| Gender | | | | | | |
| M | 11 (58) | 9 (75) | 9 (75) | 3 (30) | 10 (100) | 254 (52) |
| F | 8 (42) | 3 (25) | 3 (25) | 7 (70) | 0 | 232 (48) |
| HIV status | | | | | | |
| Positive | 9 (47) | 6 (50) | 9 (82) | 5 (50) | 5 (50) | 308 (64) |
| Negative | 10 (53) | 6 (50) | 2 (18) | 5 (50) | 4 (40) | 162 (33) |
| NA | 0 | 0 | 0 | 0 | 1 (10) | 16 (3) |
| Income | | | | | | |
| Any | 15 (79) | 5 (42) | 8 (73) | 4 (40) | 8 (80) | 360 (74) |
| None | 4 (21) | 7 (58) | 2 (18) | 6 (60) | 2 (20) | 125 (25) |
| NA | 0 | 0 | 1 (9) | 0 | 0 | 1 (<1) |
| Isoniazid | | | | | | |
| Susceptible | 16 (84) | 12 (100) | 11 (100) | 10 (100) | 10 (100) | 458 (94) |
| Resistant | 3 (16) | 0 | 0 | 0 | 0 | 28 (6) |
| Rifampin | | | | | | |
| Susceptible | 16 (84) | 12 (100) | 11 (100) | 9 (90) | 8 (80) | 456 (94) |
| Resistant | 3 (16) | 0 | 0 | 1 (10) | 2 (20) | 30 (6) |

*Values are no. (%) except as indicated. NA, not available.

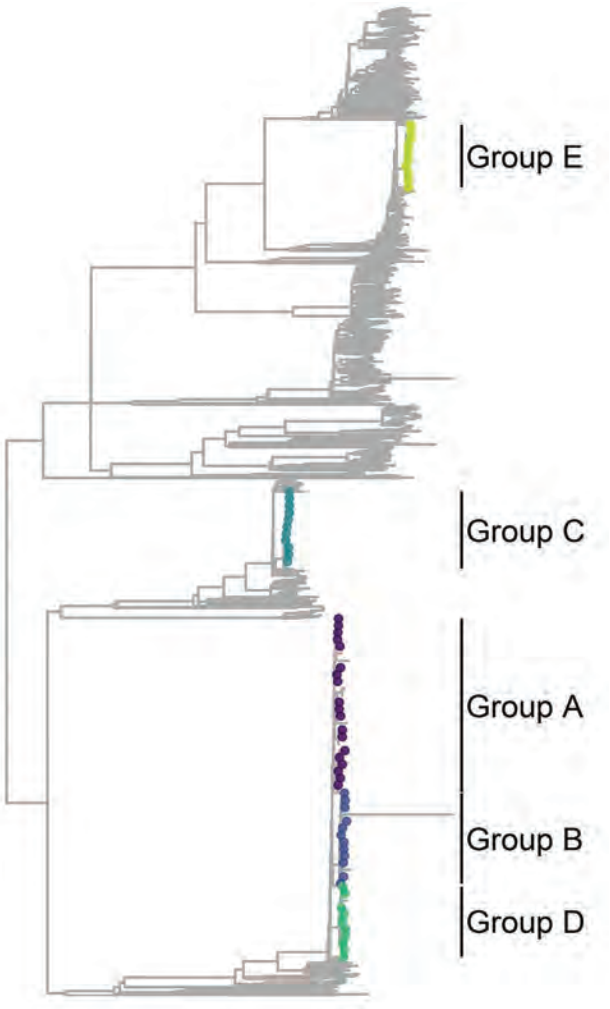


**Figure 1.** Phylogenetic tree representation for *Mycobacterium tuberculosis* lineage 4 for selected genotypic cluster groups (≤5 single-nucleotide polymorphisms) in study of high-resolution geospatial and genomic data to characterize recent tuberculosis transmission, Gaborone, Botswana, 2012–2016. Colors indicate the location of isolates in each genotypic cluster group. Branches within each of the groups are expanded for visualization.

distance threshold of ≤2 SNPs. For groups defined in this additional analysis, we estimated median center points, directional distributions, and differences in K-functions. We performed initial mapping and descriptive spatial analysis including median center, directional distribution, and kernel density using ArcGIS version 10.7.1 and performed additional analysis and data visualization in R statistical software version 4.1.2 (The R Project for Statistical computing, https://www.r-project.org). We calculated pairwise geographic distances by using R package fields (https://cran.r-project.org/web/packages/fields/index.html) and pairwise SNP distances by using ape (https://cran.r-project.org/web/packages/ape/index.html) (*23*). We used splancs (https://cran.r-project.org/web/packages/splancs/index.html) and smacpod (https://cran.r-project.org/web/packages/smacpod/index.html) for K-function analysis. Boxplots and scatter plots were displayed using ggplot2 (https://ggplot2.tidyverse.org) and egg (https://cran.r-project.org/package=egg) with the viridis (http://www.iqtree.org/https://sjmgarnier.github.io/viridis) color palette.

### Phylogenetic Analysis

We generated a maximum-likelihood phylogenetic tree using IQ-TREE version 1.6.12 (http://www.iqtree.org) (*24*) to represent genetic relationships among *M. tuberculosis* strains. We specified a Hasegawa-Kishino-Yano substitution model, which allows for unequal base frequencies and unequal transition rates, and corrected for ascertainment bias (*25*). To construct the phylogenetic tree, we used a midpoint rooting approach and expanded our dataset to include all participants with *M. tuberculosis* strains belonging to lineage 4, after excluding isolates with evidence of possible mixed infection. We highlighted the location within the tree of the main outbreak groups in our analysis and vertically expanded branches from the node representing the estimated most recent common ancestor for each group to enable detailed visualization. We then projected phylogenetic trees onto geographic maps for each of the groups, displaying the location in the tree of each *M. tuberculosis* isolate linked with its corresponding geographic location. We used R packages ggtree (https://github.com/YuLab-SMU/ggtree) (*26*), phytools (https://cran.r-project.org/web/packages/phytools/index.html) (*27*), rgdal (https://cran.r-project.org/package=rgdal), mapdata (https://cran.r-project.org/web/packages/mapdata/index.html), and prettymapr (https://cran.r-project.org/package=prettymapr) to annotate and visualize the tree.

### Epidemiologic Links

We analyzed data on occupation, places of employment, and social gathering places (e.g., markets, places of worship, taverns) to provide additional context for interpreting WGS and geospatial data (*28*). We used common occupational groups and social gathering places shared by ≥2 participants to identify potential epidemiologic links (*28*).

## Results

A total of 1,449 participants with culture-confirmed TB and primary residence in greater Gaborone had valid GPS coordinates, of which 946 (65%) had WGS data available and were thus eligible for this analysis

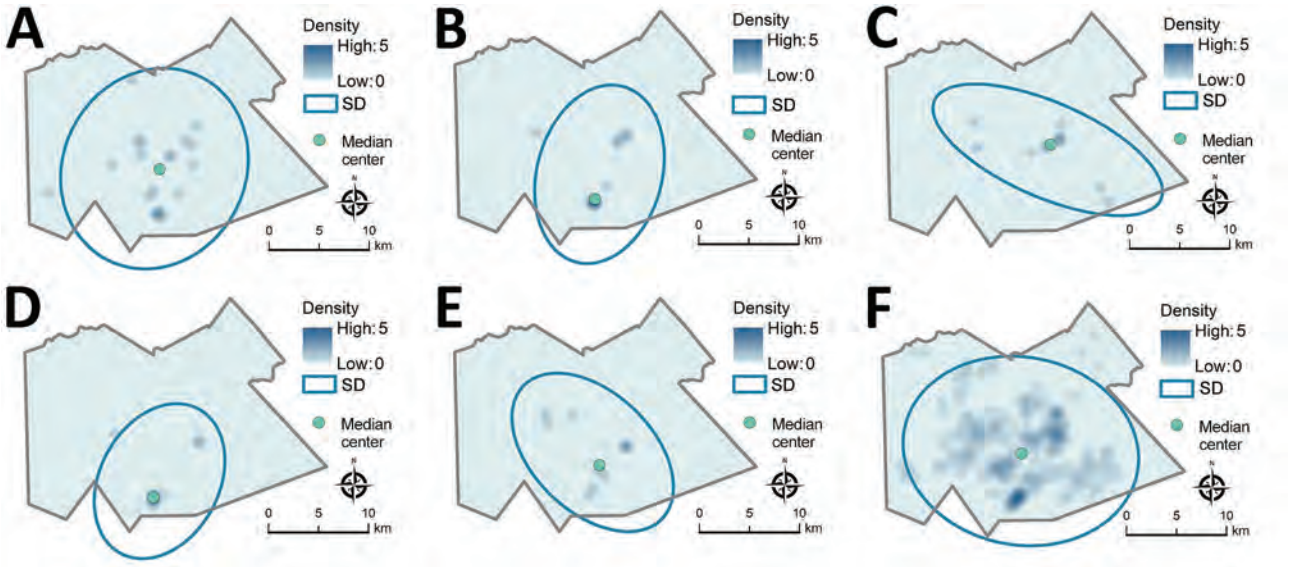


**Figure 2.** Kernel density map, median center point, and directional distribution for genotypic groups A–E (≤5 single-nucleotide polymorphisms) (panels A–E) and genotypically ungrouped *Mycobacterium tuberculosis* strains (F) in study of high-resolution geospatial and genomic data to characterize recent tuberculosis transmission, Gaborone, Botswana, 2012–2016. The blue ovals encompass the area within the SD ellipse, representing the geographic distance and directional orientation of participant locations within each group. Density is shown on a different scale (up to 35 cases/km$^2$) for ungrouped participants than for participants in the genotypic cluster groups (up to 5 cases/km$^2$) because of differences in size of the datasets.

(*5*,*14*). We determined that participants with WGS data were geographically representative of participants overall and that distributions of age, sex, HIV status, and income were similar between participants with and without WGS data (Appendix Table 1; https://wwwnc.cdc.gov/EID/article/29/5/22-0796-App1.pdf). We excluded 29 participants with evidence of possible mixed-strain infections. There were 431 participants that belonged to genotype-specific groups of 2–19 persons, including 62 participants belonging to 5 large groups of ≥10 persons, which we considered outbreaks. Data from the 62 participants comprising outbreak groups A–E and the 486 in a control group of participants who did not belong to any genotype-specific group, a total of 548 participants, were the focus of our primary analysis (Table 1).

Median age among ungrouped participants was 35 years (IQR 28–42 years); 52% were male, 25% reported no income, and 64% had diagnosed TB/HIV co-infection (Table 1). On the basis of genotypic prediction, we estimated that most had *M. tuberculosis* susceptible to first-line antimicrobial drugs isoniazid (94%) and rifampin (94%). Among participants in the 5 genotypic groups, median age ranged from 29 years in group A to 39 years in group E (Table 1). Participants in group E were exclusively men; D was the only group with more women than men (70%); group C had the most participants with diagnosed TB/HIV coinfection (9/11; 82%). The percentage of participants reporting no income ranged from 18% in group C to 60% in group D. Three participants in group A had multidrug-resistant TB with predicted resistance to both isoniazid and rifampin.

The maximum-likelihood phylogenetic tree for lineage 4 (Figure 1) shows the genetic location of isolates in each outbreak group, highlighted with different colors corresponding to each group. Groups

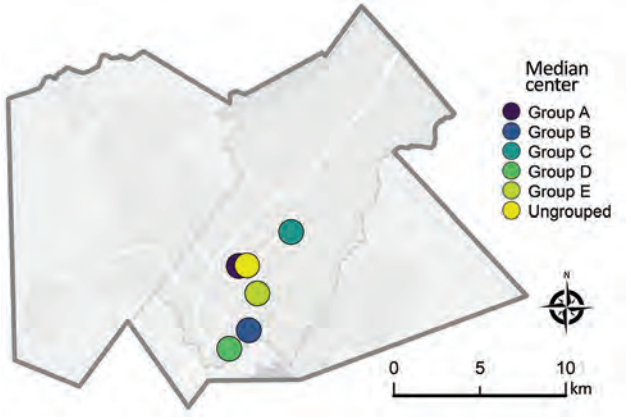


**Figure 3.** Median center points for *Mycobacterium tuberculosis* genotypic groups A–E (≤5 single-nucleotide polymorphisms) and genotypically ungrouped strains in study of high-resolution geospatial and genomic data to characterize recent tuberculosis transmission, Gaborone, Botswana, 2012–2016. The median center represents a centralized geographic location that is estimated by minimizing the distance to all other participant locations being analyzed.

**Table 2.** Spatial summary for each *Mycobacterium tuberculosis* outbreak group (≤5 SNP) in study of high-resolution geospatial and genomic data to characterize recent tuberculosis transmission, by distance rank from reference, Gaborone, Botswana, 2012–2016

| Distance rank | Group | Median center distance, m | X span, m | Y span, m | Rotation, degrees |
|---|---|---|---|---|---|
| 1 | Group A | 458 | 9120 | 10,263 | 28 |
| 2 | Group E | 1,633 | 9,597 | 5,983 | 134 |
| 3 | Group C | 3,143 | 12,431 | 4,768 | 111 |
| 4 | Group B | 3,788 | 6,251 | 9,077 | 15 |
| 5 | Group D | 4,979 | 5,946 | 8,197 | 29 |
| Referent | Ungrouped | Referent | 11,786 | 9,507 | 103 |

A, B, and D all belonged to sublineage 4.1.1.3 (Euro-American [X-type]) and were located near each other in the tree; group C belonged to sublineage 4.1.2.1 (Euro-American [Haarlem]) and group E to 4.3.4.1 (American [LAM]) (*29*) and were located at greater genetic distances from the other groups.

As displayed in maps showing kernel density estimations, median center points, and directional distributions for each outbreak group and for ungrouped participants (Figure 2), we detected significant spatial segregation among outbreak groups ($p = 0.038$). There was also spatial segregation among center points for each group (Figure 3) and different directional distributions (Figure 2) among groups. For example, participants in group C were spread over 12 km in an elongated east–west distribution, but groups B and D both had a more compact (<10 km) north–south spread (Table 2; Figure 2). In contrast, residential locations for ungrouped participants were widely spread across the study area (Table 2; Figure 2). The distance between the center points for ungrouped participants and each of the genotypic groups ranged from <0.5 km for group A to ≈5 km for group D (Table 2; Figure 3).

Locations of potential spatial clusters of participants within each group were visually apparent from estimations of kernel density, especially for groups B and D in the south-central part of the map (Figure 2). The presence of spatial clustering in those groups was also supported by results of the K-function analysis (Figure 4). Differences in K-functions indicated participants in groups B and D had significantly greater spatial clustering than participants with ungrouped strains at relatively close distances (up to ≈4 km). Geographic distance between the first and subsequent case diagnoses over time varied by group (Figure 5). Although group C had an overall pattern of increasing distance over time of detection, all subsequently diagnosed cases in group D were located relatively near the first participant; subsequent participants in group B were located at relatively large but equal distances from the first diagnosed case-patient.

Median distance within groups was <5 SNPs for all groups except A, which had a median of 7 (Figure 6). Group A also had higher variability in pairwise SNP distances compared with other groups. We observed low positive correlation between geographic

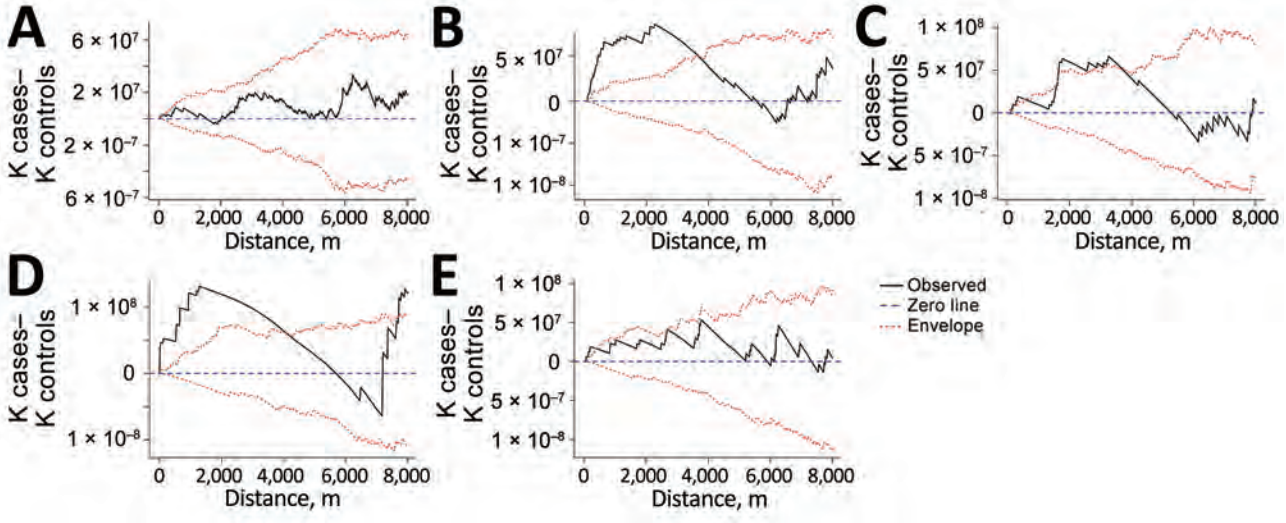


**Figure 4.** K-function differences for *Mycobacterium tuberculosis* genotypic groups A–E (≤5 single-nucleotide polymorphisms) compared with ungrouped strains in study of high-resolution geospatial and genomic data to characterize recent tuberculosis transmission, Gaborone, Botswana, 2012–2016. Differences in K-functions were used to assess geospatial clustering among participants in each group relative to participants with ungrouped strains. Observations falling above the upper 95% envelope indicate significant spatial clustering.

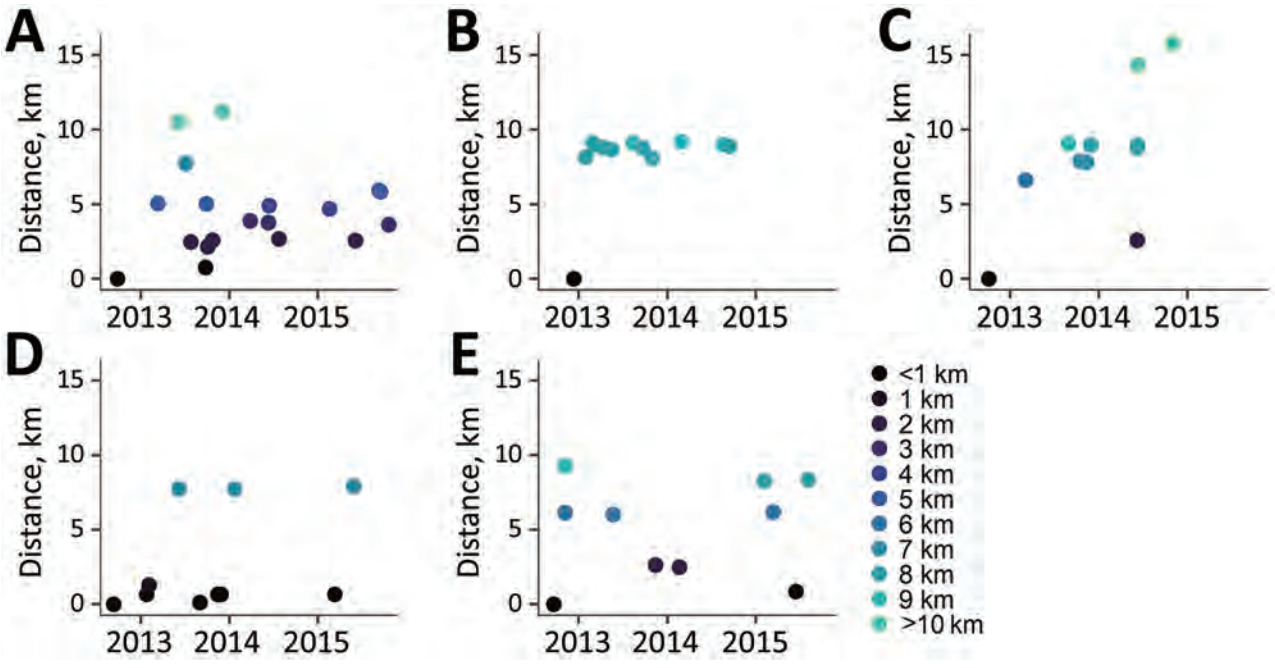


**Figure 5.** Incident tuberculosis by geographic distance from first study participant by genotypic cluster group (≤5 single-nucleotide polymorphisms) in study of high-resolution geospatial and genomic data to characterize recent tuberculosis transmission, Gaborone, Botswana, 2012–2016. Plots represent each participant by date of tuberculosis diagnosis and by geographic distance (based on participant's primary residence) from the first participant (shown in each plot at a distance of 0 km) in each genotypic cluster group.

and SNP pairwise distances overall (ρ = 0.1; p = 0.06) (Figure 7). However, this correlation varied by group; groups A (ρ = 0.26; p = 0.001) and E (ρ = 0.3; p = 0.045) displayed low to modest positive correlation, whereas group C showed negative correlation (ρ = −0.33; p = 0.015).

Phylogenetic tree displays linked to spatial maps (Figure 8) show heterogenous genotypic and geographic patterns in the different groups. In group E, closely related *M. tuberculosis* isolates were generally located closer in space and separate areas of potential geographic clustering were visible. In group D, most isolates appeared to aggregate in a single geographic cluster, regardless of within-group genetic relatedness. We observed a similar pattern in group B with 2 potential spatial clusters. In groups A and C, closely related isolates were generally dispersed more broadly over the geographic area. We visually identified distinct subclusters of spatially and phylogenetically linked cases in all groups. Potential epidemiologic links were identified in each of the outbreak groups. At least 2 participants in all groups but C had similar occupations (Appendix Table 2). Each group had >1 participant associated with 3–6 social gathering places (Appendix Table 3). In group E, 2 participants with the same occupation also had 2 social gathering sites in common (alcohol-related venues).

Results of the sensitivity analysis indicated genotypic groups defined using a ≤2 SNP threshold also displayed distinct geographic characteristics. Fewer participants overall were identified as belonging to a genotype-specific group using the lower SNP threshold. There were 50 participants total in the largest groups (labeled groups A2–G2, with 6–9 participants each), and 643 ungrouped participants (Appendix Table 2). Similar to our primary outbreak group analysis, those groups displayed significant spatial segregation (p = 0.049), different directional distributions, and spatially varied median center points (Appendix Figure 1). Groups A2, B2, D2, and F2 had significant spatial clustering at shorter distances (0.5–4.0 km).

## Discussion

In our analysis, outbreak groups of patients infected with closely related *M. tuberculosis* strains displayed distinct geospatial characteristics. Less genetic and spatial heterogeneity among participants in 2 of the outbreak groups might indicate localized areas of more recent transmission compared with outbreak groups that were less closely spatially clustered, which might reflect a more advanced stage in the transmission trajectory. Geographic distance between first and subsequent cases varied by group. The first case in group B was located at a relatively large but equal

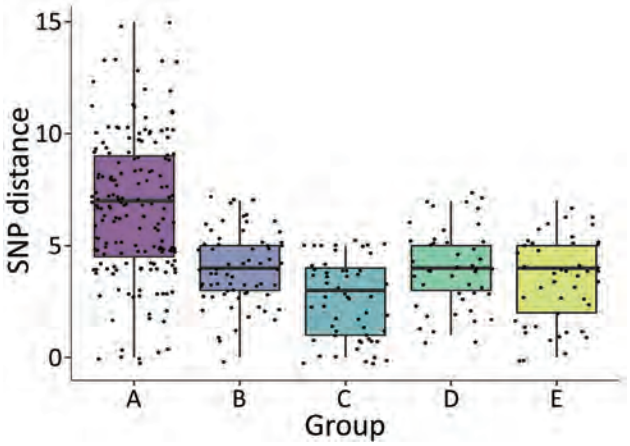


**Figure 6.** Pairwise SNP distances by ≤5 single-nucleotide polymorphism (SNP) genotypic cluster group in study of high-resolution geospatial and genomic data to characterize recent tuberculosis transmission, Gaborone, Botswana, 2012–2016. Box plots with individual data points superimposed display SNP distance summaries by group. Median within-group SNP distance was <5 SNPs for all groups except group A, which had a median of 7 SNPs. Horizontal lines within boxes indicate medians; box tops and bottoms indicate interquartile ranges; error bars indicate 95% CIs.

distance from all subsequent cases. Further mapping efforts could incorporate direction as well as distance to subsequent cases to help examine whether the first case may have potentially introduced TB to ≥1 areas of localized transmission. However, this observation could alternatively be explained by timing of recorded sampling, missed cases, or incomplete spatial data. A location-based approach using the most recently diagnosed instead of the first diagnosed case has been suggested as an alternative, high-yield approach for active case finding (*30*).

Our results support findings from a previous analysis (*5*) that found evidence of localized transmission by detecting spatial clustering of genotypic groups identified using MIRU-VNTR typing. Although overall areas of spatial aggregation were similar, our analysis incorporated higher-resolution genomic sequencing data to detect finer-scale spatial patterns and describe the geographic distribution of distinct genotypic groups. Our results also align with recent studies combining spatial and WGS data to study TB transmission in several other high-burden settings, including China (*31*,*32*), Ghana (*33*), and along the Thailand-Myanmar border (*34*). Observed spatial patterns among related *M. tuberculosis* strains have included local and regional distributions of outbreak groups (*31*,*33*) and lineages (*34*), and associations between residential proximity and genetic similarity (*31*,*32*). In contrast, a study in China found that the majority of genotypic groups included participants from separate geographic districts (*28*). However, that study differed from ours because it specifically analyzed multidrug-resistant TB, and 70% of participants had migrated from other provinces (*28*).

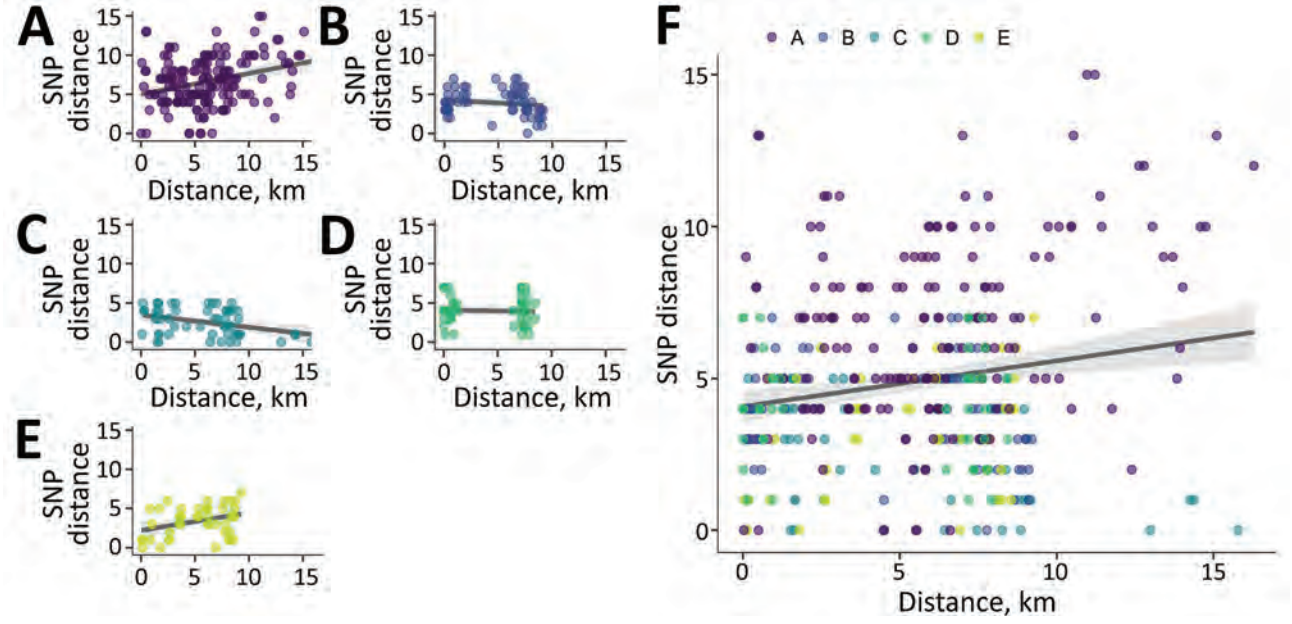


**Figure 7.** Correlation between pairwise single-nucleotide polymorphisms (SNP) distance and pairwise geographic distance for genotypic cluster groups ≤5 SNP (A–E) and ungrouped cases (F) in study of high-resolution geospatial and genomic data to characterize recent tuberculosis transmission, Gaborone, Botswana, 2012–2016. Points represent measurements for within-group pairs. There was low positive correlation between pairwise geographic and SNP distances overall (Spearman ρ = 0.1; p = 0.06). SNP, single-nucleotide polymorphism.

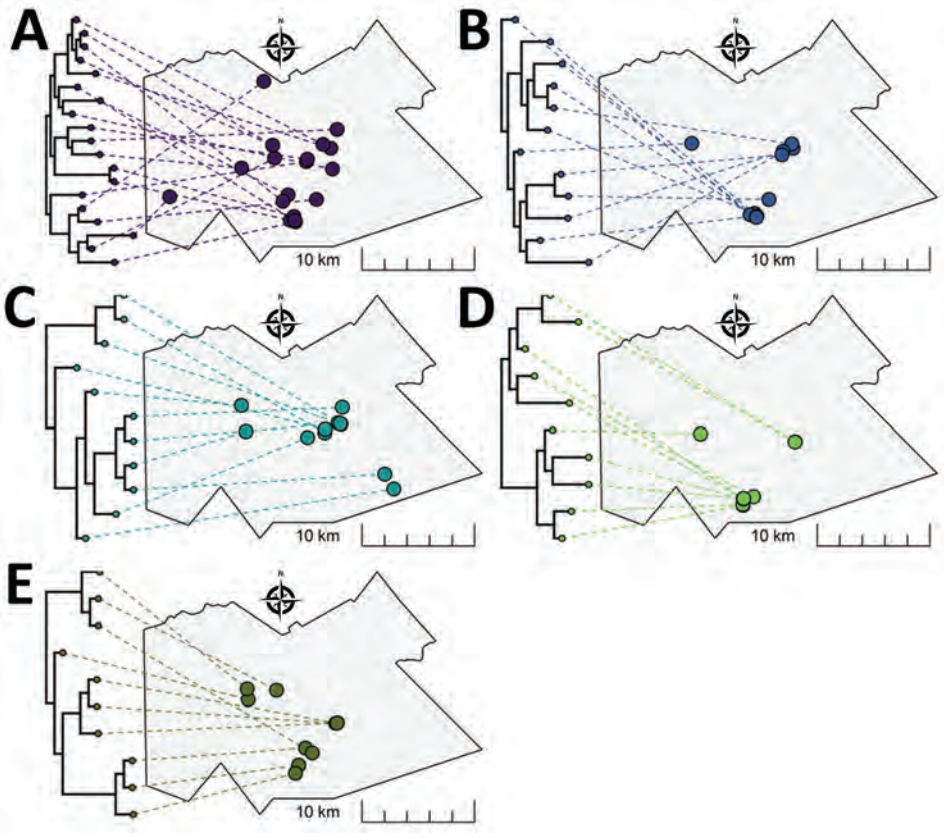


**Figure 8.** Representation of phylogenetic trees for *Mycobacterium tuberculosis* genotypic cluster groups A–E (≤5 single-nucleotide polymorphisms) projected onto geographic maps in study of high-resolution geospatial and genomic data to characterize recent tuberculosis transmission, Gaborone, Botswana, 2012–2016. The location of each *M. tuberculosis* isolate in the tree is displayed with a link drawn to its corresponding geographic location. Tree tips on the same bifurcating branches represent the most closely related isolates.

Phylogenetic trees and geographic maps are often presented as complementary but separate displays of data. We generated phylogenetic trees linked to spatial maps that produced a high-resolution display for each genotypic cluster that could guide public health activities. For example, potential subgroups of closely related strains within outbreak groups could be linked with corresponding geographic locations to help identify high-risk areas for targeted interventions, including active case finding for early diagnosis and treatment, contact investigations, and TB-prevention therapies.

Multiple strata of data are missing from our analysis that might have affected results on detection and geospatial characterization of outbreak groups. Although the original study had relatively high enrollment (4,331/5,515 persons diagnosed during the study period), not every person with TB was captured, including those diagnosed but not enrolled and an unknown number of undetected cases. We excluded participants not culture-confirmed (n = 2,169), which reduced the sample size but helped ensure persons misdiagnosed with TB were not included in the analysis. WGS results were available for culture-confirmed participants with samples containing sufficient DNA (n = 1,426). We further excluded participants for whom we had no geographic coordinates and those with possible mixed-strain infections (*18*,*35*). More complete data could have led to detecting larger or additional outbreak groups or alternate geospatial patterns. However, we believe that the data available are representative of the largest genotypic clusters in the study area and reflect real geographic patterns. We also did not have detailed social contact data. Although we did analyze occupational and social gathering data to identify potential epidemiologic links, additional WGS and epidemiologic data incorporating spatial and social network analysis might have helped us better reconstruct potential transmission chains (*36*).

In conclusion, integrating genomic and geospatial data presents a promising approach for studying TB transmission in high-burden settings. We used this approach to identify heterogeneity among multiple *M. tuberculosis* transmission chains. We identified geographically clustered strains of *M. tuberculosis* representing localized areas of recent transmission. Although barriers remain, substantial progress has been made toward increasing capacity for genomic technologies in low- and middle-income countries

(*37*,*38*). Integrated genomic/geospatial combined approaches used in near real time could help TB-prevention programs identify emerging outbreaks and plan and mobilize interventions to interrupt ongoing transmission (*37*,*38*).

### Acknowledgments

We acknowledge the contributions of study participants and the research team involved in data collection who made this study possible.

Research reported in this publication was supported by the US National Institute of Allergy and Infectious Diseases of the National Institutes of Health under award no. R01AI147336 and R01AI097045 and the President's Emergency Plan for AIDS Relief through the Centers for Disease Control and Prevention.

## About the Author

Ms. Baker is a predoctoral student at the Sue and Bill Gross School of Nursing at the University of California, Irvine. Her research interests include infectious disease epidemiology, spatial analysis, and global health.

### References

1. World Health Organization. Global tuberculosis report 2021 [cited 2021 Oct 19]. https://www.who.int/publications-detail-redirect/9789240037021
2. Auld SC, Kasmar AG, Dowdy DW, Mathema B, Gandhi NR, Churchyard GJ, et al. Research roadmap for tuberculosis transmission science: where do we go from here and how will we know when we're there? J Infect Dis. 2017;216(suppl_6):S662–8. https://doi.org/10.1093/infdis/jix353
3. Auld SC, Shah NS, Cohen T, Martinson NA, Gandhi NR. Where is tuberculosis transmission happening? Insights from the literature, new tools to study transmission and implications for the elimination of tuberculosis. Respirology. 2018;23:807–17. https://doi.org/10.1111/resp.13333
4. Shaweno D, Trauer JM, Doan TN, Denholm JT, McBryde ES. Geospatial clustering and modelling provide policy guidance to distribute funding for active TB case finding in Ethiopia. Epidemics. 2021;36:100470. https://doi.org/10.1016/j.epidem.2021.100470
5. Zetola NM, Moonan PK, Click E, Oeltmann JE, Basotli J, Wen XJ, et al. Population-based geospatial and molecular epidemiologic study of tuberculosis transmission dynamics, Botswana, 2012–2016. Emerg Infect Dis. 2021;27:835–44. https://doi.org/10.3201/eid2703.203840
6. Vesga JF, Hallett TB, Reid MJA, Sachdeva KS, Rao R, Khaparde S, et al. Assessing tuberculosis control priorities in high-burden settings: a modelling approach. Lancet Glob Health. 2019;7:e585–95. https://doi.org/10.1016/S2214-109X(19)30037-3
7. Gardy JL, Johnston JC, Ho Sui SJ, Cook VJ, Shah L, Brodkin E, et al. Whole-genome sequencing and social-network analysis of a tuberculosis outbreak. N Engl J Med. 2011;364:730–9. https://doi.org/10.1056/NEJMoa1003176
8. Guthrie JL, Gardy JL. A brief primer on genomic epidemiology: lessons learned from *Mycobacterium tuberculosis*. Ann N Y Acad Sci. 2017;1388:59–77. https://doi.org/10.1111/nyas.13273
9. Shaweno D, Karmakar M, Alene KA, Ragonnet R, Clements AC, Trauer JM, et al. Methods used in the spatial analysis of tuberculosis epidemiology: a systematic review. BMC Med. 2018;16:193. https://doi.org/10.1186/s12916-018-1178-4
10. Trauer JM, Dodd PJ, Gomes MGM, Gomez GB, Houben RMGJ, McBryde ES, et al. The importance of heterogeneity to the epidemiology of tuberculosis. Clin Infect Dis. 2019;69:159–66. https://doi.org/10.1093/cid/ciy938
11. Dowdy DW, Golub JE, Chaisson RE, Saraceni V. Heterogeneity in tuberculosis transmission and the role of geographic hotspots in propagating epidemics. Proc Natl Acad Sci U S A. 2012;109:9557–62. https://doi.org/10.1073/pnas.1203517109
12. Shrestha S, Reja M, Gomes I, Baik Y, Pennington J, Islam S, et al. Quantifying geographic heterogeneity in TB incidence and the potential impact of geographically targeted interventions in South and North City Corporations of Dhaka, Bangladesh: a model-based study. Epidemiol Infect. 2021;149:e106. https://doi.org/10.1017/S0950268821000832
13. Reid MJA, Arinaminpathy N, Bloom A, Bloom BR, Boehme C, Chaisson R, et al. Building a tuberculosis-free world: The Lancet Commission on tuberculosis. Lancet. 2019;393:1331–84. https://doi.org/10.1016/S0140-6736(19)30024-8
14. Zetola NM, Modongo C, Moonan PK, Click E, Oeltmann JE, Shepherd J, et al. Protocol for a population-based molecular epidemiology study of tuberculosis transmission in a high HIV-burden setting: the Botswana Kopanyo study. BMJ Open. 2016;6:e010046. https://doi.org/10.1136/bmjopen-2015-010046
15. Click ES, Finlay A, Oeltmann JE, Basotli J, Modongo C, Boyd R, et al. Phylogenetic diversity of *Mycobacterium tuberculosis* in two geographically distinct locations in Botswana—The Kopanyo Study. Infect Genet Evol. 2020;81:104232. https://doi.org/10.1016/j.meegid.2020.104232
16. Kohl TA, Utpatel C, Schleusener V, De Filippo MR, Beckert P, Cirillo DM, et al. MTBseq: a comprehensive pipeline for whole genome sequence analysis of *Mycobacterium tuberculosis* complex isolates. PeerJ. 2018;6:e5895. https://doi.org/10.7717/peerj.5895
17. Grobbel HP, Merker M, Köhler N, Andres S, Hoffmann H, Heyckendorf J, et al. Design of multidrug-resistant tuberculosis treatment regimens based on DNA sequencing. Clin Infect Dis. 2021;73:1194–202. https://doi.org/10.1093/cid/ciab359
18. Baik Y, Modongo C, Moonan PK, Click ES, Tobias JL, Boyd R, et al. Possible transmission mechanisms of mixed *Mycobacterium tuberculosis* infection in high HIV prevalence country, Botswana. Emerg Infect Dis. 2020;26:953–60. https://doi.org/10.3201/eid2605.191638
19. Dreyer V, Utpatel C, Kohl TA, Barilar I, Gröschel MI, Feuerriegel S, et al. Detection of low-frequency resistance-mediating SNPs in next-generation sequencing data of *Mycobacterium tuberculosis* complex strains with binoSNP. Sci Rep. 2020;10:7874. https://doi.org/10.1038/s41598-020-64708-8
20. Diggle P, Zheng P, Durr P. Nonparametric estimation of spatial segregation in a multivariate point process: bovine tuberculosis in Cornwall, UK. J R Stat Soc Ser C Appl Stat. 2005;54:645–58. https://doi.org/10.1111/j.1467-9876.2005.05373.x
21. Waller L. Detection of clustering in spatial data. In: Rogerson P, Fotheringham S, editors. The SAGE handbook of spatial

analysis. London: SAGE Publications, Ltd; 2009.
22. Wheeler DC. A comparison of spatial clustering and cluster detection techniques for childhood leukemia incidence in Ohio, 1996–2003. Int J Health Geogr. 2007;6:13. https://doi.org/10.1186/1476-072X-6-13
23. Paradis E, Schliep K. ape 5.0: an environment for modern phylogenetics and evolutionary analyses in R. Bioinformatics. 2019;35:526–8. https://doi.org/10.1093/bioinformatics/bty633
24. Nguyen LT, Schmidt HA, von Haeseler A, Minh BQ. IQ-TREE: a fast and effective stochastic algorithm for estimating maximum-likelihood phylogenies. Mol Biol Evol. 2015;32:268–74. https://doi.org/10.1093/molbev/msu300
25. Crispell J, Zadoks RN, Harris SR, Paterson B, Collins DM, de-Lisle GW, et al. Using whole genome sequencing to investigate transmission in a multi-host system: bovine tuberculosis in New Zealand. BMC Genomics. 2017;18:180. https://doi.org/10.1186/s12864-017-3569-x
26. Yu G. Using ggtree to visualize data on tree-like structures. Curr Protoc Bioinformatics. 2020;69:e96. https://doi.org/10.1002/cpbi.96
27. Revell LJ. phytools: An R package for phylogenetic comparative biology (and other things). Methods Ecol Evol. 2012;3:217–23. https://doi.org/10.1111/j.2041-210X.2011.00169.x
28. Jiang Q, Liu Q, Ji L, Li J, Zeng Y, Meng L, et al. Citywide transmission of multidrug-resistant tuberculosis under China's rapid urbanization: a retrospective population-based genomic spatial epidemiological study. Clin Infect Dis. 2020;71:142–51. https://doi.org/10.1093/cid/ciz790
29. Coll F, McNerney R, Guerra-Assunção JA, Glynn JR, Perdigão J, Viveiros M, et al. A robust SNP barcode for typing *Mycobacterium tuberculosis* complex strains. Nat Commun. 2014;5:4812. https://doi.org/10.1038/ncomms5812
30. Moonan PK, Zetola NM, Tobias JL, Basotli J, Boyd R, Click ES, et al. A neighbor-based approach to identify tuberculosis exposure, the Kopanyo Study. Emerg Infect Dis. 2020;26:1010–3. https://doi.org/10.3201/eid2605.191568
31. Zhou Y, Anthony R, Wang S, Ou X, Liu D, Zhao Y, et al. The epidemic of multidrug resistant tuberculosis in China in historical and phylogenetic perspectives. J Infect. 2020;80:444–53. [Erratum in J Infect. 2022;85:609.] https://doi.org/10.1016/j.jinf.2019.11.022
32. Yang C, Lu L, Warren JL, Wu J, Jiang Q, Zuo T, et al. Internal migration and transmission dynamics of tuberculosis in Shanghai, China: an epidemiological, spatial, genomic analysis. Lancet Infect Dis. 2018;18:788–95. https://doi.org/10.1016/S1473-3099(18)30218-4
33. Asare P, Otchere ID, Bedeley E, Brites D, Loiseau C, Baddoo NA, et al. Whole genome sequencing and spatial analysis identifies recent tuberculosis transmission hotspots in Ghana. Front Med (Lausanne). 2020;7:161. https://doi.org/10.3389/fmed.2020.00161
34. Maung HMW, Palittapongarnpim P, Aung HL, Surachat K, Nyunt WW, Chongsuvivatwong V. Geno-spatial distribution of *Mycobacterium tuberculosis* and drug resistance profiles in Myanmar–Thai border area. Trop Med Infect Dis. 2020;5:153. https://doi.org/10.3390/tropicalmed5040153
35. Lee RS, Proulx JF, McIntosh F, Behr MA, Hanage WP. Previously undetected super-spreading of *Mycobacterium tuberculosis* revealed by deep sequencing. eLife. 2020;9:e53245. https://doi.org/10.7554/eLife.53245
36. Hatherell HA, Colijn C, Stagg HR, Jackson C, Winter JR, Abubakar I. Interpreting whole genome sequencing for investigating tuberculosis transmission: a systematic review. BMC Med. 2016;14:21. https://doi.org/10.1186/s12916-016-0566-x
37. Inzaule SC, Tessema SK, Kebede Y, Ogwell Ouma AE, Nkengasong JN. Genomic-informed pathogen surveillance in Africa: opportunities and challenges. Lancet Infect Dis. 2021;21:e281–9. https://doi.org/10.1016/S1473-3099(20)30939-7
38. Gardy JL, Loman NJ. Towards a genomics-informed, real-time, global pathogen surveillance system. Nat Rev Genet. 2018;19:9–20. https://doi.org/10.1038/nrg.2017.88

Address for correspondence: Sanghyuk Shin, Associate Professor, Sue & Bill Gross School of Nursing, Director, UCI Infectious Disease Science Initiative, University of California Irvine, 106F Berk Hall, Irvine, CA 92697, USA; email: ssshin2@uci.edu

# Cutaneous Leishmaniasis Caused by *Leishmania infantum*, Israel, 2018–2021

Michal Solomon, Nadav Astman, Karin Warshavsky, Aviv Barzilai, Tal Meningher, Dror Avni, Eli Schwartz

Cutaneous leishmaniasis (CL) is endemic to Israel. Previously, CL caused by *Leishmania infantum* had been reported in Israel only once (in 2016). We report 8 *L. infantum* CL cases; 7 occurred during 2020–2021. None of the patients had systemic disease. *L. infantum* CL may be an emerging infection in Israel.

*Leishmania* is a protozoan that causes a wide variety of diseases. Clinical manifestations include cutaneous leishmaniasis (CL), visceral leishmaniasis (VL), or mucocutaneous leishmaniasis, depending mainly on the specific causative leishmania species (*1*). Old World CL is classically attributable to *L. major* and *L. tropica*. However, *L. infantum*, which usually causes VL, recently has been considered as a causative agent of CL (*2*).

CL is endemic to Israel and has been attributed almost exclusively to infection with *L. major* and, more recently, to *L. tropica* (*3*). However, human VL caused by an *L. donovani* substrain, *L. infantum*, has been reported, albeit rarely, in Israel (*4*). The reservoir is dogs, and the epidemiology of the disease among dogs indicates wide distribution in Israel (*5*). Nevertheless, cases of CL caused by *L. infantum* were previously reported in the Middle East and worldwide. In Israel, CL caused by *L. infantum* was reported in 2016 (*6*); that infection was acquired in the southern part of Israel, known to be endemic for *L. major*. In this article, we report 8 cases of *L. infantum* CL observed in Israel during 2018–2021.

## The Study

All patients were seen at Chaim Sheba Medical Center (Tel Hashomer, Israel). We defined *L. infantum* CL as cutaneous lesions (ulcers, nodules, or papules) clinically compatible with leishmaniasis and a PCR result positive for *L. infantum*. The study was approved by the Chaim Sheba Medical Center Institutional Review Board (protocol approval no. 7274–09).

We took tissue specimens from suspected skin lesions and extracted DNA from dried blood spots by using the QIAamp DNA Mini Kit (QIAGEN, https://www.qiagen.com). We analyzed the samples for internal transcribed spacer 1 PCR by using 10 μM primers (LITSR 5′-CTGGATCATTTTCCGATG-3′ and L5.8S 5′-TGATACCACTTATCGCACTT-3′) (*7*). We analyzed the amplicons on 4% agarose gel. We sent the *L. infantum*–positive samples to Hylabs (Rehovot, Israel) for a second validation and sequencing.

During 2016–2021, our laboratory at Chaim Sheba Medical Center diagnosed 609 cases of leishmania (Table 1). Among those, 8 cases (1.3%) were attributable to *L. infantum*. All of the cases were confirmed by PCR and further sequencing.

One case was diagnosed in 2018 and the other 7 cases during 2020–2021. Of the 8 patients, 6 were male and 2 female. The infections were acquired in different regions of Israel, including the southern region (Negev and Arava areas), where *L. major* is endemic, and the central region (east of Tel Aviv), where *L. tropica* is endemic (Figure 1).

The mean age of patients at diagnosis was 31 years (range 10–56 years; median 28.5 years). The average number of lesions was 2 (range 1–6). The lesions were commonly located on the limbs (6 patients); in 2 patients, the lesions were located on the face (Table 2; Figure 2).

Two patients recovered within a short period (≈3 months) without any treatment, 3 patients were treated with topical therapy (intralesional sodium stibogluconate and liquid nitrogen), and the other 3 patients were treated with systemic therapy (oral miltefosine and intravenous liposomal amphotericin B). Systemic therapy was initiated when topical

Author affiliations: Chaim Sheba Medical Center, Tel Hashomer, Israel (M. Solomon, N. Astman, K. Warshavsky, A. Barzilai, T. Meningher, D. Avni, E. Schwartz); Tel Aviv University, Tel Aviv, Israel (M. Solomon, N. Astman, K. Warshavsky, A. Barzilai, D. Avni, E. Schwartz)

DOI: https://doi.org/10.3201/eid2905.221812

**Table 1.** Leishmaniasis cases diagnosed (N = 609), by *Leishmania* species, at the laboratory at Chaim Sheba Medical Center, Tel Hashomer, Israel, 2016–2021*

| *Leishmania* species | No. (%) cases |
|---|---|
| *L. major* | 403 (66.1) |
| *L. tropica* | 175 (28.7) |
| *L. braziliensis* | 23 (3.7) |
| *L. infantum* | 8 (1.3) |

treatment failed or intralesional sodium stibogluconate injection was not feasible because of the anatomic location of the lesions (e.g., on the face or eyelid). All patients who received systemic therapy had a good response. None of the patients had systemic disease.

## Conclusions

The first known case of CL attributable to *L. infantum* infection in southern Israel was reported in 2016 (*6*). We describe a case series of 8 patients with *L. infantum* CL in Israel. The disease was acquired in different parts of Israel, and all but 1 case occurred during 2020–2021, pointing to a possible emergence of a new species causing CL in Israel. Canids, including domestic dogs and wild canids, are reservoirs for *L. infantum*. Recently, cats were also reported as a reservoir (*5*).

The known vectors of *L. infantum* are *Phlebotomus syriacus*, *P. tobbi*, and *P. perfilliewi* flies, all of which exist in Israel (*9*) Because both the reservoir and the vector for *L. infantum* have existed in Israel for years, the reason for this outbreak of CL is not well understood. Of note, in several countries, including Saudi Arabia, Turkey, and Yemen, *L. infantum* as a causative agent for CL has already been described (*10*–*12*), whereas Israel historically has not documented this disease.

Diagnosis of this *Leishmania* species in skin lesions can be made mainly by PCR testing. In Israel, PCR tests have been available since 2003 (*7*). At Chaim Sheba Medical Center, molecular diagnosis has been available since 2016, and it was only recently that the emergence of *L. infantum* CL was observed, thus excluding a diagnostic bias as a cause for this phenomenon. In addition, a query of 3 other centers in Israel where molecular diagnosis is performed indicated that cases of *L. infantum* caused by CL were seen only as of 2020 (E. Schwartz, pers. comm., email, 2022 Nov 1).

Clinical pleomorphism is a major feature of *Leishmania* parasites, a phenomenon particularly well illustrated in the case of *L. infantum*. This species is endemic in countries around the Mediterranean Basin and is most commonly known to cause VL, which is fatal if untreated. Host factors play an important role in this pleomorphism (*13*). However, some reports suggest a possible contribution of parasite factors attributable to different subspecies. Among the different *L. infantum* zymodemes (groups of strains showing the same isoenzymatic profile), some are restricted to cutaneous cases, such as MON-1, MON-24, MON-29, and MON-33 (*14*). However, the major and ubiquitous MON-1 zymodeme, mostly associated with VL, was also found in CL cases (*14*).

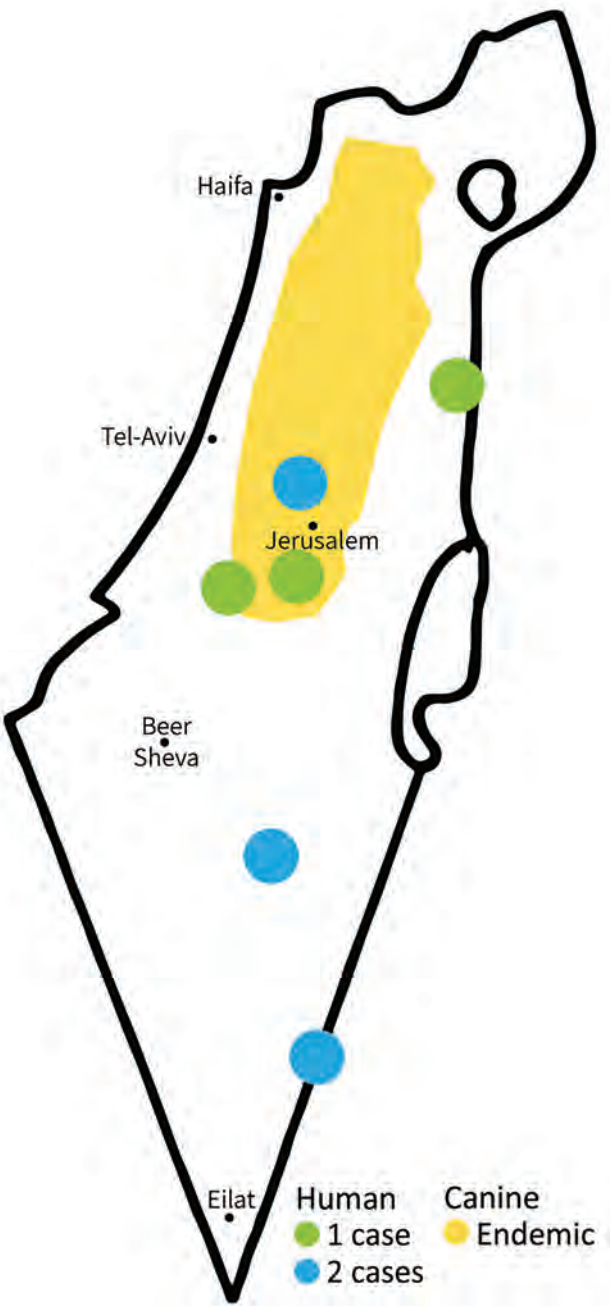


**Figure 1.** Foci of cutaneous leishmaniasis caused by *Leishmania infantum*, Israel, 2018–2021. Distribution of canine *L. infantum* in Israel based on Jaffe et al (*8*).

**Table 2**. Clinical and demographic characteristics of 8 patients with cutaneous leishmaniasis caused by *Leishmania infantum*, Israel, 2018–2021

| Characteristic | Value |
|---|---|
| Mean age, y (range) | 31.8 (10–56) |
| Sex, no. patients | |
| M | 6 |
| F | 2 |
| Exposure area | Southern and eastern Israel |
| Mean no. lesions (range) | 2 (1–6) |
| Anatomic location, no. patients* | |
| Head and neck | 2 |
| Upper limbs | 3 |
| Lower limbs | 4 |

*Includes multiple locations per patient.

Transmission of *L. infantum* infection is considered predominantly zoonotic, and domestic animals are the major reservoir. The disease spreads through expansion of the zoonotic or the anthroponotic cycles (*15*) to regions where local vectors (phlebotomine species) can contribute to *L. infantum* transmission.

No specific recommendations exist regarding treatment of CL caused by *L. infantum*. The treatment regimen we chose was based on disease severity. In mild cases, no treatment was given, and the lesions healed spontaneously and rapidly within 3 months. In moderate cases, topical treatment was used (intralesional sodium stibogluconate and liquid nitrogen). In severe cases or in cases that were refractory to local treatment, systemic treatment was given (oral miltefosine and intravenous liposomal amphotericin B), all with good responses. None of the patients had systemic involvement. The treatment protocols for severe lesions were similar to those used in *L. donovani* CL cases and in severe cases of *L. major* and *L. tropica* CL. Although *L. infantum* can cause VL, none of the patients had systemic disease. Therefore, a nonsystemic treatment (topical or intralesional) seems to be an adequate treatment in most cases.

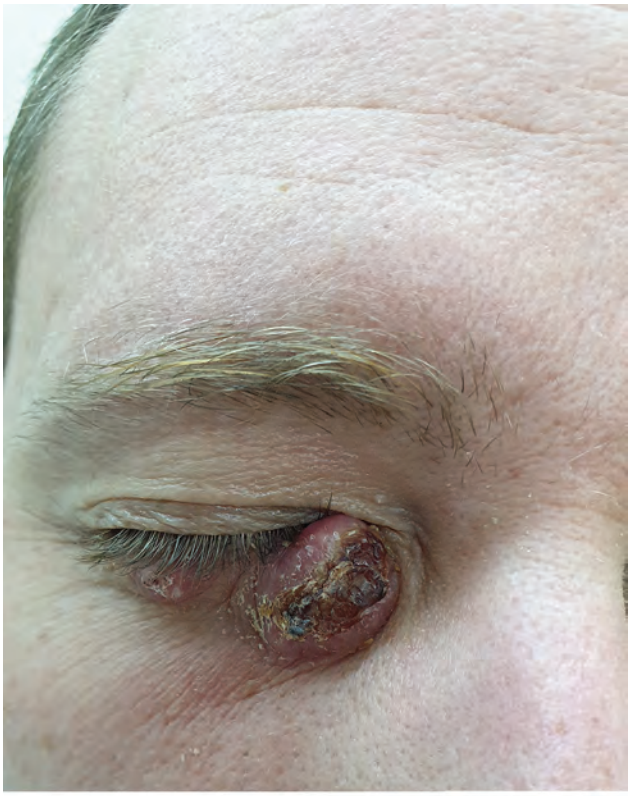

**Figure 2.** Cutaneous lesion caused by *Leishmania infantum* on the right lower eyelid of a patient seen at Chaim Sheba Medical Center, Israel, 2021.

In conclusion, the increasing number of *L. infantum* CL cases since 2020, occurring in different parts of Israel, point to an emerging new leishmania species in Israel. Clinicians should include this pathogen in the differential diagnosis of patients with cutaneous lesions clinically compatible with leishmaniasis.

## About the Author

Dr. Solomon is dermatologist at Chaim Sheba Medical Center in Israel. Her primary research interests include cutaneous leishmaniasis and tropical skin diseases.

## References

1. Reithinger R, Dujardin JC, Louzir H, Pirmez C, Alexander B, Brooker S. Cutaneous leishmaniasis. Lancet Infect Dis. 2007;7:581–96. https://doi.org/10.1016/S1473-3099(07)70209-8
2. del Giudice P, Marty P, Lacour JP, Perrin C, Pratlong F, Haas H, et al. Cutaneous leishmaniasis due to *Leishmania infantum*. Case reports and literature review. Arch Dermatol. 1998;134:193–8. https://doi.org/10.1001/archderm.134.2.193
3. Solomon M, Pavlotsky F, Leshem E, Ephros M, Trau H, Schwartz E. Liposomal amphotericin B treatment of cutaneous leishmaniasis due to *Leishmania tropica*. J Eur Acad Dermatol Venereol. 2011;25:973–7. https://doi.org/10.1111/j.1468-3083.2010.03908.x
4. Nasereddin A, Baneth G, Schönian G, Kanaan M, Jaffe CL. Molecular fingerprinting of *Leishmania infantum* strains following an outbreak of visceral leishmaniasis in central Israel. J Clin Microbiol. 2005;43:6054–9. https://doi.org/10.1128/JCM.43.12.6054-6059.2005
5. Baneth G, Nachum-Biala Y, Zuberi A, Zipori-Barki N, Orshan L, Kleinerman G, et al. *Leishmania* infection in cats and dogs housed together in an animal shelter reveals a higher parasite load in infected dogs despite a greater seroprevalence among cats. Parasit Vectors. 2020;13:115. https://doi.org/10.1186/s13071-020-3989-3
6. Ben-Shimol S, Sagi O, Horev A, Avni YS, Ziv M, Riesenberg K. Cutaneous leishmaniasis caused by *Leishmania infantum* in southern Israel. Acta Parasitol. 2016;61:855–8. https://doi.org/10.1515/ap-2016-0118
7. Schönian G, Nasereddin A, Dinse N, Schweynoch C, Schallig HD, Presber W, et al. PCR diagnosis and characterization of *Leishmania* in local and imported clinical samples. Diagn Microbiol Infect Dis. 2003;47:349–58. https://doi.org/10.1016/S0732-8893(03)00093-2

8. Jaffe CL, Baneth G, Abdeen ZA, Schlein Y, Warburg A. Leishmaniasis in Israel and the Palestinian Authority. Trends Parasitol. 2004;20:328–32. https://doi.org/10.1016/j.pt.2004.05.001
9. Orshan L, Szekely D, Khalfa Z, Bitton S. Distribution and seasonality of *Phlebotomus* sand flies in cutaneous leishmaniasis foci, Judean Desert, Israel. J Med Entomol. 2010;47:319–28. https://doi.org/10.1093/jmedent/47.3.319
10. Eroglu F, Koltas IS, Alabaz D, Uzun S, Karakas M. Clinical manifestations and genetic variation of *Leishmania infantum* and *Leishmania tropica* in southern Turkey. Exp Parasitol. 2015;154:67–74. https://doi.org/10.1016/j.exppara.2015.04.014
11. Khatri ML, Di Muccio T, Gramiccia M. Cutaneous leishmaniasis in North-Western Yemen: a clinicoepidemiologic study and *Leishmania* species identification by polymerase chain reaction-restriction fragment length polymorphism analysis. J Am Acad Dermatol. 2009;61:e15–21. https://doi.org/10.1016/j.jaad.2009.04.047
12. Rasheed Z, Ahmed AA, Salem T, Al-Dhubaibi MS, Al Robaee AA, Alzolibani AA. Prevalence of *Leishmania* species among patients with cutaneous leishmaniasis in Qassim Province of Saudi Arabia. BMC Public Health. 2019;19:384. https://doi.org/10.1186/s12889-019-6710-8
13. Pratlong F, Dedet JP, Marty P, Portús M, Deniau M, Dereure J, et al. *Leishmania*-human immunodeficiency virus coinfection in the Mediterranean Basin: isoenzymatic characterization of 100 isolates of the *Leishmania infantum* complex. J Infect Dis. 1995;172:323–6. https://doi.org/10.1093/infdis/172.1.323
14. Rioux JA, Moreno G, Lanotte G, Pratlong F, Dereure J, Rispail P. Two episodes of cutaneous leishmaniasis in man caused by different zymodemes of *Leishmania infantum* s.1. Trans R Soc Trop Med Hyg. 1986;80:1004–5. https://doi.org/10.1016/0035-9203(86)90300-7
15. Svobodová M, Alten B, Zídková L, Dvorák V, Hlavacková J, Mysková J, et al. Cutaneous leishmaniasis caused by *Leishmania infantum* transmitted by *Phlebotomus tobbi*. Int J Parasitol. 2009;39:251–6. https://doi.org/10.1016/j.ijpara.2008.06.016


Address for correspondence: Michal Solomon, Department of Dermatology, The Chaim Sheba Medical Center, Tel Hashomer 52621, Israel; email: solomondr1@gmail.com

# Fatal Case of Heartland Virus Disease Acquired in the Mid-Atlantic Region, United States

Sichen Liu,[1] Suraj Kannan,[1] Monica Meeks, Sandra Sanchez, Kyle W. Girone, James C. Broyhill, Roosecelis Brasil Martines, Joshua Bernick, Lori Flammia, Julia Murphy, Susan L. Hills, Kristen L. Burkhalter, Janeen J. Laven, David Gaines, Christopher J. Hoffmann

Heartland virus (HRTV) disease is an emerging tickborne illness in the midwestern and southern United States. We describe a reported fatal case of HRTV infection in the Maryland and Virginia region, states not widely recognized to have human HRTV disease cases. The range of HRTV could be expanding in the United States.

Heartland virus (HRTV) is a bandavirus spread by *Amblyomma americanum* (lone star) ticks in the midwestern and southern United States (*1*). Many cases of HRTV infection have been characterized by severe illness or death, mostly among men >50 years of age with multiple underlying conditions (*1*–*7*). HRTV infection in humans typically manifests as a nonspecific febrile illness characterized by malaise, myalgias, arthralgias, and gastrointestinal distress, along with thrombocytopenia, leukopenia, hyponatremia, and elevated liver transaminases (*3*). Most reported hospitalized patients recover, but deaths have occurred and have been associated with secondary hemophagocytic lymphohistiocytosis (HLH) (*4*,*5*).

Since HRTV was discovered in 2009 in Missouri, USA, human HRTV disease cases have also been reported in Kansas, Oklahoma, Arkansas, Tennessee, Kentucky, Indiana, Illinois, Iowa, Georgia, Pennsylvania, New York, and North Carolina according to the Centers for Disease Control and Prevention (CDC; https://www.cdc.gov/heartland-virus/statistics/index.html). Studies have documented HRTV RNA in *A. americanum* ticks and HRTV-neutralizing antibodies in vertebrate animals in these states (*8*–*13*). However, the distribution of *A. americanum* ticks is wider and growing, possibly because of climate change, which could lead to HRTV range expansion (*3*,*11*). Of note, vertebrate animals with neutralizing antibodies to HRTV have been documented in states without confirmed human cases, including Texas, Florida, South Carolina, and Louisiana in the south and Vermont, New Hampshire, and Maine in the northeast (*12*,*13*). To date, no seropositive animals have been reported from Maryland or Virginia in the mid-Atlantic region. We describe a fatal human case of HRTV infection with secondary HLH in which initial infection likely occurred in either Maryland or Virginia.

## The Study

The patient was a man in his late 60s who had a medical history of splenectomy from remote trauma, coronary artery disease, and hypertension. He was seen at an emergency department in November 2021 for 5 days of fever, nonbloody diarrhea, dyspnea, myalgias, and malaise. At initial examination, he appeared fatigued but was alert and oriented. Laboratory results were notable for hyponatremia, mildly elevated liver enzymes, leukopenia, and thrombocytopenia (Table). The patient had homes in rural areas of Maryland and Virginia and had not traveled outside of this area in the previous 3 months. He spent time outdoors on his properties but did not recall attached ticks or tick bites. Despite the lack of known tick bites, the symptom constellation and potential exposure led clinicians to highly suspect tickborne illness; they prescribed doxycycline and discharged the patient home.

Author affiliations: National Institute of Allergy and Infectious Diseases, Bethesda, Maryland, USA (S. Liu); Johns Hopkins University School of Medicine, Baltimore, Maryland, USA (S. Kannan, M. Meeks, S. Sanchez, C.J. Hoffman); Virginia Department of Health, Richmond, Virginia, USA (K.W. Girone, J.C. Broyhill, J. Bernick, L. Flammia, J. Murphy, D. Gaines); Centers for Disease Control and Prevention, Atlanta, Georgia, USA (R.B. Martines); Centers for Disease Control and Prevention, Fort Collins, Colorado, USA (S.L. Hills, K.L. Burkhalter, J.J. Laven)

DOI: https://doi.org/10.3201/eid2905.221488

[1]These first authors contributed equally to this article.

Two days later, on day 7 after symptom onset, the patient returned to the emergency department with confusion, an unsteady gait, and new fecal and urinary incontinence; he was admitted for inpatient management. He had progressive encephalopathy with hyponatremia and rising transaminases (Table). Results of neurologic workup and imaging were unremarkable (Table). Computed tomography imaging of the abdomen and pelvis showed new pelvic and inguinal lymphadenopathy. The patient was treated with hypertonic saline, intravenous doxycycline, and piperacillin/tazobactam.

Because of clinical deterioration, he was transferred to a tertiary care center. At arrival at the tertiary center, he was fatigued and disoriented. Physical examination demonstrated new hepatomegaly and lower extremity livedo reticularis. Results of broad testing for infectious etiologies was negative (Appendix Table, https://wwwnc.cdc.gov/EID/article/29/5/22-1488-App1.pdf). Laboratory results demonstrated increased creatine kinase (9,567 U/L), lactate (2.5 mg/dL), lactate dehydrogenase (1,709 U/L), and ferritin (47,445 ng/mL). Interleukin 2 receptor, a marker for HLH, was also elevated (9,390 pg/mL) (Table). Immunosuppressive agents for management of likely secondary HLH were deferred while clinicians conducted a diagnostic workup of the underlying disease process. An arboviral disease was the leading diagnostic consideration, but limited availability of commercial diagnostic testing for tickborne diseases delayed diagnosis.

The patient's clinical course continued to deteriorate. He had acute respiratory failure, renal failure, and a cardiac arrest. He was transitioned to comfort care and died on day 13 after symptom onset.

Because of concern for arboviral illness, the Virginia Department of Health (VDH) initiated an investigation and sent a serum specimen to CDC for testing (Appendix). Quantitative reverse transcription PCR was notably positive for HRTV RNA (Appendix Table). Autopsy findings identified

**Table.** Laboratory findings in a fatal case of heartland virus disease acquired in the mid-Atlantic region, United States*

| Test | Reference range | Days after symptom onset | | | | |
|---|---|---|---|---|---|---|
| | | 5 | 7 | 9 | 11 | 13 |
| Temperature, °C | 35.5–38.3 | 36.8 | 38.5 | 38.5 | 39.1 | 36.9 |
| Blood cell counts | | | | | | |
| Leukocyte count, × $10^3$ cells/μL | 4.50–11.00 | 2.4 | 3.7 | 3.5 | 2.48 | 3.25 |
| Absolute neutrophil count, cells/μL | 1.50–7.80 | ND | ND | ND | 0.99 | 0.88 |
| Absolute lymphocyte count, cells/μL | 1.10–4.80 | ND | ND | ND | 1.22 | 1.76 |
| Hemoglobin, g/dL | 13.9–16.3 | 14.5 | 14.9 | 14.6 | 14.4 | 11.7 |
| Platelets, × $10^3$/μL | 150–350 | 178 | 106 | 82 | 59 | 61 |
| Blood chemistry test results | | | | | | |
| Sodium, mmol/L | 135–148 | 126 | 115 | 120 | 129 | 136 |
| Potassium, mmol/L | 3.5–5.1 | 3.7 | 3.3 | 4.2 | 4.4 | 4.4 |
| Carbon dioxide, mmol/L | 21–31 | 22 | 22 | 20 | 17 | 18 |
| Anion gap, mmol/L | 7–16 | 13 | 15 | 12 | 12 | 11 |
| Blood urea nitrogen, mg/dL | 7–22 | 12 | 12 | 16 | 26 | 68 |
| Creatinine, mg/dL | 0.6–1.3 | 1.0 | 1.3 | 1.2 | 1.4 | 4.4 |
| Aspartate aminotransferase, units/L | ≤37 | 45 | 359 | 434 | 590 | 617 |
| Alanine aminotransferase, units/L | ≤40 | 46 | 238 | 262 | 209 | 156 |
| Alkaline phosphatase, units/L | 30–120 | 69 | 64 | 53 | 67 | 89 |
| Cerebrospinal fluid test results | | | | | | |
| Leukocyte count, cells/$mm^3$ | 0–5 | ND | 2 | ND | ND | ND |
| Glucose, mg/dL | 40–70 | ND | 80 | ND | ND | ND |
| Protein, mg/dL | 12–60 | ND | 58 | ND | ND | ND |
| Cardiac test results | | | | | | |
| Troponin I, ng/mL | <0.04 | ND | ND | ND | 0.21 | 0.38 |
| Troponin T, high sensitivity, ng/L | 0–19 | 14 | 22 | 30 | ND | ND |
| Pro-BNP, pg/mL | 5–125 | ND | ND | ND | 4,258 | ND |
| Lipid panel test results | | | | | | |
| Cholesterol, total, mg/dL | ≤200 | ND | ND | ND | 69 | ND |
| Triglycerides, mg/dL | ≤150 | ND | ND | ND | 147 | ND |
| Other test results | | | | | | |
| D-dimer, mg/L | 0.00–0.49 | ND | ND | 2.72 | 3.71 | ND |
| Creatine kinase, U/L | 24–195 | ND | ND | ND | 8,727 | 11,083 |
| Lactic acid, mmol/L | 0.5–2.0 | 1.6 | 1.8 | ND | 2.5 | 2.4 |
| Lactate dehydrogenase, U/L | 118–273 | ND | ND | 1,412 | 1,709 | ND |
| Ferritin, ng/mL | 30–400 | ND | ND | ND | 47,445 | 174,957 |
| Fibrinogen, mg/dL | 170–422 | ND | ND | 199 | 224 | 170 |
| C-reactive protein, mg/dL | <0.5 | ND | 1.2 | 0.6 | 0.5 | ND |
| Interleukin 2 receptor, pg/mL | 532–1,891 | ND | ND | ND | 9,390 | ND |

*BNP, B-type natriuretic peptide; ND, not done.

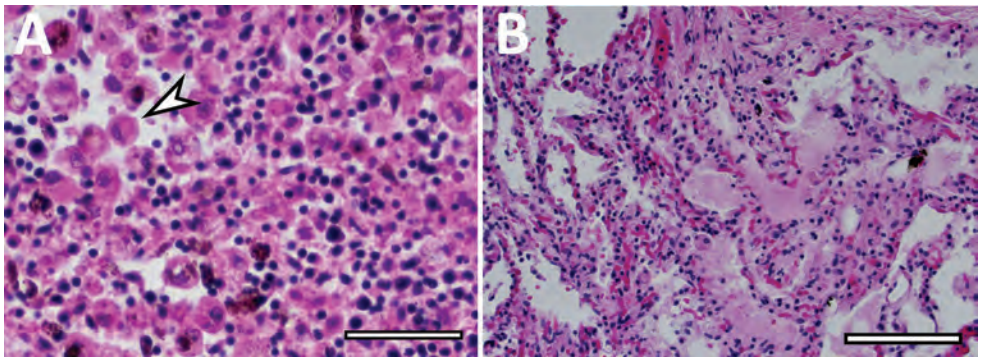


**Figure 1.** Postmortem autopsy findings in a fatal case of heartland virus disease acquired in the mid-Atlantic region, United States. A) Hematoxylin and eosin stain of patient accessory spleen; arrow indicates congestion with hemophagocytic histiocytes. Scale bar indicates 50 μm. B) Hematoxylin and eosin stain showing pulmonary hyperinflammation, including pleural thickening and adhesions, and pulmonary fibrosis, edema, and calcifications. Scale bar indicates 125 μm.

markedly congested accessory spleens with abundant histiocytes, phagocytosing erythrocytes, and pulmonary hyperinflammation (Figure 1). Immunohistochemistry testing of heart, spleen, kidney, and liver samples were positive for HRTV at CDC (Figure 2). Immunohistochemistry of the spleen was negative for Epstein-Barr virus (EBV) at the clinical institution. The autopsy report concluded that the cause of death was respiratory failure secondary to hyperinflammation due to HLH, likely triggered by HRTV infection.

VDH performed tick drags at the patient's 2 properties in eastern Maryland and central Virginia during early- to mid-June 2022. VDH collected a total of 193 ticks across the properties, which were sent to CDC for testing (Appendix). The tick pools collected from both properties tested negative for HRTV RNA.

## Conclusions

HRTV disease has been reported in >50 patients in states across the midwestern and southern United States (*1*–*7*). A bite from an *A. americanum* tick is the only known means of environmental HRTV transmission (*1*). Corresponding to *A. americanum* tick seasonal activity, all reported cases have occurred during April–September, and symptoms developed during June in most case-patients (*1*,*3*). Because the incubation period for HRTV is estimated to be 2 weeks, this patient was likely infected in late October. Adult ticks are minimally active at that time; however, larval ticks can become infected with HRTV and can still be observed during October (*1*,*14*). We suspect this patient was bitten by larval ticks unknowingly because of their small size, and that the bite marks healed before his clinical signs and symptoms appeared.

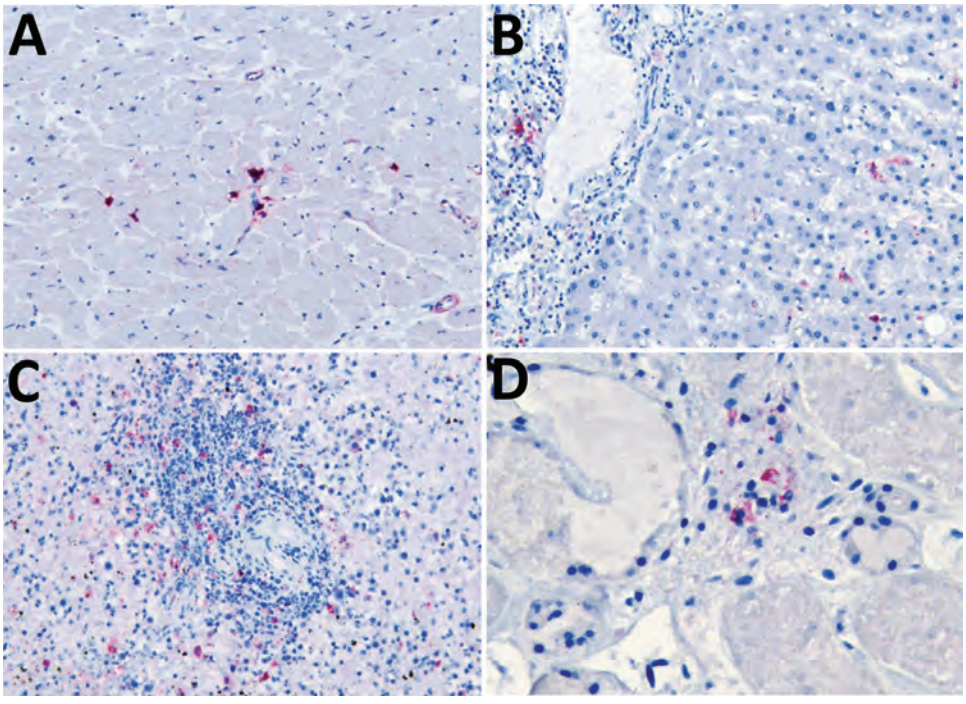


**Figure 2.** Viral immunostaining of samples from a fatal case of heartland virus disease acquired in the mid-Atlantic region, United States. Heartland virus antigen was detected in multiple organs. A) Mononuclear interstitial inflammatory cell of myocardium. Original magnification ×20. B) Periportal macrophages and Kupffer cells in liver. Original magnification ×20. C) Large hematopoietic cells of spleen. Original magnification ×20. D) Inflammatory interstitial cells of kidney. Original magnification ×40.

Maryland and Virginia fall within the *A. americanum* tick distribution area, but we found no previous reports of HRTV illness from those states during a literature search, and CDC had no reported cases from those states. Among 193 ticks collected during tick drags of both properties, no HRTV-infected vectors were found, but this result does not exclude HRTV in either state. Previous studies report low overall minimum infection rates among *A. americanum* ticks from other states, ranging from 0.4 to 11/1,000 ticks (1 infected tick/90–2,174 collected) (*1*,*8*,*10*,*11*). We suspect the Virginia property was the likely location of infection, based on the number of ticks VDH collected while sampling an area that the patient frequented 10–14 days before symptom onset and because fewer ticks were collected from the Maryland property (Appendix).

The patient's clinical and laboratory findings were consistent with HLH secondary to HRTV infection. HLH has been documented in several cases of infection with the related *Bandavirus*, severe fever with thrombocytopenia syndrome virus, and in at least 1 case of HRTV infection (*1*,*4*). Reports showed corticosteroids and ribavirin did not effectively treat severe fever with thrombocytopenia syndrome–triggered HLH, but preliminary clinical data shows potential benefit from favipiravir (*1*,*15*). Currently, clinical management for HRTV infection is supportive care (*3*).

We hypothesize that HRTV infection is underrecognized and mainly diagnosed when severe disease leads to additional testing at referral centers. Although lack of responsiveness to appropriate antimicrobial agents for bacterial tickborne illness might suggest severe disease (*2*), self-limited disease likely is undiagnosed or diagnosed as another tickborne disease. Because tick ranges are increasing overall, incidence of previously regional tickborne infections, such as HRTV, likely will continue to increase. Expanding testing capabilities for arbovirus and tickborne infections, including multiplex testing, would enable real-time assessment and management of patients with potential arboviral and other tickborne infections.

### Acknowledgments

We thank the patient's family for their kindness with this study. We also thank Luciana Silva-Flannery for performing immunohistochemistry for HRTV, and the manuscript's anonymous reviewers.

## About the Authors

Dr. Liu is an infectious disease fellow at the National Institute of Allergy and Infectious Diseases, National Institutes of Health, Bethesda, Maryland, USA. His research interest is in local, targeted antimicrobial therapy. Mr. Kannan is an MD candidate at the Johns Hopkins School of Medicine and a PhD candidate in the Johns Hopkins Department of Biomedical Engineering, Baltimore, Maryland, USA. His research interests include internal medicine and the interface of evidence-based medicine and patient-centered decision-making.

## References

1. Brault AC, Savage HM, Duggal NK, Eisen RJ, Staples JE. Heartland virus epidemiology, vector association, and disease potential. Viruses. 2018;10:1–17. https://doi.org/10.3390/v10090498
2. McMullan LK, Folk SM, Kelly AJ, MacNeil A, Goldsmith CS, Metcalfe MG, et al. A new phlebovirus associated with severe febrile illness in Missouri. N Engl J Med. 2012;367:834–41. https://doi.org/10.1056/NEJMoa1203378
3. Staples JE, Pastula DM, Panella AJ, Rabe IB, Kosoy OI, Walker WL, et al. Investigation of heartland virus disease throughout the United States, 2013–2017. Open Forum Infect Dis. 2020;7:a125. https://doi.org/10.1093/ofid/ofaa125
4. Carlson AL, Pastula DM, Lambert AJ, Staples JE, Muehlenbachs A, Turabelidze G, et al. Heartland virus and hemophagocytic lymphohistiocytosis in immunocompromised patient, Missouri, USA. Emerg Infect Dis. 2018;24:893–7. https://doi.org/10.3201/eid2405.171802
5. Fill MA, Compton ML, McDonald EC, Moncayo AC, Dunn JR, Schaffner W, et al. Novel clinical and pathologic findings in a heartland virus-associated death. Clin Infect Dis. 2017;64:510–2.
6. Muehlenbachs A, Fata CR, Lambert AJ, Paddock CD, Velez JO, Blau DM, et al. Heartland virus-associated death in Tennessee. Clin Infect Dis. 2014;59:845–50. https://doi.org/10.1093/cid/ciu434
7. Decker MD, Morton CT, Moncayo AC. One confirmed and 2 suspected cases of heartland virus disease. Clin Infect Dis. 2020;71:3237–40. https://doi.org/10.1093/cid/ciaa647
8. Dupuis AP II, Prusinski MA, O'Connor C, Maffei JG, Ngo KA, Koetzner CA, et al. Heartland virus transmission, Suffolk County, New York, USA. Emerg Infect Dis. 2021;27:3128–32. https://doi.org/10.3201/eid2712.211426
9. Newman BC, Sutton WB, Moncayo AC, Hughes HR, Taheri A, Moore TC, et al. Heartland virus in lone star ticks, Alabama, USA. Emerg Infect Dis. 2020;26:1954–6. https://doi.org/10.3201/eid2608.200494
10. Romer Y, Adcock K, Wei Z, Mead DG, Kirstein O, Bellman S, et al. Isolation of heartland virus from lone star ticks, Georgia, USA, 2019. Emerg Infect Dis. 2022;28:786–92. https://doi.org/10.3201/eid2804.211540
11. Tuten HC, Burkhalter KL, Noel KR, Hernandez EJ, Yates S, Wojnowski K, et al. Heartland virus in humans and ticks, Illinois, USA, 2018–2019. Emerg Infect Dis. 2020;26:1548–52. https://doi.org/10.3201/eid2607.200110
12. Clarke LL, Ruder MG, Mead DG, Howerth EW. Heartland virus exposure in white-tailed deer in the Southeastern United States, 2001–2015. Am J Trop Med Hyg. 2018;99:1346–9. https://doi.org/10.4269/ajtmh.18-0555
13. Riemersma KK, Komar N. Heartland virus neutralizing antibodies in vertebrate wildlife, United States, 2009–2014. Emerg Infect Dis. 2015;21:1830–3. https://doi.org/10.3201/eid2110.150380

14. Jackson LK, Gaydon DM, Goddard J. Seasonal activity and relative abundance of *Amblyomma americanum* in Mississippi. J Med Entomol. 1996;33:128–31. https://doi.org/10.1093/jmedent/33.1.128
15. Suemori K, Saijo M, Yamanaka A, Himeji D, Kawamura M, Haku T, et al. A multicenter non-randomized, uncontrolled single arm trial for evaluation of the efficacy and the safety of the treatment with favipiravir for patients with severe fever with thrombocytopenia syndrome. PLoS Negl Trop Dis. 2021;15:e0009103. https://doi.org/10.1371/journal.pntd.0009103

Address for correspondence: Christopher J. Hoffmann, Johns Hopkins University, 1550 Orleans St, CRBII 1M11, Baltimore, MD 21205, USA; email: choffmann@jhmi.edu

# Case Report and Literature Review of Occupational Transmission of Monkeypox Virus to Healthcare Workers, South Korea

Yunsang Choi, Eun-bi Jeon, Taeyoung Kim, Seong Jin Choi, Song Mi Moon, Kyoung-Ho Song, Hong Bin Kim, Eu Suk Kim

We report a case of occupational monkeypox virus infection from a needlestick injury in a healthcare worker in South Korea and review similar reports in the literature during 2022. Postexposure prophylactic treatment with a third-generation smallpox vaccine and antiviral agent tecovirimat inhibited local virus spread and alleviated lesion pain.

In July 2022, the World Health Organization (WHO) declared the international mpox outbreak a global public health emergency (*1*). Mpox, caused by monkeypox virus, is transmitted through person-to-person contact, contaminated objects, or respiratory droplets (*2*). During the outbreak, transmission occurred through sexual contact in most reported mpox cases, especially among men who have sex with men (*3*).

By December 2022, the WHO had reported 83,497 confirmed cases of mpox, including 1,176 cases among healthcare workers (HCWs). However, most infections of HCWs occurred in the community, rather than from occupational exposure. Further investigations are needed to determine the main risk of occupational exposure to monkeypox virus in hospitals and the best responses for prevention (*4*).

Cases of HCWs who were confirmed to have monkeypox virus infections obtained through needlestick injuries or contact with a contaminated environment while collecting patient specimens have been reported recently in several countries (*5*–*10*). The first imported case of mpox was reported in South Korea in June 2022 (*11*). We report a case of occupational monkeypox virus transmission in an HCW in Korea. Furthermore, we conducted a literature review of other reported cases of healthcare-associated monkeypox virus transmission in 2022.

Author affiliations: Seoul National University Bundang Hospital, Seongnam, South Korea (Y. Choi, E.-b. Jeon, S.J. Choi, S.M. Moon, K.-H. Song, H.B. Kim, E.S. Kim); Seoul National University College of Medicine, Seoul, South Korea (Y. Choi, S.J. Choi, S.M. Moon, K.-H. Song, H.B. Kim, E.S. Kim); Korea Disease Control and Prevention Agency, Cheongju, South Korea (T. Kim)

DOI: https://doi.org/10.3201/eid2905.230028

## The Study

On November 14, 2022, a 33-year-old healthy female HCW was exposed to monkeypox virus through a needlestick (26G needle) injury on the left index finger during aspiration of an infected patient's vesicle. The HCW wore personal protective equipment consisting of a disposable gown, double gloves, and powered air-purifying respirator. Bleeding occurred after the injury, and povidone-iodine was applied to the puncture site ≈20 min after the incident. Within 20 hours after injury, the HCW received a third-generation smallpox vaccine (single-dose, subcutaneous injection of JYNNEOS; Bavarian Nordic A/S, https://www.bavarian-nordic.com) as postexposure prophylaxis. The HCW had no history of smallpox vaccination, exposure to monkeypox virus, or recent sexual contact and had not traveled abroad.

On November 17 (day 1), the HCW noticed a small papule at the needlestick site (Figure, panel A). On day 2, the papule increased in size; the HCW was admitted to the hospital isolation ward, according to Korea Disease Control and Prevention Agency policy for mpox. We performed monkeypox virus-specific PCR on blood samples and oropharynx and nasopharynx swab samples collected from the HCW. All samples were PCR-negative for monkeypox virus.

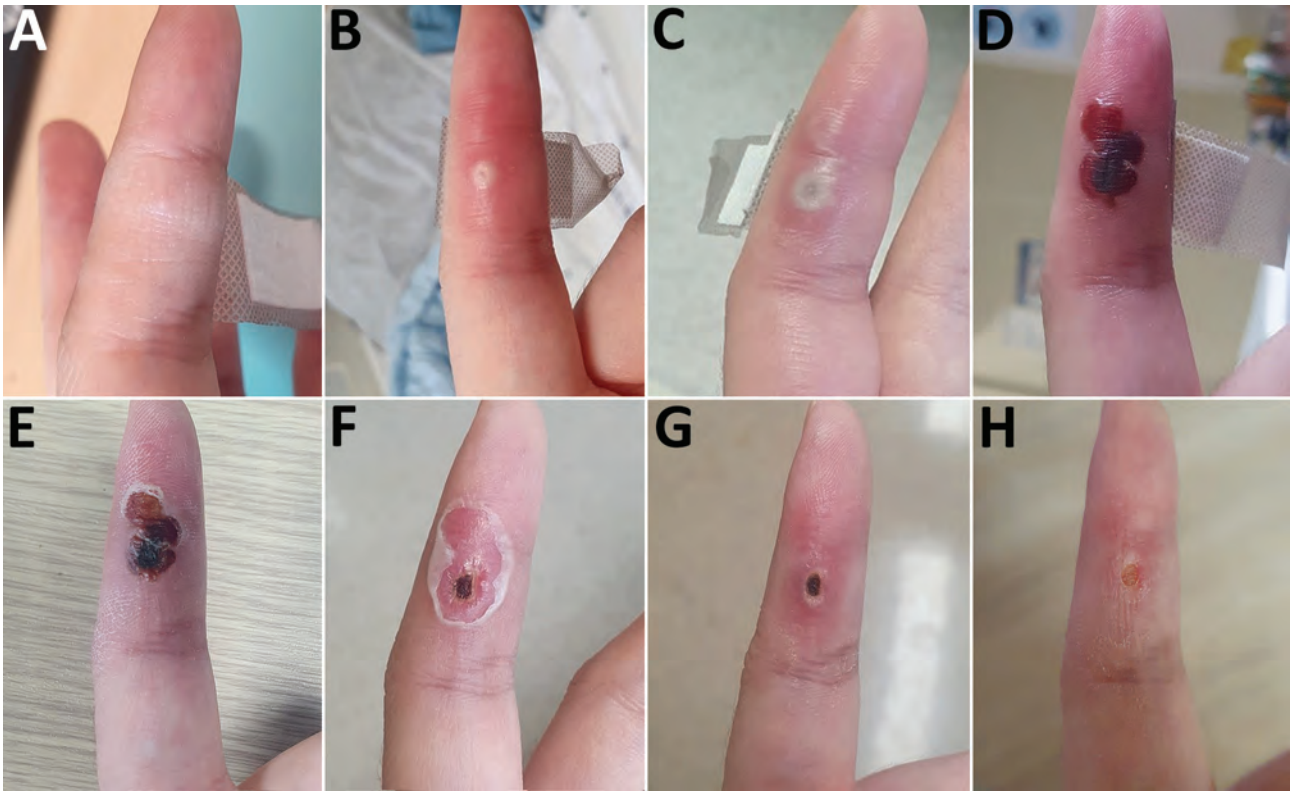


**Figure.** Progression of skin lesion caused by occupational transmission of monkeypox virus to a healthcare worker in South Korea. The healthcare worker was infected in the left index finger with monkeypox virus after a needlestick from a 26G needle during aspiration of an infected patient's vesicle. Photographs show the lesion at the inoculation site from onset to recovery. A) Day 1 (November 17, 2022); B) day 6; C) day 8; d) day 18; E) day 22; F) day 25; G) day 34; H) day 40.

On day 6, the lesion was slightly larger and had a central umbilication (Figure, panel B). We aspirated the lesion, and PCR results for the aspirate were positive for monkeypox virus. We repeated testing of blood samples and oropharyngeal and nasopharyngeal swab samples, and PCR results for those samples were negative. Monkeypox virus transmission was presumed to be occupational because no other risk factors were identified.

On day 8, a new lesion appeared immediately above the initial lesion and began to progress (Figure, panel C). Pain at the lesion site was severe; the numeric rating scale (*12*) score was 8 because of neuralgia. The HCW described a sharp pain as "the feeling of being cut with a knife" that disrupted sleep. Although no disseminated lesions were present, because of the pain intensity and local spread of infection around the initial lesion, the attending infectious disease specialist prescribed tecovirimat starting on day 9 (10 days after smallpox vaccination), which substantially alleviated the pain. By day 16, the pain was almost completely gone.

On day 18, the lesions formed a crust (Figure, panel D) and were partially debrided 4 days later (Figure, panel E). PCR of the debrided skin specimen was positive for monkeypox virus. On day 25, the crust was completely debrided. and a necrotic scab remained underneath the devitalized tissue at the puncture site (Figure, panel F). Because mpox lesions developed after postexposure vaccination, the HCW did not receive a second dose of smallpox vaccine, which was scheduled for 28 days after the first dose. PCR of a lesion site sample yielded positive results for monkeypox virus, but the possibility of virus transmission was low, and clinical progress was stable. Consequently, we discharged the HCW under the guidance of an infectious disease specialist. After the patient was discharged, the tissue around the puncture site recovered completely by day 34 (Figure, panel G), and the scab was completely eliminated by day 40 (Figure, panel H).

We conducted a literature review to evaluate the status of and response to monkeypox virus infections among HCWs during the 2022 outbreak (Table). Transmission of monkeypox virus occurred through needlestick injuries in 5/8 cases; initial lesions developed at the puncture sites in each of those cases. The median incubation period was 5 (range 3–10) days,

which was slightly shorter than the previously reported 7- (range 3–20-) day incubation period (*3*). The patient we report did not have disseminated or severe mpox. However, after administration of tecovirimat, symptoms (especially pain intensity) improved substantially and rapidly.

## Conclusions

As recommended by WHO (*1*), 3 HCWs with needlestick injuries, 2 from the literature (*5*,*8*) and the HCW in the case we report, received a third-generation smallpox vaccine promptly after needlestick injury, and only local skin lesions developed at the site of inoculation without generalized illness. However, additional reports from the literature showed that HCWs without postexposure vaccination had substantially disseminated lesions; among those, 2 HCWs (*6*,*7*) were infected by needlestick injuries. Lesions developed on the hands and wrists of the other 2 HCWs, and the mode of transmission was likely fomite contact with bare skin. The HCW from California (*10*) was immunocompromised and worked in a clinic where patients with mpox regularly visited; unrecognized exposure and spread might have occurred through respiratory droplets.

On the basis of our case report and literature review, we recommend the following procedures for HCWs who treat patients with mpox. First, the literature review revealed differences in clinical manifestations depending on the infection route and vaccination status, similar to findings from previous reports from the prairie dog–associated mpox outbreak in the United States (*13*). Therefore, prompt vaccination after exposure might prevent disease progression and should be considered for HCWs in environments requiring contact with monkeypox virus-infected patients; preexposure vaccination should also be considered. Second, precautions should be exercised when collecting specimens from patients with suspected mpox. For the safety of HCWs, instead of unroofing or aspirating the lesion with a sharp tool, the sample should be obtained by

**Table.** Case report of occupational transmission of monkeypox virus to a healthcare worker in South Korea and literature review of healthcare-associated cases of monkeypox virus transmission during the 2022 mpox outbreak*

| | Case reports | | | | | | | |
|---|---|---|---|---|---|---|---|---|
| Characteristics | 1 | 2 | 3 | 4 | 5† | 6† | 7‡ | 8 |
| Country | France | Brazil | Portugal | Florida, USA | Brazil | Brazil | California, USA | South Korea |
| Exposure date, 2022 | July | July | July | July | July | July | August | November |
| HCW, age/sex | 25/F | 20s/F | 29/M | NA | NA/F | NA/F | 40/F | 33/F |
| HCW occupation | Doctor | Nurse | Doctor | Nurse | Nurse | Nurse | Doctor | Doctor |
| Patient source, age/sex | 30/M | 20s/M | NA | NA | 40/M | 40/M | NA | 20s/F |
| Exposure | | | | | | | | |
| Type | Needlestick | Needlestick | Needlestick | Needlestick | Fomites | Fomites | Other§ | Needlestick |
| Site | Right thumb¶ | Thumb | Left index finger | Index finger | Left ring finger | Forearm | Left middle finger | Left index finger# |
| PCR results | | | | | | | | |
| Vesicle | Positive | Positive | Positive | Positive | Positive | Positive | Positive | Positive |
| Oropharynx | Negative | Positive | Negative | NA | NA | NA | NA | Negative |
| Blood | Negative | Positive | Negative | NA | NA | NA | NA | Negative |
| Incubation period, d | 4 | 5 | 4 | 10 | 5 | 5 | 7 | 3 |
| Dissemination | No | Yes | Yes | No | Yes | Yes | Yes | No |
| Vaccination** | Imvanex, <3 h | No | No | JYNNEOS, <15 h | No | No | No | JYNNEOS, <20 h |
| Isolation of HCW after symptoms, d | 21 | 19 | 24 | 19 | 21 | 22 | 20 | 26 |
| Tecovirimat treatment | No | No | No | No | No | No | Yes, 14 d | Yes, 14 d |
| Major symptoms | | | | | | | | |
| Skin lesion(s) | Yes | Yes | Yes | Yes | Yes | Yes | Yes | Yes |
| Lymphadenopathy | No | Yes | Yes | No | Yes | Yes | No | No |
| Other | Seropurulent fluid from wound | Fever | Fever, chills, myalgia | No | Hyperemia | Fever | Fever, cough, sore throat | Myalgia |
| Reference | (*5*) | (*6*) | (*7*) | (*8*) | (*9*) | (*9*) | (*10*) | This case |

*Cases 1–7 were collected from the literature; case 8 is the patient described in this report. HCW, healthcare worker; NA, not available.
†Cases 5 and 6 were described in 1 report.
‡Medical history of rheumatoid arthritis, treated with etanercept.
§Inadvertent contamination during specimen collection or contact with contaminated environment.
¶Puncture from 25G needle.
#Puncture from 26G needle.
**Postexposure prophylaxis vaccination with third-generation smallpox vaccines (JYNNEOS, also known as Imvanex; Bavarian Nordic A/S, https://www.bavarian-nordic.com) conducted within specified hours after exposure to monkeypox virus.

rubbing the surface of the lesion with a swab or collecting a scab with forceps (*14*). Because PCR is highly sensitive, a positive result can be obtained when samples are collected by using this method. Third, although tecovirimat is generally recommended for patients with severe mpox or high risk of dissemination (*10*), the drug was administered to our patient, who had localized infection, to prevent disease progression; prompt administration of tecovirimat might be necessary to maximize effectiveness. Most patients with mpox report extreme pain in the affected area. Thus, although the isolation period or the time until the virus is undetectable might not be shortened, antiviral treatment should be considered if skin lesions progress or pain is severe and no shortage of drugs exists.

In summary, we report a case of monkeypox virus infection in a HCW after a needlestick injury and a literature review of similar cases during the 2022 mpox outbreak. Although larger studies are needed to determine efficacy of postexposure vaccination prophylaxis, this case series indicates postexposure vaccination might have prevented dissemination of virus lesions. Therefore, clinicians should consider postexposure vaccination and tecovirimat or other antiviral drugs to inhibit local monkeypox virus spread and alleviate lesion pain.

### Acknowledgments

We thank the attending physicians, Eun Mi You and Sua Noh, and Yujin Kang and all nurses in the infection isolation ward at Seoul National University Bundang Hospital for their treatment efforts for this patient; Myoung Jin Shin, Su Young Kim, and infection control practitioners in the hospital infection control team for working on mpox outbreak responses; public health officials of Korea Disease Control and Prevention Agency and Gyeonggi Provincial Government for their cooperation on the mpox response; and Editage (https://www.editage.co.kr) for English language editing.

The research was approved by the Institutional Review Board of Seoul National University Bundang Hospital following the ICMJE recommendations for the protection of research participants and was conducted in accordance with the ethical standards set forth in the Declaration of Helsinki 1964 and its later amendments or equivalent ethical standards (IRB no. B-2301-805-701). The healthcare worker signed a consent form for this report. The opinions expressed by authors contributing to this journal do not necessarily reflect the opinions of the Korea Disease Control and Prevention Agency or the institutions with which the authors are affiliated.

### About the Author

Dr. Choi is a fellow of infectious disease at the Seoul National University Bundang Hospital, Bundang-gu, Seongnam, Gyeonggi-do, South Korea. Her research interests focus on nosocomial disease transmission and multidrug-resistant bacterial infections.

### References

1. WHO Emergency Response Team. Vaccines and immunization for monkeypox: interim guidance, 16 November 2022 [cited 2022 Dec 27]. https://www.who.int/publications/i/item/WHO-MPX-Immunization
2. Vivancos R, Anderson C, Blomquist P, Balasegaram S, Bell A, Bishop L, et al.; UKHSA Monkeypox Incident Management team; Monkeypox Incident Management Team. Community transmission of monkeypox in the United Kingdom, April to May 2022. Euro Surveill. 2022;27:2200422. https://doi.org/10.2807/1560-7917.ES.2022.27.22.2200422
3. Thornhill JP, Barkati S, Walmsley S, Rockstroh J, Antinori A, Harrison LB, et al.; SHARE-net Clinical Group. Monkeypox virus infection in humans across 16 countries—April–June 2022. N Engl J Med. 2022;387:679–91. https://doi.org/10.1056/NEJMoa2207323
4. World Health Organization. 2022–23 Mpox (monkeypox) outbreak: global trends [cited 2022 Dec 27]. https://worldhealthorg.shinyapps.io/mpx_global
5. Le Pluart D, Ruyer-Thompson M, Ferré VM, Mailhe M, Descamps D, Bouscarat F, et al. A healthcare-associated infection with monkeypox virus of a healthcare worker during the 2022 outbreak. Open Forum Infect Dis. 2022;9:ofac520. PubMed https://doi.org/10.1093/ofid/ofac520
6. Carvalho LB, Casadio LVB, Polly M, Nastri AC, Turdo AC, de Araujo Eliodoro RH, et al. Monkeypox virus transmission to healthcare worker through needlestick injury, Brazil. Emerg Infect Dis. 2022;28:2334–6. https://doi.org/10.3201/eid2811.221323
7. Mendoza R, Petras JK, Jenkins P, Gorensek MJ, Mableson S, Lee PA, et al. Monkeypox virus infection resulting from an occupational needlestick—Florida, 2022. MMWR Morb Mortal Wkly Rep. 2022;71:1348–9. https://doi.org/10.15585/mmwr.mm7142e2
8. Caldas JP, Valdoleiros SR, Rebelo S, Tavares M. Monkeypox after occupational needlestick injury from pustule. Emerg Infect Dis. 2022;28:2516–9. https://doi.org/10.3201/eid2812.221374
9. Salvato RS, Rodrigues Ikeda ML, Barcellos RB, Godinho FM, Sesterheim P, Bitencourt LCB, et al. Possible occupational infection of healthcare workers with monkeypox virus, Brazil. Emerg Infect Dis. 2022;28:2520–3. https://doi.org/10.3201/eid2812.221343
10. Alarcón J, Kim M, Balanji N, Davis A, Mata F, Karan A, et al. Occupational monkeypox virus transmission to healthcare worker, California, USA, 2022. Emerg Infect Dis. 2023;29:435–7. https://doi.org/10.3201/eid2902.221750
11. Jang YR, Lee M, Shin H, Kim JW, Choi MM, Kim YM, et al. The first case of monkeypox in the Republic of Korea. J Korean Med Sci. 2022;37:e224. https://doi.org/10.3346/jkms.2022.37.e224
12. Hartrick CT, Kovan JP, Shapiro S. The numeric rating scale for clinical pain measurement: a ratio measure?

Pain Pract. 2003;3:310–6. https://doi.org/10.1111/j.1530-7085.2003.03034.x
13. Reynolds MG, Yorita KL, Kuehnert MJ, Davidson WB, Huhn GD, Holman RC, et al. Clinical manifestations of human monkeypox influenced by route of infection. J Infect Dis. 2006;194:773–80. https://doi.org/10.1086/505880
14. Centers for Disease Control and Prevention. Guidelines for collecting and handling specimens for mpox testing [cited 2022 Dec 27]. https://www.cdc.gov/poxvirus/monkeypox/clinicians/prep-collection-specimens.html

Address for correspondence: Eu Suk Kim, Department of Internal Medicine, Seoul National University Bundang Hospital 82, Gumi-ro 173 Beon-gil, Bundang-gu, Seongnam, Gyeonggi-do, South Korea; email: eskim@snubh.org

# Spatiotemporal Evolution of SARS-CoV-2 Alpha and Delta Variants during Large Nationwide Outbreak of COVID-19, Vietnam, 2021

Nguyen Thi Tam,[1] Nguyen To Anh,[1] Trinh Son Tung,[1] Pham Ngoc Thach, Nguyen Thanh Dung, Van Dinh Trang, Le Manh Hung, Trinh Cong Dien, Nghiem My Ngoc, Le Van Duyet, Phan Manh Cuong, Hoang Vu Mai Phuong, Pham Quang Thai, Nguyen Le Nhu Tung, Dinh Nguyen Huy Man, Nguyen Thanh Phong, Vo Minh Quang, Pham Thi Ngoc Thoa, Nguyen Thanh Truong, Tran Nguyen Phuong Thao, Dao Phuong Linh, Ngo Tan Tai, Ho The Bao, Vo Trong Vuong, Huynh Thi Kim Nhung, Phan Nu Dieu Hong, Le Thi Phuoc Hanh, Le Thanh Chung, Nguyen Thi Thanh Nhan, Ton That Thanh, Do Thai Hung, Huynh Kim Mai, Trinh Hoang Long, Nguyen Thu Trang, Nguyen Thi Hong Thuong, Nguyen Thi Thu Hong, Le Nguyen Truc Nhu, Nguyen Thi Han Ny, Cao Thu Thuy, Le Kim Thanh, Lam Anh Nguyet, Le Thi Quynh Mai, Tang Chi Thuong, Le Hong Nga, Tran Tan Thanh, Guy Thwaites, H. Rogier van Doorn, Nguyen Van Vinh Chau, Thomas Kesteman, Le Van Tan, for the OUCRU COVID-19 Research Groups

We analyzed 1,303 SARS-CoV-2 whole-genome sequences from Vietnam, and found the Alpha and Delta variants were responsible for a large nationwide outbreak of COVID-19 in 2021. The Delta variant was confined to the AY.57 lineage and caused >1.7 million infections and >32,000 deaths. Viral transmission was strongly affected by nonpharmaceutical interventions.

After successfully controlling SARS-CoV-2 transmission in 2020 (*1*), Vietnam experienced a large nationwide outbreak of infection with SARS-CoV-2 in 2021. This outbreak was characterized by 2 distinct phases: January–April, with 1,632 infections and no deaths, and May–December, with 1,727,398 infections and 32,359 deaths (*2*).

Genomic surveillance has been one of the top priorities of the World Health Organization and has generated major insights into the spatiotemporal evolution of SARS-CoV-2 (*3*), which are critical for pandemic response. However, most of the studies published about genetic evolution of SARS-CoV-2 are based on datasets from high-income countries with relatively open borders (*4*–*6*), and little is known about the transmission dynamics of SARS-CoV-2 in

Author affiliations: Oxford University Clinical Research Unit, Hanoi, Vietnam (N.T. Tam, T.S. Tung, N.T. Trang, N.T.H. Thuong, T. Kesteman, H. R. van Doorn); National Hospital for Tropical Diseases, Hanoi (P.N. Thach, V.D. Trang, L.V. Duyet, P.M. Cuong); Vietnam Military Medical University, Hanoi (T.C. Dien); National Institute of Hygiene and Epidemiology, Hanoi (H.V.M. Phuong, L.T.Q. Mai, P.Q. Thai); Hue National Hospital, Hue, Vietnam (P.N.D. Hong, L.T.P. Hanh); Da Nang Center for Disease Control, Da Nang, Vietnam (L.T. Chung, N.T.T. Nhan, T.T. Thanh); Pasteur Institute, Nha Trang, Khanh Hoa, Vietnam (D.T. Hung, H.K. Mai, T.H. Long); Oxford University Clinical Research Unit, Ho Chi Minh City, Vietnam (N.T. Anh, N.T.T. Hong, L.N.T. Nhu, N.T.H. Ny, T.T. Thanh, C.T. Thuy, L.K. Thanh, L.A. Nguyet, G. Thwaites, L.V. Tan); Hospital for Tropical Diseases, Ho Chi Minh City (N.T. Dung, L.M. Hung, N.L.N. Tung, D.N.H. Man, N.M. Ngoc, N.T. Phong, V.M. Quang, P.T.N. Thoa, N.T. Truong, T.N.P. Thao, D.P. Linh, N.T. Tam, H.T. Bao, V.T. Vuong, H.T.K. Nhung); Department of Health, Ho Chi Minh City, (N.V.V. Chau, T.C. Thuong); Ho Chi Minh City Center for Disease Control, Ho Chi Minh City (L.H. Nga); University of Oxford, Oxford, UK (H.R. van Doorn, G. Thwaites, L.V. Tan)

DOI: https://doi.org/10.3201/eid2905.221787

[1]These authors contributed equally to this article.

[2]Members of the working group are shown at the end of this article.

countries such as Vietnam where strict nonpharmaceutical interventions were implemented. We analyzed the spatiotemporal evolution of SARS-CoV-2 in Vietnam during 2021 and mapped patterns of viral evolution and diffusion against the public health measures implemented during the study period.

## The Study

The study was conducted at the National Hospital for Tropical Diseases in Hanoi, Vietnam, and the Hospital for Tropical Diseases in Ho Chi Minh City, Vietnam. Both are tertiary referral hospitals for COVID-19 patients in northern (hospital in Hanoi) and southern (hospital in Ho Chi Minh City) Vietnam. The laboratories of the 2 hospitals were responsible for SARS-CoV-2 diagnosis and sequencing in Vietnam. We compiled detailed study methods, including public health measures (Appendix Figure 1, https://wwwnc.cdc.gov/EID/article/29/5/22-1787-App1.pdf), and demographic features of study participants (Table).

We selected 1,365 nasopharyngeal throat swab specimens for whole-genome sequencing and obtained 1,303 complete genome sequences. We detected no recombinants. Most obtained sequences belonged to Delta variant (93.8%, n = 1,222), followed by Alpha (5.7%, n = 74), A.23.1 (0.4%, n = 5), and B.1.637 (0.2%, n = 2) variants. Of the Delta sequences, 1,212 (99.2%) were assigned to AY.57 lineage by PANGO lineage (*8*). The remaining were assigned to AY.23 and AY.79 (n = 3 each), AY.6, AY.38, AY.85, and B.1.617.2 (n = 1 each).

We temporally documented the Alpha and A.23.1 sequences during January–May 2021. We detected the first 3 Delta sequences, including 2 AY.57 and 1 B.1.617.2, in late April 2021. From June on, Delta was the only variant detected, coinciding with an upsurge in the number of infections and deaths during the 2021 outbreak (Appendix Figure 2).

Maximum-likelihood phylogenetic analysis of Alpha variant sequences showed that they were closely related to the contemporary sequences detected in the region and clustered into 4 major groups, corresponding to the sporadic community transmission clusters detected in northern, central, and southern Vietnam in early 2021 (Figure 1). This finding suggested that multiple importations and exportations of the Alpha variant into Vietnam occurred during January–May 2021.

Because of the dominance of the AY.57 lineage, and the small number of AY.57 sequences reported outside Vietnam, and especially in the nearby region (Cambodia, n = 5; Thailand, n = 5; Laos, n = 0; Singapore, n = 5), we focused our phylogeographic analysis on the 1,212 Delta AY.57/1.303 sequences obtained from Vietnam. After we removed identical, low-quality, and outlier sequences, as suggested by TempEst software, (https://tempest-solutions.com), 748 nonidentical sequences were available for analysis.

Results confirmed that AY.57 viruses were introduced into the northeastern region in early 2021 (Figure 2, https://wwwnc.cdc.gov/EID/article/29/5/22-1787-F2.htm) probably by a single introduction event (Appendix Figure 4). The estimated time to the most recent common ancestor was March 14, 2021 (95% CI February 22, 2021–April 8, 2021), shortly after the discovery of the Delta variant in November 2020. In the following months, the northeastern and Red River delta regions then acted as a source seeding the virus to neighboring and southeastern provinces, with limited viral dispersal between provinces/cities (Figure 2). During July–December 2021, the southeastern region was the main source, seeding the virus back to the northern region and the rest of Vietnam. In addition, we observed the establishment of multiple localized clusters of AY.57 lineage elsewhere in the southcentral coastal region and the Red River delta (Figure 2).

A Bayesian Skyride showed a sharp increase in genetic diversity during April–August 2021 (Figure 3, panel A), reflecting the expansion of the AY.57 lineage

**Table.** Demographics of study participants for spatiotemporal evolution of SARS-CoV-2 Alpha and Delta variants during large nationwide outbreak of COVID-19, Vietnam, 2021*

| Characteristic | No. sequences, n = 1,303 | Alpha, n = 74 | AY.57, n = 1,212 |
|---|---|---|---|
| Age, y | | | |
| Median (Q1–Q3) | 43 (29–61) | 35 (30–55) | 44 (29–61) |
| Missing | 38 (2.9) | 31 (41.9) | 2 (0.2) |
| Sex | | | |
| M | 689 (52.9) | 22 (29.7) | 661 (54.5) |
| F | 578 (44.4) | 21 (28.4) | 551 (45.5) |
| Unknown | 36 (2.8) | 31 (41.9) | |
| Region | | | |
| Central | 120 (9.2) | 24 (32.4) | 94 (7.8) |
| Northern | 504 (38.7) | 44 (59.5) | 450 (37.1) |
| Southern | 679 (52.1) | 6 (8.1) | 668 (55.1) |

*Values are no. (%) unless indicated otherwise. Characteristics of A.23.1 variant–infected cases were previously reported (7). Q, quartile.

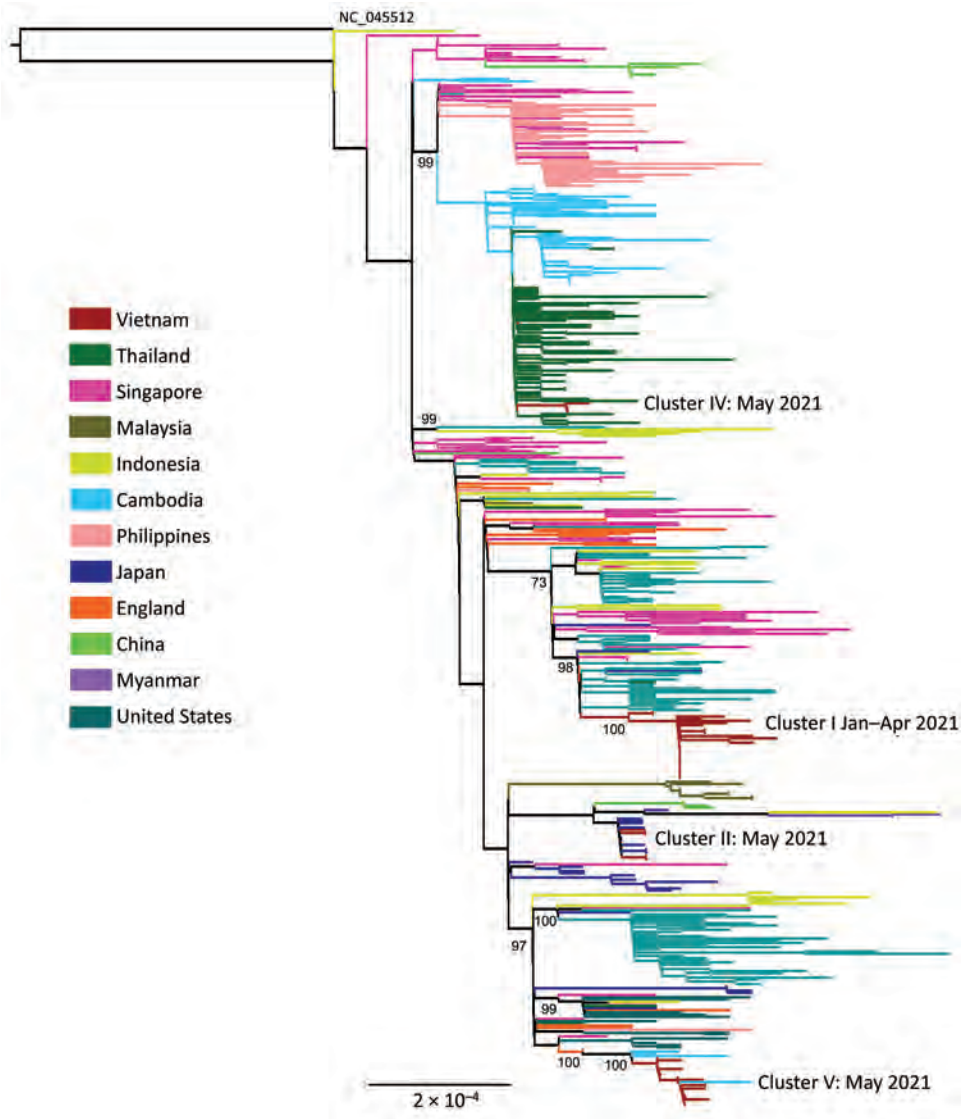


**Figure 1.** Maximum-likelihood tree of SARS-CoV-2 Alpha and Delta variants during large nationwide outbreak of COVID-19, Vietnam, 2021. Complete coding sequences of Alpha variant viruses circulating in Vietnam in 2021 are shown. Phylogenetic clusters were named accordingly to community clusters recorded during the study period shown in Appendix Figure 1, https://wwwnc.cdc.gov/EID/article/29/5/22-1787-App1.pdf). Numbers along branches are bootstrap values. Cluster II was linked with a traveler from Japan (Appendix Figure 1). Outgroup was the SARS-CoV-2 wild-type strain (GenBank accession no. NC_0455122).

across the country, paralleling the start of the large nationwide outbreak from May onward (Appendix Figures 1, 2). In the following months, the viral population size remained relative stable, despite some fluctuations in the number of viral sequences obtained (Figure 3, panel B), followed by a slight decrease in the genetic diversity during November. The estimated mean of the nonsynonymous to synonymous substitution (dN/dS) value was 0.86, albeit it varied across the genomes (Appendix Table 1), and the evolutionary rate of AY.57 coding sequences was $5.29 \times 10^{-4}$ substitutions/site/year (95% CI $4.966 \times 10^{-4}$ to $5.639 \times 10^{-4}$ substitutions/site/year).

## Conclusions

We showed that the Alpha and especially Delta variants were the main causes of SARS-CoV-2 outbreaks of >1.7 million infections and >32,000 deaths in Vietnam during 2021. The Alpha variant was introduced into Vietnam during early 2021 by different importation events but only caused sporadic community outbreaks until May, when a second wave associated with the Delta variant predominated from June on. The viruses of the Delta variant were confined to AY.57 lineage and were responsible for the major wave in 2021, probably by a single introduction event. Viral movement between provinces was not apparent. During the study period, nearly 200 sublineages of the Delta variant were documented worldwide (*9*), and in other countries, such as the United Kingdom and the United States, where use of nonpharmaceutical measures was relaxed, viral dispersal across the localities was more apparent (*10,11*). The rigorous containment approach applied in Vietnam

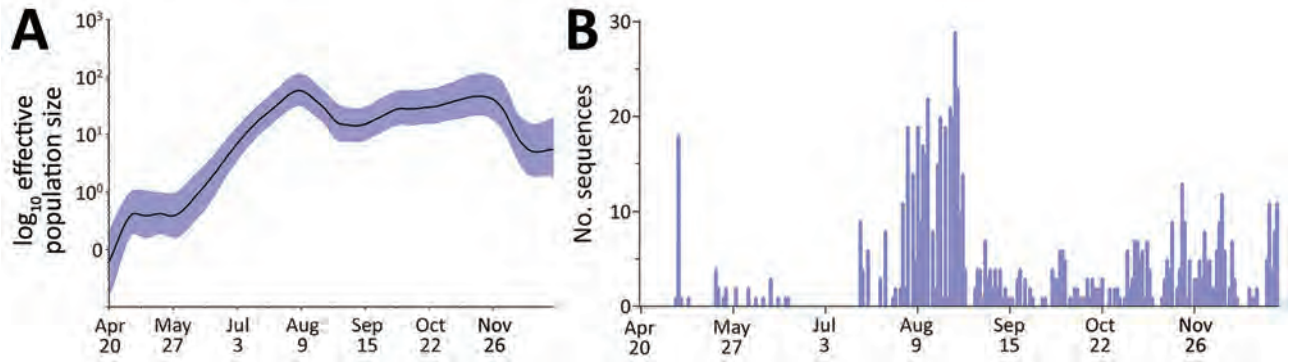


**Figure 3.** Genetic diversity and distribution of SARS-CoV-2 AY.57 lineage during large nationwide outbreak of COVID-19, Vietnam, 2021. A) Bayesian skyride plot illustrating the relative genetic diversity of AY.57 lineage in Vietnam during 2021. Purple shading indicates 95% highest posterior density interval. B) Distribution of the number of AY.57 sequences used for analysis over the study period.

in 2021, with limited domestic travels and tight border controls, was probably the key factor determining the localization of a single AY.57 lineage in Vietnam and its limited dispersal across the country.

The sharp increase in the relative genetic diversity of the AY.57 lineage during April–July 2021 marked the start of the nationwide outbreak in subsequent months despite in-country lockdown measures. Although nonpharmaceutical interventions were sufficient to prevent uncontrolled community transmission in 2020 (*1*), they were not sufficient after introduction of the Delta variant. This finding was probably caused by the much higher transmissibility of the Delta variant and the immunologically naive population in Vietnam at the time. During April–July 2021, only <1% of 97 million persons in Vietnam were vaccinated against SARS-CoV-2 (*12*).

Although our estimated evolutionary rate was AY.57-lineage specific, the result was within the range of previously estimated values for the Delta variant more broadly (*10*; N. Benazi, Institut Pasteur of Algeria, and S. Bounab, University of M'sila, pers. comm., email, 2023 Mar 1. This finding points to a fast evolution of the AY.57 lineage in Vietnam during the study. Although the role of population immune landscapes in shaping the evolution of SARS-CoV-2 merits further research, a recent report showed that vaccines had played a role in selective adaptation of the SARS-CoV-2 Delta variant (*13*).

The potential bias toward our referral-hospital based sampling approach represents a limitation of our study, which might have failed to comprehensively capture the genetic diversity of the pathogen. However, this limitation was probably modest given that our results are consistent with sequences uploaded to GISAID (https://www.gisaid.org) (*9*).

In conclusion, we report how rigorous public health measures in Vietnam influenced the introduction and spread of the Alpha and Delta variants during the large nationwide outbreak of COVID-19 in 2021. Genomic surveillance is critical to inform pandemic response.

Members of the OUCRU COVID-19 research group: Mary Chambers, Marc Choisy, Dong Huu Khanh Trinh, Dong Thi Hoai Tam, Du Hong Duc, Dung Vu Tien Viet, Jaom Fisher, Barney Flower, Ronald Geskus, Hang Vu Thi Kim, Ho Quang Chanh, Ho Thi Bich Hai, Ho Van Hien, Hung Vu Bao, Huong Dang Thao, Huynh le Anh Huy, Huynh Ngan Ha, Huynh Trung Trieu, Huynh Xuan Yen, Evelyne Kestelyn, Thomas Kesteman, Lam Anh Nguyet, Katrina Lawson, Leigh Jones, Le Kim Thanh, Le Dinh Van Khoa, Le Thanh Hoang Nhat, Le Van Tan, Sonia Odette Lewycka, Lam Minh Yen, Le Nguyen Truc Nhu, Le Thi Hoang Lan, Nam Vinh Nguyen, Ngo Thi Hoa, Nguyen Bao Tran, Nguyen Duc Manh, Nguyen Hoang Yen, Nguyen Le Thao My, Nguyen Minh Nguyet, Nguyen To Anh, Nguyen Thanh Ha, Nguyen Than Ha Quyen, Nguyen Thanh Ngoc, Nguyen Thanh Thuy Nhien, Nguyen Thi Han Ny, Nguyen Thi Hong Thuong, Nguyen Thi Hong Yen, Nguyen Thi Huyen Trang, Nguyen Thi Kim Ngoc, Nguyen Thi Kim Tuyen, Nguyen Thi Ngoc Diep, Nguyen Thi Phuong Dung, Nguyen Thi Tam, Nguyen Thi Thu Hong, Nguyen Thu Trang, Nguyen Thuy Thuong Thuong, Nguyen Xuan Truong, Nhung Doan Phuong, Ninh Thi Thanh Van, Ong Phuc Thinh, Pham Ngoc Thanh, Phan Nguyen Quoc Khanh, Phung Ho Thi Kim, Phung Khanh Lam, Phung Le Kim Yen, Phung Tran Huy Nhat, Motiur Rahman, Thuong Nguyen Thi Huyen, Guy Thwaites, Louise Thwaites, Tran Bang Huyen, Tran Dong Thai Han, Tran Kim Van Anh, Tran Minh Hien, Tran Phuong Thao, Tran Tan Thanh, Tran Thi Bich Ngoc, Tran Thi Hang, Tran Tinh Hien, Trinh Son Tung, H. Rogier van Doorn, Jennifer Van Nuil, Celine Pascale Vidaillac, Vu Thi Ngoc Bich, Vu Thi Ty Hang, and Sophie Yacoub. Members of the HTD COVID-19 research group: Nguyen Van Vinh

Chau, Nguyen Thanh Dung, Le Manh Hung, Huynh Thi Loan, Nguyen Thanh Truong, Nguyen Thanh Phong, Dinh Nguyen Huy Man, Nguyen Van Hao, Duong Bich Thuy, Nghiem My Ngoc, Nguyen Phu Huong Lan, Pham Thi Ngoc Thoa, Tran Nguyen Phuong Thao, Tran Thi Lan Phuong, Le Thi Tam Uyen, Tran Thi Thanh Tam, Bui Thi Ton That, Huynh Kim Nhung, Ngo Tan Tai, Tran Nguyen Hoang Tu, Vo Trong Vuong, Dinh Thi Bich Ty, Le Thi Dung, Thai Lam Uyen, Nguyen Thi My Tien, Ho Thi Thu Thao, Nguyen Ngoc Thao, Huynh Ngoc Thien Vuong, Huynh Trung Trieu, Pham Ngoc Phuong Thao, and Phan Minh Phuong. Members of the EOCRU COVID-19 research group: Andy Bachtiar, J. Kevin Baird, Fitri Dewi, Ragil Dien, Bimandra A. Djaafara, Iqbal E. Elyazar, Raph H. Hamers, Winahyu Handayani, Livia N. Kurniawan, Ralalicia Limato, Cindy Natasha, Nunung Nuraeni, Khairunisa Puspatriani, Mutia Rahadjani, Atika Rimainar, Saraswati Shankar, H. Anuraj, Henry Suhendra, Ida Sutrisni, Ayu Suwarti, Nicolas Tarino, Diana Timoria, and Fitri Wulandari. Members of the OUCRU-NP COVID-19 research group: Buddha Basnyat, Manish Duwal, Amit Gautum, Abhilasha Karkey, Niharika Kharel, Aakriti Pandey, Samia Rijal, Suchita Shrestha, Pratibha Thapa, Summita Udas.

### Acknowledgments

We thank Le Nguyen Minh Hoa and technicians at Department of Microbiology and Molecular, National Hospital for Tropical Diseases for collecting swab samples and initial testing of SARS-CoV-2 diagnostics; the OUCRU team for supporting whole-genome sequencing and providing data entry; data contributors and their laboratories for obtaining specimens for this study; and laboratories that submitted and shared their generated genetic sequences and metadata via GISAID, on which this research is based.

Genomic surveillance was supported by the Wellcome Trust (222574/Z/21/Z). L.V.T. and G.T. are supported by the Wellcome Trust of Great Britain (204904/Z/16/Z and 106680/B/14/Z, respectively).

## About the Author

Dr. Tam is a postdoctoral scientist at the Oxford University Clinical Research Unit, Hanoi, Vietnam. Her primary research interests are genomic surveillance of SARS-CoV-2 variants emerging in Vietnam since 2020, and situation and molecular mechanisms of antimicrobial drug resistance for bacterial pathogens in Vietnam.

### References

1. Van Tan L. COVID-19 control in Vietnam. Nat Immunol. 2021;22:261. https://doi.org/10.1038/s41590-021-00882-9
2. World Health Organization. COVID-19 in Viet Nam Situation report 101, 2022 [cited 2022 Oct 24]. https://www.who.int/vietnam/internal-publications-detail/covid-19-in-vietnam-situation-report-101
3. Attwood SW, Hill SC, Aanensen DM, Connor TR, Pybus OG. Phylogenetic and phylodynamic approaches to understanding and combating the early SARS-CoV-2 pandemic. Nat Rev Genet. 2022;23:547–62. https://doi.org/10.1038/s41576-022-00483-8
4. du Plessis L, McCrone JT, Zarebski AE, Hill V, Ruis C, Gutierrez B, et al.; COVID-19 Genomics UK (COG-UK) Consortium. Establishment and lineage dynamics of the SARS-CoV-2 epidemic in the UK. Science. 2021;371:708–12. https://doi.org/10.1126/science.abf2946
5. da Silva Filipe A, Shepherd JG, Williams T, Hughes J, Aranday-Cortes E, Asamaphan P, et al.; COVID-19 Genomics UK (COG-UK) Consortium. Genomic epidemiology reveals multiple introductions of SARS-CoV-2 from mainland Europe into Scotland. Nat Microbiol. 2021;6:112–22. https://doi.org/10.1038/s41564-020-00838-z
6. Lemey P, Ruktanonchai N, Hong SL, Colizza V, Poletto C, Van den Broeck F, et al. Untangling introductions and persistence in COVID-19 resurgence in Europe. Nature. 2021;595:713–7. https://doi.org/10.1038/s41586-021-03754-2
7. Chau NV, Hong NT, Ngoc NM, Anh NT, Trieu HT, Nhu LN, et al.; for OUCRU COVID-19 research group. Rapid whole-genome sequencing to inform COVID-19 outbreak response in Vietnam. J Infect. 2021;82:276–316. https://doi.org/10.1016/j.jinf.2021.03.017
8. Github. Co-lineages/pangolin [cited 2023 Mar 7]. https://github.com/cov-lineages/pangoli
9. COV Spectrum. Detect and analyze variants of SARS-CoV-2 [cited 2023 Mar 7]. https://cov-spectrum.org/explore/Vietnam/AllSamples/Past6M
10. Eales O, Page AJ, de Oliveira Martins L, Wang H, Bodinier B, Haw D, et al.; COVID-19 Genomics UK (COG-UK) Consortium. SARS-CoV-2 lineage dynamics in England from September to November 2021: high diversity of Delta sub-lineages and increased transmissibility of AY.4.2. B MC Infect Dis. 2022;22:647. https://doi.org/10.1186/s12879-022-07628-4
11. McCrone JT, Hill V, Bajaj S, Pena RE, Lambert BC, Inward R, et al.; COVID-19 Genomics UK (COG-UK) Consortium. Context-specific emergence and growth of the SARS-CoV-2 Delta variant. Nature. 2022;610:154–60. https://doi.org/10.1038/s41586-022-05200-3
12. Our World in Data. Vietnam: coronavirus pandemic country profile [cited 2023 Mar 7]. https://ourworldindata.org/coronavirus/country/vietnam
13. Duerr R, Dimartino D, Marier C, Zappile P, Levine S, Francois F, et al. Clinical and genomic signatures of SARS-CoV-2 Delta breakthrough infections in New York. EBioMedicine. 2022;82:104141. https://doi.org/10.1016/j.ebiom.2022.104141

Address for correspondence: Nguyen To Anh or Le Van Tan, Oxford University Clinical Research Unit, Ho Chi Minh City, Vietnam; emails: anhnt@oucru.org or tanlv@oucru.org

# Emerging Invasive Group A *Streptococcus* $M1_{UK}$ Lineage Detected by Allele-Specific PCR, England, 2020[1]

Xiangyun Zhi, Ho Kwong Li, Hanqi Li, Zuzanna Loboda, Samson Charles, Ana Vieira, Kristin Huse, Elita Jauneikaite, Lucy Reeves, Kai Yi Mok, Juliana Coelho, Theresa Lamagni, Shiranee Sriskandan

Increasing reports of invasive *Streptococcus pyogenes* infections mandate surveillance for toxigenic lineage $M1_{UK}$. An allele-specific PCR was developed to distinguish $M1_{UK}$ from other *emm*1 strains. The $M1_{UK}$ lineage represented 91% of invasive *emm*1 isolates in England in 2020. Allele-specific PCR will permit surveillance for $M1_{UK}$ without need for genome sequencing.

Upsurges in invasive group A *Streptococcus* (GAS) infections have been widely reported in England and elsewhere (*1*), emphasizing the need to examine the relationship between circulating *S. pyogenes* that cause pharyngitis and scarlet fever and cases of invasive disease. Although many factors, such as exposure history, underlying conditions, viral co-infection, and genetic susceptibility, might increase susceptibility to *S. pyogenes* infection, strain-specific virulence might also be crucial.

In England, where both scarlet fever and invasive *S. pyogenes* infections are notifiable, pronounced upsurges in scarlet fever were recorded over an 8-year period (*2*,*3*) but subsided during the COVID-19 pandemic. During the 2015–16 season, a notable increase in invasive infections was observed that had not been evident previously (*4*). Both scarlet fever and invasive infections were associated with the emergence of $M1_{UK}$, a new sublineage of *emm*1 *S. pyogenes* (*4*) that appeared to outcompete the highly successful, contemporary epidemic *emm*1 $M1_{global}$ strain, which emerged and spread globally during the 1980s (*5*,*6*). Despite an unchanged phage repertoire, $M1_{UK}$ strains produce more superantigenic scarlet fever toxin SpeA (streptococcal pyrogenic exotoxin A) than contemporary $M1_{global}$ *S. pyogenes* strains (*4*).

*emm*1 *S. pyogenes* strains are highly virulent (*5*) and disproportionately associated with invasive infections; any increase in the prevalence of *emm*1 strains in persons with pharyngitis or scarlet fever is, therefore, a public health concern. Known distribution of $M1_{UK}$ is largely limited to those countries undertaking and reporting genome sequencing (Figure 1). $M1_{UK}$ has been identified in other countries in Europe, from a single isolate in Denmark (*4*) to dominant status in the Netherlands (*7*). The lineage has also been reported in North America; the Public Health Agency of Canada reported that 17/178 (10%) of *emm*1 isolates from 2016 were $M1_{UK}$ (*8*). This finding contrasts with a reported $M1_{UK}$ frequency of just 0%–2.8% of *emm*1 isolates in the United States, according to the Active Bacterial Core surveillance system of the US Centers for Disease Control and Prevention; however, the low US frequency was associated with severe infections (*9*). Of note, most reports used genomic data that were >5 years old, so a reappraisal of prevalence is needed. A recent study in Australia using data through 2020 indicated expansion of $M1_{UK}$ in Queensland and Victoria (*10*). The authors identified acquisition of an additional phage encoding superantigen genes *ssa* and *spec* and a single-nucleotide polymorphism (SNP) implicated in SpeA upregulation in the $M1_{UK}$ lineage. Multicountry increases in GAS infections (*1*) since pandemic restrictions were lifted underscore the importance of increasing global

Author affiliations: Imperial College London, London, UK (X. Zhi, H.K. Li, H. Li, Z. Loboda, S. Charles, A. Vieira, K. Huse, E. Jauneikaite, L. Reeves, K.Y. Mok, S. Sriskandan); United Kingdom Health Security Agency, London (J. Coelho, T. Lamagni)

DOI: https://doi.org/10.3201/eid2905.221887

[1]Data from this study were presented at the 21st Lancefield International Symposium on Streptococci and Streptococcal Diseases; Stockholm, Sweden; June 7–10, 2022.

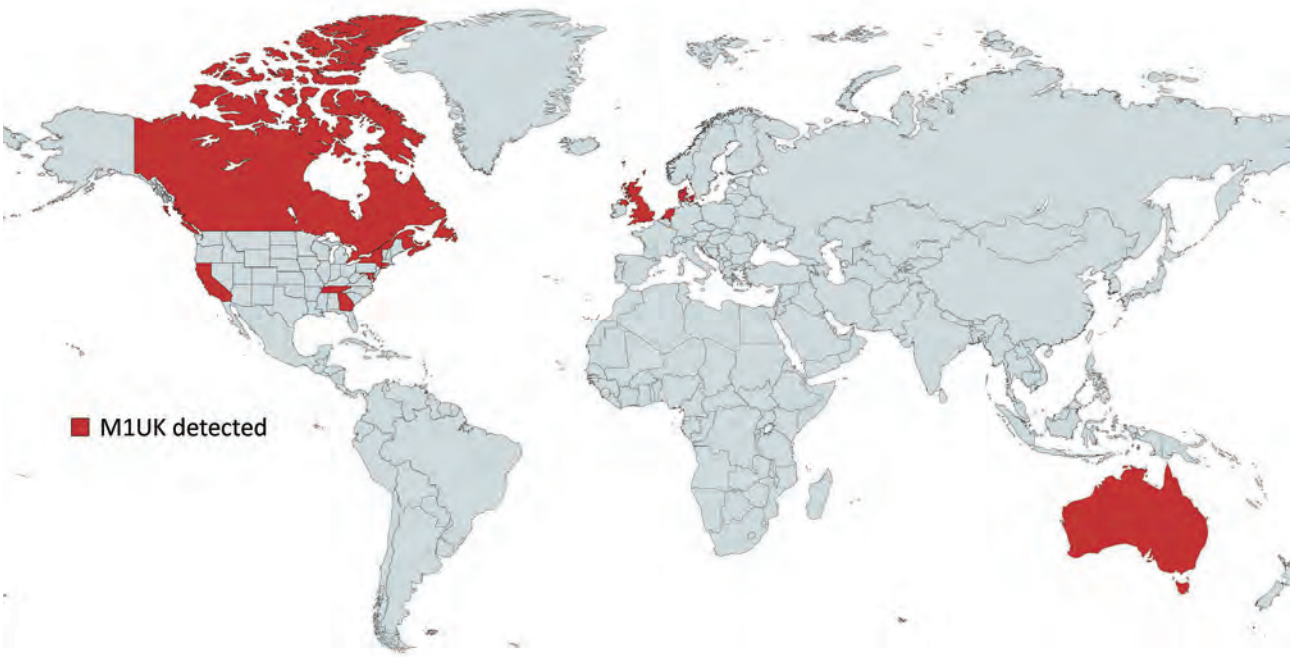


**Figure 1.** Countries and US states with reported $M1_{UK}$ *Streptococcus pyogenes* cases. Map created by using MapChart (https://www.mapchart.net) as part of a study of emerging invasive group A *Streptococcus* $M1_{UK}$ lineage detected by allele-specific PCR, England, 2020.

surveillance of lineages that have potentially enhanced fitness, such as $M1_{UK}$.

## The Study

Genetic distinction between $M1_{UK}$ and $M1_{global}$ strains is possible by using whole-genome sequencing to detect the 27 SNPs that characterize the $M1_{UK}$ lineage (*4*), but sequencing technology is not available in all countries. We designed an allele-specific PCR (AS-PCR) method to detect $M1_{UK}$-specific SNPs in the *rofA*, *gldA*, and *pstB* genes. We chose amplification targets to separate $M1_{UK}$ and $M1_{global}$ strains but also to identify strains from less common intermediate sublineages that had only 13 or 23 of the 27 $M1_{UK}$-specific SNPs (*4*). We optimized PCR conditions for each pair of amplicons by using DNA from control strains for each lineage (Table; Appendix Figure, https://wwwnc.cdc.gov/EID/article/29/5/22-1887-App1.pdf). Collecting bacterial samples from patients was part of routine clinical care; collecting surplus samples after anonymizing patient information was approved by the West London National Research Ethics Committee (approval no. 06/Q0406/20).

To evaluate allele-specific PCR, we tested whether the *rofA* and *pstB* primers correctly identified lineages of 27 newly genome-sequenced noninvasive *emm*1

**Table.** PCR primers and conditions used to differentiate $M1_{global}$ and $M1_{UK}$ *Streptococcus pyogenes* lineages in study of emerging invasive group A *Streptococcus* $M1_{UK}$ lineage detected by allele-specific PCR, England, 2020*

| Target gene | Primer type† | Sequences‡ | PCR cycle conditions | Product, bp |
|---|---|---|---|---|
| *rofA* | WT sequence | TGTTAATTGCTTGGTTAAATCA | 30 cycles of 95°C for 3 min, 45 s; 59.2°C for 30 s; 72°C for 1 min (final cycle: 5 min) | 278 |
| | Forward-SNP | 5′-TGTTAATTGCTTGGTTAAA**G**t**A**-'3 | | |
| | Forward-WT | 5′-TGTTAATTGCTTGGTTAAA**G**CA-'3 | | |
| | Reverse | 5′-GCTCATCTCCTAACGGATTCTT-'3 | | |
| *gldA* | WT sequence | AGATGGGTTAGCAACATGG | 30 cycles of 95°C for 3 min, 45 s; 61.8°C for 30 s;72°C for 1 min (final cycle: 5 min) | 292 |
| | Forward-SNP | 5′-AGATGGGTTAGCAACA**A**a**G**-'3 | | |
| | Forward-WT | 5′-AGATGGGTTAGCAACA**A**GG-'3 | | |
| | Reverse | 5′-GAATAGCACCTGTCAGCG-'3 | | |
| *pstB* | WT sequence | GATAAATCAATCTTAGACCA | 30 cycles of 95°C for 3 min, 45 s; 50°C for 30 s; 72°C for 1 min (final cycle: 5 min) | 287 |
| | Forward-SNP | 5′-GATAAATCAATCTTAGA**T**a**A**-'3 | | |
| | Forward-WT | 5′-GATAAATCAATCTTAGA**T**CA-'3 | | |
| | Reverse | 5′-CGTGAGGCTTGCTGCATTGAG-'3 | | |

*SNP, single-nucleotide polymorphism; WT, wild-type.
†Forward primers were designed to detect either the targeted SNP ($M1_{UK}$) or WT ($M1_{global}$) sequences.
‡Lowercase bold letters in primer sequences denote the base complementary to the targeted SNP in the $M1_{UK}$ sequence. Underlined uppercase letters indicate an additional mismatched base introduced into primer sequences to increase primer specificity.

*S. pyogenes* strains isolated during 2017–18 and collected by the infection bioresource at Imperial College. We artificially enriched the isolates for $M1_{global}$ strains to ensure adequate numbers of each lineage: 8/27 isolates were $M1_{global}$, and 19/27 were $M1_{UK}$. PCR amplification of *rofA* and *pstB* alleles from those isolates assigned 100% of strains to the correct lineage previously identified by sequencing (Appendix Table 1).

To evaluate the ability of AS-PCR to identify *emm*1 isolates from $M1_{global}$, $M1_{UK}$, and intermediate sublineages (*4*), we tested 16 strains from 2013–2016 that comprised 4 isolates each of $M1_{global}$, $M1_{13snps}$, $M1_{23snps}$, and $M1_{UK}$ lineages (Appendix Table 2). SNPs were correctly detected in the *rofA* gene from all $M1_{13snps}$, $M1_{23snps}$, and $M1_{UK}$ isolates (Appendix Table 3). SNPs were also correctly detected in *gldA* from all $M1_{23snps}$ and $M1_{UK}$ isolates but not $M1_{global}$ or $M1_{13snps}$ isolates. Finally, SNPs in *pstB* were only identified in $M1_{UK}$ isolates. Thus, in all cases, SNP profiles determined by AS-PCR were consistent with strain-specific genome sequences.

In England, submission of all isolates from invasive infection is requested by the UK Health Security Agency reference laboratory for *emm* genotyping. *emm*1 isolates are routinely the dominant genotype among invasive sterile-site isolates, typically representing 20%–30% of invasive infections. During 2020, when incidence of common respiratory infections was reduced by COVID-19–related public health interventions, *emm*1 *S. pyogenes* frequency varied each month from 0%–24% of all invasive infections and decreased toward the end of the year. We subjected all 305 invasive *emm*1 *S. pyogenes* isolates from 2020 that were available for this study to AS-PCR (Appendix Table 4). AS-PCR identified $M1_{UK}$-specific SNPs in *rofA*, *gldA*, and *pstB* in 278/305 (91.1%) of isolates, which were, therefore, assigned to the $M1_{UK}$ lineage. No SNPs were detected in the remaining 27 isolates, which were assigned to $M1_{global}$; no intermediate lineage *emm*1 strains were identified in isolates collected during 2020 by using AS-PCR.

We performed Western blot analysis of 10 $M1_{UK}$ isolates identified by AS-PCR. We confirmed that SpeA production was similar to $M1_{UK}$ strains tested previously; however, we did not quantify SpeA production.

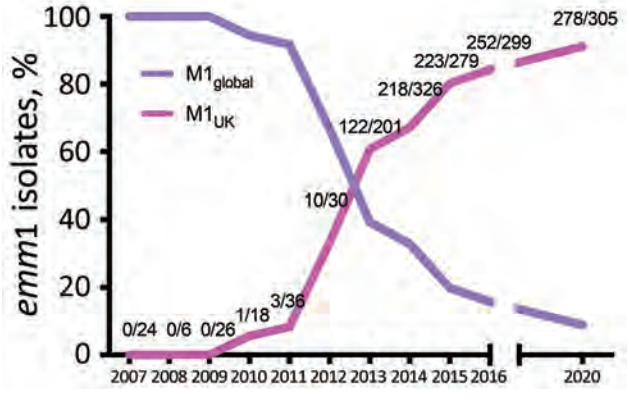


**Figure 2.** Prevalence of $M1_{UK}$ and $M1_{global}$ *Streptococcus pyogenes* lineages over time in study of emerging invasive group A *Streptococcus* $M1_{UK}$ lineage detected by allele-specific PCR, England, 2020. We determined percentages of *emm*1 isolates in England that belonged to $M1_{UK}$ or $M1_{global}$ lineages by using all available *emm*1 *S. pyogenes* genome sequences for 2007–2016 (*4*) and all available invasive isolates from 2020 that we tested by allele-specific PCR. Numbers on graph indicate number of isolates assigned as $M1_{UK}$/total number sequenced for each year. Graph was adapted and updated from data previously described (*4*).

## Conclusions

The longevity of emergent *S. pyogenes* lineages in a population is difficult to predict. Although an $emm89_{emergent}$ acapsular lineage has disseminated globally (*11*), an emergent *emm*3 SpeC-producing lineage, associated with upsurges in scarlet fever and invasive infections, ceased to be detectable within a few years (*12*). Taken together with previously reported genome-sequenced *emm*1 isolates (Figure 2), AS-PCR results indicated that the $M1_{UK}$ lineage continued to expand among invasive *S. pyogenes* isolates from 2016 to the end of 2020 in England.

Increased invasive GAS activity in several countries (*1*) indicates a need for ongoing surveillance of novel lineages, given the potential public health effects. AS-PCR provides a readily available method to detect $M1_{UK}$ that is straightforward and, for screening purposes only, can be simplified by using only *rofA* primers to identify $M1_{UK}$ or associated sublineages. A limitation of our study is that the assay requires validation in reference laboratory settings. AS-PCR does not replace genome sequencing as the preferred method for surveillance of highly pathogenic bacteria, but sequencing is not widely available and is expensive.

*emm*1 strains have accounted for >50% of invasive infections in children in England during the 2022–23 season (*13*). Our results indicate that the $M1_{UK}$ lineage remained dominant in England and expanded to the end of 2020, and contact tracing in 2018 demonstrated a high frequency of secondary acquisition of $M1_{UK}$ in school outbreak settings (*14*). Given the recognized association between *emm*1 *S. pyogenes* and fatal outcome of invasive infections (*15*), enhanced surveillance for the $M1_{UK}$ sublineage is warranted. We conclude that AS-PCR is a readily available method to determine whether *emm*1 *S. pyogenes* isolates belong to the $M1_{UK}$ clade without need for genome sequencing and will improve surveillance of invasive GAS strains.

**Acknowledgments**

We thank the National Institute for Health Research (NIHR) Imperial Biomedical Research Centre (BRC); NIHR Health Protection Research Unit (HPRU) in Healthcare-associated Infection and Antimicrobial Resistance at Imperial College London; Medical Research Council Centre for Molecular Bacteriology and Infection; scientific and biomedical staff from the NIHR BRC Colebrook laboratory, NIHR HPRU, NIHR BRC Imperial Genomics Facility, and Northwest London Pathology/Imperial College Healthcare Trust Diagnostic laboratory for contributing to the collection, biobanking, typing, and sequencing of bacterial isolates; and staff at the UK Health Security Agency reference laboratory who genotyped *emm*-invasive isolates used in this study.

This study was funded by UK Research and Innovation Medical Research Council (MR/P022669/1) and NIHR Imperial Biomedical Research Centre.

## About the Author

Dr. Zhi is a postdoctoral research associate at Imperial College London. Her research focuses on pathogenesis and vaccine prevention of *Streptococcus pyogenes* disease.

## References

1. World Health Organization. Increase in invasive group A streptococcal infections among children in Europe, including fatalities [cited 2022 Dec 14]. https://www.who.int/europe/news/item/12-12-2022-increase-in-invasive-group-a-streptococcal-infections-among-children-in-europe--including-fatalities
2. Turner CE, Pyzio M, Song B, Lamagni T, Meltzer M, Chow JY, et al. Scarlet fever upsurge in England and molecular-genetic analysis in north-west London, 2014. Emerg Infect Dis. 2016;22:1075–8. https://doi.org/10.3201/eid2206.151726
3. Lamagni T, Guy R, Chand M, Henderson KL, Chalker V, Lewis J, et al. Resurgence of scarlet fever in England, 2014–16: a population-based surveillance study. Lancet Infect Dis. 2018;18:180–7. https://doi.org/10.1016/S1473-3099(17)30693-X
4. Lynskey NN, Jauneikaite E, Li HK, Zhi X, Turner CE, Mosavie M, et al. Emergence of dominant toxigenic M1T1 *Streptococcus pyogenes* clone during increased scarlet fever activity in England: a population-based molecular epidemiological study. Lancet Infect Dis. 2019;19:1209–18. https://doi.org/10.1016/S1473-3099(19)30446-3
5. Nasser W, Beres SB, Olsen RJ, Dean MA, Rice KA, Long SW, et al. Evolutionary pathway to increased virulence and epidemic group A *Streptococcus* disease derived from 3,615 genome sequences. Proc Natl Acad Sci USA. 2014;111:E1768–76. https://doi.org/10.1073/pnas.1403138111
6. Sumby P, Porcella SF, Madrigal AG, Barbian KD, Virtaneva K, Ricklefs SM, et al. Evolutionary origin and emergence of a highly successful clone of serotype M1 group A *Streptococcus* involved multiple horizontal gene transfer events. J Infect Dis. 2005;192:771–82. https://doi.org/10.1086/432514
7. Rümke LW, de Gier B, Vestjens SMT, van der Ende A, van Sorge NM, Vlaminckx BJM, et al. Dominance of $M1_{UK}$ clade among Dutch M1 *Streptococcus pyogenes*. Lancet Infect Dis. 2020;20:539–40. https://doi.org/10.1016/S1473-3099(20)30278-4
8. Demczuk W, Martin I, Domingo FR, MacDonald D, Mulvey MR. Identification of *Streptococcus pyogenes* $M1_{UK}$ clone in Canada. Lancet Infect Dis. 2019;19:1284–5. https://doi.org/10.1016/S1473-3099(19)30622-X
9. Li Y, Nanduri SA, Van Beneden CA, Beall BW. $M1_{UK}$ lineage in invasive group A *Streptococcus* isolates from the USA. Lancet Infect Dis. 2020;20:538–9. https://doi.org/10.1016/S1473-3099(20)30279-6
10. Davies MR, Keller N, Brouwer S, Jespersen MG, Cork AJ, Hayes AJ, et al. Detection of *Streptococcus pyogenes* M1UK in Australia and characterization of the mutation driving enhanced expression of superantigen SpeA. Nat Commun. 2023;14:1051. PubMed https://doi.org/10.1038/s41467-023-36717-4
11. Turner CE, Abbott J, Lamagni T, Holden MTG, David S, Jones MD, et al. Emergence of a new highly successful acapsular group A *Streptococcus* clade of genotype *emm*89 in the United Kingdom. mBio. 2015;6:e00622. https://doi.org/10.1128/mBio.00622-15
12. Al-Shahib A, Underwood A, Afshar B, Turner CE, Lamagni T, Sriskandan S, et al. Emergence of a novel lineage containing a prophage in *emm*/M3 group A *Streptococcus* associated with upsurge in invasive disease in the UK. Microb Genom. 2016;2:e000059. https://doi.org/10.1099/mgen.0.000059
13. UK Health Security Agency. Group A streptococcal infections: second update on seasonal activity in England 2022 to 2023 [cited 2022 Dec 16]. https://www.gov.uk/government/publications/group-a-streptococcal-infections-activity-during-the-2022-to-2023-season/group-a-streptococcal-infections-second-update-on-seasonal-activity-in-england-2022-to-2023
14. Cordery R, Purba AK, Begum L, Mills E, Mosavie M, Vieira A, et al. Frequency of transmission, asymptomatic shedding, and airborne spread of *Streptococcus pyogenes* in schoolchildren exposed to scarlet fever: a prospective, longitudinal, multicohort, molecular epidemiological, contact-tracing study in England, UK. Lancet Microbe. 2022;3:e366–75. https://doi.org/10.1016/S2666-5247(21)00332-3
15. Nelson GE, Pondo T, Toews KA, Farley MM, Lindegren ML, Lynfield R, et al. Epidemiology of invasive group A streptococcal infections in the United States, 2005–2012. Clin Infect Dis. 2016;63:478–86. https://doi.org/10.1093/cid/ciw248

Address for correspondence: Shiranee Sriskandan, Section of Adult Infectious Diseases, Department of Infectious Disease, Imperial College London, Hammersmith Hospital Campus, Du Cane Road, London, W12 0NN, UK; email: s.sriskandan@imperial.ac.uk

# *Borrelia miyamotoi* Infection in Immunocompromised Man, California, USA, 2021

Luis Alberto Rubio, Anne M. Kjemtrup, Grace E. Marx, Shanna Cronan, Christopher Kilonzo, Megan E.M. Saunders, Jamie L. Choat, Elizabeth A. Dietrich, Kelly A. Liebman, Sarah Y. Park

Infection with *Borrelia miyamotoi* in California, USA, has been suggested by serologic studies. We diagnosed *B. miyamotoi* infection in an immunocompromised man in California. Diagnosis was aided by plasma microbial cell–free DNA sequencing. We conclude that the infection was acquired in California.

*Borrelia miyamotoi* is a relapsing fever spirochete; infection is recognized in Europe, Japan, and the northeastern United States as an emerging human infectious disease (*1*,*2*). First identified in Japan in 1995 in *Ixodes persulcatus* ticks, *B. miyamotoi* has since been detected in other species of *Ixodes* ticks, including *I. ricinus* in Europe, *I. scapularis* in eastern North America, and *I. pacificus* in western North America (*1*). In California, USA, *I. pacificus* ticks can harbor 2 spirochetes capable of causing human disease: *B. miyamotoi* and *Borrelia burgdorferi*, the agent that causes Lyme disease (*3*). Prevalence of *B. miyamotoi* in *I. pacificus* ticks in California is estimated to be 0.8% in adult ticks and 1.4% in nymphal ticks, similar to other parts of the world that have *Ixodes* spp. ticks and reported human cases of *B. miyamotoi* infection (*1*).

In California, tick-borne relapsing fever is usually ascribed to infection with *B. hermsii*, transmitted by soft ticks (*Ornithodoros hermsi*), found in high-elevation habitats (*4*). Although infection with *B. miyamotoi* in California has been suggested by serologic studies, clinical human cases of *B. miyamotoi* infection acquired in the western United States have not been reported in the literature (*1*,*3*,*4*). We describe *B. miyamotoi* infection, confirmed through plasma microbial cell–free DNA (mcfDNA) sequencing, in a California man with relapsing fevers. Our investigation was determined to be exempt from human subjects research by the Office of Human Research Protections of the California Health and Human Services Agency (Federalwide Assurance no. 00000681).

Author affiliations: University of California, San Francisco, San Francisco, California, USA (L.A. Rubio); California Department of Public Health, Sacramento, California, USA (A.M. Kjemtrup); Centers for Disease Control and Prevention, Fort Collins, Colorado, USA (G.E. Marx, J.L. Choat, E.A. Dietrich); County of Marin Department of Health and Human Services, San Rafael, California, USA (S. Cronan); California Department of Public Health, Richmond, California, USA (C. Kilonzo, M.E.M. Saunders); Marin-Sonoma Mosquito and Vector Control District, Cotati, California, USA (K.A. Liebman); Karius, Incorporated, Redwood City, California, USA (S.Y. Park)

DOI: https://doi.org/10.3201/eid2905.221638

## The Case

In December 2021, an adult man receiving ocrelizumab (anti-B lymphocyte CD20 monoclonal antibody) for multiple sclerosis diagnosed in 2018 sought care at a neurology clinic in San Francisco, California, USA. The patient reported having experienced new fevers up to 38.7°C beginning in October 2021. The febrile episodes typically lasted 1 day, occurred every 10–14 days, and were associated with night sweats, mild vision changes, and nausea. Results of a physical examination were unremarkable, and the patient was sent home with a recommendation to return for evaluation if fever recurred.

Given continued intermittent fevers, the neurologist referred the patient to a local hospital in Greenbrae, California, USA, 3 days later for an expedited evaluation. Although the patient was again afebrile and results of physical examination were unremarkable, laboratory results were notable for thrombocytopenia (96,000 cell/mL [reference range 150,000–400,000 cells/mL]), elevated C-reactive protein level (47.2 mg/L [reference ≤5.0 mg/L]), and elevated procalcitonin level (1.89 ng/mL [reference ≤0.10 ng/mL]). No abnormalities were noted on chest radiographs or computed tomography scans of the abdomen and pelvis. Peripheral blood cultures were

without growth, and the patient was discharged to home with a referral to the infectious disease clinic in San Francisco. At that clinic, serologic evaluation for certain bacteria, fungi, and viruses was notable only for positive Epstein-Barr viral capsid and nuclear antigen IgG. Serologic test results for *Borrelia burgdorferi*, brucellosis, and leptospirosis were negative, and results of a peripheral blood smear were unremarkable (Table 1).

Given the patient's immunocompromised status and relapsing fever history, suspicion for infection remained high and plasma mcfDNA sequencing (Karius test, https://kariusdx.com) was ordered. Results were positive for *B. miyamotoi* (56 DNA molecules/µL [reference <10 molecules/µL]). The Centers for Disease Control and Prevention performed confirmatory *Borrelia* PCR testing, results of which were also positive for *B. miyamotoi* (*5*), and multilocus sequence typing (MLST), which indicated that the sequence was 100% identical in >6,040 nucleotides to a *B. miyamotoi* isolate from an *I. pacificus* tick collected in Marin County, California (Table 2) (*6*,*7*). The sequence was distinct from *B. miyamotoi* isolates from other geographic regions, displaying 99.3% identity (44 nt differences) to isolates from the eastern United States.

After *B. miyamotoi* infection was diagnosed, a 4-week course of doxycycline was prescribed. The patient reported having 1 additional febrile episode (38.9°C) after the first dose, but fevers subsequently resolved, and all other signs/symptoms improved. After consultation with the patient's neurologist, cerebrospinal fluid testing was not performed, given resolution of visual symptoms and absence of other focal neurologic deficits. The patient returned to the clinic 1 month after having completed the course of doxycycline without any fever recurrence; laboratory

**Table 1.** Laboratory test results for patient with *Borrelia miyamotoi* Infection, California, USA, 2021*

| Blood test (reference values) | Dec 2021 | May 2022 |
|---|---|---|
| Leukocytes (4.0–11.0 k/uL) | 5.1 | 4.8 |
| Hemoglobin (13.5–18.0 g/dL) | 13.3 (low) | 15.2 |
| Hematocrit (40.0%–52.0%) | 38.5% (low) | 43.4% |
| Thrombocytes (150–400 l/uL) | 96,000 (low) | 224,000 |
| Sodium (136–145 mmol/L) | 134 (low) | 137 |
| Creatinine (0.70–1.30 mg/dL) | 0.82 | 0.98 |
| Albumin (2.8–4.7 g/dL) | 3.6 | 4.7 |
| Aspartate transaminase (≤40 U/L) | 45 (high) | 41 (high) |
| Alanine transaminase (≤65 U/L) | 46 | 46 |
| Alkaline phosphatase (≤38 U/L) | 81 | 60 |
| Total bilirubin (≤1.0 mg/dL) | 1.0 | 0.8 |
| C-reactive protein (≤5.0 mg/L) | 47.2 (high) | 0.2 |
| Procalcitonin (<0.10 ng/mL) | 1.89 (high) | <0.10 |
| COVID-19/influenza/RSV PCR | Not detected | ND |
| Peripheral blood cultures (2 cultures in Dec 2022) | No growth at 5 days | ND |
| Hepatitis B surface Ab (≥10 mIU/mL) | 113 | ND |
| Hepatitis B surface Ag | Nonreactive | ND |
| Hepatitis B core Ab | Nonreactive | ND |
| Hepatitis C Ab | Nonreactive | ND |
| EBV VCA IgM (<36 U/mL) | <36 U/mL | ND |
| EBV VCA IgG Ab (<18 U/mL) | 248 (high) | ND |
| EBV EBNA IgG (<18 U/mL | 255 (high) | ND |
| CMV IgM (<30 AU/mL) | <30 | ND |
| CMV IgG (<0.6 U/mL) | <0.6 | ND |
| *Cryptococcus* Ag | Not detected | ND |
| *Coccidioides* Ab, CF (<1:2) | <1:2 | ND |
| *Coccidioides* Ab, ID | Negative | ND |
| *Histoplasma* Ab, CF (<1:8) | <1:8 | ND |
| *Histoplasma*, ID | Negative | ND |
| *Histoplasma* Ag, urine (<0.2 ng/mL) | <0.2 | ND |
| *Blastomyces* Ab, ID | Negative | ND |
| *Bartonella* Ab | Negative | ND |
| *Coxiella burnetti* Ab IgM and IgG | Negative | ND |
| *Rickettsia* Ab panel | Negative | ND |
| Syphilis (*Treponema*) screen by RPR (nonreactive) | Nonreactive | ND |
| Quantiferon-TB Gold Plus | Negative | ND |

*Additional testing: February 2022, *Borrelia burgdorferi*, Brucella, and *Leptospira* Ab results all negative; March 2022, β-d-glucan (reference value <60 pg/mL), <31 pg/mL; galactomannan Ag (reference value <0.5), 0.018; *Coccidioides* Ag, serum, negative; sequencing of microbial cell–free DNA in plasma performed at Karius, Inc. (https://kariusdx.com) (reference value <10 DNA MPM), *Borrelia miyamotoi* 56 DNA MPM; relapsing fever PCR performed at CDC, *Borrelia* PCR positive group *B. miyamotoi* .Ab, antibody; Ag, antigen; CDC, Centers for Disease Control and Prevention; CF, complement fixation; CMV, cytomegalovirus; EBV, Epstein-Barr virus; EBNA, Epstein-Barr nuclear Ag; ID, immunodiffusion; MPM, molecules/mL; RPR, rapid plasma reagin; RSV, respiratory syncytial virus; VCA, viral capsid antigen.

**Table 2.** Primers used to amplify genes for multilocus sequencing of *Borrelia miyamotoi* that infected immunocompromised man in California, 2021*

| Gene | Forward primer, 3′ → 5′ | Reverse primer, 5′ → 3′ |
|---|---|---|
| *clpA* | TTGATCTCTTAGATGATCTTGG | CAAACATAAACCTTTTCAGCCTTTAATA |
| *clpX* | TTATCTGTTGCTGTTTATAATC | TTCAAACATAACATCTTTAAGTAATTCTTC |
| *nifS* | GAAAAAGTAAACTCCCTCAGAARGG | CAATGATGCCTGCAATATTTGGTG |
| *pepX* | AGAGACTTAAATTTAGCAGGAGTTG | TGCATTCCCCACATTGGAGTTC |
| *pyrG* | TTTAGTAATTGAGATTGGTGGTAC | TATTCCACAAACATTACGAGC |
| *recG* | TAGCATTCCTTTAGTTGAGGC | CTCAGCATGCTCAACTACC |
| *rplB* | AACTTATAGGCCAAAAACTTC | GATACAGGATGACGACCACC |
| *uvrA* | TTAAATTTTTAATTGATGTTGGACT | TCTGTAAAAAACCCAACATAAGTTGC |

*Genes derived from (*6*), with modifications to the *nifS* and *rplB* forward primers to make them more specific for *B. miyamotoi*.

testing showed resolution of thrombocytopenia and normalization of inflammatory markers. Ocrelizumab infusions were resumed after *B. miyamotoi* treatment, and symptom recurrence has not been reported.

The patient was a resident of Marin County, California, and reported having traveled 2 months before fever onset to Ohio and within California to Mendocino and Monterey Counties but reported no travel outside the United States for the previous 2 years. He reported hiking and swimming in freshwater lakes while traveling and near home but did not recall any insect or tick bites. He reported often spending time outdoors near home. He owned 2 domestic indoor cats not receiving regular tick prevention and reported no other animal exposures.

The California Department of Public Health Vector-Borne Disease Section collaborated with Marin-Sonoma Vector Control Agency to collect and test ticks from areas around the patient's residence. The habitat consisted of coastal redwood grove and understory grass and shrub vegetation. Questing ticks were collected by dragging a 1-$m^2$ white flannel cloth along the ground cover. A total of 19 *I. pacificus* ticks (12 adults, 7 nymphs) from the patient's yard and nearby trails were collected and stored in 70% ethanol until DNA extraction. PCR testing did not identify any ticks positive for *B. miyamotoi* infection but identified 1 adult tick infected with *B. burgdorferi* sensu lato (*8*).

## Conclusions

Although *B. miyamotoi* has been identified in ticks in California for >20 years, locally acquired human cases within the western United States have not been described (*1*). Our environmental investigation identified multiple *I. pacificus* ticks near this patient's residence and recreation areas in California, all in locations where *B. miyamotoi* has been documented in *I. pacificus* ticks (*1*). The *B. miyamotoi* sequence recovered from the patient was most closely related to an isolate recovered from an *I. pacificus* tick in California (*7*). Of note, the patient's travel to Ohio was during August, when seasonal activity of *Ixodes* spp. ticks in the region is low, and was to a location where *B. miyamotoi* has not been identified (*9*).

For patients with high or relapsing fever during seasons of *Ixodes* tick activity, particularly in areas where *B. miyamotoi* has been reported in local tick populations, clinicians should consider the possibility of *B. miyamotoi* infection along with other *Borrelia* spp. Laboratory confirmation of *B. miyamotoi* infection can be challenging because the spirochetes share many proteins with *B. burgdorferi* and *B. hermsii*, resulting in cross-reacting antibodies, and because few laboratories offer specific molecular diagnostic testing for *B. miyamotoi* (*10*). For this case, *B. miyamotoi* infection was diagnosed through molecular testing with unbiased plasma mcfDNA sequencing, an increasingly used tool for evaluating patients with fever of unknown etiology (*11*,*12*). The patient's immunocompromised status may have contributed to the infection chronicity, increasing our ability to detect the organism (*11*,*13*). PCR and sequencing confirmed the diagnosis.

Our study suggests that *B. miyamotoi* is an emerging human pathogen in California. Human infection is probably rare, given low seroprevalence in blood donors, even in counties to which *I. pacificus* ticks are endemic, and low prevalence of *B. miyamotoi* in ticks that is rarely >2% (*1*,*3*). Given limitations of serologic testing, clinicians should maintain an index of suspicion for *B. miyamotoi* in patients with relapsing fever without a clear etiology, should ask about potential tick exposure, and should consider molecular diagnostic testing.

### Acknowledgments

We thank Lindsey Termini for the case investigation.

The findings and conclusions in this article are those of the authors and do not necessarily represent the views or opinions of the California Department of Public Health, the California Health and Human Services Agency, County of Marin Department of Public Health, or the Centers for Disease Control and Prevention.

## About the Author

Dr. Rubio is an assistant clinical professor at University of California, San Francisco, and provides clinical care there and at the Zuckerberg San Francisco General Hospital and Trauma Center. His interests include general infectious diseases, latent tuberculosis infection, HIV primary care, and medical education.

## References


1. Padgett K, Bonilla D, Kjemtrup A, Vilvins I, Yoshimizu M, Hui L, et al. Large scale spatial risk and comparative prevalence of *Borrelia miyamotoi* and *Borrelia burgdorferi* sensu lato in *Ixodes pacificus*. PLoS One. 2014;9:e110853.
2. Sato K, Takano A, Konnai S, Nakao M, Ito T, Koyama K, et al. Human infections with *Borrelia miyamotoi*, Japan. Emerg Infect Dis. 2014;20:1391–3. https://doi.org/10.3201/eid2008.131761
3. Brummitt SI, Kjemtrup AM, Harvey DJ, Petersen J, Sexton C, Replogle A, et al. *Borrelia burgdorferi* and *Borrelia miyamotoi* seroprevalence in California blood donors. PloS One. 2020;15:e0243950.
4. Krause PJ, Carroll M, Fedorova N, Brancato J, Dumouchel C, Akosa F, et al. Human *Borrelia miyamotoi* infection in California: serodiagnosis is complicated by multiple endemic *Borrelia* species. PloS One. 2018;13:e0191725.
5. Dietrich EA, Replogle AJ, Sheldon SW, Petersen JM. Simultaneous detection and differentiation of clinically relevant relapsing fever *Borrelia* with semimultiplex real-time PCR. J Clin Microbiol. 2021;59:e0298120. https://doi.org/10.1128/JCM.02981-20
6. Margos G, Gatewood AG, Aanensen DM, Hanincová K, Terekhova D, Vollmer SA, et al. MLST of housekeeping genes captures geographic population structure and suggests a European origin of *Borrelia burgdorferi*. Proc Natl Acad Sci U S A. 2008;105:8730–5. https://doi.org/10.1073/pnas.0800323105
7. Kingry LC, Replogle A, Dolan M, Sexton C, Padgett KA, Schriefer ME. Chromosome and large linear plasmid sequences of a *Borrelia miyamotoi* strain isolated from *Ixodes pacificus* ticks from California. Genome Announc. 2017;5:e00960–17.
8. Barbour AG, Bunikis J, Travinsky B, Hoen AG, Diuk-Wasser MA, Fish D, et al. Niche partitioning of *Borrelia burgdorferi* and *Borrelia miyamotoi* in the same tick vector and mammalian reservoir species. Am J Trop Med Hyg. 2009;81:1120–31. https://doi.org/10.4269/ajtmh.2009.09-0208
9. Krause PJ, Fish D, Narasimhan S, Barbour AG. *Borrelia miyamotoi* infection in nature and in humans. Clin Microbiol Infect. 2015;21:631–9. https://doi.org/10.1016/j.cmi.2015.02.006
10. Fleshman AC, Foster E, Maes SE, Eisen RJ. Reported county-level distribution of seven human pathogens detected in host-seeking *Ixodes scapularis* and *Ixodes pacificus* (Acari: Ixodidae) in the contiguous United States. J Med Entomol. 2022;59:1328–35. https://doi.org/10.1093/jme/tjac049
11. Wright WF, Simner PJ, Carroll KC, Auwaerter PG. Progress report: next-generation sequencing, multiplex polymerase chain reaction, and broad-range molecular assays as diagnostic tools for fever of unknown origin investigations in adults. Clin Infect Dis. 2022;74:924–32. https://doi.org/10.1093/cid/ciab155
12. Haidar G, Singh N. Fever of unknown origin. N Engl J Med. 2022;386:463–77. https://doi.org/10.1056/NEJMra2111003
13. Boden K, Lobenstein S, Hermann B, Margos G, Fingerle V. *Borrelia miyamotoi*–associated neuroborreliosis in immunocompromised person. Emerg Infect Dis. 2016;22:1617–20. https://doi.org/10.3201/eid2209.152034


Address for correspondence: Luis Alberto Rubio, 2nd Fl, Box 0620, Division of Infections Disease, University of California San Francisco, 521 Parnassus Ave, San Francisco, CA 94143, USA; email: luis.rubio@ucsf.edu

# Novel Circovirus in Blood from Intravenous Drug Users, Yunnan, China

Yanpeng Li, Peng Zhang, Mei Ye, Ren-Rong Tian, Na Li, Le Cao, Yingying Ma, Feng-Liang Liu, Yong-Tang Zheng, Chiyu Zhang

We identified a novel circovirus (human-associated circovirus 2 [HuCV2]) from the blood of 2 intravenous drug users in China who were infected with HIV-1, hepatitis C virus, or both. HuCV2 is most closely related to porcine circovirus 3. Our findings underscore the risk for HuCV2 and other emerging viruses among this population.

Viral infections are major threats to human health (*1*,*2*). Because of the advent of high-throughout sequencing, researchers are identifying new viruses with an unprecedented speed (*3*), and continuous attempts at virus discovery and surveillance, especially among regions and populations at high risk for viral outbreaks, play a crucial role in early diagnosis and warning and in the treatment of emerging and reemerging viral infections.

Circoviruses belong to the *Circoviridae* family, which comprises viruses with circular, single-stranded DNA genomes. The viruses have been identified in a wide range of hosts, including birds, fish, insects, and mammals (*4*). Porcine circovirus (PCV) is the smallest known viral pathogen of *Circoviridae*, and the 4 PCV species that have been recognized (PCV1–PCV4) are widely spread worldwide (*5*). Despite lacking direct evidence of zoonotic transmission of PCVs from animal to human, several studies reported the detection of PCV1 or PCV2 in human samples, and PCV3 was demonstrated as capable of infecting nonhuman primates (*6*). These findings highlight a potential risk for zoonotic transmission of circovirus and the possible presence of novel circoviruses in humans (*7*).

Author affiliations: Shanghai Public Health Clinical Center, Fudan University, Shanghai, China (Y. Li, P. Zhang, L. Cao, Y. Ma, C. Zhang); Kunming Institute of Zoology, Chinese Academy of Sciences, Kunming, China (M. Ye, R.-R. Tian, N. Li, F.-L. Liu, Y.-T. Zheng); Kunming Medical University, Kunming (N. Li)

DOI: https://doi.org/10.3201/eid2905.221617

We report the genomic sequences of a novel circovirus from 2 intravenous drug users (IDUs) who were infected with HIV-1, hepatitis C virus, or both. Given the phylogenetic analysis and genetic distance, our finding suggests that this circovirus could represent a new species of human circovirus.

## The Study

IDUs are at high risk for bloodborne viral infections and bear a high burden of the viruses that primarily infect humans (e.g., HIV-1, hepatitis B virus, and HCV). In a previous study, we investigated the plasma viromes of 99 IDUs from several regions of Yunnan, China, which borders with Myanmar (*8*). We found that IDUs have higher plasma viral loads, and we identified (in addition to HIV-1, hepatitis B virus, and HCV) viruses of other vertebrate viral families, including *Anelloviridae*, *Flaviviridae*, *Circoviridae*, *Orthomyxoviridae*, *Papillomaviridae*, *Pneumoviridae*, *Parvoviridae*, and *Kolmioviridae*. Those data highlighted the complex circulation of bloodborne viruses among IDUs. In a subsequent analysis of the blood virome of an IDU patient (patient no. J030) from the city of Dehong in Yunnan Province who was co-infected with HIV-1 and HCV, we detected novel viral sequences related to PCV3 and assembled a complete circular genome (≈2004 nt) (isolate YN09/J030, GenBank accession no. ON226770). This circular viral genome contains 3 main open reading frames (ORFs): 981 nt ORF1 (encoding the potential replication-associated [rep] protein), 645 nt ORF2 (encoding the potential capsid [cap] protein), and 525 nt ORF3 (unknown protein).

Similar to other circoviruses, a typical stem-loop structure (CAGTATTAC) exists between ORF1 and ORF2 (Figure 1). By using the full-length genomes of isolate YN09/J030 and all the representatives of circovirus, we performed phylogenic analyses to

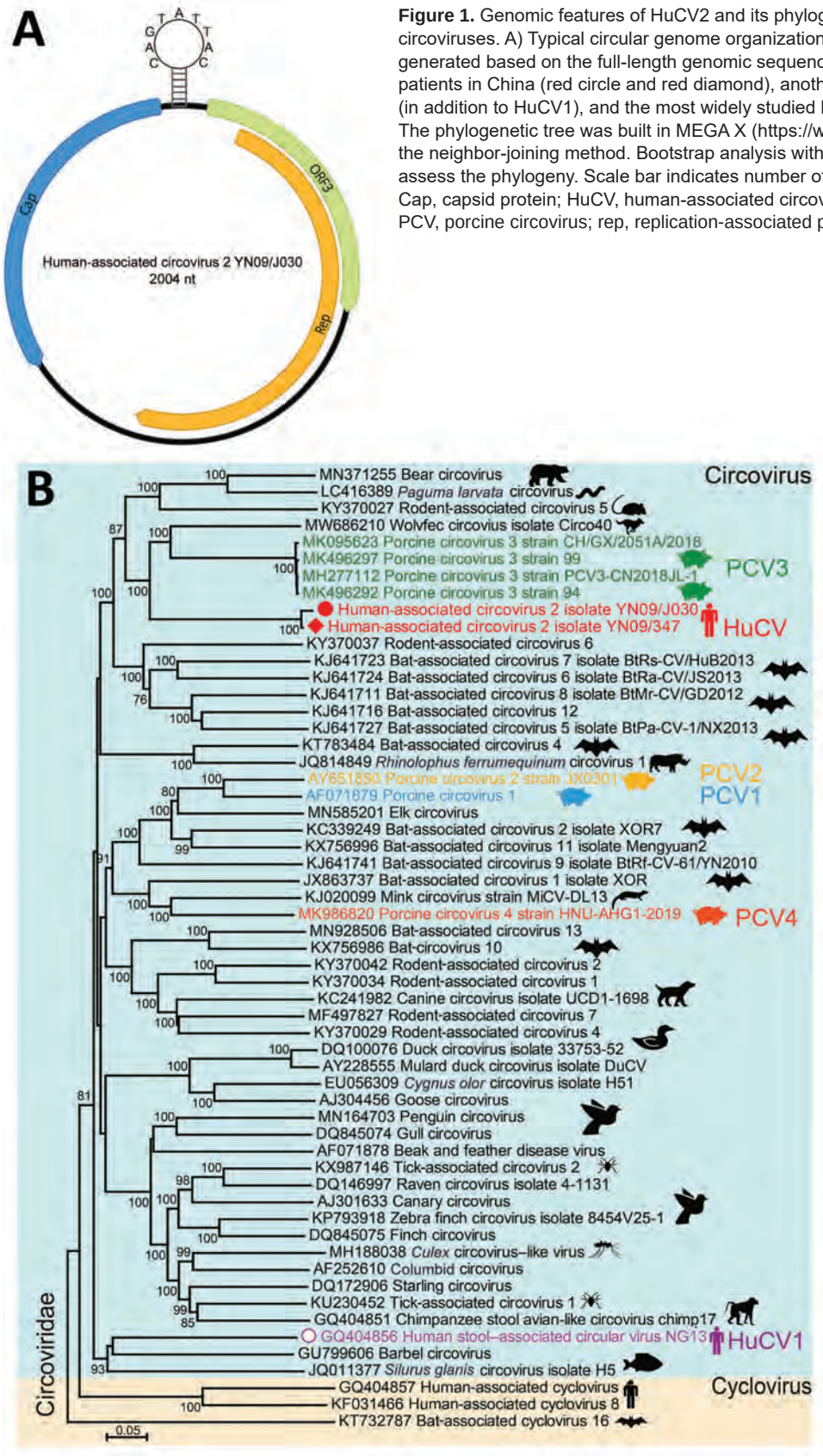


**Figure 1.** Genomic features of HuCV2 and its phylogenetic relationship with other circoviruses. A) Typical circular genome organization of HuCV2. B) Phylogenetic tree, generated based on the full-length genomic sequences, highlights HuCV2 from 2 patients in China (red circle and red diamond), another circovirus detected in humans (in addition to HuCV1), and the most widely studied known pathogens (PCV1–4). The phylogenetic tree was built in MEGA X (https://www.megasoftware.net) by using the neighbor-joining method. Bootstrap analysis with 1,000 replicates was applied to assess the phylogeny. Scale bar indicates number of nucleotide substitutions per site. Cap, capsid protein; HuCV, human-associated circovirus; ORF3, open reading frame 3; PCV, porcine circovirus; rep, replication-associated protein.

determine the evolutionary relationship of this virus. This novel virus clusters with several PCV3 strains and a circovirus from wolverines (WoCV) to form a phylogenetic clade. The virus shares 60.5% genomic sequence identity with PCV3 and 59.6% with WoCV. The first human-associated circovirus (HuCV1) was previously found in the feces of a child with acute flaccid paralysis in 2010 (*9*). Because of the nonsterile nature of feces, the origin of HuCV1 is unclear, and its association with human remains to be established. We named the newly identified virus human-associated circovirus 2 (HuCV2) (isolate YN09/J030), which we believe represents a new species of human circovirus.

Both rep and cap regions of HuCV2 clustered with the clade formed by PCV3 and WoCV. HuCV2 rep region shares 69.5% identity at the amino acid level with PCV3 and 66.7% with WoCV; the cap region shares 47% identity at the amino acid level with PCV3 and 50.4% with WoCV (Appendix Figure 1, https://wwwnc.cdc.gov/EID/article/29/5/22-1617-App1.pdf). We identified conserved regions of the rep protein, including the rolling circle replication and superfamily 3 helicase motifs. HuCV2 shares identical rolling circle replication motifs with PCV3 and WoCV, whereas Walker A motifs of HuCV2 superfamily 3 helicase have 2-residue differences with PCV3 and WoCV

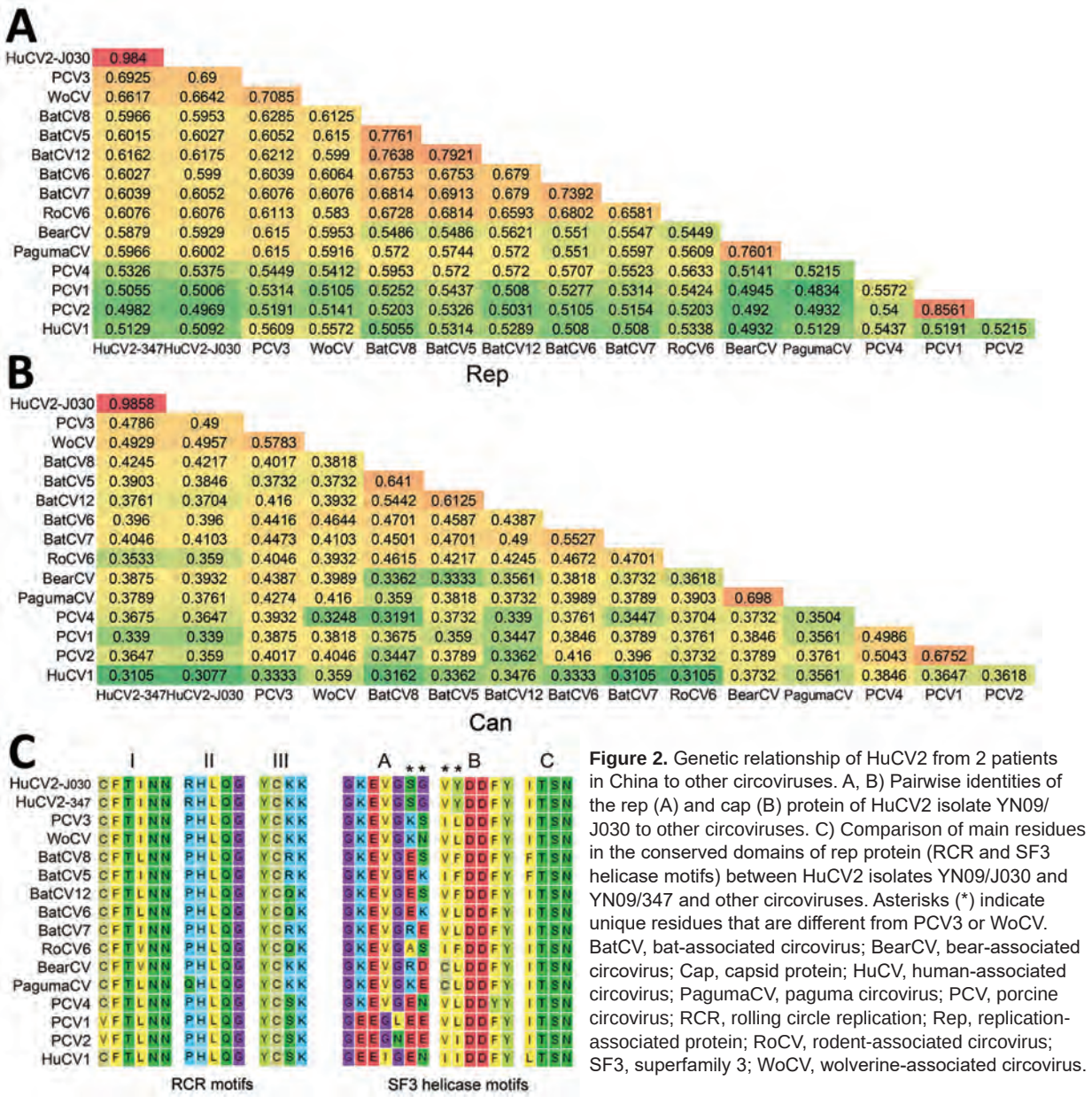


**Figure 2.** Genetic relationship of HuCV2 from 2 patients in China to other circoviruses. A, B) Pairwise identities of the rep (A) and cap (B) protein of HuCV2 isolate YN09/J030 to other circoviruses. C) Comparison of main residues in the conserved domains of rep protein (RCR and SF3 helicase motifs) between HuCV2 isolates YN09/J030 and YN09/347 and other circoviruses. Asterisks (*) indicate unique residues that are different from PCV3 or WoCV. BatCV, bat-associated circovirus; BearCV, bear-associated circovirus; Cap, capsid protein; HuCV, human-associated circovirus; PagumaCV, paguma circovirus; PCV, porcine circovirus; RCR, rolling circle replication; Rep, replication-associated protein; RoCV, rodent-associated circovirus; SF3, superfamily 3; WoCV, wolverine-associated circovirus.

**Table.** Demographic and clinical characteristics of 2 patients with novel circovirus infection, Yunnan, China*

| Characteristic | Patient 1, J030 | Patient 2, 347 |
|---|---|---|
| Sex | Male | Male |
| Ethnicity | Jingpo | Han |
| Occupation | Farmer | Farmer |
| Marriage status | Married | Single |
| Risk behaviors (drug used) | IDU (heroin) | IDU (heroin) |
| Syringe or needle sharing | Yes | Yes |
| Year of sampling | 2009 | 2009 |
| Year of 1st HIV-1 diagnosis | 2005 | 1996 |
| HIV-1† | + | – |
| HCV† | + | + |
| HuCV2 | + | + |
| Other infections | – | – |
| AIDS symptoms | No | No |
| CD4+ cell count, cells/mm$^3$ | 554 | 635 |
| HAART | No | Yes |
| Year of death | 2010 | 2014 |
| Cause of death | Unknown | Non–AIDS-related |
| HAART | No | Yes |

*HAART, highly active antiretroviral therapy; HCV, hepatitis C virus ; HuCV2, human-associated circovirus 2; injection drug use; +, positive; –, negative or below detection limit.
†Nucleic acid detection (quantitative PCR and next-generation sequencing) of the sample collected in 2009, as described in a previous study (*8*).

(Figure 2). Furthermore, we observed a 1-residue difference in HuCV2 Walker B motif from that of PCV3 and WoCV (Figure 2). We detected no recombination signals among HuCV2, PCV3 or WoCV, and circoviruses from outlying lineages, such as bat circoviruses.

To investigate HuCV2 prevalence, we developed a specific quantitative PCR method on the basis of its genomic sequence and screened 568 blood samples collected from IDUs in the same region and in several other cities of Yunnan Province (Appendix Figure 2). We detected HuCV2 sequence (cycle threshold 31) in a second patient (patient no. 347) who was co-infected with HCV. This patient was from Linxiang District of the city of Lincang and had no contact with the first case-patient. We subsequently amplified and sequenced the near full-length genome of the second circovirus isolate (isolate YN09/347, GenBank accession no. OP744467) from this patient's blood. The second HuCV2 strain shares ≈98.5% sequence identity with isolate YN09/J030 (Figure 2).

Patients J030 had HIV-1 diagnosed in 2005 and patient 347 in 1996 (Table). In our previous study (*10*), we identified both patients as HCV-positive by using quantitative reverse-transcription PCR and next-generation sequencing. Patient J030 did not receive highly active antiretroviral therapy and died in 2010. Patient 347 received the therapy but died of non–AIDS-related causes in 2014.

## Conclusions

The pathogenicity of PCVs in pigs and their potential threat to several other animals is well known, but the pathogenicity or disease association of other circoviruses is barely known. The presence of this novel circovirus HuCv2 in the blood of 2 IDUs underscore the risk for emerging viruses in this population, although the epidemiology and potential clinical importance of HuCV2 remains to be clarified.

Even though HuCV2 is more closely related to PCV3 than to other circoviruses, the low nucleotide sequence identity (60.5%) and absence of recombination between them indicate that HuCV2 could be a novel circovirus species that circulates in humans. Only 2 IDUs were detected to be HuCV2-positive, implying very low prevalence. However, all the blood samples were collected during 2009–2010, and after >10 years' storage and repeated freezing and thawing consistent with their experimental purposes, the viral genomes could be degraded. Furthermore, both patients shared needles or syringes with other IDUs (Table) and more likely spread or acquired HIV-1, HCV, and HuCV2 to or from others. Therefore, HuCV2 prevalence might be underestimated. On the other hand, whether the presence of HuCV2 in these 2 patients was associated with their health conditions or their deaths was unclear, and the infectivity and pathogenicity of HuCv2 need to be further determined. Injection drug use and other risk practices are major drivers of new bloodborne viral infections and transmission. The blood samples in our study were collected from the regions of Yunnan Province that border with Myanmar, where extensive co-infection and transmission of bloodborne viruses (e.g., HIV-1 and HCV) among IDUs were reported because of active drug trading, syringe sharing, and high-risk sexual behaviors (*10*,*11*). Thus, even though the 2 cases were reported in 2009, HuCV2 might have spread among IDUs and could be currently circulating in this population of this region, warranting further epidemiologic investigation.

In conclusion, the detection of this novel HuCV2 among IDUs raises question about its origin, prevalence, and pathogenicity in humans. In addition, HuCV2 might circulate in animals, and detection in humans may have resulted from spillover through unknown routes. Thus, screening for HuCV2 infection in animals, especially those that closely interact with humans, could be considered to determine its potential origin and host range.

**Acknowledgments**

We thank Zhizhong Song and Min Chen for their assistance. We also thank Xiaoling Zhang for her help with design of the quantitative PCR.

This study was supported by National Natural Science Foundation of China (grant nos. 32170147, 31900158, and U1302224); the Key Research and Development Program of China (grant nos. 2021YFC2300902 and 2021YFC2301303) and Yunnan (grant nos. 202103AQ100001 and 202102AA310055); and the Key Program of the Chinese Academy of Sciences (grant no. KJZD-SW-L11-02-03).

## About the Author

Dr. Li is an associate professor at Shanghai Public Health Clinical Center at Fudan University. His primary research interests are emerging viruses and the role of the virome in human health and diseases.

**References**

1. Dong XP, Soong L. Emerging and re-emerging zoonoses are major and global challenges for public health. Zoonoses. 2021;1. https://doi.org/10.15212/ZOONOSES-2021-0001
2. Dharmarajan G, Li R, Chanda E, Dean KR, Dirzo R, Jakobsen KS, et al. The animal origin of major human infectious diseases: what can past epidemics teach us about preventing the next pandemic? Zoonoses. 2022;2. https://doi.org/10.15212/ZOONOSES-2021-0028
3. Harvey E, Holmes EC. Diversity and evolution of the animal virome. Nat Rev Microbiol. 2022;20:321–34. https://doi.org/10.1038/s41579-021-00665-x
4. Breitbart M, Delwart E, Rosario K, Segalés J, Varsani A, Ictv Report C; ICTV Report Consortium. ICTV virus taxonomy profile: Circoviridae. J Gen Virol. 2017;98:1997–8. https://doi.org/10.1099/jgv.0.000871
5. Niu G, Chen S, Li X, Zhang L, Ren L. Advances in crosstalk between porcine circoviruses and host. Viruses. 2022;14:1419. https://doi.org/10.3390/v14071419
6. Krüger L, Längin M, Reichart B, Fiebig U, Kristiansen Y, Prinz C, et al. Transmission of porcine circovirus 3 (PCV3) by xenotransplantation of pig hearts into baboons. Viruses. 2019;11:650. https://doi.org/10.3390/v11070650
7. Turlewicz-Podbielska H, Augustyniak A, Pomorska-Mól M. Novel porcine circoviruses in view of lessons learned from porcine circovirus type 2—epidemiology and threat to pigs and other species. Viruses. 2022;14:261. https://doi.org/10.3390/v14020261
8. Li Y, Cao L, Ye M, Xu R, Chen X, Ma Y, et al. Plasma virome reveals blooms and transmission of anellovirus in intravenous drug users with HIV-1, HCV, and/or HBV infections. Microbiol Spectr. 2022;10:e0144722. https://doi.org/10.1128/spectrum.01447-22
9. Li L, Kapoor A, Slikas B, Bamidele OS, Wang C, Shaukat S, et al. Multiple diverse circoviruses infect farm animals and are commonly found in human and chimpanzee feces. J Virol. 2010;84:1674–82. https://doi.org/10.1128/JVI.02109-09
10. Li L, Assanangkornchai S, Duo L, McNeil E, Li J. Risk behaviors, prevalence of HIV and hepatitis C virus infection and population size of current injection drug users in a China–Myanmar border city: results from a respondent-driven sampling survey in 2012. PLoS One. 2014;9:e106899. https://doi.org/10.1371/journal.pone.0106899
11. Pang W, Zhang C, Duo L, Zhou YH, Yao ZH, Liu FL, et al. Extensive and complex HIV-1 recombination between B′, C and CRF01_AE among IDUs in south-east Asia. AIDS. 2012; 26:1121–9. https://doi.org/10.1097/QAD.0b013e3283522c97

Address for correspondence: Chiyu Zhang, Shanghai Public Health Clinical Center, Fudan University, Caolang Rd 2901, Shanghai, 201508, China; email: chiyu_zhang1999@163.com; or Yong-Tang Zheng, Key Laboratory of Animal Models and Human Disease Mechanisms, Kunming Institute of Zoology, Chinese Academy of Sciences, Longxin Rd 17, Kunming, 650223, China; email: zhengyt@mail.kiz.ac.cn

# Severe *Streptococcus equi* Subspecies *zooepidemicus* Outbreak from Unpasteurized Dairy Product Consumption, Italy

Serena Bosica, Alexandra Chiaverini, Maria Elisabetta De Angelis, Antonio Petrini, Daniela Averaimo, Michele Martino, Marco Rulli, Maria Antonietta Saletti, Maria Chiara Cantelmi, Franco Ruggeri, Fabrizio Lodi, Paolo Calistri, Francesca Cito, Cesare Cammà, Marco Di Domenico, Antonio Rinaldi, Paolo Fazii, Fabrizio Cedrone, Giuseppe Di Martino, Patrizia Accorsi, Daniela Morelli, Nicola De Luca, Francesco Pomilio, Giustino Parruti, Giovanni Savini

During November 2021–May 2022, we identified 37 clinical cases of *Streptococcus equi* subspecies *zooepidemicus* infections in central Italy. Epidemiologic investigations and whole-genome sequencing showed unpasteurized fresh dairy products were the outbreak source. Early diagnosis by using sequencing technology prevented the spread of life-threatening *S. equi* subsp. *zooepidemicus* infections.

*Streptococcus equi* subspecies *zooepidemicus* is a β-hemolytic streptococcus expressing Lancefield group C antigen and is 1 of 3 *S. equi* subspecies. *S. equi* subsp. *zooepidemicus* is an opportunistic pathogen that can infect domestic animals, pets, and wildlife (*1*–*6*). Sporadic human cases have been reported (*7*), characterized by clinical manifestations that vary from meningitis to sepsis. Human infection generally occurs through direct contact with infected animals or by consumption of contaminated unpasteurized milk or other dairy products (*8*–*10*). We report a large *S. equi* subsp. *zooepidemicus* outbreak in Italy.

Author affiliations: Istituto Zooprofilattico Sperimentale Abruzzo e Molise "G. Caporale," Teramo, Italy (S. Bosica, A. Chiaverini, M.E. De Angelis, A. Petrini, D. Aberaimo, M. Martino, M. Rulli, M.A. Saletti, M.C. Cantemi, P. Calistri, F. Cito, C. Cammà, M. Di Domenico, A. Rinaldi, D. Morelli, F. Pomilio, G. Savini); University of Teramo, Teramo (M.C. Cantelmi, F. Cito); Azienda USL di Pescara, Pescara, Italy (F. Ruggeri, F. Lodi, G. Di Martino, P. Accorsi, N. De Luca); Presidio Ospedaliero "Santo Spirito," Pescara (P. Fazii, F. Cedrone, G. Parruti)

DOI: https://doi.org/10.3201/eid2905.221338

## The Study

During November 2021–February 2022, *S. equi* subsp. *zooepidemicus* infections were detected in 18 hospitalized patients who resided in a limited area within the province of Pescara, Italy (Figure 1). A wide range of clinical manifestations were observed in the patients, including septicemia, pharyngitis, arthritis, uveitis, and endocarditis. Five of those patients died from severe meningitis. For most cases, *S. equi* subsp. *zooepidemicus* bacteremia was accompanied by ≥1 additional localized bacterial site. *S. equi* subsp. *zooepidemicus* was detected in various patient specimens, including articular effusions and cerebrospinal fluid, that were tested by hospital laboratories. A task force consisting of physicians, veterinarians, epidemiologists, scientists, microbiologists, and communication experts was created and coordinated by the local competent authority to evaluate the outbreak.

We conducted an active investigation of *S. equi* subsp. *zooepidemicus* cases, defined as patients with laboratory-confirmed infection. We identified 37 outbreak cases over a 7-month period. We completed interviews of 36 patients or their relatives by using telephone-administered questionnaires. Patients were 6–98 (median 79) years of age. Male (n = 16) and female (n = 21) patients were similarly represented (Table 1). We obtained 21 bacteria isolates from 19 hospitalized patients that were sent to Istituto Zooprofilattico Sperimentale in Teramo, Italy. We identified bacteria species by using a Biotyper matrix-assisted laser desorption/ionization time-of-flight mass spectrometer (Bruker, https://www.bruker.com).

We performed whole-genome sequencing for 21 isolates by using the Illumina platform (Illumina,

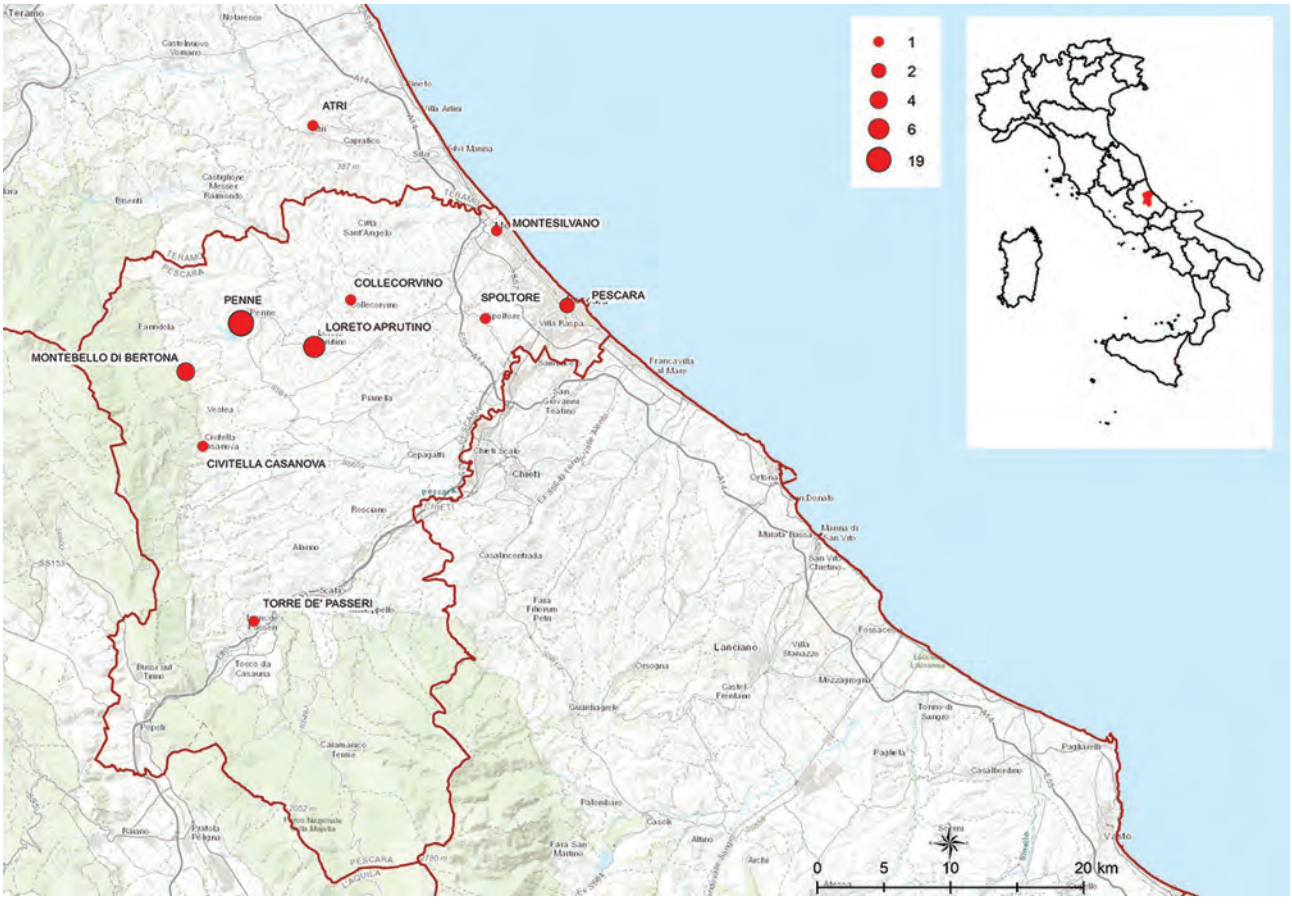


**Figure 1.** Location of residential areas in the province of Pescara and neighboring zones where outbreak cases were found in study of severe *Streptococcus equi* subspecies *zooepidemicus* outbreak from unpasteurized dairy product consumption, Italy, during November 2021–May 2022. Sizes of red dots indicate numbers (N = 37) of patients infected by location. Inset shows the outbreak area in the Vestina region of central Italy.

https://www.illumina.com) with a setting of 300 cycles (150-bp paired-end reads) (*11*). After read quality checks, we confirmed all clinical strains were *S. equi* subsp. *zooepidemicus* by using the KmerFinder tool (*12*). We assigned sequence type (ST) 61 to trains by using a multilocus sequence typing scheme (*13*) (https://pubmlst.org/streptococcus-zooepidemicus).

We confirmed correlations between human strains by performing single-nucleotide polymorphism (SNP) analysis through the US Food and Drug Administration Center for Food Safety and Applied Nutrition pipeline (*14*) and by using MinION technology (*15*) to obtain a hybrid genome from an outbreak strain as a reference. We found that all 21 clinical strains were closely related (0–3 SNPs), implying involvement of a unique source strain in the observed human cases. Moreover, the antimicrobial susceptibility test performed on all human strains gave identical results, confirming the hypothesis that 1 source strain was responsible for all human cases.

An extensive investigation was performed by public health, veterinary, and food hygiene services to identify the infection source. Epidemiologic analysis showed that 31 patients consumed soft or semi-soft cheeses purchased from local producers or dealers. A total of 8 local dairy food business operators were inspected. Samples of raw bulk milk (from cows and sheep), fresh cheese from unpasteurized and pasteurized milk, and water were obtained from each operator and sent to Istituto Zooprofilattico Sperimentale, Teramo, for bacteria detection. We cultured the samples and isolated *Streptococcus* spp. from sheep blood agar after incubation for 24 ±1 h at 37°C ±1°C in a 5% $CO_2$ enriched atmosphere. We tested all samples by using Genesig real-time PCR kits (Primerdesign Ltd, http://www. primerdesign.co.uk). We performed species identification and whole-genome sequencing as described for human samples. We detected *S. equi* subsp. *zooepidemicus* in an unpasteurized bulk cow milk sample taken from 1 dairy producer selected within the outbreak area. That

**Table 1.** Patient characteristics in study of severe *Streptococcus equi* subspecies *zooepidemicus* outbreak from unpasteurized dairy product consumption in central Italy during November 2021–May 2022*

| Characteristics | Value |
|---|---|
| Total no. patients | 37 |
| Patients with symptoms | 35 (94.6) |
| Hospitalized patients | 23 (62.2) |
| Patient deaths† | 5 (13.5) |
| Male patients | 16 (43.2) |
| Age range (median), y | 6–98 (79) |
| Age group, y | |
| ≤15 | 1 |
| 16–39 | 1 |
| 40–59 | 4 |
| 60–79 | 12 |
| ≥80 | 19 |
| Symptoms | |
| Fever | 27 (75) |
| Diarrhea | 6 (16.7) |
| Headache | 5 (13.9) |
| Vomiting | 4 (11.1) |
| Septicemia | 3 (8.3) |
| Cystitis | 2 (5.6) |
| Pharyngitis | 2 (5.6) |

*Values are no. (%) patients except as indicated.
†Number of hospitalized patients who died.

operator was then officially inspected and sampled by local competent authorities; a total of 18 *S. equi* subsp. *zooepidemicus* strains were isolated from 2 bulk milk tanks and 2 cured raw milk cheese samples. Genome sequences from those samples were also ST61; SNP analysis showed the 18 strains clustered with the clinical strains, indicating a strong correlation between the operator- and human-derived strains.

After *S. equi* subsp. *zooepidemicus* was identified as the pathogen responsible for the human cases, we reviewed data from the Istituto Zooprofilattico Sperimentale strain library. We found a strain that was isolated from the milk of a cow with mastitis in November 2021; the animal belonged to the same operator whose products tested positive. After sequencing, the strain was also identified as ST61 (Table 2) and clustered with the other trains isolated from human patients and raw milk products (Figure 2).

On the basis of epidemiologic and laboratory analyses, local competent authorities established measures to limit and prevent *S. equi* subsp. *zooepidemicus* spread by the end of February 2022. All dairy products were recalled from the market and local dealers and ripening cheeses were destroyed; local authorities required pasteurization of milk intended for cheese production.

## Conclusions

We report epidemiologic, microbiologic, and genomic findings from a *S. equi* subsp. *zooepidemicus* outbreak that involved 37 patients in Italy. We found strong genomic correlation between strains isolated from case-patients, unpasteurized milk and dairy products, and milk from infected cows that clearly indicated a zoonotic infection source. Questionnaire and laboratory data showed that human infections were caused by consuming unpasteurized fresh cheese produced from infected milk cows. We were unable to trace the origin of infection back to specific dairy food business operator livestock. The farmer who had the positive cow referred to construction work in the barn during October–November 2021, which might have caused stress, predisposing the animal to mastitis. A possible reactivation of a latent *S. equi* subsp. *zooepidemicus* infection cannot be excluded. Identifying the source of infection in a relatively short time enabled a rapid

**Table 2.** Metadata of 40 *Streptococcus equi* subspecies *zooepidemicus* strains typed by whole genome sequencing in study of severe outbreak from unpasteurized dairy product consumption, Italy*

| Identification no. | Matrix† |
|---|---|
| 2022.TE.21853.1.2 | Clinical specimen |
| 2022.TE.22318.1.2 | Clinical specimen |
| 2022.TE.22322.1.2 | Clinical specimen |
| 2022.TE.22324.1.2 | Clinical specimen |
| 2022.TE.22326.1.2 | Clinical specimen |
| 2022.TE.22327.1.2 | Clinical specimen |
| 2022.TE.22328.1.2 | Clinical specimen |
| 2022.TE.22330.1.2 | Clinical specimen |
| 2022.TE.22331.1.2 | Clinical specimen |
| 2022.TE.22332.1.2 | Clinical specimen |
| 2022.TE.22333.1.2 | Clinical specimen |
| 2022.TE.22334.1.2 | Clinical specimen |
| 2022.TE.23898.1.2 | Clinical specimen |
| 2022.TE.23902.1.2 | Mastitis milk |
| 2022.TE.24532.1.2 | Clinical specimen |
| 2022.TE.24549.1.2 | Clinical specimen |
| 2022.TE.25015.1.2 | Bulk tank raw milk no. 1 |
| 2022.TE.25536.1.2 | Clinical specimen |
| 2022.TE.26663.1.2 | Clinical specimen |
| 2022.TE.26664.1.2 | Clinical specimen |
| 2022.TE.28098.1.2 | Cured raw milk cheese no. 1 |
| 2022.TE.28099.1.2 | Cured raw milk cheese no. 1 |
| 2022.TE.28100.1.2 | Cured raw milk cheese no. 1 |
| 2022.TE.28101.1.2 | Cured raw milk cheese no. 1 |
| 2022.TE.28102.1.2 | Cured raw milk cheese no. 1 |
| 2022.TE.28103.1.2 | Cured raw milk cheese no. 1 |
| 2022.TE.28109.1.2 | Bulk tank raw milk no. 2 |
| 2022.TE.28111.1.2 | Bulk tank raw milk no. 2 |
| 2022.TE.28113.1.2 | Bulk tank raw milk no. 2 |
| 2022.TE.28116.1.2 | Bulk tank raw milk no. 2 |
| 2022.TE.28118.1.2 | Bulk tank raw milk no. 2 |
| 2022.TE.28119.1.2 | Bulk tank raw milk no. 2 |
| 2022.TE.28121.1.2 | Bulk tank raw milk no. 2 |
| 2022.TE.28123.1.2 | Bulk tank raw milk no. 2 |
| 2022.TE.29463.1.2 | Clinical specimen |
| 2022.TE.30851.1.2 | Clinical specimen |
| 2022.TE.30876.1.2 | Clinical specimen |
| 2022.TE.31297.1.2 | Cured raw milk cheese no. 2 |
| 2022.TE.31300.1.2 | Cured raw milk cheese no. 2 |
| 2022.TE.31302.1.2 | Cured raw milk cheese no. 2 |

*All 40 samples were sequence type 61.
†Strains were isolated from 2 samples each (nos. 1 and 2) taken from bulk tank raw milk and cured raw milk cheese.

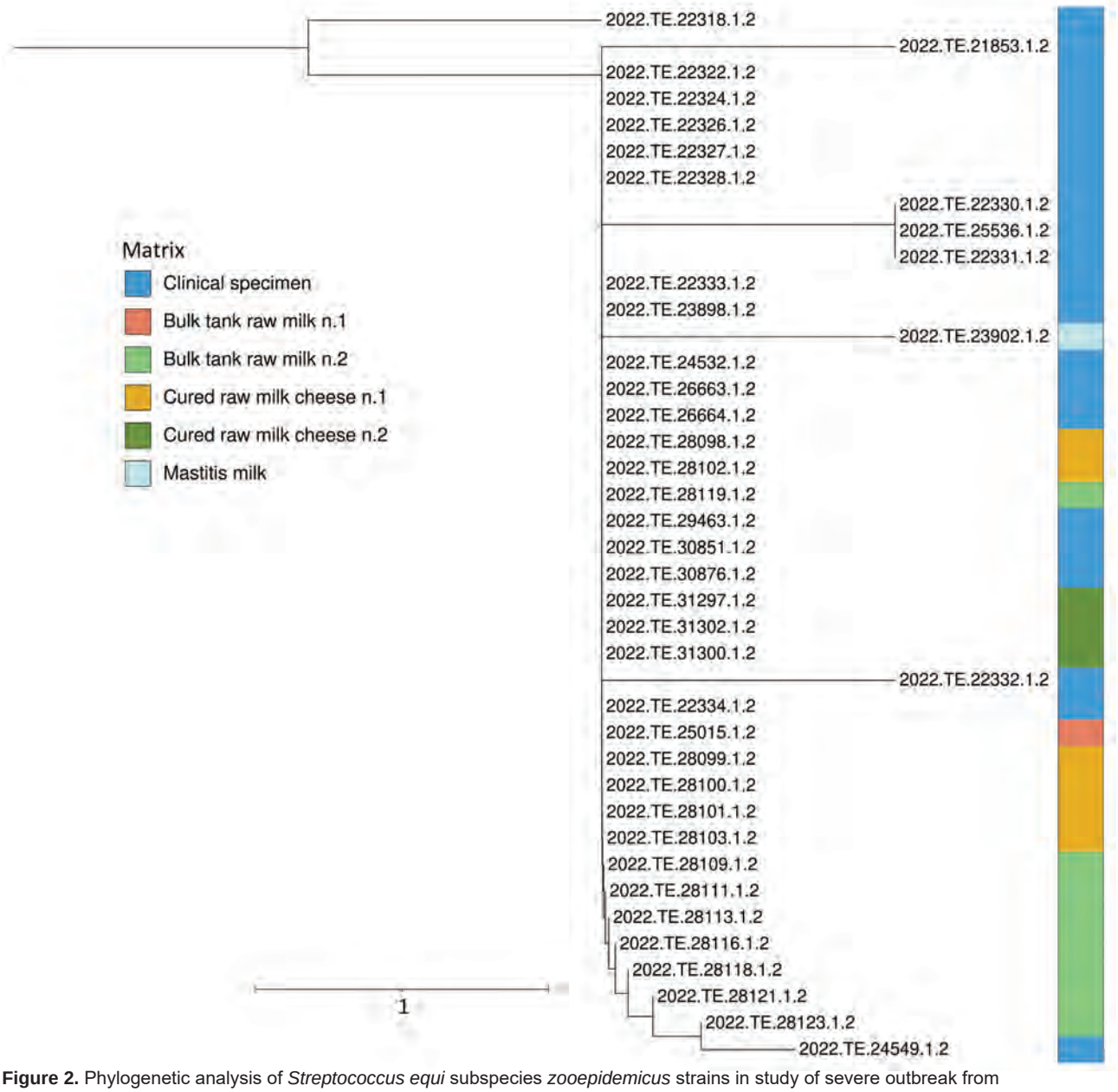


**Figure 2.** Phylogenetic analysis of *Streptococcus equi* subspecies *zooepidemicus* strains in study of severe outbreak from unpasteurized dairy product consumption, Italy. We performed whole-genome sequencing and single-nucleotide polymorphism analysis of 40 *S. equi* subsp. *zooepidemicus* strains isolated from clinical and dairy food samples (Table 2). Tree was generated by using the neighbor-joining method. Different colors indicate the different types of samples. Strains were isolated from 2 samples each taken from bulk tank raw milk and cured raw milk cheese. Tree shows clinical specimen sequences clustered with those from dairy products. Scale bar indicates nucleotide substitutions per site.

response that prevented further cases in the community. However, the outbreak in Italy was considered the largest and most severe outbreak associated with the consumption of unpasteurized fresh cheese that has been reported.

In summary, our study implicates *S. equi* subsp. *zooepidemicus* as a possible zoonotic pathogen and highlights the bacterium's virulence in humans. Awareness of individual anamnestic information and, in particular, possible contacts with domestic animals or recent consumption of unpasteurized dairy products was crucial for managing this outbreak. Equally important and of extreme value was the One Health interdisciplinary approach used to find solutions and solve community concerns. Further research is needed to gain insights into

pathogenic characteristics of the strain responsible for the outbreak. Early diagnosis and identification of bacteria by using molecular methodologies will improve medical treatment outcomes, enable timely epidemiologic disease surveillance, and prevent spread of life-threatening infections.

## About the Author

Ms. Bosica is a biologist at the Istituto Zooprofilattico Sperimentale dell'Abruzzo e del Molise "G. Caporale" in Teramo, Italy. Her interests focus on food matrix analysis for major foodborne pathogens and genetically modified organisms.

## Reference

1. Skive B, Rohde M, Molinari G, Braunstein TH, Bojesen AM. *Streptococcus equi* subsp. *zooepidemicus* invades and survives in epithelial cells. Front Cell Infect Microbiol. 2017;7:465. https://doi.org/10.3389/fcimb.2017.00465
2. Costa MO, Lage B. *Streptococcus equi* subspecies *zooepidemicus* and sudden deaths in swine, Canada. Emerg Infect Dis. 2020;26:2522–4. https://doi.org/10.3201/eid2610.191485
3. Sharp MW, Prince MJ, Gibbens J. *S zooepidemicus* infection and bovine mastitis. Vet Rec. 1995;137:128. https://doi.org/10.1136/vr.137.5.128-b
4. Las Heras A, Vela AI, Fernández E, Legaz E, Domínguez L, Fernández-Garayzábal JF. Unusual outbreak of clinical mastitis in dairy sheep caused by *Streptococcus equi* subsp. *zooepidemicus*. J Clin Microbiol. 2002;40:1106–8. https://doi.org/10.1128/JCM.40.3.1106-1108.2002
5. Pisoni G, Zadoks RN, Vimercati C, Locatelli C, Zanoni MG, Moroni P. Epidemiological investigation of *Streptococcus equi* subspecies *zooepidemicus* involved in clinical mastitis in dairy goats. J Dairy Sci. 2009;92:943–51. https://doi.org/10.3168/jds.2008-1548
6. Blum S, Elad D, Zukin N, Lysnyansky I, Weisblith L, Perl S, et al. Outbreak of *Streptococcus equi* subsp. *zooepidemicus* infections in cats. Vet Microbiol. 2010;144:236–9. https://doi.org/10.1016/j.vetmic.2009.12.040
7. Baracco GJ. Infections caused by group C and G streptococcus (*Streptococcus dysgalactiae* subsp. equisimilis and others): epidemiological and clinical aspects. Microbiol Spectr. 2019;7. PubMed https://doi.org/10.1128/microbiolspec.GPP3-0016-2018
8. Kuusi M, Lahti E, Virolainen A, Hatakka M, Vuento R, Rantala L, et al. An outbreak of *Streptococcus equi* subspecies *zooepidemicus* associated with consumption of fresh goat cheese. BMC Infect Dis. 2006;6:36. https://doi.org/10.1186/1471-2334-6-36
9. Francis AJ, Nimmo GR, Efstratiou A, Galanis V, Nuttall N. Investigation of milk-borne *Streptococcus zooepidemicus* infection associated with glomerulonephritis in Australia. J Infect. 1993;27:317–23. https://doi.org/10.1016/0163-4453(93)92358-4
10. Torres RSLA, Santos TZ, Bernardes AFL, Soares PA, Soares ACC, Dias RS. Outbreak of glomerulonephritis caused by *Streptococcus zooepidemicus* SzPHV5 type in Monte Santo de Minas, Minas Gerais, Brazil. J Clin Microbiol. 2018;56:e00845-18. https://doi.org/10.1128/JCM.00845-18
11. Chiaverini A, Guidi F, Torresi M, Acciari VA, Centorotola G, Cornacchia A, et al. Phylogenetic analysis and genome-wide association study applied to an Italian *Listeria monocytogenes* outbreak. Front Microbiol. 2021;12:750065. https://doi.org/10.3389/fmicb.2021.750065
12. Larsen MV, Cosentino S, Lukjancenko O, Saputra D, Rasmussen S, Hasman H, et al. Benchmarking of methods for genomic taxonomy. J Clin Microbiol. 2014;52:1529–39. https://doi.org/10.1128/JCM.02981-13
13. Webb K, Jolley KA, Mitchell Z, Robinson C, Newton JR, Maiden MCJ, et al. Development of an unambiguous and discriminatory multilocus sequence typing scheme for the *Streptococcus zooepidemicus* group. Microbiology. 2008;154:3016–24. PubMed https://doi.org/10.1099/mic.0.2008/018911-0
14. Davis S, Pettengill JB, Luo Y, Payne J, Shpuntoff A, Rand H, et al. CFSAN SNP pipeline: an automated method for constructing SNP matrices from next-generation sequence data. PeerJ Comput Sci. 2015;1:e20. https://doi.org/10.7717/peerj-cs.20
15. Neal-McKinney JM, Liu KC, Lock CM, Wu WH, Hu J. Comparison of MiSeq, MinION, and hybrid genome sequencing for analysis of *Campylobacter jejuni*. Sci Rep. 2021;11:5676. https://doi.org/10.1038/s41598-021-84956-6

Address for correspondence: Alexandra Chiaverini, Istituto Zooprofilattico Sperimentale Abruzzo e Molise "G. Caporale," Via Campo Boario, 64100, Teramo, Italy; email: a.chiaverini@izs.it

# Characteristics and Treatment of *Gordonia* spp. Bacteremia, France

Alia Barthel,[1] Axel Ursenbach,[1] Charlotte Kaeuffer,[1] Christelle Koebel, Alain Gravet, Dominique De Briel, Jacqueline Dubois, Elina Haerrel, Estelle Rougier,[2] Victor Gerber[1,3]

Systemic *Gordonia* spp. infections are rare and occur mostly among immunocompromised patients. We analyzed 10 cases of *Gordonia* bacteremia diagnosed in 3 tertiary care centers in France to assess risk factors, treatment, and clinical outcomes. Most patients were cured within 10 days by using β-lactam antimicrobial therapy and removing central catheters.

*Gordonia* is a slow-growing, gram-positive aerobic bacillus of the order *Mycobacteriales*. More than 40 species of this ubiquitous environmental bacterium have been described, few of which seem to infect humans (*1*). Some localized, postoperative, or traumatic infections have been described (*2*,*3*). Among immunocompromised patients, systemic bloodstream infections, although relatively uncommon, can be caused by contaminated biofilm adherent on endovascular devices (*4*,*5*). However, cases of secondary infection are more uncommon.

*Gordonia* bacteremia is not well understood because of its rarity; in addition, blood cultures may not be positive until ≥4 days after infection (*6*). The use of 16S ribosomal RNA gene sequencing has improved *Gordonia* identification rates over results from other, often insufficient, standard laboratory tests, which sometimes led to misidentification (*7*). Because no standardized recommendations for treatment exist, reported cases have been managed heterogeneously (*4*,*5*); a single treatment regimen, a 4–6-week course of an aminoglycoside combined with a carbapenem or fluoroquinolone, developed based on a 5-case series study and a literature review, has been proposed (*7*). Because some cases of severe infections have been described (*8*), to clarify risk factors and management options, we initiated this investigation describing patient characteristics to examine treatment outcomes from cases of *Gordonia* bacteremia. Our study was approved by the Ethics Committee of Medicine, Odontology and Pharmacy Faculties and Hospitals of the University Hospital of Strasbourg (project no. CE-2022-112) and declared to the Commission Nationale Informatique et Libertés.

## The Study

We retrospectively reviewed medical records from 2 tertiary care centers and 1 university hospital in northeast France. Our main purpose was to assess how *Gordonia* bacteremia cases had been managed. Our secondary purpose was to identify risk factors associated with infection. We requested information from the laboratory database of each center to collect all blood cultures testing positive for *Gordonia* spp. during January 1, 2010–May 31, 2021. We included patients with blood cultures positive for *Gordonia* sampled while hospitalized in one of the centers during the study period. We sought informed consent by mailing information about the study to patients or the parents of pediatric patients. We excluded persons opposed to participation and adults under legal guardianship or conservatorship. From medical files, we collected data on underlying diseases and immunodeficiency; presence and type of long-lasting intravascular device use, if any; clinical characteristics; antimicrobial susceptibility; treatments; and outcomes. We considered outcomes favorable when complete clinical cure was achieved, as determined by normalization of blood tests and repeated negative blood

Author affiliations: Hôpitaux universitaires de Strasbourg, Strasbourg, France (A. Barthel, A. Ursenbach, C. Koebel, E. Rougier); Groupement Hospitalier de Mulhouse et Sud-Alsace, Mulhouse, France (C. Kaeuffer, A. Gravet); Hôpitaux Civils de Colmar, Colmar, France (D. de Briel, J. Dubois, E. Haerrel, V. Gerber)

DOI: https://doi.org/10.3201/eid2905.221901

[1]These authors contributed equally to this article.

[2]Current affiliation: Hôpital Saint-Antoine, Assistance Publique des Hôpitaux de Paris, Paris, France.

[3]Current affiliation: Hôpitaux universitaires de Strasbourg, Strasbourg, France.

cultures. We sought relapses that occurred through May 31, 2022, or death of the patient.

We included 10 patients (median 49 years of age), among whom 7 had immunodeficiency and 6 had immunosuppression factors, most commonly severe malnutrition or long-term corticosteroid therapy (Tables 1, 2). Fever was the most common clinical sign; no secondary infection site was reported among case-patients. Healthcare providers considered *Gordonia* a contaminant in medical records from 5 cases; 4 patients had no central venous catheter, 3 were immunocompetent, and 1 had controlled HIV infection. We identified subspecies *G. sputi*, *G. bronchialis*, *and G. aichiensis*. Despite 16S rRNA gene sequencing, among 3 case-patients bacterium identification was limited to the genus level (i.e., *Gordonia* spp.). Nine patients were empirically prescribed antimicrobial therapy, mostly with third-generation cephalosporins and β-lactam/β-lactamase inhibitor combinations, for a median duration of 15 days. All *Gordonia* spp. were susceptible to treatment in all cases. In the 3 cases in which a long-term catheter had been removed, apyrexia without relapse was obtained within a few days of device removal; median treatment period was shorter, 13 days (range 0–15 days), for those patients who had their catheters removed than for patents who had not had their catheters removed (15 days, range 7–32 days). One patient was cured, as assessed by clinical improvement and negative repeated blood sample, by device removal alone without antimicrobial treatment. Of 2 patients who experienced relapses, 1 recovered promptly after delayed catheter removal, and the other exhibited febrile relapses with no other obvious cause of fever (e.g., venous thrombosis), clinical signs of catheter infection, and repeated blood cultures positive for *Gordonia*.

In this study, based on clinical information from an extensive series of *Gordonia* bacteremia infections among patients from several hospitals, we analyzed risk factors regardless of patient immune status. We found the main risk factors were immunosuppression and indwelling catheters of any type, consistent with findings from previous reviews (*4*,*5*,*7*,*9*). The preferred treatment, with third-generation cephalosporins or β-lactam/β-lactamase inhibitor combinations for 1–2 weeks, was of shorter duration than in most previous cases and did not match the proposed treatment

**Table 1**. Description of *Gordonia* bacteremia cases, 2010–2021, France*

| Patient no. | Patient age/sex | Immune deficiency factors | CVC type | Clinical signs | Species (no. positive samples) | AMR | Treatment | Time, d | CVC removed |
|---|---|---|---|---|---|---|---|---|---|
| Favorable outcome† | | | | | | | | | |
| 1 | 36 y/M | HIV, nephrotic syndrome | HD | CVC inflammation | *Gordonia* sp. (1) | None | None | 0 | Yes |
| 2 | 3 y/M | Hemopathy, corticosteroid, methotrexate | Central port | Fever | *G. bronchialis* (1)‡ | None | CAZ, AMC | 7 | No |
| 3 | 86 y/M | None | None | Fever, cough | *G. sputi* (1)‡ | None | AMC, 3GC | 10 | NA |
| 4 | 56 y/F | HIV | None | Fever | *G. sputi* (1) ‡ | None | 3GC | 10 | NA |
| 5 | 67 y/F | Malnutrition, hemopathy, cancer | TCVC | Acute kidney failure | *Gordonia* sp. (1) | None | 3GC, VAN | 15 | Yes |
| 6 | 75 y/M | None | None | Fever, chills | *G. aichiensis* (1)‡ | ERY, FA, FOF | PEN G, AMOX | 15 | NA |
| 7 | 42 y/M | Cirrhosis splenectomy, corticosteroid | Central port | Fever | *G. sputi* (2) | PEN, SMX | TZP, VAN | 15 | No |
| 8 | 2y/M | None | None | Knee arthritis | *Gordonia* sp. (1)‡ | § | CFZ, AMK; Tr 2¶: cefaclor | 5<br>30 | NA |
| Relapse# | | | | | | | | | |
| 9 | 3 mo/M | Nephrotic syndrome, low IgG | TCVC | Fever | *G. bronchialis* (1) | ERY, FA, FOF | AMOX; Tr 2¶: JM, polyvalent Ig | 8<br>5 | Yes |
| 10 | 61 y/F | Immunosuppressive regimen, corticosteroid, malnutrition | Central port | Fever, angiocolitis, port inflammation | *G. sputi* (2) | § | CPFX, TZP; Tr 2¶: IMP, AMK, VAN; Tr 3¶: 3GC, GEN | 15<br>10<br>7 | No |

*3GC, 3rd generation cephalosporin; AMC, amoxicillin-clavulanic acid; AMK, amikacin; AMOX, amoxicillin; AMR, antimicrobial resistance; CAZ, ceftazidime; CFZ, cefazolin; CPFX, ciprofloxacin; CVC, central venous catheter; ERY, erythromycin; FA, fusidic acid; FOF, fosfomycin; GEN, gentamicin; HD, hemodialysis; IMP, imipenem; JM, josamycin; NA, not applicable; PEN, penicillin; SMX, sulfamethoxazole; TCVC, tunneled CVC; TZP, piperacillin/tazobactam; VAN, vancomycin.
†Favorable outcome required clinical and biologic cure and repeated negative blood sample (when available), without relapse until the end of the study period (May 31, 2022).
‡In medical record, *Gordonia* sp. was considered a contaminant with no clinical significance.
§Antimicrobial susceptibility testing not performed.
¶Treatment regimens after relapse.
#Relapses through May 31, 2022.

described earlier (*4*,*7*). However, the antimicrobial drugs used were effective against all *Gordonia* species. Among 8 case-patients with favorable outcomes, only 2 received an aminoglycoside, suggesting it might be reserved for use in more severe cases. The strains' susceptibility to many antimicrobials, except for lesser susceptibility to sulfamethoxazole in some other studies, agrees with data published elsewhere (*4*,*7*,*10*,*11*). Effects after removing the central venous catheter were inconsistent but removal generally resulted in favorable outcomes. Positive effects from catheter removal has also been reported in other cases and reviews (*7*,*9*,*12*).

Our retrospective analysis of case management reflects difficulties related to late identification and uncertainty about the truly infectious nature of *Gordonia* spp. bacteria. Differences exist in the literature about whether a single positive blood culture should be considered contamination or actual infection. Some subspecies, such as *G. terrae* or *G. sputi*, seem more likely to be responsible for bacteremias; other species, such as *G. bronchialis*, are rarely represented (*4*,*5*). In this study, *G. terrae* was present in 4 patients, but *G. bronchialis* was found in at least 2 cases and was strongly considered a probable cause of true infection.

In reported cases in which *Gordonia* was considered a contaminant, empiric antimicrobial therapy was stopped after the few days required to achieve negative blood culture results, after which clinical signs regressed and repeated blood samples were negative in most cases (*9*,*13*). Whatever the significance of this microbiological result, whether specific *Gordonia* spp. are agents of infection or contaminants, short-term treatment may suffice in the absence of a central catheter or if subsequent blood samples are consistently negative, as described elsewhere (*13*).

One limitation of our retrospective study was that data were collected over >11 years, during which time variations in risk level and management strategies may have altered the experience of the small number (n = 10) of included case-patients. In addition, including cases in which *Gordonia* spp. were considered potential contaminates rather than causes of infection may have positively biased treatment outcomes. No cultures were taken from catheters to confirm their role in bacteremia, and antimicrobial susceptibility was not tested in all cases. Thus, some resistant strains might exist that have not yet been identified.

**Table 2.** Characteristics of patients with *Gordonia* bacteremia, 2010–2021, France*

| Variables | No. (%) |
|---|---|
| Median age, y (range) | 49 (0.25–86.0) |
| Sex, n = 10 | |
| M | 6 (60.0) |
| F | 4 (40.0) |
| Immunodeficiency factors, n = 7 | |
| Corticosteroids | 3 (42.8) |
| Severe malnutrition | 4 (57.1) |
| Hemodialysis | 2 (28.6) |
| Hemopathy | 2 (28.6) |
| Transplantation | 2 (28.6) |
| HIV | 2 (28.6) |
| Central venous catheter, n = 6 | |
| Central port | 3 (50.0) |
| Other central catheter | 3 (50.0) |
| Nosocomial infection,* n = 10 | |
| Y | 3 (30.0) |
| N | 7 (70.0) |
| Microbiological identification, n = 10 | |
| *G. bronchialis* | 2 (20.0) |
| *G. sputi* | 4 (40.0) |
| *G. aichiensis* | 1 (10.0) |
| Antimicrobial therapy, n = 9 | |
| 3rd/4th-generation cephalosporin | 6 (66.6) |
| β-lactam with β-lactamase inhibitor | 4 (44.4) |
| Glycopeptide | 3 (33.3) |
| Penicillin | 2 (22.2) |
| Aminoside | 2 (22.2) |
| Carbapenem | 1 (11.1) |
| Fluoroquinolone | 1 (11.1) |
| Median treatment duration, d (range) | 15 (0–35) |
| CVC ablation, n = 6 | 3 (50.0) |
| Outcome, n = 10 | |
| Favorable outcome† | 8 (80.0) |
| Relapse‡ | 2 (20.0) |

*Clinical signs of infection starting ≥48 h after hospitalization
†Favorable outcome required clinical and biologic cure and repeated negative blood sample, without relapse through the end of the study period (May 31, 2022).
‡Relapse without cure through May 31, 2022.

## Conclusions

In the absence of consensus recommendations, standardizing management of bacteremias caused by *Gordonia* spp. should be pursued. In cases with positive blood cultures, *Gordonia* should be considered infective in immunosuppressed case-patients, especially when a central venous catheter is present. β-lactam monotherapy can be empirically prescribed with aminoglycoside added in severe cases. After any central venous catheter has been removed and clinical signs improve, discontinuing antimicrobial drugs after 1–2 weeks should be considered. However, further studies are needed to clarify treatment duration and make more precise recommendations about managing a central catheter, especially when it is not removable. Studies on the effectiveness of antimicrobial lock therapy would help, possibly combined with lengthened systemic antimicrobial therapy. Given the sometimes serious nature of infection, especially among immunocompromised patients, developing treatment strategies and increasing awareness among clinicians of *Gordonia*-caused bacteremias would be of public health benefit.

## About the Author

Dr. Barthel is a medical resident who works in infectious diseases in the University Hospital of Strasbourg, with a focus on implanted devices infections.

## References


1. Arenskötter M, Bröker D, Steinbüchel A. Biology of the metabolically diverse genus *Gordonia.* Appl Environ Microbiol. 2004;70:3195–204. https://doi.org/10.1128/AEM.70.6.3195-3204.2004
2. Blanc V, Dalle M, Markarian A, Debunne MV, Duplay E, Rodriguez-Nava V, et al. *Gordonia terrae*: a difficult-to-diagnose emerging pathogen? J Clin Microbiol. 2007;45: 1076–7. https://doi.org/10.1128/JCM.02394-06
3. Choi R, Strnad L, Flaxel CJ, Lauer AK, Suhler EB. *Gordonia bronchialis*–associated endophthalmitis, Oregon, USA. Emerg Infect Dis. 2019;25:1017–9. https://doi.org/10.3201/eid2505.180340
4. Drzyzga O. The strengths and weaknesses of *Gordonia*: a review of an emerging genus with increasing biotechnological potential. Crit Rev Microbiol. 2012;38:300–16. https://doi.org/10.3109/1040841X.2012.668134
5. Johnson JA, Onderdonk AB, Cosimi LA, Yawetz S, Lasker BA, Bolcen SJ, et al. *Gordonia bronchialis* bacteremia and pleural infection: case report and review of the literature. J Clin Microbiol. 2011;49:1662–6. https://doi.org/10.1128/JCM.02121-10
6. Riegel P, Ruimy R, de Briel D, Eichler F, Bergerat JP, Christen R, et al. Bacteremia due to *Gordona sputi* in an immunocompromised patient. J Clin Microbiol. 1996;34:2045–7. https://doi.org/10.1128/jcm.34.8.2045-2047.1996
7. Blaschke AJ, Bender J, Byington CL, Korgenski K, Daly J, Petti CA, et al. *Gordonia* species: emerging pathogens in pediatric patients that are identified by 16S ribosomal RNA gene sequencing. Clin Infect Dis. 2007;45:483–6. https://doi.org/10.1086/520018
8. Grisold AJ, Roll P, Hoenigl M, Feierl G, Vicenzi-Moser R, Marth E. Isolation of *Gordonia terrae* from a patient with catheter-related bacteraemia. J Med Microbiol. 2007;56(Pt 12):1687–8. https://doi.org/10.1099/jmm.0.47388-0
9. Lai CC, Wang CY, Liu CY, Tan CK, Lin SH, Liao CH, et al. Infections caused by *Gordonia* species at a medical centre in Taiwan, 1997 to 2008. Clin Microbiol Infect. 2010;16:1448–53. https://doi.org/10.1111/j.1469-0691.2010.03085.x
10. Buchman AL, McNeil MM, Brown JM, Lasker BA, Ament ME. Central venous catheter sepsis caused by unusual *Gordona* (*Rhodococcus* species): identification with a digoxigenin-labeled rDNA probe. Clin Infect Dis. 1992;15:694–7. https://doi.org/10.1093/clind/15.4.694
11. Moser BD, Pellegrini GJ, Lasker BA, Brown JM. Pattern of antimicrobial susceptibility obtained from blood isolates of a rare but emerging human pathogen, *Gordonia polyisoprenivorans.* Antimicrob Agents Chemother. 2012;56:4991–3. https://doi.org/10.1128/AAC.01251-12
12. Pham AS, Dé I, Rolston KV, Tarrand JJ, Han XY. Catheter-related bacteremia caused by the nocardioform actinomycete *Gordonia terrae.* Clin Infect Dis. 2003;36:524–7. https://doi.org/10.1086/367543
13. Ramanan P, Deziel PJ, Wengenack NL. *Gordonia* bacteremia. J Clin Microbiol. 2013;51:3443–7. https://doi.org/10.1128/JCM.01449-13


Address for correspondence: Victor Gerber, Service de réanimation médicale, Hôpitaux Civils de Colmar, 39 avenue de la Liberté 68000 Colmar, France; email: victor_gerber@hotmail.fr

# No Substantial Histopathologic Changes in *Mops condylurus* Bats Naturally Infected with Bombali Virus, Kenya

Lauri Kareinen, Niina Airas, Sara T. Kotka, Moses M. Masika, Kirsi Aaltonen, Omu Anzala, Joseph Ogola, Paul W. Webala, Olli Vapalahti, Tarja Sironen, Kristian M. Forbes

We found similar mild perivascular inflammation in lungs of Bombali virus–positive and –negative *Mops condylurus* bats in Kenya, indicating the virus is well-tolerated. Our findings indicate *M. condylurus* bats may be a reservoir host for Bombali virus. Increased surveillance of these bats will be important to reduce potential virus spread.

Despite extensive research since the first documented human Ebola virus (EBOV) disease outbreak in 1976, animal species involved and mechanisms by which ebolaviruses spillover to humans remains enigmatic. Bats have been implicated as reservoir hosts (*1*), a suspicion supported by several types of evidence, none of which is strong alone. Evidence includes serologic and, rarely, PCR-based diagnosis of infection in wild bats; capacity for some bat species to become asymptomatically infected after laboratory inoculations; and close phylogenetic relationship between ebolaviruses and Marburg virus, which has an established fruit bat reservoir (*2*–*4*). Lack of specimens from naturally occurring ebolavirus-infected bats has precluded assessment of tissue pathology and virus distribution at a cellular level, which would normally provide insights into host roles and transmission mechanisms and permit comparisons and validation of experimental infection models.

We analyzed tissue specimens collected from wild bats in Kenya that were naturally infected with Bombali virus (BOMV), the sixth and most recent ebolavirus identified. First reported in *Mops condylurus* and *Chaerephon pumilus* bats in 2018 (*5*), BOMV has been detected by PCR at low prevalence (0.5%–6.7%) in excreta or tissue samples from *M. condylurus* bats in 4 distinct locations across sub-Saharan Africa (*5*–*8*), representing a consistent ebolavirus–bat host relationship. No further reports of infected *C. pumilus* bats or that BOMV causes human disease have been published (*6*), although prudence is warranted. All other ebolaviruses found in Africa can cause severe human disease (only 1 nonfatal infection with Taï Forest virus has been reported) (*9*). BOMV binds to the same Niemann-Pick C1 endosomal receptor for cell entry as other ebolaviruses (*5*), and recent serologic evidence of a cleared human BOMV infection has been reported (*10*).

## The Study

We captured bats by using mist nets in Busia and Taita-Taveta counties in Kenya during 2019. In brief, we captured, euthanized, and dissected bats and collected tissue samples. We screened the samples for BOMV by using reverse transcription PCR (RT-PCR) as described previously (*8*). We placed bat carcasses that had remaining tissues immediately into 10% buffered formalin, transferred them to 80% ethanol after 24–48 h, and shipped those to the University of Helsinki, Finland, for histopathologic assessment. We analyzed 3 BOMV RT-PCR–positive and 6 BOMV RT-PCR–negative *M. condylurus* bats; the BOMV-negative bats were used as negative controls (*8*).

We trimmed and processed formalin-fixed tissue samples from the 9 bats for histologic evaluation. We routinely stained tissue sections with hematoxylin and eosin. After heat-induced antigen retrieval, we also immunolabeled sections from each tissue sample

Author affiliation: Finnish Food Authority, Helsinki, Finland (L. Kareinen); University of Helsinki, Helsinki, Finland (L. Kareinen, N. Airas, S.T. Kotka, K. Aaltonen, O. Vapalahti, T. Sironen); University of Nairobi, Nairobi, Kenya (M.M. Masika, O. Anzala, J. Ogola); Maasai Mara University, Narok, Kenya (P.W. Webala); University of Arkansas, Fayetteville, Arkansas, USA (K.M. Forbes)

DOI: https://doi.org/10.3201/eid2905.221336

**Table.** Lesions found in bat tissues stained with hematoxylin and eosin in study of histopathologic changes in *Mops condylurus* bats naturally infected with BOMV, Kenya*

| Organ | Lesion | BOMV-infected† | Uninfected† |
|---|---|---|---|
| Lung | Mild perivascular and interstitial mononuclear infiltrates | 3/3 | 4/6 |
| | Scattered thickening of pulmonary vessel walls | 2/3 | 1/6 |
| | Mild peribronchial mononuclear infiltrates | 1/3 | 2/6 |
| Liver | Mild perivascular mononuclear infiltrates | 3/3 | 1/6 |
| | Moderate chronic neutrophilic infiltrates | 0/3 | 3/6 |
| | Mild hepatocellular vacuolation | 0/3 | 1/6 |
| Heart | Mild mononuclear infiltrates | 0/3 | 2/6 |
| Stomach | Moderate chronic granulomatous gastritis with intralesional nematodes | 0/3 | 2/6 |

*Comparisons were made between BOMV RT-PCR–positive (BOMV-infected) and RT-PCR–negative (uninfected) *Mops condylurus* bats. Lesions likely represent spontaneous background lesions, except for the neutrophilic infiltrates in liver tissue and granulomatous gastritis nematodiasis. BOMV, Bombali virus.
†Number of bats with lesions/total number of bats per group (infected or uninfected).

by using polyclonal rabbit serum against EBOV matrix protein VP40 (*11*) (Appendix, https://wwwnc.cdc.gov/EID/article/29/5/22-1336-App1.pdf). No BOMV isolates were available for this study, which necessitated finding a suitable, cross-reactive surrogate virus. EBOV is the most studied member in the ebolavirus family, and EBOV antibodies are readily available. EBOV and BOMV have ≈75% amino acid identity match within the VP40 protein (Appendix Figure); therefore, we considered EBOV VP40 to be a suitable antigen to detect BOMV VP40.

We observed mild perivascular and interstitial mononuclear infiltrates in all 3 BOMV RT-PCR–positive *M. condylurus* bat lung samples stained with hematoxylin and eosin (Table; Figure 1). We found similar nonspecific mononuclear infiltrates in lung tissue from 4/6 BOMV RT-PCR–negative bats. Overall, we did not observe substantial histopathologic changes in the lungs of any bats that suggested severe acute BOMV disease. We found that both BOMV RT-PCR–positive and RT-PCR–negative bats had mixed acute and chronic inflammatory lesions in other internal organs. Those lesions likely reflect natural disease in wild bats, and we interpreted those findings as incidental.

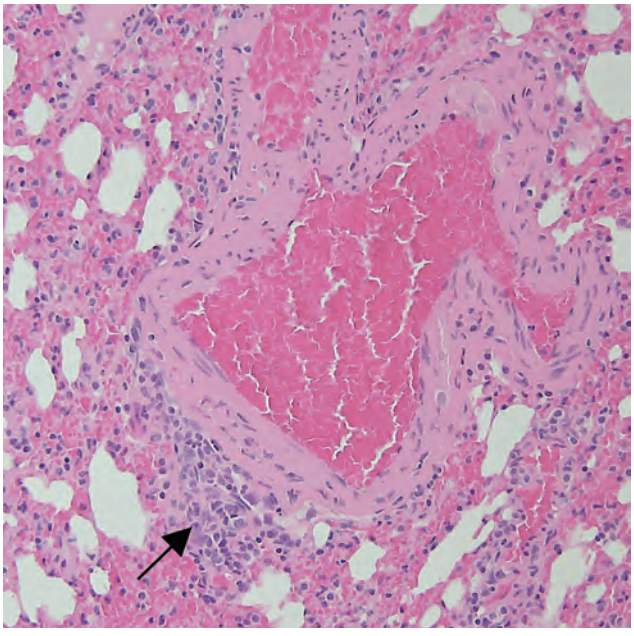

**Figure 1.** Representative tissue section from the lung of a bat in study of histopathologic changes in *Mops condylurus* bats naturally infected with Bombali virus, Kenya. We stained lung tissue sections from a Bombali virus–positive bat with hematoxylin and eosin. Arrow indicates focal minimal mononuclear cell infiltrate. Original magnification ×200.

We did not find an association between immunologic detection of EBOV VP40 antigen, used as a surrogate for BOMV, and overt histopathologic findings in BOMV RT-PCR–positive *M. condylurus* bats. We previously showed that BOMV RT-PCR–positive bats developed antibodies reactive against ebolavirus proteins from Zaire ebolavirus–infected cells (*6*). In this study, both BOMV RT-PCR–positive and RT-PCR–negative bats displayed only mild mononuclear infiltrates in lungs and exhibited mild inflammatory changes in other tissues. Those changes indicate that BOMV infection is likely well-tolerated by *M. condylurus* bats, which is consistent with expectations of a reservoir host (*12*,*13*). However, our findings should be interpreted with caution. For example, we cannot exclude the possibility that the BOMV RT-PCR–positive *M. condylurus* bats we captured had less severe pathology than infected wild conspecifics or that negative control bats might have been previously infected but cleared any residual viral antigens.

Positive immunolabeling with EBOV VP40 polyclonal antibody was observed in lungs from 2 of 3 BOMV RT-PCR–positive bats (Figure 2) but not in other tissues or in any tissues from BOMV RT-PCR–negative bats. Immunopositive-labeling occurred as granular cytoplasmic aggregates in interstitial macrophages. In contrast to their usual role in protective immunity, macrophages are directly

implicated in the pathogenesis of several viruses as either viral repositories or sites of active replication and dissemination (*14*). In humans, pathogenic filoviruses rely heavily on macrophages, which are major replication sites (*15*). Our findings suggest that macrophages might provide similar chronic reservoirs for BOMV infections in bats. However, without data showing active replication, we cannot rule out that our findings in macrophages have a different interpretation.

Positive immunolabeling in bat lungs was consistent with previous RT-PCR results (*8*). Lungs are the most frequent tissue infected by BOMV and have markedly higher viral loads than other tissues (*6*–*8*). Of note, 1 lung sample, 2 spleen samples, and 1 liver sample that were BOMV RT-PCR–positive (*8*) had no detectible EBOV VP40 antigen. Those results are most likely because immunohistochemistry has lower sensitivity than PCR, and a non–BOMV-specific antigen was used.

## Conclusions

We propose that the presence of BOMV in macrophages and absence of acute pathology typical of ebolaviruses (necrosis, thrombosis, hemorrhage, and edema) support bats as a chronic subclinical BOMV reservoir with the potential for infection and sporadic virus excretion. However, the small number of samples, absence of recovery of infectious virus, and lack of longitudinal data make interpretation of our results difficult. As for all wildlife-borne ebolaviruses, no direct evidence currently exists regarding the transmission route of BOMV between susceptible hosts. Our findings suggest the mode of transmission involves activation of replication in either macrophages or other cells and virus dispersal through saliva droplets or feces. The identification of BOMV infection in lungs and occasional virus presence in intestines further supports this hypothesis (*6*–*8*).

In summary, we showed EBOV-VP40 immunolabeling, acting as a cross-reactive surrogate for BOMV antigen, in pulmonary macrophages of wild BOMV RT-PCR–positive *M. condylurus* bats and an absence of substantial concurrent pathologic findings. Our results support *M. condylurus* bats as reservoir hosts for ebolaviruses and highlight the importance of bat surveillance to understand and mitigate potential emerging disease risks.

This research was supported by the Finnish Cultural Foundation, Jenny and Antti Wihuri Foundation, Jane and Aatos Erkko Foundation, Academy of Finland (grant no. 318726), Helsinki University Hospital Funds, University of Arkansas Funds, and Arkansas Biosciences Institute. Bat trapping and sample collections were conducted under permits from the National Commission for Science, Technology and Innovation (permit no. NACOSTI/P/18/76501/22243) and Kenya Wildlife Service (permit no. KWS/BRM/500). Bat sample imports to Finland were approved by the Finnish Food Safety Authority (EVIRA; approval nos. 4250/0460/2016 and 2809/0460/2018).

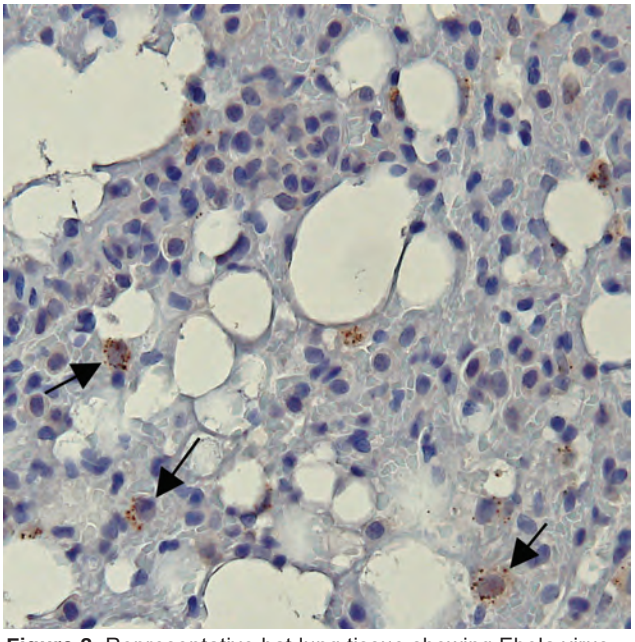

**Figure 2.** Representative bat lung tissue showing Ebola virus (EBOV) cytoplasmic granules in study of histopathologic changes in *Mops condylurus* bats naturally infected with Bombali virus, Kenya. We labeled lung tissue sections by using rabbit polyclonal serum against EBOV matrix protein VP40 and detected antigen by using a chromogenic horse radish peroxidase substrate. The sections were then counterstained with hematoxylin. Arrow indicates granular cytoplasmic immunopositivity for EBOV VP40 antigen. Original magnification ×400. VP, viral protein.

## About the Author

Dr. Kareinen is a veterinarian and PhD student at the University of Helsinki, Finland. His research interests focus on the maintenance and circulation of zoonotic viruses in bat hosts.

## References

1. Hayman DTS. Bats as viral reservoirs. Annu Rev Virol. 2016;3:77–99. https://doi.org/10.1146/annurev-virology-110615-042203
2. Swanepoel R, Leman PA, Burt FJ, Zachariades NA, Braack LE, Ksiazek TG, et al. Experimental inoculation of plants and animals with Ebola virus. Emerg Infect Dis. 1996;2:321–5. https://doi.org/10.3201/eid0204.960407

3. Leroy EM, Kumulungui B, Pourrut X, Rouquet P, Hassanin A, Yaba P, et al. Fruit bats as reservoirs of Ebola virus. Nature. 2005;438:575–6. https://doi.org/10.1038/438575a
4. Towner JS, Amman BR, Sealy TK, Carroll SAR, Comer JA, Kemp A, et al. Isolation of genetically diverse Marburg viruses from Egyptian fruit bats. PLoS Pathog. 2009;5:Se1000536. https://doi.org/10.1371/journal.ppat.1000536
5. Goldstein T, Anthony SJ, Gbakima A, Bird BH, Bangura J, Tremeau-Bravard A, et al. The discovery of Bombali virus adds further support for bats as hosts of ebolaviruses. Nat Microbiol. 2018;3:1084–9. https://doi.org/10.1038/s41564-018-0227-2
6. Forbes KM, Webala PW, Jääskeläinen AJ, Abdurahman S, Ogola J, Masika MM, et al. Bombali virus in *Mops condylurus* bat, Kenya. Emerg Infect Dis. 2019;25:955–7. https://doi.org/10.3201/eid2505.181666
7. Karan LS, Makenov MT, Korneev MG, Sacko N, Boumbaly S, Yakovlev SA, et al. Bombali virus in *Mops condylurus* bats, Guinea. Emerg Infect Dis. 2019;25:1774–5. https://doi.org/10.3201/eid2509.190581
8. Kareinen L, Ogola J, Kivistö I, Smura T, Aaltonen K, Jääskeläinen AJ, et al. Range expansion of Bombali virus in *Mops condylurus* bats, Kenya, 2019. Emerg Infect Dis. 2020;26:3007–10. https://doi.org/10.3201/eid2612.202925
9. Osterholm MT, Moore KA, Kelley NS, Brosseau LM, Wong G, Murphy FA, et al. Transmission of Ebola viruses: what we know and what we do not know. mBio. 2015;6:e00137. https://doi.org/10.1128/mBio.00137-15
10. Goldstein T, Belaganahalli MN, Syaluha EK, Lukusa JK, Greig DJ, Anthony SJ, et al. Spillover of ebolaviruses into people in eastern Democratic Republic of Congo prior to the 2018 Ebola virus disease outbreak. One Health Outlook. 2020;2:21. https://doi.org/10.1186/s42522-020-00028-1
11. Melén K, Kakkola L, He F, Airenne K, Vapalahti O, Karlberg H, et al. Production, purification and immunogenicity of recombinant Ebola virus proteins—a comparison of Freund's adjuvant and adjuvant system 03. J Virol Methods. 2017;242:35–45. https://doi.org/10.1016/j.jviromet.2016.12.014
12. Mandl JN, Ahmed R, Barreiro LB, Daszak P, Epstein JH, Virgin HW, et al. Reservoir host immune responses to emerging zoonotic viruses. Cell. 2015;160:20–35. https://doi.org/10.1016/j.cell.2014.12.003
13. Letko M, Seifert SN, Olival KJ, Plowright RK, Munster VJ. Bat-borne virus diversity, spillover and emergence. Nat Rev Microbiol. 2020;18:461–71. https://doi.org/10.1038/s41579-020-0394-z
14. Nikitina E, Larionova I, Choinzonov E, Kzhyshkowska J. Monocytes and macrophages as viral targets and reservoirs. Int J Mol Sci. 2018;19:2821. https://doi.org/10.3390/ijms19092821
15. Bray M, Geisbert TW. Ebola virus: the role of macrophages and dendritic cells in the pathogenesis of Ebola hemorrhagic fever. Int J Biochem Cell Biol. 2005;37:1560–6. https://doi.org/10.1016/j.biocel.2005.02.018

Address for correspondence: Kristian Forbes, Department of Biological Sciences, University of Arkansas, SCEN 601, 850 W Dickson St, Fayetteville, AR 16801, USA; email: kmforbes@uark.edu

# etymologia revisited

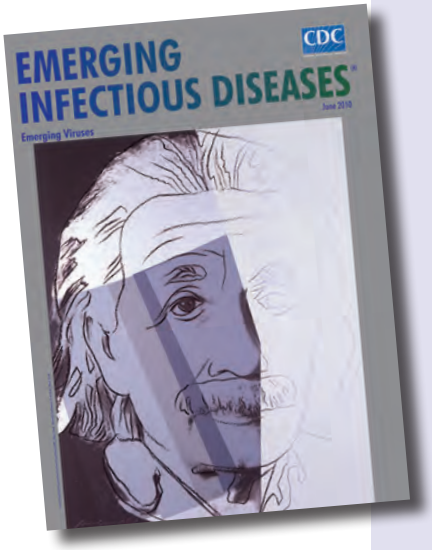


***Originally published in June 2010***

## Lassa Virus

[lah sə] virus

This virus was named after the town of Lassa at the southern end of Lake Chad in northeastern Nigeria, where the first known patient, a nurse in a mission hospital, had lived and worked when she contracted this infection in 1969. The virus was discovered as part of a plan to identify unknown viruses from Africa by collecting serum specimens from patients with fevers of unknown origin. Lassa virus, transmitted by field rats, is endemic in West Africa, where it causes up to 300,000 infections and 5,000 deaths each year.

**References:**

1 Frame JD, Baldwin JM Jr, Gocke DJ, Troup JM. Lassa fever, a new virus disease of man from West Africa. I. Clinical description and pathological findings. Am J Trop Med Hyg. 1970;19:670–6.
2. Mahy BW. The dictionary of virology, 4th ed. Burlington (MA): Elsevier; 2009.

***https://wwwnc.cdc.gov/eid/article/16/6/et-1606_article***

# Comparative Aerosol and Surface Stability of SARS-CoV-2 Variants of Concern

Trenton Bushmaker,[1] Claude Kwe Yinda,[1] Dylan H. Morris,[1] Myndi G. Holbrook, Amandine Gamble, Danielle Adney,[2] Cara Bushmaker, Neeltje van Doremalen, Robert J. Fischer, Raina K. Plowright, James O. Lloyd-Smith, Vincent J. Munster

SARS-CoV-2 transmits principally by air; contact and fomite transmission may also occur. Variants of concern are more transmissible than ancestral SARS-CoV-2. We found indications of possible increased aerosol and surface stability for early variants of concern, but not for the Delta and Omicron variants. Stability changes are unlikely to explain increased transmissibility.

Since the initial emergence of SARS-CoV-2 (lineage A), new lineages and variants have emerged (*1*), typically replacing previously circulating lineages. The World Health Organization has designated 5 virus variants as variants of concern (VOCs) (*2*). To assess whether the transmission advantage of new VOCs might have arisen partly from changes in aerosol and surface stability, we compared them directly with a lineage A ancestral virus (WA1 isolate).

## The Study

We evaluated the stability of SARS-CoV-2 variants in aerosols and on high-density polyethylene (to represent a common surface) and estimated their decay rates by using a Bayesian regression model (Appendix, https://wwwnc.cdc.gov/EID/article/29/5/22-1752-App1.pdf). We generated aerosols (<5 μm) containing SARS-CoV-2 with a 3-jet Collison nebulizer and fed them into a Goldberg drum to create an aerosolized environment (Video, https://wwwnc.cdc.gov/EID/article/29/5/22-1752-V1.htm), using an initial virus stock of $10^{5.75}$–$10^{6}$ 50% tissue-culture infectious dose ($TCID_{50}$) per mL. To measure surface stability, we deposited 50 μL containing $10^{5}$ $TCID_{50}$ of virus onto polypropylene.

For aerosol stability, we directly compared the exponential decay rate of different SARS-CoV-2 isolates (Table) by measuring virus titer at 0, 3, and 8 hours; the 8-hour time point was chosen through modeling to maximize information on decay rate given the observed 3-hour decay. We performed experiments as single runs (0-to-3 or 0-to-8 hours) and collected samples at start and finish to minimize virus loss and humidity changes from repeat sampling. We conducted all runs in triplicate. To estimate quantities of sampled virus, we analyzed air samples collected at 0, 3, or 8 hours post-aerosolization by quantitative reverse transcription PCR for the SARS-CoV-2 envelope (E) gene to quantify the genome copies within the samples. To determine the remaining concentration of infectious SARS-CoV-2 virions, we titrated samples on standard Vero E6 cells. To check robustness, we also titrated the samples on 2 Vero E6 TMPRSS2-expressing lines, yielding similar results (Appendix). We estimated exponential decay of infectious virus relative to the amount of remaining genome copies to account for particle settling and other physical loss of viruses, although we also estimated decay rates from uncorrected titration data as a robustness check, which yielded similar results (Appendix).

We recovered viable SARS-CoV-2 virus from the drum for all VOCs (Figure 1, panel A). The quantity of viable virus decayed exponentially over time (Figure 1, panel B). The half-life of the ancestral lineage WA1 in aerosols (posterior median value [2.5%–97.5%

Author affiliations: National Institute of Allergy and Infectious Diseases, National Institutes of Health, Hamilton, Montana, USA (T. Bushmaker, C.K. Yinda, M.G. Holbrook, D. Adney, N. van Doremalen, R.J. Fischer, V.J. Munster); Montana State University, Bozeman, Montana, USA (T. Bushmaker, R.K. Plowright); University of California, Los Angeles, California, USA (D.H. Morris, A. Gamble, J.O. Lloyd-Smith); Bitterroot Health—Daly Hospital, Hamilton (C. Bushmaker)

DOI: https://doi.org/10.3201/eid2905.221752

[1]These authors contributed equally to this article.

[2]Current affiliation: Lovelace Biomedical Research Institute, Albuquerque, New Mexico, USA.

**Table.** SARS-CoV-2 isolates used in study of comparative stability and their observed aerosol and surface half-lives*

| SARS-CoV-2 isolate | WHO label | PANGO label | GISAID/GenBank accession no. | Aerosol half-life, h | Surface half-life, h |
|---|---|---|---|---|---|
| hu/USA/CA_CDC_5574/2020 | | A | MN985325.1 | 3.2 9 (2.33–4.98) | 4.82 (4.23–5.49) |
| hCoV-19/USA/MT-RML-7/2020 | | B.1 | MW127503.1 | 3.99 (2.73–7.2) | 5.16 (4.48–5.96) |
| hCoV-19/England/204820464/2020 | Alpha | B.1.1.7 | EPI_ISL_683466 | 6.13 (3.14–27.5) | 5.13 (4.59–5.74) |
| hCoV-19/USA/MD-HP01542/2021 | Beta | B.1.351 | EPI_ISL_890360 | 5.13 (3.16–12.3) | 5.73 (5.01–6.72) |
| hCoV-19/USA/KY-CDC-2-4242084/2021 | Delta | B.1.617.2 | EPI_ISL_1823618 | 3.12 (2.29–4.73) | 4.38 (3.48–5.65) |
| hCoV-19/USA/WI-WSLH-221686/2021 | Omicron | B.1.1.529 | EPI_ISL_7263803 | 2.15 (1.35–4.04) | 3.58 (2.88–4.47) |

*The half-life of the aerosols or on surface is presented as posterior median value with posterior quantiles. WHO, World Health Organization.

posterior quantiles]) was 3.20 (2.33–4.98) hours. The B.1, Alpha, and Beta viruses appeared to have longer half-lives than WA1: 3.99 (2.73–7.20) hours for B.1, 6.13 (3.14–27.5) hours for Alpha, and 5.13 (3.16–12.3) hours for Beta. The half-life of Delta was similar to that of WA1: 3.12 (2.29–4.73) hours. The Omicron (BA.1) variant displayed a similar or decreased half-life compared with WA1: 2.15 (1.35–4.04) hours (Figure 1, panel B). To better quantify the magnitude and certainty of the change, we computed the posterior of the ratio for variant half-life to WA1 half-life for each variant (Figure 1, panel C). Estimated ratios were 1.25 (0.701–2.48) for B.1, 1.88 (0.859–8.75) for Alpha, 1.6 (0.838–4.01) for Beta, 0.978 (0.571–1.63) for Delta, and 0.659 (0.35–1.37) for Omicron. That is, initial spike protein divergence from WA1 (heuristically quantified by the number of amino acid substitutions) appeared to produce increased relative stability, but further evolutionary divergence reverted stability back to that of WA1, or even below it (Figure 1, panel C; Appendix Figures 1, 2).

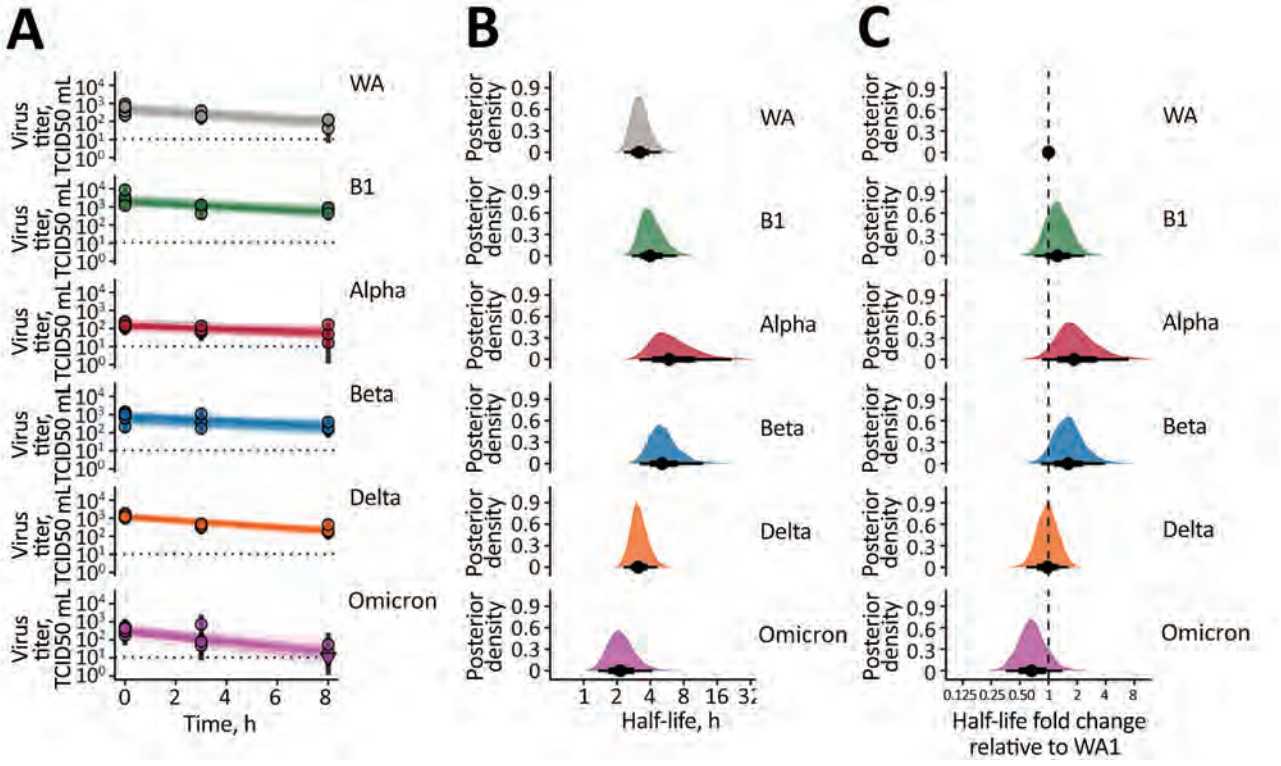


**Figure 1.** SARS-CoV-2 variant exponential decay in aerosolized form and corresponding half-lives. A) Regression lines representing predicted exponential decay of $\log_{10}$ virus titer over time compared with measured (directly inferred) virus titers. Points with black bars show individually estimated titer values (point: posterior median titer estimate; bar: 95% credible interval). Points at 3 hours and 8 hours are shifted up or down by the physical/noninactivation change in viral material estimated from quantitative reverse transcription PCR data (Appendix), to enable visual comparison with predicted decay (which reflects only inactivation effects). Semitransparent lines show random draws from the joint posterior distribution of the exponential decay rate and the drum run intercept (virus titer at $t = 0$); this visualizes the range of plausible decay patterns for each experimental condition. We performed 50 random draws and then plotted 1 line per draw for each drum run, yielding 300 plotted lines per variant. B) Inferred virus half-lives by variant, plotted on a logarithmic scale. Density plots show the shape of the posterior distribution. Dots show the posterior median half-life estimate and black lines show a 68% (thick) and 95% (thin) credible interval. C) Inferred ratio of variant virus half-lives to that of WA1 (fold-change), plotted on a logarithmic scale and centered on 1 (no change, dashed line). Dot shows the posterior median estimate and black lines show a 68% (thick) and 95% (thin) credible interval. $TCID_{50}$, 50% tissue culture infectious dose.

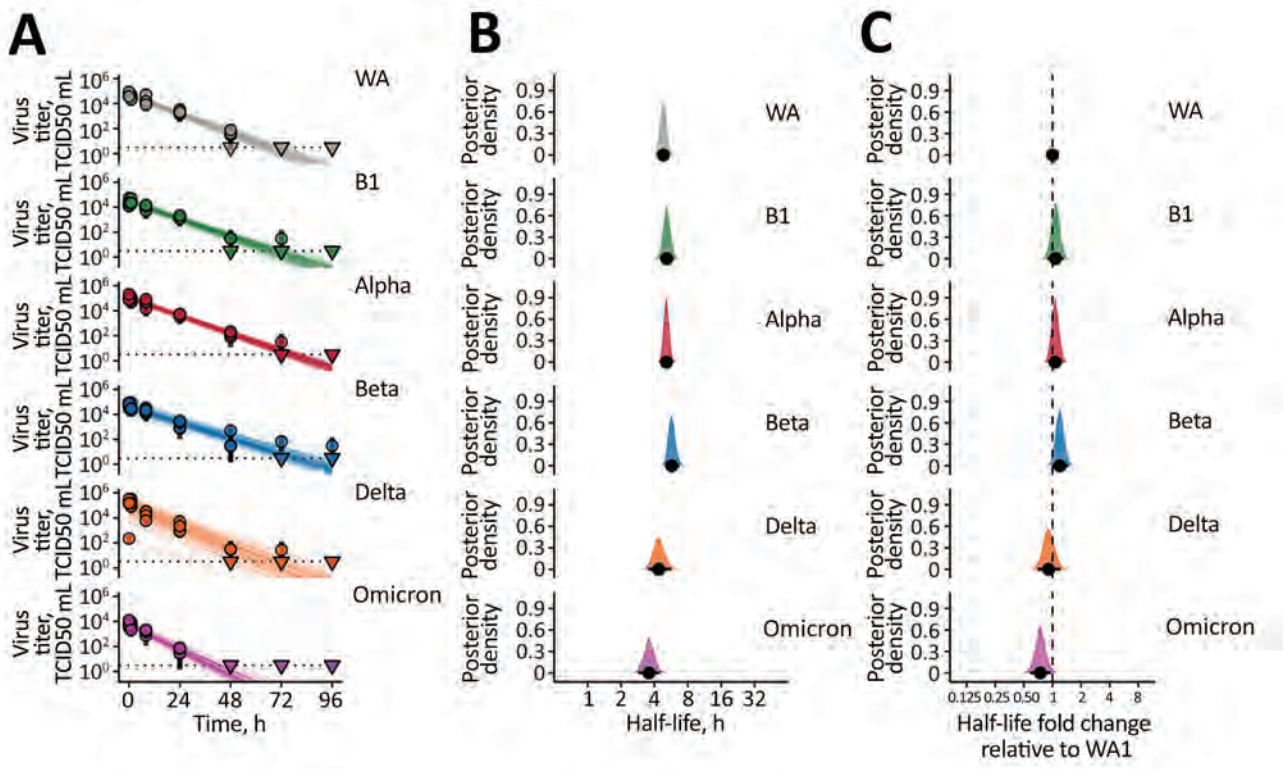


**Figure 2.** SARS-CoV-2 variant exponential decay on an inert surface and corresponding half-lives. A) Regression lines representing predicted exponential decay of $\log_{10}$ virus titer over time compared with measured (directly inferred) virus titers. Semitransparent lines show random draws from the joint posterior distribution of the virus exponential decay rate and the sample intercepts (virus titers at $t = 0$). We performed 50 random draws and then plotted 6 random initial titers per draw for each variant, yielding 300 plotted lines per variant. We chose a new group of 6 random initial titers for each new draw-variant pair. Points with black bars show individually estimated titer values (point: posterior median titer estimate; bar: 95% credible interval). Samples with no positive titration wells are plotted as triangles at the approximate LOD (dotted horizontal line). B) Inferred virus half-lives by variant, plotted on a logarithmic scale. Density plots show the shape of the posterior distribution. Dots show the posterior median half-life estimate and black lines show a 68% (thick) and 95% (thin) credible interval. C) Inferred ratio of variant virus half-lives to that of WA1 (fold-change), plotted on a logarithmic scale and centered on 1 (no change, dashed line). Dot shows the posterior median estimate and black lines show a 68% (thick) and 95% (thin) credible interval. $TCID_{50}$, 50% tissue culture infectious dose.

Next, we investigated surface stability of VOCs compared with the ancestral variant on polyethylene. Again, all variants exhibited exponential decay (Figure 2, panel A). We found a half-life of 4.82 (4.23–5.49) hours for WA1, similar to our previous estimates (Figure 2, panel B) (*3*). Early VOCs had slightly longer half-lives: 5.16 (4.48–5.96) hours for B.1, 5.13 (4.59–5.74) hours for Alpha, and 5.73 (5.01–6.72) hours for Beta (Figure 2, panel B). As with aerosols, Delta had a half-life similar to WA1 of 4.38 (3.48–5.65) hours and Omicron had a somewhat shorter half-life of 3.58 (2.88–4.47) hours (Figure 2, panel B). We again calculated posterior probabilities for the half-life ratios relative to WA1 (Figure 2, panel C). B.1 had a half-life ratio to WA1 of 1.07 (0.876–1.32), Alpha a half-life ratio of 1.07 (0.896–1.27), and Beta a half-life ratio of 1.19 (0.988–1.46). The ratios for Delta and Omicron were 0.912 (0.694–1.21) and 0.744 (0.578–0.965).

In both aerosol and surface results, the posterior 95% credible intervals for most ratios overlap 1. Experimental noise could possibly explain the apparent trend toward increased stability for B.1, Alpha, and Beta, although the clear bulk of posterior probability mass indicates greater half-lives. Conversely, the posterior ratios indicate clearly that Delta and Omicron are not markedly more stable than WA1 and might be less stable (particularly Omicron and particularly on surfaces).

## Conclusions

Several studies have analyzed the stability of SARS-CoV-2 on surfaces or in aerosols in a Goldberg rotating drum (*3*–*7*). Most have focused on the duration over which infectious virus could be detected. In this study, we paired a model-optimized experimental design with Bayesian hierarchical analysis

to systematically measure virus half-life across 6 SARS-CoV-2 variants and directly estimate relative half-lives with full error propagation. We found a small initial increase in aerosol stability from ancestral WA1 to the B.1, Alpha, and Beta variants, with some statistical uncertainty. However, we found that Delta has a half-life similar to that of WA1 and that Omicron likely has a shorter one. In surface measurements, the VOCs followed the same pattern of relative stability, confirming that the overall stability of SARS-CoV-2 variants is determined by similar factors in aerosols and on surfaces (*8*). Divergent results on the aerosol and surface stability of VOCs have been reported (*7*,*8*).

Our study suggests that aerosol stability is likely not a major factor driving the increase in transmissibility observed with several VOCs (*9*,*10*). The early rise in stability for B.1 and its descendants Alpha and Beta might have arisen incidentally from selection for other viral traits that favored higher transmission. Epidemiologic and experimental studies suggest that the window for transmission is typically relatively short (<1 hour), and thus a modest change in aerosol half-life would not have discernible epidemiologic effects (*11*). However, in specific contexts of enclosed spaces, it will remain vital to understand the temporal profile of transmission risks after the release of aerosols containing SARS-CoV-2 from an infected person. We conducted our experiments under laboratory conditions using tissue culture media, so biological factors potentially affecting decay (e.g., airway mucins and other components of airway-lining fluids) were not considered. Novel approaches studying aerosol microenvironments have reported initial rapid loss of SARS-CoV-2 infectiousness in the seconds after aerosolization (*12*); our work only addresses SARS-CoV-2 decay and stability over longer timescales, after the initial deposition loss has occurred.

Whereas evolutionary selection for previous variants favored high transmission among immunologically naive humans (*13*), since late 2021, global population-level selection has favored antigenic change (*14*) and the consequent ability to transmit among nonnaive persons. Our findings suggest that increased transmissibility through antigenic evolution might come at a tolerable cost to the virus in environmental stability. Overall, the differences in environmental stability among different VOCs, in aerosols or on surfaces, are unlikely to be driving variant population-level epidemiology.

This article was preprinted at https://doi.org/10.1101/2022.11.21.517352.

**Acknowledgments**

We thank Michele Adams for clinical specimen acquisition, Friederike Feldmann for experimental support, and Austin Athman for creation of the video. The following SARS-CoV-2 isolates were obtained through CDC: SARS-CoV-2/human/USA/WA-CDC-WA1/2020, Lineage A; BEI Resources, NIAID, NIH: SARS-CoV-2 variant Alpha (B.1.1.7) (hCoV320 19/England/204820464/2020, EPI_ISL_683466), contributed by Bassam Hallis, and variant Delta (B.1.617.2/) (hCoV-19/USA/KY-CDC-2-4242084/2021, EPI_ISL_1823618). Variant Beta (B.1.351) isolate name: hCoV-19/USA/MD-HP01542/2021, EPI_ISL_890360, was contributed by Johns Hopkins Bloomberg School of Public Health: Andrew Pekosz. Variant Omicron (B.1.1.529, alias BA.1) isolate name: hCoV-19/USA/GA-EHC-2811C/2021, EPI_ISL_7171744, was contributed by Emory University, Emory Vaccine Center: Mehul Suthar. We thank Andrew Pekosz, Mehul Suthar, Emmie de Wit, Brandi Williamson, Sujatha Rashid, Bassam Hallis, Ranjan Mukul, Kimberly Stemple, Bin Zhou, Natalie Thornburg, Sue Tong, Stacey Ricklefs, Sarah Anzick for generously sharing viruses and/or for propagating and sequence-confirming virus stocks.

This research was supported by the Intramural Research Program of the National Institute of Allergy and Infectious Diseases (NIAID), National Institutes of Health (NIH) and Defense Advanced Research Projects Agency DARPA PREEMPT # D18AC00031. Contributions of D.H.M., A.G. and J.L.S. were further supported by the National Science Foundation (DEB-1557022) and the UCLA AIDS Institute and Charity Treks. This work was part of NIAID's SARS-CoV-2 Assessment of Viral Evolution (SAVE) Program.

T.B., C.K.Y., A.G., D.H.M., R.J.F, V.M., and J.L.S. conceptualized the study; T.B., C.K.Y., M.H., and D.R.A., and R.J.F. carried out the laboratory experiments; C.I.B. and N.v.D. provided the resources; V.J.M. and R.K.P. supervised the study; T.B., C.K.Y., D.H.M., R.J.F., and A.G. curated the data; D.H.M., J.L-S. analyzed the data; T.B., C.K.Y., A.G., D.H.M., R.K.P., V.M., and J.L-S. wrote the initial draft of the manuscript, all authors reviewed and approved the final manuscript; and T.B., C.K.Y., and D.H.M made the visualizations.

## About the Author

Mr. Bushmaker is a biologist in NIAIDs Laboratory of Virology and is interested in high containment pathogens. Dr. Yinda is a postdoctoral research fellow in NIAIDs Laboratory of Virology interested in emerging viruses and their transmission potential.

## References


1. Heidari M, Sayfouri N, Jafari H. Consecutive waves of COVID-19 in Iran: various dimensions and probable causes. Disaster Med Public Health Prep. 2022;17:e136. https://doi.org/10.1017/dmp.2022.45
2. Konings F, Perkins MD, Kuhn JH, Pallen MJ, Alm EJ, Archer BN, et al. SARS-CoV-2 variants of interest and concern naming scheme conducive for global discourse. Nat Microbiol. 2021;6:821–3. https://doi.org/10.1038/s41564-021-00932-w
3. van Doremalen N, Bushmaker T, Morris DH, Holbrook MG, Gamble A, Williamson BN, et al. Aerosol and surface stability of SARS-CoV-2 as compared with SARS-CoV-1. N Engl J Med. 2020;382:1564–7. https://doi.org/10.1056/NEJMc2004973
4. Smither SJ, Eastaugh LS, Findlay JS, Lever MS. Experimental aerosol survival of SARS-CoV-2 in artificial saliva and tissue culture media at medium and high humidity. Emerg Microbes Infect. 2020;9:1415–7. https://doi.org/10.1080/22221751.2020.1777906
5. Fears AC, Klimstra WB, Duprex P, Hartman A, Weaver SC, Plante KS, et al. Persistence of severe acute respiratory syndrome coronavirus 2 in aerosol suspensions. Emerg Infect Dis. 2020;26:2168–71. https://doi.org/10.3201/eid2609.201806
6. Schuit M, Ratnesar-Shumate S, Yolitz J, Williams G, Weaver W, Green B, et al. Airborne SARS-CoV-2 is rapidly inactivated by simulated sunlight. J Infect Dis. 2020;222:564–71. https://doi.org/10.1093/infdis/jiaa334
7. Chin AWH, Lai AMY, Peiris M, Man Poon LL. Increased stability of SARS-CoV-2 Omicron variant over ancestral strain. Emerg Infect Dis. 2022;28:1515–7. https://doi.org/10.3201/eid2807.220428
8. Morris DH, Yinda KC, Gamble A, Rossine FW, Huang Q, Bushmaker T, et al. Mechanistic theory predicts the effects of temperature and humidity on inactivation of SARS-CoV-2 and other enveloped viruses. eLife. 2021;10:10. https://doi.org/10.7554/eLife.65902
9. Port JR, Yinda CK, Avanzato VA, Schulz JE, Holbrook MG, van Doremalen N, et al. Increased small particle aerosol transmission of B.1.1.7 compared with SARS-CoV-2 lineage A in vivo. Nat Microbiol. 2022;7:213–23. https://doi.org/10.1038/s41564-021-01047-y
10. Ulrich L, Halwe NJ, Taddeo A, Ebert N, Schön J, Devisme C, et al. Enhanced fitness of SARS-CoV-2 variant of concern Alpha but not Beta. Nature. 2022;602:307–13. https://doi.org/10.1038/s41586-021-04342-0
11. Jones TC, Biele G, Mühlemann B, Veith T, Schneider J, Beheim-Schwarzbach J, et al. Estimating infectiousness throughout SARS-CoV-2 infection course. Science. 2021;373:eabi5273. https://doi.org/10.1126/science.abi5273
12. Oswin HP, Haddrell AE, Otero-Fernandez M, Mann JFS, Cogan TA, Hilditch TG, et al. The dynamics of SARS-CoV-2 infectivity with changes in aerosol microenvironment. Proc Natl Acad Sci U S A. 2022;119:e2200109119. https://doi.org/10.1073/pnas.2200109119
13. Liu Y, Liu J, Plante KS, Plante JA, Xie X, Zhang X, et al. The N501Y spike substitution enhances SARS-CoV-2 infection and transmission. Nature. 2022;602:294–9. https://doi.org/10.1038/s41586-021-04245-0
14. van der Straten K, Guerra D, van Gils MJ, Bontjer I, Caniels TG, van Willigen HDG, et al. Antigenic cartography using sera from sequence-confirmed SARS-CoV-2 variants of concern infections reveals antigenic divergence of Omicron. Immunity. 2022;55:1725–1731.e4. https://doi.org/10.1016/j.immuni.2022.07.018


Address for correspondence: Vincent Munster, Rocky Mountain Laboratories, NIAID/NIH, 903S 4th St. Hamilton, MT 59840, USA, email: vincent.munster@nih.gov

# Poor Prognosis for Puumala Virus Infections Predicted by Lymphopenia and Dyspnea

Stefan Hatzl, Florian Posch, Marina Linhofer, Stephan Aberle, Ines Zollner-Schwetz, Florian Krammer, Robert Krause

We investigated a prospective cohort of 23 patients who had Puumala virus infection in Austria to determine predictors of infection outcomes. We reviewed routinely available clinical and laboratory parameters collected when patients initially sought care. Low absolute lymphocyte count and dyspnea were parameters associated with a severe course of infection.

Hantaviruses are emerging rodentborne pathogens that cause clinical illness in humans. During the past few decades, hantavirus infection outbreaks increased, demonstrating an emerging problem for healthcare systems (*1*). Human hantavirus infections cause 2 well-defined clinical syndromes: hemorrhagic fever with renal syndrome, caused by Old World hantaviruses originating in Europe and Asia; and hantavirus cardiopulmonary syndrome. Hemorrhagic fever with renal syndrome is characterized by acute renal failure, thrombocytopenia, and mortality rates of 0.1%–0.4%, and hantavirus cardiopulmonary syndrome is characterized by severe involvement of the respiratory and circulatory systems and case-fatality rates >30% (*1*).

Most cases of infection with hantavirus in Europe are caused by Puumala virus (PUUV) (*2*,*3*). Clinical manifestations of PUUV infection vary from subclinical, mild, and moderate to severe, with an urgent need for intensive care treatment. However, biomarkers or clinical parameters for risk stratification of PUUV infection are lacking. In this prospective cohort study, we aimed to clarify the prognostic value of routinely assessable clinical and laboratory values in PUUV infection requiring hospital admission.

Author affiliations: Medical University of Graz, Graz, Austria (S. Hatzl, F. Posch, M. Linhofer, I. Zollner-Schwetz, R. Krause); Medical University of Vienna, Vienna, Austria (S. Aberle); Icahn School of Medicine at Mount Sinai, New York, New York, USA (F. Krammer)

DOI: https://doi.org/10.2301/eid2905.221625

## The Study

This study was approved by the institutional review board of the Medical University of Graz (approval no. 33-329 ex 20/21). Written informed consent was obtained from all participants.

We performed a prospective, observational, pilot study, enrolling all consecutive adult patients admitted to the Department of Internal Medicine, Medical University of Graz, Austria, because of clinical suspicion of PUUV infection and detection of PUUV IgM by using point-of-care testing (Reagena POC PUUMALA IgM, https://www.reagena.com). We used a PUUV reverse transcription PCR as a confirmation test as described (*2*). Patient data were uniformly collected as described (*4*). We obtained laboratory, clinical, and radiologic data from our in-house electronic healthcare database system and from handwritten charts and inserted these data into a predefined electronic case report form by using REDCap electronic data capture (*5*,*6*). We defined a severe course of PUUV infection if a patient needed oxygen (<92% blood oxygen saturation while breathing ambient air) or hemodialysis or intensive care unit admission.

We performed statistical analyses by using Stata version 16.1 (StataCorp., https://www.stata.com). We report continuous data as medians (25th–75th percentiles) and summarized categorical data by using absolute frequencies and percentages. We applied rank-sum tests, $\chi^2$ tests, and Fisher exact tests to investigate the association between 1 continuous variable and 1 categorical variable and between 2 categorical variables. To identify variables associated with a severe course of PUUV infection among the 25 variables that were collected in the presence of multiple testing, we prespecified a Sidák corrected α of association, resulting in p

values ≤0.002 to indicate statistical significance. We used logistic models for univariate and multivariable modeling of PUUV infection severity and assessed the optimal cutoff to separate patients with and without severe course of PUUV infection by using a maximized Youdens index within a receiver operating characteristic analysis. The follow-up time was truncated at 90 days after diagnosis because no events were expected after this time interval. We computed overall survival of the cohort by using Kaplan-Meier estimators.

A total of 23 patients were included in the analysis (Table). Median age at diagnosis was 49 years (25th–75th percentile 34–59 years), and 6 (23%) patients were women. Five (22%) patients had underlying conditions (Table). Ten (44%) patients reported activities with a predisposition to rodents or rodent excreta. The most frequent symptom at diagnosis was fever, which was observed in 100% of the patients. The median body temperature at diagnosis was 39.5°C (25th–75th percentiles 39.0°C–39.7°C). Most (17/23, 74%) patients had headache and reported concomitant use of analgesics. All 3 patients who had dyspnea came to the hospital because of this primary symptom. Symptom duration was 2 (25th–75th percentile 1–3) days before admission to the hospital.

A severe course of the PUUV infection was observed in 5 (22%) of 23 patients. For these 5 patients, severe PUUV infection was diagnosed by need for oxygen therapy (n = 5), intensive care unit admission (n = 4), and renal replacement therapy (n = 2). Two of those 5 patients had to be treated with extracorporeal membrane oxygenation. Median length of in-patient hospital stay was 7 (25th–75th percentiles 4–12) days. One patient died from multiorgan failure after PUUV infection, corresponding to a 90-day overall survival rate of 96% (95% CI 73%–99%).

Dyspnea, predisposition to contact with rodents, shortened prothrombin time, and low absolute lymphocyte (ALC) count when patients sought care were associated with severe PUUV infection at the 5% level. However, because of the prespecified α corrected for multiple testing, we identified only dyspnea and a low ALC as major predictors for this outcome. Median ALC levels were 1.8 giga (G)/IL (25th–75th percentiles 0.9–2.4 G/L) for patients who had nonsevere PUUV and 0.3 G/L (25th–75th

**Table.** Baseline characteristics for patients according to clinical course and for the cohort overall in study of poor prognosis for Puumala virus infections predicted by lymphopenia and dyspnea*

| Variable | Overall, n = 23 | Mild course, n = 18 | Severe course, n = 5 | p value |
|---|---|---|---|---|
| Demographic | | | | |
| Age, y | 49 [34–59] | 51 [35–60] | 45 [24–49] | 0.087 |
| Female sex | 6 (26) | 5 (28) | 1 (20) | 1.000 |
| BMI, kg/m$^2$ | 24.9 [23.6–26.8] | 24.8 [23.4–27.0] | 25.6 [24.8–26.1] | 0.433 |
| Comorbidity | | | | |
| ≥1 | 5 (22) | 4 (22) | 1 (20) | 1.000 |
| Symptoms at diagnosis | | | | |
| Headache | 17 (74) | 12 (66) | 5 (100) | 0.133 |
| Eye pain | 2 (9) | 2 (11) | 0 | 0.435 |
| Dyspnea | 3 (13) | 0 | 3 (60) | 0.001 |
| Body temperature | 39.5 [39.0–39.7] | 39.5 [39.2–39.7] | 39.4 [39.0–39.8] | 1.000 |
| Diarrhea | 3 (13) | 3 (17) | 0 | 0.328 |
| Abdominal cramps | 3 (13) | 2 (11) | 1 (20) | 0.602 |
| Blurred vision | 3 (13) | 3 (17) | 0 | 0.328 |
| Time from first symptom to diagnosis | 2 [1–3] | 2 [1–2] | 3 [1.3–3.8] | 0.047 |
| Predisposition to contact with rodents | 10 (44) | 7 (39) | 3 (60) | 0.040 |
| Laboratory values | | | | |
| Creatinine, mg/dL | 1.2 [1.0–1.8] | 1.2 [1.0–1.9] | 1.2 [0.8–1.3] | 0.456 |
| CRP, mg/L | 60 [36–73] | 58 [42–63] | 73 [24–139] | 0.551 |
| LDH, IU | 266 [236–311] | 266 [236–312] | 258 [240–280] | 0.654 |
| Bilirubin total, mg/dL | 0.5 [0.3–0.8] | 0.3 [0.3–07] | 0.7 [0.6–0.9] | 0.107 |
| Prothrombin time, s | 105 [95–118] | 108 [105–120] | 94 [81–97] | 0.012 |
| APTT, s | 33 [31–37] | 33 [31–36] | 36 [35–41] | 0.147 |
| Blood counts | | | | |
| Leukocytes, Gg/L | 9.9 [9.9–11.8] | 9.0 [6.6–11.1] | 12.2 [9.1–13.9] | 0.371 |
| Neutrophils, G/L | 6.8 [4.1–10.7] | 6.3 [4.0–9.3] | 10.7 [7.0–12.1] | 0.168 |
| Lymphocytes, G/L | 1.0 [0.8–2.4] | 1.8 [0.9–2.4] | 0.3 [0.2–0.5] | <0.001 |
| Thrombocytes, G/L | 73 [50–130] | 63 [47–129] | 78 [73–129] | 0.911 |
| Hemoglobin, mg/dL | 14.5 [13.2–15.5] | 14.4 [13.2–15.4] | 15.5 [13.8–16.4] | 0.371 |
| Outcome | | | | |
| Died | 1 (4) | 0 | 1 (20) | 0.483 |
| Length of stay in hospital, d | 7 [4–12] | 6 [3–9] | 15 [12–17] | 0.048 |

*Values in brackets are 25th–75th percentiles; values in parentheses are percentages. APPT, activated partial thromboplastin time; BMI, body mass index; CRP, C-reactive protein; G, giga; LDH, lactate dehydrogenase.

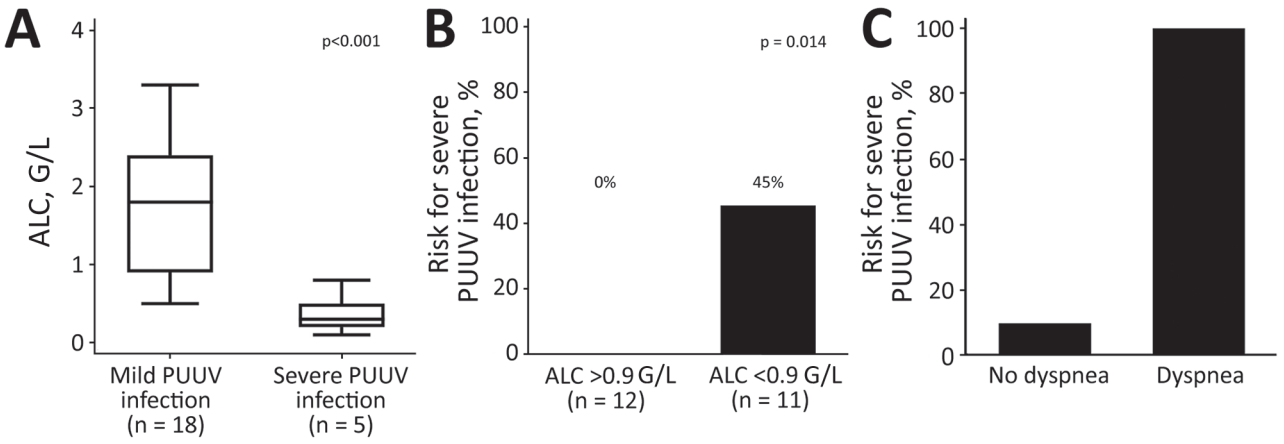


**Figure.** Poor prognosis for PUUV infections predicted by lymphopenia and dyspnea. A) Box plot showing difference in ALC between patients who had a mild clinical course and those who had a severe clinical course, showing that those with lower ALCs were more likely to have severe illness. Horizontal lines within indicate medians, top lines are maximum values, bottom lines are minimum values, and error bars indicate 25th–75th percentiles. B) Risk for severe course of PUUV infection according to the calculated ALC cutoff of 0.9 G/L, showing that lower ALC predicted increased risk for severe illness. C) Risk for developing severe PUUV infection according to dyspnea at first medical contact, showing that dyspnea predicted increased risk for severe illness. ALC, absolute lymphocyte count; G, giga; PUUV, Puumala virus.

percentiles 0.2–0.5 G/L) for patients who had severe PUUV (p<0.0001) (Figure, panel A).

Univariable logistic regression showed that a 0.1 G/L decrease in ALC predicted a 2.3-fold increase in risk for severe PUUV infection (odds ratio 2.28, 95% CI 1.03–5.03; p = 0.042). The area under the receiver operating characteristic curve for ALC for discriminating between patients with and without severe PUUV infection was 0.97, and an ALC cutoff <0.9 G/L was computed for identifying patients at high risk for severe PUUV infection. The risk for severe PUUV infection was 0% for the 12 patients who had an ALC ≥0.9 G/L and 45% for the 11 patients who had an ALC <0.9 G/L (p = 0.014) (Figure, panel B).

For the 20 patients without dyspnea at initial evaluation, 2 (10%) cases of severe PUUV infection were observed. In contrast, 3/3 (100%) patients with dyspnea at baseline showed development of severe PUUV infection (p = 0.006) (Figure, panel C).

## Conclusions

Risk stratification is crucial for personalized medicine and optimized patient allocation, especially if outpatient management might be considered. Because PUUV has a benign course in most cases, easily assessable predictors of the disease course support clinicians in their decision on patient management (*7*–*9*). We report a small but well-characterized prospective patient cohort, demonstrating lymphopenia and dyspnea at time of first medical contact and diagnosis of PUUV infection as predictors of adverse clinical course.

Most studies focusing on risk stratification in PUUV infection reported kidney injury and renal failure as clinical endpoints, although PUUV infection causes a much wider syndrome, including renal failure, respiratory failure, bleeding events, and circulatory failure (*8*,*10*,*11*). Therefore, we analyzed a composite endpoint consisting of all relevant complications of PUUV infection to support clinical decisions for admission or outpatient care.

A recent review summarized severity biomarkers in PUUV orthohantavirus infection (*12*). However, almost all mentioned biomarkers are difficult to measure, need special laboratory platforms, or are cost-intensive. In our study, we observed that low ALC and dyspnea are easily accessible markers of poor outcomes in an unbiased approach. In our approach, we used all laboratory parameters, signs, and symptoms observed at first medical contact and meticulously corrected for multiplicity. However, the case number of our study was limited, and the parameters should be seen as clinical warning signs of a potential severe clinical course of PUUV infection. The proposed biomarkers need further validation in independent cohorts to prove their utility in a clinical setting.

Our investigated biomarkers were limited to PUUV-infected patients admitted to the hospital, as described in our inclusion strategy. Because only hospitalized patients were included, the observed mortality rate of 4% is slightly higher than rates reported in epidemiologic studies (*1*,*13*).

In summary, we report a prospective cohort of 23 patients who had PUUV infection in an endemic area

in central Europe. Our findings indicate that low ALC and dyspnea are parameters associated with a severe course of PUUV infection.

The study was supported by the Styrian government (project no. ABT12-106729/2022-13).

S.H., F.K., and R.K. designed the study; S.H. and M.L. collected clinical data; S.H. performed statistical analysis; and S.H. and R.K. analyzed results and wrote the first draft of the manuscript. All authors reviewed the draft and approved the final version.

## About the Author

Dr. Hatzl is a hematology and intensive care consultant at the Department of Internal Medicine, Medical University of Graz, Graz, Austria. His primary research interest is emerging viral diseases and infectious diseases in critically ill and immunocompromised patients.

## References

1. Avšič-Županc T, Saksida A, Korva M. Hantavirus infections. Clin Microbiol Infect. 2019;21S:e6–16. https://doi.org/10.1111/1469-0691.12291
2. Camp JV, Schmon E, Krause R, Sixl W, Schmid D, Aberle SW. Genetic diversity of Puumala orthohantavirus in rodents and human patients in Austria, 2012–2019. Viruses. 2021;13:640. https://doi.org/10.3390/v13040640
3. Heyman P, Ceianu CS, Christova I, Tordo N, Beersma M, João Alves M, et al. A five-year perspective on the situation of haemorrhagic fever with renal syndrome and status of the hantavirus reservoirs in Europe, 2005–2010. Euro Surveill. 2011;16:19961. https://doi.org/10.2807/ese.16.36.19961-en
4. Hatzl S, Reisinger AC, Posch F, Prattes J, Stradner M, Pilz S, et al. Antifungal prophylaxis for prevention of COVID-19-associated pulmonary aspergillosis in critically ill patients: an observational study. Crit Care. 2021;25:335. https://doi.org/10.1186/s13054-021-03753-9
5. Harris PA, Taylor R, Thielke R, Payne J, Gonzalez N, Conde JG. Research electronic data capture (REDCap)—a metadata-driven methodology and workflow process for providing translational research informatics support. J Biomed Inform. 2009;42:377–81. https://doi.org/10.1016/j.jbi.2008.08.010
6. Harris PA, Taylor R, Minor BL, Elliott V, Fernandez M, O'Neal L, et al.; REDCap Consortium. The REDCap consortium: building an international community of software platform partners. J Biomed Inform. 2019;95:103208. https://doi.org/10.1016/j.jbi.2019.103208
7. Vaheri A, Strandin T, Hepojoki J, Sironen T, Henttonen H, Mäkelä S, et al. Uncovering the mysteries of hantavirus infections. Nat Rev Microbiol. 2013;11:539–50. https://doi.org/10.1038/nrmicro3066
8. Vaheri A, Henttonen H, Mustonen J. Hantavirus research in Finland: highlights and perspectives. Viruses. 2021;13:1452. https://doi.org/10.3390/v13081452
9. Hjertqvist M, Klein SL, Ahlm C, Klingstrom J. Mortality rate patterns for hemorrhagic fever with renal syndrome caused by Puumala virus. Emerg Infect Dis. 2010;16:1584–6. https://doi.org/10.3201/eid1610.100242
10. Mustonen J, Mäkelä S, Outinen T, Laine O, Jylhävä J, Arstila PT, et al. The pathogenesis of nephropathia epidemica: new knowledge and unanswered questions. Antiviral Res. 2013;100:589–604. https://doi.org/10.1016/j.antiviral.2013.10.001
11. Mustonen J, Outinen T, Laine O, Pörsti I, Vaheri A, Mäkelä S. Kidney disease in Puumala hantavirus infection. Infect Dis (Lond). 2017;49:321–32. https://doi.org/10.1080/23744235.2016.1274421
12. Outinen TK, Mäkelä S, Pörsti I, Vaheri A, Mustonen J. Severity biomarkers in Puumala hantavirus infection. Viruses. 2021;14:45. 10.3390/v14010045 https://doi.org/10.3390/v14010045
13. Mittler E, Wec AZ, Tynell J, Guardado-Calvo P, Wigren-Byström J, Polanco LC, et al. Human antibody recognizing a quaternary epitope in the Puumala virus glycoprotein provides broad protection against orthohantaviruses. Sci Transl Med. 2022;14:eabl5399. https://doi.org/10.1126/scitranslmed.abl5399

Address for correspondence: Robert Krause, Division of Infectious Diseases, Department of Internal Medicine, Medical University of Graz, Auenbruggerplatz 15, Graz, Austria; email: robert.krause@medunigraz.at

# Rustrela Virus as Putative Cause of Nonsuppurative Meningoencephalitis in Lions

Madeleine de le Roi, Christina Puff, Peter Wohlsein, Florian Pfaff, Martin Beer, Wolfgang Baumgärtner, Dennis Rubbenstroth

Retrospective investigation of archived tissue samples from 3 lions displaying nonsuppurative meningoencephalitis and vasculitis led to the detection of rustrela virus (RusV). We confirmed RusV antigen and RNA in cortical neurons, axons, astrocytes and Purkinje cells by reverse transcription quantitative PCR, immunohistochemistry, and in situ hybridization.

Until recently, rubella virus (RuV), an RNA virus with single-stranded RNA genome of positive orientation, was considered the only virus of the genus *Rubivirus* and the family *Matonaviridae* (*1*–*3*). Two close relatives of RuV, designated rustrela virus (RusV) and ruhugu virus (RuhV), were discovered in animals in 2020. RusV was demonstrated to cause nonsuppurative meningoencephalitis in a range of zoo animals in Germany (*1*,*4*,*5*). Furthermore, RusV was detected in domestic cats (*Felis catus*) showing clinical signs of staggering disease in Germany, Austria, and Sweden (*6*). Wild yellow-necked field mice (*Apodemus flavicollis*) and wood mice (*Apodemus sylvaticus*) are assumed to be reservoir hosts of RusV (*1*,*4*,*6*).

In the 1970s and 1980s, a series of fatal nonsuppurative encephalitis cases of undetermined cause had occurred in lions (*Panthera leo*) and tigers (*Panthera tigris*) kept in zoological gardens in Germany (*7*,*8*). We reinvestigated cases of 3 lions with nonsuppurative meningoencephalitis of unknown etiology from the 1980s for the presence of RusV.

The etiology of meningoencephalitides remains undetermined in many cases (*6*,*9*); a possible explanation is that conventional methods based on the recognition of virus-specific proteins and nucleic acids did not detect viral variants. Immunohistochemical detection of double-stranded RNA (dsRNA) is considered a virus-sensing tool irrespective of the particular virus (*10*). Therefore, we assessed the applicability of antibodies sensing dsRNA as an alternative virus detection method.

Author affiliations: University of Veterinary Medicine Hannover Foundation, Hannover, Germany (M. de le Roi, C. Puff, P. Wohlsein, W. Baumgärtner); Friedrich-Loeffler-Institut, Greifswald-Insel Riems, Germany (F. Pfaff, M. Beer, D. Rubbenstroth)

DOI: https://doi.org/10.3201/eid2905.230172

## The Study

We retrospectively investigated 3 lions for the presence of RusV. The lions were identified in 2 zoos in northern and western Germany; they exhibited neurologic signs and nonsuppurative meningoencephalitis. Lion 1 died in 1980 in a zoo in Lower Saxony, whereas lions 2 and 3 were submitted for pathological examination in 1989 by a zoo in North Rhine-Westphalia. All 3 lions displayed a mild, multifocal, lymphohistiocytic meningoencephalitis and vasculitis (Figure 1, panel A) and occasional glial nodules. Inflammatory infiltrates were most prominent in the cerebral gray matter and less prominent in cerebral white matter, cerebellum, and meninges. The spinal cord was not available for analysis. We tested archived formalin-fixed, paraffin-embedded (FFPE) tissues for the presence of RusV RNA and antigen by quantitative reverse transcription PCR (qRT-PCR), in situ hybridization (ISH) and immunohistochemistry (IHC). We included FFPE tissues originating from 8 lions without nonsuppurative meningoencephalitis (lions 4–11) as controls (Appendix, https://wwwnc.cdc.gov/EID/article/29/5/23-0172-App1.pdf).

FFPE brain samples from lions 1–3 tested positive for RusV RNA by the broadly reactive qRT-PCR assay panRusV-2 (*6*). Cycle quantification (Cq) values were 29–38. We detected no RusV RNA in central nervous system (CNS) samples from any of the 8 control animals (Appendix Table 1).

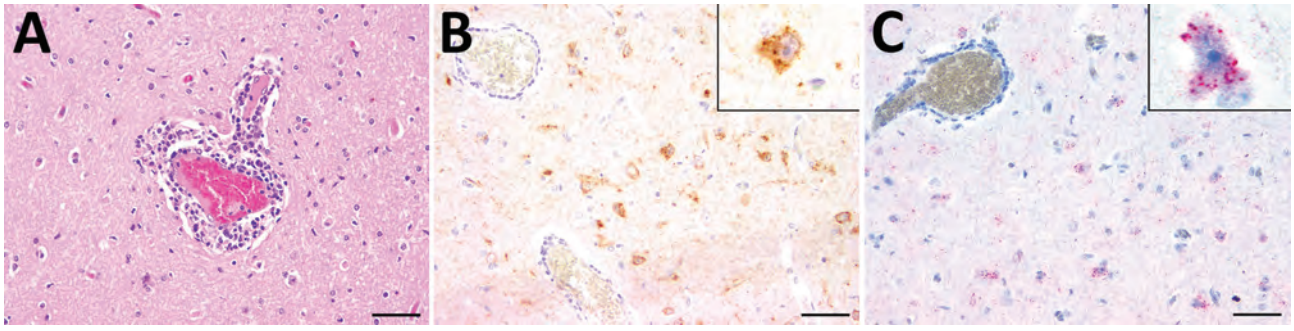


**Figure 1.** Histopathologic, immunohistochemical, and in situ hybridization findings in the cerebrum of a lion tested positive for rustrela virus (RusV) by quantitative reverse transcription PCR. A) Histopathologic analysis of cerebral sample from lion 3 indicated lymphohistiocytic meningoencephalitis and vasculitis. B) Immunohistochemistry analysis showed RusV antigen in cortical neurons and their processes. Cytoplasmic granular immunoreactivity is visible (inset). C) In situ hybridization revealed RusV RNA in cortical neurons; we observed cytoplasmic granular-positive signal (inset). Scale bars indicate 50 μm.

We determined a partial host-genome RusV sequence 409 bp long for all 3 RusV-positive animals by Sanger sequencing of overlapping RT-PCR products (Appendix). The sequences shared 97.8% nucleotide identity; phylogenetic analysis revealed all 3 sequences to form a single clade together with the sequence from a domestic cat in Hannover, Lower Saxony, in 2017 (*6*). Of note, this subclade was more closely related to sequences from cats with staggering disease in Austria than to sequences from zoo animals, domestic cats, and wild rodents in northeastern Germany (Figure 2).

IHC investigation for the presence of RusV capsid antigen using monoclonal antibody 2H11B1 (*6*) revealed multifocal, cytoplasmic, granular reactions, predominantly in cerebral cortical perikarya and their axons, in few astrocytes as well as in Purkinje cells of all 3 PCR-positive lions (Figure 1, panel B). Likewise, we detected RusV-specific RNA using a newly designed ISH probe (Appendix) in the brains of lions 2 and 3, but not of lion 1. We found viral RNA as a cytoplasmic granular signal in cortical perikarya (Figure 1, panel C). We observed RusV-specific capsid antigen and RNA in cerebral cortical neurons adjacent to perivascular infiltrates and also in neurons in more distant areas not associated with inflammatory changes. Neither IHC nor ISH revealed positive signals in any of the examined peripheral organs of the 3 RusV-positive animals and RusV-negative lion 7 (Appendix Table 1) or in the CNS of control animals. IHC staining for dsRNA using the dsRNA antibodies K1 and J2 (*11*) provided positive results in the CNS of all tested animals (Appendix Table 1). Immunolabeling with anti-dsRNA antibody 9D5 (*11*) remained negative for all 3 RusV-positive animals, whereas the RusV-negative lions 7 and 9 tested positive (Appendix Table 1).

## Conclusions

The results of this study strongly indicate RusV as the potential cause of fatal lymphohistiocytic meningoencephalitis in lions from Germany in the 1980s. The animals were reported to have had neurologic disorders characterized by fever, depression, ataxia, and prolapse of the tongue (*7*). These clinical and histopathological findings are similar to those described previously for RusV-infected zoo animals and domestic cats (*1*,*4*–*6*); they also resemble RuV-induced encephalitis in humans (*12*).

A partial colocalization of RusV antigen and RNA detection with histopathologic lesions has been observed previously (*1*,*4*,*6*). Although the pathogenesis of RusV infection has not been elucidated, a virally triggered immune response that remains present even after focal virus clearance may provide an explanation for this phenomenon (*13*). In addition, vasculitis caused by a type III hypersensitivity reaction should be considered.

The lack of viral antigen and RNA in organs other than the CNS of the infected lions is consistent with previous findings in RusV-infected zoo animals of other species, in which RusV RNA was predominantly detected in the CNS and only sporadically in other organs (*1*,*4*,*5*). These results indicate a strong neurotropism of RusV also in lions.

In this study, we consistently detected RusV RNA and antigen in the affected animals using 3 independent methods (qRT-PCR, ISH, and IHC). The lack of viral RNA detection by ISH in the brain of lion 1, positive by qRT-PCR, could be a result of lower sensitivity of ISH (*14*) or of a higher degree of RNA degradation in this >40-year-old sample. Furthermore, the crosslinking of proteins caused by formalin has been shown to influence the quality and accessibility of DNA or RNA in FFPE material (*15*).

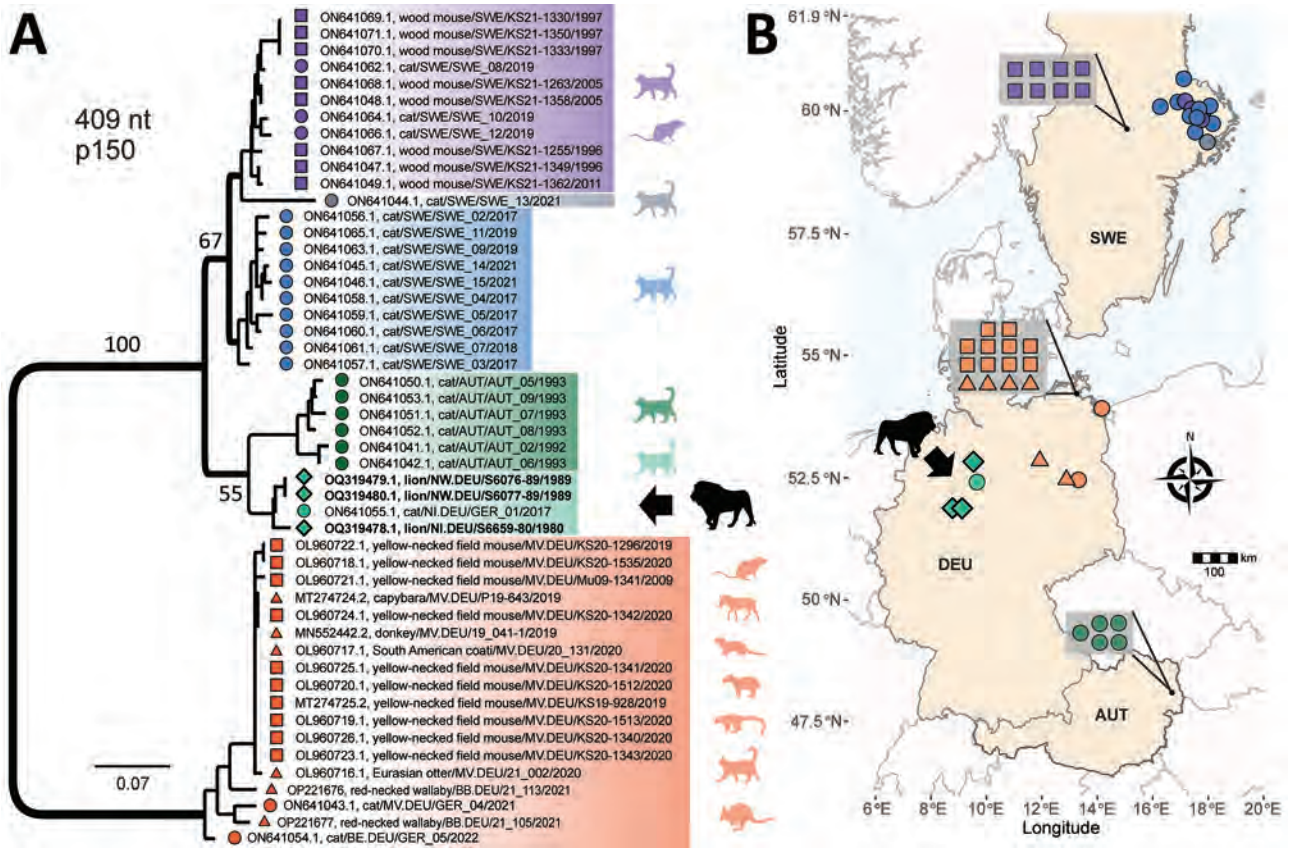


**Figure 2.** Phylogenetic analysis and spatial distribution of rustrela virus infections in Europe. A) Maximum-likelihood phylogenetic tree of partial rustrela virus (RusV) sequences (409 nt, representing genome positions 100–508 of donkey-derived RusV reference genome, GenBank accession no. MN552442.2). Only bootstrap values at major branches are shown in the phylogenetic tree. RusV sequence names are shown in the format host/ISO 1366 code of location (federal, state, country)/animal ID/year. The tree was produced using IQ-TREE version 2.2.0; transition model 2 plus empirical frequency plus gamma 4 with 1,000 bootstrap replicates. Bold text indicates sequences from this study. Scale bar indicates substitutions per site. B) Mapping of the geographic origin of RusV-positive animals in Europe. Colors represent the phylogenetic clades of the sequences. Diamonds represent lions; circles, domestic cats; triangles, other zoo animals; squares, *Apodemus* spp. rodents. Symbols in gray boxes represent individuals from the same or very close locations. AUT, Austria; BE, Berlin; DEU/GER, Germany; MV, Mecklenburg–Western Pomerania; NI, Lower Saxony; NW, North Rhine–Westphalia; SWE, Sweden.

Immunohistochemical investigation for dsRNA revealed positive results in the brains of all investigated lions, regardless of their RusV infection status. Although it is possible that the RusV-negative lions were infected by other neurotropic RNA viruses, this scenario appears unlikely because no CNS lesions were observed in control animals 4–11. Thus, this method appears unsuitable for reliable detection of viral dsRNA in the brains of lions and perhaps other animals.

In summary, our study reveals that RusV was present in northern and western Germany in the 1980s. Detecting RusV in lions indicates an even broader host range of RusV, encompassing a variety of different species (*1*,*4*–*6*) and suggests that other wild and captive felids may be susceptible to RusV infection. As described previously (*6*), fulfilling Henle-Koch's postulates by experimental reproduction of the disease has not been possible because of lack of RusV isolates. Nevertheless, the association between RusV detection and disease demonstrated in this study, combined with previous studies on RusV infections in zoo animals and domestic cats, strongly suggests RusV as a causative agent of meningoencephalitis in lions.

### Acknowledgments

We thank Julia Baskas, Petra Grünig, Jana-Svea Harre, Claudia Herrmann, Weda Hoffmann, Kerstin Rohn, Kerstin Schöne, Caroline Schütz, Philip Starcky, Kathrin Steffen, Danuta Waschke, and Melanie Woischnik for technical assistance. We are also grateful to Andrea Aebischer for providing the RusV-specific monoclonal antibody 2H11B1.

This work was in part supported by the Deutsche Forschungsgemeinschaft (DFG; German Research Foundation; -398066876/GRK 2485/1-VIPER-GRK) and by the German Federal Ministry of Education and Research, project RubiZoo (grant no. 01KI2111).

## About the Author

Ms. de le Roi is a PhD student in the Department of Pathology at the University of Veterinary Medicine Hannover Foundation, Hannover, Germany. Her research field focuses on alternative virus detection methods.

## References


1. Pfaff F, Breithaupt A, Rubbenstroth D, Nippert S, Baumbach C, Gerst S, et al. Revisiting rustrela virus: new cases of encephalitis and a solution to the capsid enigma. Microbiol Spectr. 2022;10:e0010322. https://doi.org/10.1128/spectrum.00103-22
2. Mankertz A, Chen MH, Goldberg TL, Hübschen JM, Pfaff F, Ulrich RG; ICTV Report Consortium. ICTV virus taxonomy profile: *Matonaviridae* 2022. J Gen Virol. 2022;103. In press. https://doi.org/10.1099/jgv.0.001817
3. Parkman PD, Buescher EL, Artenstein MS. Recovery of rubella virus from army recruits. Proc Soc Exp Biol Med. 1962;111:225–30. https://doi.org/10.3181/00379727-111-27750
4. Bennett AJ, Paskey AC, Ebinger A, Pfaff F, Priemer G, Höper D, et al. Relatives of rubella virus in diverse mammals. Nature. 2020;586:424–8. https://doi.org/10.1038/s41586-020-2812-9
5. Voss A, Schlieben P, Gerst S, Wylezich C, Pfaff F, Langner C, et al. Rustrela virus infection—an emerging neuropathogen of red-necked wallabies (*Macropus rufogriseus*). Transbound Emerg Dis. 2022;69:4016–21. https://doi.org/10.1111/tbed.14708
6. Matiasek K, Pfaff F, Weissenböck H, Wylezich C, Kolodziejek J, Tengstrand S, et al. Mystery of fatal "staggering disease" unravelled: novel rustrela virus causes severe meningoencephalomyelitis in domestic cats. Nat Commun. 2023;14:624. https://doi.org/10.1038/s41467-023-36204-w
7. Truyen U, Stockhofe-Zurwieden N, Kaaden OR, Pohlenz J. A case report: encephalitis in lions. Pathological and virological findings. Dtsch Tierarztl Wochenschr. 1990;97:89–91.
8. Flyr K. Encephalomyelitis bei Großkatzen. Dtsch Tierarztl Wochenschr. 1973;80:393–416.
9. Nessler J, Wohlsein P, Junginger J, Hansmann F, Erath J, Söbbeler F, et al. Meningoencephalomyelitis of unknown origin in cats: a case series describing clinical and pathological findings. Front Vet Sci. 2020;7:291. https://doi.org/10.3389/fvets.2020.00291
10. Koyama S, Ishii KJ, Coban C, Akira S. Innate immune response to viral infection. Cytokine. 2008;43:336–41. https://doi.org/10.1016/j.cyto.2008.07.009
11. Störk T, de le Roi M, Haverkamp AK, Jesse ST, Peters M, Fast C, et al. Analysis of avian Usutu virus infections in Germany from 2011 to 2018 with focus on dsRNA detection to demonstrate viral infections. Sci Rep. 2021;11:24191. https://doi.org/10.1038/s41598-021-03638-5
12. Frey TK. Neurological aspects of rubella virus infection. Intervirology. 1997;40:167–75. https://doi.org/10.1159/000150543
13. Zdora I, Raue J, Söbbeler F, Tipold A, Baumgärtner W, Nessler JN. Case report: lymphohistiocytic meningoencephalitis with central nervous system vasculitis of unknown origin in three dogs. Front Vet Sci. 2022;9:944867. https://doi.org/10.3389/fvets.2022.944867
14. Pfankuche VM, Hahn K, Bodewes R, Hansmann F, Habierski A, Haverkamp AK, et al. Comparison of different in situ hybridization techniques for the detection of various RNA and DNA viruses. Viruses. 2018;10:384. https://doi.org/10.3390/v10070384
15. Bodewes R, van Run PR, Schürch AC, Koopmans MP, Osterhaus AD, Baumgärtner W, et al. Virus characterization and discovery in formalin-fixed paraffin-embedded tissues. J Virol Methods. 2015;214:54–9. https://doi.org/10.1016/j.jviromet.2015.02.002


Address for correspondence: Dennis Rubbenstroth, Friedrich-Loeffler-Institut, Südufer 10, 17493 Greifswald-Insel Riems, Germany; email: Dennis.Rubbenstroth@fli.de

# Limited Nosocomial Transmission of Drug-Resistant Tuberculosis, Moldova

Ecaterina Noroc,[1] Dumitru Chesov,[1] Matthias Merker,[1] Matthias I. Gröschel, Ivan Barilar, Viola Dreyer, Nelly Ciobanu, Maja Reimann, Valeriu Crudu, Christoph Lange

Applying whole-genome-sequencing, we aimed to detect transmission events of multidrug-resistant/rifampin-resistant strains of *Mycobacterium tuberculosis* complex at a tuberculosis hospital in Chisinau, Moldova. We recorded ward, room, and bed information for each patient and monitored in-hospital transfers over 1 year. Detailed molecular and patient surveillance revealed only 2 nosocomial transmission events.

The main factor driving the epidemic of multidrug-resistant (MDR) and rifampin-resistant (RR) tuberculosis (TB) in Eastern Europe is active transmission of drug-resistant *Mycobacterium tuberculosis* complex (MTBC) (*1*). The role of nosocomial transmission of drug-resistant MTBC during prolonged hospitalizations remains poorly understood (*2*,*3*). We prospectively aimed to detect nosocomial transmission events at a TB referral hospital in Chisinau, the capital of Moldova.

## The Study

We performed the study at the Chiril Draganiuc Phthisiopneumology Institute, Chisinau, Moldova. From July 1, 2014, through June 30, 2015, we prospectively tracked patients' locations by room within the hospital, on the basis of the beds patients occupied each day during their hospital stays. We evaluated sputum samples by mycobacterial culture and performed phenotypic drug-susceptibility testing for all MTBC strains at admission. Sputum cultures for growth of MTBC were performed at least at the end of the second month, the fifth month, and the end of treatment in patients with drug-susceptible TB; for patients with MDR/RR TB, cultures were performed on a monthly basis until no growth of MTBC was detectable and quarterly thereafter (*4*). MTBC strains resistant to isoniazid and rifampin underwent whole-genome sequencing for genotypic prediction of drug resistance and phylogenetic comparison. All patients admitted to the study were followed up for 2 years after enrollment (Appendix 1, https://wwwnc.cdc.gov/EID/article/29/5/23-0035-App1.pdf). In total, 2,490 patients were admitted during the study period (Table 1; Appendix 1 Figure 1). The study was approved by the Research Ethical Committee of the State University of Medicine and Pharmacy (#15_49/2014), Chisinau, Moldova.

The number of patients with a confirmed diagnosis of TB by culture or the Xpert MTB/RIF assay (Cepheid, https://www.cepheid.com) was 1,016/1,379 (73.7%) (Table 1). Drug-susceptible strains of MTBC were found in 567/938 patients (60.5%), strains of mono/polydrug-resistant MTBC in 64/938 patients (6.8%), and strains of MDR/RR MTBC in 307/938 (32.7%) patients with detectable MTBC in culture. A total of 297/307 (96.7%) MDR/RR strains were available for analysis.

The median length of hospital stay was 22 days (interquartile range [IQR] 9–62 days) (Appendix 1 Figure 2, panel A). After admission, 75 patients were transferred to a different department than the one in

Author affiliations: Chiril Draganiuc Phthisiopneumology Institute, Chisinau, Moldova (E. Noroc, N. Ciobanu, V. Crudu); Nicolae Testemitanu State University of Medicine and Pharmacy, Chisinau (D. Chesov); Research Center Borstel, Borstel, Germany (D. Chesov, M. Merker, I. Barilar, V. Dreyer, M. Reimann, C. Lange); German Center for Infection Research (DZIF), Borstel (M. Merker, I. Barilar, V. Dreyer, M. Reimann, C. Lange); Harvard Medical School, Boston, Massachusetts, USA (M.I. Gröschel); Charité–Universitätsmedizin Berlin, Berlin, Germany (M.I. Gröschel); University of Lübeck, Lübeck, Germany (M. Reimann, C. Lange); Baylor College of Medicine and Texas Children's Hospital, Houston, Texas, USA (C. Lange)

DOI: https://doi.org/10.3201/eid2905.230035

[1]These first authors contributed equally to this article..

**Table 1.** Characteristics of patients by hospital departments in study of limited nosocomial transmission of drug-resistant TB, Moldova*

| Characteristic | Total, n = 2,490 | Dept 1, n = 401 | Dept 2, n = 445 | Dept 3, n = 1,127 | MDR TB dept, n = 156 | EP-TB and Surgery dept, n = 361 |
|---|---|---|---|---|---|---|
| Mean age, y (±SD) | 50.9 (±17.4) | 43.7 (±13.8) | 45.6 (±12.1) | 59.4 (±17.5) | 37.2 (±12.7) | 45.2 (±15.4) |
| Sex | | | | | | |
| M | 1,623 (65.2) | 288 (71.8) | 356 (80.0) | 609 (54.0) | 110 (70.5) | 260 (72.0) |
| F | 867 (34.8) | 113 (28.2) | 89 (20.0) | 518 (46.0) | 46 (29.5) | 101 (28.0) |
| TB | 1,379 (55.4) | 397 (99) | 442 (99.3) | 57 (5,1) | 156 (100) | 327 (90.6) |
| Culture positive TB | 938 (68.0) | 296 (74.6) | 331 (74.9) | 25 (43.9) | 142 (91) | 144 (44.0) |
| Culture negative or missed TB, Xpert positive | 78 (5.7) | 20 (5.0) | 27 (6.1) | 8 (14.0) | 9 (5.8) | 14 (4.3) |
| Patients without microbiological confirmation of TB | 363 (26.3) | 81 (20.4) | 84 (19.5) | 24 (42.9) | 5 (3.2) | 169 (51.7) |
| MDR TB by culture | 307 (31.4) | 39 (11.5) | 77 (21.3) | 7 (25) | 141 (99.3) | 43 (29.2) |
| New TB cases | 1,034 (75) | 380 (95.7) | 259 (58.6) | 52 (91.2) | 82 (52.6) | 261 (79.8) |
| Relapse TB | 233 (16.9) | 16 (4.0) | 135 (30.5) | 5 (8.9) | 30 (19.2) | 47 (14.4) |
| Retreatment after LTF | 50 (3.6) | 1 (0.3) | 23 (5.2) | 0 | 15 (9.6) | 11 (3.4) |
| Retreatment after failure | 62 (4.5) | 0 | 25 (5.7) | 0 | 29 (18.6) | 8 (2.5) |
| Pulmonary TB | 1,114 (80.8) | 369 (92.9) | 425 (96.2) | 44 (77.2) | 149 (95.5) | 127 (38.8) |
| Extrapulmonary TB | 183 (13.3) | 8 (2) | 3 (0.7) | 11 (19.6) | 1 (0.6) | 160 (49) |
| Pulmonary and extrapulmonary TB | 82 (5.9) | 20 (5.5) | 14 (3.2) | 2 (3.6) | 6 (3.9) | 40 (12.2) |

*Values are no. (%) except as indicated. Xpert, Xpert MTB/RIF assay (Cepheid, https://www.cepheid.com). Dept, department; EP-TB, extrapulmonary TB; LTF, loss to follow-up; MDR, multidrug-resistant; TB, tuberculosis.

which they were initially hospitalized (Appendix 1 Figure 2, panel B). Median length of stay until transfer to another department was 7 days (IQR 4–19 days) (Appendix 1 Figure 2, panel C).

A total of 41 patients with MDR/RR TB were initially admitted to a non–MDR TB departments. Of those, 33 patients were later transferred to the MDR TB department, and 8 patients were transferred to

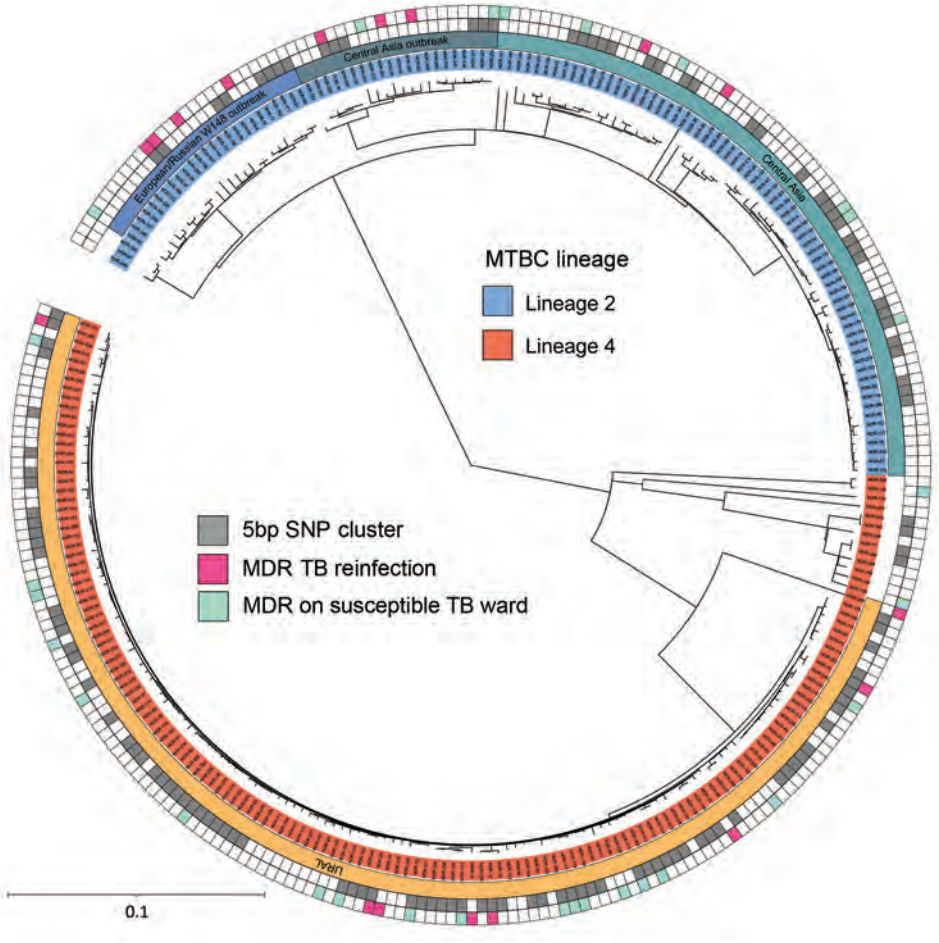


**Figure 1.** Maximum-likelihood phylogeny of 268 MDR TB isolates in study of limited nosocomial transmission of drug-resistant tuberculosis, Moldova. In outside circle, gray squares represent patient isolates with a maximum genetic distance of 5 single-nucleotide polymorphisms as a surrogate for recent transmission; pink squares indicate focus patients who acquired a new MDR MTBC strain during earlier treatment for drug-susceptible TB. Scale bar indicates number of substitutions per site. MDR, multidrug-resistant; MTBC, *Mycobacterium tuberculosis* complex; SNP, single-nucleotide polymorphism; TB, tuberculosis.

a different non–MDR TB department (Appendix 1 Figure 3, panel A). The median duration of stay for patients with MDR/RR TB in non–MDR TB departments was 7 days (IQR 4–18 days), and cumulative duration of stay was 631 days (Appendix 1 Figure 3, panel B). The median number of room-sharing contacts of patients with MDR/RR TB on non–MDR TB wards was 3 patients (IQR 2–5 patients), and the cumulative number of patients was 144.

A total of 17 patients (focus patients) with drug-susceptible MTBC strains at enrollment were found to be reinfected with an MDR/RR MTBC strain on follow-up. Only 1/144 roommates of the 41 patients with MDR/RR TB initially admitted to a non–MDR TB ward was in the same room with 1 of the 17 focus patients who potentially acquired MDR/RR TB on the non–MDR TB ward. For 297 patients with culture-confirmed MDR/RR TB at study enrollment and 17 focus patients with

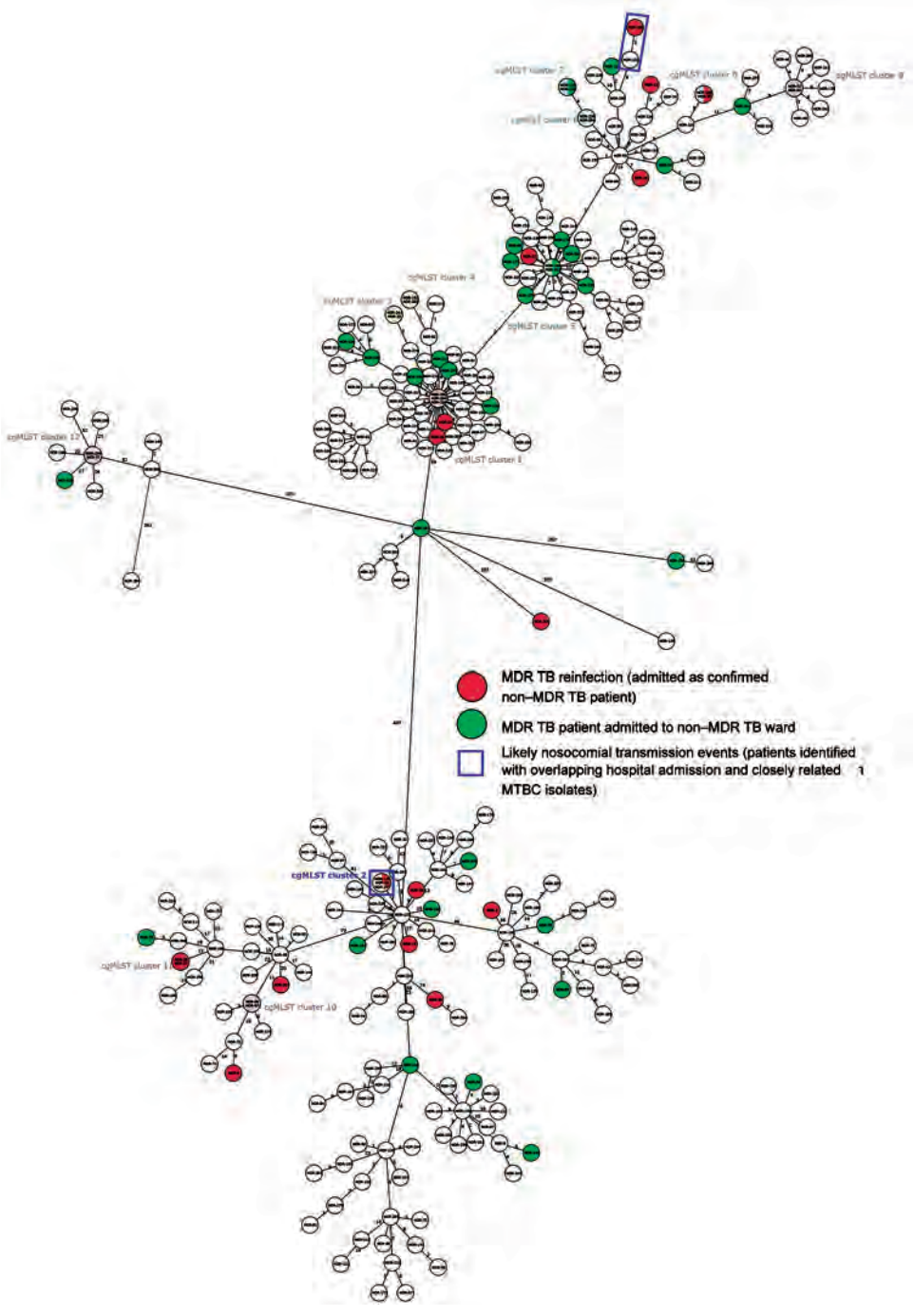


**Figure 2.** Phylogenetic network representing the genomic relatedness of all patient isolates in study of limited nosocomial transmission of drug-resistant tuberculosis, Moldova. Network is based on a core genome multilocus sequence type analysis. Pink indicates patients who acquired MDR TB, green indicates MDR TB patients initially admitted to a non–MDR TB ward; blue boxes indicate identified likely nosocomial transmission events. MDR, multidrug-resistant; MTBC, *Mycobacterium tuberculosis* complex; TB, tuberculosis.

**Table 2.** Likely nosocomial transmission events of drug-resistant TB, Moldova*

| Patient with acquired MDR TB | Possible index cases for transmission | SNP difference | Days overlap in the hospital | Days overlap on the same ward | Days overlap in the same room | Strain |
|---|---|---|---|---|---|---|
| NOR-14 | NOR-297 | 0 | 13† | 0 | 0 | 2.2.1 Central Asia outbreak |
| NOR-285 | NOR-133 | 3 | 29 | 27 | 23 | 4.2.1 URAL |

*MDR TB, multidrug-resistant tuberculosis; SNP, single-nucleotide polymorphism; TB, tuberculosis.
†Patients had already shared 52 d in the hospital before the official start of the study.

an MDR/RR MTBC reinfection detected during the follow-up period, 268 next-generation sequencing datasets were available for the molecular epidemiologic analysis (including all 17 strains from the focus patients).

The bacterial population consisted of MTBC lineage 2 isolates (116/268, 43.3%) and lineage 4 isolates (152/268, 56.7%). Isolates in lineage 2 were typed as Central Asia L2-sublineage (67/116, 57.8%), Central Asia outbreak (21/116, 18.1%), and Europe/Russia W148 outbreak (25/116, 21.6%), whereas lineage 4 almost exclusively consisted of sublineage 4.2.1, URAL genotype (139/152, 91.4%) (Figure 1). We used sequence data to predict the resistance phenotype on the basis of direct association with previously described resistance-conferring single-nucleotide polymorphisms (SNPs) (Appendix 1 Figure 4).

To highlight putative transmission events between the focus patients and concurrently admitted patients with MDR/RR TB, we performed a molecular cluster analysis on the basis of pairwise genetic distance between all isolates (Figure 2). Overall, 124/268 (46.3%) patients were part of 1 of the 28 identified clusters, including 7/17 focus patients (Appendix 2 Table, https://wwwnc.cdc.gov/EID/article/29/5/23-0035-App2.xlsx). Only 2/17 focus patients (sample ID 14 and ID 285) had a possible direct link in the hospital with a difference of <6 SNPs between the infecting MTBC strains, as well as 13 days and 29 days overlap in the hospital with their putative index case (Table 2; Appendix 1).

## Conclusions

Nosocomial transmission of MTBC infection in high-burden settings has been reported previously (*5*–*7*). We prospectively aimed to detect transmission events of MDR/RR strains of MTBC at the TB referral center in Moldova, a country of high MDR/RR TB incidence. By matching each patient with a specific ward, room, and bed in the hospital for each day of the year, we were able to identify which of 307 patients with MDR/RR TB were initially wrongly allocated to a non–MDR TB ward, potentially leading to nosocomial transmission to other patients. Forty-one patients with MDR/RR TB initially spent a total of 631 days on non–MDR TB wards before drug-resistant TB was identified and they were transferred to an MDR TB ward. By using whole-genome sequencing on MDR/RR strains of MTBC from putative index patients and patients with drug-susceptible TB in whom MDR/RR TB then developed during follow-up, we identified only 2 highly likely transmission events, indicating a low rate of nosocomial transmission of MDR/RR strains of MTBC. Systematic implementation of basic infection control measures at the Chiril Draganiuc Phthisiopneumology Institute after previous indications of nosocomial transmission of MTBC (*3*) might have been effective in reducing TB transmission (*8*). However, these findings are limited by the high clonality of MTBC strains in patients with MDR/RR TB in Moldova (*9*), where more than one third of all incident TB cases are affected by multidrug/rifampin resistance (*10*). Our results call for further community efforts to reduce transmission of drug-resistant TB.

The first limitation of this study is that isolates were sampled only in the hospital, which could have introduced selection bias with persons without access to healthcare. However, because TB care in Moldova is centralized and provided free of charge, the effect of those factors should be minimal. Second, patients admitted to the hospital might have been subsequently readmitted to another hospital, in which case transmission events would have been missed. However, use of the national TB reporting database for follow-up minimizes the potential effect of this limitation. Third, the short time frame of this study might have missed transmission events, although most cases occur within 1 year of infection. Fourth, although a diagnostic delay occurred, transmission of MDR/RR MTBC could have been reduced already if patients had received empiric partly active treatment regimens. Finally, the rate of detected transmission might have been higher if transmission from patients with MDR/RR TB to other patients with MDR/RR TB had also been assessed.

In summary, in a detailed prospective evaluation at the TB referral hospital in Chisinau, Moldova, a high burden country of drug-resistant TB, we found that the rate of nosocomial transmission of MDR/RR strains of MTBC is low. Our results indicate the need for further community efforts to reduce transmission of drug-resistant strains of MTBC in high-burden settings.

D.C., M.M., I.B., V.D., and C.L. are supported by the German Center of Infection Research (DZIF).

## About the Author

Dr. Noroc is a scientific researcher at the National Tuberculosis Reference Laboratory of the Chiril Draganuic Tuberculosis Institute in Chisinau, Moldova, and a PhD candidate at the Research Center Borstel, Germany. Her primary research interests are genotypic and phenotypic methods for the diagnosis of tuberculosis and detecting transmission chains of drug-resistant strains of *Mycobacterium tuberculosis* by molecular methods.

## References


1. Brown TS, Eldholm V, Brynildsrud O, Osnes M, Levy N, Stimson J, et al. Evolution and emergence of multidrug-resistant *Mycobacterium tuberculosis* in Chisinau, Moldova. Microb Genom. 2021;7:000620. https://doi.org/10.1099/mgen.0.000620
2. Genestet C, Paret R, Pichat C, Berland JL, Jacomo V, Carret G, et al.; Lyon TB study group. Routine survey of *Mycobacterium tuberculosis* isolates reveals nosocomial transmission. Eur Respir J. 2020;55:1901888. https://doi.org/10.1183/13993003.01888-2019
3. Crudu V, Merker M, Lange C, Noroc E, Romancenco E, Chesov D, et al. Nosocomial transmission of multidrug-resistant tuberculosis. Int J Tuberc Lung Dis. 2015;19:1520–3. https://doi.org/10.5588/ijtld.15.0327
4. Domente L, Alexandru S, Sain D, Nalivaico N, Ustian A, Moraru N, Rotaru-Lungu C. Protocol clinic național Tuberculoza la adult—PCN 123. Ministry of Health of the Republic of Moldova, Chisinau. 2012 [cited 2023 Apr 11]. https://ro.scribd.com/document/560260272/Pcn-123-Tb-Adult#
5. Bantubani N, Kabera G, Connolly C, Rustomjee R, Reddy T, Cohen T, et al. High rates of potentially infectious tuberculosis and multidrug-resistant tuberculosis (MDR-TB) among hospital inpatients in KwaZulu Natal, South Africa indicate risk of nosocomial transmission. PLoS One. 2014;9:e90868. https://doi.org/10.1371/journal.pone.0090868
6. Gandhi NR, Weissman D, Moodley P, Ramathal M, Elson I, Kreiswirth BN, et al. Nosocomial transmission of extensively drug-resistant tuberculosis in a rural hospital in South Africa. J Infect Dis. 2013;207:9–17. https://doi.org/10.1093/infdis/jis631
7. Smith JP, Modongo C, Moonan PK, Dima M, Matsiri O, Fane O, et al. Tuberculosis attributed to transmission within healthcare facilities, Botswana—The Kopanyo Study. Infect Control Hosp Epidemiol. 2022;43:1603–9. https://doi.org/10.1017/ice.2021.517
8. Fox GJ, Redwood L, Chang V, Ho J. The effectiveness of individual and environmental infection control measures in reducing the transmission of Mycobacterium tuberculosis: a systematic review. Clin Infect Dis. 2021;72:15–26.
9. Yang C, Sobkowiak B, Naidu V, Codreanu A, Ciobanu N, Gunasekera KS, et al. Phylogeography and transmission of M. tuberculosis in Moldova: a prospective genomic analysis. PLoS Med. 2022;19:e1003933. https://doi.org/10.1371/journal.pmed.1003933
10. World Health Organization. Global tuberculosis report 2022. Geneva: The Organization; 2022.


Address for correspondence: Christoph Lange, Division of Clinical Infectious Diseases, Medical Clinic, Research Center Borstel, Parkallee 35, 23845 Borstel, Germany; email: clange@fz-borstel.de

# Unknown Circovirus in Immunosuppressed Patient with Hepatitis, France, 2022

Christophe Rodriguez, Laure Boizeau,[1] Alexandre Soulier,[1] Melissa N'Debi, Vanessa Demontant, Elisabeth Trawinski, Sarah Seng, Hélène Fontaine, Paul-Louis Woerther, Sarah Marchand, Slim Fourati, Stéphane Chevaliez, Pierre Cappy, Stanislas Pol, Jean-Michel Pawlotsky

Hepatitis of undetermined origin can be caused by a wide variety of pathogens, sometimes emerging pathogens. We report the discovery, by means of routine shotgun metagenomics, of a new virus belonging to the family Circoviridae, genus *Circovirus*, in a patient in France who had acute hepatitis of unknown origin.

The world is regularly exposed to the emergence or re-emergence of known or unknown infectious agents. The COVID-19 pandemic illustrates the massive impact of such emergence on human lives, national economies, and social organizations. Infections of undetermined origin must be diagnosed early so that adapted measures are put in place to prevent the spread of potentially harmful pathogens. New diagnostic technologies such as shotgun metagenomics (SMg), which requires no prior knowledge of the agents sought, have greatly simplified diagnosis of novel pathogens. SMg has become a key tool for surveillance of viral emergence (*1*). It is regularly used in diagnosing patients with syndromes of suspected viral origin, such as encephalitis, meningitis, pneumopathies, or hepatitis. The Henri Mondor Hospital NGS Plateform laboratory has developed an original SMg technique and has used it for the past 5 years to explore complex infections not diagnosed by classical methods (*2*–*4*). We report detection of a new, yet unknown virus from the family Circoviridae in an immunosuppressed patient with acute hepatitis of unknown origin.

Author affiliations: Hôpital Henri Mondor, AP-HP, Université Paris-Est, Créteil, France (C. Rodriguez, L. Boizeau, A. Soulier, M. N'Debi, V. Demontant, E. Trawinski, S. Seng, P.-L. Woerther, S. Marchand, S. Fourati, S. Chevaliez, P. Cappy, J.-M. Pawlotsky); L'Institut Mondor de Recherche Biomédicale—INSERM U955, Créteil (C. Rodriguez, L. Boizeau, A. Soulier, S. Fourati, S. Chevaliez, P. Cappy, J.-M. Pawlotsky); Hôpital Cochin, AP-HP, Université Paris-Cité, Paris, France (H. Fontaine, S. Pol)

DOI: https://doi.org/10.3201/eid2905.221485

## The Patient

A 61-year-old woman who had undergone heart and lung transplantation for Eisenmenger syndrome 18 years earlier was hospitalized in March 2022 for acute hepatitis of unknown origin. As a result of her immunodepression, she had several infections develop in the preceding 6 months, including ganciclovir-resistant cytomegalovirus (CMV) colitis, parvovirus B19 bicytopenia, and aspergillus bronchitis. At admission, she was receiving multiple therapies, including immunosuppressive and anti-infectious drugs. Serum aminotransferase levels had progressively increased from December 2021 and peaked in April 2022 (alanine aminotransferase, 23× upper limit of normal [ULN]; aspartate aminotransferase, 47× ULN; gamma-glutamyl transpeptidase, 17× ULN; alkaline phosphatase, 1.5× ULN; bilirubin, 54 μmol/L) (Appendix Figure 1, https://wwwnc.cdc.gov/EID/article/29/5/22-1485-App1.pdf).

Results of a liver biopsy showed signs of acute hepatitis, without suggestions of a given etiology. The following markers of infection were absent: hepatitis A virus IgM, hepatitis B virus DNA, hepatitis C virus RNA, hepatitis D virus RNA, hepatitis E virus RNA, HIV RNA, herpes simplex virus 1 and 2 DNA, varicella zoster virus DNA, CMV DNA, Epstein-Barr virus DNA, human herpes virus 6 DNA, adenovirus DNA, enterovirus RNA, parvovirus B19 DNA, and markers of leptospirosis. CMV and Epstein-Barr virus DNAs were undetectable at admission but became detectable at the time of the aminotransferase peak; viral levels were 2.9 log IU/mL for CMV and 4.4 log IU/mL for Epstein-Barr virus. There were no

[1]These authors contributed equally to this article.

markers of autoimmune hepatitis, and withdrawal or diminution of potentially hepatotoxic treatments had no effect on cytolysis. Aminotransferase levels started to decrease spontaneously 7 weeks after admission. SMg testing was prescribed to identify a potential treatable cause of this acute hepatitis. The patient expressed no opposition to the use of her data and samples for this purpose.

The SMg technique has already been described (*2*–*4*). We performed preextraction mechanical, enzymatic, and chemical actions before extracting both DNAs and RNAs using a DSP DNA Midi Kit on a QiaSymphony device (both QIAGEN, https://www.qiagen.com/us). We generated DNA libraries using a Nextera XT kit nd generated RNA libraries using a TruSeq Total RNA kit (both Illumina, https://www.illumina.com). We sequenced these libraries using NextSeq 500/550 High Output Kit v2.5 300 Cycles (Illumina). We performed metagenomics data analysis using MetaMIC software (https://gitlab.com/mndebi/metamic). The software filters out poor-quality data, identifies sequences by comparison with an nucleotide-based database, reduces background noise by comparison with environmental controls, and establishes a report on the presence or absence of bacteria, viruses, fungi, and parasites.

We performed data reanalysis for genome reconstruction and phylogenetic analysis. We assembled viral DNA sequences and RNA transcripts by using Metaspades 3.15.3 software (*5*). We assembled contigs by means of iterative in-house scripts, gradually replacing the closest reference viral sequences by the patient's sequences. We checked the consensus sequence by realigning the reads with bwa-mem 0.7.17-r1188 software (https://github.com/lh3/bwa) and by manual checking using the IGV 2.9.4 tool (https://software.broadinstitute.org/software/igv/). We performed phylogenetic analysis using a library of the replicase region and full-length Circoviridae genome sequences (*6*), supplemented by the sequences closest to the newly identified virus found using BLASTn (https://blast.ncbi.nlm.nih.gov/Blast.cgi?PROGRAM=tblastn&PAGE_TYPE=BlastSearch&LINK_LOC=blasthome) and the nucleotide database from GenBank, and MUSCLE alignment (*7*) and a maximum-likelihood Kimura model phylogeny by using MEGA5 software (https://www.megasoftware.net).

SMg generated 31,431,784 DNA sequences and 78,933,526 RNA sequences. There were 579,324 DNA sequences and 191,574 RNA sequences related to the DNA genome and RNA transcripts of a yet unknown member of the Circoviridae family, distantly related to *Porcine circovirus 3*. We have provisionally called the new species *Circovirus parisii*.

The viral genome sequence of 2,021 nt could be reconstructed (GenBank accession no. ON526744) (Figure, panel A). The origin of replication located in the AGTATTAC sequence had 1 nucleotide deletion compared with other circoviruses (Figure, panel A). We identified the 2 major circovirus open reading frames (ORFs), starting at positions 140 (replicase, ORF1/rep, sense) and 2,013 (capsid protein, ORF2/cap, antisense), as well as sense ORF3, starting at position 82 (Figure, panel A). The 6 regions described as conserved within the rep region were present, identical to other species from the same genus (Figure, panel A).

By phylogenetic analysis, the new *C. parisii* clustered with other circoviruses, on the same branch as recently described wolverine circovirus (*8*), rodent circovirus (*9*), and *Porcine circovirus 3*. It was related to another branch containing bat circovirus (Figure, panel B). The genetic distances between *C. parisii* and other circoviruses were of the same order as those between different circovirus species.

The presence of the virus was confirmed by means of a specific PCR technique developed in our lab, which is based on SMg sequencing (Appendix). Sanger sequencing of PCR products yielded a sequence identical to that generated by SMg. No circovirus sequence was found in the environmental control.

## Conclusions

Our shotgun metagenomics approach enabled us to identify a putative new member of the Circoviridae family, provisionally named *C. parisii*, in a profoundly immunosuppressed patient who had self-resolving acute hepatitis. Phylogenetic analysis showed clustering of the new virus with members of the *Circovirus* genus known to infect different animal species. As for other circoviruses, the viral genome displayed an origin of replication (lacking 1 nucleotide), a replicase gene spanning 6 conserved regions, a capsid protein gene, and an ORF3, the role of which remains unknown.

Circoviruses are single-stranded DNA viruses generally transmitted via the fecal–oral route, with a potential pathogenic role in animals. Thus far, no human circovirus infections have been recorded (*10*), and serologic studies have not revealed any human contact (*11*). Nevertheless, culture of *Porcine circovirus 2* on human cell lines, including liver cells, demonstrates the ability of this virus to replicate in human cells (*12*). Various pathologies have been observed in animals infected with circoviruses, including hepatitis (*13*,*14*). *Porcine circovirus 3*, the closest known circovirus, causes respiratory and neurologic diseases, cardiac and multisystemic inflammation, reproductive failure,

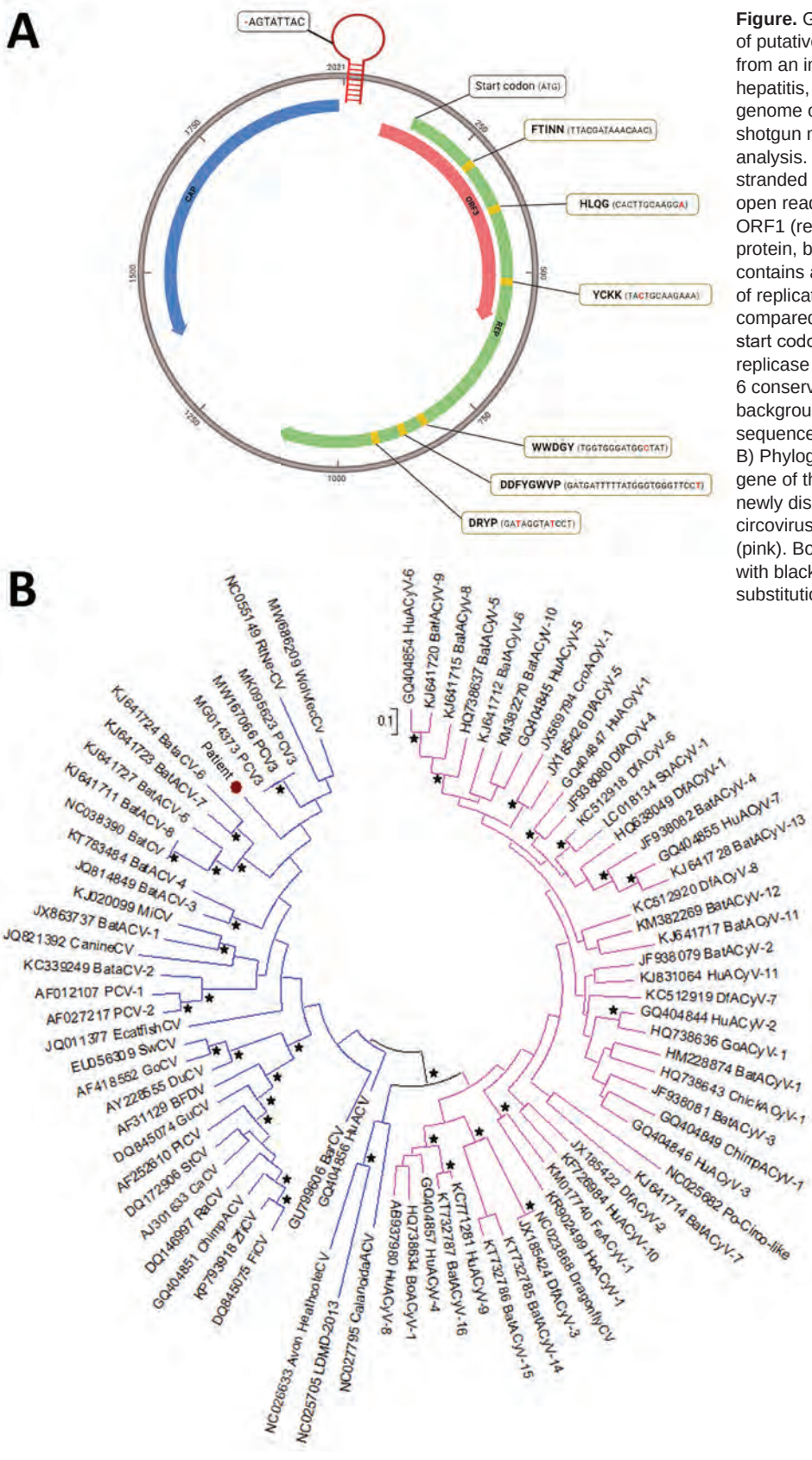


**Figure.** Genomic and phylogenetic analysis of putative novel virus, *Circovirus parisii*, from an immunocompromised patient with hepatitis, France, 2022. A) Full-length genome of *C. parisii* reconstructed from shotgun metagenomics (SMg) sequence analysis. The genome is a 2021-nt single-stranded circular DNA containing 3 predicted open reading frames (ORFs), including ORF1 (replicase, green), ORF2 (capsid protein, blue) and ORF3 (red). The stem-loop contains an AGTATTAC sequence (origin of replication) that misses 1 nt (red dash) compared with other circoviruses. An ATG start codon is located at the 5′ end of the replicase gene. The replicase gene contains 6 conserved motifs, represented with a yellow background (amino acid and nucleotide sequences), with silent substitutions in red. B) Phylogenetic analysis of the replicase gene of the Circoviridae family, including the newly discovered *C. parisii* (red dot), known circoviruses (blue), and known cycloviruses (pink). Bootstrap values >70% are indicated with black stars. Scale bar indicates substitutions per site.

and porcine dermatitis and nephropathy syndrome (*15*). The presence of the novel virus at the time of the aminotransferase peak raises questions about the causal relationship. Other techniques, such as in situ hybridization on infected tissue, might have offered some insights but were not available in our case. The source of transmission—perhaps animal, perhaps human—could not be established based on this patient's history.

## About the Author

Dr. Rodriguez is a professor at Assistance Publique-Hôpitaux de Paris, University Paris-Est Créteil, INSERM U955 Team 18. His research interests are infectious diseases, metagenomics, diagnostic, transcriptomics, virology, and emerging pathogens.

## References

1. Aarestrup FM, Bonten M, Koopmans M. Pandemics–One Health preparedness for the next. Lancet Reg Health Eur. 2021;9:100210. https://doi.org/10.1016/j.lanepe.2021.100210
2. Rodriguez C, de Prost N, Fourati S, Lamoureux C, Gricourt G, N'debi M, et al. Viral genomic, metagenomic and human transcriptomic characterization and prediction of the clinical forms of COVID-19. PLoS Pathog. 2021;17:e1009416. https://doi.org/10.1371/journal.ppat.1009416
3. Rodriguez C, Gricourt G, Ndebi M, Demontant V, Poiteau L, Burrel S, et al. Fatal encephalitis caused by cristoli virus, an emerging orthobunyavirus, France. Emerg Infect Dis. 2020;26:1287–90. https://doi.org/10.3201/eid2606.191431
4. Winter S, Lechapt E, Gricourt G, N'debi M, Boddaert N, Moshous D, et al. Fatal encephalitis caused by Newcastle disease virus in a child. Acta Neuropathol. 2021;142:605–8. https://doi.org/10.1007/s00401-021-02344-w
5. Nurk S, Meleshko D, Korobeynikov A, Pevzner PA. metaSPAdes: a new versatile metagenomic assembler. Genome Res. 2017;27:824–34. https://doi.org/10.1101/gr.213959.116
6. Rosario K, Breitbart M, Harrach B, Segalés J, Delwart E, Biagini P, et al. Revisiting the taxonomy of the family Circoviridae: establishment of the genus *Cyclovirus* and removal of the genus *Gyrovirus*. Arch Virol. 2017;162:1447–63. https://doi.org/10.1007/s00705-017-3247-y
7. Tamura K, Peterson D, Peterson N, Stecher G, Nei M, Kumar S. MEGA5: molecular evolutionary genetics analysis using maximum likelihood, evolutionary distance, and maximum parsimony methods. Mol Biol Evol. 2011;28:2731–9. https://doi.org/10.1093/molbev/msr121
8. Bandoo RA, Bautista J, Lund M, Newkirk E, Squires J, Varsani A, et al. Identification of novel circovirus and anelloviruses from wolverines using a non-invasive faecal sampling approach. Infect Genet Evol. 2021;93:104914. https://doi.org/10.1016/j.meegid.2021.104914
9. Wu Z, Lu L, Du J, Yang L, Ren X, Liu B, et al. Comparative analysis of rodent and small mammal viromes to better understand the wildlife origin of emerging infectious diseases. Microbiome. 2018;6:178. https://doi.org/10.1186/s40168-018-0554-9
10. World Organization for Animal Health. New castle disease, 2022. [cited 2022 May 23]. https://www.woah.org/en/disease/newcastle-disease/
11. Burbelo PD, Ragheb JA, Kapoor A, Zhang Y. The serological evidence in humans supports a negligible risk of zoonotic infection from porcine circovirus type 2. Biologicals. 2013;41:430–4. https://doi.org/10.1016/j.biologicals.2013.09.005
12. Liu X, Ouyang T, Ouyang H, Liu X, Niu G, Huo W, et al. Human cells are permissive for the productive infection of porcine circovirus type 2 in vitro. Sci Rep. 2019;9:5638. https://doi.org/10.1038/s41598-019-42210-0
13. Hui A, Altan E, Slovis N, Fletcher C, Deng X, Delwart E. Circovirus in blood of a febrile horse with hepatitis. Viruses. 2021;13:944. https://doi.org/10.3390/v13050944
14. Rosell C, Segalés J, Domingo M. Hepatitis and staging of hepatic damage in pigs naturally infected with porcine circovirus type 2. Vet Pathol. 2000;37:687–92. https://doi.org/10.1354/vp.37-6-687
15. Saporiti V, Franzo G, Sibila M, Segalés J. Porcine circovirus 3 (PCV-3) as a causal agent of disease in swine and a proposal of PCV-3 associated disease case definition. Transbound Emerg Dis. 2021;68:2936–48. https://doi.org/10.1111/tbed.14204

Address for correspondence: Christophe Rodriguez, Department of Microbiology, Hôpital Henri Mondor, 51 avenue du Maréchal de Lattre de Tassigny, 94010 Créteil CEDEX, France; email: christophe.rodriguez@aphp.fr

# Panton-Valentine Leukocidin–Positive CC398 MRSA in Urban Clinical Settings, the Netherlands

Jairo Gooskens, Marja M. Konstantinovski, Margriet E.M. Kraakman, Jayant S. Kalpoe, Nathalie D. van Burgel, Eric C.J. Claas, Thijs Bosch

Author affiliations: Leiden University Medical Center, Leiden, the Netherlands (J. Gooskens, M.M. Konstantinovski, M.E.M. Kraakman, E.C.J. Claas); Regional Public Health Laboratory Kennemerland, Haarlem, the Netherlands (J.S. Kalpoe); Haga Ziekenhuis, The Hague, the Netherlands (N.D. van Burgel); National Institute for Public Health and the Environment, Bilthoven, the Netherlands (T. Bosch)

DOI: https://doi.org/10.3201/eid2905.221717

We report detection of Panton-Valentine leukocidin–positive clonal complex 398 human-origin methicillin-resistant *Staphylococcus aureus* L2 in the Netherlands. This hypervirulent lineage originated in the Asia-Pacific Region and could become community-acquired in Europe after recurrent travel-related introductions. Genomic surveillance enables early detection to guide control measures and help limit the spread of pathogens in urban settings.

*Staphylococcus aureus* is a frequent cause of community- and healthcare-associated infections. Clonal complex 398 (CC398) is of particular concern because it includes common livestock-associated methicillin-resistant *S. aureus* (LA-MRSA) IIa subclades in Europe and human-origin MRSA (HO-MRSA) II-GOI subclades in the Asia-Pacific Region (*1*–*4*). Panton-Valentine leukocidin (PVL)–positive HO-MRSA L2 strains have recently emerged and are expanding geographically, causing skin and soft-tissue infections and occasional invasive disease in humans (*2*,*3*,*5*,*6*).

We report 3 patients in the Netherlands with infections caused by hypervirulent PVL-positive CC398 HO-MRSA L2 strains. The cases were detected as part of a CC398 MRSA surveillance study in a single urban area during 2014–2018 (*7*). One patient had furunculosis skin infection, 1 had a plantar abscess soft-tissue infection, and 1 patient with cystic fibrosis had recurrent bronchitis. One patient had a recent travel history to Vietnam in the Asia-Pacific Region, but none had livestock contact. Phenotypic susceptibility testing of patient samples confirmed methicillin resistance and the MRSA strains were sent to reference laboratories as part of routine molecular surveillance in the Netherlands. Whole-genome sequencing (WGS) and core genome multilocus sequence typing (cgMLST) were performed as part of the CC398 MRSA surveillance study. Detection of 3 PVL-positive CC398 isolates prompted comparative genomic analysis of single-nucleotide polymorphisms (SNPs) outside the scope of the surveillance study. The medical ethical committee of the Leiden University Medical Center approved the study protocol and waived the need for patient consent (approval no. G18.021/SH/sh).

MLST showed sequence types (STs) belonging to CC398, including ST1232 (n = 2), a single-locus variant of ST398, and ST4081 (n = 1), a double-locus variant of ST398. WGS and comparative genomic analysis of SNPs confirmed that all isolates were part of the same L2 lineage within the II-GOI clade (Figure) (*1*–*6*). We performed cgMLST on 1,861 genes, and results showed each patient had a different complex type (CT), CT6700, CT6814, and CT7459, thus ruling out direct transmission events between the patients.

The L2 strains we detected carried resistance genes on the staphylococcal cassette chromosome *mec* element type V(5C2), including *mec*A, which confers β-lactam resistance, and pT181 plasmid integrated *tet*K, which confers tetracycline resistance. In addition, on other mobile genetic elements, the L2 strains carried *erm*(A), conferring macrolide-lincosamide-streptogramin resistance; *ant*(9)-Ia, conferring spectinomycin resistance; *bla*Z, conferring β-lactam resistance; and *tet*38, conferring tetracycline resistance. All 3 strains carried the same virulence markers, including the immune evasion cluster *scn*, *chp*, and *sak*; leukocidin pro-toxin subunits lukF-PV and lukS-PV; *cna*, *ebp*, *ica*, *map*, *sdr*, and *srt*B biofilm formation or microbial surface components recognizing adhesive matrix molecules; immune modulation markers *ads*A, *cap*8, and *sbi*; exoenzymes *aur*, *geh*, *lip*, and *ssp*; and exotoxins or effector delivery components *hla*, *hld*, *hlg*, *esa*, and *esx* (*8*). We deposited the 3 isolates in GenBank (accession nos. SRR21673410, SRR21624599, and SRR21673965) (Figure).

In conclusion, clinicians should be aware of recurrent introductions and evolutionary changes of hypervirulent PVL-positive CC398 HO-MRSA L2 strains in the Netherlands. All 3 patients carrying the detected strains manifested relevant infections, but clinical outcomes were not evaluated in the surveillance study. Additional studies could investigate travel-related transmission routes, disease burden, and clinical outcomes

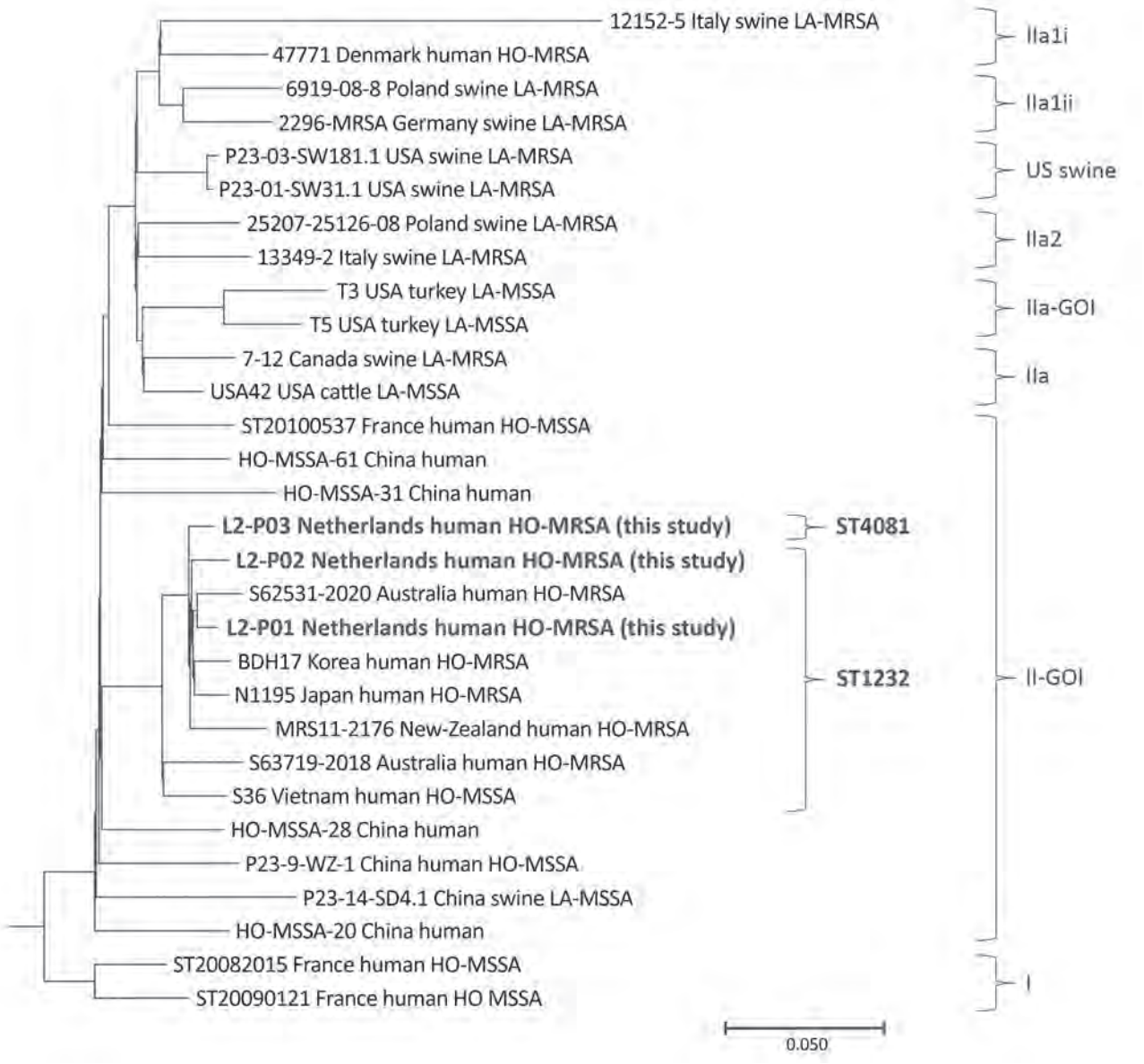


**Figure.** Maximum-parsimony tree of Panton-Valentine leukocidin–positive CC398 MRSA detected in urban clinical settings, the Netherlands. Bold text indicates 3 HO-MRSA strains detected in this study, which we deposited in GenBank (accession nos. SRR21673410 for L2-P01, SRR21624599 for L2-P02, and SRR21673965 for L2-P03); those strains were compared with 27 CC398 *Staphylococcus aureus* strains from GenBank. The tree was constructed by using GenBank accession no. AM990992.1 as a reference strain, and then rooted and grouped into clades, as previously described (*1*). Scale bar indicates nucleotide substitutions per 100 sites based on a concatenated alignment of 3,878 high-quality single-nucleotide polymorphisms. HO-MRSA, human-origin MRSA; LA-MRSA, livestock-associated MRSA; MRSA, methicillin-resistant *Staphylococcus aureus*; MSSA, methicillin-susceptible *S. aureus*; ST, sequence type.

of patients. In addition, future studies could determine if PVL-positive CC398 HO-MRSA strains are becoming established as community-acquired pathogens in urban settings in Europe. We recommend active WGS surveillance for early clinical recognition of PVL-positive CC398 MRSA, which can guide prevention and control measures and limit inter human transmission and severe clinical outcomes.

This project was partially funded by the Antibiotic Resistance Network Holland West. The Dutch Ministry of Health, Welfare and Sport provided funding through Healthcare Project 21243 (Activity E).

J.G. and M.E.M.K. conceptualized study and devised methods; J.G. prepared original manuscript draft; J.G., M.M.K., and M.E.M.K. interpreted data; J.G., M.M.K. reviewed and edited manuscript; J.G., J.S.K., N.D.v.B.,

E.C.J.C., and T.B. supervised study. All authors read and agreed to the final version of the manuscript.

## About the Author

Dr. Gooskens is a clinical microbiologist at the Department of Medical Microbiology, Leiden University Medical Center, Leiden, the Netherlands. His current research interests focus on clinical molecular diagnostics and antimicrobial resistance of CC398 *Staphylococcus aureus*.

## References


1. Price LB, Stegger M, Hasman H, Aziz M, Larsen J, Andersen PS, et al. *Staphylococcus aureus* CC398: host adaptation and emergence of methicillin resistance in livestock. MBio. 2012;3:e00305-11. https://doi.org/10.1128/mBio.00305-11
2. Møller JK, Larsen AR, Østergaard C, Møller CH, Kristensen MA, Larsen J. International travel as source of a hospital outbreak with an unusual meticillin-resistant *Staphylococcus aureus* clonal complex 398, Denmark, 2016. Euro Surveill. 2019;24:1800680. https://doi.org/10.2807/1560-7917.ES.2019.24.42.1800680
3. Coombs GW, Daley D, Shoby P, Yee NWT, Robinson JO, Murray R, et al. Genomic characterisation of CC398 MRSA causing severe disease in Australia. Int J Antimicrob Agents. 2022;59:106577. https://doi.org/10.1016/j.ijantimicag.2022.106577
4. Lu H, Zhao L, Si Y, Jian Y, Wang Y, Li T, et al. The surge of hypervirulent ST398 MRSA lineage with higher biofilm-forming ability is a critical threat to clinics. Front Microbiol. 2021;12:636788. https://doi.org/10.3389/fmicb.2021.636788
5. Williamson DA, Bakker S, Coombs GW, Tan H, Monecke S, Heffernan H. Emergence and molecular characterization of clonal complex 398 (CC398) methicillin-resistant *Staphylococcus aureus* (MRSA) in New Zealand. J Antimicrob Chemother. 2014;69:1428–30. https://doi.org/10.1093/jac/dkt499
6. Kaneko H, Kim ES, Yokomori S, Moon SM, Song KH, Jung J, et al. Comparative genomic analysis of the human variant of methicillin-resistant *Staphylococcus aureus* CC398 in Japan and Korea. Microb Drug Resist. 2022;28:330–7. https://doi.org/10.1089/mdr.2021.0203
7. Konstantinovski MM, Schouls LM, Witteveen S, Claas ECJ, Kraakman ME, Kalpoe J, et al. Livestock-associated methicillin-resistant *Staphylococcus aureus* epidemiology, genetic diversity, and clinical characteristics in an urban region. Front Microbiol. 2022;13:875775. https://doi.org/10.3389/fmicb.2022.875775
8. Strauß L, Ruffing U, Abdulla S, Alabi A, Akulenko R, Garrine M, et al. Detecting *Staphylococcus aureus* virulence and resistance genes: a comparison of whole-genome sequencing and DNA microarray technology. J Clin Microbiol. 2016;54:1008–16. https://doi.org/10.1128/JCM.03022-15


Address for correspondence: Jairo Gooskens, Department of Medical Microbiology, Leiden University Medical Center, Albinusdreef 2, Leiden 2333, the Netherlands; email: j.gooskens@lumc.nl

# Cystic Echinococcosis in Northern New Hampshire, USA

Ahmad AlSalman, Abigail Mathewson, Isabella W. Martin, Rattanaporn Mahatanan, Elizabeth A. Talbot

Author affiliations: Dartmouth Health, Lebanon, New Hampshire, USA (A. AlSalman, I.W. Martin, R. Mahatanan, E.A. Talbot); Dartmouth College, Hanover, New Hampshire, USA (A. AlSalman, I.W. Martin, R. Mahatanan, E.A. Talbot); New Hampshire Department of Health and Human Services, Concord, New Hampshire, USA (A. Mathewson, E.A. Talbot)

DOI: https://doi.org/10.3201/eid2905.221828

In April 2022 and December 2022, the New Hampshire Department of Health and Human Services confirmed 2 cases of locally acquired human pulmonary cystic echinococcosis caused by *Echinococcus granulosus* tapeworms. Both patients reported dressing locally hunted moose and exposure to dogs.

*Echinococcus granulosus* is a zoonotic cestode that lives in the intestine of its definitive host, canids (e.g., dogs, coyotes, foxes, wolves). Embryonated eggs released in canid feces are immediately infectious when consumed by an intermediate host, usually an ungulate (e.g., moose, deer, sheep) or sometimes a human (aberrant intermediate host). An ingested egg hatches in the small intestine, becoming an oncosphere that travels to organs such as the lung, liver, spleen, bone, or brain where it forms a thick-walled cyst. Canids become infected when they ingest flesh and viscera of an infected intermediate host (*1*). We report 2 human cases of *E. granulosus* tapeworm infection in northern New Hampshire, USA, during 2022.

In April 2022, an otherwise healthy middle-aged man (patient 1) from rural northern New Hampshire sought care from his primary-care physician for a routine physical examination. On chest auscultation, the physician heard localized wheezes, prompting chest radiograph and subsequent computed tomography scan; the images showed a noncalcified 4-cm mass in the lower lobe of the right lung. After initial endobronchial biopsy of the mass was nondiagnostic, the patient underwent thoracoscopic lung wedge resection. A gray cystic lesion ruptured during the procedure, releasing clear fluid. The ruptured cyst was excised, and histologic examination showed the presence of a laminated outer cyst wall and numerous daughter cysts, each containing multiple protoscolices with internal hooklets and calcareous corpuscles (Figure), features diagnostic of *E. granulosus*

tapeworm infection. The patient was prescribed a treatment course of albendazole and planned close follow-up, given the high risk for recurrence.

In December 2022, patient 2, an otherwise healthy middle-aged woman, sought medical attention for anaphylaxis that was determined to be caused by a ruptured cyst. Radiography showed 2 lung lesions and 1 small (<5 cm) liver lesion. Results of serum *Echinococcus* antibody testing was positive. A course of albendazole was prescribed (400 mg 2×/d) and, 4 weeks into therapy, the patient had the first larger pulmonary lesion successfully excised with plans for resection of the second excision.

Both patients reported similar epidemiologic risk factors of dressing locally hunted moose and being exposed to dogs in northern New Hampshire. Neither patient reported relevant travel history outside of New Hampshire. Patient 1 reported observing that the proportion of moose carcasses with extensive cystic lung lesions has increased in recent years. The stool of his 4-year-old domestic dog tested negative for *E. granulosus* through a commercial veterinary laboratory. We postulate that both patients acquired *E. granulosus* infection either by consuming produce contaminated with infected canid feces or through consumption of eggs shed in their dogs' stool. The patients gave verbal permission to publish this report.

In the United States, locally acquired human *E. granulosus* infections remain rare. However, cases in Arctic and sub-Arctic areas of Canada and Alaska are well described, mainly among Native American populations (*2*–*4*). In the contiguous United States, a few human cases are reported annually in Arizona, New Mexico, California, and Utah (*4*). *E. granulosus* infections have been described in wildlife of northern New England (*5*,*6*); in 2012, surveillance of the hunter-harvested moose population (*Alces alces*) in Maine documented the presence of the G8 genotype *E. granulosus* (Canadensis) in 21/54 (39%) of lung sets examined. Domestic dogs and eastern coyotes (*Canis latrans*) were suggested as definitive hosts, given the absence of wolves in the area (*5*). Other areas in the contiguous United States where sylvatic cycles of transmission have been confirmed include Idaho, Minnesota, California, and Montana; stable cycles were described mainly in the Arctic and sub-Arctic areas of Canada and Alaska (*2*). Information about *E. granulosus* infections in local wild canids in northern New England is lacking.

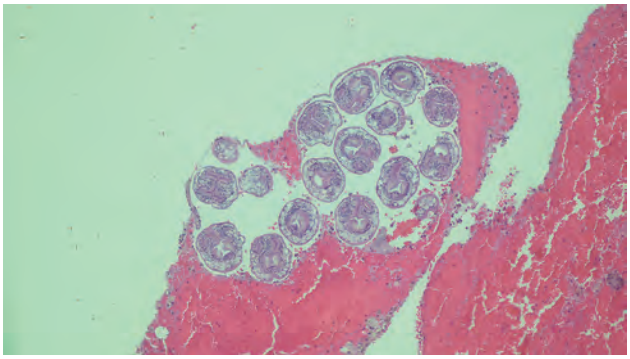

**Figure.** Lung biopsy specimen from a patient with *Echinococcus granulosus* tapeworm infection shows a daughter cyst containing multiple protoscolices with internal hooklets and calcareous corpuscles. Hematoxylin and eosin stain; original magnification ×100.

New Hampshire Department of Health and Human Services has notified healthcare providers caring for patients involved in moose hunting about preventive measures. Such measures include wearing waterproof gloves when dressing moose carcasses, preventing domestic dogs and wild canids from consuming raw viscera, disposing of all viscera in accordance with recommendations from New Hampshire Fish and Game Department, thoroughly cooking all game meat that is fed to dogs, and administering to dogs a deworming agent effective against tapeworms at least twice per year.

## About the Author

Dr. AlSalman completed a fellowship in infectious diseases as well as residency in general preventive medicine and public health at Dartmouth Health in Lebanon, New Hampshire. He is now an infectious diseases consultant at UnityPoint Health in Des Moines, Iowa.

## References


1. US Centers for Disease Control and Prevention. Echinococcosis—biology. 2019 July 16 [cited 2022 May 12]. https://www.cdc.gov/parasites/echinococcosis/biology.html
2. Cerda JR, Buttke DE, Ballweber LR. *Echinococcus* spp. tapeworms in North America. Emerg Infect Dis. 2018;24:230–5. https://doi.org/10.3201/eid2402.161126
3. Himsworth CG, Jenkins E, Hill JE, Nsungu M, Ndao M, Thompson RCA, et al. Emergence of sylvatic *Echinococcus granulosus* as a parasitic zoonosis of public health concern in an indigenous community in Canada. Am J Trop Med Hyg. 2010;82:643–5. https://doi.org/10.4269/ajtmh.2010.09-0686
4. Deplazes P, Rinaldi L, Alvarez Rojas CA, Torgerson PR, Harandi MF, Romig T, et al. Global distribution of alveolar and cystic echinococcosis. Adv Parasitol. 2017;95:315–493. https://doi.org/10.1016/bs.apar.2016.11.001
5. Lichtenwalner A, Adhikari N, Kantar L, Jenkins E, Schurer J. *Echinococcus granulosus* genotype G8 in Maine moose (*Alces alces*). Alces. 2014;50:27–33.
6. Schurer JM, Bouchard E, Bryant A, Revell S, Chavis G, Lichtenwalner A, et al. Echinococcus in wild canids in Québec (Canada) and Maine (USA). PLoS Negl Trop Dis. 2018;12:e0006712. https://doi.org/10.1371/journal.pntd.0006712


Address for correspondence: Ahmad AlSalman, Iowa Methodist Medical Center, Infectious Disease, 1221 Pleasant St, Ste 300, Des Moines IA 50309-1406, USA; email: ahmad.alsalman@dartmouth.edu

# Mpox among Public Festival Attendees, Chicago, Illinois, USA, July–August 2022

Emily A.G. Faherty, Richard A. Teran, Stephanie R. Black, Vaishali Chundi, Shamika Smith, Brandon Bernhardt, Emma Weber, Bridget Brassil, Peter Ruestow, Janna L. Kerins

Author affiliations: Centers for Disease Control and Prevention, Atlanta, Georgia, USA (E.A.G. Faherty); Chicago Department of Public Health, Chicago, Illinois, USA (E.A.G. Faherty, R.A. Teran, S.R. Black, V. Chundi, S. Smith, B. Bernhardt, E. Weber, B. Brassil, P. Ruestow, J.L. Kerins)

DOI: https://doi.org/10.3201/eid2905.221797

We investigated an mpox outbreak after a 2022 LGBTQ event in Chicago, Illinois, USA. Among case-patients, 38% had received 1 dose of mpox vaccine, none 2 doses; most reported sexual activity during the probable exposure period. Among other preventive measures, persons at risk should complete mpox vaccination 14 days before an event.

Monkeypox virus transmission may be associated with large events where at-risk or potentially infected persons engage in sexual activity at or outside the event (*1*). The Chicago Department of Public Health (CDPH) investigated an mpox outbreak associated with Market Days (MD), an annual LGBTQ outdoor festival held in Chicago, Illinois, USA, August 6–7, 2022, attended by ≈100,000 persons from across the country. We describe persons with mpox who attended the festival.

CDPH interviewed mpox case-patients (*2*) to ascertain MD attendance and conducted a supplemental survey about exposures, sexual behavior, and preventive measures. Event-attending case-patients were defined as persons with positive mpox or orthopoxvirus test results who attended MD on August 6–7 and had symptoms within 21 days before or after attendance (July 16–August 28). Illinois surveillance systems verified laboratory and JYNNEOS (https://www.jynneos.com) vaccination data. CDPH also solicited cases from other jurisdictions in a national call for cases related to the event. Event-associated case-patients were categorized by vaccination status at the time of MD. This investigation was reviewed by the Centers for Disease Control and Prevention and conducted in accordance with its policies and applicable federal law (45 C.F.R. part 46.102(l) (*2*), 21 C.F.R. part 56; 42 U.S.C. §241(d); 5 U.S.C. §552a; 44 U.S.C. §3501 et seq).

We identified 40 event-associated case-patients from Chicago and other jurisdictions who attended MD; symptom onset occurred before MD for 7 and during or after for 33 (Figure). Case-patients with symptom onset before MD had a median of 1 (interquartile range [IQR] 1–2) sex partner during MD, and case-patients with symptom onset after MD had a median of 5 (IQR 2–5) sex partners during MD (Appendix, https://wwwnc.cdc.gov/EID/article/29/5/22-1797-App1.pdf). Many case-patients were non-Hispanic/Latino White (45%), most were

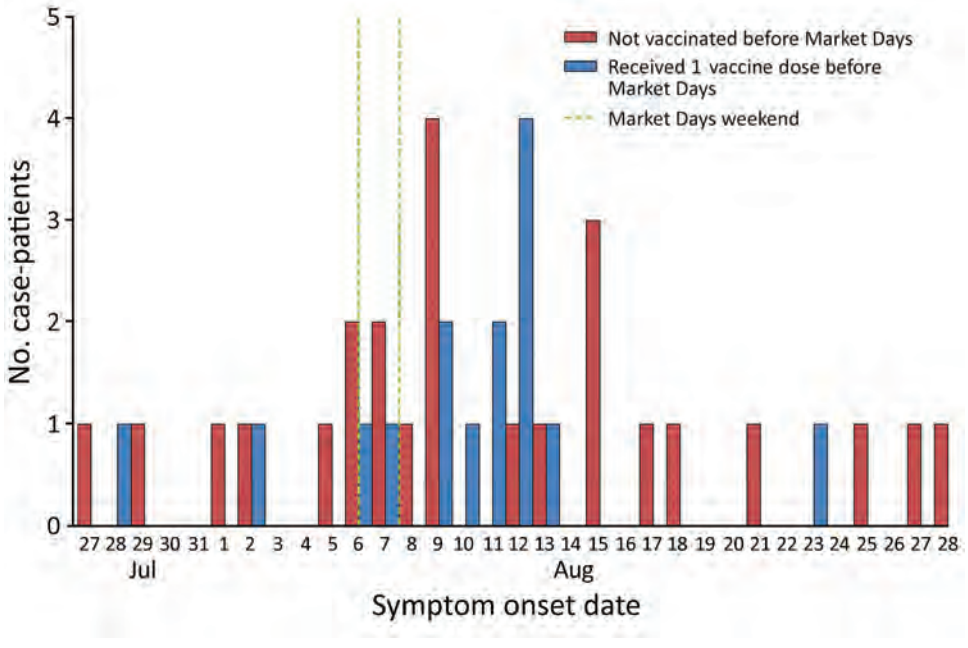


**Figure.** Epidemic curve for mpox case-patients who attended Market Days event, by symptom onset date, Chicago, Illinois, USA, July–August 2022. Vertical dashed lines indicate dates of Market Days event. Vaccine was JYNNEOS (https://www.jynneos.com).

**Table.** Characteristics of mpox case-patients attending MD event, by vaccination status before the event, Chicago, Illinois, USA, July–August 2022*

| Characteristics | All cases, n = 40 | Vaccinated before MD, n = 15 | Not vaccinated before MD, n = 25 |
|---|---|---|---|
| Demographics† | | | |
| Chicago resident | 36 (90) | 14 (93.3) | 22 (88) |
| Male sex at birth | 39 (97.5) | 15 (100) | 24 (96) |
| Median age in years, IQR | 31 (27.3–35.8) | 32 (29–35.5) | 30 (25.5–35.5) |
| Reported male-to-male sexual contact | 28 (70) | 11 (73.3) | 17 (68) |
| Race/ethnicity | | | |
| Non-Hispanic or Latino White | 18 (45) | 8 (53.3) | 10 (40) |
| Non-Hispanic or Latino Black | 9 (22.5) | 2 (13.3) | 7 (28) |
| Hispanic or Latino | 13 (32.5) | 5 (33.3) | 8 (32) |
| Sexual exposures | | | |
| Reported having sex during probable exposure period | 32 (80) | 12 (80) | 20 (80) |
| Reported having sex during MD | 14 (35) | 6 (40) | 8 (32) |
| Sex with a main partner at MD | 1 (2.5) | - | 1 (4) |
| Sex with a casual partner at MD | 3 (7.5) | 1 (6.7) | 2 (8) |
| Sex with an anonymous partner at MD | 7 (17.5) | 4 (26.7) | 3 (12) |
| Reported nonsexual skin-to-skin contact or kissing during probable exposure period | 4 (10) | 2 (13.3) | 2 (8) |
| Reported sexual activity outside probable exposure period | 1 (3) | ND | 1 (4) |
| Missing information about sexual exposures | 1 (3) | ND | 1 (4) |
| Median no. sex partners at MD (IQR) | 3.5 (1.3–5) | 4 (2.3–5) | 3 (1–5.3) |
| Met sex partners at MD | 9 (23) | 4 (26.6) | 5 (20) |
| Met at another location | 2 (5) | 2 (13.3) | ND |
| Met by using an online app | 2 (5) | 2 (13.3) | ND |
| Nonvaccine prevention measures‡ | 28 (70) | 12 (80) | 16 (64) |
| Abstained from sex | 9 (23) | 2 (13.3) | 7 (28) |
| Reduced number of sex partners | 5 (13) | 2 (13.3) | 3 (12) |
| Avoided skin-to-skin contact | 8 (20) | 4 (26.7) | 4 (16) |
| Wore more clothing | 3 (8) | 2 (13.3) | 1 (4) |
| Other measures§ | 8 (20) | 3 (20) | 5 (20) |

*Values are no. (%) except as indicated. Tests of significant differences by vaccination status were conducted by using Fisher exact tests and t-tests for continuous variables; no values were p>0.05. IQR, interquartile range; MD, Market Days; ND, no data.
†Percentages may not add up to 100% because of rounding.
‡Case-patients may have reported adopting >1 prevention measure.
§Other measures included isolating after the event and wearing protective clothing or a mask.

male at birth (98%), and most reported having sex with men (70%) (Table). Two case-patients, 1 living with HIV, were hospitalized for mpox.

Fifteen (38%) case-patients had received 1 dose of JYNNEOS vaccine before MD; none received 2 doses or were due for their second dose by MD (within 28 days of first dose). Among 1-dose recipients, 8 (53%) were vaccinated <14 days before symptom onset. Among all 1-dose recipients vaccinated before symptom onset, median time from vaccination to symptom onset was 13 (IQR 9–29) days. Fewer non-Hispanic/Latino Black case-patients were vaccinated before MD (2/15, 13%) than non-Hispanic/Latino White (8/15, 53%) or Hispanic/Latino (5/15, 33%) case-patients.

Most (32/40, 80%) case-patients reported having had sexual activity during the probable exposure period (21 days before symptom onset). Case-patient reports included sexual activity during MD (August 6–7) at any location, meeting a partner at MD, and sexual activity at the event. Only 14 (35%) case-patients reported sexual activity during MD at any location, including 3 with symptom onset before those dates. Nine (23%) persons engaged in sex with >1 partner during MD, 9 (23%) met a sex partner at MD, and 4 (10%) case-patients reported sexual activity at MD. Case-patients reporting sexual activity during MD had a median of 3.5 (IQR 1.3–5.0) partners; more had anonymous sex partners (7/14, 50%) than casual or main partners (4/14, 29%). More case-patients who received 1 vaccine dose before MD had sex with an anonymous partner during MD (4/15, 27%) than did unvaccinated case-patients (3/25, 12%).

Among all event-associated case-patients, 28 (70%) adopted nonvaccine prevention measures during MD; 9 (23%) abstained from sex, and 8 (20%) avoided skin-to-skin contact. More case-patients unvaccinated before MD abstained from sex during MD (7/25, 28%) than did 1-dose recipients (2/15, 13%). Seven (78%) of 9 case-patients who abstained from sex during MD reported having sex during the probable exposure period. Among case-patients reporting sexual activity during MD, 2 (2/14, 14%) reduced their number of sex partners and 4 (4/14, 29%) adopted other measures (e.g., isolating after MD).

Although MD might have presented more opportunities for sex partnerships, <50% of case-patients reported sex related to the event. Among case-patients who had sex during MD, most had anonymous sex partners, potentially increasing transmission (3). Most case-patients also reported adopting ≥1 prevention measure during MD but may not have maintained measures throughout the probable exposure period. For example, among 9 persons who abstained from sex at MD, 7 (78%) reported sexual activity with ≥1 partner outside the event.

More than one third of case-patients reported 1 vaccine dose before MD. Symptoms developed within 14 days after the first dose for most (8, 53%) who were partially vaccinated before MD. Although equal proportions of vaccinated and unvaccinated persons reported sex during MD, 1-dose recipients reported taking fewer precautions, such as abstaining from sex or avoiding anonymous sex.

Among study limitations, we may have undercounted event-associated case-patients. Out-of-state case-patients may not have reported or been asked about event attendance. Also, without a comparison group, we could not compare preventive measures by case-patient status. Information about prevention measures and sexual behavior were self-reported and subject to social desirability bias.

Vaccination uptake before large gatherings may affect behavior and perceived infection risk. Risk messaging should emphasize completing vaccination 14 days before an event and taking other measures to prevent mpox.

#### Acknowledgments

We thank Suzanne Beavers, Palak Panchal, Hannah Matzke, Leah Quinn, Saul Ayala, Sarah Love, Elizabeth Shane, Alexandria Davis, Andrew Weidemiller, Angelica Serra, Anthony Garcia, Ben Cammack, Cecilia Pigozzi, Dailha Acevedo, Damian Plaza, Daniel Liguori, Hallie Hutchison, Janetta Prokopowicz, Jazmine Wright, Jose Medina, Lily Fahrenwald, Maria Ferreira-Alharb, Marsha Flowers, Maureen Love, Mawiyah Coates, Salma Ali, Seliciano Douthard, Susan Woods, Tiffany Evans, and Vilma Alicea for their work on this investigation.

### About the Author

Dr. Faherty is an infectious disease epidemiologist and CDC Epidemic Intelligence Service Officer assigned to the Chicago Department of Public Health Bureau of Disease Control in the Communicable Diseases Program. Her research interests include vaccine-preventable disease and sexual and reproductive health.

#### References

1. Iñigo Martínez J, Gil Montalbán E, Jiménez Bueno S, Martín Martínez F, Nieto Juliá A, Sánchez Díaz J, et al. Monkeypox outbreak predominantly affecting men who have sex with men, Madrid, Spain, 26 April to 16 June 2022. Euro Surveill. 2022;27:2200471. https://doi.org/10.2807/1560-7917.ES.2022.27.27.2200471
2. Centers for Disease Control and Prevention. Case definitions for use in the 2022 monkeypox response [cited 2022 Oct 19]. https://www.cdc.gov/poxvirus/monkeypox/clinicians/case-definition.html
3. van Kesteren NM, Hospers HJ, Kok G. Sexual risk behavior among HIV-positive men who have sex with men: a literature review. Patient Educ Couns. 2007;65:5–20. https://doi.org/10.1016/j.pec.2006.09.003

Address for correspondence: Emily A.G. Faherty, Chicago Department of Public Health, 1340 S Damen Ave, Chicago, IL 60608, USA; tqy5@cdc.gov

# *Burkholderia pseudomallei* Laboratory Exposure, Arizona, USA

Lisa J. Speiser, Erin H. Graf, Maria Teresa Seville, Kai Singbartl, Mary L. Dalton, Denise Harrington, Melissa Kretschmer, Marina Kuljanin, Karen Zabel, Rebecca Sunenshine, Irene Ruberto, Heather Venkat, Thomas E. Grys

Author affiliations: Mayo Clinic Hospital, Phoenix, Arizona, USA (L.J. Speiser, E.H. Graf, M.T. Seville, K. Singbartl, M.L. Dalton, D. Harrington, T.E. Grys); Maricopa County Department of Public Health, Phoenix (M. Kretschmer, M. Kuljanin, K. Zabel, R. Sunenshine); Arizona Department of Health Services, Phoenix (I. Ruberto, H. Venkat); Centers for Disease Control and Prevention, Atlanta, Georgia, USA (H.Venkat)

DOI: https://doi.org/10.3201/eid2905.221865

We describe an incidental *Burkholderia pseudomallei* laboratory exposure in Arizona, USA. Because melioidosis cases are increasing in the United States and *B. pseudomallei* reservoirs have been discovered in the Gulf Coast Region, US laboratory staff could be at increased risk for *B. pseudomallei* exposure.

*Burkholderia pseudomallei* bacterium, the causative agent of melioidosis, is endemic to Australia and Thailand. However, the US Centers for Disease Control and Prevention (CDC) recently discovered positive environmental samples in the Gulf Coast Region of Mississippi, USA, when investigating 2 melioidosis cases (*1*). In 2021, 4 melioidosis cases in the United States were found to be caused by imported aromatherapy spray contaminated with *B. pseudomallei* (*2*). Because melioidosis cases are increasing in the United States, laboratory staff potentially are at risk for *B. pseudomallei* exposure. In nonendemic areas, laboratory staff are unfamiliar with *B. pseudomallei*, and the bacterium commonly is misidentified. As occurred with the 2 melioidosis cases related to aromatherapy products (*2*), matrix-assisted laser desorption/ionization time-of-flight (MALDI-TOF) libraries often misidentify *B. pseudomallei* as *B. thailandensis*. We describe an incidental *B. pseudomallei* laboratory exposure in Arizona, USA.

In mid-January 2021, the microbiology laboratory at Mayo Clinic Arizona (Phoenix, AZ, USA) identified *Burkholderia* species growing from an intraoperative periaortic swab sample obtained from a 58-year-old man with a mycotic aneurysm (*3*). Results of routine Gram stains of all specimens were negative. Aerobic cultures revealed pinpoint growth on sheep blood and chocolate agars, but not on MacConkey agar, after 18 hours. Staff performed Gram stain of the colonies, which revealed gram-negative rods. The technologist suspected an atypical *Pseudomonas* species and, on an open benchtop, performed oxidase testing, with positive results, and spot indole testing, with negative results. MALDI-TOF mass spectrometry provided an unvalidated *B. thailandensis* identification. Because of concerns that the unvalidated result could suggest *B. pseudomallei*, staff performed slide catalase testing on a fresh subculture per the Laboratory Response Network Sentinel Level Clinical Laboratory Protocol (*4*). The catalase reaction was negative, which was inconsistent with *Burkholderia* species. The laboratory then sent the isolate to the Mayo Clinic reference laboratory (Rochester, MN, USA) for definitive identification. By using a laboratory-developed MALDI-TOF database that was considered unvalidated, the reference laboratory presumptively identified the isolate as *B. pseudomallei*. The Minnesota Public Health Laboratory confirmed *B. pseudomallei* through molecular and biochemical methods. Repeat catalase testing found the isolate to be slide catalase–negative but weakly tube catalase–positive. The isolate was transferred to CDC for antimicrobial-susceptibility testing, which demonstrated a typical susceptibility profile to trimethoprim/sulfamethoxazole, doxycycline, amoxicillin/clavulanic acid, and ceftazidime. *B. pseudomallei* growth was eventually observed on both MacConkey and colistin nalidixic acid agars and on all anaerobic, mycobacterial, and fungal culture media. *B. pseudomallei* is a Select Agent, thus, the Federal Select Agent Program was notified, and all cultures were destroyed within 7 days of definitive identification.

Because of initial lack of clinical suspicion for *B. pseudomallei*, we evaluated clinical staff for exposure. We identified 30 employees who had possible exposure. We assessed each employee for exposure risk, as previously described (*5*), and identified 3 employees who were exposed in the microbiology laboratory: 1 high-risk and 2 low-risk exposures. The employee with high-risk exposure had a predisposing condition and performed an aerosolizing procedure outside of the biologic safety cabinet by subjecting the specimen to MALDI-TOF mass spectrometry without first inactivating it. The 2 employees with low-risk exposures participated in close inspection of the open plate growing *B. pseudomallei* outside of the biologic safety cabinet.

Laboratory-acquired melioidosis is extremely rare. Reports of 2 prior laboratory-acquired melioidosis cases in the United States have been published (*6*,*7*), but none have been reported since 1981. As for the high-risk exposure we describe, both published cases were attributed to aerosol exposure (*6*,*7*). *B. mallei* is considered to have greater potential for laboratory infection than *B. pseudomallei* (*8*).

In animal models, postexposure prophylaxis (PEP) has been shown to effectively prevent acute melioidosis if administered within 24 hours of exposure (*9*). However, PEP fails to prevent latent or persistent infection (*10*); nonetheless, consensus recommendations are to offer PEP to all employees with high- and low-risk incidents, regardless of their predisposing risk for melioidosis (*5*). After explaining risks versus benefits, we offered the employee with high-risk exposure a 3-week duration of trimethoprim/sulfamethoxazole PEP (*5*,*9*). However, the employee stopped PEP after 1 week because of insomnia; no subsequent PEP was prescribed because the employee stopped PEP without consulting a medical provider. On the basis of guidance from the Maricopa County Department of Public Health, we offered PEP to the employees with low-risk exposures; 1 elected to take doxycycline, and the other declined PEP.

We instructed exposed employees to monitor their temperatures 2 times a day for 21 days and notify the hospital's occupational health department if symptoms occurred. None of the employees reported symptoms during the monitoring period.

Because *B. pseudomallei* can persist intracellularly for extended periods before causing clinical disease, we requested assistance from the Arizona Department of Health Services, Maricopa County Department of Public Health, and CDC to offer serologic monitoring to the exposed employees; 2 elected to undergo serologic monitoring. After 6 weeks, neither employee seroconverted.

In conclusion, lack of clinical and laboratory suspicion for *B. pseudomallei* resulted in incidental laboratory exposure of 3 employees. US laboratories should remain vigilant for and aware of the growth characteristics associated with *B. pseudomallei* to help avoid occupational exposure.

### About the Author

Dr. Speiser is an assistant professor of medicine at the Mayo Clinic College of Medicine, Phoenix, Arizona, USA, and serves as a senior associate consultant in the Department of Infectious Diseases and medical director of Infection Prevention and Control at the Mayo Clinic, Phoenix. Her research interests include hospital-acquired infections and emerging infectious diseases.

### References


1. Centers for Disease Control and Prevention. Bacteria that causes rare disease melioidosis discovered in U.S. environmental samples [cited 2022 Sep 21]. https://www.cdc.gov/media/releases/2022/p0727-Melioidosis.html
2. Gee JE, Bower WA, Kunkel A, Petras J, Gettings J, Bye M, et al. Multistate outbreak of melioidosis associated with imported aromatherapy spray. N Engl J Med. 2022;386:861–8. https://doi.org/10.1056/NEJMoa2116130
3. Speiser LS, Kasule S, Hall CM, Sahl JW, Wagner DM, Saling C, et al. A case of *Burkholderia pseudomallei* mycotic aneurysm linked to exposure in the Caribbean via whole-genome sequencing. Open Forum Infect Dis. 2022;9:ofac136. https://doi.org/10.1093/ofid/ofac136
4. American Society for Microbiology. Sentinel level clinical laboratory guidelines for suspected agents of bioterrorism and emerging infectious diseases; *Burkholderia mallei* and *Burkholderia pseudomallei* [cited 2021 Sep 29]. https://www.asm.org/Articles/Policy/Laboratory-Response-Network-LRN-Sentinel-Level-C
5. Peacock SJ, Schweizer HP, Dance DA, Smith TL, Gee JE, Wuthiekanun V, et al. Management of accidental laboratory exposure to *Burkholderia pseudomallei* and *B. mallei*. Emerg Infect Dis. 2008;7:e2. https://doi.org/10.3201/eid1407.071501
6. Green RN, Tuffnell PG. Laboratory acquired melioidosis. Am J Med. 1968;44:599–605. https://doi.org/10.1016/0002-9343(68)90060-0
7. Schlech WF III, Turchik JB, Westlake RE Jr, Klein GC, Band JD, Weaver RE. Laboratory-acquired infection with *Pseudomonas pseudomallei* (melioidosis). N Engl J Med. 1981;305:1133–5. https://doi.org/10.1056/NEJM198111053051907
8. Srinivasan A, Kraus CN, DeShazer D, Becker PM, Dick JD, Spacek L, et al. Glanders in a military research microbiologist. N Engl J Med. 2001;345:256–8. https://doi.org/10.1056/NEJM200107263450404
9. Sivalingam SP, Sim SH, Jasper LC, Wang D, Liu Y, Ooi EE. Pre- and post-exposure prophylaxis of experimental *Burkholderia pseudomallei* infection with doxycycline, amoxicillin/clavulanic acid and co-trimoxazole. J Antimicrob Chemother. 2008;61:674–8. https://doi.org/10.1093/jac/dkm527
10. Barnes KB, Steward J, Thwaite JE, Lever MS, Davies CH, Armstrong SJ, et al. Trimethoprim/sulfamethoxazole (co-trimoxazole) prophylaxis is effective against acute murine inhalational melioidosis and glanders. Int J Antimicrob Agents. 2013;41:552–7. https://doi.org/10.1016/j.ijantimicag.2013.02.007


Address for correspondence: Lisa Speiser, Infectious Diseases Department, Mayo Clinic, 5777 East Mayo Blvd, Phoenix, AZ 85054, USA; email: speiser.lisa@mayo.edu

# Epizootic Hemorrhagic Disease Virus Serotype 8, Italy, 2022

Alessio Lorusso, Stefano Cappai, Federica Loi, Luigia Pinna, Angelo Ruiu, Giantonella Puggioni, Annalisa Guercio, Giuseppa Purpari, Domenico Vicari, Soufien Sghaier, Stephan Zientara, Massimo Spedicato, Salah Hammami, Thameur Ben Hassine, Ottavio Portanti, Emmanuel Breard, Corinne Sailleu, Massimo Ancora, Daria Di Sabatino, Daniela Morelli, Paolo Calistri, Giovanni Savini

Author affiliations: Istituto Zooprofilattico Sperimentale dell'Abruzzo e del Molise "Giuseppe Caporale", Teramo, Italy (A. Lorusso, M. Spedicato, O. Portanti, M. Ancora, D. Di Sabatino, D. Morelli, P. Calistri, G. Savini); Istituto Zooprofilattico Sperimentale della Sardegna, Sassari, Italy (S. Cappai, F. Loi, L. Pinna, A. Ruiu, G. Puggioni); Istituto Zooprofilattico Sperimentale della Sicilia, Palermo, Italy (A. Guercio, G. Purpari, D. Vicari); Institut de la Recherche Vétérinaire de Tunisie, Tunis, Tunisia (S. Sghaier); Laboratoire de Santé Animale, Maisons–Alfort, France (S. Zientara, E. Breard, C. Sailleu); Universitè de la Manouba, Tunisia (S. Hammami); Commissariat Régional au Développement Agricole de Nabeul, Nabeul, Tunisia (T. Ben Hassine)

DOI: https://doi.org/10.3201/eid2905.221773

We describe the detection of epizootic hemorrhagic disease virus (EHDV) serotype 8 in cattle farms in Sardinia and Sicily in October–November 2022. The virus has a direct origin in North Africa; its genome is identical (>99.9% nucleotide sequence identity) to EHDV serotype 8 strains detected in Tunisia in 2021.

The World Organisation for Animal Health (WOAH) lists epizootic hemorrhagic disease (EHD) as a disease of wild and domestic ruminants caused by EHD virus (EHDV). EHDV is related to bluetongue virus (BTV), the etiologic agent of bluetongue, a disease of ruminants. Both viruses belong to the genus *Orbivirus* and circulate in multiple serotypes (*1*,*2*). Their viral genomes consist of 10 segments (S1–S10) of double-strand RNA; the structural outer capsid protein (coded by S2) determines serotype specificity. Both viruses cause similar clinical signs in cattle and are transmitted by *Culicoides* spp. biting midges. Bluetongue primarily affects sheep and in recent decades has been described multiple times in the European Union (EU), causing devastating repercussions on animal trade (*3*). Most bluetongue outbreaks in Europe had a direct origin in North Africa because of wind-driven dissemination of BTV-infected midges from this region (*1*,*4*–*7*). We describe detection of EHDV serotype 8 (EHDV-8) in cattle in Italy, as a follow-up to our previous studies on EHDV-8 (GenBank accession nos. OP381190–9) in Tunisia in 2021 (*8*).

On October 25, 2022, respiratory distress, erosions of the muzzle and oral mucosa, and drooling were reported in 3 cattle at farm 1, located near the city of Trapani, Sicily (Figure); serum and whole blood samples were collected. On October 28, 2022, clinical signs consisting of inappetence, cyanosis and edema of the tongue, conjunctivitis, and fever were reported in an animal at farm 2, located in Arbus Municipality of Sardinia (Figure). On November 3, that animal died; spleen was collected at necropsy, along with whole blood from 3 additional symptomatic cattle on the farm. On November 4, at farm 3 (in Arbus Municipality) and farm 4 (in nearby Guspini Municipality), 3 cattle showed similar signs, and whole blood and serum samples were collected (Figure).

We tested 1 EDTA blood sample per animal and spleen samples for EHDV RNA by using a VetMAX EHDV Kit (Thermo Fisher Scientific, https://www.thermofisher.com). We developed a real-time reverse transcription PCR (rRT-PCR) specific for the S2 of the EHDV-8 strain detected in Tunisia in 2021 (EHDV-8 TUN 2021) because the available test designed for the S2 segment of the EHDV-8 reference serotype (isolated in Australia in 1982) did not detect EHDV-8 TUN 2021 (*8*). Primer nucleotide sequences were EHDV_Ser8varNEW_fwd AGAGATGAAGATCGCGAGGA and EHDV_Ser8varNEW_rev GAATCACACGCGCTCACTAA; the probe nucleotide sequence was EHDV_Ser8varNEW_Probe FAM-ACGGATGAGATACGGAACATACGGGG-TAMRA. We prepared the master mix by using TaqMan Fast Virus 1-Step (Thermo Fisher Scientific)

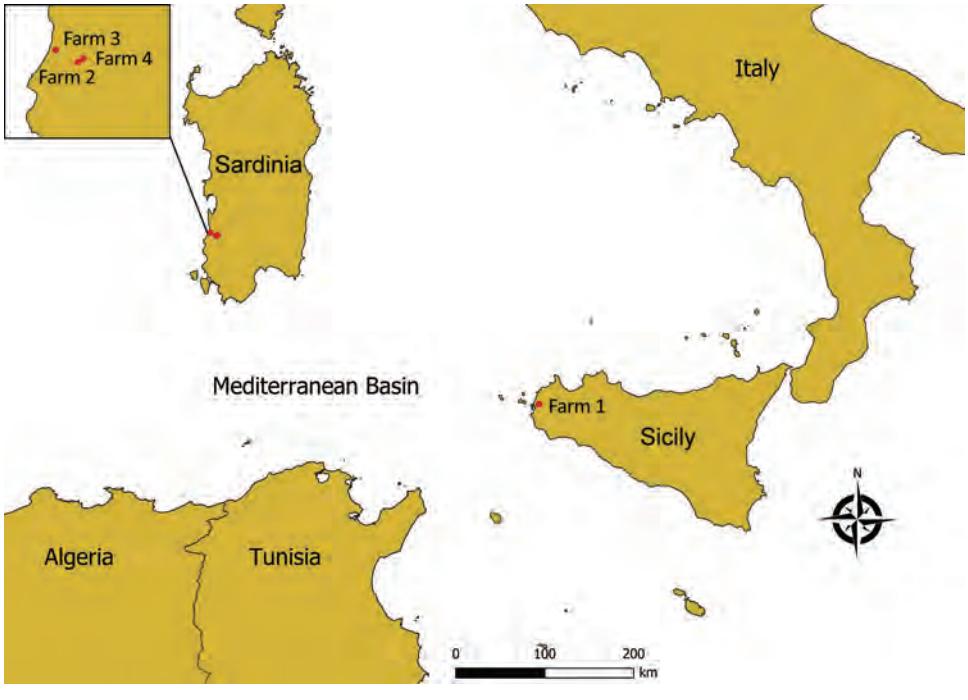


**Figure.** Geographic locations for detection of epizootic hemorrhagic disease virus serotype 8, Italy, 2022. Red dots indicate locations of the 4 farms involved. Inset map details locations of the 3 farms affected in the Arbus Municipality of Sardinia.

and a final concentration of 400 nmol (primers) and 200 nmol (probe). After we performed RNA denaturation at 95°C for 3 min, we added 5 μL of RNA to 20 μL of mix and achieved amplification as follows: 45°C for 10 min, 95°C for 10 min, then 40 cycles of 95°C for 15 s, and finally 60°C for 1 min. We performed whole-genome sequencing (WGS) (*9*) on selected samples. We tested serum samples collected from all animals with a competitive ELISA, ID Screen EHDV Competition (Innovative Diagnostics, https://www.innovative-diagnostics.com), and by virus neutralization (*10*). We attempted virus isolation by using rRT-PCR–positive blood samples on Vero cells (*8*).

All sampled animals from Sardinia and Sicily were positive for EHDV RNA (cycle threshold 23–28). Genotyping confirmed the presence of EHDV-8 TUN 2021–like strains. We reported the outbreak to Italy's Ministry of Health, which notified WOAH and the European Commission, which imposed animal movement restrictions within a 150-km radius of the outbreak sites. We selected 1 EHDV-8–positive blood sample from Sardinia for WGS; results confirmed that the Sardinia EHDV-8 strain (GenBank accession nos. OP897265–74) shares high nucleotide sequence identity (>99.9%) with multiple EHDV-8 TUN 2021–like strains. WGS of the Sicily strains is ongoing. We isolated the virus from all rRT-PCR–positive blood samples; all serum samples tested positive by ELISA and by virus neutralization (antibody titer 10–20).

Confirmation of novel *Orbivirus* incursion into the EU sustained by EHDV-8 was predictable, considering the distribution of this virus in Tunisia and likely in neighboring countries (*8*). On November 18, 2022, EHD was also reported in the Andalusia region of Spain, in the cities of Cadiz and Seville. Predicting future scenarios for the EU cattle production system is difficult, but EHD will probably pose new challenges to EU veterinary authorities. The lessons learned with bluetongue should be a reference for choosing proper control and prevention strategies for EHD. Overall, these events further emphasize the importance for countries in Europe to have robust collaborations with authorities in North Africa on public and animal health. The prompt detection of EHDV-8 in Sardinia and Sicily is the most recent example of the benefits that such relationships could yield. This collaboration proved crucial; it led to development of a specific and accurate molecular test for detecting EHDV-8, given that knowledge of the genome constellation and the genomic relatedness of EHDV-8 with extant EHDV serotypes had already been achieved. Vaccine development needs to be boosted because vaccination is the only strategy to reduce virus circulation and prevent direct and indirect economic losses.

This work was supported by the Prima Foundation through project BlueMed and by Italy's Ministry of Health through project Ricerca Corrente EpiTraP and project Ricerca Finalizzata ArtOmic.

## About the Author

Dr. Lorusso is a virologist and doctor of veterinary medicine at the Istituto Zooprofilattico Sperimentale dell'Abruzzo e del Molise "Giuseppe Caporale". His research interests include the surveillance and characterization of viruses of public health interest.

## References

1. MacLachlan NJ, Mayo CE, Daniels PW, Savini G, Zientara S, Gibbs EP. Bluetongue. Rev Sci Tech. 2015;34:329–40. https://doi.org/10.20506/rst.34.2.2360
2. Savini G, Afonso A, Mellor P, Aradaib I, Yadin H, Sanaa M, et al. Epizootic haemorrhagic disease. Res Vet Sci. 2011;91:1–17. https://doi.org/10.1016/j.rvsc.2011.05.004
3. Rushton J, Lyons N. Economic impact of bluetongue: a review of the effects on production. Vet Ital. 2015;51:401–6.
4. Lorusso A, Guercio A, Purpari G, Cammà C, Calistri P, D'Alterio N, et al. Bluetongue virus serotype 3 in western Sicily, November 2017. Vet Ital. 2017;53:273–5.
5. Lorusso A, Sghaier S, Di Domenico M, Barbria ME, Zaccaria G, Megdich A, et al. Analysis of bluetongue serotype 3 spread in Tunisia and discovery of a novel strain related to the bluetongue virus isolated from a commercial sheep pox vaccine. Infect Genet Evol. 2018;59:63–71. https://doi.org/10.1016/j.meegid.2018.01.025
6. Cappai S, Rolesu S, Loi F, Liciardi M, Leone A, Marcacci M, et al. Western bluetongue virus serotype 3 in Sardinia, diagnosis and characterization. Transbound Emerg Dis. 2019;66:1426–31. https://doi.org/10.1111/tbed.13156
7. Calistri P, Giovannini A, Conte A, Nannini D, Santucci U, Patta C, et al. Bluetongue in Italy: part I. Vet Ital. 2004;40:243–51.
8. Sghaier S, Sailleau C, Marcacci M, Thabet S, Curini V, Ben Hassine T, et al. Epizootic haemorrhagic disease virus serotype 8 in Tunisia, 2021. Viruses. 2022;15:16. https://doi.org/10.3390/v15010016
9. Marcacci M, De Luca E, Zaccaria G, Di Tommaso M, Mangone I, Aste G, et al. Genome characterization of feline morbillivirus from Italy. J Virol Methods. 2016;234:160–3. https://doi.org/10.1016/j.jviromet.2016.05.002
10. World Organisation for Animal Health. Manual of diagnostic tests and vaccines for terrestrial animals 2022 [cited 2022 Nov 12]. https://www.woah.org/en/what-we-do/standards/codes-and-manuals/terrestrial-manual-online-access

Address for correspondence: Alessio Lorusso, Istituto Zooprofilattico Sperimentale dell'Abruzzo e del Molise "Giuseppe Caporale", Via Campo Boario 1, Teramo 64100, Italy; email: a.lorusso@izs.it

# Human-to-Animal Transmission of SARS-CoV-2, South Korea, 2021

Jinsun Bae,[1] Changseek Ro,[1] Yunhee Kang, Eulhae Ga, Woonsung Na, Daesub Song

Author affiliations: Seoul Metropolitan Government, Seoul, South Korea (J. Bae, C. Ro, Y. Kang); Chonnam National University, Gwangju, South Korea (E. Ga, W. Na); Seoul National University, Seoul (D. Song)

DOI: https://doi.org/10.3201/eid2905.221359

To investigate SARS-CoV-2 transmission from humans to animals in Seoul, South Korea, we submitted samples from companion animals owned by persons with confirmed COVID-19. Real-time PCR indicated higher SARS-CoV-2 viral infection rates for dogs and cats than previously reported from the United States and Europe. Host-specific adaptations could introduce mutant SARS-CoV-2 to humans.

The risk for zoonoses (animal-to-human transmission) is increasing as human and wildlife habitats overlap with more human and animal migration and industrial food animals worldwide. Reverse zoonosis (human-to-animal transmission) also occurs (*1*–*5*), including the possibility that an animal could act as a carrier and reinfect a person.

According to South Korea government health policy, every confirmed human case of COVID-19 is reported to the regional public health center, and epidemiologic investigations began in February 2021. To determine possible human-to-animal transmission of SARS-CoV-2, we surveyed SARS-CoV-2 results for companion animals (dogs and cats) owned by persons with confirmed COVID-19 who were living in Seoul during February–November 2021. We assessed only companion animals for which owners were confirmed and for which owners had requested testing. A total of 375 companion animals (271 dogs and 104 cats) were tested for SARS-CoV-2 by real-time PCR.

When a companion animal exhibits suspected clinical signs and its owner requests a test, the Seoul city animal specimen collection team is dispatched to collect samples. For this study, the veterinarian managing the protection facility collected samples from companion animals whose owners had been confirmed to have COVID-19 and transferred the animals to separate protection facilities. Sampling was conducted according to guidelines of the World Organisation for Animal Health (*6*). Samples were collected by swabbing 3 locations on the animals: the oropharynx, nasal cavity, and rectum. The samples were transferred to individual virus transport media (1 mL), packaged in 3-layer biosafety packaging containers, and transported to the testing facility while refrigeration was maintained.

The COVID-19 diagnosis was established by using the real-time PCR method recommended by the World Health Organization to determine the presence or absence of SARS-CovV-2 virus antigens (*7*). Among the amplification genes, both RdRp (RNA-dependent RNA polymerase) and E genes were detected, indicating SARS-CoV-2 positivity; cycle threshold for each was $\leq$38. When PCR was positive for samples from $\geq$1 of the 3 sampling sites, the animal was determined to have a positive result.

Using SPSS Statistics 24 (IBM, https://www.ibm.com), we cross-tabulated and statistically analyzed the COVID-19 infection rate for companion dogs and cats owned by persons with confirmed cases of COVID-19. We found that 102 (27.2%) of 375 animals examined had positive results for SARS-CoV-2 infection: 65 (24%) dogs and 37 (35.6%) cats (Table). When we compared the positivity rates for the 2 species, we found that the positivity rate for cats was significantly higher than that for dogs ($p<0.024$).

We also investigated the rate of positivity detection according to sampling site. The positivity rate was higher for samples collected from the oropharynx (72.41%) and nasal cavity (84.85%) of dogs and from the oropharynx (83.33%) and nasal cavity (75.0%) of cats than from the rectum from either species (30.3% for dogs and 51.43% for cats).

This study reveals SARS-CoV-2 positivity rates of 24.0% for dogs and 35.6% for cats in South Korea, higher than rates previously reported from studies of dogs and cats. Although the animals in our study were already known to have been exposed to SARS-CoV-2 because their owners were confirmed to have COVID-19, the rate of positivity is high compared with rates determined in previous studies of animals with SARS-CoV-2–positive owners (*8*,*9*). This finding emphasizes the value and necessity of managing infectious diseases in companion animals as well as in humans because the risk for reverse zoonoses increases when companion animals are in prolonged and close contact with their owners.

[1]These authors contributed equally to this article.

**Table.** Positivity rates for companion animals owned by SARS-CoV-2–positive persons in study of human-to-animal transmission of SARS-CoV-2, South Korea, 2021*

| Animal | Test results, no. (%) | | $\chi^2$ distribution | p value |
|---|---|---|---|---|
| | Positive | Negative | | |
| Dogs, n = 271 | 65 (24.0) | 206 (76.0) | 5.100 | 0.024 |
| Cats, n = 104 | 37 (35.6) | 67 (64.4) | | |
| Total, n = 375 | 102 (27.2) | 273 (72.8) | | |

*Positivity rate for cats was significantly (p = 0.024) higher than that for dogs.

Our study was limited by having been conducted with animals consigned to the protection facilities of the Seoul City Government and those whose tests were requested by their owners because of the animals' clinical signs. Owner bias might have affected the population in this setting.

Our study could provide epidemiologically meaningful data for public health. As SARS-CoV-2 spreads as a pandemic, reverse zoonotic infections will continue, and viruses will mutate to adapt to the new host. For companion animals living near humans, continuous epidemiologic investigations and monitoring will be needed.

This research was supported by COVID-19 Animal Inspection Project of Seoul Metropolitan Government.

## About the Author

Dr. Bae is a leader of the veterinary public health section of the Seoul Metropolitan government. Her research interests include the epidemiology of zoonoses, infectious disease prevention policies and administrative affairs such as quarantine.

## References

1. Segalés J, Puig M, Rodon J, Avila-Nieto C, Carrillo J, Cantero G, et al. Detection of SARS-CoV-2 in a cat owned by a COVID-19–affected patient in Spain. Proc Natl Acad Sci U S A. 2020;117:24790–3. https://doi.org/10.1073/pnas.2010817117
2. Hamer SA, Pauvolid-Corrêa A, Zecca IB, Davila E, Auckland LD, Roundy CM, et al. SARS-CoV-2 infections and viral isolations among serially tested cats and dogs in households with infected owners in Texas, USA. Viruses. 2021;13:938. https://doi.org/10.3390/v13050938
3. Calvet GA, Pereira SA, Ogrzewalska M, Pauvolid-Corrêa A, Resende PC, Tassinari WS, et al. Investigation of SARS-CoV-2 infection in dogs and cats of humans diagnosed with COVID-19 in Rio de Janeiro, Brazil. PLoS One. 2021; 16:e0250853. https://doi.org/10.1371/journal.pone.0250853
4. Colitti B, Bertolotti L, Mannelli A, Ferrara G, Vercelli A, Grassi A, et al. Cross-sectional serosurvey of companion animals housed with SARS-CoV-2–infected owners, Italy. Emerg Infect Dis. 2021;27:1919–22. https://doi.org/10.3201/eid2707.203314
5. Bessière P, Vergne T, Battini M, Brun J, Averso J, Joly E, et al. SARS-CoV-2 infection in companion animals: prospective serological survey and risk factor analysis in France. Viruses. 2022;14:1178. https://doi.org/10.3390/v14061178
6. World Organisation for Animal Health. Consideration for sampling, testing, and reporting of SARS-CoV-2 in animals [cited 2023 Mar 9]. https://rr-asia.woah.org/wp-content/uploads/2020/05/sampling_testing_and_reporting_of_sars-cov-2_in_animals_7may_2020.pdf
7. Corman V, Bleicker T, Brünink S, Drosten C, Zambon M. Diagnostic detection of 2019-nCoV by real-time RT-PCR [cited 2023 Mar 9]. https://www.who.int/docs/default-source/coronaviruse/protocol-v2-1.pdf
8. Meisner J, Baszler TV, Kuehl KE, Ramirez V, Baines A, Frisbie LA, et al. Household transmission of SARS-CoV-2 from humans to pets, Washington and Idaho, USA. Emerg Infect Dis. 2022;28:2425–34.
9. Kannekens-Jager MM, de Rooij MMT, de Groot Y, Biesbroeck E, de Jong MK, Pijnacker T, et al. SARS-CoV-2 infection in dogs and cats is associated with contact to COVID-19–positive household members. Transbound Emerg Dis. 2022;69:4034–40. https://doi.org/10.1111/tbed.14713

Address for correspondence: Woonsung Na, College of Veterinary Medicine, Chonnam National University, Gwangju 61186, South Korea; email: wsungna@jnu.ac.kr; and Daesub Song, College of Veterinary Medicine, Seoul National University, Seoul 08826, South Korea; email: sds@snu.ac.kr

# Norovirus GII.3[P25] in Patients and Produce, Chanthaburi Province, Thailand, 2022

Watchaporn Chuchaona, Sarawut Khongwichit, Woraya Luang-on, Sompong Vongpunsawad, Yong Poovorawan

Author affiliations: Chulalongkorn University, Bangkok, Thailand (W. Chuchaona, S. Khongwichit, S. Vongpunsawad, Y. Poovorawan); Ministry of Public Health, Nonthaburi, Thailand (W. Luang-on)

DOI: https://doi.org/10.3201/eid2905.221291

An increase in acute gastroenteritis occurred in Chanthaburi Province, Thailand, during December 2021–January 2022. Of the norovirus genotypes we identified in hospitalized patients and produce from local markets, genotype GII.3[P25] accounted for one third. We found no traceable link between patients and produce but found evidence of potential viral intake.

Noroviruses are the leading cause of sporadic and outbreak-associated, acute, nonbacterial gastroenteritis (*1*). They are genetically diverse and are classified into 10 genogroups (GI–GX) representing >40 genotypes, although most human noroviruses are GI and GII (*2*). Emergence of recombinant strains that have different combinations of the RNA-dependent RNA polymerase (RdRp) and viral protein 1 (VP1) genes can cause upsurge of new infections (*3*). In 2020, during the early months of the COVID-19 pandemic, public health measures resulted in the drastic reduction of norovirus outbreaks (*4*). We report a resurgence of norovirus in Chanthaburi Province, Thailand

During December 2021–January 2022, local health authorities in Chanthaburi Province contacted the university for assistance in investigating an increase of vomiting and diarrhea requiring hospitalization among healthy adults. Because preliminary findings by local officials over several weeks had not identified an obvious single-infection source, we suspected norovirus because of rapid widespread community infection. Subsequently, we obtained fecal samples from 34 patients for testing with the approval from the Institutional Review Board of Chulalongkorn University (approval no. 549/62).

Because many patients reported dining out at eateries serving uncooked vegetables, health officials suspected produce as a potential source of infection. Therefore, 24 samples of fresh produce (e.g., salad greens, basil, parsley, napa cabbage, and tomato) from open-air markets near the infection cluster were sent from local health officials for testing to determine a potential norovirus source.

We crushed vegetables in 1 mL nuclease-free water before RNA extraction. We used a bag of ice cubes, which we melted and concentrated from 1 L to 1 mL by using an Amicon Centrifugation Filtration Device (Merck Millipore, https://www.emdmillipore.com) before testing.

After we performed automated viral RNA extraction by using a magLEAD 12 gC Instrument (Precision System Science, https://www.pss.co.jp), we tested for noroviruses by using a real-time reverse transcription PCR (RT-PCR) (*5*). We dual-typed norovirus-positive samples for the RdRp and VP1 genes by using a conventional RT-PCR (*6*). We genotyped Sanger-sequenced nucleotide sequences by using the Norovirus Genotyping Tool (http://www.rivm.nl/mpf/norovirus/typingtool) and deposited them in GenBank (accession nos. OP210707–54, OP210788–834, OP218773–7, and OP218813–7). We performed phylogenetic analysis by using the maximum-likelihood method and 1,000 bootstrap replicates implemented in MEGA 11 (http://www.megasoftware.net).

A total of 32/34 patients (age range 1–82 years, mean age ±SD 31.4 ±19.7 years) were positive for norovirus; they had GI only (2/32), GII only (23/32), and GI and GII (7/32) infections. We ascertained nucleotide sequences for all 30 GII-positive samples (Table).

Analysis of the RdRp gene identified GII.P25 (10/30), GII.P7 (8/30), GII.P17 (6/30), and 2 each of GII.P12, GII.P21, and GII.P31 (Appendix Figure, https://wwwnc.cdc.gov/EID/article/29/5/22-1291-App1.pdf). Analysis of the VP1 gene identified GII.3 (15/30), GII.6 (4/30), GII.21 (4/30), GII.17 (2/30), GII.4 Sydney (2/30), GII.4 Hong Kong (2/30), and GII.7 (1/30). Defined genotypes were GII.6[P7] (3/30); 2 each of GII.3[P7], GII.3[P12], GII.17[P17], GII.21[P17], and GII.21[P21]; and 1 each of GII.3[P17], GII.3[P31], GII.4 Sydney[P7], GII.4 Sydney[P25], GII.4 Hong Kong [P7], GII.4 Hong Kong [P31], GII.6[P17], and GII.7[P7]. We also observed the relatively rare GII.3[P25] genotype (9/30) (*7*).

**Table.** Detection of GII noroviruses in patients and produce samples, Chanthaburi Province, Thailand, 2022*

| | RdRp gene | | | | | |
|---|---|---|---|---|---|---|
| VP1 | P7 | P12 | P17 | P21 | P25 | P31 |
| GII.3 | 2/4 | 2/ND | 1/1 | ND | 9/1 | 1/ND |
| GII.4 Hong Kong | 1/ND | ND | ND/1 | ND | ND | 1/2 |
| GII.4 Sydney | 1/ND | ND | ND | ND | 1/ND | ND |
| GII.6 | 3/5 | ND | 1/1 | ND | ND/1 | ND |
| GII.7 | 1/ND | ND | ND | ND | ND | ND |
| GII.17 | ND | ND | 2/1 | ND | ND | ND |
| GII.21 | ND/1 | ND | 2/ND | 2/ND | ND | ND |

*Values indicate patient samples/produce samples positive for norovirus (e.g., the GII.3[P7] combination was detected in 2 patient and 4 produce samples). Several VP1 and RdRp combinations are detected in patient and produce samples. Produce samples were obtained from open-air markets near the infection cluster and sent by local health officials for testing to determine a potential norovirus source. ND, not detected; P, polymerase; RdRp, RNA-dependent RNA polymerase; VP, viral protein.

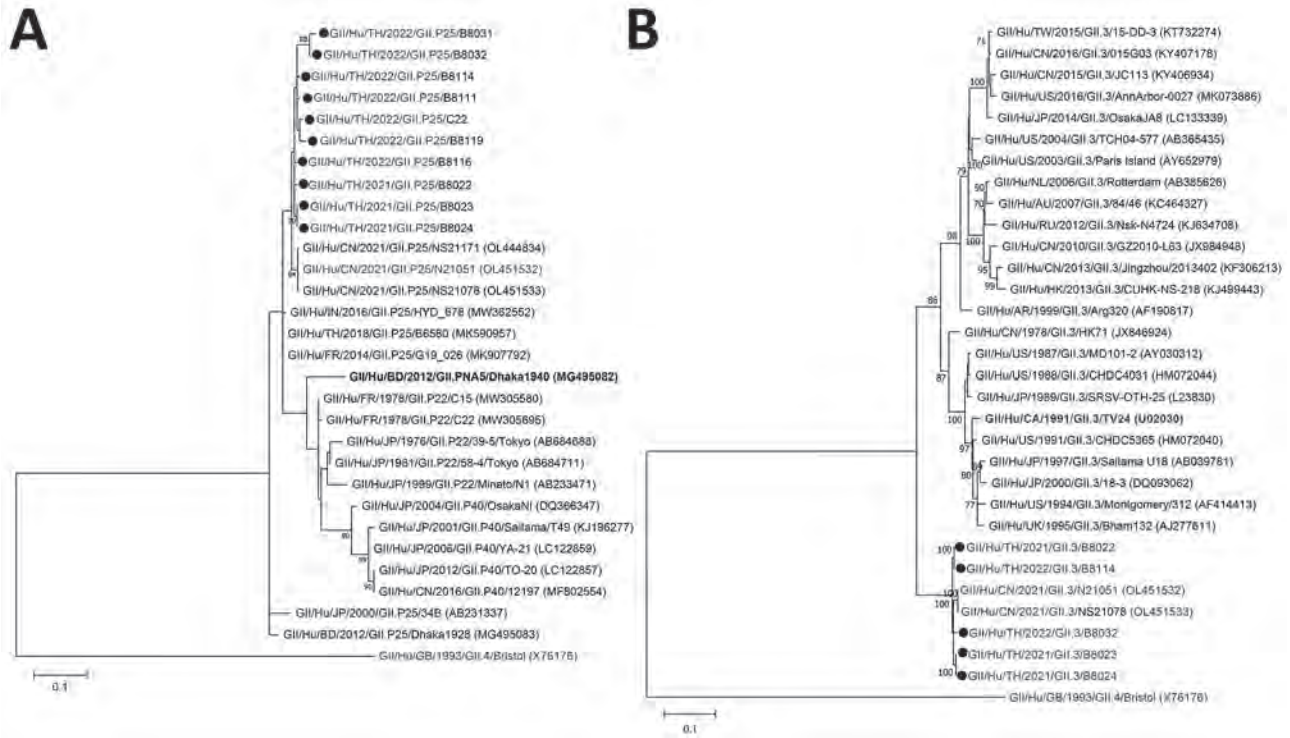


**Figure.** Phylogenetic analysis of norovirus strains, Chanthaburi Province, Thailand, 2022. A) Partial sequence of the RNA-dependent RNA polymerase gene (187 bp). B) Complete sequence of the capsid gene (1,644 bp). Strains identified in this study (black circles) were compared with the reference (bold) and global strains. GenBank accession numbers for strains are indicated in parentheses. Trees were generated by using the maximum-likelihood method with 1,000 bootstrap replicates implemented in MEGA 11 (https://www.megasoftware.net). Bootstrap values ≥70 are indicated at the nodes. Only strains of sufficient nucleotide sequence length needed for analysis are included. Scale bars indicate nucleotide substitutions per site.

Testing for a possible source showed that 8/24 produce samples and ice were norovirus-positive; GII.3[P25] was identified in a tomato (Appendix Table). Partial RdRp genes and entire VP1 genes showed closest phylogeny with unpublished GenBank sequences OL451532 and OL451533, which were deposited by health authorities in China during November 2021. GII.3[P25] from Thailand and China clustered away from global strains (Figure).

Although only 5 GII.3[P25] strains from Thailand yielded full-length VP1 sequences, deduced amino acid residues in the P2 domain (residues 385–420) were possible for all 10 strains. Alignments showed residue changes D388N, Q391M, N404T, E405D, S412I, N415R, and F420V compared with the prototypic GII.3/TV24 (GenBank accession no. U02030) and more recent GII.3 VP1 strains.

Many different norovirus genotypes found in samples from patients during this investigation did not implicate an overwhelmingly predominant strain responsible for the infection cluster. However, emergence of GII.3[P25] in Thailand identified in patients and produce (sample C22) indicated a potential source of infection. The diversity of norovirus strains in produce sampled warrants increased awareness of food safety in preventing norovirus infection. In addition, we identified GII.4 Hong Kong [P31] and 2 novel variants, GII.4 Hong Kong [P7] (patient B8045) and GII.4 Hong Kong [P17] (sample C30), which were reported recently (*8*,*9*), and GII.21[P17], previously reported in South Korea (*10*).

Combined investigation of illness in patients and of potential sources of infection is often challenging. A limitation of our study was low viral loads (cycle threshold ≥30) for many of the samples, which hindered confirmation of minor recombinants found. Our study was also limited by the lack of a definitive traceable link between patients and produce but does provide evidence of potential ingestion of the virus. Although contaminated fruits and vegetables can serve as a source of outbreaks in countries in temperate zones, this study paralleled similar transmission, but in a tropical country. Continuous molecular and epidemiologic surveillance of emerging norovirus variants is needed to detect future outbreaks.

### Acknowledgments

We thank staff members of the Chanthaburi Provincial Health Office and the Office of Disease Prevention and Control Region 6 Chonburi for supporting sample collection.

This study was supported by the Center of Excellence in Clinical Virology of Chulalongkorn University and Hospital. W.C. was supported by Chulalongkorn University's Second Century Fund (C2F).

### About the Author

Dr. Chuchaona is a postdoctoral fellow at the Center of Excellence in Clinical Virology in the Faculty of Medicine at Chulalongkorn University, Bangkok, Thailand. Her primary research interests are molecular epidemiology and evolution of human noroviruses.

### References

1. Ahmed SM, Hall AJ, Robinson AE, Verhoef L, Premkumar P, Parashar UD, et al. Global prevalence of norovirus in cases of gastroenteritis: a systematic review and meta-analysis. Lancet Infect Dis. 2014;14:725–30. https://doi.org/10.1016/S1473-3099(14)70767-4
2. Chhabra P, de Graaf M, Parra GI, Chan MC, Green K, Martella V, et al. Updated classification of norovirus genogroups and genotypes. J Gen Virol. 2019;100:1393–406. https://doi.org/10.1099/jgv.0.001318
3. Bull RA, White PA. Mechanisms of GII.4 norovirus evolution. Trends Microbiol. 2011;19:233–40. https://doi.org/10.1016/j.tim.2011.01.002
4. Kraay AN, Han P, Kambhampati AK, Wikswo ME, Mirza SA, Lopman BA. Impact of nonpharmaceutical interventions for severe acute respiratory syndrome coronavirus 2 on norovirus outbreaks: an analysis of outbreaks reported by 9 US States. J Infect Dis. 2021;224:9–13. https://doi.org/10.1093/infdis/jiab093
5. Debbink K, Costantini V, Swanstrom J, Agnihothram S, Vinjé J, Baric R, et al. Human norovirus detection and production, quantification, and storage of virus-like particles. Curr Protoc Microbiol Clin Virol. 2013;31:15K1.1–15K1.45. https://doi.org/10.1002/9780471729259.mc15k01s31
6. Chhabra P, Browne H, Huynh T, Diez-Valcarce M, Barclay L, Kosek MN, et al. Single-step RT-PCR assay for dual genotyping of GI and GII norovirus strains. J Clin Virol. 2021;134:104689. https://doi.org/10.1016/j.jcv.2020.104689
7. Kendra JA, Tohma K, Parra GI. Global and regional circulation trends of norovirus genotypes and recombinants, 1995–2019: a comprehensive review of sequences from public databases. Rev Med Virol. 2022;32:e2354. https://doi.org/10.1002/rmv.2354
8. Chan MC, Roy S, Bonifacio J, Zhang LY, Chhabra P, Chan JC, et al.; for NOROPATROL2. Detection of norovirus variant GII.4 Hong Kong in Asia and Europe, 2017–2019. Emerg Infect Dis. 2021;27:289–93. https://doi.org/10.3201/eid2701.203351
9. Mabasa VV, van Zyl WB, Ismail A, Allam M, Taylor MB, Mans J. Multiple novel human norovirus recombinants identified in wastewater in Pretoria, South Africa by next-generation sequencing. Viruses. 2022;14:2732. https://doi.org/10.3390/v14122732
10. Koo ES, Kim MS, Choi YS, Park KS, Jeong YS. Occurrence of novel GII.17 and GII.21 norovirus variants in the coastal environment of South Korea in 2015. PLoS One. 2017;12:e0172237. https://doi.org/10.1371/journal.pone.0172237

Address for correspondence: Yong Poovorawan, Center of Excellence in Clinical Virology, Faculty of Medicine, Chulalongkorn University, 1873 Rama 4 Rd, Pathumwan, Bangkok 10330, Thailand; email: yong.p@chula.ac.th

# COVID-19 Vaccine Uptake by Infection Status in New South Wales, Australia

Heather F. Gidding, Sandrine Stepien, Jiahui Qian, Kristine K. Macartney, Bette Liu

Author affiliations: University of Sydney Northern Clinical School, St. Leonards, New South Wales, Australia (H.F. Gidding); National Centre for Immunisation Research and Surveillance, Westmead, New South Wales, Australia (H.F. Gidding, S. Stepien, J. Qian, K.K. Macartney, B. Liu); University of New South Wales School of Population Health, Kensington, New South Wales, Australia (H.F. Gidding, J. Qian, B. Liu); University of Sydney Faculty of Medicine and Health, Camperdown, New South Wales, Australia (H.F. Gidding, K.K. Macartney)

DOI: https://doi.org/10.3201/eid2905.230047

Using linked public health data from Australia to measure uptake of COVID-19 vaccination by infection status, we found coverage considerably lower among infected than uninfected persons for all ages. Increasing uptake of scheduled doses, including among previously infected persons after the recommended postinfection delay, is needed to reduce COVID-19 illness rates.

Although coverage with 2 doses of COVID-19 vaccine rapidly reached >95% in adults in Australia by late 2021 (*1*), by December 4, 2022, uptake had slowed and plateaued at much lower levels for 2 doses among children 5–15 years of age (52.1%) and for boost-

ers among adults (72.4% for dose 3 and 44.3% for dose 4) (*1*). At the time of this analysis, deferring a scheduled COVID-19 vaccination by 3 months after SARS-CoV-2 infection was recommended; that period has now been changed to 6 months (*2*,*3*). Because a history of infection can influence perceptions about protection against and risk of future infection, we aimed to examine whether timing and uptake of vaccination were affected among persons with recent SARS-CoV-2 infection. We obtained ethics approval for this study from the New South Wales (Australia) Population Health Services Research Ethics Committee (project 2022/ETH00584).

We linked Australian Immunisation Register (AIR) data and COVID-19 notifications for residents ≥5 years of age on January 1, 2022, living in either the Greater Sydney Metropolitan or Hunter New England areas of New South Wales. AIR includes data on COVID-19 vaccine receipt (by vaccination date, brand, and dose number) among persons registered on Medicare, Australia's national health insurance program, and for unregistered persons who reported having received a COVID-19 vaccine. Reporting COVID vaccinations to AIR and positive COVID-19 PCR or rapid antigen test results to public health authorities was mandatory during the study period. Study data were available through May 29, 2022.

We calculated the cumulative percentages of study participants who received the next recommended COVID-19 vaccine dose by infection status and by time after the current dose (i.e., dose 1 for the 5–11 and 12–15 year age groups; dose 2 for the 16–39, 40–64, and ≥65 year age groups; and dose 3 for ≥65 year age group) (Figure). We based infection status on data from COVID-19 notifications as follows: no infection before receiving the next scheduled dose or, if the person did not receive the next dose, by the end of follow-up; infected before current dose; infected after current dose but before the due date for the next dose; or infected after exceeding the due date for the next dose (Table).

Most study participants were uninfected, but distribution by infection status varied by cohort (Table). In all cohorts, vaccine uptake was most rapid and coverage plateaued at the highest levels among uninfected participants, but the level at which coverage plateaued among uninfected participants differed by cohort (range 36%–98%) (Figure). Even after accounting for the recommended 3-month delay between infection and vaccination, we found coverage among infected persons plateaued at considerably lower levels than among uninfected persons. Among children 5–15 years of age, those infected after the due date for dose 2 had substantially lower uptake (11%–13%) than did the subcohorts

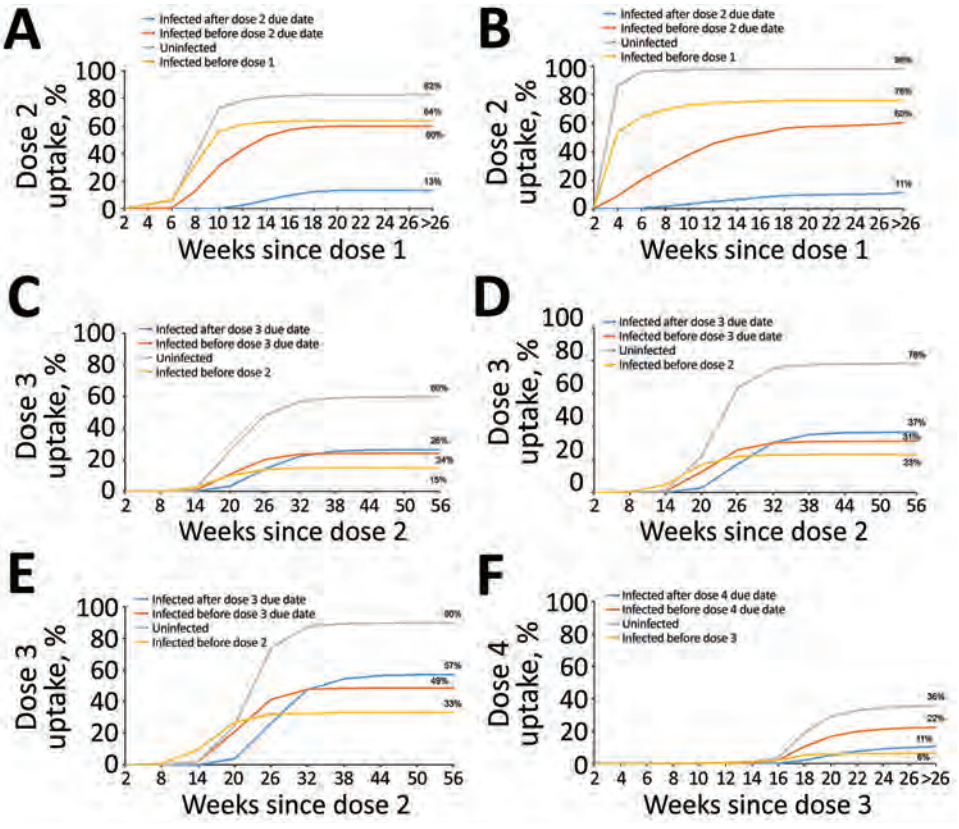


**Figure.** Cumulative uptake of next dose by time since current dose in study of COVID-19 vaccine uptake, by age group and infection status as at May 29, 2022, Greater Sydney Metropolitan and Hunter New England areas of New South Wales, Australia: A, B) Dose 2 uptake for the 5–11-year (A) and 12–15-year (B) age groups; C–E) dose 3 uptake for the 16–39-year (C), 40–64-year (D), and ≥65-year (E) age groups; F) dose 4 uptake for the ≥65-year age group.

**Table.** Age and dose specific cohorts and their distribution in study of COVID-19 vaccine uptake, by infection status on May 29, 2022, Greater Sydney Metropolitan and Hunter New England areas, New South Wales, Australia

| Age group, y | Current dose* | Next dose* | Recommended time between current and next dose, d | Total cohort | Uninfected, no. (%) | Infected, no. (%) | | |
|---|---|---|---|---|---|---|---|---|
| | | | | | | Before current dose | Before next dose due | After next dose due |
| 5–11 | Dose 1 | Dose 2 | 63† | 285,638 | 210,004 (73.5) | 18,611 (6.5) | 49,888 (17.5) | 7,135 (2.5) |
| 12–15 | Dose 1 | Dose 2 | 28‡ | 241,490 | 236,900 (98.1) | 1,962 (0.8) | 889 (0.4) | 1,739 (0.7) |
| 16–39 | Dose 2 | Dose 3 | 91§ | 1864,335 | 1,413,329 (75.8) | 15,345 (0.8) | 68,578 (3.7) | 367,083 (19.7) |
| 40–64 | Dose 2 | Dose 3 | 91§ | 1,727,123 | 1,503,582 (87.1) | 7,968 (0.5) | 21,456 (1.2) | 194,117 (11.2) |
| ≥65 | Dose 2 | Dose 3 | 91§ | 885,564 | 841,931 (95.1) | 1,689 (0.2) | 5,544 (0.6) | 36,400 (4.1) |
| | Dose 3 | Dose 4 | 91§ | 779,649 | 679,155 (87.1) | 24,042 (3.1) | 42,464 (5.4) | 33,988 (4.4) |

*Cohorts were assembled based on the current dose under consideration and retrospectively followed up to determine if they received the next dose.
†Children 5–11 y of age: recommended interval between doses 1 and 2 was 8 wk so dose 2 due date was set at 9 wk (63 d).
‡Most children 12–15 y of age: recommended interval between doses 1 and 2 was 3 wk so the dose 2 due date was set at 4 wk (28 d).
§For persons ≥16 y of age: recommended interval between doses 2 and 3 changed from November 2021 to January 2022 to 3 mo so the dose 3 due date was set at 91 d; 3 mo was also the most recently recommended interval between doses 3 and 4.

infected before dose 1 or between doses 1 and 2 (≥60%). Among all the adult cohorts (≥16 years of age), uptake was more similar among the 3 infected subcohorts; coverage plateaued lowest (range 6%–33%) among those infected before the current dose.

Our use of population-level data was a primary strength of this study. Two international studies reporting on whether SARS-CoV-2 infection status influences vaccination uptake levels were cross-sectional surveys with low response rates or performed among only healthcare workers (*4*,*5*). Unlike this study, those studies did not examine cumulative vaccine uptake by timing of infection, but they also found previous SARS-CoV-2 infection was associated with lower vaccination uptake.

Our study was limited by a lack of information on reasons for vaccination decisions, and data were available only through May 29, 2022. In addition, COVID-19 notifications were not linked to national public health databases before June 2021, although relatively few infections occurred in New South Wales before that period (*6*); data only represent infections reported. Although reporting positive PCR and rapid antigen tests was mandatory during the study period, positive results were likely underreported. In addition, persons more likely to be tested and have results reported might also have been more likely to get vaccinated, possibly resulting in an underestimation of true discrepancies among subcohorts.

In conclusion, our study shows that persons with previous SARS-CoV-2 infection were less likely to take up subsequent recommended vaccine doses than uninfected persons. Because previous infection alone is unlikely to provide sufficient protection against severe disease (*2*), greater adherence to vaccine recommendations is required to reduce health effects from COVID-19. Ongoing monitoring of vaccination uptake and timely linkage to infection status could help better understand gaps between SARS-CoV-2 population immunity and vaccine recommendations. Those data, together with information from surveys to identify drivers of delayed vaccination among infected populations, would enable development of appropriately targeted public health campaigns to reduce COVID-19–related illness rates.

### Acknowledgments

We would like to thank the New South Wales Health Linked Data for Vaccine Effectiveness Reference Group for their guidance and Shayal Prasad for her help preparing the figures. We acknowledge the staff at the New South Wales Centre for Health Record Linkage and the Australian Government Department of Health and Aged Care and New South Wales Ministry of Health, who provided advice and data for the project.

H.G. was funded through an APPRISE CRE Fellowship (NHMRC grant no. APP1116530).

### About the Author

Dr. Gidding is an infectious disease epidemiologist and associate professor at the University of Sydney and National Centre for Immunisation Research and Surveillance. Her primary research interests include maximizing use of linked routinely collected administrative data sets to evaluate vaccination programs.

### References

1. Australian Government Department of Health and Aged Care. Vaccination numbers and statistics [cited 2023 Jan 12]. https://www.health.gov.au/initiatives-and-programs/covid-19-vaccines/numbers-statistics
2. Australian Government Department of Health and Aged Care. Australian Technical Advisory Group on Immunisation (ATAGI) updated recommendations for a winter dose of COVID-19 vaccine [cited 2022 Sep 28]. https://www.health.gov.au/news/atagi-updated-recommendations-for-a-winter-dose-of-covid-19-vaccine
3. Australian Government Department of Health and Aged Care. Australian Technical Advisory Group on Immunisation (ATAGI) updated recommendations for vaccination after COVID-19 infection [cited 2023 Mar 20]. https://www.

health.gov.au/our-work/covid-19-vaccines/getting-your-vaccination/vaccination-after-covid-19-infection
4. Nguyen KH, Huang J, Mansfield K, Corlin L, Allen JD. COVID-19 Vaccination coverage, behaviors, and intentions among adults with previous diagnosis, United States. Emerg Infect Dis. 2022;28:631–8. https://doi.org/10.3201/eid2803.211561
5. Hall VJ, Foulkes S, Saei A, Andrews N, Oguti B, Charlett A, et al.; SIREN Study Group. COVID-19 vaccine coverage in health-care workers in England and effectiveness of BNT162b2 mRNA vaccine against infection (SIREN): a prospective, multicentre, cohort study. Lancet. 2021; 397:1725–35. https://doi.org/10.1016/S0140-6736(21)00790-X
6. Our World in Data. Australia: coronavirus pandemic country profile [cited 2022 Sep 28]. https://ourworldindata.org/coronavirus/country/australia

Address for correspondence: Heather Gidding, National Centre for Immunisation Research and Surveillance of Vaccine Preventable Diseases, Cnr Hawkesbury Rd and Hainsworth St, Westmead, NSW 2145, Australia; email: heather.gidding@sydney.edu.au

# Presence of *Burkholderia pseudomallei* in Soil, Nigeria, 2019

Jelmer Savelkoel,[1] Rita O. Oladele,[1] Chiedozie K. Ojide, Rebecca F. Peters, Daan W. Notermans, Justina O. Makinwa, Maaike C. de Vries, Marion A.E. Sunter, Sébastien Matamoros, Nasiru Abdullahi, Uche S. Unigwe, Alani S. Akanmu, W. Joost Wiersinga,[2] Emma Birnie[2]

Author affiliations: Amsterdam UMC location University of Amsterdam, Amsterdam, the Netherlands (J. Savelkoel, D.W. Notermans, S. Matamoros, W.J. Wiersinga, E. Birnie); Lagos University Teaching Hospital, Lagos, Nigeria (R.O. Oladele, R.F. Peters, J.O. Makinwa, A.S. Akanmu); College of Medicine University of Lagos, Lagos, Nigeria (R.O. Oladele, A.S. Akanmu); Ebonyi State University, Abakaliki, Nigeria (C.K. Ojide); Alex Ekwueme Federal University Teaching Hospital, Abakaliki, Nigeria (C.K. Ojide, U.S. Unigwe); National Institute for Public Health and the Environment (RIVM), Bilthoven, the Netherlands (D.W. Notermans, M.C. de Vries, M.A.E. Sunter); Federal Medical Centre, Abuja, Nigeria (N. Abdullahi); University of Nigeria Teaching Hospital, Enugu, Nigeria (U.S. Unigwe)

DOI: http://doi.org/10.3201/eid2905.221138

Melioidosis, caused by the soil-dwelling bacterium *Burkholderia pseudomallei*, is predicted to be endemic in Nigeria but is only occasionally reported. This report documents the systematic identification of the presence of *B. pseudomallei* and *B. thailandensis* in the soil across multiple states in Nigeria.

The gram-negative, soil-dwelling bacterium *Burkholderia pseudomallei* is the causative agent of melioidosis, which is an important cause of lethal community-acquired sepsis throughout the tropics (*1*). Melioidosis is predicted to be endemic in Nigeria, a country with the highest estimated annual incidence, mortality, and disease burden in Africa, partly explained by its suitable environment and large population (*2*–*4*). Clinical evidence of melioidosis in Nigeria is scarce and based only on traveler-associated cases in the United Kingdom and reports from Nigeria presuming the presence of *B. pseudomallei* (*4*–*7*). This study was a collaborative effort prompted by the African Melioidosis Workshop in Lagos, Nigeria (*4*); our goal was to determine the environmental presence of *B. pseudomallei* in Nigeria. Ethics approval was obtained from the National Health Research Ethics Committee of Nigeria (approval no. NHREC/01/01/2007-26/03/2019).

We performed an environmental soil sampling study based on consensus guidelines for the identification of *B. pseudomallei* (*8*). We consulted local residents and maps to select sites associated with the occurrence of *B. pseudomallei*, as we have done previously (*9*). Using a fixed interval grid and samples taken 5 meters apart, we collected 100 soil samples per site across 8 sites in Nigeria during the rainy season in April–May 2019 (Table; Appendix, https://wwwnc.cdc.gov/EID/article/29/5/22-1138-App1.pdf). We collected a total of 800 samples in the northwestern state Kebbi, southwestern state Ogun, and southeastern states Ebonyi and Enugu. We collected soil at a depth of 65 cm and processed 10 g of soil within 7 days to enable selective enriched culture (*8*,*10*). We screened isolates by using colony morphology and, if results were suspect, used matrix-assisted laser desorption/ionization-time of flight mass spectrometry (MALDI Biotyper Compass v4.1 and Compass Library v10; Bruker Daltonics, https://www.bruker.com). We subjected all presumptive *B. pseudomallei* isolates to real-time multiplex PCR and performed whole-genome sequencing on 9 *B. pseudomallei* isolates and 3 *B. thailandensis* isolates by using the NextSeq 500/550 platform (Illumina, https://www.illumina.com) (Appendix). We then included

[1]These first authors contributed equally to this article.

[2]These senior authors contributed equally to this article.

**Table.** Site characteristics and distribution of *Burkholderia pseudomallei* at 8 sampling sites in Nigeria, 2019

| Site | Location | State | Place | Site characteristics | Sample holes positive for *B. pseudomallei* |
|---|---|---|---|---|---|
| A | Southwestern | Ogun | Lufoko | Rice field, dry | 0 |
| B | Southwestern | Ogun | Ige | Rice field, dry | 0 |
| C | Northwestern | Kebbi | Birnin Kebbi* | Rice field, moist | 4 |
| D | Northwestern | Kebbi | Birnin Kebbi* | Rice field, moist | 1 |
| E | Southwestern | Ogun | Sunmoge | Cattle, grassland next to river, moist | 0 |
| F | Southeastern | Ebonyi | Abakaliki | Rice field and cassava crops, moist | 38 |
| G | Southeastern | Ebonyi | Abakaliki | Rice swamp, wet | 1 |
| H | Southeastern | Enugu | Nenwe | Rice field, moist | 14 |

*The sampling sites in Birnin Kebbi were located 3 km apart from each other. An overview of the geographic distribution of sampling sites for *Burkholderia pseudomallei* can be found in the Appendix (https://wwwnc.cdc.gov/EID/article/29/5/22-1138-App1.pdf).

the same *B. pseudomallei* isolates in our phylogenetic comparison and used them for antimicrobial susceptibility testing (Appendix). Sequences for the samples in this study are available on the European Nucleotide Archive database (project number PRJEB54705, sample accession nos. ERS12451640–51; https://www.ebi.ac.uk/ena/browser/home).

By using the methods described, we isolated *B. pseudomallei* from 58 (7.3%) of 800 samples in 5 (62.5%) of the 8 sampling sites (Table; Appendix). We observed the highest positivity in the southeastern states, with rates as high as 38% in Ebonyi and 14% in Enugu. We also isolated the nonpathogenic *B. thailandensis* from 193 (24.1%) of 800 samples in 4 (50%) of the 8 sampling sites. Antimicrobial susceptibility of the *B. pseudomallei* isolates displayed overall sensitivity against antibiotic agents commonly used for the treatment of melioidosis, such as ceftazidime, meropenem, and trimethoprim/sulfamethoxazole (Appendix).

We conducted phylogenetic analysis of our 9 sequenced *B. pseudomallei* isolates and 13 additional genomes originating from Africa, all retrieved from the European Nucleotide Archive database. The phylogenetic tree revealed a cluster of predominantly continental African origin that included all of the soil isolates from Nigeria and a cluster of strains derived mainly from the Indian Ocean region (Figure). Our *B. pseudomallei* isolates did not closely match the previously sequenced traveler-associated strain from Nigeria (ERR298772) (*7*): the genome differed by 8,370 to 9,431 core single-nucle-otide polymorphisms. We speculated that the higher positivity in the southeastern states re lects the relative-

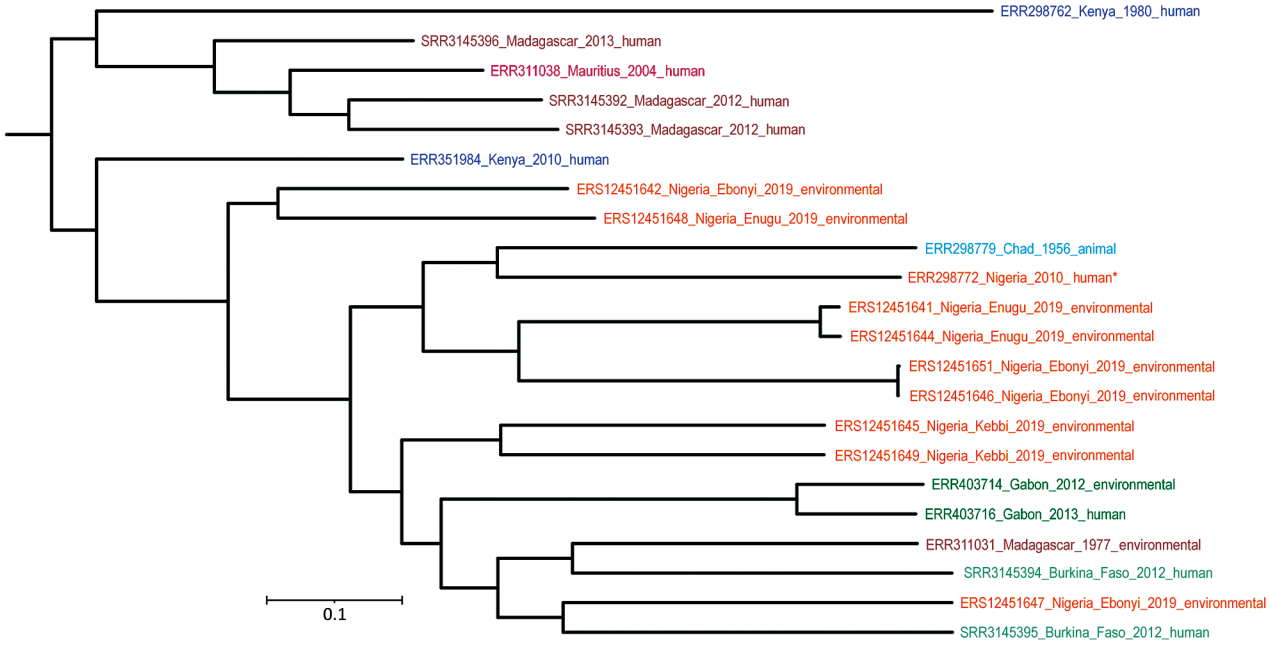


**Figure.** Phylogenetic tree of *Burkholderia pseudomallei* genomes from Nigeria (orange text) and additional genomes originating from Africa, all retrieved from the European Nucleotide Archive database. Tree generated by FastTree (http://www.microbesonline.org/fasttree) based on core single-nucleotide polymorphisms distance and visualized with iTOL (https://itol.embl.de). Colors indicate countries of origin. Asterisk indicates a previously sequenced, traveler-associated strain. Scale bar indicates number of nucleotide substitutions per site.

ly high annual precipitation in southeastern Nigeria as compared with sampling sites in the northwestern and southwestern states (Appendix).

Adopting a culture-based approach, combined with matrix-assisted laser desorption/ionization-time of flight mass spectrometry, real-time PCR, and whole genome sequencing allowed us to identify the environmental presence of *B. pseudomallei*. Limitations of our study include possible sampling errors and false-negative samples because we relied on a culture-based approach instead of using an additional quantitative PCR on soil samples (*9*). Moreover, we did not collect soil samples in multiple seasons to investigate a seasonal pattern, nor did we collect water or air samples.

In conclusion, we documented the systematic confirmation of the environmental presence of *B. pseudomallei* and *B. thailandensis* across multiple states in Nigeria. We identified the highest *B. pseudomallei* positivity rates in the southeastern states Ebonyi and Enugu. Phylogenetic analysis clustered our *B. pseudomallei* isolates with previous genomes that originated mostly from continental Africa. Our results highlight the probability of unrecognized melioidosis in Nigeria and warrant the attention of health workers and public health officials. Improving capacity and increasing awareness, together with environmental, serologic, and disease surveillance, is needed to increase our understanding of the melioidosis burden within Nigeria.

### Acknowledgments

We thank all participants of the African Melioidosis Workshop in Lagos, Nigeria, and everyone who helped with the soil sampling. We also express our gratitude to Michelle B.S. Menig, Cornelia M. Prtenjaca Wolbers, Maaike J.C. van den Beld, and Frans A.G. Reubsaet for their expert technical assistance.

This work was supported by an Amsterdam UMC PhD Scholarship to Jelmer Savelkoel in 2021 and a research grant from the European Society of Clinical Microbiology and Infectious Diseases to Emma Birnie in 2018.

## About the Author

Mr. Savelkoel is a researcher at the Center for Experimental and Molecular Medicine of Amsterdam UMC. His research interests include the global distribution and global health aspects of melioidosis.

### References

1. Wiersinga WJ, Virk HS, Torres AG, Currie BJ, Peacock SJ, Dance DAB, et al. Melioidosis. Nat Rev Dis Primers. 2018;4:17107. https://doi.org/10.1038/nrdp.2017.107
2. Limmathurotsakul D, Golding N, Dance DA, Messina JP, Pigott DM, Moyes CL, et al. Predicted global distribution of *Burkholderia pseudomallei* and burden of melioidosis. Nat Microbiol. 2016;1:15008. https://doi.org/10.1038/nmicrobiol.2015.8
3. Birnie E, Virk HS, Savelkoel J, Spijker R, Bertherat E, Dance DAB, et al. Global burden of melioidosis in 2015: a systematic review and data synthesis. Lancet Infect Dis. 2019;19:892–902. https://doi.org/10.1016/S1473-3099(19)30157-4
4. Birnie E, James A, Peters F, Olajumoke M, Traore T, Bertherat E, et al. Melioidosis in Africa: time to raise awareness and build capacity for its detection, diagnosis, and treatment. Am J Trop Med Hyg. 2022;106:394–7. https://doi.org/10.4269/ajtmh.21-0673
5. Adejobi A, Ojo O, Alaka O, Odetoyin B, Onipede A. Antibiotic resistance pattern of *Pseudomonas* spp. from patients in a tertiary hospital in South-West Nigeria. Germs. 2021;11:238–45. https://doi.org/10.18683/germs.2021.1260
6. Osunla AC, Akinmolayemi AT, Makinde OA, Abioye OE, Olotu EJ, Ikuesan FA. Occurrence and antibiotics resistance signatures of *Burkholderia pseudomallei* isolated from selected hospital final effluents in Akoko metropolis within Ondo State Nigeria. Int J Public Health Res. 2021;11:1309–16.
7. Salam AP, Khan N, Malnick H, Kenna DT, Dance DA, Klein JL. Melioidosis acquired by traveler to Nigeria. Emerg Infect Dis. 2011;17:1296–8. https://doi.org/10.3201/eid1707.110502
8. Limmathurotsakul D, Dance DA, Wuthiekanun V, Kaestli M, Mayo M, Warner J, et al. Systematic review and consensus guidelines for environmental sampling of *Burkholderia pseudomallei*. PLoS Negl Trop Dis. 2013;7:e2105. https://doi.org/10.1371/journal.pntd.0002105
9. Wiersinga WJ, Birnie E, Weehuizen TA, Alabi AS, Huson MA, Huis in 't Veld RA, et al. Clinical, environmental, and serologic surveillance studies of melioidosis in Gabon, 2012–2013. Emerg Infect Dis. 2015;21:40–7. https://doi.org/10.3201/eid2101.140762
10. Manivanh L, Pierret A, Rattanavong S, Kounnavongsa O, Buisson Y, Elliott I, et al. *Burkholderia pseudomallei* in a lowland rice paddy: seasonal changes and influence of soil depth and physico-chemical properties. Sci Rep. 2017;7:3031. https://doi.org/10.1038/s41598-017-02946-z

Address for correspondence: Jelmer Savelkoel, Amsterdam UMC location University of Amsterdam, Center for Experimental and Molecular Medicine, Meibergdreef 9, 1105 AZ, Room T1.0-234, Amsterdam, the Netherlands; email: j.savelkoel@amsterdamumc.nl

# Genome Analysis of Triploid Hybrid *Leishmania* Parasite from the Neotropics

Frederik Van den Broeck, Senne Heeren, Ilse Maes, Mandy Sanders, James A. Cotton,[1] Elisa Cupolillo, Eugenia Alvarez, Lineth Garcia, Maureen Tasia, Alice Marneffe, Jean-Claude Dujardin, Gert Van der Auwera

Author affiliations: Katholieke Universiteit Leuven, Leuven, Belgium (F. Van den Broeck, S. Heeren); Institute of Tropical Medicine, Antwerp, Belgium (F. Van den Broeck, S. Heeren, I. Maes, J.-C. Dujardin, G. Van der Auwera); Wellcome Sanger Institute, Hinxton, UK (M. Sanders, J.A. Cotton); Instituto Oswaldo Cruz–Fiocruz, Rio de Janeiro, Brazil (E. Cupolillo); Cayetano Heredia University, Lima, Peru (E. Alvarez); Universidad Mayor de San Simon, Cochabamba, Bolivia (L. Garcia); Centre Hospitalier Universitaire St. Pierre, Brussels, Belgium (M. Tasia, A. Marneffe)

DOI: https://doi.org/10.3201/eid2905.221456

We discovered a hybrid *Leishmania* parasite in Costa Rica that is genetically similar to hybrids from Panama. Genome analyses demonstrated the hybrid is triploid and identified *L. braziliensis* and *L. guyanensis*–related strains as parents. Our findings highlight the existence of poorly sampled *Leishmania* (*Viannia*) variants infectious to humans.

*Leishmania* are intracellular protozoan parasites that cause the vectorborne disease leishmaniasis, which occurs in ≈88 countries (*1*). Human infection can result in 2 main forms of disease, cutaneous and visceral leishmaniasis, and different *Leishmania* species cause diverse clinical manifestations and sequelae (*1*). Correct species typing is thus required to clinically manage leishmaniasis (*2*).

In August 2020, a patient returning from Costa Rica sought care at the Hospital St. Pierre (Brussels, Belgium) with a single, well-demarcated, ulcerated erythematous plaque on the left flank indicative of cutaneous leishmaniasis. Molecular diagnosis confirmed the presence of *Leishmania* parasites on the basis of 18S ribosomal DNA (*3*). A 1,245-bp fragment of the multicopy heat-shock protein 70 gene (*hsp70*) was sequenced for species typing (*4*). This sequencing revealed an atypical sequence related to both the *L. guyanensis* and *L. braziliensis* species that showed sequence variation across copies at 10 positions, suggesting either a mixed infection or hybrid parasite. Despite the atypical nature of the infecting species, the patient had good therapeutic response after 5 intralesional injections with meglumine antimoniate (Glucantime, Sanofi, https://www.sanofi.com), leaving only a slightly hyperpigmented scar. The clinical sample was cultured in vitro (referred to as MHOM/CR/2020/StPierre) and subjected to HSP70 typing (*4*) and whole-genome sequencing (*5*).

Compared with results for the clinical sample, the consensus sequence of the *hsp70* locus in the cultured isolate revealed sequence variation in 1 extra site, bringing the total to 11 (Appendix 1, https://wwwnc.cdc.gov/EID/article/29/5/22-1456-App1.pdf). Of those sites, 10 were shared with 6 cutaneous leishmaniasis strains described from Panama (*6*). Comparison with all available *Leishmania hsp70* sequences from GenBank (Appendix 1) revealed 2 monophyletic groups as the possible origin of the different *hsp70* copies in the Costa Rica sequence: first, a subgroup of the *L. guyanensis* species complex found in Ecuador, Panama, and Colombia; and second, a subgroup of the *L. braziliensis* species complex described from Panama, Guatemala, and Brazil. Even though such analysis is biased by available sequences and the use of a single chromosomal locus, the geography of the hypothetical parents is compatible with Costa Rica. To further investigate the nature of the Costa Rica isolate, we resorted to genome analysis.

We identified 125,632 single-nucleotide polymorphisms (SNPs) within the sample from Costa Rica after mapping genomic sequences against the *L. braziliensis* M2904 reference genome (*5*) (Appendix 2, https://wwwnc.cdc.gov/EID/article/29/5/22-1456-App2.pdf). This total included 21,168 homozygous SNPs (both haplotypes were different from M2904) and 104,464 heterozygous SNPs (one haplotype was similar to M2904 and the other different). Chromosomes 1 and 11, the first 140 kb of chromosome 20, and the last 60 kb of chromosome 27 were highly homozygous, almost completely lacking in heterozygous variants, whereas most variants in the rest of the genome were heterozygous (Appendix 2). This observation of a largely heterozygous genome that is interrupted by homozygous stretches strongly suggests that the isolate is a hybrid parasite, rather than the result of a mixed infection (*7*).

We investigated chromosome copy numbers by using the distribution of allelic read depth frequencies at heterozygous sites (*7*), which should be centered around 0.5 in diploid organisms (both alleles represented equally). However, we discovered a bimodal distribution with modes 0.33 and 0.67 (Appendix 2), suggesting that the hybrid is triploid (*7*).

We analyzed the genomic ancestry of the hybrid compared with 40 genomes of 7 *Leishmania* (*Viannia*) species (Appendix 2) using phylogenies based on ge-

[1]Current affiliation: Wellcome Center for Integrative Parasitology, University of Glasgow, Glasgow, Scotland, UK.

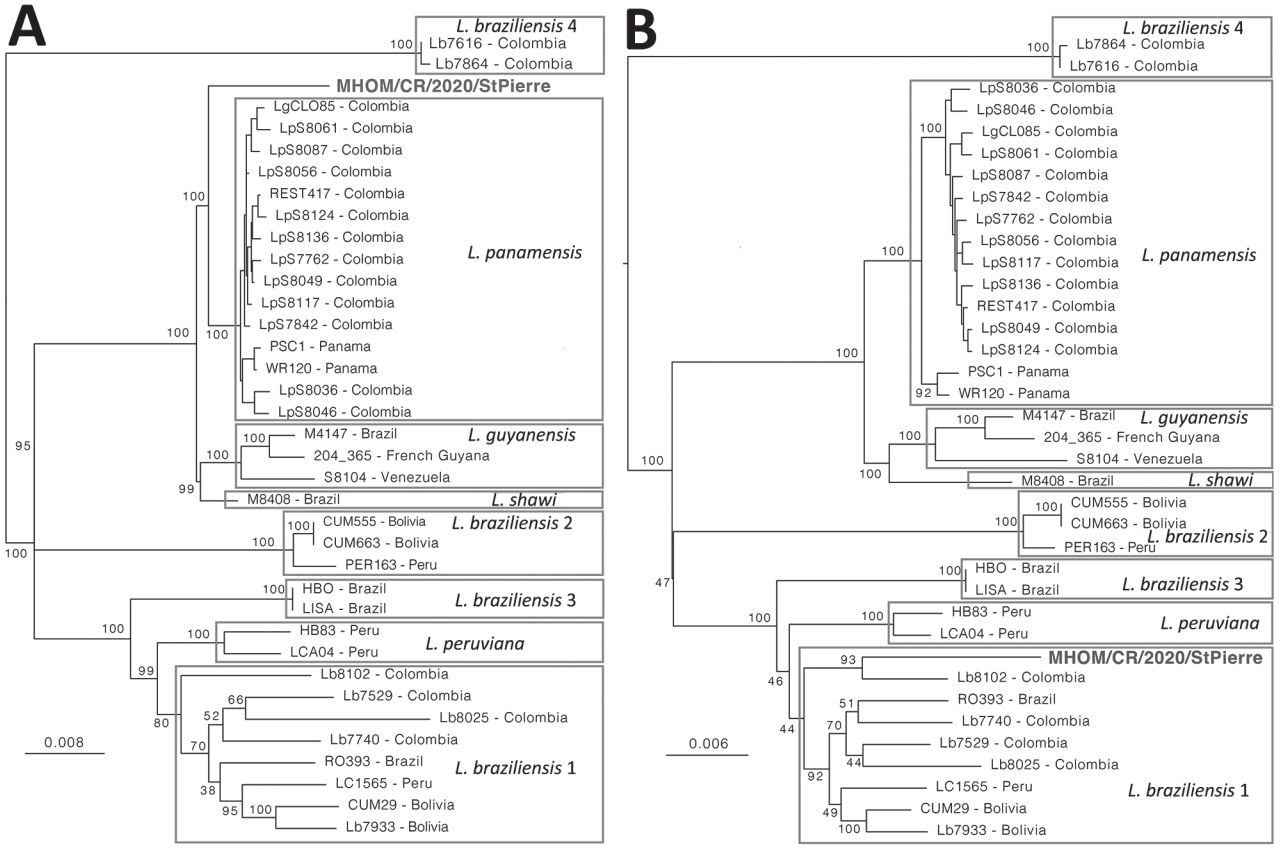


**Figure.** Midpoint rooted maximum-likelihood phylogenetic trees based on single-nucleotide polymorphisms called in chromosome 1 and the first 140kb of the telomeric region of chromosome 20 of a hybrid *Leishmania* parasite from Costa Rica. For each strain, sequences were composed based on concatenated single-nucleotide polymorphisms that were each coded by 2 base pairs, after which invariant sites were removed, resulting in 2,382 bp sequences for chromosome 1 and 3,015 bp sequences for chromosome 20. Consensus phylogenetic trees were generated from 1,000 bootstrap trees using IQ-TREE (http://www.iqtree.org) with 37 taxa (excluding *L. naiffi* and *L. lainsoni* strains) under the transversion with empirical base frequencies, ascertainment bias correction, and discrete gamma with 4 rate categories substitution model, which was the best-fit model revealed by ModelFinder as implemented in IQTREE. Branch support values are presented near each node following 1,000 bootstrap replicates; bootstrap values within the clade containing *L. panamensis* strains were omitted for clarity reasons. Scale bar indicates number of substitutions per site. Appendix 2 (https://wwwnc.cdc.gov/EID/article/29/5/22-1456-App2.pdf) includes a description of the *L. braziliensis* 1–4 lineages.

nomic regions that were homozygous in the hybrid (where both haplotypes originate from the same parental species). In the chromosome 20 phylogeny, the Costa Rica hybrid clusters with *L. braziliensis* 1 strain Lb8102 from Colombia (Figure; Appendix 2 Figure 8), which could be close to one of the parental strains. The ancestry of the other parental genome remains unclear, because in the chromosome 1 phylogeny it clusters with *L. panamensis* strains from Colombia and Panama (Figure), even though it is also tightly linked with a cluster of *L. guyanensis* strains from Venezuela, Brazil, and French Guiana in the mitochondrial maxicircle phylogeny (Appendix 2 Figures 3, 9). We could not resolve the geographic origin of the 2 parents in greater detail because of the lack of available *Leishmania* (*Viannia*) genomes.

Our study provides a detailed genomic description of a hybrid between the *L. braziliensis* and the *L. guyanensis* species complexes. The first report of such hybrids in Central America dates back to the early 1990s, concerning putative *L. braziliensis*–*L. panamensis* hybrids from the north of Nicaragua (*8*). Those hybrids were reported again in 2021 in Panama (*6*). Further, parasites with signatures from both *L. braziliensis* and *L. guyanensis* relatives have been described in South America, more specifically from Ecuador, Peru, Brazil, and Venezuela (*9*,*10*). Together with our report from Costa Rica, these reports point to a widespread circulation in the Neotropical region of recombinant strains, the epidemiology and clinical significance of which remain elusive.

**Acknowledgments**

We thank Pieter Monsieurs for help with generating whole-genome sequence data and Isabel Micalessi and Lara Balcaen for molecular diagnosis of the case.

Genomic sequence reads of MHOM/CR/2020/StPierre are available on the European Nucleotide Archive (https://www.ebi.ac.uk/ena) under accession no. PRJNA881292. The *hsp70* sequence is available from GenBank under accession no. OQ200658.

F.V.D.B. and S.H. acknowledge support from the Research Foundation Flanders (grant nos. 1226120N and G092921N).

## About the Author

Dr. Van den Broeck is a researcher specializing in genetics and population genomics of eukaryote parasites, particularly parasites that cause neglected tropical diseases. He has contributed multiple research papers investigating the complex hybrid ancestry of protozoan parasites, such as *Trypanosoma cruzi* (agent of Chagas disease) and *Leishmania braziliensis* (agent of cutaneous leishmaniasis).

**References**

1. Torres-Guerrero E, Quintanilla-Cedillo MR, Ruiz-Esmenjaud J, Arenas R. Leishmaniasis: a review. F1000 Res. 2017;6:750. https://doi.org/10.12688/f1000research.11120.1
2. Pan American Health Organization. Guideline for the treatment of leishmaniasis in the Americas. 2nd ed. Washington: The Organization; 2022.
3. van Griensven J, van Henten S, Mengesha B, Kassa M, Adem E, Endris Seid M, et al. Longitudinal evaluation of asymptomatic Leishmania infection in HIV-infected individuals in North-West Ethiopia: a pilot study. PLoS Negl Trop Dis. 2019;13:e0007765. https://doi.org/10.1371/journal.pntd.0007765
4. Van der Auwera G, Maes I, De Doncker S, Ravel C, Cnops L, Van Esbroeck M, et al. Heat-shock protein 70 gene sequencing for Leishmania species typing in European tropical infectious disease clinics. Euro Surveill. 2013;18:20543. https://doi.org/10.2807/1560-7917.ES2013.18.30.20543
5. Van den Broeck F, Savill NJ, Imamura H, Sanders M, Maes I, Cooper S, et al. Ecological divergence and hybridization of Neotropical *Leishmania* parasites. Proc Natl Acad Sci U S A. 2020;117:25159–68. https://doi.org/10.1073/pnas.1920136117
6. Miranda ADC, González KA, Samudio F, Pineda VJ, Calzada JE, Capitan-Barrios Z, et al. Molecular identification of parasites causing cutaneous leishmaniasis in Panama. Am J Trop Med Hyg. 2021;104:1326–34. https://doi.org/10.4269/ajtmh.20-1336
7. Tihon E, Imamura H, Dujardin JC, Van Den Abbeele J, Van den Broeck F. Discovery and genomic analyses of hybridization between divergent lineages of *Trypanosoma congolense*, causative agent of Animal African Trypanosomiasis. Mol Ecol. 2017;26:6524–38. https://doi.org/10.1111/mec.14271
8. Belli AA, Miles MA, Kelly JM. A putative *Leishmania panamensis*/*Leishmania braziliensis* hybrid is a causative agent of human cutaneous leishmaniasis in Nicaragua. Parasitology. 1994;109:435–42. https://doi.org/10.1017/S0031182000080689
9. Brito MEF, Andrade MS, Mendonça MG, Silva CJ, Almeida EL, Lima BS, et al. Species diversity of *Leishmania* (*Viannia*) parasites circulating in an endemic area for cutaneous leishmaniasis located in the Atlantic rainforest region of northeastern Brazil. Trop Med Int Health. 2009;14:1278–86. https://doi.org/10.1111/j.1365-3156.2009.02361.x
10. Tabbabi A, Cáceres AG, Bustamante Chauca TP, Seki C, Choochartpong Y, Mizushima D, et al. Nuclear and kinetoplast DNA analyses reveal genetically complex Leishmania strains with hybrid and mito-nuclear discordance in Peru. PLoS Negl Trop Dis. 2020;14:e0008797. https://doi.org/10.1371/journal.pntd.0008797

Address for correspondence: Frederik Van den Broeck or Gert Van der Auwera, Institute of Tropical Medicine, Nationalestraat 155, 2000 Antwerp, Belgium; email: fvandenbroeck@gmail.com or gvdauwera@itg.be

# New Genotype of *Coxiella burnetii* Causing Epizootic Q Fever Outbreak in Rodents, Northern Senegal

Joa Mangombi-Pambou, Laurent Granjon, Clément Labarrere, Mamadou Kane, Youssoupha Niang, Pierre-Edouard Fournier, Jérémy Delerce, Florence Fenollar, Oleg Mediannikov

Author affiliations: Centre Interdisciplinaire de Recherches Médicales de Franceville, Franceville, Gabon (J. Mangombi-Pambou); Aix-Marseille University, Marseille, France (J. Mangombi-Pambou, C. Labarrere, P.-E. Fournier, J. Delerce, F. Fenollar, O. Mediannikov); University Hospital Institute Méditerranée Infection, Marseille (J. Mangombi-Pambou, C. Labarrere, P.-E. Fournier, F. Fenollar, O. Mediannikov); Centre de Biologie pour la Gestion des Populations, Montpellier, France (L. Granjon); Biologie des Populations Animales Sahelo-Soudaniennes, Dakar, Senegal (M. Kane, Y. Niang)

DOI: https://doi.org/10.3201/eid2905.221034

In Senegal, *Coxiella burnetii*, which causes Q fever, has often been identified in ticks and humans near livestock, which are considered to be reservoirs and main sources of infection. We describe the emergence of *C. burnetii* in rodents, not previously known to carry this pathogen, and describe 2 new genotypes.

*Coxiella burnetii* is a causative agent of Q fever, a worldwide zoonosis. The disease may be acute (relatively benign) or chronic (with a wide range of clinical manifestations that can lead to high human mortality) (*1*). Humans are infected by inhaling contaminated environmental dust and aerosol particles from the birth products of infected animals, as well as through direct contact with milk, urine, or feces containing *C. burnetii* (*2*,*3*). Humans are not considered natural hosts of *C. burnetii* (*4*). A wide spectrum of animals can serve as hosts (*4*), but the reservoirs are livestock, mainly sheep, cattle, and goats (*3*), which are also the main sources of human infection (*1*).

In Senegal, *C. burnetii* has been reported in humans (*4*–*6*) and ticks (*4*). It has been isolated from rodent-associated soft ticks (*Ornithodoros sonrai*) and detected in several species of hard ticks collected from ruminants (*4*). Our previous study of zoonotic pathogens in rodents collected in 2017 revealed no presence of *C. burnetii* in rodent populations from the Ferlo region in northern Senegal (*7*). However, in this study, we tested rodent samples collected during 2019–2020 from the same region and found high prevalence of a new *C. burnetii* genotype, which might indicate an ongoing epizootic outbreak.

We screened 125 rodent samples for *C. burnetii*; the rodents were collected in the Ferlo region in northern Senegal near Widou Thiengoly (15.99°N, 15.32°W) under framework agreements between the French National Research Institute for Development and Senegal (*7*). None of the rodent species investigated were listed as protected with the International Union for Conservation of Nature or the Convention on International Trade in Endangered Species of Wild Fauna and Flora. Handling procedures were performed under Centre de Biologie Pour la Gestion des Populations agreement no. D-34-169-1 for experiments on wild animals and followed the guidelines of the American Society of Mammologists (*8*).

Rodents sampled belonged to the species *Arvicanthis niloticus* (n = 29), *Desmodilliscus braueri* (n = 3), *Gerbillus nancillus* (n = 9), *G. nigeriae* (n = 71), *Jaculus jaculus* (n = 4), *Taterillus* spp. (probably *T. pygargus*) (n = 8), and *Xerus erythropus* (n = 1). We extracted DNA from the spleen as described elsewhere (*7*) and stored it at −20°C. We detected bacterial DNA using *C. burnetii*–specific quantitative real-time PCR with primers and probes targeting IS1111 and IS30A spacers (*4*). For positive samples with a cycle threshold value <38, we first amplified 3 pairs of intergenic spacer primers, Cox2F/R, Cox5F/R, and Cox18F/R (*5*). Multispacer sequence typing (MST) genotyping of *C. burnetii* strains using sequences from the amplification of these 3 primer pairs revealed a potential new genotype. We amplified the other 7 primer pairs, Cox20F/R, Cox22F/R, Cox37F/R, Cox51F/R, Cox56F/R, Cox57F/R, and Cox61F/R, to describe this genotype.

Overall, 22.4% (28/125 for IS1111) and 19.2% (24/125 for IS30A) of rodents screened were positive for *C. burnetii*–specific quantitative PCR: *Desmodilliscus braueri* (33.3%; 1/3), *G. nancillus* (33.3%; 3/9), *G. nigeriae* (28.2%; 20/71), *Jaculus jaculus* (25%; 1/4), and *Taterillus* spp. (37.5%, 3/8). We found no *Arvicanthis niloticus* or *Xerus erythropus* rodents positive for *C. burnetii*. We performed complete MST genotyping of positive *C. burnetii* strain samples, and the sequences obtained from the primer pairs showed 100% identity for all positive samples. Nevertheless, 1 sample showed an insertion of 5 nucleotide bases in the amplified sequence of Cox56 spacer (Table), indicating

**Table.** Characterization of new *Coxiella burnetii* MST75 and MST76 genotypes described in study of new genotype of *C. burnetii* causing epizootic Q fever outbreak in rodents, northern Senegal*

| Species | No. | Is1111 positive, no. (%) | Profile of spacers | | | | | | | | | | |
|---|---|---|---|---|---|---|---|---|---|---|---|---|---|
| | | | Cox2 | Cox5 | Cox18 | Cox20 | Cox22 | Cox37 | Cox51 | Cox56 | Cox57 | Cox61 | Genotype |
| *Arvicanthis niloticus* | 29 | NA | NA | NA | NA | NA | NA | NA | NA | NA | NA | NA | NA |
| *Desmodilliscus braueri* | 3 | 1 (33.3) | 3 | 14 | 6 | 6 | 5 | 4 | 10 | 10 | 13 | 5 | MST75 |
| *Gerbillus nancillus* | 9 | 3 (33.3) | 3 | 14 | 6 | 6 | 5 | 4 | 10 | 10 | 13 | 5 | MST75 |
| *G. nigeriae*† | 71 | 20 (28.2) | 3 | 14 | 6 | 6 | 5 | 4 | 10 | 20/21‡ | 13 | 5 | MST75/ MST76‡ |
| *Jaculus jaculus* | 4 | 1 (25) | 3 | 14 | 6 | 6 | 5 | 4 | 10 | 10 | 13 | 5 | MST75 |
| *Taterillus* spp. | 8 | 3 (37.5) | 3 | 14 | 6 | 6 | 5 | .4 | 10 | 10 | 13 | 5 | MST75 |
| *Xerus erythropus* | 1 | NA | NA | NA | NA | NA | NA | NA | NA | NA | NA | NA | NA |
| Total | 125 | 28 | NA | NA | NA | NA | NA | NA | NA | NA | NA | NA | NA |

*MST, multispacer sequence typing; NA, not applicable.
†Invasive (expanding) species.
‡Genotype MST76 has the same profile as MST75 except for Cox 56.

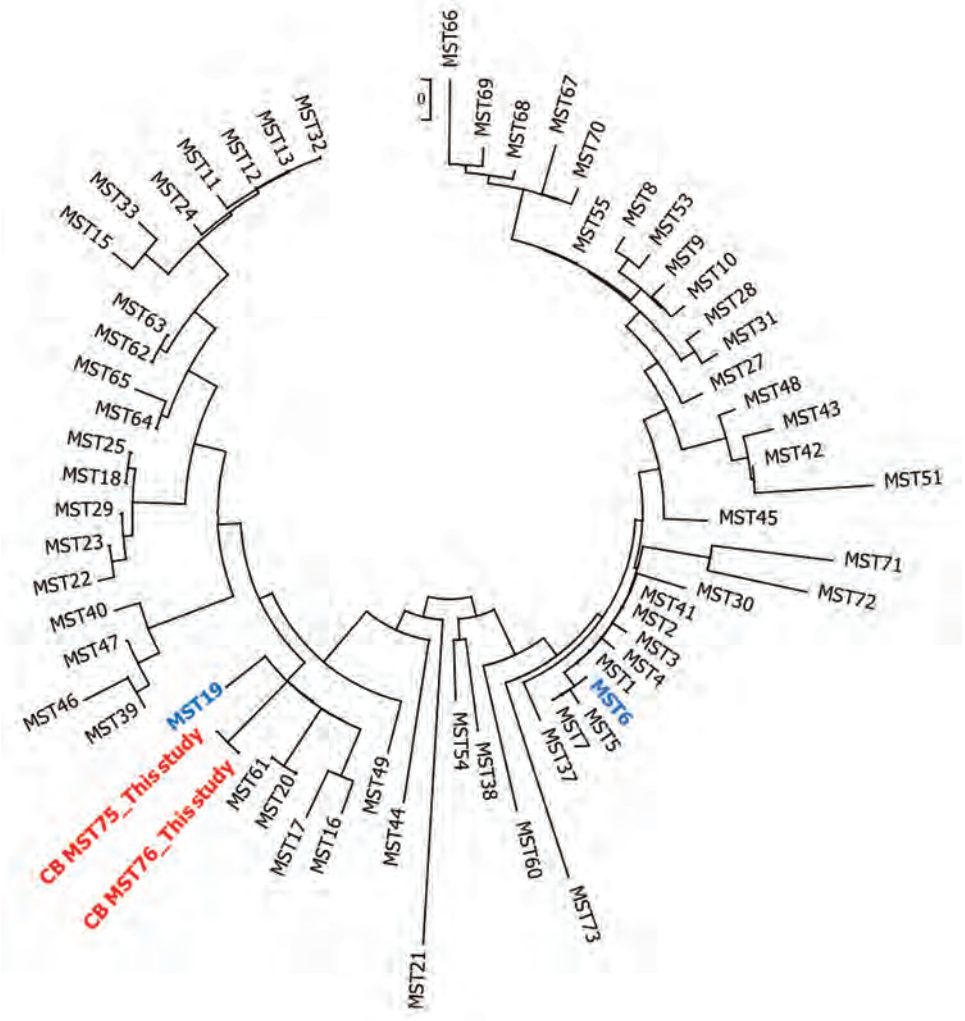


**Figure.** Neighbor-joining circular unrooted tree showing the relationship between *Coxiella burnetii* genotypes described in study of new genotype of *C. burnetii* causing epizootic Q fever outbreak in rodents, northern Senegal. MST75 and MST76 (red) were compared with genotypes already found in Senegal, MST19 and MST6 (blue), and other genotypes. The analysis involved 64 nt sequences. All positions containing gaps and missing data were eliminated. There were a total of 4,692 positions in the final dataset. Evolutionary analyses were conducted in MEGA7 (https://www.megasoftware.net). MST, multispacer sequence typing.

the presence of a probable variant. All of these sequences demonstrated the presence of ≥1 new genotypes of *C. burnetii* according to the BLAST database (https://ifr48.timone.univ-mrs.fr/mst/coxiellaburnetii/blast.html). Phylogenetic analysis based on concatenated sequences of spacers revealed that the new genotypes, MST75 (major) and MST76 (with an insertion), are close together and cluster with other genotypes, including those already found in Senegal, such as MST19, and those infecting animals and humans, such as MST16, MST17, MST20, and MST61 (Figure).

Our finding of *C. burnetii* MST75 and MST76 genotypes in the Ferlo rodent community suggests the emergence of a Q fever epizootic outbreak. Previously identified *C. burnetii* strains in Senegal were related to the proximity of livestock near the villages of Dielmo and Ndiop (*9*). In Ferlo, a previous study conducted on rodents sampled in 2017 did not find *C. burnetii* (*7*), indicating a relatively recent, possibly still ongoing epizootic outbreak. High *C. burnetii* prevalences (28%–38%) were observed in different species of gerbilline rodents, including *G. nigeriae*, which has recently colonized northern Senegal and is now the dominant species in outdoor rodent communities of Ferlo (*10*). The possibility of animal transmission from farms located near the rodent sampling area should also be explored. Our study shows the emergence in Senegal of new *C. burnetii* genotypes in susceptible animals, such as rodents (*1*), which might be a source of human infections. Although the pathogenicity of these new genotypes for humans is yet unknown, our findings signal the urgent need for epidemiologic surveillance for *C. burnetii* infection in humans in Senegal and neighboring countries.

## Acknowledgments

We thank Philippe Gauthier for precise taxonomic identification of some rodent specimens using barcoding (based on cyt*b* sequences), and Fabien Flirden for his technical support on molecular biology.

This study was supported by the Institut Hospitalo-Universitaire Méditerranée Infection, the French National Research Agency under the Investissements d'avenir programme, (reference ANR-10-IAHU-03), and the fourth Make Our Planet Great Again (MOPGA 4) program. This work was cofunded by the Labex Dispositif de Recherche Interdisciplinaire sur les Interactions Hommes-Milieux, and the Investissements d'Avenir program (ANR-11-LABX-0010), which is managed by the Agence nationale de la recherche.

### About the Author

Dr. Mangombi-Pambou is a postdoctoral researcher at the Institut Hospitalo Universitaire Méditérranée Infection in Marseille, France. His research interests include infectious diseases of zoonotic origin and the ecology and role of rodents in the dynamics of zoonotic diseases.

### References

1. Angelakis E, Raoult D. Q fever. Vet Microbiol. 2010;140:297–309. https://doi.org/10.1016/j.vetmic.2009.07.016
2. Tissot-Dupont H, Raoult D. Q fever. Infect Dis Clin North Am. 2008;22:505–14, ix. https://doi.org/10.1016/j.idc.2008.03.002
3. Vanderburg S, Rubach MP, Halliday JEB, Cleaveland S, Reddy EA, Crump JA. Epidemiology of *Coxiella burnetii* infection in Africa: a OneHealth systematic review. PLoS Negl Trop Dis. 2014;8:e2787. https://doi.org/10.1371/journal.pntd.0002787
4. Mediannikov O, Fenollar F, Socolovschi C, Diatta G, Bassene H, Molez J-F, et al. *Coxiella burnetii* in humans and ticks in rural Senegal. PLoS Negl Trop Dis. 2010;4:e654. https://doi.org/10.1371/journal.pntd.0000654
5. Angelakis E, Mediannikov O, Socolovschi C, Mouffok N, Bassene H, Tall A, et al. *Coxiella burnetii*–positive PCR in febrile patients in rural and urban Africa. Int J Infect Dis. 2014;28:107–10. https://doi.org/10.1016/j.ijid.2014.05.029
6. Sokhna C, Mediannikov O, Fenollar F, Bassene H, Diatta G, Tall A, et al. Point-of-care laboratory of pathogen diagnosis in rural Senegal. PLoS Negl Trop Dis. 2013;7:e1999. https://doi.org/10.1371/journal.pntd.0001999
7. Dahmana H, Granjon L, Diagne C, Davoust B, Fenollar F, Mediannikov O. Rodents as hosts of pathogens and related zoonotic disease risk. Pathogens. 2020;9:202. https://doi.org/10.3390/pathogens9030202
8. Sikes RS, Gannon WL; Animal Care and Use Committee of the American Society of Mammologists. Guidelines of the American Society of Mammologists for the use of wild mammals in research. J Mammal. 2011;92:235–53. https://doi.org/10.1644/10-MAMM-F-355.1
9. Diouf FS, Ndiaye EHI, Hammoud A, Diamanka A, Bassene H, Ndiaye M, et al. Detection of *Coxiella burnetii* and *Borrelia* spp. DNA in cutaneous samples and in household dust in rural areas, Senegal. Vector Borne Zoonotic Dis. 2021;21:659–66. https://doi.org/10.1089/vbz.2020.2723
10. Granjon L, Ba K, Diagne C, Ndiaye A, Piry S, Thiam M. The Ferlo small rodent community: historical trends and characteristics of the current population [in French]. In: Boëtsch G, Duboz P, Guissé A, Sarr P, editors. The Great Green Wall, an African response to climate change [in French]. Paris: Centre national de la recherche scientifique; 2019. p. 1–19.

Address for correspondence: Oleg Mediannikov, IHU Méditerranée Infection, 19-21 Boulevard Jean Moulin, 13005 Marseille, France; email: olegusss1@gmail.com

# Therapeutic Failure and Acquired Bedaquiline and Delamanid Resistance in Treatment of Drug-Resistant TB

James Millard, Stephanie Rimmer, Camus Nimmo, Max O'Donnell

Author affiliations: Guys and St Thomas' NHS Foundation Trust, London, UK (J. Millard); Wellcome Trust Liverpool Glasgow Centre for Global Health Research, Liverpool, UK (J. Millard); University of Liverpool, Liverpool (J. Millard); Africa Health Research Institute, Durban, South Africa (J. Millard, C. Nimmo); Imperial College Healthcare, London (S. Rimmer); Francis Crick Institute, London (C. Nimmo); University College London, London (C. Nimmo); Columbia University Medical Center, New York, New York, USA (M. O'Donnell); CAPRISA MRC-HIV-TB Pathogenesis and Treatment Research Unit, Durban (M. O'Donnell)

DOI: http://doi.org/10.3201/eid2905.221716

New classes of antitubercular drugs, diarylquinolines and nitroimidazoles, have been associated with improved outcomes in the treatment of drug-resistant tuberculosis, but that success is threatened by emerging drug resistance. We report a case of bedaquiline and delamanid resistance in a 55-year-old woman in South Africa with extensively drug-resistant tuberculosis and known HIV.

Major improvements have been achieved in drug-resistant tuberculosis (TB) treatment in recent years; 2 new drug classes, diarylquinolines (bedaquilline) and nitroimidazoles (pretomanid and delamanid), have been central to this success (*1*). The ZeNiX trial demonstrated cure rates of >90% in complex

drug-resistant TB when a bedaquiline, pretomanid, and linezolid (BPaL) regimen was given for just 6 months (*2*); the TB-PRACTECAL trial used BPaL plus moxifloxacin to treat multidrug-resistant (MDR) TB and achieved cure rates of 89% versus 50% in controls (*3*). These regimens have been recommended as the preferred treatment option for drug-resistant TB by the World Health Organization (*4*).

Threatening those recent successes, resistance can emerge to bedaquiline through mutations in *atpE*, *pepQ*, or *Rv0678* (with mutations in *Rv0678* being by far the most common in clinical isolates) and to pretomanid and delamanid through mutations of *fbiA/B/C*, *ddn*, and *fgd1*. Bedaquiline resistance has been increasingly reported, but only a handful of cases of resistance to both classes of agents in TB patients have been reported (*4*–*8*). All of those reports have described prolonged infections treated with differing drug combinations over time, and none were cases where all 3 components of BPaL were administered concurrently. We present the case of a patient with pre-XDR TB (resistant to rifampin, isoniazid, and fluoroquinolones) in South Africa whose treatment regimen failed when bedaquiline resistance and subsequent delamanid resistance developed, despite treatment with bedaquiline, delamanid, and linezolid beginning early in therapy.

A 55-year-old woman sought care in July 2018 for weight loss and fatigue. She had completed treatment for drug-susceptible TB in 2007 and received an HIV diagnosis in 2012 (initial viral load 31,222 copies/mL and CD4 count 174 cells/μL) that was treated with efavirenz/emtricitabine/tenofovir. Chest radiography revealed extensive cavitary pulmonary TB. She had no other medical diagnoses. Initial sputum smear showed 3+ acid-fast bacilli and was culture-positive for *Mycobacterium tuberculosis* consistent with rifampin resistance by the Xpert MTB/RIF assay (Cepheid, https://www.cepheid.com).

A 9-month oral regimen consisting of bedaquiline, linezolid, clofazimine, levofloxacin, ethionamide, and pyrazinamide was commenced in line with guidelines in South Africa at the time, and the patient was enrolled in the PRAXIS study, a randomized controlled trial of bedaquiline adherence support (*9*). Antiretroviral drugs were changed to nevirapine/emtricitabine/tenofovir to manage interactions with bedaquiline. GenoType MTBDRplus and MTBDRsl (Hain Lifescience, https://www.hain-lifescience.de) line probe assay results and phenotypic drug susceptibility testing (DST) on the baseline culture confirmed resistance to rifampin, isoniazid, and fluoroquinolones. Because of fluoroquinolone resistance, we changed

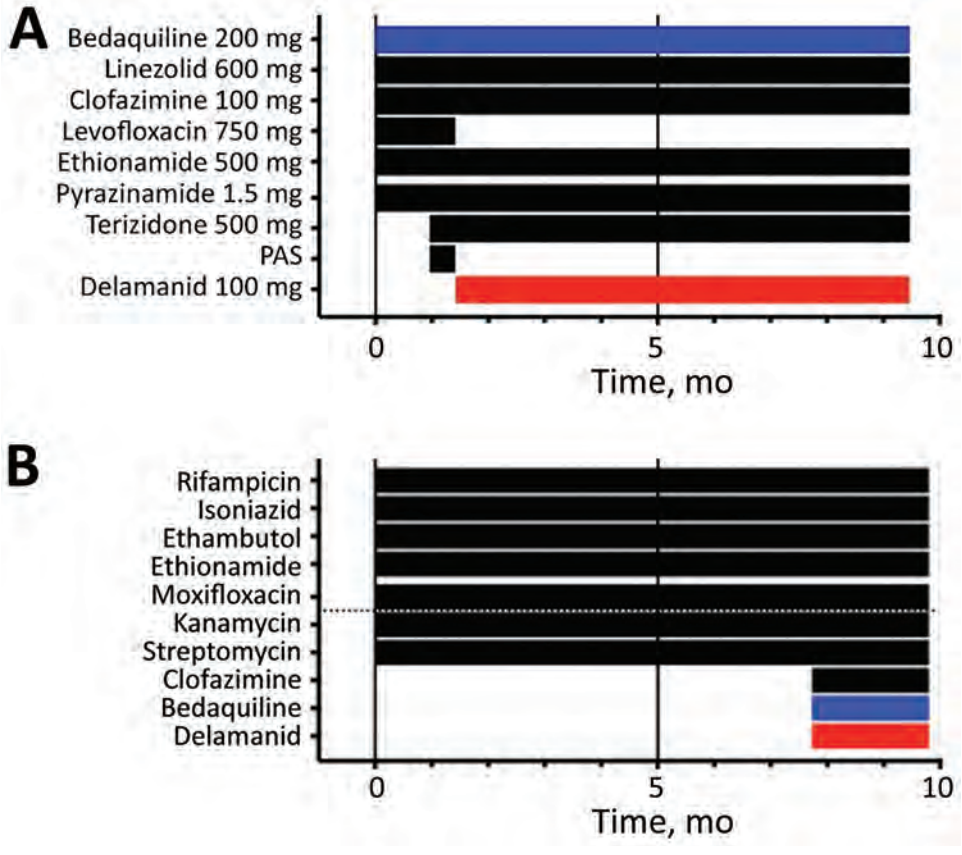


**Figure.** Drug regime over time of patient with drug-resistant tuberculosis, South Africa. A) Drug treatment history by month. B) Development of drug resistance according to phenotypic drug susceptibility testing per month. Red indicates delamanid, blue indicates bedaquiline. PAS, P-aminosalicylic acid.

treatment to a modified World Health Organization long regimen (minimum 18 months) and added terizidone and p-aminosalicylic acid. Delamanid became available through an expanded-access program and was added at week 6 when levofloxacin and p-aminosalicylic acid were stopped.

We assessed adherence to bedaquiline and antiretrovirals using a Wisepill medication dispenser (Wisepill Technologies, https://www.wisepill.com). We conducted extended-phenotypic DST at weeks 6 and 34 and performed whole-genome sequencing (WGS) at weeks 6, 14, and 34. We assessed MICs for a range of drugs on week 6 isolates and week 34 isolates by using a microtiter plate (*9*). Phenotypic DST at week 6 demonstrated additional resistance to moxifloxacin, ethionamide, ethambutol, streptomycin, and kanamycin; we observed corresponding mutations in *rpoB*, *katG*, *gyrA*, *ethA*, *embB*, and rrs (Figure; Appendix Figure, https://wwwnc.cdc.gov/EID/article/29/5/22-1716-App1.pdf). At week 10, the patient was discharged from hospital for outpatient management.

Despite therapy, she remained smear-positive and culture-positive at week 34 and had lost a further 5 kg. We extended bedaquiline to 9 months. Bedaquiline adherence from initiation of therapy was 45%. WGS at week 14 identified acquisition of 2 bedaquiline resistance-associated variants (RAVs) in *Rv0678*: one was a single-nucleotide variation (Gln22Pro) and the other was an insertion (Asp47frameshift). WGS at week 34 demonstrated acquisition of a further 6 *Rv0678* bedaquiline RAVs (Ala57Glu, Arg72Trp, Asp88frameshift, Asp88Ala, Gly121Arg, Leu122Pro) and the emergence of 2 heterozygous *fbiC* loss-of-function mutations (Ala487frameshift, 25%; Ser534stop, 12%). Phenotypic DST at week 34 confirmed emergent resistance to bedaquiline and clofazimine, which commonly demonstrates cross-resistance with bedaquiline because of *Rv0678* mutations (Figure). Delamanid phenotypic DST by microtiter plate confirmed an increase in delamanid MIC from 0.015 to >0.5 μg/mL, consistent with resistance (*10*). The patient died ≈10 months after initial diagnosis and treatment initiation.

Recent clinical trial evidence from ZeNix-TB and TB-PRACTECAL has been extremely encouraging for the development of an effective, 6-month regimen for complex drug-resistant TB (2,3). Despite promising clinical trial results, this case highlights the ease with which resistance can develop in real-world implementation, likely because of the complex interplay of factors such as inadequate regimens caused by delayed or limited DST, drug pharmacokinetics, lesion penetration of drugs, and medication adherence. As regimens based on BPaL are rolled out more widely, combining this treatment with contemporaneous access to rapid DST for all agents, and access to adherence support, is essential to limit the development of resistance and loss of these effective new regimens.

M.O. is supported by National Institutes of Health/National Institute of Allergy and Infectious Diseases (R01AI124413, R01AI167795) and by the National Center for Advancing Translational Sciences (UL1TR001873). This work was supported by grants from the Wellcome Trust to C.N. (203583/Z/16/Z) and J.M. (203919/Z/16/Z). C.N. is supported by the Francis Crick Institute, which receives its core funding from Cancer Research UK (CC2169), the UK Medical Research Council (CC2169), and the Wellcome Trust (CC2169).

## About the Author

Dr. Millard is an infectious disease clinician at Guys and St Thomas' NHS Foundation Trust. He has research interests in tuberculosis, particularly resistance and therapeutics.

## References

1. World Health Organization. Rapid communication: key changes to the treatment of drug-resistant tuberculosis. Geneva: The Organization; 2022 [cited 2022 Oct 6]. https://www.who.int/publications/i/item/WHO-UCN-TB-2022-2
2. Conradie F, Bagdasaryan TR, Borisov S, Howell P, Mikiashvili L, Ngubane N, et al.; ZeNix Trial Team. Bedaquiline–pretomanid–linezolid regimens for drug-resistant tuberculosis. N Engl J Med. 2022;387:810–23. https://doi.org/10.1056/NEJMoa2119430
3. Nyang'wa B-T, Berry C, Kazounis E, Motta I, Parpieva N, Tigay Z, et al.; TB-PRACTECAL Study Collaborators. A 24-week, all oral regimen for rifampicin-resistant tuberculosis. N Engl J Med. 2022;387:2331–43. https://doi.org/10.1056/NEJMoa2117166
4. Nimmo C, Millard J, van Dorp L, Brien K, Moodley S, Wolf A, et al. Population-level emergence of bedaquiline and clofazimine resistance-associated variants among patients with drug-resistant tuberculosis in southern Africa: a phenotypic and phylogenetic analysis. Lancet Microbe. 2020;1:e165–74. https://doi.org/10.1016/S2666-5247(20)30031-8
5. Bloemberg GV, Keller PM, Stucki D, Trauner A, Borrell S, Latshang T, et al. Acquired resistance to bedaquiline and delamanid in therapy for tuberculosis. N Engl J Med. 2015;373:1986–8. https://doi.org/10.1056/NEJMc1505196
6. Polsfuss S, Hofmann-Thiel S, Merker M, Krieger D, Niemann S, Rüssmann H, et al. Emergence of low-level delamanid and bedaquiline resistance during extremely drug-resistant tuberculosis treatment. Clin Infect Dis. 2019;69:1229–31. https://doi.org/10.1093/cid/ciz074
7. Yoshiyama T, Takaki A, Aono A, Mitarai S, Okumura M, Ohta K, et al. Multidrug resistant tuberculosis with simultaneously acquired drug resistance to bedaquiline and delamanid. Clin Infect Dis. 2021;73:2329–31. https://doi.org/10.1093/cid/ciaa1064
8. Omar SV, Ismail F, Ndjeka N, Kaniga K, Ismail NA. Bedaquiline-resistant tuberculosis associated with Rv0678

mutations. N Engl J Med. 2022;386:93–4. https://doi.org/10.1056/NEJMc2103049
9. O'Donnell MR, Padayatchi N, Wolf A, Zelnick J, Daftary A, Orrell C, et al. Bedaquiline adherence measured by electronic dose monitoring predicts clinical outcomes in the treatment of patients with multidrug-resistant tuberculosis and HIV/AIDS. J Acquir Immune Defic Syndr. 2022;90:325–32. https://doi.org/10.1097/QAI.0000000000002940
10. Fowler P; CRyPTIC Consortium. Epidemiological cut-off values for a 96-well broth microdilution plate for high-throughput research antibiotic susceptibility testing of *M. tuberculosis*. Eur Respir J. 2022;60:2200239. https://doi.org/10.1183/13993003.00239-2022

Address for correspondence: James Millard, Dept of Infectious Diseases, St Thomas' Hospital, Westminster Bridge Rd, London, SE1 7EH, UK; email: jmillard@liverpool.ac.uk

## COMMENT LETTER

# Nomenclature for Human Infections Caused by Relapsing Fever *Borrelia*

Paul S. Mead

Author affiliation: Centers for Disease Control and Prevention, Fort Collins, Colorado, USA

DOI: https://doi.org/10.3201/eid2905.230195

**To the Editor:** Vazquez et al. report a convincing case of relapsing fever caused by *Borrelia lonestari* bacteria (*1*). This discovery highlights an existing problem with the nomenclature for relapsing fever.

Tick-borne relapsing fever (TBRF) is the name given to illness caused by several genospecies of relapsing fever *Borrelia* bacteria, all of which are transmitted by argasid (soft) ticks (*2*). The limitations of this term became apparent after discovery of *B. miyamotoi*, a related genospecies that is transmitted by ixodid (hard) ticks and causes illness that differs epidemiologically from traditional TBRF (*3*). Consequently, 3 terms are used in the scientific literature to describe *B. miyamotoi* infections: *Borrelia miyamotoi* disease, hard tick–borne relapsing fever, and hard tick relapsing fever (*3*,*4*). In the interest of standard nomenclature, it is worth considering objectively the relative merits of each term.

The term *Borrelia miyamotoi* disease (BMD) is problematic because it is species specific and cannot accommodate the discovery of related pathogens transmitted by ixodid ticks, including potentially *B. lonestari* (*1*,*3*). Disease names are most serviceable as umbrella terms that exist above the species level (e.g., Lyme disease, shigellosis).

The term hard tick–borne relapsing fever has a different problem, a grammatical one. The word hard rightly modifies tick, not tick-borne, which is a mode of transmission. This problem is solved by shortening to hard tick relapsing fever. The suffix "-borne" is not essential for clarity, as demonstrated by other established names (e.g., sand fly fever, Colorado tick fever) (*2*).

In the absence of a formal nomenclature decision by the World Health Organization, the following terms are consistent with precedent, epidemiologically useful, linguistically sensible replacements for TBRF: hard tick relapsing fever (HTRF) for illness caused by relapsing fever–clade *Borrelia* transmitted by ixodid ticks, and its congener, soft tick relapsing fever (STRF), for related agents transmitted by argasid ticks.

### References

1. Vazquez Guillamet LJ, Marx GE, Benjamin W, Pappas P, Lieberman N, Bachiashvili K, et al. Relapsing fever caused by *Borrelia lonestari* after tick bite in Alabama, USA. Emerg Infect Dis. 2023;29:441–4. https://doi.org/10.3201/eid2902.221281
2. World Health Organization. International Classification of Diseases, 11th revision. 2022 [cited Jan 31]. https://icd.who.int
3. Telford SR III, Molloy PJ, Berardi VP. *Borrelia miyamotoi*. Ann Intern Med. 2015;163:963–4. https://doi.org/10.7326/L15-5187
4. Rodino KG, Pritt BS. When to think about other *Borrelia*: hard tick relapsing fever (*Borrelia miyamotoi*), *Borrelia mayonii*, and beyond. Infect Dis Clin North Am. 2022;36:689–701. https://doi.org/10.1016/j.idc.2022.04.002

Address for correspondence: Paul S. Mead, Centers for Disease Control and Prevention, 3156 Rampart Rd, Fort Collins, CO 80521, USA; email: pmead@cdc.gov

## Correction

### Vol. 26, No. 12

The Figure had an incorrect x-axis scale in Laboratory Features of Trichinellosis and Eosinophilia Threshold for Testing, Nunavik, Quebec, Canada, 2009–2019 (L.B. Harrison et al.). The article has been corrected online (https://wwwnc.cdc.gov/eid/article/28/12/22-1144_article).

**Franz Xaver Winterhalter (1805–1873), *Princess Alice (1843–78), later Grand Duchess of Hesse*, 1861.** Oil on canvas, 46.9 in x 34.9 in/119.0 cm x 88.6 cm. Royal Collection Trust, Buckingham Palace, London, United Kingdom.

# A Deadly Kiss

Byron Breedlove

Diphtheria, a serious infection caused by the bacterium *Corynebacterium diphtheriae*, was described by Hippocrates early in the 5th century BCE. In 1826, French physician Pierre Bretonneau named the disease *diphtérite*, derived from the Greek word for "leather" or "hide" because of the coating that appears in the throats of infected people. Before then, various names were ascribed to the disease or its aftermath, such as *El Año de los Garrotillos* (The Year of Strangulations) to characterize a 1613 epidemic in Spain. Before the availability of vaccines, diphtheria was a leading cause of childhood death. The most common type of diphtheria is the classic respiratory disease, and another type of infection, called cutaneous diphtheria, causes skin ulcers.

An outbreak of diphtheria in 1878 claimed many lives, not just among the youngest and poorest. Historically, diphtheria mortality rates have been typically higher among people in younger than older age groups. Among the victims were Princess Alice (Alice Maud Mary), whose 1861 portrait appears as this month's cover image, and her young daughter, Marie. This painting is one of an estimated 120 portraits completed by German artist Franz Xaver Winterhalter for members of the English royal family. His exclusive clientele, which also included members of the royal families in Germany, France, and Belgium, made him a wealthy celebrity.

Born in Menzenschwand village in Germany's Black Forest in 1805, Winterhalter was encouraged to draw from a young age. In 1818, he received art instruction in Fribourg, and in 1823, he moved to Munich to attend the Academy of Fine Arts, where one of his instructors was portraitist Josef Stieler. After traveling in Germany and Italy, Winterhalter moved to Paris and soon enjoyed the patronage of King Louis-Philippe. According to the Getty Museum, "In 1835, after he painted the German Grand Duke and Duchess of Baden, Winterhalter's international career as a court portrait painter was launched."

The Getty Museum notes that "Winterhalter's portraits were prized for their subtle intimacy, but his popularity among patrons came from his ability to create the image his sitters wished or needed to

Author affiliation: Centers for Disease Control and Prevention, Atlanta, Georgia, USA

DOI: https://doi.org/10.3201/eid2905.AC2905

project to their subjects. He was able to capture the moral and political climate of each court, adapting his style to each client until it seemed as if his paintings acted as press releases, issued by a master of public relations."

Completed in June 1861, Winterhalter's portrait shows a calm, beatific Princess Alice during an eventful year. Alice had acted as companion and caretaker for her maternal grandmother, Victoria, Duchess of Kent, who died in March. Alice's engagement in April 1861 to Prince Louis IV of Hesse no doubt helped dispel the gloom from that loss. In December, however, Alice again found herself as caregiver, this time for her father, Prince Albert, who died in December.

The Royal Trust Collection, home to this painting, notes that Alice "is wearing the dress in which she appeared at her first Drawing-Room (a formal reception where ladies were presented at court) on 7 May 1859. She was the third child and second daughter of Queen Victoria and Prince Albert. Known for her sweet nature, she often took on the role of peacekeeper in the royal household." Alice, poised and composed, is wearing a white iridescent ball dress and a black shawl with a ringlet of flowers. Winterhalter's skills are revealed by the textures and tones in Alice's skin, hair, and clothes, the facets and reflections from her jewelry, and careful rendering of the flowers.

After their wedding in 1862, Alice and Prince Louis moved to Germany. During the Austro-Prussian War in 1866, also known as Seven Weeks' War, while Alice was pregnant with her third child, her father-in-law, Louis III, Grand Duke of Hesse, sided with the Austrians, and Prince Louis served as a commander for the Hessian Calvary, leaving Alice with the children. The Royal Museums Greenwich notes that "During this time, she befriended Florence Nightingale and played an active role in the region's military hospitals." Afterward, Alice helped create a center to train nurses and sometimes personally helped care for the destitute.

Prince Louis' father and older brother both died in 1877, and Louis became Grand Duke and Alice Duchess of Hesse, a position she would only briefly hold. In November 1878, diphtheria spread throughout the royal household. The first stricken was Alice's oldest daughter, Victoria, followed by Alix, Marie, Irene, Ernest, and her husband Louis. Marie died from diphtheria on November 15, although Alice initially did not reveal Marie's death to her other children. When Ernest heard the news, he proved devastated; accounts suggest that Alice comforted her son with a kiss that would prove deadly. Whether that contact infected her remains a point of conjecture, but Alice nonetheless contracted diphtheria and died on December 14, 1878, the 17th anniversary of her father's death.

Five years after Alice's death, bacteriologists Edwin Klebs and Friedrich Löffler identified the bacterium that causes diphtheria and named it Klebs–Löffler bacillus (now called *Corynebacterium diphtheriae*). Diphtheria is now largely preventable by an effective vaccine regimen and treatable with antibiotics and an antitoxin. Recent data from the World Health Organization reported that, in 2021, there were 8,638 cases globally. Although diphtheria is now rare in industrialized nations and its global burden has declined dramatically, in locales where vaccination coverage is inadequate or vaccination is disrupted or unavailable because of conflict, population displacement, or misinformation, recent outbreaks have been reported and resurgence of diphtheria remains possible.

## Bibliography


1. Acosta AM, Moro PL, Hariri S, Tiwari TS. Chapter 7: Diphtheria. In: Hall E, Wodi AP, Hamborsky J, Morelli V, Schillie S, editors. Epidemiology and prevention of vaccine-preventable diseases. 14th ed. Washington: Centers for Disease Control and Prevention. 2021 [cited 2023 Apr 3]. https://www.cdc.gov/vaccines/pubs/pinkbook/dip.html
2. Centers for Disease Control and Prevention. Diphtheria [cited 2023 Apr 3]. https://www.cdc.gov/diphtheria/index.html
3. Clarke KE, MacNeil A, Hadler S, Scott C, Tiwari TS, Cherian T. Global epidemiology of diphtheria, 2000–2017. Emerg Infect Dis. 2019;25:1834–42. https://doi.org/10.3201/eid2510.190271
4. Klass P. How science conquered diphtheria, the plague among children [cited 2023 Apr 3]. https://www.smithsonianmag.com/science-nature/science-diphtheria-plague-among-children-180978572
5. Maramraj KK, Latha ML, Reddy R, Sodha SV, Kaur S, Dikid T, et al. Addressing reemergence of diphtheria among adolescents through program integration in India. Emerg Infect Dis. 2021;27:953–6. https://doi.org/10.3201/eid2703.203205
6. New York Times. The Princess Alice dead. Fatal termination of an attack of diphtheria—mourning in England and Canada—the life of the dead princess. December 15, 1878 [cited 2023 Mar 26]. https://timesmachine.nytimes.com/timesmachine/1878/12/15/issue.html
7. Royal Collection Trust. Princess Alice (1843–78), later Grand Duchess of Hesse [cited 2023 Mar 20]. https://www.rct.uk/collection/404579/princess-alice-1843-78-later-grand-duchess-of-hesse
8. World Health Organization. Diphtheria reported cases and incidence [cited 2023 Mar 23]. https://immunizationdata.who.int/pages/incidence/DIPHTHERIA.html?CODE=Global&YEAR=


Address for correspondence: Byron Breedlove, EID Journal, Centers for Disease Control and Prevention, 1600 Clifton Rd NE, Mailstop H16-2, Atlanta, GA 30329-4027, USA; email: wbb1@cdc.gov

# EMERGING INFECTIOUS DISEASES®

## Upcoming Issue

- Association of Persistent Symptoms after Lyme Neuroborreliosis and Increased Levels of Interferon-α in Blood.
- Probable Transmission of SARS-CoV-2 from African Lion to Zoo Employees
- Case Studies and Literature Review of *Francisella tularensis*–Related Prosthetic Joint Infection
- Epidemiologic Characteristics of Mpox Infections among People Experiencing Homelessness, Los Angeles County, California, USA, 2022
- Prevalence of Nonfalciparum and *Plasmodium falciparum* Malaria Infections among Schoolchildren, Tanzania
- Rising Incidence of *Sporothrix brasiliensis* Infections, 2011–2022, Curitiba, Brazil
- SARS-CoV-2 Seroprevalence Studies in Pets, Spain
- Evolution of Avian Influenza Virus (H3) with Spillover into Humans, China
- Results of PCR Analysis of Mpox Clinical Samples, Sweden, 2022
- Tanapox, South Africa, 2022
- MERS-CoV–Specific T-Cell Responses in Camels after Single MVA-MERS-S Vaccination
- Detection of Novel Poxvirus from Gray Seal (*Halichoerus grypus*), Germany
- Tropism and Replication Competence of Novel Zoonotic-like Avian Influenza A(H3N8) in Ex Vivo Human Bronchus and Lung
- Detection of *Leishmania* RNA Virus 1 in *Leishmania* (*Viannia*) *panamensis* Isolates, Panama
- *Baylisascaris procyonis* Roundworm Infection in Child with Autism Spectrum Disorder, Washington, USA, 2022
- Limited Cutaneous Leishmaniasis as Ulcerated Verrucous Plaque on Leg, Tucson, Arizona, USA
- Genomic Surveillance of Monkeypox Virus, Minas Gerais, Brazil, 2022
- Manifestations and Management of Trimethoprim/Sulfamethoxazole–Resistant *Nocardia otitidiscaviarum* Infection
- Antimicrobial-Resistant Infections after Turkey/Syria Earthquakes, 2023

**Complete list of articles in the June issue at https://wwwnc.cdc.gov/eid/#issue-299**

## Earning CME Credit

To obtain credit, you should first read the journal article. After reading the article, you should be able to answer the following, related, multiple-choice questions. To complete the questions (with a minimum 75% passing score) and earn continuing medical education (CME) credit, please go to http://www.medscape.org/journal/eid. Credit cannot be obtained for tests completed on paper, although you may use the worksheet below to keep a record of your answers.

You must be a registered user on http://www.medscape.org. If you are not registered on http://www.medscape.org, please click on the "Register" link on the right hand side of the website.

Only one answer is correct for each question. Once you successfully answer all post-test questions, you will be able to view and/or print your certificate. For questions regarding this activity, contact the accredited provider, CME@medscape.net. For technical assistance, contact CME@medscape.net. American Medical Association's Physician's Recognition Award (AMA PRA) credits are accepted in the US as evidence of participation in CME activities. For further information on this award, please go to https://www.ama-assn.org. The AMA has determined that physicians not licensed in the US who participate in this CME activity are eligible for *AMA PRA Category 1 Credits*™. Through agreements that the AMA has made with agencies in some countries, AMA PRA credit may be acceptable as evidence of participation in CME activities. If you are not licensed in the US, please complete the questions online, print the AMA PRA CME credit certificate, and present it to your national medical association for review.

## Article Title

### Trends in and Risk Factors for Recurrent *Clostridioides difficile* Infection, New Haven County, Connecticut, USA, 2015–2020

## CME Questions

**1. Which one of the following trends in the epidemiology of *Clostridioides difficile* infection (CDI) in the current is most accurate?**

A. Rates of healthcare-facility-onset (HCFO) CDI generally declined over time, whereas rates of community-associated (CA) CDI remained stable
B. Rates of HCFO CDI remained over time, whereas rates of CA-CDI increased
C. Rates of recurrent CDI (RCDI) were higher in cases of CA-CDI vs HCFO CDI
D. The overall rate of RCDI was 12%

**2. Which one of the following trends was noted in the prevalence of RCDI in the current study?**

A. Black race was associated with lower rates of RCDI compared with White race
B. There was no race-based difference in the rate of RCDI
C. There was a steady increase in the risk for RCDI from 2015 to 2020
D. The rate of RCDI declined precipitously from 2019 to 2020

**3. Which one of the following medical conditions was most associated with a higher risk for RCDI in the current study?**

A. Immunocompromise
B. Malignancy
C. Cognitive impairment
D. Stroke

## Earning CME Credit

To obtain credit, you should first read the journal article. After reading the article, you should be able to answer the following, related, multiple-choice questions. To complete the questions (with a minimum 75% passing score) and earn continuing medical education (CME) credit, please go to http://www.medscape.org/journal/eid. Credit cannot be obtained for tests completed on paper, although you may use the worksheet below to keep a record of your answers.

You must be a registered user on http://www.medscape.org. If you are not registered on http://www.medscape.org, please click on the "Register" link on the right hand side of the website.

Only one answer is correct for each question. Once you successfully answer all post-test questions, you will be able to view and/or print your certificate. For questions regarding this activity, contact the accredited provider, CME@medscape.net. For technical assistance, contact CME@medscape.net. American Medical Association's Physician's Recognition Award (AMA PRA) credits are accepted in the US as evidence of participation in CME activities. For further information on this award, please go to https://www.ama-assn.org. The AMA has determined that physicians not licensed in the US who participate in this CME activity are eligible for *AMA PRA Category 1 Credits*™. Through agreements that the AMA has made with agencies in some countries, AMA PRA credit may be acceptable as evidence of participation in CME activities. If you are not licensed in the US, please complete the questions online, print the AMA PRA CME credit certificate, and present it to your national medical association for review.

## Article Title

### Emergence of Erythromycin-Resistant Invasive Group A *Streptococcus*, West Virginia, USA, 2020–2021

## CME Questions

**1. Your patient is a 37-year-old man with a history of intravenous drug use (IVDU) who was just diagnosed with invasive group A *Streptococcus pyogenes* (iGAS) infection. On the basis of the study at J.W. Ruby Memorial Hospital in West Virginia from 2020 to 2021 by Powell and colleagues, which one of the following statements about the clinicoepidemiology of iGAS infections is correct?**

A. Most patients were elderly
B. More than half of patients were experiencing homelessness at the time of culture; 20% had recent or remote IVDU
C. The most common infection source was respiratory
D. Antimicrobial therapy varied considerably by patient acuity, length of hospitalization, IV catheter availability, and initial treatment response

**2. According to the study at J.W. Ruby Memorial Hospital in West Virginia from 2020 to 2021 by Powell and colleagues, which one of the following statements about the specific phenotypic and genotypic antimicrobial resistance traits of available isolates from iGAS infections is correct?**

A. 76% of isolates were simultaneously resistant to erythromycin and clindamycin
B. Susceptible isolates were primarily *emm11*
C. All *emm92* and *emm89* isolates were simultaneously resistant to erythromycin and clindamycin
D. Macrolide-resistant isolates were typically sensitive to tetracycline and aminoglycosides

**3. On the basis of the study at J.W. Ruby Memorial Hospital in West Virginia from 2020 to 2021 by Powell and colleagues, which one of the following statements about clinical and public health implications of the clinicoepidemiology of iGAS infections and specific phenotypic and genotypic antimicrobial resistance traits of corresponding available isolates is correct?**

A. The study findings do not corroborate Active Bacterial Core (ABC)-Centers for Disease Control and Prevention (CDC) national data
B. Predominance of erythromycin resistance and *emm92* suggest increased emergence of resistance and clonal dissemination
C. Across all populations, *emm*-type distribution remained stable compared with historical reports
D. The findings do not suggest predisposition to iGAS infections based on socioeconomic status

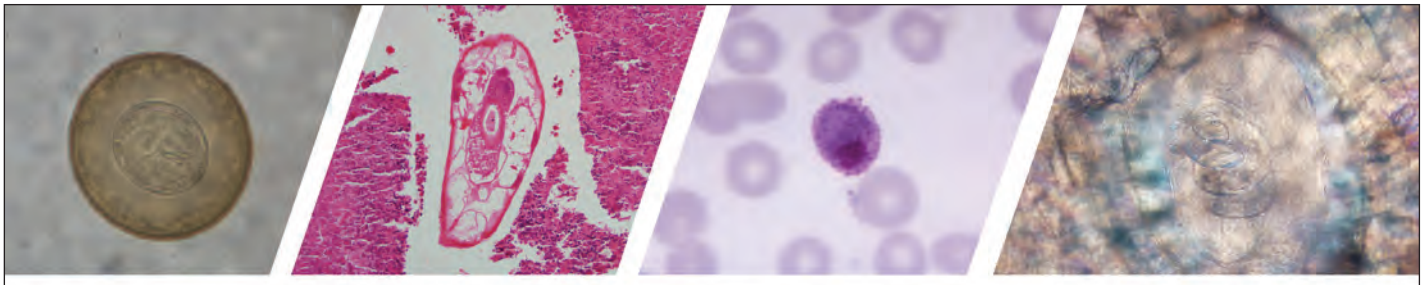

DPDx

# Diagnostic Assistance and Training in Laboratory Identification of Parasites

A free service of CDC available to laboratorians, pathologists, and other health professionals in the United States and abroad

- Diagnosis from photographs of worms, histological sections, fecal, blood, and other specimen types
- Expert diagnostic review
- Formal diagnostic laboratory report
- Submission of samples via secure file share

Visit the DPDx website for information on laboratory diagnosis, geographic distribution, clinical features, parasite life cycles, and training via Monthly Case Studies of parasitic diseases.

www.cdc.gov/dpdx
dpdx@cdc.gov

U.S. Department of Health and Human Services
Centers for Disease Control and Prevention

CS272346-DE